ANALYTICAL APPLICATION OF PROTON-INDUCED PROMPT PHOTON SPECTROMETRY

A thesis submitted to the

UNIVERSITY OF CAPE TOWN

in fulfilment of the requirements for the degree of

DOCTOR OF PHILOSOPHY

by

DHERENDRA GIHWALA

Department of Analytical Science
University of Cape Town
Rondebosch 7700
South Africa

March 1982

Acknowledgements

I wish to express my gratitude to :

Dr. Max Peisach, for the guidance, active participation and continuous support during his supervision of this investigation;

Dr. J.J. Kritzinger and the technical personnel of the Southern Universities Nuclear Institute, for their friendly assistance and efficient operation of the accelerator;

Dr. C.L. Olivier and Mr. C. Pineda, for their many stimulating discussions on prompt techniques;

Messrs S. Allie and G.J. Boulle for their help with computer programming;

Miss A. Hanmer for the kind assistance in tabulating the survey data;

Mr. L. Jacobson, of the Windhoek Museum, for providing the archaeological specimens;

Mr. P. Groenewald for his patient and expert execution of the drawings;

Mr. S. Hendricks for the photography of the drawings and preparation of the final figures;

Mrs. A. Alhadeff for the meticulous and prompt way in which she completed the typing;

The Council for Scientific and Industrial Research, for financial assistance; and,

My family and friends for their forbearance and moral support.

ABSTRACT

Prompt gamma-rays emitted under bombardment with 3.5 to 6.0 MeV protons from the 77 stable non-gaseous elements were evaluated for analytical application. The compilation included the yields of about 2200 gamma-rays and their detection limit for analysis. Because the data were measured under identical experimental conditions, the relative values may be generally applicable. For each element, the gamma-ray spectrum and the numerical data are presented in tables listing identified gamma-rays with yields and detection limits for E_p = 4.5 MeV, the gamma-yields as a function of proton energy for the most intense gamma-rays, and, the polynomial coefficients of the function relating the detection limit to the bombarding energy. An Atlas of Spectra and a Catalogue of gamma-rays summarised the data.

Because steels contain a variety of minor components, they represent a good matrix in which to test the method for multi-elemental analysis. The minor components that were determined were silicon, vanadium, chromium, manganese and cobalt and sources of interference were discussed.

The manufacture of cements requires rapid analysis of raw materials and products, for process control. Under bombardment with 4.75-MeV protons, fluorine, sodium, magnesium, aluminium, silicon, phosphorus and calcium were determined in cement standards. Under 5-MeV alpha particle bombardment confirmatory results were obtained for fluorine, sodium, magnesium and aluminium in the same samples whilst oxygen was directly measured.

Archaeological specimens were analysed to use the elemental composition as a means to characterise the samples. With the external beam technique prompt X-rays and prompt gamma-rays were simultaneously recorded. From X-ray spectra, potassium, calcium, titanium, iron, copper, zinc, gallium, rubidium, strontium and zirconium were determined and from gamma-ray spectrometry, boron, fluorine, sodium, magnesium, aluminium, silicon and copper. The same analytical data were subjected to multivariate statistical methods of cluster analysis, multi-dimensional scaling and correspondance analysis.

Lithium was determined in sugilite, a rare gem mineral, by prompt alpha particle spectrometry from the reaction $^{7}Li(p,\alpha)^{4}He$ induced by 1-MeV protons, and by prompt gamma-ray spectrometry using the 479-keV ^{7}Li p(1,0) gamma-ray induced by 1- and 4.5-MeV protons and the 429-keV ^{7}Li n(1,0) gamma-ray induced by 4.5-MeV protons.

SUMMARY

Prompt gamma-rays emitted under bombardment with protons from 3.5 to 6.0 MeV, from the 77 stable non-gaseous elements were evaluated for analytical application from the data from the bombardment of thick targets of the elements or pure simple compounds. Included in the compilation were the yields of about 2200 gamma-rays and the attainable sensitivity of analysis as given by the concentration of the element producing an integrated gamma-ray count equivalent to three times the standard deviation of the background against which it was measured. The importance of the data lies in the fact that the yields were measured under identical experimental conditions. Accordingly, the relative values may be applicable for data from complex matrices and under altered experimental conditions.

For each element, arranged in order of atomic number, the gamma-ray spectrum is discussed and thereafter the numerical data are presented in three tables; the first lists the identified gamma-rays in order of gamma-ray energy together with the yield for E_p = 4.5 MeV ; the second lists the gamma-ray yields as a function of proton energy for the five most intense gamma-rays and, where applicable, additional gamma-rays for which the sensitivity is better than 1000 $\mu g.g^{-1}$; and, the third table, the polynomial co-efficients of the function relating the attainable sensitivity to the bombarding energy, as obtained from a least squares fit of the experimental data. The minimum sensitivity and the corresponding proton energy are included in the third table. All the data are summarized in an Atlas of

Spectra and a Catalogue of Gamma-rays.

With the compilation it was possible to carry out the following analyses as examples.

Steels represent a good system in which the multi-elemental nature of the method could be tested because most steels contain a variety of minor components in a matrix consisting largely of iron. A number of standard steel samples, many of which contained the same element but in widely varying concentrations were analysed by this technique. The minor components that were determined were silicon, vanadium, chromium, manganese and cobalt. Use was made of the data in the survey to discuss, in detail, possible sources of interference.

With Ge(Li) and intrinsic germanium detectors it was possible to record simultaneously two different energy regions of the gamma-ray spectrum with improved resolution and thereby extend the number of analytically useful gamma-rays.

The manufacture of cements involves the processing of geological material from different sources. The exact composition of the ores may have a profound effect on the performance of the final product so that rapid analysis of raw materials and products is vital for process control. Since the present technique is in principle rapid, non-destructive and experimentally simple for multi-elemental analysis, its application to cement analysis was checked with standard cements obtained from the U.S. Bureau of Standards. Under bombardment with 4.75-MeV protons, flourine, sodium, magnesium, aluminium, silicon, phosphorus and

calcium were determined. When the same samples were again analysed but by using 5-MeV alpha particles to excite the prompt gamma-rays, confimatory results were obtained for flourine, sodium, magnesium and aluminium, and in addition, the oxygen content was directly measured.

Archaeological specimens were analysed in order to use the elemental composition as a means to characterise the samples. This formed part of a wider study to chart trade and migration routes of early inhabitants of South West Africa/Namibia. By using the external beam technique with a Si(Li) detector to record prompt X-rays and a Ge(Li) detector to record prompt gamma-rays simultaneously, the number of elements determined in a single sample was increased. The bombarding beam of 4-MeV protons was more energetic than was normally used to excite prompt X-rays, but this energy was chosen to increase the yield of X-rays of medium weight elements while at the same time approximating to optimal conditions for prompt gamma-ray excitation.

The elements that were determined by measuring X-ray spectra were potassium, calcium, titanium, iron, copper, zinc, gallium, rubidium, strontium and zirconium, while those determined by gamma-ray spectrometry were boron, flourine, sodium, magnesium, aluminium, silicon and copper.

The same analytical data were then subjected to multivariate statistical methods of cluster analysis, multidimensional scaling and correspondance analysis.

Sugilite, a sodium potassium, ferric silicate gem mineral, is known to contain lithium but the concentration was determined by differences, with the result that the value was subject to a large relative error. Because of the rarity of the gem, non-destructive (nuclear) methods were preferred.

Lithium was determined under proton bombardment by two complementary methods, the spectrometry of prompt alpha particles from the reaction $^{7}Li(p,\alpha)^{4}He$ and the simultaneous measurement of the 479-keV ^{7}Li p(1,0) prompt gamma-ray induced by 1 meV protons. The analysis was repeated with 4.5 MeV protons to make use of the second intense gamma-ray, 429-keV ^{7}Li n(1,0).

CONTENTS

CHAPTER I

INTRODUCTION

The present day analyst is confronted with an ever-increasing number of methods and techniques based on physical, chemical and biological sampling. His primary interest is to solve his problem by the most expenditious route. Thus, for an analytical method to be accepted in the practical world it must compete favourably with all the other methods in the arsenal of the analyst. However, a method will also find wide acceptance if it presents unique advantages in areas such as sensitivity, speed, cost, low matrix effects, preservation of the sample and so on. The advantage which nuclear analysis with charged particles of a few MeV has to offer is due to the fact that the bombarding particle rapidly loses its energy in matter. It can thus be used to analyse surfaces and near-surface layers. This region is of no small importance because all interactions with solids in heterogeneous systems, whether physical or chemical, occur at surfaces. If in addition, the surface layers are representative of the bulk of the material, the same method can be applied for bulk analysis.

Not surprisingly, therefore, charged-particle nuclear analysis is progressing from extensive exploration and development to applications in a variety of research activities [Wo 75, Bi 78, Pe 81a]. The impetus for this change comes not only from a more widespread realisation and understanding of the special merits of the analytical technique, but also from a substantial increase in the availability of the means by which such analyses can be carried out. Furthermore, although significant additions to the methodology are still being made [e.g., Zi 78] there already exists a sufficiently large bank of information for the routine application of nuclear analysis with charged particles. It is this availability of information and instruments, together with the special advantages inherent in the method, that has led to the growth of the number of applications.

Conventional activation analysis involves the measurement of radio-activity generated in the sample. The radiative emission proceeds

slowly being determined by the half-life of the decaying species and hence allows time for the sample to be removed from the place of irradiation to the place of analysis. However, many nuclear transitions occur too rapidly (with half-lives less than nano-seconds). These rapid decays can provide much information of analytical interest, but for a long time received little attention because 'prompt' radiation of this kind must be counted in situ while the irradiation takes place. It may be noted that chemical separation which enhances the sensitivity of classical activation analysis by enabling the required activity to be isolated, cannot be used with prompt radiation. Nevertheless over recent years [Bo 80, Gi 78a, Pe 81b] there has been a continuous growth of interest in prompt methods. Of particular interest is the measurement of prompt gamma radiations emitted during the de-excitation of excited nuclear states, because the energy and the yields of the gamma-rays supply information on the types and amounts of nuclei present in the sample, but unlike most other nuclear processes, the radiation is relatively easy to measure since it leaves the reaction site with little or no distortion in energy or intensity.

PROPERTIES OF NUCLEAR REACTIONS

KINEMATICAL RELATIONSHIPS

A characteristic nuclear reaction yielding prompt gamma-rays may be written in the style of a chemical reaction as

$$A + a \rightarrow B + b + \gamma + Q \qquad (1)$$

where Q is the energy released during the reaction of an incident particle, a, impinging on a target nucleus A to yield a product nucleus B with the emission of light products, b accompanying the gamma-ray(s). Symbollically this is written as :

$$A(p,b\gamma)B$$

In the non-relativistic case, and for those reactions where b is a single particle, the kinematic relationships between the reactants and products may be deduced from the laws of conservation of energy and momentum [Ev 55]. For a reaction on a target nucleus at rest (in the laboratory system of co-ordinates) the conservation of total energy requires that

$$E_a + Q = E_b + E_B + E_\gamma \qquad (2)$$

where

$$Q = (M_A + M_a - M_b - M_B)c^2, \qquad (3)$$

c is the velocity of light in a vacuum, E_γ is the energy of the gamma-ray(s) and E and M refer respectively to the kinetic energy and mass of the particles denoted by the subscripts.

If Q in equation (3) is positive, the reaction is said to be exoergic and kinetic energy is gained in the reaction. If Q is negative, the reaction is said to be endogenic and there is a threshold energy E_{th}, for the incident particle, below which the reaction cannot occur. This threshold energy is always greater than |Q| and is given by the relationship :

$$E_{th} = -Q \frac{M_B + M_b}{M_B + M_b - M_a} \qquad (4)$$

Values of Q have been tabulated for most of the commonly used reactions [Go 72 a]

Since the momentum also has to be conserved :

$$M_b V_b \text{ Cos } \theta + M_B V_B \text{ Cos } \phi = M_a V_a \qquad (5)$$

and

$$M_b V_b \text{ Sin } \theta + M_B V_B \text{ Sin } \phi = 0 , \qquad (6)$$

where V is the velocity denoted by the subscripts. θ and ϕ are the directions, in the laboratory co-ordinate system, of the particles b and B respectively, relative to the direction of incidence.

NUCLEAR REACTION CROSS SECTION

The probability of a nuclear reaction occurring is proportional to the product of a number of incident particles and the number of target nuclei.

For a bombarding beam of $\underline{\Phi}_a$ particles per second, of energy $\underline{E}_a$, incident on unit area of a slab of target material of thickness $\underline{dx}$ containing $\underline{N}_A$ nuclei per unit volume, the number, $\underline{dn}$, of nuclear reactions of the type A(a,bγ)B occurring per second in the slab is given by :

$$dn \propto \Phi_a N_A dx \tag{7}$$

$$\therefore \quad dn = \sigma(E_a) \Phi_a N_A dx \tag{8}$$

where the proportionality constant $\underline{\sigma}(E_a)$ has the dimension of area and is called the cross-section of a reaction for a bombarding energy $\underline{E}_a$.

It is usual to express the cross-section in barns where

$$1 \text{ barn} = 10^{-28} \text{ m}^2 \tag{9}$$

The relationship between cross-section and bombarding energy is called the excitation function of a specific nuclear reaction. At a fixed energy the yield of such a reaction is proportional to the reaction cross-section. In practice the analyst is more concerned with the variation of the cross-section than with the absolute value. Thus instead of calculating cross-sections, it has become the accepted practice to measure the relative yields to obtain the shape of the excitation function which may be relatively smooth or may show large peaks called resonances, corresponding to excited states of the compound nucleus formed as an intermediate stage in the reaction. In the latter case, careful choice of incident particle energy can maximise the yield from one reaction whilst minimising that of others. References to reaction cross-sections are given in [Go 72 a]while information on cross-sections themselves is available for charged-particle reactions [eg. La 66]

CHARGED PARTICLE REACTIONS

The interaction between accelerated charged particles and target nuclei leads, through nuclear interactions, to the emission of prompt gamma-rays which are characteristic of the product nuclei, and, through a knowledge of the nuclear reaction taking place, are also indicative of the target.

Figure (1) is a schematic representation of a proton-induced reaction, A(p,bγ)B.

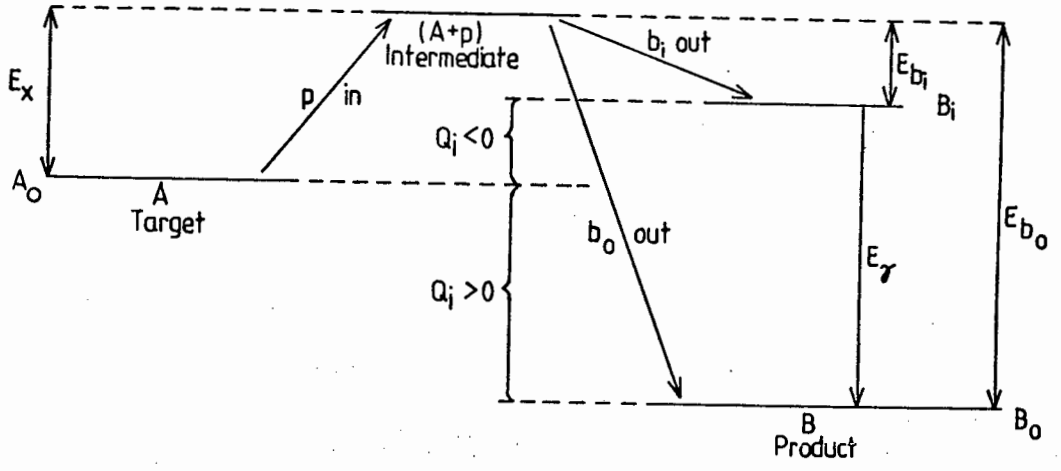

FIGURE 1 : Schematic representation of the nuclear reaction A(p,bγ)B by compound nucleus formation showing the kinetic energies involved and the energies of the gamma-rays produced. E_x is the excitation energy of the compound nucleus, which is the sum of the binding energy and a term proportional to the kinetic energy, E_p, of the bombarding particle.

The target nucleus A is bombarded with protons ,p, of energy E_p. At the time the proton enters the target nucleus, an intermediate nucleus is formed, which emits particle b almost instantaneously as a prompt light product and forms the heavy product nucleus in its ground state (B_o) or in its excited state (B_i). The corresponding light product is labelled b_o and b_i in Figure 1. The emission of prompt particles b_i will be followed by the decay of

the excited level to a lower state through the emission of the prompt gamma-rays $\underline{E}_\gamma$ as shown in the figure. The excited states correspond to a unique set of well-defined energy levels, so that the prompt gamma-rays which are emitted are characteristic of the product nucleus. A knowledge of the reaction parameters and the energy levels of the product nucleus thus permit the identification of the emitted gamma-rays.

Three special cases of nuclear interactions with bombarding proton beams that have some relevance to elemental analysis deserve mentioning :

(a) where the light product particle ,b, is a proton and only part of the energy of the bombarding proton is transferred to the target nucleus. The target nucleus is left in an excited nuclear state which subsequently decays, usually by the emission of gamma-rays. The interaction may be written as

$$p + A \longrightarrow p' + A^* + Q$$

followed by $$A^* \longrightarrow A + \gamma \qquad (10)$$

where $\underline{p}'$ refers to the outgoing proton and $\underline{A}^*$ decays to the excited state of the target nucleus. Such interactions are obviously endoergic and are called 'inelastic scattering'. The term 'Coulomb excitation' is also used for such interactions except when the mechanism involves the formation of a compound nucleus. The importance of the interaction to analysis is that the gamma-rays may be excited at bombarding energies appreciably below the Coulomb barrier (q.v.)

(b) where the only light products are gamma-rays and the proton undergoes capture by the target nucleus. Such reactions are usually exoergic and the product nucleus is produced in a highly excited state. Relatively high energy gamma-rays are frequently emitted in such reactions, and their analytical significance lies in the fact that interfering radiations of equivalent energies are unlikely.

(c) where the interaction results merely in an exchange of kinetic energy without nuclear excitation of the target nucleus. Such interactions are called 'elastic scattering' and are important for analysis because the extent of energy loss of the bombarding particle provides information on the mass of the scattering nucleus.

GAMMA-RAY EMISSION

The excitation of atomic nuclei by impinging charged particles proceeds only by means of the interaction between the electromagnetic field of the projectile and nuclear protons [Al 56]. The electrostatic Coulomb barrier, C_b, between the positively charged bombarding particle and the nuclear charge may be calculated by [Ri 68] :

$$C_b(\text{MeV}) = \frac{0.959 k Z_1 Z_2}{A_1^{1/3} + A_2^{1/3}} \qquad (11)$$

where Z and A are atomic and mass numbers respectively, the subscripts 1 and 2 refer to the bombarding and target nuclei and k is a constant related to the quantum-mechanical penetration of the barrier [Do 59]. As was indicated earlier, Coulomb excitation involves a scattering process whereby the incident projectile energies are sufficiently below the Coulomb barrier, so that the projectile is outside the range of nuclear forces. Occurrence of this scattering process can be detected by radiation from low-lying excited state(s) of the nucleus, each excited state being characterised by its energy excess above the ground state, and by spins and parity.

The mechanism described below for gamma emission is essentially the same whether the excited state is formed by Coulomb excitation or as a result of nuclear reactions.

Since gamma-rays are electromagnetic radiation, their emission by nuclei is due to the oscillation of electric charge. "The complex oscillation of electric charge in nuclei may be broken down into the backward and forward motion of charges and into the fluctuation

of the electric current flowing in closed loops" (Quoted verbatim from [Ha 62]). The distribution of charge may be expressed in terms of electric multipoles (E) and the distribution of closed current loops defines the magnetic multipoles (M). Electromagnetic theory of radiation for an oscillating charge or current loop in the nucleus shows [Ha 62] that the emitted quanta carry away angular momentum , l, as well as energy in such a way that for each quantum of energy emitted, there is an emission of one unit of angular momentum. Furthermore, there may or may not be a change in parity and spin between the initial and final states of the nucleus. Thus the general rules [Ha 62] connecting the ground and excited states of the nucleus are :

1. $I_i + I_f \geq l \geq |I_i - I_f|$
2. $\pi_i + \pi_f + l$ is even for radiation by electric radiation.
3. $\pi_i + \pi_f + l$ is odd for radiation by magnetic radiation. (12)

where I and π represent the spins and parities respectively and subscripts i and f denote respectively the initial and final states of the nucleus. The terminology commonly used to describe the type of transition taking place are En and Mn where n is a number representing the angular momentum quanta carried away. The terminology for gamma-ray processes can thus be summarised [Ha 62] :

Radiation type	Name	Angular momentum carried away	Does nuclear parity change?
E1	Electric dipole	1	Yes
M1	Magnetic dipole	1	No
E2	Electric quadrupole	2	No
M2	Magnetic quadrupole	2	Yes
E3	Electric octupole	3	Yes
M3	Magnetic octupole	3	No
E4	Electric 2^4-pole	4	No
M4	Magnetic 2^4-pole	4	Yes

Table 1 : Gamma-ray emission rules.

It should be noted that the minimum angular momentum which can be carried away by a gamma-ray photon is one unit, hence transitions are forbidden between two levels both of which have zero spin.

Recent tabulations have listed the strengths of gamma-rays classified according to the character of the transition [En 79a, En 79b, En 81].

NUCLEAR ANALYSIS WITH CHARGED PARTICLES

The main difference between analysis with charged particles and that using other activation methods, stems from the characteristically strong Coulomb interaction of the bombarding ions with electric charges in matter. Whereas neutrons and photons penetrate matter easily, charged particles are slowed down and stopped within a relatively short distance. Thus, while the nuclear cross-section may be considered essentially constant throughout the samples for neutrons and photons, it should be expected to vary drastically with depth as the charged particle energy is degraded within the sample.

THICK TARGET YIELDS

When the nuclei $\underline{A}$ of a thin target interact with a beam of charged particles of energy $\underline{E}_i$, the yield of gamma-rays (Y) is proportional to the rate of reaction as defined in equation (7). The beam is degraded only slightly in a thin target so $\underline{\sigma}$ in equation (8) can be considered constant. Since, however, the analyst is more often than not confronted with the analysis of thick samples (infinitely thick with respect to the beam), the rate of gamma-ray production is given by :

$$Y(E_i) = N_o \Phi_A \int_0^R \sigma(x)dx \qquad (13)$$

where $\underline{N}_o$ is the number of nuclei per unit mass of target and $\underline{R}$ is the effective range of the bombarding particle in the thick target beyond which the energy is insufficient to cause nuclear

excitation. Experimentally the yield that is measured, y, is related to the above but corrected for the solid angle Ω, subtended by the detector and the fractional efficiency of detection of the gamma-ray, ε. Thus

$$y = \frac{Y\Omega\varepsilon}{4\pi} \tag{14}$$

Since the particle energy at $x = R$ is E_{th}, the yield may be rewritten in terms of energy as :

$$Y(E_i) = N_o \Phi_A \int_{E_i}^{E_{th}} \sigma(E) \left(\frac{dE(x)}{\rho dx} \right)^{-1} dE \tag{15}$$

where $\frac{dE(x)}{\rho dx}$ is the stopping power with $E(x)$ as the kinetic energy of a charged particle at depth x in the sample and ρ, the sample density. The stopping power, i.e. the energy loss per unit length is given by [Fa 63] :

$$-\frac{dE(x)}{dx} = \frac{4\pi e^4 Z_1^2 n}{M_e v^2} \times \left[\ln \left(\frac{2M_e v^2}{q} \right) + \ln \left(\frac{1}{1-\beta^2} \right) - \beta^2 \right] \tag{16}$$

where e = charge on the electron

n = number of electrons per unit volume of the sample

M_e = mass of the electron

q = the effective ionization potential of the atoms in the target material

v = the velocity (non-relativistic) of the projectile

β = v/c, where c is the velocity of light.

Multiplying and dividing both fractions on the right by M_1, the incident particle mass, and remembering that $E = \frac{1}{2} M_1 v^2$, equation (16) is converted to :

$$-\frac{dE(x)}{dx} = nK \frac{Z_1^2 M_1}{E} \times \left[\ln \frac{4M_e E}{M_1 q} + \ln \left(\frac{1}{1-\beta^2} \right) - \beta^2 \right] \tag{17}$$

where $K = \frac{2\pi e^4}{M_e}$

Thus it is clear that the stopping power depends on the nature of the matrix (n,q), and on the nature (Z_1,M_1) and kinetic energy (E) of the bombarding particle.

QUANTITATIVE ANALYSIS

The measured yield, y, from a nuclide w in a sample is given [Is 78a] by modifying equation (15) to :

$$y = \Phi P_w \frac{1}{M_w} \int_{E_i}^{E_{th}} \sigma(E) \left(\frac{\rho dx}{dE(x)} \right) dE \qquad (18)$$

where P_w is the concentration of w in the sample and M_w its atomic mass.
The ratio between the measured yields induced in a sample, s, and in a standard can be written as :

$$\frac{y_s}{y^0} = \frac{\Phi_s}{\Phi^0} \frac{(P_w)_s}{(P_w)^0} \frac{U_s}{U^0} \qquad (19)$$

where the superscript 0 refers to the standard, and the subscript s to the sample, and where the effective quantity U is defined as :

$$U = \int_{E_i}^{E_{th}} \sigma(E) \left(\frac{\rho dx}{dE(x)} \right) dE \qquad (20)$$

Various mathematical methods have been applied to cope with the problem of correcting for range effects of charged particles in different matrices. The best known procedures are :

(1) the method of equivalent thicknesses [En 65]. This method is not easy to apply and has the disadvantage that the errors of the analysis depend directly on the errors of the calculated equivalent thickness. Consequently this method is not often used.

(2) the method of average cross-sections [Ri 65, Ri 67], and,

(3) the method of average stopping power [Is 78a].

The latter two methods are closely related.

From equation (20) it can be seen that $\underline{U}$ is composed of a cross-section and a stopping power factor. If now the value of the cross-section is replaced by the average cross-section $\langle\sigma\rangle$ we obtain :

$$U = \langle\sigma\rangle \int_{E_i}^{E_{th}} \frac{\rho dx}{dE(x)} \, dE \tag{21}$$

which expresses $\underline{U}$ according to the method of average cross-sections. Alternatively, if the average stopping power $\left\langle \frac{dE(x)}{\rho dx} \right\rangle$ is substituted for the stopping power factor we obtain :

$$U = \left\langle \frac{dE(x)}{\rho dx} \right\rangle^{-1} \int_{E_i}^{E_{th}} \sigma(E) \, dE \tag{22}$$

which expresses $\underline{U}$ according to the method of average stopping powers.

In a detailed discussion [Is 78a] it was shown that the assumptions inherent in the method of average cross-sections reduces the value of the correction factor to

$$\frac{U_s}{U^0} = \frac{R_s}{R^0} \quad , \tag{23}$$

while the assumptions of the method of average stopping powers reduced the value of the correction factor to

$$\frac{U_s}{U^0} = \frac{\left(\frac{dE}{\rho dx}\right)_s}{\left(\frac{dE}{\rho dx}\right)^0} \qquad \text{at } E = E_m \tag{24}$$

where the mean energy $\underline{E}_m$ at which the ratio of the stopping powers have to be calculated, is given by :

$$E_m = \frac{\int_0^{E_i} E\sigma(E) \, dE}{\int_0^{E_i} \sigma(E) \, dE} \tag{25}$$

Experimental evaluation of these two approaches for oxygen determination in different matrices by triton activation [Is 78a] showed that the method of average stopping powers was clearly the more accurate. For this reason the method of average stopping powers was used in this investigation.

It may be noted that $\underline{E}_m$ depends only on the excitation function and is independent of the matrix in which the analysis may be carried out. For this reason universally applicable $\underline{E}_m$ values may be compiled as a function of bombarding energy from excitation function data.

Since the accuracy of an analysis will depend on the accuracy of the stopping power factor it is important that the most accurate data on stopping powers should be used. The most recent compilation [Zi 77] of such data give values for a variety of particles for matrices of each pure element. The data can readily be converted by Bragg's Law for any matrix of known composition.

If in any particular analysis it is feared that systematic errors may be introduced by even the best available stopping power data, it has been shown [Is 78b] that the use of stopping power data can be avoided provided the products of several nuclear reactions are simultaneously measured.

PROTON-INDUCED PROMPT GAMMA-RAY SPECTROMETRY

Interest in prompt gamma-ray spectrometry has been growing steadily over the past 25 years primarily because it is so simple to apply and also because it is potentially a rapid method. Among the earliest applications were the determination of beryllium in airborne dust by the measurement of the gamma-rays emitted during the irradiation with alpha particles from ^{210}Po [Go 57] and the determination of flourine in glasses by measuring the energetic gamma-rays emitted under proton bombardment [Ru 57]. Since then interest in the technique has grown apace but most of the literature on the subject was published over the past decade. Accelerated protons and to a lesser extent, helium ions were at first the favoured

means of excitation but with improved accelerator techniques more attention was given to heavier ions as well.

A comprehensive bibliography [Bi 78] which included the literature published to the end of 1976 revealed that most investigations made use of proton beams and of these many of the investigations were confined to studies on low-Z elements such as fluorine, sodium, aluminium and silicon. Furthermore, relatively low bombarding energies were used in these investigations. A notable exception was the use of cyclotron beams of up to 8 MeV [Sh 73].

In recent years there has appeared a series of surveys each extending the knowledge of prompt gamma-ray spectrometry to areas of application that had previously been poorly documented. Thus the prompt radiations from a wide range of elements under bombardment with protons up to 4 MeV were studied [Cl 75] and attempts were made at estimating the attainable sensitivities. The data obtained from the wide-ranging investigation from the Belgium group were summarised [De 78] in a survey covering the elements Ti to Zn. In that study, data was provided on the bombardment of thick targets with protons up to 3.5 MeV. The paucity of analytical data for alpha particle ($^4He^+$) bombardment was largely remedied by a systematic survey [Gi 79a] in which the gamma-rays induced by 5 MeV beams were summarised. Further data were also reported [Gi 78a] for beams of 12 and 16 MeV. In the case of triton irradiation at energies of a few MeV the most likely reactions are (t,n), (t,p), (t,d) and (t,α), all of which are so exoergic that complex gamma-ray spectra may be expected from the decay of their products. This may explain why only one application of this technique [Pe 72] appeared in the literature prior to the publication of a systematic study covering over 30 elements [Bo 78] and providing information for irradiation with tritons up to 3.5 MeV. The analytical possibilities of Coulomb excitation with heavy ions was demonstrated for beams of 55-MeV ^{35}Cl ions in a study [Bo 79a] covering over 40 elements.

A recent review article [Bo 80] dealt with the prompt gamma-rays produced during the bombardment of most elements by a variety of charged particles and the use of prompt gamma-ray spectrometry as

an analytical tool. In this review analytical possibilities were enumerated and the expected sensitivities were reported. Even a casual reading of this article [Bo 80] revealed that whilst much effort has gone into the study of the analytical possibilities of prompt gamma-ray spectrometry with beams of a specialised nature available only from selected accelerators, the use of simple proton beams at energies above 4 MeV was ignored. This observation confirmed earlier impressions gained from the examination of the bibliography on ion-induced prompt gamma-rays for nuclear analysis [Bi 78], where only a single article [Sh 73] described the use of a few elements with 6 and 8 MeV protons.

A need thus existed to extend the work done by previous users of proton beams to energies exceeding 4 MeV. The Van de Graaff accelerator of the Southern Universities Nuclear Institute is capable of providing beams up to 6 MeV. Accordingly this work was undertaken to study proton-induced prompt gamma-ray spectrometry with beams of up to 6 MeV and to evaluate the analytical possibilities.

SCOPE OF THIS INVESTIGATION

Nuclear physics research has established the energy levels of most nuclei to fairly high energies of excitation and their decay by gamma-ray emission but for analytical purposes this mass of data is not readily assimilable because most frequently the original measurements were carried out on thin targets and under conditions of irradiation selected in terms of the requirements of the original investigation. What the analyst needs is a normalisation of the gamma-ray yields to a single set of experimental conditions. Furthermore, since most analyses are not carried out on thin targets the aforementioned normalised data would be more useful when relating to thick targets. In such a compilation the absolute accuracy of the data though important would be secondary to the relative yields of gamma-rays emitted from different elements under constant conditions of irradiation. Such relative values could then readily be applied to any analysis of thick targets using bombarding beams of the same energy.

For the above reasons the primary purpose of this investigation was to identify the proton-induced gamma-rays and to measure their yields under uniform experimental conditions for as many elements as possible. The usefulness of the data would increase with the increasing range of proton energies and for this reason the investigations were extended to 6 MeV, being the highest proton energy routinely accessable with the Van de Graaff accelerator of the Southern Universities Nuclear Institute. To provide an overlap with previously published [Bi 78, De 78, An 81] compilations a lower energy of 3.5 MeV was decided upon. Proton energies below the latter value were however not excluded for cases of special interest.

The characteristic features of a gamma-ray spectrum are sharp peaks superimposed on a continuum. Since the intensities of the gamma-rays have to be measured against the continuum, the sensitivity of analysis attainable through the use of a particular gamma-ray will not increase uniformly with increasing yield but will also depend on the manner in which the intensity of the continuum changes. Accordingly, the variation of attainable sensitivity with bombarding energy had to be determined.

Every naturally-occurring element was studied except hydrogen, the nucleus of which has no excited state, the noble gases and the radioactive heavy elements; polonium, radium, actinium and protactinium. The investigation thus covered 77 elements.

Once the data had been evaluated practical application of the technique had to be studied.

The experimental procedures are described in Chapter 2. The main features of the results obtained for each element are described element-for-element in Chapter 3. Under each element are listed the observed and identified gamma-rays and the yield data pertaining to 4.5 MeV protons. The yield of gamma-rays showing the best for potential analytical application are given as a function of bombarding energy from 3.5 to 6 MeV. For these gamma-rays sensitivity

data are presented as co-efficients of a polynomial fitted to the experimental data by the method of least squares.

The information contained in the survey was applied for the determination of minor components in steels. This work is described in Chapter 4 and illustrates how two different detectors can be used for spectrometry of different energy regions in the gamma-ray spectra. In Chapter 5, the application of the technique to the determination of major and minor components in cements is described and illustrated how two different irradiation conditions could be used to increase the number of elements analysed. Two different analytical techniques of photon spectrometry were used for the analysis of archaeological samples and this work is described in Chapter 6, while comparison between prompt gamma spectrometry and prompt charged-particle spectrometry was illustrated by the analysis of a gemstone mineral, as described in Chapter 7.

It was realised that a systematic compilation of the data would be of archival value. For this reason an Atlas of Spectra recorded under bombardment with 4 MeV protons is given for the elements investigated in order of atomic number in Appendix I. A Catalogue of all observed and identified gamma-rays is given in Appendix II in order of gamma-ray energy. To facilitate the use of the Catalogue for evaluating possible interferences, yields and attainable sensitivities at a proton energy of 4.5 MeV are included in the listing.

CHAPTER 2

EXPERIMENTAL

SELECTION OF MATERIALS

In order to obtain quantitative data, targets of pure elements were preferred. Where metals were available, these were used. In some cases the pure elements were available in powdered form and these were compressed into tablets for use, provided the tablet could withstand the temperatures generated during bombardment.

Where the elements were either chemically reactive or unsuitable for irradiation, simple compounds such as oxides, halides or other salts were used. The exact chemical form of the target is described for each element in Chapter 3.

PREPARATION OF SAMPLES FOR IRRADIATION

(a) Pure solid samples

Pure metals were usually obtained in flat sheet form, 1 - 2 mm thick and measuring 25 mm square. These were machined to fit the target holders (q.v.), and washed by immersion in absolute alcohol.

Standard steel samples were obtained from the U.S. Bureau of Standards, Washington and Harwell, England. They were cut into discs of 2 mm thick and about 13 mm diameter, except when the original dimensions were smaller. The surface of the samples were mechanically polished with diamond paste to give a smooth, mirror-like finish, and thereafter were carefully washed under ultra-sonic agitation with water containing detergents to remove the remaining traces of abrasives. This process was repeated using hot organic solvents to remove surface greases. Silicon was obtained in the form of pure solid wafers whereas pure germanium and hafnium targets were machined to a convenient size out of lumps of pure element.

(b) Pellets of pure elements and simple compounds

Elements that were obtained in a granular form or coarse lumps were crushed, and powdered portions of about 15 g were pressed into pellets having the same dimensions as the machined discs, by means of a Beckman 13 mm die and 25 ton hydraulic press, shown diagrammatically in Figure 2.

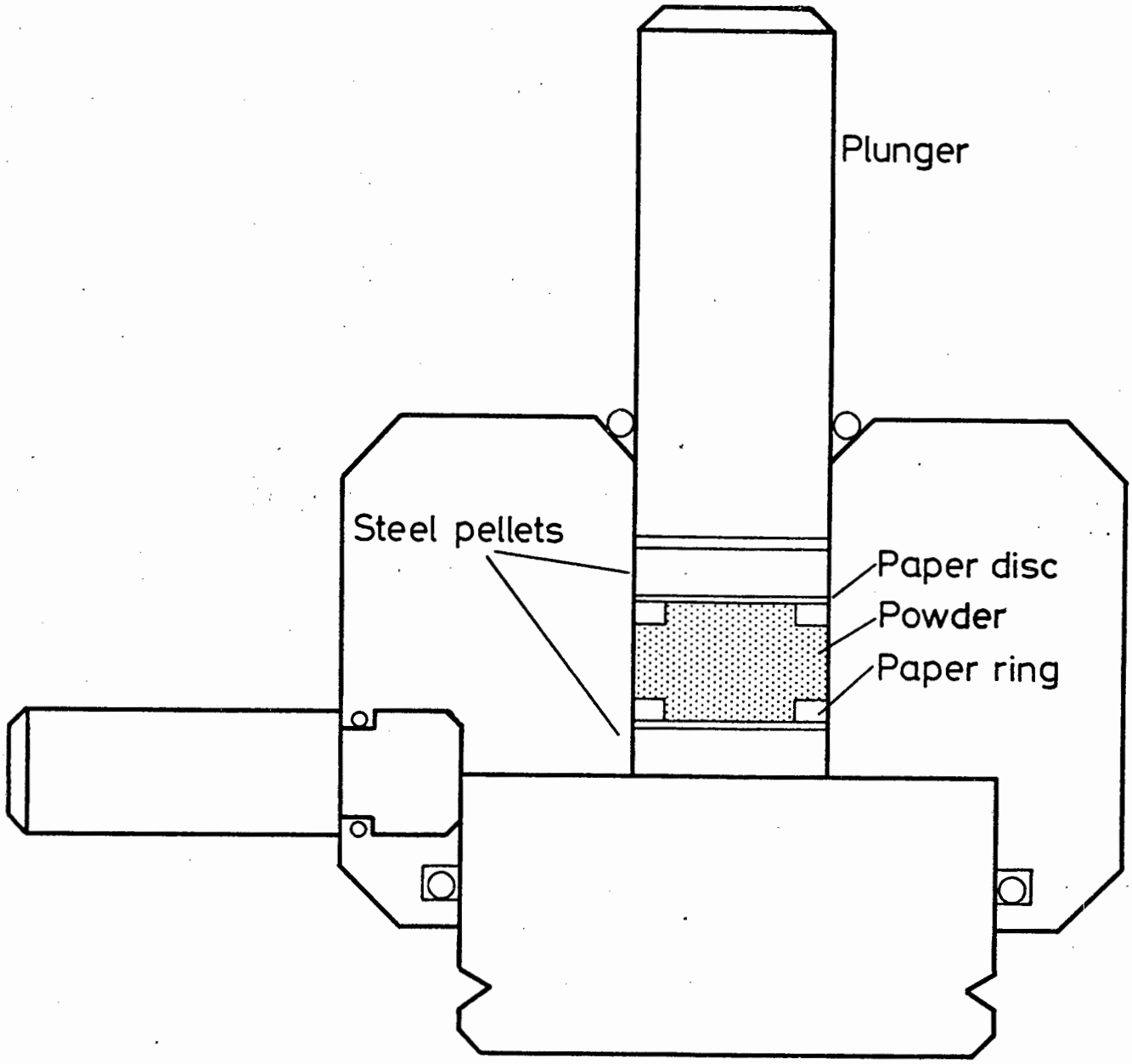

FIGURE 2 : Schematic representation of the die used for making target pellets.

The paper rings and discs shown in the figure were used to give extra mechanical strength to allow for safer handling of the final pellet. The paper discs also served to protect the die from any damage by small crystals of harder materials, and overall, to decrease the possibility of cross-contamination between samples. Compression of material was carried out under vacuum to remove trapped air. A uniform pressure of ten tons was applied since this was the maximum permissible for the die used. After the preparation of each pellet, the whole apparatus was thoroughly cleaned and washed with water and alcohol to remove all traces of remaining powder.

Standard reference cement samples were obtained from the U.S. Bureau of Standards, Washington, U.S.A. and were pressed into pellets.

It was assumed that all the sample specimens were homogeneous. Prior to irradiation, all the targets were kept in a vacuum dessicator to prevent contamination from dust.

(c) Thin targets of pure elements

For the qualitative study of some of the pure elements, use was made of thin targets. Foils of 5 μm thick, mounted on permanent supports of epoxyresin of about 1 mm thick were obtained from Messrs. Goodfellow Metals, Cambridge, England. The only handling that was required on these targets was to cut them to fit on the target holder. Some thin targets of pure compounds were made by evaporating the material onto backing of tantalum in vacuum under electron bombardment.

(d) Archaeological Specimens

Source materials such as soapstone and clay samples were obtained from several areas of South West Africa/Namibia. From the soapstone rocks obtained, smooth slabs were cut measuring about 20 mm wide and varying in length between 150 and 200 mm. The clay specimens were compressed into pellets by the technique previously described. Unlike source

materials, archaeological specimens of artefacts, potsherds and clays were analysed *without treatment*, but care was taken to mount the specimens in such a way that the bombarding beam fell onto a relatively flat area.

(e) Gemstone mineral

Sugilite, a sodium potassium, ferric silicate mineral from the Kuruman district of the Northern Cape was analysed for its previously undetermined lithium content. The single sample had been polished and thus presented smooth faces for bombardment. Standards for comparison were prepared by making homogeneous mixtures of the known constituents in a bore-mill and compressing the mixtures into pellets.

THE FACILITIES FOR IRRADIATION AND MEASUREMENT

THE SCATTERING CHAMBER

Irradiations were carried out in a scattering chamber (Figure 3) which was specially designed for optimum efficiency and for the simultaneous use with five detectors. The aluminium chamber was electrically insulated from the beam line and all detectors, so that it serves as a self-contained Faraday cup. It was thus possible to integrate the bombarding current directly. The bombarding beam was collimated outside the chamber in the beam tubes, by a series of tantalum diaphragms The final beam spot diameter was defined by a variable collimator just outside the chamber, in front of which was placed a copper grid, charged to -300 V, to prevent entry into the chamber of secondary electrons produced by glancing collisions of imperfectly focused beams on the beam tubes.

The chamber was easily isolated from the remainder of the accelerator vacuum system with a single-stroke hand-operated vacuum lock. The size and position of the beam could be viewed on a quartz window at the rear of the chamber.

Since the archaeological samples, that could be analysed in vacuum, were limited in shape and size by the geometry of the vacuum

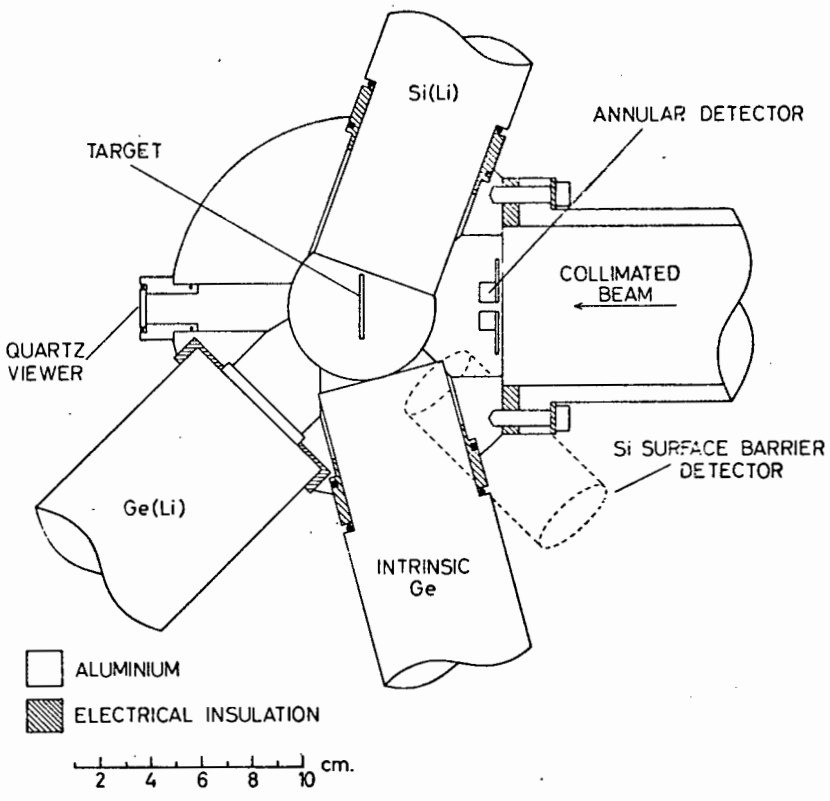

FIGURE 3 : Insulated scattering chamber specially designed for analytical use with up to five different detectors.

chamber, most samples were analysed externally [Bo 79c]. The quartz viewer at the rear of the chamber was then removed and replaced by an exit window made of 0.01 mm thick beryllium foil (1.85 mg.cm^2). After emerging through the window, the beam was collimated by a 3 mm hole in a perspex plate and allowed to fall on the target mounted at an angle of 45^o to the direction of incidence of the beam. Samples which were awkward in shape and size could now be easily mounted manually.

THE DETECTORS

To measure the prompt gamma-rays, use was made of a lithium-drifted germanium detector [Ge(Li)], and a high-resolution intrinsic germanium detector [IG].

The 80-cm^3 Ge(Li) detector had a resolution of 2.3 keV at 1332 keV

and was of the type which has been in common use over the past decade.

For energy calibration, standard reference sources, ^{22}Na, ^{57}Co, ^{60}Co, ^{137}Cs, and others were used.

To calculate the relative yields of the various prompt gamma-rays that were studied, the absolute efficiency of the detector had to be measured, using calibrated sources. A plot of the % efficiency as a function of gamma-ray energy is shown in Figure 4.

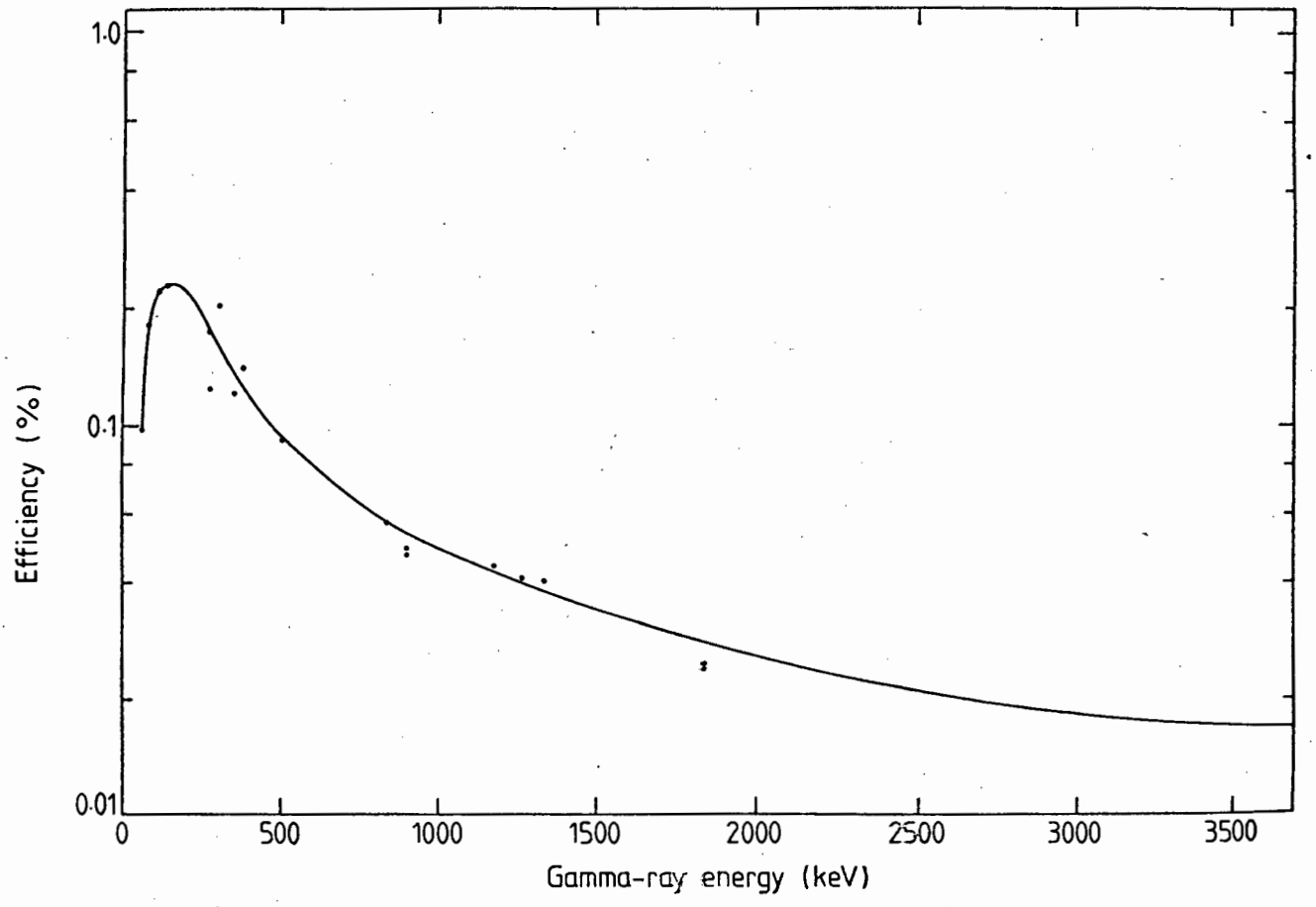

FIGURE 4 : The measured efficiency of the Ge(Li) detector as a function of gamma-ray energy.

The Ge(Li) detector was positioned at 45° to the beam where the aluminium chamber was specially thinned so as to reduce the absorption of lower energy gamma-rays. It was also found that in

this position, the effect of neutrons from the target was small.

For high-resolution work, a Princeton Gamma-Tech intrinsic germanium detector was used having an active area of 300 mm^2 and a thickness of 10 mm. The resolution at 5.9 keV was 266 eV and at 122 keV, 534 eV. Initially the IG spectrometer was placed in a port of the scattering chamber, positioned at 105^{o} to the beam. However, in this position the detector was subject to vibration from the vacuum pumps, which resulted in high microphonic background in the gamma-ray spectrum. Accordingly, the detector was shifted to a free-standing 45^{o} position.

Other detectors used in the present study were :

(a) a lithium-drifted silicon detector, Si(Li), for the measurement of prompt X-rays. The detector was used simultaneously with the Ge(Li) in the study of archaeological specimens.

(b) a silicon surface barrier detector for the measurement of prompt alpha particles. A gold absorber of appropriate thickness was placed in front of the detector to prevent back-scattered protons from penetrating to the detector. This detector was used simultaneously with the Ge(Li) spectrometer in the determination of lithium in a gem mineral.

THE AUTOMATIC SAMPLE CHANGER

The samples were mounted normal to the beam on a vertical ladder which had space for ten holders with an additional vacant position for beam alignment. The ladder was fitted into the shaft of a motor drive and kept accurately at the centre of the scattering chamber by nylon-grooved wheels on either side (Figure 5).

The position of the ladder was controlled by a stepping motor operating at six pulses per mm, through a 25:1 gear, thereby enabling the target to be positioned accurately within about 6 μm, at a speed of 1 to 400 steps per second. By moving the ladder in the chamber under remote control, it was possible to bombard

ten targets without disruption of the vacuum system.

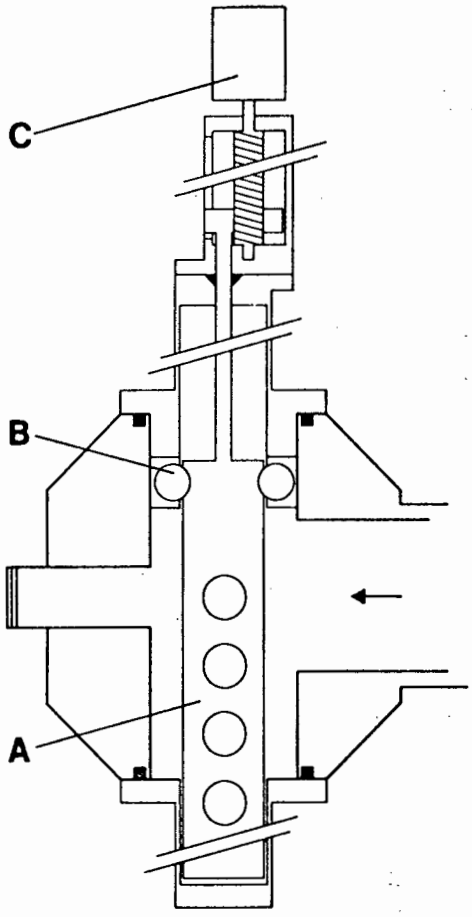

FIGURE 5 : Automatic Sample Changer
A - Sample Ladder
B - Nylon positioning wheels
C - Stepping motor

THE ELECTRONIC MEASURING SYSTEM

A block diagram of the electronic system used for prompt gamma-ray spectrometry is shown in Figure 6.

The output pulses from the Ge(Li) detector, were transmitted through a low noise pre-amplifier to a high resolution linear research amplifier (ORTEC Model 450), both of which were able to handle high count rates without appreciable loss of energy resolution. These pulses were then transmitted to a 4096-channel pulse-height analyser through an anologue to digital converter. A current integrator, set to count for either a pre-determined time or to accumulate a pre-determined total current, automatically switched off the measuring system when the value was reached. An identical arrangement was used with the IG detector.

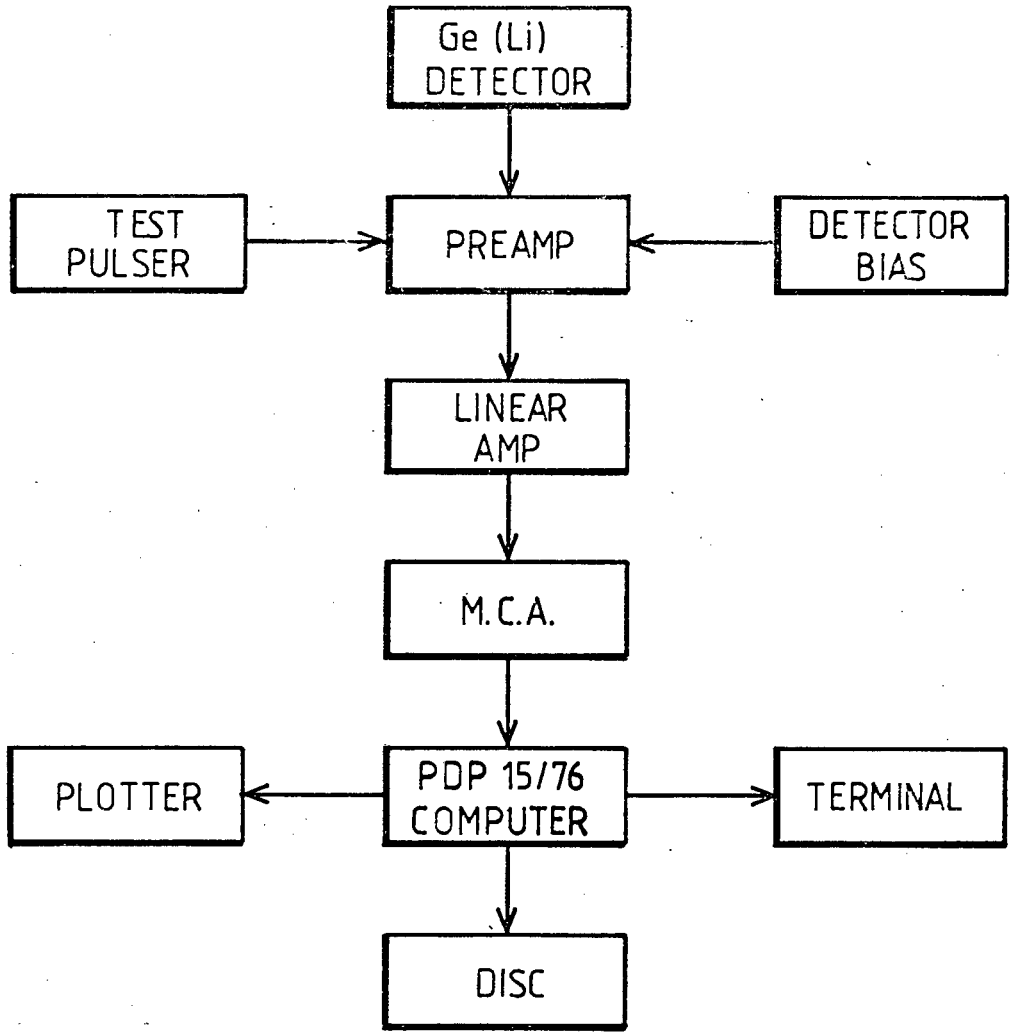

FIGURE 6 : Block diagram of eletronic and computation equipment for gamma-ray measurement. For low energy gamma-ray measurements, an intrinsic germanium detector was used.

IRRADIATION

A proton beam of variable energy was produced by the 6 MV Van de Graaff accelerator of the Southern Universities Nuclear Institute. The accelerated beam was reduced by collimation and focused to a circular cross-section of 3.5 mm. The beam impinging on the target was measured with a current integrator and the current was so adjusted that system dead-time losses in the multi-channel analyser did not exceed 10%. As there was some variation in the proton beam current with time, it was often more convenient for determining the duration of the irradiation by the integrated charge falling on the target rather than by the clock time. Depending on the type of target under investigation, beam currents ranged from about 0.5 to 3 nA. Counting required 10 to 15 minutes per sample depending on the nature of the sample under scrutiny

and in particular on the concentration levels at which the elements were to be determined.
For the survey, proton beams of 3500 keV to 6000 keV were used, whilst for excitation curve data, targets were bombarded with protons of 2500 keV to 5700 keV in steps of 100 keV. The bombarding energies used in the actual analysis for specific elements, were selected according to the sensitivity curve data obtained in the Survey (see Chapter 3).

At the end of each run, the spectrum was recorded on magnetic tape. The UNIVAC 1105 computer of the University of Cape Town was used to process the data off-line.

COMPUTATION

The availability of the PDP-11 and PDP-15 on-line systems at SUNI assisted materially in the smooth running of the experiment by instantaneously supplying information such as peak position, peak areas and energy calibrations on demand.

The PDP-15 computer, under the operating system RSX PLUS III, was also used to compile programs to assist in the calculation of the survey data. One such program was written to calculate stopping powers of compounds using Ziegler co-efficients [Zi 77] and Bragg's Law, while another was for computing the co-efficients of polynomials fitted to sensitivity functions by the method of least squares.

The computer program routinely used for the determination of peak areas was a modified version of SAMPO [Ro 69]. The program fitted modified Gaussian peaks and curved baselines to the observed data, by iteration until the chi square value reached a minimum. Input information included a series of well-defined single peaks, approximate peak centres, resolution and two parameters describing deviation from true Gaussian shape as obtained from radioactive standards. Using this information, the program computed a calculated spectrum, and compared it with the observed spectrum, a calculated baseline, and the best fit parameters, centroids and areas of spectrum peaks. An important advantage of the program

was that it enabled up to six close-lying or even overlapping peaks to be resolved and separately integrated.

CHAPTER 3

SURVEY OF THE ELEMENTS

The objective of the present study was two-fold. The first need was to make available to the analyst added information of a kind that would make decisions on selectivity and sensitivity possible. Since what information was available was widely scattered from many investigations under different experimental conditions, the second need was to establish a consistent bank of data so as to make possible comparison of the gamma-ray intensities from different elements in a single matrix.

When investigations were carried out at bombarding energies above 3500 keV, not only did the yield of gamma-rays increase with energy, but the number of gamma-rays available for analysis also increased. With increasing complexity of the gamma-ray spectra at higher proton energy, the probability of the inter-element interferences increased as well. To evaluate the extent of possible interferences, it was necessary to study as many elements as possible and to extend the study over a wide range of bombarding energies. In the survey that follows, attainable sensitivities and yields of gamma-rays from all stable, non-gaseous elements under bombardment with protons from 3500 to 6000 keV are presented.

SENSITIVITY OF ANALYSIS

It is usual to express the sensitivity of an analytical method as the minimum amount of material that can be determined. In the present context the sensitivity of an analysis, based on the measurement of a particular gamma-ray, will depend on the integrated area under the relevant spectrum peak, but since the peak is measured against a background continuum it may be expected that the intensity of the background will determine the sensitivity of the measurement. The usual method of determining the nett area under the peak in the spectrum is to integrate the total peak area in the required energy region and to subtract from it the integrated background, the shape of the background spectrum being inferred from adjacent energy regions.

It can readily be shown that for a large number of counts, the standard deviation is given by $\sqrt{\underline{C}}$ where $\underline{C}$ is the expected average value of the measured count. In practice, the relationship is approximately true when $\underline{C}$ refers to the measured number of counts.

Since $$C_{nett} = C_{total} - C_{bg} \quad ,$$

where the subscripts refer respectively to the nett integrated count under the peak, gross integrated count and the integrated background count, the standard deviation of the nett count, σ_{nett}, is given by

$$\sigma_{nett} = \sqrt{\sigma^2_{total} + \sigma^2_{bg}} \qquad (26)$$

and therefore

$$\sigma_{nett} = \sqrt{C_{nett} + 2\, C_{bg}} \qquad (27)$$

It thus follows that the background is the most important parameter affecting the sensitivity.

For an analytical method three levels of concentration can be considered [Cu 68] :

(a) a concentration region where the nett peak is sufficiently precise to enable quantitative analysis to be carried out with relative standard deviation of less than 10% ,

(b) a lower level of concentration where the nett peak is sufficiently intense for qualitative analysis but where quantitative analysis become more inexact, and ,

(c) the lowest concentration region where the definition of the nett peak is indistinct and qualitative analysis becomes unreliable.

From a thorough investigation of sensitivity limits in these regions [Cu 68] using well-known blanks and accepting the restriction that (a) should have a minimum precision of 10%, it was shown that :

In region (a) $$C_{nett} \geq 10\sigma_{bg}$$

In region (b) $$10\sigma_{bg} > C_{nett} \geq 3.29\sigma_{bg}$$

In region (c) $$3.29\sigma_{bg} > C_{nett} \geq 1.64\sigma_{bg}$$

In this work 'sensitivity' as applied to a gamma-ray refers to the concentration of the target element for which

$$C_{nett} = 3\sqrt{C_{bg}} \qquad (28)$$

and approximates to the lower limit of region (b). These values were obtained from spectra of thick targets of pure elements, and this approach is justified because the spectrum that would be generated from the element under consideration in any concentration would approximate to that of the pure element if, ideally, that element alone contributed to the gamma-ray spectrum. Therefore the sensitivity limits given here are *practical* limits albeit from an idealised matrix. In these targets, the same elements would be detectable with a greater sensitivity.

The analytical definition of sensitivity as accepted by the International Union of Pure and Applied Chemistry refers to the rate of change of signal with concentration as given by the slope of a calibration line [An 76]. Such a definition by implication refers to region (a) above but cannot apply when no calibration line had been constructed, as is the case in this survey. The 'limit of detection' as defined in the same document [An 76] gives a lower value than that given by equation (28) and refers to region (c) above. As has been mentioned above, the term here

refers approximately to the region (b).

FACTORS INFLUENCING SENSITIVITY

For a prevailing level of background the sensitivity would be improved if the peak spanned the least possible expanse of the continuum i.e. the detector should be of optimum resolution. Poor sensitivity resulted from the measurement of Doppler broadened prompt gamma-rays in cases where the extent of broadening exceeded the resolution of the detector. The Doppler effect is prominent in $(p,\alpha\gamma)$ nuclear reactions on light target nuclei.

When an excitation function contained marked resonances, advantages could be taken of the high yields obtainable at resonance energies in thin target analysis.

In thick target bombardment the yield of prompt photons increased with bombarding energy and accordingly the attainable sensitivities might have been expected to improve. However, with higher bombarding energy there was an increase in the flux and number of prompt gamma-rays with the result that the intensity of the Compton continuum also increased. The optimum bombarding energy was the energy where the best compromise between increased yield and increased background was attained. To determine the optimal bombarding conditions interference-free sensitivities were calculated as a function of bombarding energy. An n-order polynomial, with n = 3 in most cases was fitted to the experimental data by the method of least squares. In the survey that follows the co-efficients of the corresponding curve for the polynomial

$$S = \sum_{i=o}^{n} a_i E^i \qquad (29)$$

are listed for each element. The proton energy at which the minimum sensitivity, S_{min}, is attainable, is given for each gamma-ray considered. It may however be pointed out that the use of bombarding energies higher than that for optimal sensitivity, has the advantage that data may be accumulated faster, because of the increased reaction cross-section, for a relatively small loss of

sensitivity. Such conditions may be preferred when higher concentrations have to be determined.

Because the intensity of the background is so important to the measurement of sensitivity it may be appropriate to discuss the backgrounds that are generated by the irradiating beam and that caused by radioactivity in the vicinity, before proceeding to the element-by-element survey.

BEAM-INDUCED BACKGROUND

The background counts (see background) in the previous section refer to the level of the continuum in the spectrum against which the peak of interest had to be integrated. The intensity of this continuum is made up of contributions from the following beam-induced counts :

(i) gamma-rays produced in the target having energies greater than the gamma-ray under investigation.

Since a flux of monoenergetic gamma-rays interacting with the detector will produce a spectrum consisting of a photopeak representing the energy of a gamma-ray and a continuum caused mainly by Compton events in the detector, the background continuum under a selected peak would consist largely of a sum of the continua generated by each gamma-ray of higher energy in the region of interest. Such a background is unavoidable and in the case of a pure element would represent the lowest attainable intensity.

(ii) gamma-rays and X-rays produced by the bombarding particles on materials other than the target.

The interaction of the bombarding beam with the collimator material and with the material of construction of the beam tube and scattering chamber produce photons from tantalum and aluminium as background radiation. In addition sodium was a common contaminant of sample surfaces and where present produced sodium gamma-rays as an added background. Although

it is not always possible to eliminate such causes of background, the intensity can be appreciably reduced by taking proper experimental precaution and giving attention to beam-optics by careful steering.

(iii) gamma-rays from radioactivity induced by bombardment.

Radionuclides with different half-lives of up to about 1 day were generated inside the scattering chamber with increasing intensity during a series of measurements and resulted in an increased level of background with time.

(iv) Prompt gamma-rays generated in the detector by neutrons formed in the irradiating system.

RADIOACTIVE BACKGROUND

Natural radioactivity that contributed to the background consisted of radiation from ^{40}K and from the 4n and the (4n + 2) radioactivity series present in the construction material of the building and in the lead-shielding. Also detected was the cosmogenic radionuclide ^{7}Be which emitted a 478-keV gamma-ray. Other radionuclides present in the surroundings were those of long half-lives accumulated as a result of fast neutron activation of materials present and included the nuclides ^{54}Mn and ^{208}Bi.

A full description of the gamma-ray background pertaining to the SUNI facility has already been discussed [Gi 78a]and the assignment and origin of the background peaks are given in Table 2. The assignment of prompt gamma-rays in Table 2 follows the nomenclature described below.

NOMENCLATURE OF PROMPT GAMMA-RAYS

Prompt gamma-rays are emitted from the product nucleus of a nuclear reaction, but the analyst is rarely concerned with the exact identity of the nucleus undergoing de-excitation. What is of greater importance to the analyst is the identity of the target

TABLE 2 : Assigmnent and origin of peaks in the background spectra.

E_γ(keV)	Assignment	Origin or natural decay chain
57	Ta Kα X-ray	chamber lining
66	Ta Kβ X-ray	chamber lining
74	^{208}Bi; ^{212}Pb	^{209}Bi(n, 2n)^{208}Bi; 4n unresolved Kα X-rays
86	^{208}Bi; ^{212}Pb	^{209}Bi(n, 2n)^{209}Bi; 4n unresolved Kβ X-rays
129	^{228}Ac	4n
136	^{181}Ta p,p′(1,0)	collimators and chamber lining
186	^{226}Ra	(4n + 2)
239	^{212}Pb; ^{214}Pb	4n; (4n + 2)
277	^{108}Ti; ^{228}Ac	4n; 4n
285	^{214}Bi	(4n + 2)
296	^{210}Ti; ^{214}Pb	(4n + 2); (4n + 2)
301	^{188}Ta p,p′(4,0)	collimators and chamber lining
328	^{228}Ac	4n
339	^{228}Ac	4n
352	^{214}Pb	(4n + 2)
440	^{23}Na p,p′(1,0)	sodium contamination of target
463	^{228}Ac	4n
478	^{7}Be	cosmic-ray produced
511	β^+; ^{208}Tl	various; 4n
563	^{76}Ge n,n′(1,0)	neutron bombardment of detector
583	^{208}Tl	4n
596	^{74}Ge n,n′(1,0)	neutron bombardment of detector
608	^{74}Ge n,n′(2,1)	neutron bombardment of detector
609	^{214}Bi	(4n + 2)
666	^{214}Bi	(4n + 2)
691	^{72}Ge n,n′(1,0)	neutron bombardment of detector
727	^{212}Bi	4n
769	^{214}Bi	(4n + 2)
795	^{210}Ti; ^{228}Ac	(4n + 2); 4n
834	^{72}Ge n,n′(2,0)	neutron bombardment of detector
835	^{54}Mn	^{54}Fe(n,p)^{54}Mn by fast neutrons
844	^{27}Al p,p′(1,0)	scattered proton excitation of chamber
861	^{208}Ti	4n
911	^{228}Ac	4n
935	^{214}Bi	(4n + 2)
969	^{228}Ac	4n
1015	^{27}Al p,p′(2,0)	scattered-proton excitation of chamber
1120	^{214}Bi	(4n + 2)
1155	^{214}Bi	(4n + 2)
1214	(2236-2m_e)	^{27}Al
1223	^{24}Na	^{27}Al(n,αγ)^{24}Na by fast neutrons

TABLE 2 (Continued)

Eγ (KeV)	Assignment	Origin or natural decay chain
1238	^{214}Bi	(4n + 2)
1275	^{24}Na	^{27}Al(n,αγ)^{24}Na by fast neutrons
1369	^{24}Na	^{27}Al(n,α)^{24}Na by fast neutrons
1378	^{214}Bi	(4n + 2)
1408	^{214}Bi	(4n + 2)
1461	^{40}K	0.012 atom % of natural K
1464	^{72}Ge n,n´(3,0)	neutron bombardment of detector
1509	^{214}Bi	(4n + 2)
1588	^{228}Ac	4n
1592	(2614-2m_e)	^{208}Bi; ^{208}Ti
1693	(2204-m_e)	^{214}Bi
1725	(2236-m_e)	^{27}Al
1732	(2754-2m_e),^{214}Bi	^{24}Na; (4n + 2)
1764	^{214}Bi	(4n + 2)
1850	^{214}Bi	(4n + 2)
2103	(2614-m_e)	^{208}Bi; ^{208}Tl
2210	^{214}Bi	(4n + 2)
2210	^{27}Al p,p´(3,0)	scattered-proton excitation of chamber
2243	(2754-m_e)	^{24}Na
2614	^{208}Bi; ^{208}Tl	^{209}Bi(n,2n)^{208}Bi by fast neutrons; 4n
2754	^{24}Na	^{27}Al(n,α)^{24}Na by fast neutrons

nuclide in the sample on which the nuclear reaction was induced. Accordingly, for analytical purposes it is more meaningful to label the spectral peaks with the target nucleus. In defining the conditions of the analysis the nature of the bombarding beam is known and need not be stressed, thus the reaction is uniquely identified if the light product particle is given. Accordingly the following convention [Pe 81b]is used for peak assignment. In the nuclear reaction A(a,bγ)B, peak assignment is written as A b(r,s) where b is the prompt light particle of the reaction and the gamma-ray quantum is emitted by de-excitation of the heavy product nucleus from level r to level s. When the target nucleus can be inferred unambiguously it may be omitted from the nomenclature. When gamma-rays arise from a reaction not directly induced by the incident beam then both incident and product particles are specified, e.g. the 608-keV gamma-ray generated in a Ge(Li) detector by neutrons formed at the target may be labelled as ^{74}Ge n,n´(2,1).

Lithium : - The target was a pellet of lithium oxide. Lithium has two naturally - occurring isotopes viz. ^{7}Li (92.5 atom %) and ^{6}Li (7.5 atom %). The more abundant isotope produced an intense gamma-ray corresponding to 478 keV, resulting from the de-excitation of the first level of ^{7}Li, and one of 429 keV produced from the (p,nγ) reaction on ^{7}Li. The threshold energy for the generation of the latter gamma-ray was 2370 keV which explained the absence of this gamma-ray when beams of 1000-keV protons were used. However, at higher bombarding energies the sensitivities of analysis obtained when both the 429- and 478-keV gamma-rays were used, offered good analytical potential in such materials as geological ores. Gamma-rays from the ^{7}Li(p,γ)^{8}Be reaction, with energies between 14000 and 18000 keV were measured with a NaI counter [Go 72b] but the sensitivities obtained using those gamma-rays were less than that which was attained in the present investigation (See Chapter 7).

Eγ keV	Assignment	Yield. quanta $sr^{-1}nC^{-1}$	Sensitivity $\mu g.g^{-1}mC^{-1}$	Eγ keV	Assignment	Yield. quanta $sr^{-1}nC^{-1}$	Sensitivity $\mu g.g^{-1}mC^{-1}$
429	^{6}Li γ(1,0)	154 300	13	478	^{7}Li p(1,0)	521 800	5
429	^{7}Li n(1,0)						

E_γ(keV) \ E_p(keV)	Yield (quanta $sr^{-1}nC^{-1}$)					
	3 500	4 000	4 500	5 000	5 500	6 000
429	109 200	150 000	154 300	160 100	188 700	201 200
478	450 500	488 500	521 800	523 600	528 300	619 400

E_γ (keV)	Co-efficients of polynomials fitted to Sensitivity Functions			$S_{min.}/\mu g.g^{-1}$	E_p at $S_{min.}$ (keV)
	a_0	a_1	a_2		
429	+65	-26	+3.2	11	4 030
478	+15.9	- 6.9	+0.96	3.5	3 500

Beryllium : - Beryllium powder was compressed into a tablet and irradiated. No gamma-rays were observed from the Coulomb-excitation process or from the (p,nγ) reaction.

Gamma-rays in the spectrum were from the proton-capture reaction on ^9Be and from the $^9Be(p,\alpha\gamma)^6Li$ reaction but these were of such low intensity that they were considered to be of little analytical value.

Eγ keV	Assignment	Yield. quanta $sr^{-1}nC^{-1}$	Sensitivity $\mu g.g^{-1}mC^{-1}$	Eγ keV	Assignment	Yield. quanta $sr^{-1}nC^{-1}$	Sensitivity $\mu g.g^{-1}mC^{-1}$
415	^9Be γ(3,2)	14	43 700	1022	^9Be γ(2,1)	2.1	120 400
718	^9Be γ(1,0)	5.3	90 300	3562	^9Be α(2,0)	11	40 300

E_γ (keV) \ E_p (keV)	Yield (quanta $sr^{-1}nC^{-1}$)					
	3 500	4 000	4 500	5 000	5 500	6 000
415	9.3	10	14	18	23	36
718	2.1	3.6	5.3	7.8	11	17
1022	1.3	1.9	2.1	4.6	8.1	12
3562	7.8	9.4	11	14	19	22

E_γ (keV)	Co-efficients of polynomials fitted to Sensitivity Functions				$S_{min.}/\mu g.g^{-1}$	E_p at $S_{min.}$ (keV)
	a_0	a_1	a_2	a_3		
415	- 63 040	+63 551	-12 792	+871	40 300	3 500
718	+144 446	-19 207	+ 1 604	0	86 800	6 000
1022	+188 028	-25 356	+ 2 259	0	116 000	5 500
3562	+ 73 376	- 9 333	+ 472	0	34 000	6 000

Boron : Bombardment of a pure boron pellet led to the production of gamma-rays from both stable isotopes of the element. The most intense gamma-ray was one of 2125 keV which resulted from the decay of the first excited level of ^{11}B. The sensitivity calculated for the characteristically shaped

spectrum peak, due to Doppler broadening, was about 50 ug.g^{-1} with little change over a bombarding energy range of 3500 to 6000 keV. Because of the breadth of this peak, it was subject to interference from other gamma-rays in its vicinity, the most likely being from sulphur and chlorine both of which produced moderately intense gamma-rays of 2127 keV. This interference was, however, not serious when these elements were present in low concentrations.

Eγ keV	Assignment	Yield. quanta sr^{-1}nC^{-1}	Sensitivity µg.g^{-1}mC^{-1}	Eγ keV	Assignment	Yield. quanta sr^{-1}nC^{-1}	Sensitivity µg.g^{-1}mC^{-1}
414	^{10}B p(3,2)	490	2 400	1102	^{11}B - 2m$_e$	1 960	1 470
429	^{10}B α(1,0)	26 600	90	1613	^{11}B - m$_e$	3 100	1 480
598	^{10}B α(2,1)	1 200	1 310	2125	^{11}B p(1,0)	47 800	50
719	^{10}B p(1,0)	15 300	120	2320	^{11}B γ(2,1)	42	4 100
1021	^{10}B p(2,1)	2 140	860				

Eγ(keV) \ E_p(keV)	Yield (quanta sr^{-1}nC^{-1})					
	3 500	4 000	4 500	5 000	5 500	6 000
429	20 900	22 400	26 600	32 800	34 000	36 700
598	470	640	1 200	1 840	2 760	3 100
719	6 800	8 960	15 300	19 200	22 400	24 600
1021	400	1 760	2 140	2 690	3 700	4 210
2125	34 500	44 800	47 800	73 600	100 400	136 300

Another peak in the spectrum which was Doppler broadened was that due to the 478-keV ^{10}B α(1,0) gamma-ray. Because of the broadness of this peak, interference was possible from gamma-rays, the energies of which differ from that of ^{10}B by more than the resolution of the detector. Hence in a matrix containing manganese for example, the intense 411.5-keV ^{55}Mn n(1,0) gamma-ray could cause serious interference. Similarly in light matrices, containing sodium, magnesium, or both, the intense 440-keV gamma-rays from ^{23}Na p(1,0) and ^{25}Mg α(1,0) would detrimentally affect use of the boron gamma-ray for analysis.

E_γ (keV)	Co-efficients of polynomials fitted to Sensitivity Functions				$S_{min.}/\mu g.g^{-1}$	E_p at $S_{min.}$ (keV)
	a_0	a_1	a_2	a_3		
429	+ 2 984	- 1 843	+ 382	- 26	84	4 100
598	+79 666	-43 462	+ 7 955	-482	960	5 050
719	+ 8 030	- 4 753	+ 939	- 61	120	4 500
1021	+95 792	-56 248	+10 988	-705	860	4 500
2125	+ 430	- 209	+ 39	+ 2.2	48	4 950

The extent of possible interference with the 718-keV ^{10}B p(1,0) gamma-ray was appreciably less, the likely interfering elements producing gamma-rays of low intensity. An important consideration was, however, the formation of neutron-induced prompt gamma-rays from germanium, of 691 and 741 keV, which influenced the accurate stripping of the photopeak of boron.

Because of the presence of intense gamma-rays from both the boron isotopes, it was possible to determine them simultaneously [Ra 81].

Carbon : - Bombardment of a plug of graphite with protons yielded gamma-rays mostly from the very low abundant ^{13}C isotope. In fact, the only gamma-rays which were observed from ^{12}C were two low yield proton-capture photons. Although the threshold for the 4439-keV ^{12}C p(1,0) gamma-ray was 4809 keV no such gamma-ray was observed even at higher energies.

Eγ keV	Assignment	Yield. quanta $sr^{-1}nC^{-1}$	Sensitivity $\mu g.g^{-1}mC^{-1}$	Eγ keV	Assignment	Yield. quanta $sr^{-1}nC^{-1}$	Sensitivity $\mu g.g^{-1}mC^{-1}$
1629	^{13}C γ(2,1)	15	47 400	3087	^{13}C p(1,0)	54	16 600
1742	^{13}C γ(5,2)	19	39 600	3180	^{13}C p(4,2)	26	27 300
2313	^{13}C γ(1,0)	24	36 300	3511	^{12}C γ(2,0)	75	21 500
2365	^{13}C γ(1,0)	29	27 500	3685	^{13}C p(2,0)	30	31 100
2605	^{13}C γ(3,1)	47	13 700	5106	^{13}C γ(4,0)	12	11 700

The decay of the first excited level of ^{13}C produced gamma-rays of 3087 keV but in the bombarding energy range covered in this investigation, the sensitivities attainable were poor.

Most of the gamma-rays in the spectrum resulted from the proton-capture reaction on ^{13}C but these photons were too feeble to be considered for analytical application.

E_γ (keV) \ E_p (keV)	Yield (quanta $sr^{-1}nC^{-1}$)					
	3 500	4 000	4 500	5 000	5 500	6 000
2313	15	20	24	32	40	54
2602	38	42	47	51	58	65
3087	26	33	54	65	80	95
3511	58	62	75	83	98	130
5106	6.1	11	12	16	23	36

E_γ (keV)	Co-efficients of polynomials fitted to Sensitivity Functions				$S_{min.}/\mu g.g^{-1}$	E_p at $S_{min.}$ (keV)
	a_0	a_1	a_2	a_3		
2313	- 93 952	+110 624	-26 568	+1 849	12 900	6 000
2602	- 4 992	+ 21 408	- 5 898	+ 458	9 800	6 000
3087	+ 42 345	- 7 904	+ 529	0	13 700	6 000
3511	-140 256	+113 168	-24 784	+1 683	10 900	6 000
5106	+112 048	- 66 056	+14 488	-1 060	8 610	6 000

Nitrogen : - To investigate the gamma-ray spectrum from nitrogen, a stack of foils each 1.052 mg/cm^2 thick of KAPTON ($C_{22}H_{10}N_2O_4$) was bombarded. This material contained 7.65 % nitrogen by mass.

Decay of the first level of ^{14}N (99.64 atom % in nature) provided the most sensitive gamma-ray for analysis.

Coulomb excitation of ^{15}N produced high energy gamma-rays of 5270 and 5298 keV. Although these were of low intensity, the peaks could be integrated together to produce a reasonable sensitivity for analysis of nitrogen.

Proton-capture on ^{15}N was the only other source of gamma-rays, the resulting peaks being of low intensity.

Eγ keV	Assignment	Yield. quanta $sr^{-1}nC^{-1}$	Sensitivity $\mu g.g^{-1}mC^{-1}$	Eγ keV	Assignment	Yield. quanta $sr^{-1}nC^{-1}$	Sensitivity $\mu g.g^{-1}mC^{-1}$
429	^{15}N γ(2,0)	710	1 880	5270	^{15}N p(1,0)	63	13 700
710	^{15}N γ(3,0)	340	4 320	5299	^{15}N p(2,0)	72	7 370
2313	^{15}N p(1,0)	520	1 850				

E_γ (keV) \ E_p (keV)	Yield (quanta $sr^{-1}nC^{-1}$)					
	3 500	4 000	4 500	5 000	5 500	6 000
429	520	630	710	1 050	1 180	1 280
710	63	110	340	380	930	940
2313	340	460	520	600	1 770	2 370
5270	48	56	63	74	79	87
5299	33	49	72	98	110	150

E_γ (keV)	Co-efficients of polynomials fitted to Sensitivity Functions				$S_{min.}/\mu g.g^{-1}$	E_p at $S_{min.}$ (keV)
	a_0	a_1	a_2	a_3		
429	+ 2 454	- 804	+ 139	0	1 290	3 500
710	+107 392	-42 792	+4 822	- 87	3 300	5 100
2313	+ 17 116	- 8 946	+1 734	-111	1 830	6 000
5270	+ 15 734	- 401	- 9.5	0	12 950	6 000
5299	+ 19 112	- 4 616	+ 532	- 16	6 940	6 000

Oxygen : - Since ytterbium yielded only one gamma-ray of low intensity (see page 214) the target used for the spectrum of oxygen was a tablet of ytterbium oxide. Gamma-rays originated from Coulomb excitation and reactions on all three stable oxygen isotopes.

Proton capture on ^{18}O resulted in excited nuclei of ^{19}F which emitted gamma-rays of 110 and 197 keV. These gamma-rays were of low intensity and not usable for analysis because the same gamma-rays are emitted with high intensity by Coulomb excitation of fluorine (q.v.).

The first levels of both ^{17}O and ^{18}O decayed by emitting gamma-rays of 870 keV and 1982 keV respectively. Both photopeaks, although not very intense, were situated in that region of the spectrum where the background continuum was sufficiently low. As a result of this, sensitivities of about 200 $\mu g.g^{-1}$ could be attained.

Proton capture on ^{16}O resulted in a gamma-ray of 497 keV which was considered to be sensitive for oxygen analysis.

The majority of the other oxygen gamma-rays originated from the decay of the lower levels of ^{18}F, the nuclide formed by the reactions, $^{17}O(p,\gamma)^{18}F$ and $^{18}O(p,n\gamma)^{18}F$. Many of these gamma-rays provided a sensitivity of better than the $mg.g^{-1}$ level. All gamma rays labelled ^{18}O n(r,s) could also have been labelled ^{17}O γ(r,s). The former label was used because ^{18}O occurs in nature at a higher concentration.

Eγ keV	Assignment	Yield. quanta $sr^{-1}nC^{-1}$	Sensitivity $\mu g.g^{-1}mC^{-1}$	Eγ keV	Assignment	Yield. quanta $sr^{-1}nC^{-1}$	Sensitivity $\mu g.g^{-1}mC^{-1}$
110	^{18}O γ(1,0)	21	11 700	937	^{18}O n(1,0)	900	280
197	^{18}O γ(2,0)	73	2 700	1042	^{18}O n(2,0)	1 230	230
495	^{16}O γ(1,0)	270	850	1081	^{18}O n(3,0)	270	960
579	^{17}O n(5,4)	62	3 800	1122	^{18}O n(4,0)	43	6 900
620	^{18}O n(5,3)	130	2 100	1471	^{18}O - m_e	340	810
659	^{18}O n(5,2)	120	2 400	1982	^{18}O p(1,0)	2 950	120
764	^{18}O n(5,1)	22	13 100	2313	^{17}O α(1,0)	10	16 300
870	^{17}O p(1,0)	380	700				

E_γ (keV) \ E_p (keV)	Yield (quanta $sr^{-1}nC^{-1}$)					
	3 500	4 000	4 500	5 000	5 500	6 000
495	160	220	270	310	430	580
870	165	270	380	610	1 000	1 130
937	22	210	900	1 520	2 930	3 460
1042	16	88	1 230	3 100	9 560	9 710
1081	26	110	270	610	1 150	1 390
1471	240	280	340	380	630	650
1982	500	1 990	2 950	5 100	8 700	9 640

E_γ (keV)	Co-efficients of polynomials fitted to Sensitivity Functions				$S_{min.}/\mu g.g^{-1}$	E_p at $S_{min.}$ (keV)
	a_0	a_1	a_2	a_3		
495	+52 086	-31 521	+6 371	-422	750	4 000
870	+ 40	+ 1 018	- 328	+ 29	600	5 230
937	+40 884	-22 897	+4 285	-266	200	6 000
1042	+69 726	-38 997	+7 256	-448	80	5 500
1081	+66 416	-35 584	+6 377	-379	460	5 000
1471	+36 010	-21 062	+4 127	-263	800	4 430
1982	+11 656	- 6 804	+1 324	- 85	100	4 670

Fluorine : - The target used to provide the fluorine spectrum was gadolinium fluoride. The observed fluorine peaks resulted from Coulomb excitation and from the reaction $^{19}F(p,\alpha\gamma)^{16}O$.

The most important gamma-rays, from an analytical point of view, were those resulting from the decay of the first and second levels of ^{19}F having energies of 110 keV and 197 keV. Absolute sensitivities of analysis using these gamma-rays were calculated to be between 10^{-1} and 60 $\mu g.g^{-1}$. A possible source of interference is the $^{18}O(p,\gamma)^{19}F$ reaction with the emission the 110-keV and-197 keV gamma-rays. These gamma-rays were, however, of low intensity and would not seriously affect the determination of fluorine except when low concentrations of F have to be determined in the presence of large amounts of oxygen.

Three distinct peaks were seen in the spectrum from the reaction $^{19}F(p,\alpha\gamma)^{16}O$ and these occurred at 6130, 6720 and 7117 keV. The three gamma-rays were strongly affected by Doppler broadening and offered reasonable sensitivities.

Eγ keV	Assignment	Yield. quanta $sr^{-1}nC^{-1}$	Sensitivity $\mu g.g^{-1}mC^{-1}$	Eγ keV	Assignment	Yield. quanta $sr^{-1}nC^{-1}$	Sensitivity $\mu g.g^{-1}mC^{-1}$
110	^{19}F p(1,0)	84 500	70	1444	^{19}F p(5,1)	176	3 800
197	^{19}F p(2,0)	483 000	10	1457	^{19}F p(4,0)	298	2 300
1236	^{19}F p(3,1)	55 000	130	1554	^{19}F p(5,0)	56	11 100
1261	^{19}F p(4,2)	62	10 600	6130	^{19}F α(2,0)	880	1 800
1346	^{19}F p(3,0)	2 400	330	6720	^{19}F α(3,0)	860	1 900
1349	^{19}F p(4,1)			7117	^{19}F α(4,0)	710	2 900
1356	^{19}F p(5,2)	2.2	128 000				

Since the fluorine gamma-rays were easily detectable and intense, numerous analytical applications were made of these gamma-rays as cited in ref [Bi 78].

E_p (keV) / E_γ (keV)	Yield (quanta $sr^{-1}nC^{-1}$)					
	3 500	4 000	4 500	5 000	5 500	6 000
110	20 600	43 600	84 500	96 500	127 400	198 400
197	150 200	302 000	483 000	571 400	690 300	771 200
1236	31 400	48 900	55 000	66 300	72 900	93 300
1346 / 1349	1 630	1 980	2 400	2 870	3 190	3 640
6130	560	710	880	1 290	1 460	1 720

E_γ (keV)	Co-efficients of polynomials fitted to Sensitivity Functions				$S_{min.}/\mu g.g^{-1}$	E_p at $S_{min.}$ (keV)
	a_0	a_1	a_2	a_3		
110	- 420	+ 386	- 92	+ 6.9	57	5 580
197	- 10	+ 12.8	- 2.2	+ 8.7	5	6 000
1236	+ 1 971	- 1 397	+ 331	-250	73	3 500
1346 / 1349	- 1 134	+ 924	- 192	+ 13	290	4 000
6130	+46 145	-32 062	+7 219	-518	150	3 500

Sodium : - Analysis of the spectrum of sodium chloride, bombarded with protons showed that gamma-rays were emitted as a result of Coulomb excitation of ^{23}Na in addition to those from the reactions $^{23}Na(p,\alpha\gamma)^{20}Ne$ and $^{23}Na(p,\gamma)^{24}$. The most distinctive feature in the spectrum was the very intense peak corresponding to an energy of 440 keV and resulting from the excitation of the first level of ^{23}Na by inelastic scattering. Although this peak was situated on a high Compton continuum, it offered a sensitivity of $16\mu g.g^{-1}$ at a bombarding energy of 4500 keV.

Of the other four gamma-rays that were observed, the 1634-keV ^{23}Na $\alpha(1,0)$ photon was also very intense and the peak corresponding to this energy had its area increased by an unresolved peak corresponding to 1637 keV resulting from Coulomb excitation of the second excited level of ^{23}Na.

Use of the intense gamma-ray of 440 keV for the analysis of sodium in archaeological specimens was made [Ch 72] where a sensitivity of 10-50 $\mu g.g^{-1}$ was predicted. The prompt gamma-ray technique was particularly useful in that study because of the preference of keeping specimens intact and non-radioactive for museum purposes.

E_γ (keV)	Co-efficients of polynomials fitted to Sensitivity Functions				$S_{min.}/\mu g.g^{-1}$	E_p at $S_{min.}$ (keV)
	a_0	a_1	a_2	a_3		
440	+ 83	- 28	+ 2.9	0	16	4 500
614	+ 33 703	- 15 464	+ 1 928	0	3 050	4 500
1128	+140 384	- 74 711	+14 760	-1 012	4 900	6 000
1369	-720 064	+293 920	+38 568	-1 548	9 650	6 000
1634 / 1637	- 102	+ 110	- 25	+ 1.7	14	6 000

E_γ (keV) \ E_p (keV)	Yield (quanta $sr^{-1}nC^{-1}$)					
	3 500	4 000	4 500	5 000	5 500	6 000
440	36 800	50 200	92 600	12 600	194 800	220 000
614	290	450	690	1 170	2 900	4 200
1128	240	660	780	950	11 100	14 200
1369	22	31	42	44	47	63
1634 / 1637	11 200	49 200	80 600	118 000	13 700	185 000

E_γ keV	Assignment	Yield. quanta $sr^{-1}nC^{-1}$	Sensitivity $\mu g.g^{-1}mC^{-1}$	E_γ keV	Assignment	Yield. quanta $sr^{-1}nC^{-1}$	Sensitivity $\mu g.g^{-1}mC^{-1}$
440	^{23}Na p(1,0)	92 600	16	1369	^{23}Na $\gamma(1,0)$	42	34 900
614	^{23}Na - $2m_e$	690	2 400	1634	^{23}Na $\alpha(1,0)$	80 600	37
1128	^{23}Na - m_e	780	10 400	1637	^{23}Na p(2,1)		

Magnesium : - Magnesium hydroxide was compressed into a tablet and bombarded to obtain data for the gamma-ray spectrum of magnesium. Most of the intense gamma-rays were produced by the inelastic scattering process on ^{25}Mg, especially the 585-keV ^{25}Mg p(1,0) gamma-ray which offered a sensitivity of better than 100 $\mu g.g^{-1}$.

Eγ keV	Assignment	Yield. quanta $sr^{-1}nC^{-1}$	Sensitivity $\mu g.g^{-1}mC^{-1}$	Eγ keV	Assignment	Yield. quanta $sr^{-1}nC^{-1}$	Sensitivity $\mu g.g^{-1}mC^{-1}$
390	^{25}Mg p(2,1)	1 260	620	1612	^{25}Mg p(3,0)	2 790	470
440	^{26}Mg α(1,0)	130	6 720	1637	^{26}Mg α(2,1)	27	34 000
585	^{25}Mg p(1,0)	3 200	310	1809	^{26}Mg p(1,0)	410	2 430
844	^{26}Mg γ(1,0)	350	3 800	1965	^{25}Mg p(4,0)	180	3 400
975	^{25}Mg p(2,0)	1 360	1 290	1979	^{25}Mg p(5,1)	110	6 100
990	^{25}Mg p(4,2)	290	4 800	2210	^{26}Mg γ(3,0)	530	1 540
1014	^{26}Mg γ(2,0)	820	2 200				
1369	^{24}Mg p(1,0)	21 800	86				
1369	^{26}Mg γ(3,1)						

Gamma-rays originating from reactions on ^{26}Mg were generally of low intensity but the 1369-keV ^{26}Mg γ(3,1) gamma-ray was considered important, because, when coupled with a gamma-ray of the same energy originating from ^{24}Mg, it had a very high yield photopeak which had a sensitivity of 50 $\mu g.g^{-1}$.

Great care was required in the determination of magnesium in a matrix containing aluminium because reactions on the latter produced identical gamma-rays.

E_p(keV) / E_γ(keV)	Yield (quanta $sr^{-1}nC^{-1}$)					
	3 500	4 000	4 500	5 000	5 500	6 000
390	540	860	1 260	1 750	2 510	3 740
585	1 820	2 417	3 200	4 910	6 380	11 300
975	510	840	1 360	1 970	2 210	3 760
1369	2 170	9 620	21 800	32 600	43 400	88 200
1612	810	1 930	2 790	36 900	49 700	64 600

Analysis of mixtures of magnesium with aluminium could thus be attempted only be means of peak-ratio methods.

E_γ (keV)	Co-efficients of polynomials fitted to Sensitivity Functions				$S_{min.}/\mu g.g^{-1}$	E_p at $S_{min.}$ (keV)
	a_0	a_1	a_2	a_3		
390	+13 021	- 6 383	+1 086	-63	320	6 000
585	+ 9 182	- 4 077	+ 589	-27	73	5 700
975	+22 874	+10 568	+1 698	-92	720	6 000
1369	+ 3 389	- 1 868	+ 352	-22	54	6 000
1612	+ 7 546	- 3 437	+ 542	-29	260	6 000

Aluminium : - Bombardment of an aluminium target produced gamma-rays from Coulomb excitation and proton capture.

Decay of the first five levels of ^{27}Al resulted in the production of the analytically most useful gamma-rays. It should be noted that these gamma-rays were also emitted from (p,γ) reactions on ^{26}Mg and were therefore subject to interference from magnesium. However, the contribution of magnesium counts could be corrected for by considering the ratios of yields relative to that of interference-free magnesium gamma-rays.

The main source of interference on the 844-keV aluminium peak was the very intense 847-keV peak associated with ^{56}Fe, if this element were present.

E_γ keV	Assignment	Yield. quanta $sr^{-1}nC^{-1}$	Sensitivity $\mu g.g^{-1}mC^{-1}$	E_γ keV	Assignment	Yield. quanta $sr^{-1}nC^{-1}$	Sensitivity $\mu g.g^{-1}mC^{-1}$
171	^{27}Al p(2,1)	660	1 790	1367	^{27}Al p(3,1)	10 300	230
720	^{27}Al p(5,2)	21	120 300	1699	^{27}Al - m_e	530	5 700
754	^{27}Al - $2m_e$	33	112 500	1720	^{27}Al p(4,2)	610	4 200
844	^{27}Al p(1,0)	8 080	390	1779	^{27}Al γ(1,0)	760	4 500
1015	^{27}Al p(2,0)	22 700	110	2210	^{27}Al p(3,0)	8 750	200
1196	^{27}Al p(3,2)	280	9 400	2735	^{27}Al p(4,0)	310	7 200
1268	^{27}Al - m_e	340	6 700	2982	^{27}Al p(5,0)	44	27 300

In general, sensitivities up to 100 $\mu g.g^{-1}$ were calculated.

E_γ (keV) \ E_p (keV)	Yield (quanta $sr^{-1}nC^{-1}$)					
	3 500	4 000	4 500	5 000	5 500	6 000
171	320	470	660	1 290	1 730	2 210
844	3 950	6 520	8 080	14 900	23 700	31 200
1015	11 200	15 900	22 700	33 600	51 300	73 700
1367	3 300	6 220	10 300	15 000	21 600	27 800
2210	1 560	4 450	8 750	12 100	17 200	21 400

E_γ (keV)	Co-efficients of polynomials fitted to Sensitivity Functions				$S_{min.}/\mu g.g^{-1}$	E_p at $S_{min.}$ (keV)
	a_0	a_1	a_2	a_3		
171	-14 314	+11 257	-2 504	+176	1 090	6 000
844	-14 160	+ 9 171	-1 888	+127	230	3 500
1015	+ 149	- 10.1	+ 0.375	0	100	6 000
1367	+ 5 115	- 2 816	+ 536	- 33.7	230	4 750
2210	+ 5 122	- 2 940	+ 582	- 38.5	140	6 000

Silicon : - A representative spectrum of the element was obtained from the bombardment of a wafer of elemental silicon. The spectrum was dominated by the intense 1779-keV ^{28}Si p(1,0) gamma-ray. This gamma-ray was also formed as a result of the raction $^{31}P(p,\alpha\gamma)^{28}Si$ and would therefore be subjected to correction for interference from phosphorus.

Earlier silicon analysis with protons, mainly used bombarding

Eγ keV	Assignment	Yield. quanta $sr^{-1}nC^{-1}$	Sensitivity $\mu g.g^{-1}mC^{-1}$	Eγ keV	Assignment	Yield. quanta $sr^{-1}nC^{-1}$	Sensitivity $\mu g.g^{-1}mC^{-1}$
756	^{29}Si p(2,1)	720	2 100	1779	^{28}Si p(1,0)	31 900	75
844	^{30}Si α(1,0)	150	19 100	2028	^{29}Si p(2,0)	690	1 600
1015	^{30}Si α(2,0)	460	7 500	2240	^{30}Si p(1,0)	570	1 700
1273	^{29}Si p(1,0)	3 600	750	2430	^{29}Si p(3,0)	170	4 900

E_γ (keV) \ E_p (keV)	Yield (quanta $sr^{-1}nC^{-1}$)					
	3 500	4 000	4 500	5 000	5 500	6 000
756	280	420	720	1 120	1 340	1 610
1273	1 590	2 430	3 600	5 790	6 900	7 470
1779	16 800	26 610	31 900	63 600	67 200	81 400
2028	96	260	690	1 620	1 960	2 170
2240	66	190	570	610	790	1 010

particles of low energies, usually of less than 500 keV (Pi 65) and was based on measurements of gamma-lines emitted from (p,γ) and (p,αγ) reactions. However, in the present study, at higher bombarding energies, Coulomb excitation resulted in a very intense gamma-ray of 1779 keV which offered much better sensitivity.

E_γ (keV)	Co-efficients of polynomials fitted to Sensitivity Functions				$S_{min.}/\mu g.g^{-1}$	E_p at $S_{min.}$ (keV)
	a_0	a_1	a_2	a_3		
756	+ 11 764	- 3 182	+ 144	+ 20	1 800	5 000
1273	- 339	+ 1 855	- 622	+ 58	560	5 000
1779	+ 207	+ 50	+ 2.7	+ 0.24	50	5 000
2028	+ 58 680	-29 070	+ 4 805	-259	1 010	5 000
2240	+133 740	-74 532	+13 900	-855	1 660	4 870

Moreover, it is hardly likely that the feeble gamma-rays from the (p,αγ) reaction could be used in the presence of aluminium because these photons have exactly the same energies as the very intense Coulomb excited gamma-rays from ^{27}Al.

Phosphorus : - The target irradiated to give data on the gamma-rays from phosphorus was mercurous phosphate. Mono-isotopic phosphorus was represented by three very intense peaks in the spectrum. Of these, the most analytical significant gamma-ray was of 1266 keV from the decay of the first level of ^{31}P.

Over a bombarding energy range of between 3500 keV and 6000 keV there was a gradual increase in the sensitivity with increasing bombarding energy with a best sensitivity of about 20 $\mu g.g^{-1}$.

The 1778-keV gamma-ray resulting from the (p,$\alpha\gamma$) reaction offered a sensitivity of about 125 $\mu g.g^{-1}$. However, care had to be taken when using this photon for analysis, because of the very intense gamma-ray of 1779 keV from silicon (a very likely source of interference in geological material) and aluminium.

The intensity of a gamma-ray of 2230 keV increased rapidly with increasing bombarding energy but was accompanied by a moderate increase in the sensitivity. Counts from the Coulomb-excited gamma-ray of 2234 keV were integrated together with those from the 2230-keV gamma-ray.

Eγ keV	Assignment	Yield. quanta $sr^{-1}nC^{-1}$	Sensitivity $\mu g.g^{-1}mC^{-1}$	Eγ keV	Assignment	Yield. quanta $sr^{-1}nC^{-1}$	Sensitivity $\mu g.g^{-1}mC^{-1}$
1266	^{31}P p(1,0)	39 100	25	2230	^{31}P γ(1,0)	7 600	40
1778	^{31}P α(1,0)	7 720	140	2234	^{31}P p(3,0)		

E_γ (keV) \ E_p (keV)	Yield (quanta $sr^{-1}nC^{-1}$)					
	3 500	4 000	4 500	5 000	5 500	6 000
1266	26 100	29 600	39 100	52 200	73 600	101 100
1778	2 640	3 150	7 720	12 500	17 900	26 400
2230 } 2234 }	2 390	4 270	7 600	17 800	28 400	36 900

E_γ (keV)	Co-efficients of polynomials fitted to Sensitivity Functions				$S_{min.}/\mu g.g^{-1}$	E_p at $S_{min.}$ (keV)
	a_0	a_1	a_2	a_3		
1266	+128	- 57	+11	-0.76	18	6 000
1778	+ 96	+139	-47	+4	120	5 650
2230 } 2234 }	+756	-370	+64	-3.7	28	6 000

Sulphur : - Targets of pure sulphur were bombarded.

A very intense gamma-ray resulted from the decay of the first excited state of ^{32}S which was the isotope with highest natural abundance. The peak of this gamma-ray was further enhanced by contribution from the 2229-keV gamma-ray also formed by Coulomb excitation of the same isotope.

E_γ keV	Assignment	Yield. quanta $sr^{-1}nC^{-1}$	Sensitivity $\mu g.g^{-1}mC^{-1}$	E_γ keV	Assignment	Yield. quanta $sr^{-1}nC^{-1}$	Sensitivity $\mu g.g^{-1}mC^{-1}$
346	^{33}S p(3,2)	3	336 000	1719	^{32}S - m_e	950	2 300
811	^{32}S γ(1,0)	105	7 100	1787	^{34}S p(3,1)	140	10 400
841	^{33}S p(1,0)	1 410	620	1966	^{33}S p(2,0)	35	46 300
1107	^{36}S α(1,0)	8	146 000	2127	^{34}S p(1,0)	830	2 000
1208	^{32}S - $2m_e$	620	2 030	2229	^{32}S p(4,1)	15 700	80
1472	^{33}S p(3,1)	870	1 100	2230	^{32}S p(1,0)		
1543	^{32}S p(2,1)	27	52 000	2313	^{33}S p(3,0)	17	22 100

E_γ(keV) \ E_p(keV)	Yield (quanta $sr^{-1}nC^{-1}$)					
	3 500	4 000	4 500	5 000	5 500	6 000
841	280	960	1 410	3 290	6 190	9 310
1208	49	110	620	2 760	4 210	7 120
1719	48	87	950	2 350	2 680	3 100
2127	27	320	830	1 430	1 630	2 040
2230	3 250	10 900	15 700	35 600	39 400	48 600

E_γ (keV)	Co-efficients of polynomials fitted to Sensitivity Functions				$S_{min.}/\mu g.g^{-1}$	E_p at $S_{min.}$ (keV).
	a_0	a_1	a_2	a_3		
841	+ 18 833	- 10 763	+ 2 107	- 137	570	4 800
1208	+ 67 978	- 31 512	+ 4 852	- 247	270	6 000
1719	+ 160	+ 7 606	- 2 582	+ 222	730	5 785
2127	+244 280	-137 536	+25 841	-1 607	1 820	4 920
2230	+ 4 039	- 2 029	+ 335	- 18	52	5 070

The first three levels of ^{33}S were excited and the p(1,0) gamma-ray provided a sensitivity of about 600 $\mu g.g^{-1}$. Two peaks of moderate intensity were observed from the Coulomb excitation of ^{34}S. Because of the low natural concentration of ^{36}S, only one gamma-ray of low intensity and little analytical use resulted from the isotope.

Chlorine : - A tablet of barium chloride was bombarded to obtain data for chlorine. Both isotopes of chlorine provided sufficiently intense gamma-rays for chlorine determination at a concentration level of 100 $\mu g.g^{-1}$. Coulomb excitation of ^{35}Cl resulted in the production of many gamma-rays but the bombarding energy was too low for the (p,nγ) reaction (threshold = 8152 keV). In the case of the (p,αγ) reaction on this isotope, a strong Doppler broadened gamma-ray of 2230 keV was observed.

Eγ keV	Assignment	Yield. quanta $sr^{-1}nC^{-1}$	Sensitivity $\mu g.g^{-1}mC^{-1}$	Eγ keV	Assignment	Yield. quanta $sr^{-1}nC^{-1}$	Sensitivity $\mu g.g^{-1}mC^{-1}$
883	^{35}Cl p(3,2)	72	14 600	2230	^{35}Cl α(1,0)	6.7	49 600
930	^{35}Cl p(4,2)	81	14 300	2491	^{37}Cl n(4,0)	190	3 100
1219	^{35}Cl p(1,0)	10 500	130	2646	^{35}Cl p(3,0)	950	640
1410	^{37}Cl n(1,0)	1 950	640	2693 2698	^{35}Cl p(4,0) ^{35}Cl p(7,2)	290	1 420
1611	^{37}Cl n(2,0)	2 660	420	2796	^{37}Cl n(5,0)	230	2 100
1727	^{37}Cl p(1,0)	750	1 000	3003	^{35}Cl p(5,0)	8.4	32 500
1763	^{35}Cl p(2,0)	7 420	180	3087	^{37}Cl p(2,0)	290	1 370
2127	^{37}Cl α(1,0)	1 780	560	3163	^{35}Cl p(6,0)	34	9 500
2217	^{37}Cl n(3,0)	400	2 240				

E_γ (keV) \ E_p (keV)	Yield (quanta $sr^{-1}nC^{-1}$)					
	3 500	4 000	4 500	5 000	5 500	6 000
1219	1 930	5 120	10 500	12 405	18 300	24 105
1410	35	420	1 950	3 260	6 120	9 840
1611	70	415	2 665	4 540	7 510	10 400
1763	710	2 560	7 420	12 200	16 105	18 300
2646	15	540	950	3 165	4 620	6 715

This was also the case of the 2127-keV gamma-ray that was produced by the same reaction on ^{37}Cl. Most of the other gamma-rays from this isotope were produced by the (p,nγ) reaction.

E_γ (keV)	Co-efficients of polynomials fitted to Sensitivity Functions				$S_{min.}/\mu g.g^{-1}$	E_p at $S_{min.}$ (keV)
	a_0	a_1	a_2	a_3		
1219	+ 1 578	- 824	+ 158	- 10.3	100	6 000
1410	+26 964	-15 283	+2 952	-190	480	6 000
1611	+31 500	-17 840	+3 400	-215	320	6 000
1763	+ 6 769	- 3 691	+ 688	- 43	90	6 000
2646	+37 808	+20 316	+3 687	-224	140	6 000

Potassium : - ^{39}K, the most abundant of the stable potassium isotopes, yielded only one gamma-ray when a tablet of potassium bromide was bombarded. The gamma-ray originated from the the decay of first level of ^{36}Ar from the reaction $^{39}K(p,\alpha\gamma)^{36}Ar$ The threshold of the (p,nγ) reaction, 7492 keV, was too high for the production of any gamma-rays.

Because of the very low natural abundance of ^{40}K(0.012 atom %) no intense gamma-rays were expected. However, only one gamma-ray of 1410 keV was observed which was tentatively identified as ^{40}K α(1,0).

Up to seven levels of ^{41}K were excited but only the decay of the lower levels produced gamma-rays of reasonable intensity. No gamma-rays were observed due to the excitation of the fifth level of ^{41}K.

Eγ keV	Assignment	Yield. quanta $sr^{-1}nC^{-1}$	Sensitivity $\mu g.g^{-1}mC^{-1}$	Eγ keV	Assignment	Yield. quanta $sr^{-1}nC^{-1}$	Sensitivity $\mu g.g^{-1}mC^{-1}$
267	^{41}K p(3,2)	22	27 300	695	^{41}K p(7,1)	92	2 600
384	^{41}K p(6,2)	230	2 500	980	^{41}K p(1,0)	135	1 360
404	^{41}K p(7,2)	52	15 400	1294	^{41}K p(2,0)	69	2 980
580	^{41}K p(3,1)	30	4 960	1410	^{40}K α(1,0)	78	2 130
602	^{41}K p(4,1)	35	5 900	1970	^{39}K α(1,0)	110	1 470

E_p (keV) / E_γ (keV)	Yield (quanta $sr^{-1}nC^{-1}$)					
	3 500	4 000	4 500	5 000	5 500	6 000
384	42	100	230	310	405	720
695	10	52	92	190	380	560
980	8.3	74	135	260	340	420
1410	16	37	78	94	120	240
1970	21	66	110	190	460	810

E_γ (keV)	Co-efficients of polynomials fitted to Sensitivity Functions				$S_{min.}/\mu g.g^{-1}$	E_p at $S_{min.}$ (keV)
	a_0	a_1	a_2	a_3		
384	+ 88 252	-46 716	+ 8 465	-512	1 940	6 000
695	+136 020	-75 056	+14 054	-878	1 960	6 000
980	+ 41 636	-21 566	+ 3 839	-229	920	6 000
1410	+136 256	-75 063	+13 938	-858	1 950	6 000
1970	+ 1 122	+ 1 764	- 593	+ 49	930	6 000

Calcium : - Gamma-rays of calcium from five of its six naturally-occurring isotopes were observed when a target of calcium hydroxide was bombarded. The only isotope that did not produce any photons was ^{46}Ca which had a natural abundance of 0.003 atom %. On the other hand, the most abundant isotope, ^{40}Ca, produced no gamma-rays from Coulomb excitation because both the ground state and the first excited state at 3354 keV are 0^+ states, between which, gamma-ray decay is forbidden. The first excited state decays by pair-emission [Be 55].

The most useful gamma-ray was from the decay of the first excited state of ^{44}Ca with the sensitivity limit of 200 $\mu g.g^{-1}$ even though the isotopic abundance was only 2.08 atom %.

^{48}Ca provided relatively intense photopeaks in the low energy region of the spectrum.

A composite peak from the contribution of two gamma-rays, from different isotopes, was sufficiently intense for analysis of calcium at concentrations somewhat below 1000 $\mu g.g^{-1}$.

Eγ keV	Assignment	Yield. quanta $sr^{-1}nC^{-1}$	Sensitivity $\mu g.g^{-1}mC^{-1}$	Eγ keV	Assignment	Yield. quanta $sr^{-1}nC^{-1}$	Sensitivity $\mu g.g^{-1}mC^{-1}$
121	^{48}Ca n(2,1)	290	630	593	^{43}Ca p(2,0)	38	8 500
131	^{48}Ca n(1,0)	310	590	729	^{43}Ca n(5,1)	35	9 100
373	^{43}Ca p(1,0)	180	930	787	^{40}Ca p(6,3)	29	10 600
376	^{44}Ca γ(2,0)			1157	^{44}Ca p(1,0)	560	500
397	^{49}Ca p(3,2)	6.9	94 200	1525	^{42}Ca p(1,0)	140	1 540
520	^{48}Ca n(4,3)	64	5 700	1811	^{48}Ca n(8,2)	35	8 300

E_γ (keV) \ E_p (keV)	Yield (quanta $sr^{-1}nC^{-1}$)					
	3 500	4 000	4 500	5 000	5 500	6 000
121	95	110	290	340	615	790
131	130	250	310	610	940	1 120
373 } 376 }	64	115	180	260	360	480
1157	125	280	560	1 380	1 620	1 860
1525	39	62	140	235	360	525

E_γ (keV)	Co-efficients of polynomials fitted to Sensitivity Functions				$S_{min.}/\mu g.g^{-1}$	E_p at $S_{min.}$ (keV)
	a_0	a_1	a_2	a_3		
121	+ 3 387	- 1 097	+ 107	0	520	5 000
131	-10 408	+ 6 773	-1 352	+ 86	230	6 000
373 } 376 }	+ 7 131	- 2 822	+ 378	- 13	840	5 050
1157	+26 652	-14 936	+2 827	-178	220	6 000
1525	+13 308	- 2 810	- 140	+ 44	900	5 780

Scandium : - In order to obtain the prompt gamma-ray spectrum, a piece of pure scandium metal sheet was bombarded.

Any photon emission from the first excited state of ^{45}Sc at 12.4 keV would have been below the threshold of the Ge(Li) spectrometer and would not have been observed.

By far the most gamma-rays were produced by Coulomb excitation, many of which were of such intensity that they provided sensitivities in the order of 300 $\mu g.g^{-1}$ improving to about 150 $\mu g.g^{-1}$ at proton bombarding energies of 6000 keV.

No gamma-rays were observed resulting from the excitation of the twelfth level of ^{45}Sc.

E_γ keV	Assignment	Yield. quanta $sr^{-1}nC^{-1}$	Sensitivity $\mu g.g^{-1}mC^{-1}$	E_γ keV	Assignment	Yield. quanta $sr^{-1}nC^{-1}$	Sensitivity $\mu g.g^{-1}mC^{-1}$
293	^{45}Sc n(3,1)	4 000	300	927	^{45}Sc p(5,0)	350	3 300
347	^{45}Sc p(7,4)	270	3 700	962	^{45}Sc p(6,1)	1 400	860
364	^{45}Sc p(2,1)	3 200	340	974	^{45}Sc p(6,0)	2 500	490
377	^{45}Sc p(2,0)	380	2 500	1033	^{45}Sc p(10,2)	63	7 300
415	^{45}Sc n(4,2)	1 900	570	1056	^{45}Sc p(16,6)	310	4 400
425	^{45}Sc p(13,8)	250	3 400	1121	^{45}Sc γ(2,1)	280	4 500
432	^{45}Sc p(6,3)	530	1 900	1237	^{45}Sc p(8,0)	3 200	360
459	^{45}Sc p(11,6)	470	2 300	1290	^{45}Sc p(9,0)	120	7 500
531	^{45}Sc p(3,1)	3 800	300	1409	^{45}Sc p(10,0)	1 500	730
543	^{45}Sc p(3,0)	2 700	420	1434	^{45}Sc p(11,0)	160	5 200
597	^{45}Sc p(15,11)	530	2 300	1525	^{45}Sc α(1,0)	130	5 700
689	^{45}Sc p(10,4)	940	1 500	1662	^{45}Sc p(13,0)	770	950
691	^{45}Sc p(7,2)			1788	^{45}Sc p(14,1)	8.3	55 000
707	^{45}Sc n(4,1)	250	5 000	1800	^{45}Sc p(14,0)	68	10 500
720	^{45}Sc p(4,0)	3 800	400	1837	^{45}Sc α(2,0)	51	14 900
760	^{45}Sc p(9,3)	250	4 800	1936	^{45}Sc p(15,0)	9.7	50 100
889	^{45}Sc γ(1,0)	2 100	640				
890	^{45}Sc p(11,3)						

E_γ (keV) \ E_p (keV)	Yield (quanta $sr^{-1}nC^{-1}$)					
	3 500	4 000	4 500	5 000	5 500	6 000
293	83	900	4 000	6 400	13 700	16 500
364	1 000	1 740	3 200	3 400	10 500	12 500
415	1 090	1 470	1 900	2 170	2 410	2 920
531	870	1 700	3 800	3 920	4 300	6 450
543	570	1 340	2 700	2 860	5 500	5 810
720	1 200	2 150	3 800	4 200	6 400	7 500
889	600	1 060	2 100	3 200	6 900	8 240
962	220	550	1 400	1 570	2 110	3 250
974	540	1 160	2 500	2 700	4 600	5 200
1237	530	1 350	3 200	4 030	7 880	9 920
1409	230	730	1 500	2 060	3 570	5 220
1662	72	290	770	1 310	2 320	2 770

E_γ (keV)	Co-efficients of polynomials fitted to Sensitivity Functions				$S_{min.}/\mu g.g^{-1}$	E_p at $S_{min.}$ (keV)
	a_0	a_1	a_2	a_3		
293	+39 914	-22 122	+4 098	-253	140	6 000
364	- 510	+ 548	- 74	0	130	6 000
415	- 7 120	+ 4 968	-1 089	+ 81	410	3 500
531	+12 604	- 8 744	+2 105	-164	420	6 000
543	+18 854	-10 534	+1 990	-124	420	4 500
720	+ 3 556	- 1 843	+ 353	- 22	380	4 500
889	+ 2 240	- 651	+ 98	- 6.8	420	6 000
962	+74 564	-42 108	+7 886	-481	860	4 500
974	+19 460	-11 147	+2 162	-137	490	4 500
1237	+17 251	-10 139	+2 037	-136	320	6 000
1409	+35 382	-20 007	+3 866	-250	530	6 000
1662	+17 325	- 6 228	+ 584	0	730	5 330

Titanium : - The titanium spectrum showed a mass of peaks, many of them of such high intensity that the element could easily be determined to a limit of $25 \mu g.g^{-1}$. Most of the intense peaks were composite in nature represented by the sums of intensities of gamma-ray groups. This was possible because natural titanium consists of five isotopes each of which had an appreciable natural abundance.

A peak at about 88 keV was intense and suited for titanium determination above 420 $\mu g.g^{-1}$. Its intensity was further enhanced by the contribution of counts from gamma-rays from similar reactions on the ^{48}Ti - ^{49}Ti pair. This photopeak of 90 keV could not be resolved from the 88-keV peak and were integrated together.

De-excitation of the first levels of both the ^{47}Ti and ^{48}Ti isotopes resulted in relatively intense gamma-rays of 159 and 985 keV respectively, the latter offering the best sensitivity for titanium analysis.

The $(p,n\gamma)$ reaction on ^{49}Ti produced a gamma-ray at 226 keV and the peak in the spectrum was integrated together with the 227-keV photopeak from the $(p,\alpha\gamma)$ reaction on ^{49}Ti. The

Eγ keV	Assignment	Yield. quanta $sr^{-1}nC^{-1}$	Sensitivity $\mu g.g^{-1}mC^{-1}$	Eγ keV	Assignment	Yield. quanta $sr^{-1}nC^{-1}$	Sensitivity $\mu g.g^{-1}mC^{-1}$
88	^{47}Ti n(1,0)	2 890	420	1049	^{46}Ti p(5,2)	88	8 700
88	^{46}Ti γ(1,0)			1049	^{49}Ti n(5,1)		
90	^{49}Ti n(1,0)			1049	^{48}Ti γ(5,1)		
90	^{48}Ti γ(1,0)			1065	^{48}Ti p(7,2)	110	7 100
94	^{50}Ti n(2,1)	560	2 200	1065	^{49}Ti n(6,1)		
98	^{48}Ti n(4,2)			1092	^{47}Ti p(2,1)	180	4 200
152	^{49}Ti n(2,0)	475	1 200	1121	^{46}Ti p(2,1)	50	15 400
152	^{46}Ti γ(2,0)			1140	^{48}Ti γ(5,0)	165	4 800
152	^{48}Ti γ(2,0)			1140	^{49}Ti n(5,0)		
159	^{47}Ti p(1,0)	2 110	350	1155	^{48}Ti γ(6,0)	380	1 900
160	^{49}Ti p(2,1)			1155	^{49}Ti n(6,0)		
204	^{49}Ti p(3,1)	12	19 200	1312	^{48}Ti p(2,1)	160	4 700
210	^{47}Ti γ(3,1)	8	30 500	1361	^{49}Ti n(7,2)	20	37 100
226	^{50}Ti n(1,0)	1 570	420	1361	^{49}Ti γ(7,2)		
227	^{49}Ti α(1,0)			1394	^{47}Ti p(4,1)	55	12 700
308	^{48}Ti n(1,0)	18	33 200	1424	^{48}Ti γ(7,1)	15	33 300
308	^{47}Ti γ(1,0)			1424	^{49}Ti n(7,1)		
320	^{50}Ti γ(1,0)	64	11 200	1438	^{48}Ti p(3,1)	370	1 700
320	^{50}Ti n(2,0)			1491	^{48}Ti γ(8,2)	50	14 100
354	^{48}Ti α(2,1)	8	112 000	1491	^{48}Ti n(8,2)		
368	^{48}Ti α(2,0)	10	89 800	1492	^{50}Ti γ(3,1)		
393	^{48}Ti γ(5,3)	26	30 900	1509	^{48}Ti γ(9,2)	195	3 400
393	^{49}Ti n(5,3)			1512	^{49}Ti n(7,0)		
543	^{48}Ti α(3,0)	8	100 000	1512	^{48}Ti γ(7,0)		
595	^{49}Ti n(3,2)	170	6 800	1512	^{49}Ti n(8,1)		
595	^{48}Ti γ(3,2)			1542	^{49}Ti p(2,0)	15	48 500
658	^{48}Ti γ(3,1)	120	11 900	1553	^{48}Ti γ(8,1)	315	2 400
658	^{49}Ti n(3,1)			1554	^{50}Ti p(1,0)		
661	^{46}Ti γ(4,0)			1570	^{46}Ti p(11,2)	50	12 300
748	^{48}Ti γ(3,0)	12	124 000	1570	^{49}Ti n(10,0)		
774	^{50}Ti α(1,0)	13	110 000	1571	^{48}Ti γ(10,1)		
889	^{46}Ti p(1,0)	1 990	560	1571	^{49}Ti n(10,1)		
928	^{48}Ti p(4,2)	20	49 200	1601	^{47}Ti n(9,2)	65	8 700
929	^{50}Ti γ(2,0)			1602	^{49}Ti n(8,0)		
945	^{48}Ti p(5,2)	40	22 800	1602	^{48}Ti γ(8,0)		
986	^{48}Ti γ(5,2)	17 700	54	1623	^{49}Ti p(4,0)	10	46 700
984	^{48}Ti p(1,0)			1762	^{49}Ti p(6,0)	8.3	67 400
986	^{49}Ti n(5,2)			1796	^{48}Ti γ(11,0)	20	36 200
1021	^{48}Ti γ(4,0)	470	1 800	1841	^{48}Ti γ(12,1)	20	34 200
1021	^{49}Ti n(4,0)			1903	^{48}Ti γ(12,0)	10	63 000

combined area of these peaks were of such intensity that a sensitivity of 110 $\mu g.g^{-1}$ was attained with 6000 keV. The composite peak at 986 keV represented the gamma-rays ^{48}Ti

p(1,0), ^{48}Ti γ(5,2) and ^{49}Ti n(5,2) of which the major contribution was from Coulomb excitation of ^{48}Ti occurring with the highest natural abundance of 73.7 atom %.

E_γ (keV) \ E_p (keV)	Yield (quanta $sr^{-1}nC^{-1}$)					
	3 500	4 000	4 500	5 000	5 500	6 000
88, 90, 91	125	790	2 890	3 740	4 240	9 680
159, 160	410	1 015	2 110	2 550	4 040	7 420
226, 227	220	710	1 570	2 690	5 520	8 760
889	560	1 210	1 990	3 120	5 850	12 600
983, 984, 986	1 260	9 620	17 700	28 200	49 900	84 600

E_γ (keV)	Co-efficients of polynomials fitted to Sensitivity Functions				$S_{min.}/\mu g.g^{-1}$	E_p at $S_{min.}$ (keV)
	a_0	a_1	a_2	a_3		
88, 90, 91	- 4 592	+ 3 480	- 762	+ 52	170	6 000
159, 160	+ 3 992	- 2 076	+ 398	-260	290	6 000
226, 227	+39 747	-21 934	+4 074	-253	110	6 000
889	+18 538	- 8 969	+1 477	- 81	320	6 000
983, 984, 986	+ 616	- 314	+ 62	- 4.3	20	6 000

Vanadium : - A pure vanadium metal sheet was bombarded to yield the gamma-ray spectrum.

No gamma-ray from the low abundance ^{50}V isotope was observed. The Coulomb-excited 320-keV ^{51}V p(1,0) gamma-ray, which was used for analytical purposes under alpha bombardment [Gi 78a]

was again observed with appreciable intensity, but in this case there was extensive overlap in the spectrum with the peak from the 316-keV ^{51}V n(5,3) gamma-ray. This overlap does not, however, constitute interference because the relative intensity of these two gamma-rays are constant for a constant bombarding energy. The combined areas under these two spectrum peaks could thus be used as a measure of vanadium content.

Of the several gamma-rays available for interference-free analysis, the one at 750 keV was most intense. A detailed description of vanadium analysis in steels is given in Chapter 4 (see page 146).

Eγ keV	Assignment	Yield. quanta $sr^{-1}nC^{-1}$	Sensitivity $\mu g.g^{-1}mC^{-1}$	Eγ keV	Assignment	Yield. quanta $sr^{-1}nC^{-1}$	Sensitivity $\mu g.g^{-1}mC^{-1}$
198	^{51}V γ(4,3)	380	1 800	1148	^{51}V n(10,3)	420	1 800
204	^{51}V n(6,4)	710	3 300	1165	^{51}V n(3,0)	1 420	210
206	^{51}V p(4,3)			1333	^{51}V γ(3,1)	35	12 000
316	^{51}V n(5,3)	3 310	540	1353	^{51}V n(4,0)	1 120	790
320	^{51}V p(1,0)	4 100	370	1434	^{51}V γ(1,0)	500	1 400
576	^{51}V n(4,2)	550	4 400	1480	^{51}V n(5,0)	4 960	880
603	^{51}V n(4,1)	3 570	860	1481	^{51}V p(5,2)		
609	^{51}V p(2,1)	3 610	920	1493	^{51}V p(4,1)	410	1 300
749	^{51}V n(1,0)	3 380	210	1558	^{51}V n(6,0)	1 020	2 100
775	^{51}V n(9,5)	150	5 100	1608	^{51}V p(3,0)	750	3 400
808	^{51}V n(6,1)	5 240	600	1814	^{51}V p(4,0)	930	1 000
929	^{51}V p(2,0)	410	1 730	1899	^{51}V n(7,0)	630	3 100
935	^{51}V γ(2,1)	320	2 200	2002	^{51}V n(8,0)	1 050	1 300

E_γ(keV) \ E_p(keV)	Yield (quanta $sr^{-1}nC^{-1}$)					
	3 500	4 000	4 500	5 000	5 500	6 000
316	2 320	2 930	3 310	3 745	4 740	8 105
320	2 760	3 305	4 100	6 950	9 040	11 120
603	1 040	2 170	3 570	4 710	7 320	9 813
609	390	2 010	3 610	4 980	6 030	7 910
749	160	2 270	3 380	3 535	3 740	4 010
808	3 315	4 040	5 240	7 965	11 610	13 730
1165	840	1 290	1 420	2 125	2 910	3 175
1353	95	180	1 120	2 710	4 730	6 970
1480 / 1483	410	2 160	4 960	5 310	7 430	10 730

E_γ (keV)	Co-efficients of polynomials fitted to Sensitivity Functions				$S_{min.}/\mu g.g^{-1}$	E_p at $S_{min.}$ (keV)
	a_0	a_1	a_2	a_3		
316	+12 969	- 6 948	+1 239	+ 71	280	4 750
320	+10 389	- 6 660	+1 426	- 97	320	3 900
603	+17 556	- 7 964	+1 224	- 62	620	6 000
609	+21 940	-11 355	+2 031	-120	920	5 130
749	+ 2 711	- 1 561	+ 315	- 21	190	4 200
808	+10 309	- 5 119	+ 878	- 49	490	5 250
1165	+31 800	-18 806	+3 693	-238	190	4 600
1353	+58 172	-32 922	+6 257	-394	760	4 870
1480 1483	+22 192	-11 639	+2 115	-129	640	6 000

Chromium : - Metallic chromium was irradiated to produce the gamma-ray spectra. Most of the intense gamma-rays were

Eγ keV	Assignment	Yield. quanta $sr^{-1}nC^{-1}$	Sensitivity $\mu g.g^{-1}mC^{-1}$	Eγ keV	Assignment	Yield. quanta $sr^{-1}nC^{-1}$	Sensitivity $\mu g.g^{-1}mC^{-1}$
55	^{54}Cr n(1,0)	380	4 800	955	^{54}Cr n(6,1)	22	
55	^{53}Cr γ(1,0)			955	^{53}Cr γ(6,1)		
154	^{52}Cr α(2,0)	540	2 600	1006	^{53}Cr n(6,2)	430	6 000
156	^{54}Cr n(2,0)			1116	^{53}Cr p(2,0)	460	6 600
156	^{53}Cr γ(2,0)			1213	^{52}Cr p(3,1)	140	24 400
211	^{54}Cr n(3,2)	75	16 600	1288	^{53}Cr n(2,0)	2 300	1 300
211	^{53}Cr γ(3,2)			1288	^{52}Cr γ(2,0)		
250	^{54}Cr n(4,2)	210	6 300	1332	^{52}Cr p(4,1)	230	10 500
250	^{53}Cr γ(4,2)			1335	^{54}Cr n(8,1)		
253	^{53}Cr γ(4,1)			1375	^{54}Cr n(7,0)		
378	^{53}Cr n(1,0)	8 050	260	1400	^{54}Cr n(9,1)	135	18 700
378	^{52}Cr γ(1,0)			1434	^{52}Cr p(1,0)	36 600	140
406	^{54}Cr n(4,0)	160	9 300	1440	^{53}Cr n(3,0)		
406	^{53}Cr γ(4,0)			1619	^{53}Cr n(4,0)	660	3 200
564	^{53}Cr p(1,0)	700	3 400	1894	^{53}Cr n(5,1)	115	15 900
783	^{50}Cr p(1,0)	3 060	1 100	1894	^{52}Cr γ(5,1)		
839	^{54}Cr n(5,0)	690	3 700	2194	^{53}Cr n(7,1)	95	18 000
839	^{53}Cr γ(5,0)			2194	^{52}Cr γ(7,1)		
854	^{54}Cr n(6,2)	760	3 300	2274	^{52}Cr γ(5,0)	490	4 050
854	^{53}Cr γ(6,2)			2274	^{53}Cr n(5,0)		
911	^{53}Cr n(2,1)	1 750	1 800	2405	^{53}Cr n(6,0)	180	13 100
911	^{52}Cr γ(2,1)			2405	^{52}Cr γ(6,0)		
935	^{52}Cr p(2,1)	180	13 500				

due to reaction with ^{52}Cr which has a natural abundance of 83.79 atom % in nature. The intensities of the prominent gamma-rays were enhanced by the fortunate chance that radiations from ^{53}Cr, the next most abundant isotope (9.50 atom %) frequently had energies very close to those from ^{52}Cr. Apart from the very intense 783-keV ^{50}Cr p(1,0) gamma-ray, all the other radiations from reactions with this isotope and with ^{54}Cr were relatively weak.

The gamma-ray of 155 keV was ascribed to ^{52}Cr α(2,0) but the corresponding gamma-ray ^{52}Cr α(1,0) with an energy of 91 keV which should have been excited was not observed. A similar result was also obtained [De 78] at a bombarding energy of 3200 keV.

E_γ (keV) \ E_p (keV)	Yield (quanta $sr^{-1}nC^{-1}$)					
	3 500	4 000	4 500	5 000	5 500	6 000
378	1 010	3 420	8 050	11 760	15 700	27 350
783	360	1 140	3 060	3 810	4 750	6 210
911 / 912	360	1 120	1 750	2 360	4 100	6 240
1288 / 1290	780	1 160	2 300	2 930	4 140	6 180
1435 / 1440	11 310	21 760	36 600	43 730	54 310	79 340

E_γ (keV)	Co-efficients of polynomials fitted to Sensitivity Functions				$S_{min.}$/μg.g^{-1}	E_p at $S_{min.}$ (keV)
	a_0	a_1	a_2	a_3		
378	+ 220	- 201	+ 73	+ 6	180	3 650
783	+53 736	-61 540	+14 994	-1 191	940	3 550
911 / 913	+14 008	- 3 248	- 1 042	+ 259	800	3 760
1288 / 1290	+47 972	-32 914	+ 7 513	+ 550	760	3 830
1435 / 1440	+ 1 749	- 590	+ 52	0	70	5 700

If all the intense gamma-rays were to be considered for analysis, a compromise bombarding energy of 4000 keV was suggested.

The determination of chromium in steels where this bombarding energy was used, is discussed in Chapter 4 (see page 153).

Manganese : - Chips of electrolytic manganese was bombarded to obtain the gamma-ray spectra. Since stable manganese is mono-isotopic all the recorded gamma-rays resulted from the interaction with ^{55}Mn. The nuclear reactions from which gamma-rays were detected were Coulomb-excitation of ^{55}Mn, proton-capture and the reaction $^{55}Mn(p,n\gamma)^{55}Fe$. In all the cases the gamma-rays that were observed are in accordance with the evaluated data. The first 6 levels, to 2199 keV, of ^{55}Mn were excited by Coulomb excitation. Of the expected decay gamma-rays only two were not observed viz., the 308-keV p(3,2) and the 1759-keV p(5,1) because of their low intensities. The proton-capture reaction led to the population of the first 2 excited states to 2085 keV and the decay of these states were observed.[Au 77]

Eγ keV	Assignment	Yield. quanta $sr^{-1}nC^{-1}$	Sensitivity $\mu g.g^{-1}mC^{-1}$	Eγ keV	Assignment	Yield. quanta $sr^{-1}nC^{-1}$	Sensitivity $\mu g.g^{-1}mC^{-1}$
92	^{55}Mn n(4,3)	3 400	7 800	1238	^{55}Mn γ(2,1)	2 800	6 600
126	^{55}Mn p(1,0)	5 900	250	1316	^{55}Mn n(3,0)	13 400	210
385	^{55}Mn n(3,2)	930	1 800	1370	^{55}Mn n(9,2)	1 900	550
412	^{55}Mn n(1,0)	7 600	190	1408	^{55}Mn n(4,0)	5 400	450
477	^{55}Mn n(4,2)	6 000	270	1508	^{55}Mn n(5,1)	510	3 700
521	^{55}Mn n(2,1)	310	5 800	1528	^{55}Mn p(4,0)	290	2 900
803	^{55}Mn n(8,4)	2 400	950	1640	^{55}Mn n(6,1)	1 700	1 300
828	^{55}Mn n(7,3)	1 700	1 300	1733	^{55}Mn n(7,1)	1 480	11 000
847	^{55}Mn γ(1,0)	670	4 100	1883	^{55}Mn p(5,0)	1 250	10 000
858	^{55}Mn p(2,1)	1 100	1 800	1918	^{55}Mn n(5,0)	930	2 100
931	^{55}Mn n(2,0)	3 400	90	2051	^{55}Mn n(6,0)	690	2 400
984	^{55}Mn p(2,0)	260	9 000	2143	^{55}Mn n(7,0)	1 700	1 100
985	^{55}Mn n(9,3)			2168	^{55}Mn n(12,1)	1 090	6 600
1166	^{55}Mn p(3,1)	50	59 000	2199	^{55}Mn p(6,0)	1 210	5 800
1214	^{55}Mn n(7,2)	1 800	1 300	2470	^{55}Mn n(10,0)	980	1 800
1225	^{55}Mn n(11,3)	990	2 300	2578	^{55}Mn n(12,0)	1 290	1 200

E_p (kev) / E_γ (keV)	Yield (quanta $sr^{-1}nC^{-1}$)					
	3 500	4 000	4 500	5 000	5 500	6 000
126	1 950	4 930	5 950	7 780	13 700	14 100
412	2 170	4 810	7 600	9 270	11 100	15 500
477	1 740	2 620	6 000	9 770	14 400	20 700
803	760	1 420	2 400	3 430	8 360	10 400
931	25 200	30 000	33 900	34 100	37 800	41 800
1316	4 810	10 600	13 400	14 500	15 700	17 300
1370	640	1 170	1 900	2 460	4 680	9 940
1408	1 860	4 360	5 400	7 280	12 600	14 050

Most of the gamma-rays originate from the(p,nγ) reaction which resulted in the excitation of 12 levels above the ground state of the product nucleus. Virtually all the gamma-rays [Ko 76] from the decay of these levels were observed with the exception of low-intensity transitions from the 8th excited state at 2211-keV and the unconfirmed transitions from excited states 8 and 9.

E_γ (keV)	Co-efficients of polynomials fitted to Sensitivity Functions				$S_{min.}/\mu g.g^{-1}$	E_p at $S_{min.}$ (keV)
	a_0	a_1	a_2	a_3		
126	+10 246	- 6 372	+1 323	- 89	230	4 120
412	+ 3 315	- 1 419	+ 161	0	185	4 400
477	+12 470	- 7 947	+1 706	-121	260	4 200
803	+23 516	-11 497	+1 900	-101	850	5 100
931	+ 1 610	+ 1 516	- 424	+ 38	90	4 500
1316	+12 085	- 7 623	+1 609	-112	180	4 400
1370	+21 747	-13 791	+2 914	-200	410	4 000
1408	+27 880	-14 990	+2 712	-163	310	5 500

Iron : - Although the bombardment of iron yielded a gamma-ray spectrum in which only one peak was very prominent viz., 847-keV ^{56}Fe p(1,0), the formation of even low intensity gamma-rays was of importance because the element was likely to constitute the major component in a matrix such as steel. Thus, for example, the appearance of two minor peaks in the spectrum-corresponding to 122-keV ^{57}Fe p(2,1) and 127.3-keV ^{56}Fe γ(3,2) entirely eliminated the possibility of manganese analysis using the intense manganese gamma-ray of 126 keV.

E_γ keV	Assignment	Yield quanta $sr^{-1}nC^{-1}$	Sensitivity $\mu g.g^{-1}mC^{-1}$	E_γ keV	Assignment	Yield quanta $sr^{-1}nC^{-1}$	Sensitivity $\mu g.g^{-1}mC^{-1}$
112	^{57}Fe γ(3,0)	5.6	90 500	847	^{56}Fe p(1,0)	21 800	40
112	^{58}Fe n(3,0)			970	^{56}Fe n(4,0)	35	25 400
123	^{57}Fe p(2,1)	8.3	72 400	1224	^{56}Fe γ(1,0)	44	15 900
127	^{56}Fe γ(3,2)	79	10 200	1224	^{57}Fe n(1,0)		
127	^{57}Fe n(3,2)			1238	^{56}Fe p(2,1)	190	2 900
352	^{57}Fe p(3,1)	88	8 900	1328	^{58}Fe α(4,2)	86	5 100
366	^{57}Fe γ(4,0)	19	44 900	1377	^{56}Fe γ(2,0)	590	860
366	^{58}Fe n(4,0)			1377	^{57}Fe n(2,0)		
367	^{57}Fe p(3,0)			1408	^{54}Fe p(1,0)	530	900
380	^{56}Fe γ(5,2)	31	29 600	1757	^{56}Fe γ(5,0)	220	2 560
380	^{57}Fe n(5,2)			1757	^{57}Fe n(5,0)		
412	^{54}Fe p(4,2)	82	12 500	1810	^{56}Fe p(3,1)	33	14 500
466	^{56}Fe γ(4,1)	74	13 800	1897	^{56}Fe γ(6,0)	18	20 800
466	^{57}Fe n(4,1)			1897	^{57}Fe n(6,0)		
673	^{56}Fe γ(6,1)	34	39 700	1918	^{57}Fe n(7,0)	115	4 100
673	^{57}Fe n(6,1)			1919	^{56}Fe γ(7,0)		
692	^{57}Fe p(4,1)	42	33 200	2111	^{56}Fe p(4,1)	44	10 200
812	^{58}Fe p(1,0)	36	27 600	2133	^{56}Fe γ(8,0)	59	7 600
				2133	^{57}Fe n(8,0)		

E_γ (keV) \ E_p (keV)	Yield (quanta $sr^{-1}nC^{-1}$)					
	3 500	4 000	4 500	5 000	5 500	6 000
847	1 980	9 570	21 800	28 900	98 800	101 400
1238	37	73	190	550	3 280	5 620
1377	80	270	590	610	1 590	2 190
1408	27	120	530	880	3 590	4 220
1757	5	87	220	270	770	1 120

E_γ (keV)	Co-efficients of polynomials fitted to Sensitivity Functions				$S_{min.}/\mu g.g^{-1}$	E_p at $S_{min.}$ (keV)
	a_0	a_1	a_2	a_3		
847	+ 144	+ 9.6	- 12.6	+ 1.3	20	6 000
1238	+163 444	-77 840	+12 289	-641	300	6 000
1377	+ 28 702	-16 260	+ 3 148	-202	860	4 500
1408	+107 232	-58 760	+10 783	-659	390	6 000
1757	+ 93 088	-49 996	+ 9 139	-556	1 980	6 000

Proton-capture reactions on the ^{56}Fe isotope and $(p,n\gamma)$ reactions on the lesser abundant ^{57}Fe isotope (2.19 atom %) yielded the same gamma-rays and since most of the peaks from these reactions appearin that region of the spectrum where the intensity of the continuum had decreased considerably, they offered moderate sensitivities.

Cobalt : - The spectra were obtained from the bombardment of metallic cobalt. The element is mono-isotopic in nature and gamma-rays were emitted as a result of Coulomb excitation as well as from the reactions; $^{59}Co(p,n\gamma)^{59}Ni$; $^{59}Co(p,\gamma)^{60}Ni$ and $^{59}Co(p,n\gamma)^{56}Fe$. Although the decay of the fourth excited level of the Coulomb excited nuclide resulted in an intense-gamma-ray, careful consideration had to be given when using it for analytical purposes because of the presence of a very intense gamma-ray from chromium in the vicinity of the 1429-keV cobalt peak.

Eγ keV	Assignment	Yield. quanta $sr^{-1}nC^{-1}$	Sensitivity $\mu g.g^{-1}mC^{-1}$	Eγ keV	Assignment	Yield. quanta $sr^{-1}nC^{-1}$	Sensitivity $\mu g.g^{-1}mC^{-1}$
197	^{59}Co p(3,1)	72	7 400	1291	^{59}Co p(3,0)	95	12 800
312	^{59}Co n(4,3)	110	10 000	1301	^{59}Co n(5,0)	150	7 200
339	^{59}Co n(1,0)	14 800	80	1332	^{59}Co γ(1,0)	750	1 290
430	^{59}Co n(8,5)	153	6 000	1337	^{59}Co n(6,1)	3 730	380
465	^{59}Co n(2,0)	910	1 200	1432	^{59}Co p(4,0)	3 380	390
760	^{59}Co n(11,4)	120	12 200	1461	^{59}Co p(5,0)	680	1 560
826	^{59}Co γ(2,1)	88	13 500	1480	^{59}Co p(6,0)	190	5 900
842	^{59}Co α(1,0)	140	12 100	1608	^{59}Co n(11,1)	440	2 100
878	^{59}Co n(3,0)	2 210	710	1680	^{59}Co n(7,0)	240	3 800
997	^{59}Co n(5,1)	4 500	370	1735	^{59}Co n(8,0)	170	6 200
1099	^{59}Co p(1,0)	270	5 700	1746	^{59}Co n(9,0)	39	18 000
1173	^{59}Co γ(3,1)	410	6 900	1773	^{59}Co α(9,2)	710	1 120
1189	^{59}Co n(4,0)	4 920	360	1778	^{59}Co n(10,0)	650	1 700
1190	^{59}Co p(2,0)			1948	^{59}Co n(11,0)	1 200	640
1272	^{59}Co n(8,2)	96	12 600				

E_γ (keV) \ E_p (keV)	Yield (quanta $sr^{-1}nC^{-1}$)					
	3 500	4 000	4 500	5 000	5 500	6 000
339	1 210	3 230	14 800	25 200	26 100	29 800
878	310	1 100	2 210	3 870	5 740	8 310
997	380	1 990	4 500	7 830	8 740	11 900
1189 / 1190	510	2 100	4 920	7 390	10 100	16 700
1337	440	1 530	3 730	5 210	7 980	8 670
1432	370	960	3 380	5 340	7 120	8 390
1948	260	470	1 200	3 030	7 590	12 400

Many levels of ^{59}Ni, produced by the (p,nγ) reaction on ^{59}Co, were excited and decay of the lower states yielded the most intense gamma-rays. The most important of these was a gamma-ray of 339 keV which offered a sensitivity of 70 $\mu g.g.^{-1}$ at an optimum bombarding energy of 5100 keV. Because the 1332-and 1337-keV photons are so close to each other, the peaks from these gamma-rays could be integrated together so that this doublet could be potentially useful for the determination of the element. A mean bombarding energy of 5000 keV is suggested if all the intense gamma-rays are to be utilized for the analysis of cobalt.

E_γ (keV)	Co-efficients of polynomials fitted to Sensitivity Functions				$S_{min.}/\mu g.g^{-1}$	E_p at $S_{min.}$ (keV)
	a_0	a_1	a_2	a_3		
339	+ 830	- 298	+ 29	0	70	5 100
878	+32 190	-17 879	+3 340	-205	610	4 800
997	+40 822	-23 873	+4 657	-301	300	4 700
1189 / 1190	+14 510	- 7 692	+1 365	- 79	280	4 950
1337	+13 743	- 7 063	+1 212	- 67	320	4 960
1432	+14 933	- 7 108	+1 436	- 88	290	6 000
1948	+10 056	- 5 499	+1 072	- 70	550	6 000

Nickel : - Bombardment of a pure nickel plate led to the production of many low intensity gamma-rays with the exception of two analytically useful ones corresponding to 1333 keV and 1454 keV. These resulted from the Coulomb excitation of the first levels of ^{60}Ni and ^{58}Ni respectively. Both of these gamma-rays would provide a sensitivity of analysis of less than 500 $\mu g.g^{-1}$ at a proton energy of 4500 keV. With increasing bombarding energy the sensitivity increased, because the background against which these gamma-rays were measured, was relatively little affected by the Compton continuum contributed from higher energy gamma-rays.

Eγ keV	Assignment	Yield. quanta $sr^{-1}nC^{-1}$	Sensitivity $\mu g.g^{-1}mC^{-1}$	Eγ keV	Assignment	Yield. quanta $sr^{-1}nC^{-1}$	Sensitivity $\mu g.g^{-1}mC^{-1}$
53	^{61}Ni α(1,0)	6.3	93 000	750	^{62}Ni p(6,3)	10	62 000
59	^{61}Ni α(3,2)	7.4	69 000	771	^{64}Ni γ(1,0)	12	43 000
111	^{61}Ni α(3,0)	6.4	52 000	826	^{60}Ni p(2,1)	100	6 200
147	^{62}Ni n(4,2)	1.3	217 000	870	^{62}Ni p(2,1)	29	24 100
159	^{64}Ni n(1,0)	130	2 800	873	^{61}Ni n(3,1)		
185	^{64}Ni n(3,1)	1.3	212 000	914	^{58}Ni γ(2,0)	72	10 100
197	^{62}Ni α(2,1)	38	7 800	961	^{62}Ni γ(2,0)	18	47 000
265	^{61}Ni n(5,4)	1.5	188 000	970	^{60}Ni γ(2,0)	10	91 600
274	^{64}Ni n(2,0)	140	3 100	1027	^{64}Ni p(1,0)	5.1	174 000
313	^{61}Ni α(4,2)	4.3	72 000	1173	^{62}Ni p(1,0)	350	3 000
341	^{62}Ni α(4,1)	47	6 600	1314	^{61}Ni n(3,0)	20	29 500
349	^{62}Ni n(4,1)	6.5	51 800	1321	^{58}Ni p(3,1)	10	41 100
373	^{61}Ni p(3,2)	20	19 600	1333	^{60}Ni p(1,0)	2 100	320
423	^{58}Ni γ(2,1)	22	17 200	1412	^{62}Ni γ(4,0)	7.1	44 300
477	^{61}Ni n(1,0)	43	10 100	1454	^{58}Ni p(1,0)	4 360	110
491	^{58}Ni γ(1,0)	11	35 900	1547	^{62}Ni γ(5,0)	8.1	45 000
588	^{61}Ni p(3,1)	29	18 900	1640	^{61}Ni γ(5,0)	8.2	30 400
659	^{61}Ni p(3,0)	3.4	155 000	1774	^{58}Ni γ(6,1)	12	18 900
669	^{63}Ni γ(1,0)	3.2	161 000				

E_p(keV) / E_γ(keV)	Yield (quanta $sr^{-1}nC^{-1}$)					
	3 500	4 000	4 500	5 000	5 500	6 000
159	20	69	130	370	480	890
274	19	67	140	260	400	500
1173	40	170	350	1 190	1 680	1 990
1333	98	520	2 100	7 500	13 900	19 800
1454	410	1 750	4 360	17 500	25 200	37 600

E_γ (keV)	Co-efficients of polynomials fitted to Sensitivity Functions				$S_{min.}$/µg.g^{-1}	E_p at $S_{min.}$ (keV)
	a_0	a_1	a_2	a_3		
159	+ 41 073	- 14 316	+ 1 300	0	1 550	5 500
274	+228 144	-126 588	+23 698	-1 479	2 100	6 000
1173	+ 95 016	- 51 264	+ 9 406	- 577	1 440	6 000
1333	+ 53 546	- 29 642	+ 5 482	- 388	100	6 000
1454	+ 4 009	- 1 442	+ 130	0	45	6 000

Copper : - Each of the two copper isotopes produced gamma-

Eγ keV	Assignment	Yield. quanta sr^{-1}nC^{-1}	Sensitivity µg.g^{-1}mC^{-1}	Eγ keV	Assignment	Yield. quanta sr^{-1}nC^{-1}	Sensitivity µg.g^{-1}mC^{-1}
54	^{65}Cu n(1,0)	5	76 000	962	^{63}Cu p(2,0)	18 800	500
55	^{63}Cu n(2,1)			992	^{63}Cu γ(1,0)	4 400	900
115	^{65}Cu n(2,0)	6 400	390	1039	^{65}Cu γ(1,0)	650	5 500
153	^{65}Cu n(3,1)	4 800	580	1048	^{65}Cu n(8,0)	2 600	1 700
194	^{63}Cu n(1,0)	290	4 800	1048	^{65}Cu n(10,3)		
201	^{65}Cu n(8,6)	740	2 600	1049	^{63}Cu p(7,2)		
207	^{65}Cu n(3,0)	380	2 700	1114	^{65}Cu p(2,0)	600	7 000
249	^{63}Cu n(2,0)	80	25 000	1119	^{63}Cu p(9,2)		
365	^{63}Cu p(3,1)	960	3 600	1137	^{65}Cu n(12,3)	710	5 000
369	^{65}Cu p(3,1)			1138	^{65}Cu n(10,2)		
450	^{63}Cu p(4,2)	270	4 900	1174	^{65}Cu α(1,0)	590	6 500
484	^{65}Cu n(9,4)	470	8 500	1177	^{63}Cu α(4,1)	420	8 000
509	^{65}Cu p(4,2)	5 450	2 500	1229	^{65}Cu n(12,2)	1 500	2 500
585	^{63}Cu p(5,2)	530	7 100	1254	^{65}Cu n(13,2)	1 900	1 700
611	^{65}Cu p(5,2)	280	11 600	1263	^{65}Cu n(4,3)	1 300	2 200
639	^{63}Cu n(4,0)	400	6 800	1264	^{65}Cu n(11,0)		
652	^{63}Cu n(5,0)	2 560	1 900	1310	^{63}Cu γ(1,0)	910	3 900
654	^{65}Cu n(4,2)			1327	^{63}Cu p(3,0)	9 900	950
670	^{63}Cu p(1,0)	12 300	770	1329	^{63}Cu α(1,0)	5 600	960
703	^{65}Cu n(6,3)	1 500	2 500	1343	^{63}Cu p(7,1)	550	5 300
715	^{65}Cu n(4,1)	640	6 800	1344	^{65}Cu n(12,0)		
742	^{63}Cu p(4,1)	170	2 100	1355	^{65}Cu n(14,2)	1 200	2 500
752	^{65}Cu n(5,4)	3 800	1 200	1370	^{65}Cu n(13,0)	1 300	2 400
754	^{63}Cu p(9,3)			1412	^{63}Cu p(4,0)	4 300	770
769	^{65}Cu n(4,0)	4 520	970	1463	^{63}Cu α(5,1)	370	7 200
771	^{65}Cu p(1,0)			1470	^{65}Cu n(14,0)	170	15 000
795	^{65}Cu n(6,2)	1 360	2 900	1473	^{65}Cu n(16,2)		
808	^{63}Cu γ(2,1)	1 000	3 600	1523	^{65}Cu n(15,1)	290	10 000
831	^{63}Cu α(2,1)	530	6 300	1547	^{63}Cu p(5,0)	2 160	1 300
840	^{65}Cu α(2,1)	950	4 100	1577	^{65}Cu n(15,0)	590	4 800
852	^{65}Cu p(4,1)	870	3 700	1588	^{65}Cu n(16,0)	670	3 700
856	^{65}Cu n(7,1)			1623	^{65}Cu p(4,0)	150	18 000
865	^{65}Cu n(5,0)	4 300	900	1725	^{65}Cu p(5,0)	60	91 000
899	^{63}Cu p(6,2)	480	6 800	1799	^{65}Cu γ(2,0)	430	5 400
910	^{65}Cu n(6,0)	2 800	1 500	1861	^{63}Cu p(6,0)	620	3 200
932	^{65}Cu n(8,2)	2 500	1 600				

rays many of which were of sufficient intensity to offer reasonable sensitivity for analysis of the element.

Sensitivities ~~of less~~ better than 1000 $\mu g.g^{-1}$ were obtained for those gamma-rays which originated from the decay of the first four excited levels of ^{63}Cu. The reactions that produced other gamma-rays from this isotope were: $^{63}Cu(p,n\gamma)^{64}Zn$ which did not produce any intense gamma-rays; $^{63}Cu(p,\alpha\gamma)^{60}Ni$ which produced a gamma-ray of 1329 keV that could usefully be integrated together with the photopeak of 1329-keV ^{63}Cu p(3,0), and proton-capture of ^{63}Cu which resulted in an analytically useful gamma-ray of 992 keV.

E_p(keV) / E_γ(keV)	Yield (quanta $sr^{-1}nC^{-1}$)					
	3 500	4 000	4 500	5 000	5 500	6 000
115	1 050	2 300	6 400	11 700	18 200	21 600
153	2 300	3 100	4 800	5 700	7 300	9 600
769 / 771	1 300	3 300	4 520	10 800	12 400	16 700
865	940	2 160	4 300	10 070	13 600	26 400
962	905	12 400	18 800	27 500	36 300	49 700
992	840	2 210	4 400	8 640	12 700	20 100
1327	1 160	3 570	9 900	13 400	26 300	31 700
1329	960	2 170	5 600	7 210	8 470	12 400
1412	630	1 950	4 300	4 960	6 200	9 900

E_γ (keV)	Co-efficients of polynomials fitted to Sensitivity Functions				$S_{min.}/\mu g.g^{-1}$	E_p at $S_{min.}$ (keV)
	a_0	a_1	a_2	a_3		
115	+ 8 987	- 4 802	+ 886	- 54.7	270	6 000
153	+ 910	+ 469	- 225	+ 22.2	390	5 450
769 / 771	+ 9 542	- 4 993	+ 969	- 62.7	390	5 450
865	+ 1 821	- 284	+ 17.7	0	750	6 000
962	+61 757	-35 691	+6 892	-441	400	6 000
992	+16 290	- 8 798	+1 662	-104	860	4 880
1327	+ 2 988	- 732	+ 61.2		800	6 000
1329	+ 7 422	- 3 505	+ 631	- 38	890	6 000
1412	+17 444	- 9 584	+1 836	-118	600	6 000

De-excitation of the first level of ^{65}Cu at 771 keV provided the analytically most useful gamma-ray from this isotope, particularly so because its peak could easily be coupled with the 769-keV photopeak from the (p,nγ) reaction.

Zinc : - A pure metal sheet was bombarded to produce the gamma-rays. Zinc has 5 naturally-occurring isotopes all of which yielded observed gamma-rays on bombardment with protons. Excitation of the first level of the highest abundant isotope, ^{64}Zn (48.89 atom %) resulted in a very intense peak corresponding to a gamma-ray of 992 keV. A comparable photopeak was observed for the next most abundant isotope ^{66}Zn (27.8 atom %) while the third gamma-ray, useful for analysis, was produced by the same process on ^{68}Zn (18.57 atom %). Of the two less abundant isotopes, the 360-keV ^{67}Zn n(2,0) gamma-ray may be useful

Eγ keV	Assignment	Yield. quanta $sr^{-1}nC^{-1}$	Sensitivity $\mu g.g^{-1}mC^{-1}$	Eγ keV	Assignment	Yield. quanta $sr^{-1}nC^{-1}$	Sensitivity $\mu g.g^{-1}mC^{-1}$
169	^{66}Zn γ(1,0)	290	3 500	828	^{67}Zn n(3,0)	64	1 900
169	^{67}Zn n(1,0)			834	^{66}Zn p(2,1)	220	8 600
175	^{67}Zn γ(1,0)	1 210	1 200	843	^{67}Zn n(5,2)	200	10 200
175	^{68}Zn n(1,0)			871	^{67}Zn p(5,0)	300	7 400
185	^{67}Zn p(2,0)	110	10 300	871	^{68}Zn γ(3,0)		
193	^{64}Zn γ(1,0)	100	12 400	888	^{67}Zn p(6,0)	130	12 600
237	^{68}Zn γ(5,3)	44	16 700	910	^{70}Zn γ(5,0)	79	3 200
320	^{68}Zn γ(1,0)	930	2 200	911	^{67}Zn n(4,0)		
321	^{68}Zn n(5,1)			992	^{64}Zn p(1,0)	10 200	210
321	^{67}Zn γ(5,1)			1039	^{66}Zn p(1,0)	5 220	320
				1053	^{67}Zn n(6,2)	100	10 300
324	^{67}Zn γ(2,0)			1077	^{68}Zn p(1,0)	1 630	1 100
360	^{67}Zn n(2,0)	1 540	980	1107	^{68}Zn γ(5,0)	320	7 800
508	^{70}Zn n(1,0)	1 270	1 000	1107	^{70}Zn γ(7,0)		
574	^{68}Zn γ(2,0)	400	7 100	1160	^{67}Zn n(7,2)	230	4 300
578	^{68}Zn p(2,1)			1196	^{67}Zn n(8,2)	110	15 000
585	^{68}Zn n(8,0)	100	19 700	1202	^{69}Zn n(5,0)	450	4 000
651	^{70}Zn n(2,0)	83	22 600	1206	^{68}Zn γ(7,1)	12	32 600
691	^{70}Zn n(3,0)	170	13 100	1333	^{66}Zn p(3,1)	180	8 800
710	^{68}Zn γ(4,1)	24	42 400	1335	^{68}Zn γ(6,0)		
807	^{68}Zn p(3,1)	480	5 800	1412	^{66}Zn p(4,1)	160	12 400
809	^{64}Zn p(2,1)			1413	^{67}Zn n(6,0)		
				1555	^{67}Zn n(8,0)	130	14 700

especially if ^{67}Zn is enriched in the target, but ^{70}Zn yielded only low intensity gamma-rays because its natural abundance was only 0.62 atom %.

The most serious sources of interferences when considering using any of the intense photopeaks for analysis, would be the presence of copper which, through proton capture reactions on ^{63}Cu and ^{65}Cu, produced gamma-rays of 992 and 360 keV respectively. The presence of gallium in the matrix would interfere with the use of the 992-and 1037-keV gamma-rays but to a lesser extent [Ch 72].

E_γ (keV) \ E_p (keV)	Yield (quanta $sr^{-1}nC^{-1}$)					
	3 500	4 000	4 500	5 000	5 500	6 000
175	38	160	1 210	1 510	1 940	2 310
320, 321, 324	24	220	930	1 040	1 120	1 460
360	33	98	1 540	1 620	1 780	1 990
508	45	730	1 270	1 470	2 120	2 430
992	2 110	4 710	10 200	14 900	17 400	21 300
1039	780	2 110	5 220	7 900	9 420	12 600

E_γ (keV)	Co-efficients of polynomials fitted to Sensitivity Functions				$S_{min.}/\mu g.g^{-1}$	E_p at $S_{min.}$ (kev)
	a_0	a_1	a_2	a_3		
175	+134 960	-74 400	+13 756	- 850	210	6 000
320, 321, 324	- 22 016	+22 028	-55 947	+ 424	320	5 820
360	+157 752	-89 433	+16 945	-1 069	240	6 000
508	+ 58 504	-32 066	+ 5 846	- 345	910	4 750
992	+ 20 125	-10 757	+ 1 930	- 116	92	6 000
1039	+ 51 883	-30 112	+ 5 840	- 376	150	6 000

Gallium : - Both isotopes of gallium provided a number of gamma-rays, many of which were of sufficient intensity to

determine the element to below 300 $\mu g.g^{-1}$. Of the lower abundant isotope, the photon that originated from the decay of the first transition state was the only Coulomb-excited gamma-ray which offered a sensitivity of below the $mg.g^{-1}$ range. No gamma-rays from the reaction $^{71}Ga(p,n\gamma)^{71}Ge$ could be detected.

Both Coulomb-excition and reactions on the higher abundant isotope of mass 69, provided gamma-rays of good analytical potential, the best of which was the 176-keV ^{69}Ga $\gamma(2,1)$ gamma-ray, which, although situated on a high Compton continuum, showed increasing sensitivity with increasing bombarding energy.

Eγ keV	Assignment	Yield. quanta $sr^{-1}nC^{-1}$	Sensitivity $\mu g.g^{-1}mC^{-1}$	Eγ keV	Assignment	Yield. quanta $sr^{-1}nC^{-1}$	Sensitivity $\mu g.g^{-1}mC^{-1}$
87	^{69}Ga n(1,0)	230	2 300	812	^{69}Ga n(5,0)	280	2 100
113	^{71}Ga γ(8,6)	100	4 400	834	^{71}Ga γ(2,0)	280	2 000
143	^{71}Ga γ(2,1)	330	1 300	872	^{69}Ga p(3,0)	110	4 300
146	^{69}Ga n(2,1)			894	^{71}Ga γ(4,2)	72	6 300
176	^{69}Ga γ(2,1)	2 250	140	927	^{69}Ga n(9,2)	140	3 800
233	^{69}Ga n(2,0)	790	400	941	^{69}Ga γ(4,2)	140	3 300
247	^{69}Ga p(13,9)	110	3 100	965	^{71}Ga p(5,0)	44	10 600
287	^{69}Ga n(3,2)	970	450	995	^{69}Ga n(8,0)	23	22 500
307	^{69}Ga p(6,4)	100	3 400	1027	^{69}Ga p(4,0)	1 540	381
318	^{69}Ga p(1,0)	250	1 800	1040	^{69}Ga γ(1,0)	600	970
374	^{69}Ga n(3,0)	300	1 200	1099	^{69}Ga γ(11,3)	260	2 200
390	^{71}Ga p(1,0)	560	700	1106	^{69}Ga p(5,0)	120	1 400
398	^{69}Ga n(4,0)	540	750	1113	^{69}Ga γ(4,1)	84	1 800
500	^{69}Ga p(7,4)	950	490	1140	^{69}Ga γ(6,1)	190	1 750
512	^{71}Ga p(3,0)	180	2 300	1182	^{69}Ga n(13,2)	42	6 700
521	^{71}Ga p(4,1)	370	1 100	1208	^{69}Ga p(7,1)	16	17 900
532	^{69}Ga p(5,2)	91	4 400	1216	^{69}Ga γ(2,0)	39	7 300
574	^{69}Ga p(2,0)	400	1 230	1230	^{71}Ga γ(5,2)	15	17 800
596	^{71}Ga p(6,3)	250	1 800	1307	^{69}Ga n(12,0)	140	2 200
620	^{71}Ga p(6,2)	120	4 200	1332	^{69}Ga γ(13,4)	78	36 700
668	^{69}Ga γ(3,1)	100	5 200	1336	^{69}Ga p(6,0)		
691	^{71}Ga γ(1,0)	230	2 500	1339	^{69}Ga γ(9,3)		
708	^{69}Ga p(4,1)	420	1 400	1412	^{69}Ga γ(8,1)	63	4 300
744	^{69}Ga γ(8,3)	68	5 500	1464	^{71}Ga γ(3,0)	33	7 300
786	^{71}Ga γ(8,4)	70	7 700	1527	^{69}Ga p(7,0)	64	4 100
788	^{69}Ga p(5,1)			1708	^{69}Ga γ(3,0)	82	3 700

E_p (keV) / E_γ (keV)	Yield (quanta $sr^{-1}nC^{-1}$)					
	3 500	4 000	4 500	5 000	5 500	6 000
176	700	1 800	2 250	7 170	11 100	17 200
233	130	710	790	2 300	4 300	8 700
287	57	570	970	2 990	5 470	10 900
390	145	310	560	730	1 025	2 140
398	200	370	540	710	780	1 160
500	43	320	950	1 140	1 370	1 705
1027	405	635	1 540	1 715	2 280	4 340
1040	140	360	600	775	990	1 140

E_γ (keV)	Co-efficients of polynomials fitted to Sensitivity Functions				$S_{min.}/\mu g.g^{-1}$	E_p at $S_{min.}$ (keV)
	a_0	a_1	a_2	a_3		
176	+ 1 946	- 825	+ 116	- 5.1	60	6 000
233	- 6 062	+ 4 121	- 846	+ 55	160	6 000
287	+19 958	-11 145	+2 109	-133	210	6 000
390	+10 706	- 5 927	+1 170	- 77	550	6 000
398	+ 6 213	- 2 611	+ 408	- 21	640	6 000
500	+19 098	-10 214	+1 858	-112	450	6 000
1027	+22 465	-12 044	+2 184	-132	270	6 000
1040	+10 434	- 5 763	+1 183	- 82	650	6 000

Germanium : - A disc, cut from a pure germanium crystal was bombarded to obtain the gamma-ray spectra. Three of the five naturally-occurring isotopes of the element were Coulomb excited to yield gamma-rays. The radiation from the first three levels of ^{73}Ge were too low in energy to be detected by the gamma-ray spectrometer, and those photons which were observed were of low intensity. It appeared that the best sensitivity for the analysis of germanium was offered by a gamma-ray which originated from the $(p,n\gamma)$ reaction on ^{73}Ge, but its energy was 510 keV, and could not be resolved from the annihilation gamma-rays of 511 keV. Therefore this gamma-ray served little analytical purpose.

The first excited state of ^{74}Ge had the correct spin and

parity values for an E2 transition but no gamma-ray of 596-keV was observed from this level. In fact, only two photopeaks from this isotope, which had the highest natural abundance, were present in the spectrum and both of these were of low intensity.

Eγ keV	Assignment	Yield. quanta $sr^{-1}nC^{-1}$	Sensitivity $\mu g.g^{-1}mC^{-1}$	Eγ keV	Assignment	Yield. quanta $sr^{-1}nC^{-1}$	Sensitivity $\mu g.g^{-1}mC^{-1}$
46	^{76}Ge n(1,0)	290	5 500	354	^{73}Ge p(4,0)	3	65 000
87	^{76}Ge n(2,0)	23	21 800	442	^{73}Ge n(5,1)	15	22 300
109	^{76}Ge p(6,5)	0.3	968 000	510	^{73}Ge n(5,0)	1 530	230
121	^{76}Ge n(3,0)	0.3	880 000	546	^{76}Ge p(2,1)	1	214 000
166	^{76}Ge n(4,0)	8	40 000	563	^{76}Ge p(1,0)	0.7	258 000
202	^{74}Ge n(3,0)	0.5	651 000	578	^{73}Ge n(7,0)	15	21 000
236	^{76}Ge n(8,3)	41	4 000	609	^{74}Ge p(2,1)	30	11 400
254	^{73}Ge n(3,0)	34	12 000	770	^{73}Ge n(10,0)	6	57 000
295	^{73}Ge p(5,3)	28	9 300	847	^{76}Ge p(3,1)	160	2 300
302	^{76}Ge p(3,2)	11	25 000	911	^{76}Ge p(6,2)	18	17 000
351	^{73}Ge p(5,1)	14	20 000				

Most of the observed gamma-rays were produced from inelastic scattering and the (p,nγ) reaction on ^{76}Ge. Of these, the reaction $^{76}Ge(p,n\gamma)^{76}As$ produced a gamma-ray from which a sensitivity of 3100 $\mu g.g^{-1}$ was calculated. The 847 keV gamma-ray, also produced from the latter reaction, provided a sensitivity of below 2000 $\mu g.g^{-1}$ but even this lower value was not attainable in practice because of the presence of the intense 844-keV gamma-ray from aluminium, the material used for the construction of the scattering chamber.

E_γ (keV) \ E_p (keV)	Yield (quanta $sr^{-1}nC^{-1}$)					
	3 500	4 000	4 500	5 000	5 500	6 000
46	18	78	290	690	870	1 010
236	6.9	27	41	85	170	490
295	7.3	21	34	110	210	360
510	120	1 130	1 530	1 930	2 550	2 700
2300	21	54	160	195	210	390

E_γ (keV)	Co-efficients of polynomials fitted to Sensitivity Functions				$S_{min.}/\mu g.g^{-1}$	E_p at $S_{min.}$ (keV)
	a_0	a_1	a_2	a_3		
46	+437 776	-247 184	+46 984	-2 976	3 100	6 000
236	+374 504	-211 624	+40 021	-2 507	3 800	4 900
295	- 66 720	+ 84 576	-23 104	+1 856	9 300	5 000
510	+ 614	- 131	10.6	0	210	6 000
2300	+250 368	-141 868	+26 916	-1 695	2 000	6 000

Arsenic : - Although the element has only one naturally-

E_γ keV	Assignment	Yield. quanta $sr^{-1}nC^{-1}$	Sensitivity $\mu g.g^{-1}mC^{-1}$
113	^{75}As n(1,0)	3 200	270
133	^{75}As n(2,0)	148	4 100
136	^{75}As p(5,2)		
141	^{75}As n(5,3)	1 380	570
189	^{75}As p(6,3)	32	14 600
199	^{75}As p(1,0)	190	3 300
203	^{75}As p(5,1)	48	12 100
204	^{75}As p(6,2)		
229	^{75}As n(13,7)	50	11 300
236	^{75}As n(9,5)	110	5 500
265	^{75}As p(2,0)	71	7 200
280	^{75}As p(3,0)	330	1 400
287	^{75}As n(3,0)	4 900	100
293	^{75}As n(4,0)	470	1 200
304	^{75}As p(4,0)	8	58 000
314	^{75}As p(13,7)	315	2 000
316	^{75}As n(5,1)		
338	^{75}As p(9,3)	180	3 600
374	^{75}As p(7,1)	460	1 300
397	^{75}As p(12,6)	13	39 400
401	^{75}As p(5,0)	25	18 300
418	^{75}As p(13,6)	9	40 500
418	^{75}As p(9,1)		
426	^{75}As p(14,9)	830	820
428	^{75}As n(5,0)		
460	^{75}As p(11,5)	130	4 500
466	^{75}As p(12,5)	45	11 300
469	^{75}As p(6,0)		
471	^{75}As p(14,7)		
486	^{75}As p(13,5)	120	5 000
557	^{75}As p(11,4)		
557	^{75}As p(10,2)	75	8 100
558	^{75}As γ(1,0)		
561	^{75}As p(12,4)		
563	^{75}As γ(2,1)		
572	^{75}As p(7,0)	285	2 400
575	^{75}As p(14,6)		
581	^{75}As p(11,3)	28	19 000
582	^{75}As p(13,4)		
585	^{75}As p(12,3)		
586	^{75}As p(6,0)		
596	^{75}As p(11,2)	120	4 980
603	^{75}As p(12,2)	670	1 100
607	^{75}As p(13,3)		
615	^{75}As n(7,0)	85	6 600
618	^{75}As p(9,0)		
621	^{75}As p(13,2)	230	2 900
623	^{75}As p(10,1)		
643	^{75}As p(14,5)	88	6 700
657	^{75}As γ(3,1)	130	4 500
662	^{75}As p(11,1)	32	15 600
666	^{75}As p(12,1)		
688	^{75}As p(13,1)	250	2 800
691	^{75}As α(1,0)	125	5 500
740	^{75}As p(14,4)	105	6 400
764	^{75}As p(14,3)	75	8 100
772	^{75}As γ(1,0)	70	8 500
778	^{75}As p(14,2)	12	43 700
822	^{75}As p(10,0)	125	5 100
845	^{75}As p(14,1)	500	1 400
856	^{75}As p(11,0)	130	4 800
863	^{75}As p(12,0)	105	5 800
886	^{75}As p(13,0)	210	3 100
1044	^{75}As p(14,0)	74	9 100

Eγ keV	Assignment	Yield. quanta $sr^{-1}nC^{-1}$	Sensitivity $\mu g.g^{-1}mC^{-1}$
133	^{74}Se γ(1,0)	81	9 300
148	^{74}Se α(2,0)	12	51 400
149	^{77}Se n(4,0)		
149	^{78}Se n(4,1)		
158	^{77}Se α(1,0)	15	39 200
162	^{77}Se p(1,0)	67	9 700
170	^{76}Se α(4,2)	63	10 000
195	^{80}Se α(1,0)	68	8 400
197	^{80}Se n(9,5)		
207	^{77}Se α(6,0)	830	1 000
212	^{80}Se n(10,5)	150	4 600
216	^{80}Se α(2,0)	1 030	820
219	^{80}Se n(3,1)	25	18 700
219	^{74}Se p(2,1)		
234	^{80}Se n(4,1)	22	17 300
235	^{76}Se α(5,3)		
244	^{80}Se n(5,1)	225	3 700
247	^{82}Se n(3,1)		
261	^{80}Se γ(2,1)	4.6	97 500
269	^{76}Se α(6,3)	150	4 800
271	^{80}Se n(4,2)	22	35 500
276	^{80}Se γ(1,0)	24	25 200
286	^{76}Se α(8,4)	36	20 200
290	^{80}Se γ(4,1)		
293	^{82}Se n(8,0)	18	41 100
294	^{80}Se n(8,2)		
299	^{82}Se n(4,2)	5.4	84 800
308	^{82}Se γ(5,2)	12	48 200
309	^{76}Se α(5,2)		
315	^{80}Se n(6,0)	150	5 700
323	^{74}Se α(4,3)	3.8	101 200
327	^{76}Se α(5,1)	1.9	150 600
329	^{80}Se n(7,1)		
331	^{82}Se n(4,1)		
336	^{78}Se n(12,1)	17	27 400
343	^{80}Se n(8,1)	24	23 600
344	^{76}Se α(6,2)		
347	^{82}Se n(5,2)	4.3	95 700
351	^{82}Se γ(7,2)		
357	^{82}Se γ(1,0)	1.9	162 800
359	^{74}Se α(3,1)		
361	^{76}Se α(6,1)		
366	^{80}Se n(7,0)	160	5 200
377	^{82}Se n(4,0)	42	13 900
391	^{77}Se n(13,0)	3.2	112 400

Eγ keV	Assignment	Yield. quanta $sr^{-1}nC^{-1}$	Sensitivity $\mu g.g^{-1}mC^{-1}$
393	^{76}Se α(5,0)	3.4	111 200
398	^{82}Se n(6,2)		
407	^{80}Se n(16,6)	5.2	87 300
425	^{82}Se n(5,0)	21	41 300
425	^{73}Se α(7,2)		
428	^{76}Se α(6,0)	9.8	52 300
430	^{82}Se n(6,1)		
432	^{80}Se n(9,1)		
456	^{80}Se n(10,1)	15	32 300
467	^{80}Se n(9,0)	100	9 900
470	^{82}Se n(7,2)		
484	^{74}Se α(8,3)	9.2	85 600
492	^{80}Se γ(6,1)	3.9	112 500
493	^{80}Se n(10,0)		
521	^{77}Se p(7,0)	6.4	92 600
525			
538	^{80}Se γ(3,0)	82	8 100
543	^{82}Se α(2,1)	68	6 200
552	^{80}Se γ(8,1)	84	8 300
559	^{76}Se p(1,0)	210	5 000
561	^{80}Se γ(9,1)		
563	^{76}Se p(2,1)		
614	^{78}Se p(1,0)	1 240	930
635	^{74}Se p(1,0)	24	21 400
638	^{82}Se n(8,0)		
646	^{82}Se n(9,1)	4.2	114 300
650	^{80}Se γ(5,0)	4.8	105 900
655	^{82}Se p(1,0)	19.2	32 800
666	^{80}Se p(1,0)	310	3 300
681	^{74}Se α(4,1)	44	20 800
684	^{82}Se γ(2,0)		
693	^{78}Se p(2,1)	66	13 700
696	^{82}Se γ(8,1)		
701	^{82}Se n(16,3)	59	7 300
728	^{74}Se p(4,1)	47	10 400
767	^{80}Se γ(6,0)	28	29 700
783	^{80}Se n(2,1)	4.6	96 900
813	^{80}Se p(3,1)	50	18 400
828	^{80}Se γ(7,0)	12	56 500
830	^{74}Se α(7,4)		
830	^{82}Se p(11,0)		
831	^{74}Se α(7,4)		
886	^{78}Se p(3,1)	40	17 200
978	^{74}Se α(7,0)	54	12 300
988	^{82}Se γ(5,0)	14	49 300
991	^{74}Se α(8,0)		

E_γ (keV) \ E_p (keV)	Yield (quanta $sr^{-1}nC^{-1}$)					
	3 500	4 000	4 500	5 000	5 500	6 000
216, 219	53	275	1 030	1 940	2 160	2 670
244, 247	125	220	225	370	620	890
559, 561, 563	61	125	210	370	420	650
614	210	680	1 240	1 310	1 520	1 780
666	125	250	310	450	610	980

E_γ (keV)	Co-efficients of polynomials fitted to Sensitivity Functions				$S_{min.}/\mu g.g^{-1}$	E_p at $S_{min.}$ (keV)
	a_0	a_1	a_2	a_3		
216, 219	+ 44 288	-24 713	+ 4 669	- 294	690	6 000
244, 247	+175 680	-98 552	+18 595	-1 166	1 910	6 000
559, 561, 563	+ 23 616	- 7 912	+ 1 130	- 63.4	3 170	6 000
614	+ 11 049	- 3 603	+ 317	0	820	5 680
666	+ 88 328	-45 852	+ 8 195	- 489	2 610	6 000

Bromine : - Analysis of the spectrum of potassium bromide showed that bromine gamma-rays were emitted as a result of inelastic scattering and the (p,nγ) reactions on both the ^{79}Br and ^{81}Br isotopes. In addition, proton capture on ^{79}Br provided a photon of low intensity.

Eγ keV	Assignment	Yield. quanta $sr^{-1}nC^{-1}$	Sensitivity $\mu g.g^{-1}mC^{-1}$	Eγ keV	Assignment	Yield. quanta $sr^{-1}nC^{-1}$	Sensitivity $\mu g.g^{-1}mC^{-1}$
111	^{79}Br n(6,4)	115	4 700	445	^{81}Br n(8,3)	490	1 600
130	^{79}Br n(1,0)	420	2 200	446	^{81}Br n(5,1)		
144	^{79}Br n(4,2)	740	1 300	457	^{81}Br n(2,0)	240	2 100
147	^{79}Br n(2,0)			477	^{79}Br n(9,3)	63	10 700
161	^{79}Br n(4,1)	120	4 000	511	^{81}Br n(6,1)	900	720
183	^{79}Br n(3,0)	1 020	760	512	^{79}Br n(12,3)		
190	^{81}Br n(1,0)	1 040	760	513	^{79}Br n(9,2)		
217	^{79}Br p(2,0)	210	2 200	523	^{79}Br p(6,0)	92	7 800
219	^{79}Br n(6,3)			537	^{81}Br n(8,2)	98	7 700
262	^{79}Br p(3,0)	44	10 600	538	^{81}Br p(3,0)		
276	^{81}Br p(1,0)	145	3 300	549	^{81}Br n(3,0)	370	2 100
276	^{79}Br n(9,5)			569	^{81}Br n(9,2)	83	8 500
303	^{79}Br n(7,2)	130	5 800	605	^{79}Br p(7,0)	420	2 200
306	^{79}Br p(4,0)	15	61 800	608	^{81}Br n(4,0)		
320	^{79}Br n(7,1)	50	12 500	616	^{79}Br γ(1,0)	120	6 100
351	^{79}Br n(8,3)	150	4 400	695	^{79}Br n(12,0)	140	7 900
384	^{79}Br n(5,0)	490	1 700	729	^{81}Br n(7,1)	430	2 100
385	^{79}Br n(10,4)			835	^{81}Br n(9,1)	91	8 400
402	^{79}Br n(6,0)	180	3 900	837	^{81}Br p(7,0)		
				1107	^{81}Br n(10,0)	73	12 000

In the case of ^{81}Br the second excited state [Ro 72] of 536.1 keV and spin and parity of $9/2^+$ has a half-life of 36 μs and decays to the first state of 276.4 keV by an M2 transition, with the emission of a 260-keV gamma-ray. The first excited state [Co 74] of ^{79}Br at 207.2 keV has a spin and parity of $9/2^+$ and decays with a half-life of 4.88s with an E3 transition to the ground state. Both these levels were not excited by inelastic scattering.

From an analytical point of view, the gamma-rays resulting from the (p,nγ) reaction on both nuclides were more significant than the gamma-rays from Coulomb excitation. Sensitivities of about 360 $\mu g.g^{-1}$ were achieved using the 190-keV ^{81}Br n(1,0) gamma-ray. The good sensitivity values for those gamma-rays which were considered useful for analysis of bromine were in some cases due to the coupling of gamma-rays, such as the 145-keV

E_p (keV) / E_γ (keV)	Yield (quanta $sr^{-1}nC^{-1}$)					
	3 500	4 000	4 500	5 000	5 500	6 000
144 147	85	130	740		1 670	3 040
183	100	430	1 020		2 450	4 150
190	95	560	1 040		2 890	3 830
384 385	35	215	490		980	3 700
445 446	50	410	900		1 820	4 170

E_γ (keV)	Co-efficients of polynomials fitted to Sensitivity Functions				$S_{min.}/\mu g.g^{-1}$	E_p at $S_{min.}$ (keV)
	a_0	a_1	a_2	a_3		
144 147	- 1 154	+ 2 274	- 558	0	940	6 000
183	+ 3 988	- 1 198	120	- 3	470	6 000
190	- 4 118	+ 3 967	- 955	+ 70	360	6 000
384 385	+27 058	-13 472	+2 395	-145	1 100	6 000
445 446	48 104	-27 441	+5 285	-339	390	5 900

pair ^{79}Br n(4,2) and n(2,0); the 384-keV pair ^{79}Br n(5,0) and n(10,4) and the 445-keV ^{81}Br n(8,3) and n(5,1).

Rubidium : - Gamma-rays from the decay of the first level of both stable isotopes of rubidium were observed when a target of rubidium sulphate was bombarded, but these were of low intensity and little analytical importance.

Two different reactions on ^{87}Rb provided gamma-rays of 484 keV and 485 keV. Since these two photons were close to each other in energy, and their respective photopeaks were integrated together and gave a combined sensitivity of about 400 $\mu g.g^{-1}$

Eγ keV	Assignment	Yield. quanta $sr^{-1}nC^{-1}$	Sensitivity $\mu g.g^{-1}mC^{-1}$	Eγ keV	Assignment	Yield. quanta $sr^{-1}nC^{-1}$	Sensitivity $\mu g.g^{-1}mC^{-1}$
151	^{85}Rb p(1,0)	71	2 600	504	^{85}Rb n(3,2)	440	820
232	^{85}Rb n(1,0)	1 300	240	537	^{85}Rb n(5,1)	320	1 200
239	^{85}Rb n(2,0)	28	10 000	550	^{85}Rb n(9,5)	360	1 100
355	^{87}Rb n(3,2)	51	7 200	769	^{85}Rb n(5,0)	270	1 510
355	^{85}Rb p(3,2)			865	^{87}Rb n(4,1)	130	3 800
380	^{85}Rb (6,3)	43	7 900	914	^{85}Rb n(8,0)	190	2 200
381	^{87}Rb n(4,2)			1031	^{85}Rb n(9,1)	75	3 600
388	^{87}Rb n(1,0)	39	8 000	1077	^{85}Rb γ(1,0)	66	7 200
403	^{87}Rb p(1,0)	12	24 800	1229	^{87}Rb n(3,0)	150	3 600
439	^{85}Rb γ(8,4)	47	9 400	1238	^{87}Rb n(7,2)	17	23 900
484	^{87}Rb γ(4,2)	340	980	1296	^{87}Rb n(8,2)	52	10 000
485	^{87}Rb n(2,1)			1771	^{87}Rb n(5,0)	72	10 600

The most intense gamma-rays originated from the (p,nγ) reaction on the more abundant isotope, ^{85}Rb (72.17 atom %) when using the 232 keV-^{85}Rb n(1,0) gamma-ray, an analytical sensitivity of 170$\mu g.g^{-1}$ could be expected.

E_γ (keV) \ E_p (keV)	Yield (quanta $sr^{-1}nC^{-1}$)					
	3 500	4 000	4 500	5 000	5 500	6 000
232	240	560	1 300	3 160	4 960	6 010
484 / 485	57	120	340	710	1 300	1 620
504	55	160	440	990	1 520	1 990
537	56	140	320	610	800	1 360
550	51	83	360	790	1 630	3 290

E_γ (keV)	Co-efficients of polynomials fitted to Sensitivity Functions				$S_{min.}/\mu g.g^{-1}$	E_p at $S_{min.}$ (keV)
	a_0	a_1	a_2	a_3		
232	+ 6 551	- 3 356	+ 585	- 34	170	5 320
484 / 485	+13 614	- 5 081	+ 586	- 17	640	6 000
504	+44 798	-24 459	+4 497	-274	600	5 100
537	+20 556	-10 205	+1 750	- 98	960	5 000
550	+12 858	- 4 352	+ 386	0	630	5 500

Strontium : - Bombardment of a strontium chloride target produced strontium gamma-rays from Coulomb excitation the (p,nγ) reaction and by proton-capture. Strontium has four stable isotopes and the most dominant peaks in the spectrum were from gamma-rays resulting from the decay of levels of ^{87}Sr. These offered sensitivities of about 3000 $\mu g.g^{-1}$. The most useful gamma-ray, however, was one due to the (p,nγ)

Eγ keV	Assignment	Yield. quanta $sr^{-1}nC^{-1}$	Sensitivity $\mu g.g^{-1}mC^{-1}$	Eγ keV	Assignment	Yield. quanta $sr^{-1}nC^{-1}$	Sensitivity $\mu g.g^{-1}mC^{-1}$
232	^{87}Sr γ(1,0)	300	530	843	^{87}Sr γ(7,0)	42	5 650
232	^{88}Sr n(1,0)			843	^{88}Sr n(7,0)		
336	^{88}Sr p(5,3)	7	64 300	873	^{87}Sr p(2,0)	14	24 600
388	^{87}Sr p(1,0)	15	22 600	1229	^{87}Sr p(3,0)	16	22 240
602	^{84}Sr p(4,2)	13	22 800	1740	^{87}Sr p(5,0)	13	20 960
792	^{86}Sr γ(2,0)	18	20 700	1771	^{87}Sr p(7,0)	14	17 970
792	^{87}Sr n(2,0)						
793	^{84}Sr n(1,0)						
793	^{84}Sr p(1,0)						

reaction on ^{88}Sr, the most abundant isotope. Proton-capture on ^{87}Sr provided exactly the same gamma-ray which contributed to the peak area of the photopeak, rendering it sensitive to about 400 $\mu g.g^{-1}$ at a bombarding energy of 6000 keV.

The apparently intense spectrum peaks corresponding to gamma-rays of 1229, 1740 and 1771 keV are not useful for analysis because, by co-incidence intense gamma-rays from chlorine are formed with similar energies.

E_p (keV) / E_γ (keV)	Yield (quanta $sr^{-1}nC^{-1}$)					
	3 500	4 000	4 500	5 000	5 500	6 000
232	50	77	300	480	520	610
843	5.9	9	42	57	88	110
1229	3.6	9.8	16	21	31	42
1740	5.3	10	13	17	19	22
1771	9.5	11	14	17	22	40

E_γ (keV)	Co-efficients of polynomials fitted to Sensitivity Functions				$S_{min.}/\mu g.g^{-1}$	E_p at $S_{min.}$ (keV)
	a_0	a_1	a_2	a_3		
232	+ 21 348	- 10 509	+ 1 745	- 96	380	6 000
843	+443 904	-240 664	+ 43 722	-2 628	5 160	5 070
1229	+ 48 552	- 25 308	+ 4 572	- 273	20 180	5 100
1740	+990 000	-692 464	+121 324	-7 066	21 920	6 000
1771	+133 776	- 49 880	+ 5 522	- 140	22 910	5 800

Yttrium : - A target of yttrium oxide was used to obtain the gamma-ray spectra. Coulomb excitation of the first two levels of ^{89}Y resulted in relatively weak gamma-rays. The most important gamma-rays originated from the proton-capture reaction on the isotope and of the gamma-rays produced the 420-, 564-and 2179 keV photons were analytically the most significant. However, even under the most appropiate bombarding energies, the best sensitivities that could be achieved was in the $mg.g^{-1}$ region.

Eγ keV	Assignment	Yield. quanta $sr^{-1}nC^{-1}$	Sensitivity $\mu g.g^{-1}mC^{-1}$	Eγ keV	Assignment	Yield. quanta $sr^{-1}nC^{-1}$	Sensitivity $\mu g.g^{-1}mC^{-1}$
357	^{89}Y n(3,2)	5.3	32 400	891	^{89}Y γ(6,2)	12	15 800
420	^{89}Y γ(4,3)	46	5 300	908	^{89}Y p(1,0)	20	10 900
506	^{89}Y n(2,1)	280	940	1122	^{89}Y γ(7,2)	22	14 700
564	^{89}Y γ(5,2)	73	2 600	1507	^{89}Y p(2,0)	58	2 200
588	^{89}Y n(1,0)	260	1 200	1511	^{89}Y n(4,0)		
770	^{89}Y n(8,2)	15	11 800	1759	^{89}Y γ(1,0)	11	29 700
864	^{89}Y n(3,1)	13	19 400	2179	^{89}Y γ(2,0)	110	1 700

E_p(keV) / E (keV)	Yield (quanta $sr^{-1}nC^{-1}$)					
	3 500	4 000	4 500	5 000	5 500	6 000
506	70	110	280	430	670	810
564	29	38	73	110	140	190
588	43	100	260	3 740	6 170	8 710
1507 } 1511 }	3	5	58	360	730	990
2179	37	96	110	160	220	410

E_γ (keV)	Co-efficients of polynomials fitted to Sensitivity Functions				$S_{min.}/\mu g.g^{-1}$	E_p at $S_{min.}$ (keV)
	a_0	a_1	a_2	a_3		
506	+109 480	- 5 696	+ 1 056	- 63	910	4 620
564	+128 220	- 70 424	+13 064	- 803	2 310	5 020
588	+127 348	- 69 174	+12 520	- 747	1 190	5 000
1507 } 1511 }	+229 116	-126 968	+23 566	-1 456	1 080	6 000
2179	+ 7 694	- 357	+ 732	- 52	1 430	6 000

Zirconium : - This element has five naturally-occurring stable isotopes ranging in abundance from 2.8 to 51.4 atom %.

Gamma-rays were observed from all these isotopes.

The first excited levels of all the zirconium isotopes yielded gamma-rays of moderate intensities.

Eγ keV	Assignment	Yield. quanta $sr^{-1}nC^{-1}$	Sensitivity $\mu g.g^{-1}mC^{-1}$	Eγ keV	Assignment	Yield. quanta $sr^{-1}nC^{-1}$	Sensitivity $\mu g.g^{-1}mC^{-1}$
92	^{92}Zr n(2,1)	200	2 000	560	^{92}Zr p(3,1)	14	21 900
105	^{91}Zr n(1,0)	350	1 100	616	^{96}Zr p(4,1)	10	33 800
151	^{92}Zr n(3,1)	120	2 600	642	^{94}Zr n(10,0)	92	4 400
163	^{90}Zr n(3,1)	160	1 700	751	^{94}Zr p(4,1)	85	5 100
164	^{96}Zr p(2,1)			804	^{92}Zr n(9,3)	8.6	44 800
165	^{92}Zr n(5,2)			918	^{94}Zr p(1,0)	18.7	17 300
180	^{96}Zr n(2,0)	32	7 500	934	^{92}Zr p(1,0)	60	6 500
195	^{92}Zr n(6,3)	29	9 100	979	^{93}Zr n(7,0)	6.9	53 900
233	^{96}Zr n(3,0)	3.5	68 300	1083	^{91}Zr n(2,1)	205	1 900
234	^{94}Zr γ(1,0)			1129	^{90}Zr p(6,3)	23	18 800
253	^{94}Zr n(6,2)	55	5 500	1205	^{91}Zr p(1,0)	175	2 300
293	^{94}Zr n(7,1)	190	1 500	1385	^{92}Zr p(2,0)	28	11 900
305	^{96}Zr p(4,3)	6.7	43 100	1466	^{91}Zr p(2,0)	24	15 400
311	^{96}Zr p(3,1)	105	2 800	1508	^{91}Zr n(5,1)	86	4 400
329	^{94}Zr n(10,4)	84	3 500	1594	^{96}Zr p(1,0)	66	4 900
344	^{94}Zr n(7,0)	15	17 600	1758	^{96}Zr p(2,0)	25	15 200
357	^{92}Zr n(4,0)	22	12 700	1761	^{90}Zr p(1,0)		
452	^{96}Zr p(4,2)	35	8 200	1778	^{92}Zr p(3,0)	17	19 400
535	^{96}Zr p(6,3)	105	3 100	1848	^{92}Zr p(4,0)	6.6	43 300

E_γ(keV) \ E_p(keV)	Yield (quanta $sr^{-1}nC^{-1}$)					
	3 500	4 000	4 500	5 000	5 500	6 000
92	35	110	200	310	450	570
105	75	190	350	460	590	780
163, 164, 165	40	83	160	210	275	340
293	85	160	190	310	460	525
1083	80	170	205	310	480	510

Most of the Coulomb-excited gamma-rays were from ^{96}Zr, the isotope with the lowest natural abundance, and thus were of low intensity.

Gamma-rays from the (p,nγ) reaction were generally more intense than from Coulomb excitation. The best sensitivities for the analysis of zirconium were attained at the maximum bombarding energies.

E_γ (keV)	Co-efficients of polynomials fitted to Sensitivity Functions				$S_{min.}/\mu g.g^{-1}$	E_p at $S_{min.}$ (keV)
	a_0	a_1	a_2	a_3		
92	+26 652	-13 716	+2 568	-164	1 370	6 000
105	+ 5 363	- 1 407	+ 104	0	670	6 000
163, 164, 165	+23 890	-12 400	+2 318	-146	1 290	6 000
293	+24 146	-12 852	+2 459	-160	970	6 000
1083	+ 9 826	- 2 618	+ 189	0	940	6 000

Niobium : - The target of niobium oxide, compressed into a pellet was irradiated with protons. Although the decay of the first excited state of ^{93}Nb was E2 in character, no gamma-ray from this level was observed. The gamma-rays of 1364, 1429 and 1530 keV provided the best potential sensitivities for analysis.

Eγ keV	Assignment	Yield. quanta $sr^{-1}nC^{-1}$	Sensitivity $\mu g.g^{-1}mC^{-1}$	Eγ keV	Assignment	Yield. quanta $sr^{-1}nC^{-1}$	Sensitivity $\mu g.g^{-1}mC^{-1}$
93	^{93}Nb γ(6,5)	1.6	95 800	726	^{93}Nb γ(5,2)	22	28 800
110	^{93}Nb n(3,2)	6.6	56 300	744	^{93}Nb p(3,0)	11	12 600
123	^{93}Nb γ(7,5)	30	14 200	780	^{93}Nb p(4,1)	230	2 600
203	^{93}Nb γ(4,3)	25	15 100	809	^{93}Nb p(4,0)	14	31 400
204	^{93}Nb p(7,4)			850	^{93}Nb γ(7,2)	20	21 900
235	^{93}Nb p(7,3)	27	16 300	871	^{93}Nb γ(1,0)	90	7 800
268	^{93}Nb γ(9,5)	64	11 500	944	^{93}Nb n(1,0)	40	16 900
291	^{93}Nb γ(3,2)	8.3	39 600	950	^{93}Nb p(6,0)	110	4 900
318	^{93}Nb p(8,3)	7.4	42 300	979	^{93}Nb γ(3,1)	46	14 200
326	^{93}Nb γ(6,4)	8.8	38 100	993	^{93}Nb γ(4,1)	14	32 600
339	^{93}Nb p(5,1)	12	32 800	1034	^{93}Nb p(8,1)	85	6 800
436	^{93}Nb γ(5,3)	12.3	27 300	1083	^{93}Nb p(8,0)	120	4 400
494	^{93}Nb γ(4,2)	8.2	43 300	1364	^{93}Nb n(2,0)	1 270	610
686	^{93}Nb p(2,0)	110	6 200	1429	^{93}Nb γ(5,1)	1 420	420
703, 704	^{93}Nb γ(2,1), ^{93}Nb γ(9,3)	106	6 700	1530	^{93}Nb γ(6,1)	1 360	530

E_γ (keV) \ E_p (keV)	Yield (quanta $sr^{-1}nC^{-1}$)					
	3 500	4 000	4 500	5 000	5 500	6 000
780	100	145	230	275	320	405
1083	40	85	120	180	210	305
1364	220	805	1 270	1 590	2 230	2 790
1429	215	740	1 420	1 820	2 400	2 960
1530	205	840	1 360	1 730	2 190	2 610

E_γ (keV)	Co-efficients of polynomials fitted to Sensitivity Functions				$S_{min.}/\mu g.g^{-1}$	E_p at $S_{min.}$ (keV)
	a_0	a_1	a_2	a_3		
780	+1 780	+3 394	-1 110	+ 87	1 010	6 000
1083	+3 056	+4 680	-1 487	+114	2 170	6 000
1364	+6 011	-2 516	+ 374	- 18	470	5 800
1429	+ 837	- 88	+ 3.2	- 0.41	320	6 000
1530	+3 500	-1 509	+ 253	- 14	480	6 000

Molybdenum : - Because natural molybdenum is composed of

E_γ keV	Assignment	Yield. quanta $sr^{-1}nC^{-1}$	Sensitivity $\mu g.g^{-1}mC^{-1}$	E_γ keV	Assignment	Yield. quanta $sr^{-1}nC^{-1}$	Sensitivity $\mu g.g^{-1}mC^{-1}$
139	^{98}Mo n(5,0)	13	20 600	567	^{95}Mo p(2,1)	55	8 200
140	^{98}Mo γ(1,0)			585	^{95}Mo γ(3,1)	25	8 300
181	^{98}Mo γ(3,0)	180	2 400	592	^{95}Mo p(3,1)	11	16 300
203	^{95}Mo n(4,3)	80	3 100	630	^{95}Mo n(3,0)	175	2 100
204	^{95}Mo p(1,0)			630	^{94}Mo γ(3,0)		
216	^{96}Mo γ(2,0)	50	6 000	669	^{97}Mo n(10,6)	40	9 600
216	^{97}Mo n(2,0)			703	^{94}Mo p(2,1)	60	6 200
216	^{96}Mo γ(2,0)			723	^{98}Mo p(3,1)	30	12 100
228	^{96}Mo γ(3,1)	6	40 000	767	^{95}Mo p(2,0)	80	4 200
242	^{92}Mo p(3,2)	22	34 800	773	^{92}Mo p(2,1)		
294	^{95}Mo n(3,2)	36	5 800	778	^{96}Mo p(1,0)	100	4 500
298	^{94}Mo γ(2,1)	22	16 300	786	^{95}Mo p(3,0)	6.7	49 700
324	^{96}Mo γ(3,0)	105	3 900	787	^{98}Mo p(1,0)		
324	^{97}Mo n(3,0)			843	^{96}Mo p(2,1)	26	11 600
336	^{95}Mo n(2,0)	135	2 500	871	^{94}Mo p(1,0)	7.7	22 200
336	^{94}Mo γ(2,0)			972	^{98}Mo p(4,1)	2.7	53 500
353	^{98}Mo n(9,0)	17	20 900	1230	^{98}Mo p(5,1)	4.6	38 300
480	^{92}Mo p(10,7)	70	5 900	1372	^{100}Mo p(5,1)	21	20 500
481	^{97}Mo p(1,0)			1583	^{92}Mo p(7,1)	12	28 100
537	^{100}Mo p(1,0)	15	22 400	1760	^{98}Mo p(4,0)	14	24 600

E_γ (keV) \ E_p (keV)	Yield (quanta $sr^{-1}nC^{-1}$)					
	3 500	4 000	4 500	5 000	5 500	6 000
181	74	120	180	285	460	790
324	40	75	105	130	320	720
336	52	80	135	235	550	620
630 } 631 }	31	60	175	340	800	1 010
778	38	49	100	125	240	360

seven stable isotopes, ranging in abundance from 9.1 to 24.4 atom %, it was not surprising that all the nuclides contributed to the gamma-ray spectrum. Of the Coulomb-excited gamma-rays that were produced, the decay of the first excited state of all the nuclides, except for ^{92}Mo, were observed. The only useful gamma-ray, due to the inelastic process was the 778-keV gamma-ray.

The ^{98}Mo $\gamma(3,0)$ gamma-ray of 181 keV offered reasonable sensitivity. The gamma-ray of 336 keV showed the best potential for determination of molybdenum.

E_γ (keV)	Co-efficients of polynomials fitted to Sensitivity Functions				$S_{min.}/\mu g.g^{-1}$	E_p at $S_{min.}$ (keV)
	a_0	a_1	a_2	a_3		
181	+26 994	-15 500	+3 163	-217	1 280	6 000
324	+50 288	-23 800	+4 126	-251	1 780	6 000
336	+92 240	-46 848	+8 074	-467	1 240	6 000
630 } 631 }	- 8 612	+ 8 562	-2 033	+147	1 280	6 000
778	+51 560	-28 084	+5 689	-395	2 730	6 000

Ruthenium : – Ruthenium sponge was compressed into a pellet and this was bombarded to examine the gamma-ray spectra of this element. Most of the Coulomb excited gamma-rays were from the decay of the lower levels and the only isotope that did not produce any detectable photons from the decay of the first excited state was ^{96}Ru.

Eγ keV	Assignment	Yield. quanta $sr^{-1}nC^{-1}$	Sensitivity $\mu g.g^{-1}mC^{-1}$
89	^{99}Ru p(1,0)	25	15 400
97	^{104}Ru n(2,0)	20	19 300
120	^{96}Ru n(6,4)	2.8	26 200
127	^{101}Ru p(1,0)	50	9 100
129	^{104}Ru n(3,0)		
130	^{104}Ru γ(1,0)		
151	^{99}Ru γ(3,0)	2.0	45 700
181	^{104}Ru n(4,0)	74	5 200
182	^{101}Ru n(2,0)		
182	^{100}Ru γ(2,0)		
197	^{101}Ru n(3,1)	10	19 300
197	^{100}Ru γ(3,1)		
198	^{101}Ru p(4,1)		
217	^{96}Ru p(5,4)	45	7 700
264	^{99}Ru n(4,2)	31	11 200
264	^{98}Ru γ(4,2)		
297	^{102}Ru γ(3,0)	100	3 800
305	^{101}Ru n(3,0)	110	3 400
305	^{100}Ru γ(3,0)		
307	^{101}Ru p(2,0)		
355	^{101}Ru n(4,0)	500	800
355	^{100}Ru γ(4,0)		
358	^{104}Ru p(1,0)		
410	^{104}Ru γ(4,0)	23	13 200
422	^{101}Ru p(6,0)	12	23 100
427	^{99}Ru n(3,0)	48	7 000
427	^{98}Ru γ(3,0)		
441	^{96}Ru p(6,5)	89	5 400
475	^{102}Ru p(1,0)	330	910
496	^{101}Ru n(7,3)	31	14 200
496	^{100}Ru γ(7,3)		
540	^{100}Ru p(1,0)	140	3 300
545	^{101}Ru p(10,0)	12	10 300
546	^{101}Ru n(7,2)		
546	^{100}Ru γ(7,2)		
610	^{102}Ru γ(6,0)	9.6	13 300
616	^{101}Ru p(11,0)	62	5 900
617	^{99}Ru p(6,0)		
653	^{98}Ru p(1,0)	190	3 200
690	^{100}Ru p(3,1)	35	17 400
694	^{101}Ru n(7,1)		
694	^{100}Ru γ(7,1)		
719	^{99}Ru p(8,0)	42	13 100
720	^{101}Ru p(16,0)		
826	^{100}Ru p(4,1)	28	14 800
851	^{101}Ru n(7,0)	4.3	31 200
851	^{100}Ru γ(7,0)		
1004	Ru	5.7	35 600
1013	^{96}Ru n(4,1)	55	5 300
1645	Ru	8.6	32 100
1756	^{96}Ru p(6,1)	13	23 600

De-exciation of the first level of three of the ruthenium isotopes, those of mass number 98,102 and 104, resulted in

E_γ (keV) \ E_p (keV)	Yield (quanta $sr^{-1}nC^{-1}$)					
	3 500	4000	4 500	5 000	5 500	6 000
297	25	55	100	310	540	670
305 } 307	35	70	110	375	720	890
357 } 358	160	270	500	710	1 090	1 430
475	130	230	330	560	880	1 160
653	20	52	190	130	690	950

gamma-rays of such intensity that the element could be determined to below 1000 $\mu g.g^{-1}$.

The intensity of the spectrum peak corresponding to 355 keV was due to the summing of yields of the gamma-rays ^{101}Ru n(4,0) and ^{104}Ru p(1,0).

E_γ (keV)	Co-efficients of polynomials fitted to Sensitivity Functions				$S_{min.}/\mu g.g^{-1}$	E_p at $S_{min.}$ (keV)
	a_0	a_1	a_2	a_3		
297	+ 9 568	- 336	- 372	+ 34	1 760	6 000
305, 307	+43 980	-23 924	+4 801	-330	2 100	6 000
357, 358	+ 3 752	- 1 226	+ 139	- 3	700	5 330
475	+ 1 608	- 105	- 49	+ 8	910	4 770
653	+19 180	- 7 223	+1 109	- 63	2 050	6 000

Rhodium : – The rhodium gamma-ray spectrum was dominated by two gamma-rays originating from de-excitation of the third and fourth levels of ^{103}Rh. While many other levels were also excited, the gamma-rays produced were of such low intensity that many of them were not observed over the background continuum of the spectrum and those which were observed were of little analytical value.

Although the observed spectrum showed that the 12th excited state of ^{103}Rh was excited by inelastic scattering of protons

Eγ keV	Assignment	Yield. quanta $sr^{-1}nC^{-1}$	Sensitivity $\mu g.g^{-1}mC^{-1}$	Eγ keV	Assignment	Yield. quanta $sr^{-1}nC^{-1}$	Sensitivity $\mu g.g^{-1}mC^{-1}$
119	^{103}Rh n(1,0)	620	950	385	^{103}Rh n(5,1)	71	5 400
148	^{103}Rh n(3,1)	150	3 100	504	^{103}Rh n(5,0)	30	16 500
244	^{103}Rh n(2,0)	100	3 800	532	^{103}Rh n(6,0)	66	9 700
267	^{103}Rh n(3,0)	83	5 200	608	^{103}Rh p(7,1)	65	10 600
295	^{103}Rh p(3,0)	590	710	626	^{103}Rh n(7,0)	52	14 000
357	^{103}Rh p(4,0)	690	700	880	^{103}Rh p(12,0)	4	142 000
380	^{103}Rh n(4,1)	95	4 100				

E_p(keV) / E_γ(keV)	Yield (quanta $sr^{-1}nC^{-1}$)					
	3 500	4 000	4 500	5 000	5 500	6 000
119	140	370	620	870	1 520	2 350
148	25	95	150	320	530	750
244	27	85	100	270	560	850
295	120	490	590	640	690	780
357	210	560	690	790	870	1 040

E_γ (keV)	Co-efficients of polynomials fitted to Sensitivity Functions				$S_{min.}/\mu g.g^{-1}$	E_p at $S_{min.}$ (keV)
	a_0	a_1	a_2	a_3		
119	+19 560	- 9 135	+1 462	- 78	520	6 000
148	- 3 856	+14 908	-4 750	+398	400	5 820
244	+ 8 808	+ 1 260	- 884	+ 78	1 400	6 000
295	+11 128	- 7 001	+1 466	- 97	360	3 900
357	+10 009	- 4 772	+ 587	0	310	4 000

only the 3rd, 4th and 7th excited states were populated by the same process. The excitation energy for the first excited state is 40 keV, but this energy gamma-ray emitted in its decay was not detected because the energy lay below the detection threshold. All the remaining states could not be reached by Coulomb excitation [Th 67].

No gamma-rays were attributable to the $(p,\alpha\gamma)$ reaction or proton-capture but most of the peaks in the spectrum were from gamma-rays from the $(p,n\gamma)$ reaction, of which those of 119 keV and 148 keV were analytically the most important, especially because there was a substantial increase in their yields with increasing bombarding energies.

Palladium : - Coulomb excitation and reaction gamma-rays were observed from all of the seven naturally-occurring stable isotopes of palladium. Decay gamma-rays from the first level

Eγ keV	Assignment	Yield. quanta $sr^{-1}nC^{-1}$	Sensitivity $\mu g.g^{-1}mC^{-1}$	Eγ keV	Assignment	Yield. quanta $sr^{-1}nC^{-1}$	Sensitivity $\mu g.g^{-1}mC^{-1}$
79	^{106}Pd n(1,0)	17	54 300	345	^{105}Pd p(4,0)	25	39 500
93	^{106}Pd γ(2,0)	74	14 100	346	^{105}Pd n(3,0)		
93	^{110}Pd γ(1,0)			378	^{110}Pd p(1,0)	1 290	1 100
113	^{109}Pd p(1,0)	105	8 300	423	^{105}Pd γ(4,0)	130	7 300
189	^{109}Pd p(2,0)	215	6 900	433	^{105}Pd p(5,0)	2 700	260
191	^{110}Pd n(2,0)			433	^{105}Pd n(5,0)		
193	^{108}Pd n(4,0)			434	^{108}Pd p(1,0)		
195	^{106}Pd γ(3,1)	17	65 100	442	^{105}Pd p(6,0)	470	2 100
198	^{110}Pd n(3,0)	275	4 400	498	^{108}Pd p(2,1)	93	11 100
206	^{106}Pd n(3,0)	140	8 600	512	^{106}Pd p(1,0)	2 025	630
235	^{110}Pd n(4,0)	150	8 100	550	^{106}Pd γ(8,4)	130	7 500
237	^{110}Pd n(5,0)			556	^{104}Pd p(1,0)	560	2 300
248	^{110}Pd n(6,0)	105	10 100	556	^{102}Pd p(1,0)		
267	^{110}Pd n(7,0)	85	12 200	768	^{104}Pd p(2,1)	25	46 300
281	^{105}Pd p(1,0)	180	7 100	786	^{104}Pd p(4,1)	85	14 600
321	^{104}Pd γ(3,1)	9.6	88 700	786	^{106}Pd γ(5,0)		
325	^{106}Pd γ(3,0)	130	9 900				

of all the nuclides were observed and ^{104}Pd and ^{102}Pd which by chance had equal excitation energies for their first excited states produced gamma-rays of 556 keV.

The 378-keV ^{110}Pd p(1,0) photon was reasonably intense and a determination limit of less than 1000 $\mu g.g^{-1}$ was achieved. The most sensitive gamma-ray was one of 433 keV. The photopeak of this gamma-ray was substantially increased by contribution of counts from three sources viz., the gamma-ray from the decay of the fifth level of ^{105}Pd; the gamma-ray formed by the (p,nγ) reaction on ^{105}Pd; and, the Coulomb excited gamma-ray from the decay of the high abundant ^{108}Pd isotope.

E_p (keV) / E_γ (Kev)	Yield (quanta $sr^{-1}nC^{-1}$)					
	3 500	4 000	4 500	5 000	5 500	6 000
198	8	46	275	320	490	760
378	240	440	1 290	1 490	1 860	2 340
433 } 434 }	310	750	2 700	3 300	4 120	6 420
442	46	100	470	630	780	1 190
556	75	150	560	880	1 190	1 640

E_γ (keV)	Co-efficients of polynomials fitted to Sensitivity Functions				$S_{min.}/\mu g.g^{-1}$	E_p at $S_{min.}$ (keV)
	a_0	a_1	a_2	a_3		
198	+585 408	-325 856	+60 564	-3 748	1 070	6 000
378	+ 11 718	- 5 258	+ 872	- 51	610	6 000
433 } 434 }	+ 14 853	- 8 157	+ 1 513	- 93	180	6 000
442	+ 13 806	- 4 143	+ 359	0	1 840	6 000
556	+ 19 724	- 10 816	+ 2 278	- 164	1 430	6 000

Silver : - The element produced a large number of gamma-rays within the first 1000 keV of the spectrum. Most of the photons were fairly weak with the exception of two prominent pairs between 300 and 450 keV.

Eγ keV	Assignment	Yield. quanta $sr^{-1}nC^{-1}$	Sensitivity $\mu g.g^{-1}mC^{-1}$	Eγ keV	Assignment	Yield. quanta $sr^{-1}nC^{-1}$	Sensitivity $\mu g.g^{-1}mC^{-1}$
93	^{107}Ag p(1,0)	17	14 500	505	^{107}Ag n(4,0)	31	9 300
98	^{107}Ag p(3,2)	1.7	93 300	526	^{107}Ag p(5,3)	1	122 000
144	^{109}Ag n(2,1)	1.9	84 300	614	^{109}Ag n(7,1)	27	10 200
203	^{109}Ag n(2,0)	87	2 600	623	^{109}Ag n(6,0)	14	20 800
205	^{107}Ag n(1,0)			625	^{107}Ag p(5,2)		
247	^{109}Ag n(7,4)			633	^{107}Ag γ(1,0)	8.4	32 200
259	^{109}Ag n(5,2)	7.4	24 700	702	^{109}Ag p(5,0)	43	7 300
285	^{109}Ag p(5,4)	16	12 800	722	^{109}Ag n(8,0)	16	18 500
288	^{109}Ag n(3,1)	29	5 900	724	^{107}Ag p(7,3)		
311	^{109}Ag p(3,0)			738	^{107}Ag p(8,3)	12.8	23 200
325	^{107}Ag p(2,0)	230	930	786	^{107}Ag p(4,0)	10	30 200
325	^{107}Ag n(2,0)	290	830	832	^{109}Ag n(10,1)	20	13 300
348	^{109}Ag n(3,0)			834	^{107}Ag p(8,2)		
362	^{107}Ag p(4,3)	43	4 300	872	^{107}Ag p(2,1)	9.9	90 000
366	^{107}Ag n(3,0)	140	1 300	891	^{109}Ag n(10,0)	14	17 900
367	^{109}Ag n(4,1)			909	^{109}Ag p(9,4)	20	25 300
391	^{109}Ag p(5,3)	1.3	90 500	927	^{109}Ag n(11,0)	11	22 800
415	^{109}Ag p(4,0)	260	730	974	^{107}Ag p(6,0)	8.0	31 300
423	^{107}Ag p(3,0)	280	805	997	^{109}Ag n(13,0)	7.3	29 300
426	^{109}Ag n(4,0)			1013	^{107}Ag p(9,3)	4.8	35 600
447	^{109}Ag p(6,4)	2.2	73 100				
462	^{107}Ag p(4,2)	14	12 600				
462	^{109}Ag n(5,0)						

The heavier of the two naturally-occurring isotopes of silver, that of mass number 107, gave gamma-rays of 325 and 423 keV with reasonable sensitivities. These resulted respectively from the transition from the second and third levels to the ground state.

E_p (keV) / E_γ (keV)	Yield (quanta $sr^{-1}nC^{-1}$)					
	3 500	4 000	4 500	5 000	5 500	6 000
311	110	160	230	320	440	580
325	93	170	290	320	455	560
415	105	180	260	390	550	670
423, 426	105	165	280	360	420	490
362, 366, 367	75	100	140	180	210	320

E_γ (keV)	Co-efficients of polynomials fitted to Sensitivity Functions				$S_{min.}/\mu g.g^{-1}$	E_p at $S_{min.}$ (keV)
	a_0	a_1	a_2	a_3		
311	+ 8 391	- 4 780	+ 987	- 66	840	4 000
325	+17 698	-10 249	+2 028	-129	830	4 500
415	+12 785	- 7 363	+1 464	- 94	700	4 000
423, 426	+21 838	-13 606	+2 853	-192	800	4 500
362, 366, 367	+ 6 442	- 1 612	+ 56	+ 10	1 090	5 600

The gamma-ray of importance was of 325 keV from the $(p,n\gamma)$ reaction on ^{107}Ag and was the same energy as another gamma-ray from Coulomb excitation of the same isotope.

The decay of the third and fourth levels to the ground state of ^{109}Ag resulted in gamma-rays which provided the best sensitivity

for analysis of silver. These gamma-rays have energies of 311 keV and 415 keV respectively. The first two levels of ^{109}Ag were not populated by Coulomb excitation because they had spin and parity values of $7/2^+$ and $9/2^+$ compared to $1/2^-$ of the ground state.

Sensitivity limits in general did not reach below the $mg.g^{-1}$ level even with increasing bombarding beams.

Cadmium : - All eight stable isotopes of cadmium were

Eγ keV	Assignment	Yield. quanta $sr^{-1}nC^{-1}$	Sensitivity $\mu g.g^{-1}mC^{-1}$
96	^{111}Cd p(2,1)	8.3	7 000
102	^{106}Cd p(4,2)	8.9	5 300
145	^{106}Cd p(7,5)	5.1	11 900
246	^{111}Cd p(1,0)	8.4	6 900
255	^{112}Cd γ(2,1)	18	3 100
255	^{113}Cd n(2,1)		
264	^{113}Cd p(1,0)	23	2 800
278	^{114}Cd n(2,0)	12	4 300
278	^{113}Cd γ(2,0)		
289	^{116}Cd n(9,1)	45	1 300
299	^{113}Cd p(2,0)	18	3 100
311	^{114}Cd γ(2,1)	19	5 100
316	^{113}Cd p(3,0)		
342	^{111}Cd p(2,0)	22	2 900
345	^{114}Cd γ(3,1)		
377	^{114}Cd n(5,0)	5.3	11 200
377	^{113}Cd γ(5,0)		
392	^{112}Cd γ(1,0)	8.1	9 400
392	^{113}Cd n(1,0)		
513	^{111}Cd p(7,2)	125	670
514	^{116}Cd p(1,0)		
538	^{110}Cd γ(1,0)	19	2 900
538	^{111}Cd n(1,0)		
559	^{114}Cd p(1,0)	120	640
584	^{113}Cd p(5,0)	21	3 500
616	^{106}Cd p(2,1)	92	900
617	^{112}Cd p(1,0)		
621	^{111}Cd p(4,0)	270	590
633	^{106}Cd p(1,0)	20	4 000
633	^{108}Cd p(1,0)		
650	^{111}Cd n(5,1)	21	2 400
650	^{110}Cd γ(5,1)		
650	^{108}Cd γ(1,0)		
650	^{114}Cd p(3,1)		
658	^{110}Cd p(1,0)	39	1 600
660	^{116}Cd γ(3,0)		
671	^{108}Cd γ(6,1)	4	13 700
695	^{112}Cd p(2,1)	20	3 400
730	^{114}Cd n(7,0)	6	11 300
730	^{113}Cd γ(7,0)		
742	^{111}Cd γ(8,0)	7	9 600
742	^{112}Cd n(8,0)		
770	^{116}Cd p(4,1)	4	4 500
782	^{106}Cd p(8,2)	2	36 100
818	^{110}Cd p(2,1)	4	16 900
826	^{114}Cd n(9,0)	8	8 000
826	^{113}Cd γ(9,0)		
853	^{111}Cd p(7,0)	5	11 400
881	^{116}Cd n(6,0)	3	24 800
963	^{112}Cd n(10,0)	2	67 900
963	^{111}Cd γ(10,0)		
1026	^{112}Cd γ(3,0)	16	3 200
1026	^{113}Cd n(3,0)		
1026	^{108}Cd n(3,0)		
1063	^{108}Cd γ(12,1)	7	12 200
1101	^{111}Cd n(3,0)	33	2 200
1101	^{110}Cd γ(3,0)		
1132	^{112}Cd γ(4,0)	11	15 700
1132	^{113}Cd n(4,0)		
1218	^{111}Cd n(6,0)	11	6 100
1218	^{110}Cd γ(6,0)		
1220	^{116}Cd p(2,0)		
1509	^{108}Cd p(2,0)	4	14 600
1542	^{111}Cd n(9,0)	4	10 600
1542	^{110}Cd γ(9,0)		

Coulomb-excited or underwent reaction to yield a large amount of gamma-rays.

Decay of the first level of all the nuclides resulted in gamma-rays, some of which were of such intensity that they offered good potential for the determination of cadmium. The three gamma-rays of particular interest were the 559-keV, 617-keV and 658-keV photons from the ^{114}Cd, ^{112}Cd and ^{110}Cd isotopes respectively. The sensitivities derived from two of the three mentioned gamma-rays were further enhanced by contribution from other gamma-rays. Decay of the first level of ^{116}Cd produced a gamma-ray of 514 keV which was difficult to resolve from the erratic 511-keV annihilation photon.

E_p (keV) / E_γ (keV)	Yield (quanta $sr^{-1}nC^{-1}$)					
	3 500	4 000	4 500	5 000	5 500	6 000
289	7.3	29	45	110	190	310
559	25	64	120	180	270	420
616 } 617	23	55	92	140	210	390
621	43	165	270	370	420	630
658 } 660	8.3	16	39	54	120	175

E_γ (keV)	Co-efficients of polynomials fitted to Sensitivity Functions				$S_{min.}/\mu g.g^{-1}$	E_p at $S_{min.}$ (keV)
	a_0	a_1	a_2	a_3		
289	- 7 634	+ 6 829	-1 687	+136	1 300	4 500
554	+24 146	-13 926	+2 750	0	320	6 000
616 } 617	+21 274	-11 441	+2 144	-135	660	6 000
621	+10 974	- 6 075	+1 190	- 79	420	6 000
658 } 660	+13 036	- 5 634	+ 915	- 49	1 420	6 000

Indium : - It was not surprising to find that the majority of the gamma-rays produced, when a target of pure indium metal was bombarded, originated from reactions on the heavier of the two isotopes since the lower abundant isotope only had a natural abundance of 4.8 atom %. In fact, only one gamma-ray 496-keV ^{113}In n(4,0), was assigned to this isotope.

Eγ keV	Assignment	Yield. quanta $sr^{-1}nC^{-1}$	Sensitivity $\mu g.g^{-1}mC^{-1}$	Eγ keV	Assignment	Yield. quanta $sr^{-1}nC^{-1}$	Sensitivity $\mu g.g^{-1}mC^{-1}$
115	^{115}In n(2,1)	150	2 000	933	^{115}In p(5,0)	33	8 900
336	^{115}In p(1,0)	7.4	28 700	972	^{115}In γ(5,1)	10	35 500
355	^{115}In γ(4,2)	2.3	83 300	986	^{115}In n(4,0)	30	11 200
444	^{115}In p(7,2)	17	15 200	1077	^{115}In p(4,0)	50	7 200
489	^{115}In n(4,1)	51	5 800	1132	^{115}In p(9,0)	26	11 800
496	^{113}In n(4,0)	870	340	1280	^{115}In n(5,0)	29	10 500
497	^{115}In n(1,0)			1463	^{115}In p(14,0)	21	13 600
612	^{115}In n(2,0)	4	6 900	1633	^{115}In n(7,0)	48	6 500
705	^{115}In n(7,1)	6.9	43 000	1757	^{115}In (2,0)	6.9	49 300
719	^{115}In n(3,0)	3.7	78 600				

E_γ(keV) \ E_p(keV)	Yield (quanta $sr^{-1}nC^{-1}$)					
	3 500	4 000	4 500	5 000	5 500	6 000
115	25	87	150	310	470	620
489	13	24	51	73	101	182
496 } 497	100	420	870	1 273	1 344	1 604
1078	10.4	28	50	72	109	147
1633	27	34	48	56	73	92

E_γ (keV)	Co-efficients of polynomials fitted to Sensitivity Functions				$S_{min.}/\mu g.g^{-1}$	E_p at $S_{min.}$ (keV)
	a_0	a_1	a_2	a_3		
115	+62 448	-34 258	+6 451	-404	1 770	6 000
489	+45 198	-14 622	+1 319	0	4 800	6 000
496 } 497	+ 3 352	- 1 036	+ 86	0	250	6 000
1078	+50 129	-15 037	+1 234	0	4 260	6 000
1633	+66 928	-34 200	+6 427	-403	6 130	6 000

Gamma-rays from the more abundant isotope were in general, of low intensity with the exception of the 497-keV ^{115}In n(1,0) gamma-ray. Possibly this gamma-ray was contributed by the 496 keV gamma-ray from ^{113}In.

Tin : - Gamma-ray production from most of the stable isotopes of tin were observed during the bombardment of a sheet of pure metal.

The first levels of six of the nuclides were excited by inelastic scattering. ^{119}Sn has its first level at 23.9 keV the gamma-ray of which was too low in energy to be observed by the Ge(Li) detector used. No gamma-ray was observed from the first excited state of ^{122}Sn and ^{124}Sn probably because of their relatively low natural abundance of 4.7 and 5.8 atom % respectively.

Eγ keV	Assignment	Yield. quanta $sr^{-1}nC^{-1}$	Sensitivity $\mu g.g^{-1}mC^{-1}$	Eγ keV	Assignment	Yield. quanta $sr^{-1}nC^{-1}$	Sensitivity $\mu g.g^{-1}mC^{-1}$
115	^{122}Sn n(7,2)	3.4	18 700	683	^{119}Sn n(7,2)	30	16 100
116	^{115}Sn p(2,1)			700	^{119}Sn n(3,0)	240	2 500
122	^{122}Sn n(3,0)	1.7	27 600	719	^{117}Sn n(2,0)	100	5 800
159	^{117}Sn p(1,0)	5.3	9 400	724	^{115}Sn n(1,0)		
160	^{122}Sn γ(1,0)			897	^{119}Sn p(4,1)	15	32 600
167	^{122}Sn n(6,0)	20	17 900	898	^{119}Sn p(5,1)		
194	^{122}Sn n(9,1)	10	34 100	921	^{119}Sn p(4,0)	105	6 000
256	^{122}Sn n(9,0)	30	14 500	923	^{117}Sn n(3,0)		
270	^{119}Sn n(1,0)	150	3 200	970	^{114}Sn p(6,1)	20	23 400
273	^{115}Sn n(2,1)			971	^{119}Sn n(4,0)		
273	^{116}Sn γ(2,1)			987	^{115}Sn p(4,0)	10	33 400
				1049	^{113}Sn n(5,0)	65	8 900
332	^{124}Sn γ(1,0)	25	15 900	1090	^{113}Sn p(7,0)	50	10 600
382	^{122}Sn γ(2,1)	5.7	78 900	1172	^{126}Sn p(1,0)	60	8 200
439	^{120}Sn γ(4,2)	4.2	121 000	1213	^{119}Sn n(6,0)	15	28 400
447	Sn	35	13 400	1230	^{118}Sn p(1,0)	45	12 600
497	^{115}Sn p(1,0)	45	7 800	1293	^{116}Sn p(1,0)	25	20 600
527	^{117}Sn n(1,0)	85	5 600	1300	^{114}Sn p(1,0)		
542	^{122}Sn γ(2,0)	35	12 700	1339	^{115}Sn n(8,0)	50	12 200
573	^{120}Sn γ(3,0)	25	15 700	1413	^{115}Sn n(9,0)	55	11 500
643	^{124}Sn γ(2,0)	190	2 600	1750	^{113}Sn n(12,0)	30	26 300
644	^{119}Sn n(2,0)						

The gamma-rays produced from proton-capture and (p,nγ) reactions on the various tin nuclides proved to be of greater intensity than Coulomb-excited gamma-rays and thus offered the best analytical potential.

E_γ (keV) \ E_p (keV)	Yield (quanta $sr^{-1}nC^{-1}$)					
	3 500	4 000	4 500	5 000	5 500	6 000
270, 271, 273	10	65	150	225	1 220	1 870
527	15	25	85	175	780	1 160
643, 644	8.2	25	190	570	990	1 630
700	30	145	240	890	1 410	1 940
719, 724	4.8	30	100	205	960	1 710

E_γ (keV)	Co-efficients of polynomials fitted to Sensitivity Functions				$S_{min.}/\mu g.g^{-1}$	E_p at $S_{min.}$ (keV)
	a_0	a_1	a_2	a_3		
270, 271, 273	+ 58 414	- 20 458	+ 1 836	0	1 610	6 000
527	+ 19 328	+ 15 060	- 6 982	+ 664	1 730	6 000
643, 644	+633 664	-351 248	+64 810	-3 974	920	6 000
700	+172 488	- 89 922	+15 712	- 915	710	6 000
719, 724	+ 51 940	- 10 872	- 899	+ 216	730	6 000

Antimony : - The element has 2 naturally occurring stable isotopes of comparable abundances viz. ^{121}Sb (≲ 7.3% by mass) and ^{123}Sb (42.7%). On bombardment of antimony in its pure metallic form, gamma-rays were produced with relatively weak intensities in the low energy region of the spectrum (122 keV).

The higher intensity gamma-rays were due to the (p,nγ) reaction on both the isotopes. Sensitivities were confined to above the $\mu g.g^{-1}$ concentration range in all cases. The best sensitivity was offered by that photopeak which resulted from the combined contribution of the 438-keV ^{121}Sb n(4,0) and 440-keV ^{123}Sb n(3,0) gamma-rays.

E_γ keV	Assignment	Yield. quanta $sr^{-1}nC^{-1}$	Sensitivity $\mu g.g^{-1}mC^{-1}$	E_γ keV	Assignment	Yield. quanta $sr^{-1}nC^{-1}$	Sensitivity $\mu g.g^{-1}mC^{-1}$
65	^{123}Sb n(5,3)	15	12 200	438	^{121}Sb n(4,0)	1 460	770
66	^{121}Sb p(3,2)			440	^{123}Sb n(3,0)		
159	^{123}Sb n (1,0)	220	4 500	464	^{121}Sb n(6,0)	130	7 600
160	^{123}Sb p(1,0)			470	^{121}Sb p(2,1)		
212	^{121}Sb n(1,0)	540	1 900	475	^{121}Sb n(7,0)	210	4 800
231	^{121}Sb n(5,1)	110	7 700	507	^{121}Sb p(2,0)	110	8 600
245	^{121}Sb n(2,0)	560	1 900	532	^{121}Sb n(8,0)	79	10 200
248	^{123}Sb n(2,0)			537	^{121}Sb p(3,1)	82	9 400
281	^{123}Sb n(3,1)	220	4 700	542	^{123}Sb p(2,0)		
294	^{121}Sb n(3,0)	250	4 400	573	^{121}Sb p(3,0)	105	6 700
332	^{121}Sb p(4,1)	210	4 500	594	^{121}Sb n(9,0)	95	9 500
382	^{123}Sb p(2,1)	180	3 600	681	^{121}Sb n(10,0)	53	14 900
382	^{121}Sb n(9,1)			1000	^{121}Sb p(5,1)	15	30 900
				1102	^{121}Sb p(6,1)	27	23 800

E_γ(keV) \ E_p(keV)	Yield (quanta $sr^{-1}nC^{-1}$)					
	3 500	4 000	4 500	5 000	5 500	6 000
212	37	86	540	550	710	820
245, 248	20	35	560	610	730	890
294	24	71	250	440	570	760
382	23	40	180	210	380	460
438, 440	290	580	1 460	2 010	2 820	3 640

E_γ (keV)	Co-efficients of polynomials fitted to Sensitivity Functions				$S_{min.}/\mu g.g^{-1}$	E_p at $S_{min.}$ (keV)
	a_0	a_1	a_2	a_3		
212	+122 464	- 66 854	+12 292	- 750	1 700	6 000
245, 248	+125 164	- 67 808	+12 382	- 755	1 100	6 000
294	+211 520	-120 008	+22 945	-1 465	1 090	6 000
382	- 41 964	+ 32 596	- 7 332	+ 519	1 840	6 000
438, 440	+ 22 482	- 14 238	+ 3 040	- 211	640	4 000

Tellurium : - Pure tellurium powder, compressed into a pellet was used as a target. In general, the peaks in the spectra

were small. The decay of the first levels of six of the eight stable isotopes resulted in observed gamma-rays.

In the case of ^{125}Te, the p(1,0) gamma-ray had an energy below the detection limit of the Ge(Li) detector and ^{123}Te was present in low concentrations, having a natural abundance of 0.89 atom %.

Eγ keV	Assignment	Yield. quanta $sr^{-1}nC^{-1}$	Sensitivity $\mu g.g^{-1}mC^{-1}$	Eγ keV	Assignment	Yield. quanta $sr^{-1}nC^{-1}$	Sensitivity $\mu g.g^{-1}mC^{-1}$
109	^{125}Te p(2,1)	32	24 100	463	^{125}Te p(5,0)	34	22 200
114	^{125}Te n(1,0)			505	^{123}Te p(5,0)	43	11 700
133	^{120}Te γ(2,0)	43	18 700	539	^{123}Te p(6,1)	74	9 100
173	^{125}Te p(7,5)	62	11 700	560	^{120}Te p(1,0)	120	5 600
176	^{125}Te p(3,0)			564	^{122}Te p(1,0)		
211	^{125}Te n(6,3)	23	28 500	603	^{124}Te p(1,0)	110	6 300
349	^{130}Te p(6,3)	72	13 400	603	^{130}Te γ(3,0)		
372	^{125}Te n(4,0)	45	24 600	636	^{125}Te n(6,4)	63	11 300
384	^{130}Te γ(6,2)	21	31 600	667	^{126}Te p(1,0)	390	1 900
393	^{130}Te p(6,2)	14	48 400	743	^{128}Te p(1,0)	400	1 980
408	^{125}Te p(4,1)	27	24 500	839	^{130}Te p(1,0)	230	3 400
428	^{125}Te p(5,1)	46	15 600	1633	^{130}Te p(3,0)	220	6 500
443	^{125}Te p(4,0)	93	8 600				
452	^{130}Te γ(3,1)	13	50 200				
454	^{125}Te n(5,0)						

E_γ (keV) \ E_p (keV)	Yield (quanta $sr^{-1}nC^{-1}$)					
	3 500	4 000	4 500	5 000	5 500	6 000
560 } 564	30	70	120	160	180	210
603	15	65	110	180	220	280
667	32	130	390	425	515	620
743	37	140	400	625	760	890
839	16	25	230	410	540	780

E_γ (keV)	Co-efficients of polynomials fitted to Sensitivity Functions				$S_{min.}/\mu g.g^{-1}$	E_p at $S_{min.}$ (keV)
	a_0	a_1	a_2	a_3		
560 } 564	+ 26 695	- 8 004	+ 748	0	5 300	5 350
603	+ 34 816	-14 976	+2 616	-154	5 830	6 000
667	+ 4 264	- 1 342	+ 280	- 22	1 600	6 000
743	+ 11 208	- 4 604	+ 765	- 43	1 770	6 000
839	+100 520	-52 372	+9 324	-553	2 560	5 450

Iodine : - Iodine crystals were crushed and compressed into a pellet which was bombarded. The beam current was kept low because the element sublimes very easily when being heated.

Eγ keV	Assignment	Yield. quanta $sr^{-1}nC^{-1}$	Sensitivity $\mu g.g^{-1}mC^{-1}$	Eγ keV	Assignment	Yield. quanta $sr^{-1}nC^{-1}$	Sensitivity $\mu g.g^{-1}mC^{-1}$
114	^{127}I n(4,2)	2 620	280	865	I	560	2 200
125	^{127}I n(1,0)	160	3 900	874	^{127}I n(7,4)	36	28 200
146	^{127}I p(2,1)	1 200	450	892	^{127}I n(8,4)	5.4	124 600
173	^{127}I n(2,1)	300	1 200	898	^{127}I n(11,2)	52	22 100
173	^{127}I p(3,2)			908	^{127}I p(25,9)	480	2 200
196	^{127}I n(3,1)	43	10 000	920	^{127}I p(13,2)	39	32 500
201	^{127}I p(5,4)	210	1 900	929	^{127}I n(9,8)	320	3 200
204	^{127}I p(2,0)			933	^{127}I p(10,1)	330	3 200
216	^{127}I p(4,2)	240	1 800	970	^{127}I γ(2,1)	2 140	430
244	^{127}I p(5,3)	12	34 000	987	^{127}I p(11,1)	240	4 400
317	^{127}I p(3,1)	200	2 400	991	^{127}I p(10,0)	1 980	480
321	^{127}I n(3,0)			1016	^{127}I p(15,2)	100	10 200
360	^{127}I p(4,1)	240	2 800	1037	^{127}I p(12,1)	980	1 400
370	^{127}I p(9,3)	61	8 300	1044	^{127}I p(11,0)		
375	^{127}I p(3,0)	84	7 500	1054	^{127}I α(5,1)	48	14 100
411	^{127}I n(4,0)	6.4	73 000	1066	^{127}I p(13,1)	4.6	106 100
413	^{127}I p(5,2)	6.1	71 000	1070	^{127}I n(7,1)	100	9 900
418	^{127}I p(4,0)	12	55 000	1095	^{127}I p(12,0)	110	10 000
443	^{127}I p(12,7)	600	8 700	1110	^{127}I n(9,4)	39	19 500
462	^{127}I n(5,1)	66	10 200	1124	^{127}I p(13,0)	41	19 300
490	^{127}I p(17,9)	62	11 100	1125	^{127}I p(14,1)		
513	^{127}I p(8,2)	860	1 000	1139	^{127}I p(24,3)	37	16 300
571	^{127}I p(6,1)	65	10 300	1143	^{127}I γ(3,1)	23	22 100
587	^{127}I n(5,0)	46	12 100	1161	^{127}I p(15,1)	38	16 800
594	^{127}I p(7,1)	83	8 800	1178	^{127}I n(8,1)	270	4 300
600	^{127}I p(15,5)	180	3 900	1183	^{127}I p(14,0)	370	2 600
629	^{127}I p(6,0)	140	5 200	1196	^{127}I n(7,0)	250	5 100
659	^{127}I p(8,1)	240	2 200	1213	^{127}I n(10,3)	9.3	42 000
677	^{127}I p(12,4)	1 490	700	1219	^{127}I p(15,0)	6.7	91 300
687	^{127}I p(4,1)	90	15 800	1230	^{127}I p(16,0)	190	4 400
695	^{127}I α(7,4)	200	5 700	1261	^{127}I n(11,4)	200	3 900
706	^{127}I p(13,4)	230	5 500	1326	^{127}I n(18,3)	180	5 400
717	^{127}I p(8,0)	81	22 300	1350	^{127}I p(19,1)	170	2 500
720	^{127}I p(12,3)			1394	^{127}I n(20,4)	20	42 800
745	^{127}I p(9,0)	460	2 900	1409	^{127}I n(10,1)	210	3 800
749	^{127}I p(13,3)	650	1 800	1453	^{127}I n(12,4)	154	10 900
765	^{127}I p(14,4)	630	2 200	1535	^{127}I n(10,0)	220	3 800
788	^{127}I p(10,2)	180	6 600	1582	^{127}I n(15,0)	9.6	46 500
804	^{127}I n(6,1)	300	4 200	1585	^{127}I n(17,1)	4.5	105 200
808	^{127}I p(14,3)			1629	^{127}I n(22,2)	35	30 300
841	^{127}I p(11,2)	55	19 800	1778	^{127}I n(12,0)	40	15 600
856	^{127}I p(18,4)	35	27 300	1975	^{127}I n(23,0)	25	59 800

E_p (keV) / E_γ (keV)	Yield (quanta $sr^{-1}nC^{-1}$)					
	3 500	4 000	4 500	5 000	5 500	6 000
114	490	1 280	2 620	4 780	7 540	9 620
146	310	690	1 200	2 150	3 480	4 620
513	170	440	860	1 240	1 420	1 530
677	180	840	1 500	2 380	3 960	4 670
970	190	920	2 140	4 100	7 000	9 100
991	360	830	1 980	4 290	8 910	11 700

E_γ (keV)	Co-efficients of polynomials fitted to Sensitivity Functions				$S_{min.}$/µg.g^{-1}	E_p at $S_{min.}$ (keV)
	a_0	a_1	a_2	a_3		
114	+ 9 347	- 4 825	+ 851	- 50	200	6 000
146	+ 8 533	- 4 092	+ 688	- 39	350	6 000
513	-25 066	+19 181	-4 350	+312	500	5 730
677	+17 596	- 9 340	+1 724	-107	520	6 000
970	+ 6 985	- 3 089	+ 473	- 24	250	6 000
991	+ 1 460	+ 574	- 306	+ 29	210	6 000

Many levels of ^{127}I (100 atom % in nature) were excited by inelastic scattering and some gamma-rays which were produced by this process were of such a high intensity that they could be used to determine iodine at concentrations above 250 µg.g^{-1}.

Most of the other gamma-rays were due to the (p,nγ) reaction. Of these, the 114-keV ^{127}I n(4,2) gamma-ray was analytically the most important, offering a sensitivity of 200 µg.g^{-1} at a bombarding energy of 6000 keV.

Caesium : - This mono-isotopic element was studied by examining the gamma-ray spectrum for caesium carbonate. Coulomb excitation populated many levels of ^{133}Cs although there was no sign of a gamma-ray resulting from the decay of the first level at 81 keV.

E_γ keV	Assignment	Yield. quanta $sr^{-1}nC^{-1}$	Sensitivity $\mu g.g^{-1}mC^{-1}$	E_γ keV	Assignment	Yield. quanta $sr^{-1}nC^{-1}$	Sensitivity $\mu g.g^{-1}mC^{-1}$
161	^{133}Cs p(2,0)	65	6 600	339	^{133}Cs n(6,3)	38	10 500
276	^{133}Cs p(4,2)	16	17 300	356	^{133}Cs p(4,1)	14	26 100
276	^{133}Cs n(2,1)			384	^{133}Cs p(3,0)	12	30 400
279	^{133}Cs n(3,1)	18	14 200	560	^{133}Cs p(7,1)	14	32 700
286	^{133}Cs n(5,3)			564	^{133}Cs n(5,1)		
290	^{133}Cs n(4,1)			605	^{133}Cs p(5,0)	42	11 300
291	^{133}Cs n(3,0)			633	^{133}Cs p(6,0)	140	3 900
302	^{133}Cs n(4,0)	44	7 800	769	^{133}Cs p(10,0)	20	23 500
303	^{133}Cs p(3,1)			872	^{133}Cs p(13,0)	10	37 600

E_γ (keV) \ E_p (keV)	Yield (quanta $sr^{-1}nC^{-1}$)					
	3 500	4 000	4 500	5 000	5 500	6 000
161	10	32	65	105	165	210
302, 303	25	37	44	110	185	250
339	6.7	22	38	48	75	160
605	6.3	26	42	76	92	110
633	54	75	140	210	260	320

E_γ (keV)	Co-efficients of polynomials fitted to Sensitivity Functions				$S_{min.}/\mu g.g^{-1}$	E_p at $S_{min.}$ (keV)
	a_0	a_1	a_2	a_3		
161	+177 304	-94 232	+17 294	-1 064	4 310	6 000
302, 303	+ 29 912	-15 504	+ 3 772	- 314	5 000	6 000
339	+ 87 646	-27 986	+ 2 449	0	7 630	6 000
605	+ 99 840	-30 296	+ 2 252	+ 32	6 010	6 000
633	+ 7 216	- 1 820	+ 452	- 48	2 110	6 000

Gamma-rays also resulted from the $^{133}Cs(p,n\gamma)^{133}Ba$ reaction but these photons were not very intense and of little analytical value.

Barium : - When a target of barium nitrate was bombarded, gamma-rays originated from Coulomb excitation and reactions on all of the seven natural isotopes of barium. Most of the gamma-rays, however, were of low intensity and offered little potential analytical use, except as a source of interference in other determinations. Sensitivity of about 3000 $\mu g.g^{-1}$ was achieved at bombarding energies of 6000 keV.

Eγ keV	Assignment	Yield. quanta $sr^{-1}nC^{-1}$	Sensitivity $\mu g.g^{-1}mC^{-1}$	Eγ keV	Assignment	Yield. quanta $sr^{-1}nC^{-1}$	Sensitivity $\mu g.g^{-1}mC^{-1}$
120	^{135}Ba n(1,0)	11	62 100	707	^{130}Ba n(16,5)	35	18 100
155	^{132}Ba n(1,0)	6.6	75 600	717	^{135}Ba p(5,0)	33	18 900
170	^{130}Ba γ(3,1)	18	24 900	751	^{137}Ba γ(14,1)	37	18 400
177	^{138}Ba n(6,2)	11	41 300	753	^{134}Ba γ(12,1)		
182	^{133}Ba n(1,0)	8.6	52 000	753	^{135}Ba n(12,1)		
207	^{135}Ba γ(2,0)	18	26 500	761	^{136}Ba p(3,1)	41	15 800
245	^{130}Ba γ(6,3)	35	16 900	796	^{134}Ba p(3,2)	40	16 100
279	^{137}Ba p(1,0)	23	24 900	842	^{138}Ba n(15,0)	45	13 400
304	^{130}Ba γ(4,0)	24	24 400	855	^{135}Ba p(6,0)	44	14 800
310	^{138}Ba n(9,4)	19	31 900	866	^{138}Ba n(20,4)	44	14 600
336	^{130}Ba γ(8,4)	15	38 200	908	^{130}Ba p(3,0)	43	14 900
341	^{138}Ba n(7,1)	13	41 900	936	^{138}Ba n(16,0)	44	14 500
357	^{130}Ba p(1,0)	21	25 300	941	^{138}Ba n(19,2)	57	10 300
438	^{138}Ba n(9,1)	31	21 200	961	^{138}Ba n(19,0)	44	15 400
448	^{137}Ba n(2,0)	31	20 100	990	^{132}Ba p(2,0)	45	15 100
481	^{135}Ba p(3,0)	29	22 500	1039	^{134}Ba p(4,1)	75	6 400
480	^{136}Ba n(2,0)	34	16 500	1048	^{136}Ba p(4,1)	82	6 100
576	^{136}Ba n(12,3)	35	19 300	1173	^{130}Ba γ(11,0)	93	5 900
588	^{135}Ba p(4,0)	21	27 900	1235	^{136}Ba p(6,1)	120	4 700
605	^{134}Ba p(1,0)	22	23 400	1261	^{136}Ba p(7,1)	66	7 100
654	^{135}Ba p(7,1)	24	27 300	1309	^{136}Ba p(8,1)	260	2 900
671	^{130}Ba γ(9,0)	26	24 600	1550	^{136}Ba p(2,0)	230	3 500
671	^{136}Ba p(9,2)						

E_γ(keV) \ E_p(keV)	Yield (quanta $sr^{-1}nC^{-1}$)					
	3 500	4 000	4 500	5 000	5 500	6 000
1048	10	47	82	120	180	210
1173	14	61	93	225	410	610
1235	11	67	120	180	220	280
1309	17	99	260	310	710	840
1550	41	120	230	360	420	720

E_γ (keV)	Co-efficients of polynomials fitted to Sensitivity Functions				$S_{min.}/\mu g.g^{-1}$	E_p at $S_{min.}$ (keV)
	a_0	a_1	a_2	a_3		
1048	+ 48 000	15 580	+ 1 482	+ 16.1	4 000	6 000
1173	+132 840	- 66 040	+11 336	- 651	4 100	6 000
1235	+233 592	-128 304	+23 857	-1 474	4 330	6 000
1309	+106 216	- 63 904	+13 065	- 883	2 370	6 000
1550	+118 464	- 66 488	+12 749	0	2 970	6 000

Lanthanum : - The element has two isotopes ^{139}La(99.911 atom %) and ^{138}La(0.089 atom %). The target used for the study of lanthanum was lanthanum oxide. Coulomb excitation resulted in very weak gamma-rays, all of which were of such low intensity that they were useless for analytical purposes.

Eγ. keV	Assignment	Yield. quanta $sr^{-1}nC^{-1}$	Sensitivity $\mu g.g^{-1}mC^{-1}$	Eγ keV	Assignment	Yield. quanta $sr^{-1}nC^{-1}$	Sensitivity $\mu g.g^{-1}mC^{-1}$
116	^{138}La p(2,0)	5.3	29 100	789	^{138}La n(1,0)	2.7	58 000
139	^{139}La γ(1,0)	3.4	37 400	1231	^{139}La n(12,3)	4.4	75 900
195	^{138}La γ(2,1)	3.1	36 100	1231	^{138}La γ(12,3)		
230	^{138}La p(5,0)	13	23 200	1320	^{139}La n(5,0)	7.1	24 600
255	^{139}La n(1,0)	5.8	26 800	1320	^{138}La γ(5,0)		
255	^{138}La γ(1,0)			1347	^{139}La n(6,0)	6.4	33 700
290	^{139}La n(5,4)	3.2	42 000	1347	^{138}La γ(6,0)		
290	^{139}La γ(5,4)			1597	^{138}La n(7,0)	4.3	34 400
479	^{138}La p(8,0)	3.7	38 000	1597	^{139}La γ(7,0)		
500	^{139}La n(3,1)	3.1	41 000	1631	^{139}La n(8,0)	4.2	46 964
500	^{138}La γ(3,1)			1631	^{138}La γ(8,0)		
511	^{138}La p(9,0)	74	4 800	1730	^{139}La n(12,1)	2.6	54 600
580	^{139}La n(4,2)	4.5	46 000	1730	^{138}La γ(12,1)		
580	^{138}La γ(4,2)			1985	^{139}La n(12,0)	3.6	17 100
642	^{138}La p(11,0)	5.8	33 800	1985	^{138}La γ(12,0)		
754	^{139}La n(3,0)	18	23 000				
754	^{138}La γ(3,0)						

E_γ(keV) \ E_p(keV)	Yield (quanta $sr^{-1}nC^{-1}$)					
	3 500	4 000	4 500	5 000	5 500	6 000
116	0.46	2.7	5.3	9.3	16	27
230	4.3	8.2	13	24	37	51
255	0.73	1.3	5.8	12	21	47
754	3.2	9.8	18	24	43	62
1320	1.2	3.1	7.1	16	21	37

E_γ (keV)	Co-efficients of polynomials fitted to Sensitivity Functions				$S_{min.}/\mu g.g^{-1}$	E_p at $S_{min.}$ (keV)
	a_0	a_1	a_2	a_3		
116	+381 952	-194 144	+ 35 792	-2 255	19 200	6 000
230	+800 320	-428 384	+ 78 383	-4 788	17 900	6 000
255	+381 056	-144 672	+ 17 380	- 587	12 700	6 000
754	+995 000	-751 616	+141 536	-8 917	11 500	6 000
1320	+990 000	-606 144	+118 240	-7 690	18 200	6 000

Cerium : - Under irradiation with protons, a pellet of cerium sulphate emitted few gamma-rays all of which were of low intensity and little analytical value.

Eγ keV	Assignment	Yield. quanta $sr^{-1}nC^{-1}$	Sensitivity $\mu g.g^{-1}mC^{-1}$	Eγ keV	Assignment	Yield. quanta $sr^{-1}nC^{-1}$	Sensitivity $\mu g.g^{-1}mC^{-1}$
109	^{136}Ce n(3,1)	9.2	4 900	200	^{138}Ce n(2,0)	21	22 600
124	^{142}Ce n(7,0)	11	38 500	295	^{136}Ce n(5,1)	13	53 500
126	^{138}Ce n(3,2)						

E_γ(keV) \ E_p(keV)	Yield (quanta $sr^{-1}nC^{-1}$)					
	3 500	4 000	4 500	5 000	5 500	6 000
110	2.9	6.5	9.2	11	13	17
124 } 126 }	2.1	5.4	11	12	17	25
200	8.8	14	21	26	29	41
295	3.8	4.9	13	18	22	35

E_γ (keV)	Co-efficients of polynomials fitted to Sensitivity Functions				$S_{min.}/\mu g.g^{-1}$	E_p at $S_{min.}$ (keV)
	a_0	a_1	a_2	a_3		
110	+129 320	- 68 664	+ 12 636	- 784	2 990	6 000
124 } 126 }	+994 000	-612 320	+118 784	-7 741	22 700	6 000
200	+235 538	- 111 494	+ 27 174	-3 528	21 040	6 000
295	+262 592	-134 528	+ 26 904	-1 844	25 500	6 000

Praseodymium : - The single isotope element of mass 141 was investigated by analysing the spectrum obtained from the bombardment of praseodymium oxide. Coulomb excitation of the first three levels resulted in few gamma-rays, all of which were too weak to be used for analysis. Of slightly higher intensities were the gamma-rays that originated from the (p,nγ) reaction but even with these, sensitivities of better than the $mg.g^{-1}$ limit were not achieved.

Eγ keV	Assignment	Yield. quanta $sr^{-1}nC^{-1}$	Sensitivity $\mu g.g^{-1}mC^{-1}$	Eγ keV	Assignment	Yield. quanta $sr^{-1}nC^{-1}$	Sensitivity $\mu g.g^{-1}mC^{-1}$
108	^{141}Pr γ(4,2)	3.7	45 600	1036	^{141}Pr γ(5,4)	110	2 200
145	^{141}Pr p(1,0)	2.6	61 000	1127	^{141}Pr p(3,0)	27	10 200
194	^{141}Pr n(1,0)	4.8	34 200	1223	^{141}Pr n(3,0)	21	10 600
197	^{141}Pr n(5,3)	4.6	36 100	1345	^{141}Pr n(4,0)	15	13 200
508	^{141}Pr γ(2,1)	3.4	48 600	1371	^{141}Pr n(5,1)	240	1 100
525	^{141}Pr γ(3,1)	8.1	24 500	1403	^{141}Pr n(7,1)	10	16 900
597	^{141}Pr n(9,3)	21	14 200	1470	^{141}Pr γ(15,1)	90	2 600
757	^{141}Pr n(2,0)	32	7 100	1576	^{141}Pr γ(1,0)	25	8 400
971	^{141}Pr p(2,1)	80	2 800	1626	^{141}Pr n(9,1)	8	36 600

E_γ (keV) \ E_p (keV)	Yield (quanta $sr^{-1}nC^{-1}$)					
	3 500	4 000	4 500	5 000	5 500	6 000
757	10	18	32	42	64	89
971	17	40	80	110	194	310
1036	27	54	110	180	260	405
1371	40	90	240	410	570	740
1470	35	50	90	125	310	430

E_γ (keV)	Co-efficients of polynomials fitted to Sensitivity Functions				$S_{min.}/\mu g.g^{-1}$	E_p at $S_{min.}$ (keV)
	a_0	a_1	a_2	a_3		
757	+71 712	-32 968	+5 814	-366	4 000	6 000
971	+35 056	-17 806	+3 342	-218	1 320	6 000
1036	+18 120	+ 7 442	+1 146	- 61	1 560	6 000
1371	+ 6 660	- 1 957	+ 162	0	740	6 000
1470	-12 604	+10 692	-2 312	156	2 020	6 000

Neodymium : - Four of the seven stable neodymium isotopes yielded gamma-rays when a target of neodymium nitrate was bombarded. All the gamma-rays were due to Coulomb excitation. Of these, the 130-keV gamma-ray from the lowest abundant isotope, ^{150}Nd, was the only gamma-ray that could be used to calculate a sensitivity of analysis and even then the sensitivity was no better than the $mg.g^{-1}$ range.

E_γ keV	Assignment	Yield. quanta $sr^{-1}nC^{-1}$	Sensitivity $\mu g.g^{-1}mC^{-1}$	E_γ keV	Assignment	Yield. quanta $sr^{-1}nC^{-1}$	Sensitivity $\mu g.g^{-1}mC^{-1}$
130	^{150}Nd p(1,0)	110	1 800	697	^{144}Nd p(1,0)	51	6 900
302	^{148}Nd p(1,0)	73	2 800	864	^{144}Nd p(4,1)	45	6 400
454	^{146}Nd p(1,0)	100	2 200	1042	^{146}Nd p(2,0)	15	8 800

E_γ(keV) \ E_p(keV)	Yield (quanta $sr^{-1}nC^{-1}$)					
	3 500	4 000	4 500	5 000	5 500	6 000
130	48	52	110	160	210	280
302	33	37	73	110	170	210
454	34	40	100	145	185	218
697	26	33	51	72	96	105
864	11	21	45	51	73	94

E_γ (keV)	Co-efficients of polynomials fitted to Sensitivity Functions				$S_{min.}/\mu g.g^{-1}$	E_p at $S_{min.}$ (keV)
	a_0	a_1	a_2	a_3		
130	+ 34 388	- 15 716	+ 2 470	- 130	970	6 000
302	- 9 388	+ 13 026	- 3 583	+ 283	940	5 770
454	- 3 968	- 9 368	- 2 832	+ 235	920	5 720
697	+464 640	-256 768	+47 796	-2 965	4 250	6 000
864	+218 144	-123 288	+24 058	-1 580	3 230	6 000

Samarium : - Gamma-rays were observed from all seven naturally-occurring samarium isotopes during the bombarding of a target of samarium III oxide (Sm_2O_3). De-excitation from the first level to the ground state of the most abundant isotope, ^{152}Sm, provided a potentially useful gamma-ray of 122 keV.

The first and second levels of ^{147}Sm were both Coulomb excited and by a fortunate chance the ^{147}Sm p(1,0) gamma-ray had an energy very close to the 122-keV gamma-ray from the ^{152}Sm isotope mentioned above, thus enhancing its analytically significance. A similar type of overlapping occurred at 333 keV from ^{144}Sm n(1,0) and ^{150}Sm p(1,0). The sensitivities attainable

Eγ keV	Assignment	Yield. quanta $sr^{-1}nC^{-1}$	Sensitivity $\mu g.g^{-1}mC^{-1}$	Eγ keV	Assignment	Yield. quanta $sr^{-1}nC^{-1}$	Sensitivity $\mu g.g^{-1}mC^{-1}$
68	^{154}Sm n(1,0)	50	8 300	328	^{149}Sm p(3,1)	22	12 200
121	^{147}Sm p(1,0)	380	790	333	^{144}Sm n(1,0)	500	550
122	^{152}Sm p(1,0)			334	^{150}Sm p(1,0)		
197	^{147}Sm p(2,0)	53	4 600	350	^{149}Sm p(3,0)	11	20 900
229	^{147}Sm n(1,0)	7.4	30 800	550	^{148}Sm p(1,0)	240	1 200

E_γ (keV) \ E_p (keV)	Yield (quanta $sr^{-1}nC^{-1}$)					
	3 500	4 000	4 500	5 000	5 500	6 000
68	13	31	50	61	68	82
121, 122	200	270	380	490	1 240	2 560
197	15	42	53	150	210	315
333, 334	170	480	500	740	960	1 290
550	56	125	240	410	570	840

E_γ (keV)	Co-efficients of polynomials fitted to Sensitivity Functions				$S_{min.}/\mu g.g^{-1}$	E_p at $S_{min.}$ (keV)
	a_0	a_1	a_2	a_3		
68	+ 22 181	- 5 567	+ 676	0	10 700	4 000
121, 122	+ 3 353	- 1 448	+ 270	- 16	840	4 000
197	+210 744	-111 112	+19 750	-1 156	4 600	4 500
333, 334	+ 8 993	- 4 915	+ 944	- 59	570	4 500
550	+ 10 730	- 3 563	+ 322	0	880	5 530

using these gamma-rays were 840 and 570 $\mu g.g^{-1}$ respectively. A gamma-ray which might be considered for analytical use was the 550-keV ^{148}Sm p(1,0) photon for which a sensitivity of 880 $\mu g.g^{-1}$ was calculated.

Europium : - Europium oxide pellets were used as targets. The Coulomb excited ^{153}Eu gamma-rays of 84 keV were relatively intense and interference-free. By contrast the corresponding ^{131}Eu p(1,0) gamma-ray was not observed because the energy threshold of the Ge(Li) detector. The gamma-ray that

Eγ keV	Assignment	Yield. quanta $sr^{-1}nC^{-1}$	Sensitivity $\mu g.g^{-1}mC^{-1}$	Eγ keV	Assignment	Yield. quanta $sr^{-1}nC^{-1}$	Sensitivity $\mu g.g^{-1}mC^{-1}$
84	^{153}Eu p(1,0)	480	1 100	197	^{151}Eu p(2,0)	250	1 420
110	^{151}Eu p(3,0)	120	3 500	286	^{151}Eu p(4,1)	275	1 310
110	^{151}Eu p(4,2)			308	^{151}Eu p(4,0)	190	2 100
135	^{151}Eu n(5,0)	49	6 300	512	^{151}Eu n(7,1)	500	1 000
175	^{151}Eu p(2,1)	38	9 400				

E_γ(keV) \ E_p(keV)	Yield (quanta $sr^{-1}nC^{-1}$)					
	3 500	4 000	4 500	5 000	5 500	6 000
84	205	310	480	980	1 460	2 120
110	44	95	120	135	210	460
197	48	160	250	340	530	610
268	36	110	275	390	480	620
308	80	150	190	340	570	870

E_γ (keV)	Co-efficients of polynomials fitted to Sensitivity Functions				$S_{min.}/\mu g.g^{-1}$	E_p at $S_{min.}$ (keV)
	a_0	a_1	a_2	a_3		
84	+26 350	-11 602	+1 720	- 82	780	6 000
110	+58 860	-34 024	+7 106	- 506	1 280	6 000
197	- 1 736	+ 5 194	-1 478	+ 113	660	6 000
268	+30 658	+15 080	+2 572	-1 487	640	6 000
308	-19 020	+17 356	-1 435	+ 302	1 400	6 000

originated from the decay of the second level of 197 keV was interferred with by the ^{18}O p(2,0) photon of 197 keV. Best sensitivities for analysis were achieved at the highest available bombarding energies.

Gadolinium : - A target of gadolinium oxide (Gd_2O_3) was bombarded. The majority of the gamma-rays were produced by Coulomb excitation. All the photons, however, were of low intensity and the sensitivities offered for gadolinium analysis were poor even at the highest available bombarding energies.

Eγ keV	Assignment	Yield. quanta $sr^{-1}nC^{-1}$	Sensitivity $\mu g.g^{-1}mC^{-1}$	Eγ keV	Assignment	Yield. quanta $sr^{-1}nC^{-1}$	Sensitivity $\mu g.g^{-1}mC^{-1}$
65	^{155}Gd n(1,0)	25	21 700	232	^{154}Gd p(6,4)	18	19 000
105	^{155}Gd p(3,2)	3.7	94 600	296	^{156}Gd p(3,2)	22	17 300
123	^{154}Gd p(1,0)	16	21 900	322	^{155}Gd p(4,0)	33	12 100
131	^{157}Gd p(2,0)	2.5	100 100	347	^{154}Gd p(3,2)	10	42 800
146	^{155}Gd p(2,0)	13	29 000				

E_γ(keV) \ E_p(keV)	Yield (quanta $sr^{-1}nC^{-1}$)					
	3 500	4 000	4 500	5 000	5 500	6 000
65	8.9	13	25	30	37	43
123	4.1	11	16	22	29	38
232	5.7	10	18	30	38	50
296	6.5	16	22	30	42	78
322	8.2	17	33	49	65	90

E_γ (keV)	Co-efficients of polynomials fitted to Sensitivity Functions				$S_{min.}/\mu g.g^{-1}$	E_p at $S_{min.}$ (keV)
	a_0	a_1	a_2	a_3		
65	+946 816	-530 592	+101 428	- 6 478	15 400	6 000
123	+180 000	- 76 560	+ 12 564	- 738	13 300	6 000
232	+ 47 328	- 8 968	+ 594	0	15 000	6 000
296	+148 352	- 55 248	+ 7 072	- 278	12 000	6 000
322	-961 088	+748 960	-186 896	+15 207	89 200	6 000

Terbium : - A target of terbium peroxide (Tb_4O_7) was compressed into a pellet and bombarded. The element has a single naturally-occurring isotope, ^{159}Tb, and all the gamma-rays originated either from Coulomb excitation or from the (p,nγ) reaction on this isotope. Decay of the first level of ^{159}Tb resulted in a relatively low intensity photon and was not of much analytical significance. Far more useful were the gamma-rays which resulted from the decay of the second level to the first level and to the ground level. By a fortunate chance both the gamma-rays, of 136 and 80 keV respectively, were analytically enhanced by gamma-rays of the same energies due to the (p,nγ) reaction. Little improvement in sensitivity limits were attained when higher energy bombarding beams were used. The use of a high resolution intrinsic germanium detector would have been useful for analysis not only because most of the photopeaks were situated in the low energy region of the spectrum but also because of the possibility of using the Tb X-rays for the determination of this element.

Eγ keV	Assignment	Yield. quanta $sr^{-1}nC^{-1}$	Sensitivity $\mu g.g^{-1}mC^{-1}$	Eγ keV	Assignment	Yield. quanta $sr^{-1}nC^{-1}$	Sensitivity $\mu g.g^{-1}mC^{-1}$
57	^{159}Tb n(1,0)	26	22 600	136	^{159}Tb n(2,0)	181	1 800
58	^{159}Tb p(1,0)			138	^{159}Tb p(2,0)		
80	^{159}Tb p(2,1)	220	2 700	348	^{159}Tb p(4,0)	15	7 200
80	^{159}Tb n(2,1)			371	^{159}Tb p(6,1)	9.1	33 000
104	^{159}Tb p(3,2)	14	25 800	560	^{159}Tb p(9,1)	7.7	38 900
121	^{159}Tb n(3,1)	19	17 400	580	^{159}Tb p(8,0)	50	5 300
122	^{159}Tb p(5,3)			617	^{159}Tb p(9,0)	15	19 300

E_γ (keV) \ E_p (keV)	Yield (quanta $sr^{-1}nC^{-1}$)					
	3 500	4 000	4 500	5 000	5 500	6 000
80	80	113	220	250	290	400
121 / 122	0.8	2.1	19	72	280	940
136 / 138	81	125	180	235	300	430
348	5.1	9.3	15	27	83	115
580	20	30	50	81	120	195

E_γ (keV)	Co-efficients of polynomials fitted to Sensitivity Functions				$S_{min.}/\mu g.g^{-1}$	E_p at $S_{min.}$ (keV)
	a_0	a_1	a_2	a_3		
80	+17 736	- 9 320	+1 926	-133	2 510	6 000
121, 122	-15 008	+20 544	-3 568	+135	9 000	6 000
136, 138	+16 036	- 7 924	+1 437	- 84	1 760	4 500
348	+86 384	-39 976	+6 716	-381	6 000	6 000
580	+39 328	-18 844	+3 613	-240	4 290	6 000

Dysprosium : - The majority of the gamma-rays that were produced when a target of dysprosium oxide (Dy_2O_3) was bombarded, were as a result of Coulomb excitation on five of the seven

Eγ keV	Assignment	Yield. quanta $sr^{-1}nC^{-1}$	Sensitivity $\mu g.g^{-1}mC^{-1}$	Eγ keV	Assignment	Yield. quanta $sr^{-1}nC^{-1}$	Sensitivity $\mu g.g^{-1}mC^{-1}$
73	^{164}Dy p(1,0)	100	4 300	390	^{163}Dy p(5,0)	15	9 600
94	^{163}Dy p(2,1)	15	11 300	422	^{163}Dy p(7,0)	5.8	23 800
95	^{163}Dy n(1,0)			440	^{163}Dy n(3,0)	6.2	19 500
114	^{163}Dy p(3,2)	30	5 800	538	^{156}Dy p(3,1)	7.9	11 300
167	^{163}Dy p(2,0)	330	1 640	674	^{164}Dy p(6,2)	10	11 200
169	^{164}Dy p(2,1)			689	^{164}Dy p(4,1)	10	9 200
185	^{162}Dy p(2,1)	13	11 500	762	^{164}Dy p(4,0)	11	12 400
197	^{160}Dy p(2,1)	13	11 200	843	^{164}Dy p(6,1)	12	11 900
242	^{164}Dy p(2,0)	18	8 600	871	^{160}Dy p(7,2)	12	11 800
297	^{160}Dy p(3,1)	14	11 700	884	^{156}Dy p(7,1)	16	6 900
298	^{163}Dy n(2,0)			891	^{156}Dy p(6,0)	14	8 700
342	^{164}Dy p(5,3)	20	8 600	962	^{160}Dy p(6,1)	40	5 600
351	^{163}Dy p(4,0)	25	6 500				

E_γ(keV) \ E_p(keV)	Yield (quanta $sr^{-1}nC^{-1}$)					
	3 500	4 000	4 500	5 000	5 500	6 000
73.	25	61	100	135	220	300
114	7.5	15	30	40	55	140
167, 168	87	165	330	420	550	610
351	6.7	15	25	29	41	67
962	9.2	23	40	60	120	160

E_γ (keV)	Co-efficients of polynomials fitted to Sensitivity Functions				$S_{min.}/\mu g.g^{-1}$	E_p at $S_{min.}$ (keV)
	a_0	a_1	a_2	a_3		
73	+ 16 920	- 5 948	+ 929	- 52	3 480	6 000
114	+309 456	-169 224	+31 246	-1 918	4 890	6 000
167 } 168 }	+ 39 168	- 21 776	+ 4 149	- 259	1 540	5 000
351	+198 448	-118 320	+24 100	-1 621	6 000	6 000
962	+ 79 008	- 35 068	+ 5 175	- 243	2 437	6 000

stable isotopes of the element. Two other gamma-rays from the reaction, ^{163}Dy(p,nγ)^{163}Ho were detected but were of low intensity. The most prominent peak in the spectrum was that of 167-keV, ^{163}Dy p(2,0). Decay of the ^{164}Dy isotope resulted in a gamma-ray of 169 keV. Both of these integrated together gave a sensitivity of 1500 $\mu g.g^{-1}$ for a bombarding energy of 5000 keV.

Holmium : - This single-isotope lanthanide was investigated by the bombardment of a holmium oxide (Ho_2O) pellet. Gamma-rays were produced either by Coulomb-excitation or by the (p,nγ) reaction. The gamma-rays originating from the latter were weak and of little analytical value. Intense peaks were observed corresponding to 115 keV and 154 keV resulting from Coulomb excitation of the second level of ^{165}Ho.

Using these gamma-rays, good sensitivity for holmium analysis was offered, improving with increasing bombarding energy.

Eγ keV	Assignment	Yield. quanta $sr^{-1}nC^{-1}$	Sensitivity $\mu g.g^{-1}mC^{-1}$	Eγ keV	Assignment	Yield. quanta $sr^{-1}nC^{-1}$	Sensitivity $\mu g.g^{-1}mC^{-1}$
95	^{165}Ho p(1,0)	145	4 900	472	^{165}Ho p(7,1)	15	43 000
115	^{165}Ho p(2,1)	220	2 800	516	^{165}Ho p(6,0)	12	47 000
154	^{165}Ho p(5,3)	690	700	535	^{165}Ho n(13,0)	5.3	110 000
210	^{165}Ho p(2,0)	130	2 900	567	^{165}Ho p(7,0)	6.1	108 000
289	^{165}Ho p(5,2)	4.7	86 000	594	^{165}Ho p(10,2)	40	17 900
296	^{165}Ho n(6,0)	6.1	68 000	608	^{165}Ho n(15,0)	16	42 100
357	^{165}Ho n(8,0)	60	8 400	689	^{165}Ho p(10,0)	22	37 000
361	^{165}Ho p(4,0)	45	10 400				

E_γ (keV) \ E_p (keV)	Yield (quanta $sr^{-1}nC^{-1}$)					
	3 500	4 000	4 500	5 000	5 500	6 000
95	81	105	145	250	290	320
115	75	140	220	1 970	2 790	3 640
154	100	220	690	840	1 210	1 590
210	28	47	130	140	170	210
357	18	20	60	80	180	230

E_γ (keV)	Co-efficients of polynomials fitted to Sensitivity Functions				$S_{min.}/\mu g.g^{-1}$	E_p at $S_{min.}$ (keV)
	a_0	a_1	a_2	a_3		
95	+ 9 368	- 2 176	+ 2 115	0	3 790	5 150
115	+40 152	+22 618	+ 4 286	- 270	300	6 000
154	+51 600	-28 445	+ 5 286	- 326	640	6 000
210	+32 040	-12 012	+ 1 687	- 77	3 940	6 000
357	-72 623	+63 960	-15 238	+1 181	4 120	6 000

Erbium : - A target of erbium oxide (Er_2O_3) was bombarded for the study of erbium. The excitation of the first levels of four of the six naturally occurring isotopes produced gamma-rays which are shown as a common peak in the spectrum. The peak, however, was of very low intensity and like all the other detected gamma-rays, was too weak to be of any significance for the determination of erbium.

Eγ keV	Assignment	Yield. quanta $sr^{-1}nC^{-1}$	Sensitivity $\mu g.g^{-1}mC^{-1}$	Eγ keV	Assignment	Yield. quanta $sr^{-1}nC^{-1}$	Sensitivity $\mu g.g^{-1}mC^{-1}$
78	^{164}Er n(3,0)	11	28 900	200	^{164}Er p(2,1)	2.1	102 300
79	^{170}Er p(1,0)			495	^{167}Er p(6,1)	13	21 800
79	^{167}Er p(1,0)			532	^{167}Er p(5,0)	1.9	126 400
80	^{168}Er p(1,0)			562	^{167}Er p(7,1)	2.1	121 400
81	^{166}Er p(1,0)			705	^{166}Er p(4,1)	16	22 600
90	^{164}Er p(1,0)	5.4	75 800	786	^{166}Er p(4,0)	3.4	97 600
178	^{167}Er p(2,0)	32	20 600				
178	^{162}Er n(5,0)						

E_γ (keV) \ E_p (keV)	Yield (quanta $sr^{-1}nC^{-1}$)					
	3 500	4 000	4 500	5 000	5 500	6 000
78, 79, 80, 81	6.3	8.9	11	14	17	23
90	1.7	3.1	5.4	7.3	11	14
178	3.8	18	32	44	47	57
495	5.4	8.8	13	16	20	27
705	8.1	12	16	18	27	34

E_γ (keV)	Co-efficients of polynomials fitted to Sensitivity Functions				$S_{min.}/\mu g.g^{-1}$	E_p at $S_{min.}$ (keV)
	a_0	a_1	a_2	a_3		
78, 79, 80, 81	+555 776	-296 896	+55 872	-3 535	22 100	6 000
90	+ 33 792	+ 82 368	-25 280	+2 084	67 700	5 830
178	+632 736	-334 272	+60 323	-3 650	9 880	6 000
495	+250 496	-108 352	+16 716	- 881	11 900	6 000
705	+134 850	- 37 802	+ 2 830	0	10 500	6 000

Thullium : - The single isotope element was studied by bombarding a pellet of thulia (Tm_2O_3). All the gamma-rays originated from Coulomb excitation. The first excited state (at 8.4 keV) of the ^{169}Tm isotope was well below the threshold of the Ge(Li) detector used, and the peak of this energy could, therefore, not be observed in the spectrum. The decay of the second level produced the two most intense gamma-rays, that of 110 and 118 keV. These, together with Tm X-rays of 50 keV offered the best analytical potential with calculated sensitivities of the order of 600 $\mu g.g^{-1}$. It is likely that the use of a detector specially designed for low energy photons, such as a thin Ge(Li) or intrinsic germanium detector could greatly improve the potential sensitivity of analysis.

E_γ keV	Assignment	Yield. quanta $sr^{-1}nC^{-1}$	Sensitivity $\mu g.g^{-1}mC^{-1}$	E_γ keV	Assignment	Yield. quanta $sr^{-1}nC^{-1}$	Sensitivity $\mu g.g^{-1}mC^{-1}$
110	^{169}Tm p(2,1)	520	550	453	^{169}Tm p(6,2)	10	22 100
118	^{169}Tm p(2,0)	93	2 500	563	^{169}Tm p(6,1)	25	9 500
130	^{169}Tm p(3,2)	6.7	30 400	571	^{169}Tm p(6,0)	30	8 300
193	^{169}Tm p(4,3)	7.6	28 900	625	^{169}Tm p(7,1)	9.3	26 300
228	^{169}Tm p(5,2)	7.3	33 000				

E_γ (keV) \ E_p (keV)	Yield (quanta $sr^{-1}nC^{-1}$)					
	3 500	4 000	4 500	5 000	5 500	6 000
110	252	480	520	537	643	1 090
118	44	75	93	100	120	190
453	5.4	7.2	10	12	17	77
563	6	8	25	46	65	130
571	5	12	30	52	77	140

E_γ (keV)	Co-efficients of polynomials fitted to Sensitivity Functions				$S_{min.}/\mu g.g^{-1}$	E_p at $S_{min.}$ (keV)
	a_0	a_1	a_2	a_3		
110	+ 2 979	- 1 002	+ 104	0	550	4 500
118	+ 27 452	- 14 700	+ 2 888	- 184	3 000	4 500
453	+244 416	-145 408	+30 788	-2 092	22 100	4 500
563	+154 192	- 65 336	+ 9 378	- 438	4 960	6 000
571	+320 496	-165 880	+29 160	-1 712	4 850	6 000

Ytterbium : - Although the element had seven naturally occurring isotopes, only a single low intensity gamma-ray from ytterbium was observed during the bombardment of ytterbium III oxide. The photopeak originated from the Coulomb excitation of the most abundant isotope, ^{174}Yb, and produced a gamma-ray of 177 keV. The excitation of 52-keV X-rays appeared to be more applicable for analytical purposes.

E_γ keV	Assignment	Yield. quanta $sr^{-1}nC^{-1}$	Sensitivity $\mu g.g^{-1}mC^{-1}$	E_γ keV	Assignment	Yield. quanta $sr^{-1}nC^{-1}$	Sensitivity $\mu g.g^{-1}mC^{-1}$
177	^{174}Yb p(2,1)	11	16 300				

E_γ(keV) \ E_p(keV)	Yield (quanta $sr^{-1}nC^{-1}$)					
	3 500	4 000	4 500	5 000	5 500	6 000
177	6.3	7.1	11	15	26	40

E_γ (keV)	Co-efficients of polynomials fitted to Sensitivity Functions				$S_{min.}/\mu g.g^{-1}$	E_p at $S_{min.}$ (keV)
	a_0	a_1	a_2	a_3		
177	+108 928	-59 008	+12 676	-918	12 800	6 000

Lutetium : - A pellet of high purity lutetium III oxide (Lu_2O_3) was bombarded. The element has two naturally occurring isotopes viz. ^{175}Lu (97.4 atom %) and ^{176}Lu (2.59 atom %). De-excitation of the first two levels of ^{175}Lu produced the most useful gamma-rays for analysis.

A single gamma-ray of 82 keV resulted from the decay of the first level to the ground level of ^{176}Lu. The photopeak from this gamma-ray was, however, feeble even though there was a contribution from another gamma-ray of the same energy from the $(p,n\gamma)$ reaction on ^{175}Lu.

Of the other gamma-rays originating from reactions on ^{176}Lu, the one of 190 keV was analytically useful.

Use of the 114-,138-and 252-keV gamma-rays gave sensitivities of below 1000 $\mu g.g^{-1}$ at a proton bombarding energy of 4500 keV, improving steadily with higher bombarding energies. It should also be noted that for the analytical determination of this element, effective use could be made of the intense X-rays

Eγ keV	Assignment	Yield. quanta $sr^{-1}nC^{-1}$	Sensitivity $\mu g.g^{-1}mC^{-1}$	Eγ keV	Assignment	Yield. quanta $sr^{-1}nC^{-1}$	Sensitivity $\mu g.g^{-1}mC^{-1}$
82	^{175}Lu n(1,0)	4	98 500	190	^{176}Lu p(2,1)	110	2 100
82	^{176}Lu p(1,0)			252	^{175}Lu p(2,0)	560	500
114	^{175}Lu p(1,0)	730	470	293	^{176}Lu p(3,2)	4.4	58 800
138	^{175}Lu p(2,1)	290	990	390	^{176}Lu p(4,2)	11	21 300
186	^{175}Lu n(3,0)	105	2 400	597	^{175}Lu p(4,0)	14	19 200

of about 54 keV. Since the intense gamma-rays are of low energy (<300 keV) a high resolution intrinsic germanium detector could be used for measuring both the X-rays and gamma-rays simultaneously and might lead to enhanced sensitivity.

E_p(keV) / E_γ(keV)	Yield (quanta $sr^{-1}nC^{-1}$)					
	3 500	4 000	4 500	5 000	5 500	6 000
114	311	535	730	1 000	1 540	1 960
138	100	190	290	380	640	1 440
186	42	67	105	150	200	275
190	41	67	110	150	184	239
252	200	350	560	790	1 090	1 480

E_γ (keV)	Co-efficients of polynomials fitted to Sensitivity Functions				$S_{min.}/\mu g.g^{-1}$	E_p at $S_{min.}$ (keV)
	a_0	a_1	a_2	a_3		
114	+ 7 591	- 4 192	+ 822	- 54	370	6 000
138	+16 264	- 8 046	+1 375	- 77	800	5 000
186	+14 164	- 4 610	+ 441	0	2 000	5 000
190	+26 744	-12 780	+2 104	-108	1 770	5 000
252	+ 5 707	- 2 914	+ 538	- 33	380	5 000

Hafnium : - Gamma-rays were observed from all six naturally-occurring hafnium isotopes during the bombardment of a lump of pure hafnium metal.

Of the many gamma-rays, some offered potential sensitivity of below the $mg.g^{-1}$ range. Of special merit were those gamma-rays which had identical energies but were formed by different reactions on different isotopes, as was the case for the 172-and 181-keV gamma-rays. Both of these yielded sensitivities of less than 400 $\mu g.g^{-1}$ with 6000 keV protons.

Peaks from the gamma-rays of 207 and 208 keV were integrated together and a sensitivity of 170 $\mu g.g^{-1}$ was calculated at a bombarding energy of 6000 keV.

Gamma-rays of 401,445 and 520 keV remained unassigned.

Eγ keV	Assignment	Yield. quanta $sr^{-1}nC^{-1}$	Sensitivity $\mu g.g^{-1}mC^{-1}$
51	^{174}Hf γ(2,0)	140	13 300
66	Hf k_β	290	4 050
69	^{174}Hf γ(3,0)		
71	^{176}Hf γ(1,0)		
71	^{177}Hf n(1,0)		
87	^{174}Hf γ(4,1)	420	3 300
88	^{176}Hf p(1,0)		
91	^{174}Hf p(1,0)		
93	^{178}Hf p(1,0)		
93	^{180}Hf p(1,0)		
123	^{179}Hf p(1,0)	510	1 850
124	^{174}Hf γ(1,0)		
131	^{177}Hf n(3,0)	180	4 620
131	^{176}Hf γ(3,0)		
133	^{179}Hf n(2,0)		
134	^{178}Hf γ(2,0)		
136	^{180}Hf γ(2,0)		
137	^{177}Hf p(2,1)		
146	^{179}Hf p(3,1)	740	1 150
159	^{180}Hf γ(3,0)	260	6 700
165	^{180}Hf γ(4,2)	320	5 300
172	^{176}Hf γ(4,0)	1 520	490
172	^{177}Hf n(4,0)		
181	^{178}Hf γ(3,0)	2 100	380
181	^{179}Hf n(3,0)		
202	^{176}Hf p(2,1)	2 560	300
203	^{180}Hf γ(5,2)		
207	^{174}Hf p(2,1)	3 370	240
208	^{177}Hf p(3,1)		
210	^{178}Hf γ(6,2)		
215	^{180}Hf p(2,1)	830	910
237	^{178}Hf γ(4,0)	60	7 900
237	^{179}Hf n(4,0)		
249	^{177}Hf p(2,0)	570	1 300
269	^{179}Hf p(3,0)	570	1 270
277	^{177}Hf p(5,1)	620	1 080
301	^{180}Hf γ(4,0)	50	8 300
306	^{178}Hf p(2,0)		
321	^{177}Hf p(3,0)	40	13 000
338	^{180}Hf p(3,2)	80	5 800
339	^{180}Hf γ(5,0)		
344	^{179}Hf n(6,0)		
344	^{178}Hf γ(6,0)		
356	^{178}Hf γ(7,0)	280	2 100
356	^{179}Hf n(7,0)		
375	^{179}Hf p(5,0)	82	6 400
390	^{177}Hf p(5,0)	300	2 000
401	Hf	220	2 700
421	^{179}Hf p(6,0)	80	6 500
426	^{178}Hf p(4,3)	160	3 400
427	^{177}Hf p(7,0)		
445	Hf	120	5 000
520	Hf	250	2 500
548	^{180}Hf p(3,1)	100	6 000
597	^{176}Hf p(3,0)	510	700
608	^{174}Hf p(3,0)	250	2 100
615	^{180}Hf γ(9,0)	220	2 100
632	^{178}Hf p(3,0)	96	6 500
680	^{179}Hf p(15,0)	105	6 900
701	^{179}Hf p(16,0)	200	4 000
708	^{176}Hf p(4,2)	200	3 700
849	^{180}Hf p(6,2)	160	1 600
892	^{180}Hf p(9,2)	115	5 400
983	^{180}Hf p(11,2)	65	8 500
991	^{180}Hf p(4,1)	300	1 250
1046	^{180}Hf p(5,1)	160	3 800
1090	^{180}Hf p(7,1)	120	7 000
1107	^{180}Hf p(9,1)	250	2 500

E_γ (keV) \ E_p (keV)	Yield (quanta $sr^{-1}nC^{-1}$)					
	3 500	4 000	4 500	5 000	5 500	6 000
172	42	505	1 520	2 940	3 460	5 430
181	93	450	2 100	5 210	7 130	10 200
202 + 203	780	1 010	2 560	4 790	5 700	7 980
207 + 208 + 210	340	790	3 370	6 720	8 930	11 200
215	87	247	830	1 290	1 750	2 310
597	250	450	510	1 680	2 520	3 980

E_γ (keV)	Co-efficients of polynomials fitted to Sensitivity Functions				$S_{min.}/\mu g.g^{-1}$	E_p at $S_{min.}$ (keV)
	a_0	a_1	a_2	a_3		
172	+ 63 048	- 36 586	+ 7 100	- 457	370	6 000
181	+ 39 007	- 22 017	+ 4 162	- 262	220	6 000
202, 203	+ 48 712	- 27 333	+ 5 109	- 317	170	6 000
207, 208, 210	+ 45 476	- 25 926	+ 4 929	- 311	190	6 000
215	+778 056	-449 711	+86 180	-5 469	1 010	6 000
597	- 5 249	+ 4 311	- 970	+ 68	390	6 000

Tantalum : - Intense low energy gamma-rays were excited by inelastic scattering during the bombardment of a pure tantalum sheet.

Indications are that use can be made of the 136-keV photopeak for the determination of the element to below the $\mu g.g^{-1}$ level with improving sensitivities at higher bombarding energies. Such analysis, of course, would necessitate that all collimators be replaced with materials other than the tantalum ones used in this investigation.

The lack of gamma-rays of higher energy gave an indication that tantalum would be the useful backing on which other materials could be deposited for analysis by proton-induced prompt gamma-ray spectrometry.

Eγ keV	Assignment	Yield. quanta $sr^{-1}nC^{-1}$	Sensitivity $\mu g.g^{-1}mC^{-1}$	Eγ keV	Assignment	Yield. quanta $sr^{-1}nC^{-1}$	Sensitivity $\mu g.g^{-1}mC^{-1}$
136	^{181}Ta p(2,0)	810	1 020	301	^{181}Ta p(4,0)	170	4 500
165	^{181}Ta p(4,2)	110	6 300				

E_γ (keV) \ E_p (keV)	Yield (quanta $sr^{-1}nC^{-1}$)					
	3 500	4 000	4 500	5 000	5 500	6 000
136	720	805	810	1 090	1 260	1 730
165	27	88	110	320	470	540
301	38	96	170	250	390	670

E_γ (keV)	Co-efficients of polynomials fitted to Sensitivity Functions				$S_{min.}/\mu g.g^{-1}$	E_p at $S_{min.}$ (keV)
	a_0	a_1	a_2	a_3		
136	+17 076	- 8 754	+1 588	- 97	800	6 000
165	+ 4 096	+ 1 844	- 203	- 22	3 100	6 000
301	+44 584	-22 712	+4 445	-304	2 520	6 000

Tungsten : - The three most useful gamma-rays for analysis were those with energies falling within the first 150 keV of the spectrum. Of these the ^{186}W p(1,0) gamma-ray provided the best sensitivity but care had to be taken when using this gamma-ray for the determination of tungsten in a iron matrix because of interference from the ^{57}Fe p(2,1) gamma-ray.

Eγ keV	Assignment	Yield. quanta $sr^{-1}nC^{-1}$	Sensitivity $\mu g.g^{-1}mC^{-1}$	Eγ keV	Assignment	Yield. quanta $sr^{-1}nC^{-1}$	Sensitivity $\mu g.g^{-1}mC^{-1}$
99	^{183}W p(2,0)	105	3 200	292	^{183}W p(4,0)	3	63 900
100	^{182}W p(1,0)			338	^{180}W p(2,0)	3	50 500
104	^{180}W p(1,0)			341	^{186}W p(3,2)		
111	^{184}W p(1,0)	300	1 300	351	^{182}W p(3,2)	12	12 200
122	^{186}W p(1,0)	480	700	585	^{180}W p(3,1)	1	126 000
234	^{180}W p(2,1)	12	13 900	615	^{186}W p(3,1)	19	10 600
236	^{184}W n(6,0)	1	149 000	1121	^{182}W p(4,1)	3	38 800

E_p (keV) / E_γ (keV)	Yield (quanta $sr^{-1}nC^{-1}$)					
	3 500	4 000	4 500	5 000	5 500	6 000
99, 100, 104	58	72	105	180	225	510
111	139	215	300	620	1 230	1 730
122	74	210	480	590	640	1 270
351	1.9	8.9	12	115	305	410
615	2.3	13	19	150	260	350

Because the intense gamma-rays were in the low energy region of the spectrum, where the W X-rays also featured prominently, use could be made of an intrinsic germanium detector to measure the photons. Analysis using these X-rays were carried out using lithium-drifted and intrinsic germanium detectors [Gi 79b].

E_γ (keV)	Co-efficients of polynomials fitted to Sensitivity Functions				$S_{min.}/\mu g.g^{-1}$	E_p at $S_{min.}$ (keV)
	a_0	a_1	a_2	a_3		
99, 100, 104	+ 35 984	- 18 800	+ 3 601	- 231	2 840	6 000
111	+ 6 416	- 3 238	+ 680	- 47.4	1 220	6 000
122	+ 570	+ 194	- 45.1	2.26	630	6 000
351	+496 464	-284 160	55 288	-3 583	7 740	6 000
615	+182 640	- 87 200	14 556	- 819	7 000	6 000

Rhenium : - The data for this element were obtained from the bombardment of targets of the pure metal.

Coulomb excitation of ^{187}Re resulted in the formation of a 72-keV gamma-ray which corresponded closely to the energy of the Re k_β X-rays. The values for yields and sensitivities as given in the tables were based on the nett integrated counts of both the X- and gamma-rays.

E_γ keV	Assignment	Yield. quanta $sr^{-1}nC^{-1}$	Sensitivity $\mu g.g^{-1}mC^{-1}$	E_γ keV	Assignment	Yield. quanta $sr^{-1}nC^{-1}$	Sensitivity $\mu g.g^{-1}mC^{-1}$
70	Re k_β	1 630	880	159	^{185}Re p(2,1)	205	1 960
72	^{187}Re p(2,1)			167	^{187}Re p(3,1)	360	1 180
116	^{187}Re n(5,0)	310	2 310	206	^{187}Re p(2,0)	380	950
125	^{185}Re p(1,0)	1 040	780	285	^{185}Re p(2,0)	39	8 200
134	^{187}Re p(1,0)	1 200	440	301	^{187}Re p(3,0)	74	5 000
137	^{185}Re γ(1,0)			323	^{187}Re γ(2,1)	31	11 200
155	^{187}Re γ(1,0)	180	2 350	359	^{187}Re n(8,3)	51	7 100
157	^{187}Re n(4,3)			512	^{187}Re p(6,0)	510	890

The gamma-ray offering the best sensitivity originated from the decay of the first level of ^{187}Re. The area of the photopeak from the 134-keV ^{187}Re p(1,0) gamma-ray was enhanced by the close-lying photopeak from the ^{185}Re γ(1,0) gamma-ray.

E_γ (keV) \ E_p (keV)	Yield (quanta $sr^{-1}nC^{-1}$)					
	3 500	4 000	4 500	5 000	5 500	6 000
70, 72	870	1 420	1 630	2 100	2 650	3 150
125	420	890	1 040	1 630	2 120	2 730
134, 137	305	720	1 200	1 890	2 210	2 470
167	130	280	360	560	880	1 160
206	145	260	380	480	720	980

E_γ (keV)	Co-efficients of polynomials fitted to Sensitivity Functions				$S_{min.}/\mu g.g^{-1}$	E_p at $S_{min.}$ (keV)
	a_0	a_1	a_2	a_3		
70, 72	- 2 821	+3 113	- 753	+55	540	6 000
125	+11 038	-5 683	+1 049	-65	620	6 000
134, 137	+ 4 284	-2 111	+ 388	-24	360	6 000
167	- 262	+1 595	- 432	+32	740	6 000
206	+12 358	-5 691	+ 960	-55	810	6 000

Osmium : - Powdered osmium was compressed into a pellet which was bombarded to provide the gamma-ray spectra. All the isotopes of this element have close-lying nuclear excitation states of low excitation energy. As a result several of the intense photopeaks represent composite yields from different isotopes.

The X-rays of osmium were useful for analysis not only because of their high yield but also because of the formation of several gamma-rays which combined to give unresolved spectrum peaks of 65 keV and of 72 keV.

Since the photopeaks are within the first 250 keV of the spectrum, a high resolution intrinsic germanium detector could be used for analysis to good effect.

Eγ keV	Assignment	Yield. quanta $sr^{-1}nC^{-1}$	Sensitivity $\mu g.g^{-1}mC^{-1}$
65	Os kα	3 300	240
65	^{187}Os p(2,1)		
70	^{189}Os p(2,0)	3 020	460
72	^{189}Os n(6,4)		
73	Os k_β		
74	^{187}Os p(2,0)		
112	^{187}Os p(5,1)	5.9	47 000
114	^{189}Os n(2,0)		
120	^{184}Os p(1,0)	5.8	50 400
155	^{188}Os p(1,0)	65	4 600
157	^{187}Os p(8,4)		
187	^{189}Os n(4,2)	160	2 000
187	^{188}Os γ(4,2)		
187	^{190}Os p(1,0)		
187	^{187}Os n(3,0)		
187	^{186}Os γ(3,0)		
187	^{187}Os p(6,0)		
188	^{188}Os n(3,0)		
188	^{187}Os γ(3,0)		
189	^{187}Os p(7,0)		
189	^{189}Os p(4,1)		
206	^{192}Os p(1,0)	230	1 400
219	^{189}Os p(4,0)	21	12 600
223	^{189}Os n(5,1)		
281	^{188}Os n(5,0)	4.7	56 400
281	^{187}Os γ(5,0)		
283	^{192}Os p(2,1)		
297	^{186}Os p(2,1)	2.2	94 100
354	^{186}Os p(12,7)	3.9	61 500
375	^{192}Os p(3,1)	2.9	84 700
396	^{190}Os p(5,3)	1.4	160 000
420	^{192}Os p(5,2)	1.7	152 000
435	^{186}Os p(4,2)	3.2	95 900
462	^{188}Os p(4,2)	2.9	92 700
478	^{188}Os p(3,1)	2.6	108 000
487	^{190}Os p(5,2)	9.4	42 600
487	^{188}Os n(7,0)		
487	^{187}Os γ(7,0)		
489	^{192}Os p(2,0)		
490	^{186}Os p(11,6)		
491	^{187}Os p(8,1)		
530	^{187}Os n(13,5)	0.6	179 000
530	^{186}Os γ(13,5)		
557	^{186}Os p(12,6)	4.0	73 400
558	^{190}Os p(3,0)		
568	^{190}Os p(4,1)	1.2	210 000
569	^{192}Os p(12,8)		
580	^{192}Os p(6,2)	9.4	48 300
608	^{189}Os n(11,1)	11.4	43 900
608	^{188}Os γ(11,1)		
630	^{186}Os p(3,1)	1.4	210 000
633	^{188}Os p(3,0)		
743	Os	1.7	250 000
767	^{190}Os p(5,1)	2.1	185 000
767	^{186}Os p(3,0)		

E_γ (keV) \ E_p (keV)	Yield (quanta $sr^{-1}nC^{-1}$)					
	3 500	4 000	4 500	5 000	5 500	6 000
65	1 650	1 960	3 300	4 510	6 270	8 990
70, 72, 73, 74	1 490	2 170	3 020	4 750	6 190	9 130
155, 157	17	34	65	86	225	540
187, 188, 189	50	80	160	320	610	900
206	110	180	230	360	540	910

E_γ (keV)	Co-efficients of polynomials fitted to Sensitivity Functions				$S_{min.}/\mu g.g^{-1}$	E_p at $S_{min.}$ (keV)
	a_0	a_1	a_2	a_3		
65	+ 5.5	+ 290	- 79	+ 5.9	160	6 000
70, 72, 73, 74	+ 4 570	- 2 385	+ 470	- 32	300	6 000
155, 157	+ 8 068	+ 4 276	-1 697	+132	1 010	6 000
187, 188, 189	+43 464	-21 684	-3 795	-226	1 110	6 000
206	- 312	+ 2 804	- 835	+ 67	890	6 000

Iridium : - Bombardment of iridium metal resulted in a small flux of low energy Coulomb-excited gamma-rays. The energy of the first excited state of ^{193}Ir co-incided exactly with that of the Ir K_β X-rays, therefore the data for yield and sensitivity in the tables represent the combined value of both gamma- and X-rays. This was also the case for the 67-keV gamma-ray, the peak of which overlapped with that of the K_α X-ray of iridium. In order to use the low energy photons efficiently, the intrinsic germanium detector would be preferred.

Eγ keV	Assignment	Yield. quanta $sr^{-1}nC^{-1}$	Sensitivity $\mu g.g^{-1}mC^{-1}$	Eγ keV	Assignment	Yield. quanta $sr^{-1}nC^{-1}$	Sensitivity $\mu g.g^{-1}mC^{-1}$
67	^{193}Ir p(3,1)	5 400	110	299	^{193}Ir p(5,0)	23	8 400
73	^{193}Ir p(1,0)	1 760	330	343	^{191}Ir p(5,0)	34	5 700
129	^{191}Ir p(2,0)	61	4 900	351	^{191}Ir p(6,0)	30	6 600
139	^{193}Ir p(3,0)	115	2 200	358	^{193}Ir p(6,0)	66	3 300
214	^{191}Ir p(4,2)	51	6 200	391	^{191}Ir p(7,0)	4	90 500
219	^{193}Ir p(5,2)	57	5 700	588	^{191}Ir p(9,0)	7	49 000

E_γ(keV) \ E_p(keV)	Yield (quanta $sr^{-1}nC^{-1}$)					
	3 500	4 000	4 500	5 000	5 500	6 000
67	1 470	3 300	5 400	10 100	15 800	17 400
73	540	1 100	1 760	3 300	5 100	8 400
129	34	53	61	105	135	172
139	46	87	115	190	260	310
358	17	29	66	83	87	92

E_γ (keV)	Co-efficients of polynomials fitted to Sensitivity Functions				$S_{min.}/\mu g.g^{-1}$	E_p at $S_{min.}$ (keV)
	a_0	a_1	a_2	a_3		
67	+ 1 138	- 375	+ 33	0	62	5 750
73	+ 2 644	- 775	+ 59	0	120	6 000
129	-48 016	+35 892	-7 767	+534	2 980	6 000
139	+13 339	- 3 827	+ 302	0	1 240	6 000
358	+41 654	-13 158	+1 086	0	1 840	6 000

Platinum : - Gamma-rays were observed from excitation of levels of most of the stable isotopes, although the very low abundant ^{190}Pt was not detected. Decay of the first levels of ^{194}Pt and ^{196}Pt resulted in analytically significant gamma-

Eγ keV	Assignment	Yield. quanta $sr^{-1}nC^{-1}$	Sensitivity $\mu g.g^{-1}mC^{-1}$	Eγ keV	Assignment	Yield. quanta $sr^{-1}nC^{-1}$	Sensitivity $\mu g.g^{-1}mC^{-1}$
173	^{192}Pt p(3,2)	53	10 800	407	^{198}Pt p(1,0)	160	3 500
211	^{195}Pt p(4,0)	290	1 870	587	^{192}Pt p(5,2)	21	31 500
239	^{195}Pt p(5,0)	170	2 500	608	^{194}Pt p(5,2)	17	37 300
329	^{194}Pt p(1,0)	1 410	390	612	^{192}Pt p(2,0)		
356	^{196}Pt p(1,0)	960	490	908	^{196}Pt p(6,1)	20	32 000

rays of 329 and 356 keV respectively. Both these photons offered a sensitivity of about 500 $\mu g.g^{-1}$. The Pt X-rays again featured prominently and could be used for platinum determinations.

E_γ (keV) \ E_p (keV)	Yield (quanta $sr^{-1}nC^{-1}$)					
	3 500	4 000	4 500	5 000	5 500	6 000
211	190	260	290	380	590	900
239	50	110	170	180	205	290
329	650	1 140	1 410	2 050	2 820	3 330
356	3 690	710	960	1 410	1 770	2 250
407	60	110	160	290	410	830

E_γ (keV)	Co-efficients of polynomials fitted to Sensitivity Functions				$S_{min.}/\mu g.g^{-1}$	E_p at $S_{min.}$ (keV)
	a_0	a_1	a_2	a_3		
211	+ 2 230	+ 222	- 94	+ 6.9	1 640	6 000
239	+209 536	-22 140	+23 512	-1 469	2 140	4 470
329	+ 14 983	- 8 543	+ 1 647	- 103	380	4 680
356	+ 8 725	- 4 840	+ 924	- 58	390	4 500
407	+ 97 872	-52 804	+ 9 833	- 616	2 110	6 000

Gold : - This noble metal has a single natural isotope of mass 197 . Several levels of gold was excited by Coulomb excitation. The energy of the first excited state co-incided exactly with that of the gold k_β X-rays so that the data given for yield and sensitivity are the sum of both gamma and X-rays.

Promiment photopeaks were recorded corresponding to the decay of the 3rd and 6th excited level at 279 keV and 548 keV respectively. The level at 409 keV had a parity of $^{1}1/2^-$ compared to $3/2^+$, $1/2^+$, $3/2^+$ and $5/2^+$ of the ground and the first three excited states respectively and, thus it was not excited by proton inelastic scattering. The existence of the fifth level at 502 keV was not well established [Ha 77] and therefore failure to observe any gamma-rays from this level was not surprising.

The p(1,0) gamma-rays of ^{198}Hg, ^{199}Hg, ^{200}Hg and ^{202}Hg offered the best sensitivities for analysis though the sensitivities attained were no better than 1200 $\mu g.g^{-1}$. This value was calculated from the combined yields of four gamma-rays having energies between 364 and 368 keV.

The K_β X-rays of mercury also formed a doublet with a gamma-ray of 82 keV. Since these two photopeaks could not be stripped from each other, they were integrated together providing a sensitivity of 500 $\mu g.g^{-1}$ at a bombarding energy of 6000 keV.

Eγ keV	Assignment	Yield. quanta $sr^{-1}nC^{-1}$	Sensitivity $\mu g.g^{-1}mC^{-1}$	Eγ keV	Assignment	Yield. quanta $sr^{-1}nC^{-1}$	Sensitivity $\mu g.g^{-1}mC^{-1}$
80	Hg k_β	470	620	426	^{196}Hg p(1,0)	96	1 800
82	^{200}Hg p(3,2)			440	^{202}Hg p(1,0)	240	1 300
158	^{199}Hg p(1,0)	20	9 800	491	^{202}Hg p(4,0)	22	9 900
208	^{199}Hg p(2,0)	2.7	43 300	491	^{202}Hg n(4,0)		
248	^{199}Hg p(5,2)	18	12 700	543	^{203}Hg p(4,0)	58	4 200
285	^{199}Hg p(6,2)	22	8 500	579	^{200}Hg p(2,1)	8.3	23 300
315	^{202}Hg n(2,0)	43	3 100	588	^{201}Hg n(3,1)	12	16 700
331	^{201}Hg n(1,0)	39	3 400	608	^{196}Hg γ(2,0)	4.8	76 700
351	^{202}Hg n(3,0)	21	8 800	611	^{196}Hg p(2,1)		
364	^{202}Hg γ(4,0)	190	1 400	787	^{202}Hg γ(4,1)	14	18 300
367	^{198}Hg γ(1,0)			1029	^{200}Hg p(3,0)	6.7	52 300
367	^{199}Hg n(1,0)			1121	^{199}Hg n(3,0)	8.4	46 000
368	^{200}Hg p(1,0)						
386	^{196}Hg γ(1,0)	4.4	45 000				
412	^{198}Hg p(1,0)	120	2 400				

E_p(keV) / E_γ(keV)	Yield (quanta $sr^{-1}nC^{-1}$)					
	3 500	4 000	4 500	5 000	5 500	6 000
80	210	360	470	585	720	940
315	9.8	25	43	57	78	125
364, 367, 368	59	92	190	210	340	515
412	39	48	120	190	265	340
426	36	75	96	120	180	240
440	45	170	240	325	515	760

E_γ (keV)	Co-efficients of polynomials fitted to Sensitivity Functions				$S_{min.}/\mu g.g^{-1}$	E_p at $S_{min.}$ (keV)
	a_0	a_1	a_2	a_3		
80	- 1 504	+ 1 570	- 354	+ 24.8	520	6 000
315	+78 136	-42 036	+ 7 853	-491	2 540	6 000
364, 367, 368	- 206	+ 2 386	- 712	+ 59.2	1 230	6 000
412	+94 888	-53 590	+10 302	-659	1 840	6 000
426	+ 6 396	- 1 756	+ 188	- 5.3	1 490	6 000
440	+11 038	- 5 893	+ 1 172	- 76.3	1 300	4 500

Thallium : - Gamma-rays from both stable isotopes of thallium were observed when a tablet of thallium sulphate was bombarded. The gamma-rays were of low intensity and offered poor sensitivities.

Eγ keV	Assignment	Yield. quanta $sr^{-1}nC^{-1}$	Sensitivity $\mu g.g^{-1}mC^{-1}$	Eγ keV	Assignment	Yield. quanta $sr^{-1}nC^{-1}$	Sensitivity $\mu g.g^{-1}mC^{-1}$
89	^{203}Tl γ(9,8)	37	10 900	441	^{205}Tl n(4,2)	45	3 100
185	^{205}Tl n(5,3)	19	19 500	619	^{205}Tl p(3,0)	7.8	17 400
187	^{203}Tl n(2,0)			663	^{203}Tl γ(4,1)	10	61 800
209	^{203}Tl γ(4,3)	100	5 800	663	^{205}Tl γ(4,1)		
225	^{203}Tl n(4,3)	65	7 300	680	^{203}Tl n(6,2)	5.4	38 100
236	^{205}Tl γ(6,4)	63	7 500	681	^{203}Tl p(2,0)		
261	^{205}Tl n(2,1)	120	4 300	699	^{203}Tl n(5,1)	22	35 400
272	^{203}Tl n(6,3)	92	5 000	710	^{203}Tl n(7,2)	30	24 500
279	^{203}Tl p(1,0)	125	3 600	740	^{203}Tl n(6,1)	30	24 600
296	^{205}Tl n(8,4)	41	9 900	761	^{205}Tl n(4,0)	35	11 700
308	^{203}Tl γ(5,2)	12	9 900	765	^{203}Tl p(3,1)	27	20 200
317	^{205}Tl γ(7,4)	9.1	13 400	770	^{203}Tl n(7,1)	28	26 300
338	^{203}Tl n(8,3)	7.4	17 300	803	^{205}Tl γ(1,0)	41	25 500
401	^{203}Tl p(2,1)	15	8 700	1663	^{205}Tl γ(7,0)	43	22 700
409	^{203}Tl n(3,2)	13	8 500				

E_γ (keV) \ E_p (keV)	Yield (quanta $sr^{-1}nC^{-1}$)					
	3 500	4 000	4 500	5 000	5 500	6 000
209	24	73	100	125	140	175
261	17	63	120	140	170	210
272	18	35	92	100	110	160
279	23	74	125	170	220	270
441	9.8	31	45	57	73	88

E_γ (keV)	Co-efficients of polynomials fitted to Sensitivity Functions				$S_{min.}/\mu g.g^{-1}$	E_p at $S_{min.}$ (keV)
	a_0	a_1	a_2	a_3		
209	+19 944	- 3 604	- 41	+ 28	3 200	6 000
261	+14 440	- 4 236	+ 550	- 24	3 670	6 000
272	+32 912	-15 108	+2 710	-163	4 770	6 000
279	+ 9 952	- 2 640	+ 386	- 24	2 800	6 000
441	+85 752	-43 508	+7 589	-440	2 700	6 000

Lead : - Elemental lead was bombarded but all the gamma-rays were of low intensity and served little analytical use.

$E\gamma$ keV	Assignment	Yield. quanta $sr^{-1}nC^{-1}$	Sensitivity $\mu g.g^{-1}mC^{-1}$	$E\gamma$ keV	Assignment	Yield. quanta $sr^{-1}nC^{-1}$	Sensitivity $\mu g.g^{-1}mC^{-1}$
446	^{208}Pb n(1,0)	20	6 980	570	^{207}Pb p(1,0)	2.3	42 300
510	^{208}Pb n(2,0)	110	1 380	603	^{208}Pb n(3,0)	4.5	30 400

E_γ (keV) \ E_p (keV)	Yield (quanta $sr^{-1}nC^{-1}$)					
	3 500	4 000	4 500	5 000	5 500	6 000
443	7.3	14	20	25	32	37
569	1.1	1.6	2.3	4.5	5.8	7.9
603	2.0	3.7	4.5	6.9	8.9	12

E_γ (keV)	Co-efficients of polynomials fitted to Sensitivity Functions				$S_{min.}/\mu g.g^{-1}$	E_p at $S_{min.}$ (keV)
	a_0	a_1	a_2	a_3		
443	+ 33 440	- 10 228	+ 1 158	- 49	3 220	6 000
569	+962 624	-492 288	+88 247	-5 375	26 700	6 000
603	+180 512	-719 040	+11 768	- 710	20 800	6 000

Bismuth : - A pure bismuth target was irradiated for the study of gamma-rays of the element. Gamma-rays were emitted as a result of Coulomb excitation of ^{209}Bi but in addition there were gamma-rays from $^{209}Bi(p,n\gamma)^{209}Po$ and from proton-capture reactions.

All the gamma-rays were of low intensity and of little analytical significance.

Eγ keV	Assignment	Yield. quanta $sr^{-1}nC^{-1}$	Sensitivity $\mu g.g^{-1}mC^{-1}$	Eγ keV	Assignment	Yield. quanta $sr^{-1}nC^{-1}$	Sensitivity $\mu g.g^{-1}mC^{-1}$
80	^{209}Bi γ(4,3)	3.2	101 000	816	^{209}Bi n(13,3)	20	23 100
82	^{209}Bi n(6,5)			863	^{209}Bi n(6,1)	5.6	84 900
146	^{209}Bi n(8,5)	52	5 900	873	^{209}Bi n(7,1)	31	16 300
195	^{209}Bi n(9,5)	27	12 100	896	^{209}Bi p(1,0)	82	6 300
195	^{209}Bi n(6,4)			992	^{209}Bi p(6,2)	6.8	43 000
242	^{209}Bi n(7,3)	50	6 100	1139	^{209}Bi γ(7,1)	33	12 400
246	^{209}Bi γ(2,1)	2.8	150 000	1213	^{209}Bi n(4,0)	23	11 500
292	^{209}Bi γ(3,1)	13	24 300	1327	^{209}Bi n(5,0)	38	8 700
297	^{209}Bi n(8,3)	4.9	80 400	1418	^{209}Bi n(7,0)	16	30 100
520	^{209}Bi n(12,7)	3.5	99 000	1609	^{209}Bi p(2,0)	39	14 000
545	^{209}Bi n(1,0)	5.2	61 600	1687	^{209}Bi p(5,1)	5.6	82 600
753	^{209}Bi γ(5,2)	68	7 500	2061	^{209}Bi n(15,0)	18	19 900

E_γ (keV) \ E_p (keV)	Yield (quanta $sr^{-1}nC^{-1}$)					
	3 500	4 000	4 500	5 000	5 500	6 000
146	9.8	19	52	73	84	105
242	12	27	50	63	89	140
753	21	48	68	93	110	160
896	7.3	26	82	140	205	270
1327	3.6	15	38	51	83	120

E_γ (keV)	Co-efficients of polynomials fitted to Sensitivity Functions				$S_{min.}/\mu g.g^{-1}$	E_p at $S_{min.}$ (keV)
	a_0	a_1	a_2	a_3		
146	+ 82 704	- 35 576	+ 5 402	- 274	4 660	6 000
242	+ 60 261	- 19 679	+ 1 712	0	3 730	6 000
753	+248 816	-135 384	+25 190	-1 557	6 940	6 000
896	+158 704	- 89 378	+17 370	-1 121	5 950	6 000
1327	+ 12 790	- 912	+ 22	0	8 050	6 000

Thorium : - A pellet of thorium nitrate, $Th(NO_3)_4$, was irradiated to produce the gamma-ray spectra of thorium. This element is mono-isotopic in nature and the gamma-rays that were generated were either from Coulomb excitation or from proton-capture. Since the levels of the isotope are very close-lying, a large number of gamma-rays were excited, but most of them were not intense.

Sensitivities of below 1000 $\mu g.g^{-1}$ were achieved using some of the Coulomb excited gamma-rays with the expectation of better sensitivities for higher energy proton beams.

E_γ keV	Assignment	Yield. quanta $sr^{-1}nC^{-1}$	Sensitivity $\mu g.g^{-1}mC^{-1}$	E_γ keV	Assignment	Yield. quanta $sr^{-1}nC^{-1}$	Sensitivity $\mu g.g^{-1}mC^{-1}$
64	^{232}Th γ(3,1)	180	6 300	681	^{232}Th p(5,1)	2 500	390
113	^{232}Th p(2,1)	250	2 800	714	^{232}Th p(4,0)	49	20 200
131	^{232}Th γ(12,3)	27	18 100	725	^{232}Th p(6,1)	105	8 600
163	^{232}Th γ(8,0)	600	1 100	774	^{232}Th p(6,0)	800	1 400
169	^{232}Th γ(9,0)	160	3 400	780	^{232}Th p(8,0)	890	1 300
273	^{232}Th γ(16,0)	320	1 800	824	^{232}Th p(9,1)	420	2 400
290	^{232}Th γ(17,0)	140	4 700	890	^{232}Th p(12,0)	730	1 300
304	^{232}Th γ(20,0)	130	3 700	943	^{232}Th p(13,2)	540	1 610
310	^{232}Th γ(23,2)	55	10 700	981	^{232}Th p(19,2)	3 700	270
320	^{232}Th γ(24,4)	73	7 900	1029	^{232}Th p(15,1)	3 750	260
380	^{232}Th γ(27,3)	220	3 800	1056	^{232}Th p(20,1)	310	2 800
447	^{232}Th γ(26,0)	240	3 100	1076	^{232}Th p(18,1)	1 120	1 000
519	^{232}Th γ(30,1)	57	13 600	1122	^{232}Th p(18,0)	110	10 000
529	^{232}Th γ(31,0)	76	10 200	1143	^{232}Th p(21,0)	460	1 900
569	^{232}Th γ(34,0)	82	8 700	1338	^{232}Th p(26,1)	150	6 100
586	^{232}Th γ(36,0)	390	2 400	1392	^{232}Th p(32,2)	230	3 900
612	^{232}Th p(6,2)	84	11 400	1440	^{232}Th p(30,1)	870	1 400
627	^{232}Th p(12,3)	72	13 200	1448	^{232}Th p(37,2)	290	2 400
665	^{232}Th p(4,1)	465	2 100				

E_γ (keV) \ E_p (keV)	Yield (quanta $sr^{-1}nC^{-1}$)					
	3 500	4 000	4 500	5 000	5 500	6 000
163	210	460	600	720	930	1 100
681	160	270	465	540	610	640
981	2 200	2 710	3 700	4 210	4 830	5 730
1029	2 005	2 730	3 750	4 380	5 430	7 110
1076	810	970	1 120	1 420	1 780	2 370

E_γ (keV)	Co-efficients of polynomials fitted to Sensitivity Functions				$S_{min.}/\mu g.g^{-1}$	E_p at $S_{min.}$ (keV)
	a_0	a_1	a_2	a_3		
163	+53 954	-28 666	+5 156	+308	920	6 000
681	+ 4 684	- 1 925	+ 264	- 10	340	5 000
981	+13 142	- 7 212	+1 345	- 84	160	6 000
1029	+17 023	- 9 578	+1 821	-116	150	6 000
1076	+51 128	-27 192	+4 900	-294	800	6 000

Uranium : - The spectrum of uranium dioxide (UO_2) revealed the presence of several gamma-rays concentrated in the low energy region (i.e.< 300 keV). These gamma-rays were of low intensity and offered poor sensitivity for the analysis of uranium.

Eγ keV	Assignment	Yield. quanta $sr^{-1}nC^{-1}$	Sensitivity $\mu g.g^{-1}mC^{-1}$	Eγ keV	Assignment	Yield. quanta $sr^{-1}nC^{-1}$	Sensitivity $\mu g.g^{-1}mC^{-1}$
68	^{235}U n(7,6)	4.7	53 200	122	^{235}U n(7,3)	23	10 400
68	^{234}U γ(7,6)			122	^{234}U γ(7,3)		
79	^{235}U n(3,0)	7.5	44 900	133	^{235}U n(5,0)	14	15 400
79	^{234}U γ(3,0)			133	^{234}U γ(5,0)		
92	^{235}U n(4,0)	85	4 800	152	^{235}U n(7,2)	25	7 500
92	^{234}U γ(4,0)			152	^{234}U γ(7,2)		
98	^{235}U n(6,2)	140	2 900	167	^{235}U n(7,1)	22	10 200
98	^{234}U γ(6,2)			167	^{234}U γ(7,1)		
98	U kα			189	^{235}U p(25,13)	70	5 100
99	^{235}U n(5,1)			201	^{235}U n(6,0)	8.3	27 200
99	^{234}U γ(5,1)			201	^{234}U γ(6,0)	60	5 200
109	^{235}U n(7,4)	150	2 400	232	U	30	17 300
109	^{234}U γ(7,4)			241	^{238}U γ(9,0)		
113	^{235}U n(6,1)	150	2 100				
113	^{234}U γ(6,1)						
113	U k_β						

E_γ(keV) \ E_p(keV)	Yield (quanta $sr^{-1}nC^{-1}$)					
	3 500	4 000	4 500	5 000	5 500	6 000
92	34	42	85	160	210	240
98, 99	16	28	140	140	180	220
109	40	80	150	175	220	270
189	35	64	70	125	170	210
232	12	22	60	75	85	110

E_γ (keV)	Co-efficients of polynomials fitted to Sensitivity Functions				$S_{min.}/\mu g.g^{-1}$	E_p at $S_{min.}$ (keV)
	a_0	a_1	a_2	a_3		
92	+115 880	-53 696	+8 373	-417	4 800	4 500
98, 99	+ 91 236	-42 016	+6 430	-320	1 330	6 000
109	+ 49 912	-27 528	+5 304	-341	2 000	6 000
189	+ 27 808	-11 660	+1 994	-119	4 100	6 000
232	+ 28 528	- 3 444	-1 160	+170	2 970	6 000

CHAPTER 4

STEEL ANALYSIS

The inclusion of minor components in steel alloys changes the characteristics of the metal and enables specialized steels to be made with properties to suit the purpose for which the steel is used. As a result, a wide range of steel types is produced with a variety of minor elements in concentrations ranging from a few tenths of a part per million to several per cent. Obviously, therefore, the elemental composition of steels is important for the steel industry, and fast methods of analysis will be favoured, not only because they can contribute to the control of production, but also because of the large volume of analyses that have to be carried out.

The attractiveness of non-destructive methods and the ability to perform simultaneous multi-element determinations has led to an extensive application of nuclear techniques. In the past, neutron activation analysis [Ho 61] and particle-induced X-ray emission spectrometry (PIXE) [Ah 77] have become established methods of analysis and more recently the method of charged particle induced prompt gamma-ray spectrometry has found application. [Gi 78a]. Of these methods, the duration of the analysis by neutron activation will largely be determined by the half-life of the generated radioactive nuclide, and in general such analyses will be time-consuming when used as a multi-elemental technique, because it is unlikely that all the required elements will yield short-lived radioactive products. By contrast, the real time required for charged particle activation analysis using prompt X-rays or gamma-rays is usually short and is determined by the precision required and the elemental concentration measured. The experimental tehcnique most often used for these analyses is that of energy-dispersive spectrometry and has the important advantages of selectivity, sensitivity, speed and ease of application, in addition to being multi-elemental and non-destructive.

A comparison [Gi 80] of accuracy, precision and sensitivity between proton-induced X-ray excitation and alpha-induced prompt gamma-ray excitation had shown that in the determination of vanadium, chromium, manganese, molybdenum and tungsten, both methods were equally accurate, but the latter was superior with regard to precision and sensitivity when applied to the analysis of steels. Despite this result, it was considered that further improvement in sensitivity could be attained if protons were used to generate prompt gamma-rays. However, a compilation [De 78] of the yields of prompt gamma-rays from the light elements (Ti to Zn) under proton bombardment failed to support such an assumption because the proton energies used were limited to about 3000 keV. At this energy the cross-sections for nuclear reaction with the elements under consideration, and hence the expected gamma-ray yields, were low. The present investigation was undertaken as part of a study on the analytical application of prompt gamma-rays induced by protons between 3500 and 6000 keV.

From the survey results it was apparent that for most elements of the first transition group, optimal sensitivity was attained for $4000 < E_p < 4500$ keV. Subsequently, the determination of silicon, vanadium, chromium, manganese and cobalt was performed with 4000 keV and 4500 keV protons.

RESULTS

The spectrum from the bombardment of the standard steel D837, with protons of 4000 keV and measured with a Ge(Li) detector is shown in Figure 7. The identity and origin of the numbered peaks in the spectrum are listed below the spectrum in Table 3. A spectrum of the same steel but measured with an intrinsic germanium detector is shown in Figure 8.

SILICON

Silicon is a desirable alloying element in steels because it improves the tensile stress and abrasion resistance and at the same time it diminishes the conductivity with a result that the

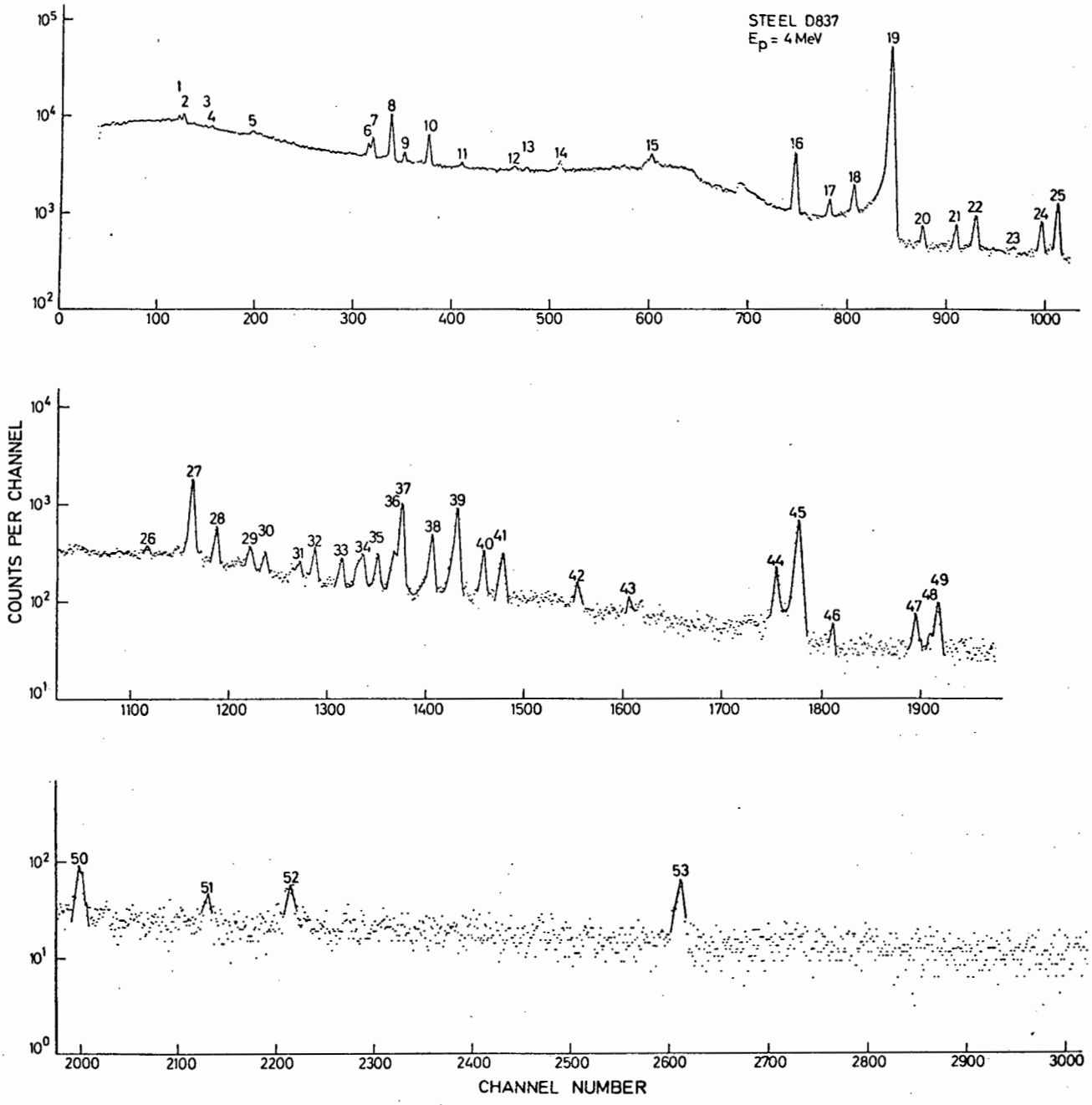

FIGURE 7 : Prompt gamma-ray spectrum from the irradiation of the standard steel D837 with 4000-keV protons measured with a Ge(Li) detector. The identity of peaks as marked in the figure, are given in Table 3.

TABLE 3 : Identity of peaks as marked in Figure 7.

Element	Gamma-ray Energy (keV)	Assignment	Peak number	Remarks
Aluminium	844	^{27}Al p(1,0)	19	
	1015	^{27}Al p(2,0)	25	
	1367	^{27}Al p(3,1)	36	

TABLE 3 (Continued)

Element	Gamma-ray Energy (keV)	Assignment	Peak number	Remarks
Silicon	1273	^{29}Si p(1,0)	31	
	1779	^{28}Si p(1,0)	45	used for analysis
	2240	^{30}Si p(1,0)	52	
Titanium	320	^{50}Ti n(2,0)	7	
	983	^{48}Ti p(1,0)	24	
	1552	^{47}Ti p(1,0)	42	
Vanadium	316	^{51}V n(5,3)	6	used for analysis
	320	^{51}V p(1,0)	7	used for analysis
	609	^{51}V p(2,1)	15	see also Ge
	750	^{51}V n(1,0)	16	used for analysis
	1165	^{51}V n(3,0)	26	used for analysis
	1353	^{51}V n(4,0)	35	used for analysis
	1481	^{51}V p(5,0)	41	used for analysis
	2001	^{51} n(7,0)	50	
Chromium	156	^{54}Cr n(2,0)	4	
	378	^{53}Cr n(1,0)	10	used for analysis
	783	^{50}Cr p(1,0)	17	used for analysis
	911	^{53}Cr n(2,1)	21	used for analysis
	1288	^{53}Cr n(2,0)	32	see also Co
	1440	^{52}Cr p(1,0)	40	used for analysis
	1619	^{53}Cr n(4,1)	43	used for analysis
	1894	^{53}Cr n(5,1)	47	
Manganese	126	^{55}Mn p(1,0)	2	see also Fe
	411	^{55}Mn n(1,0)	11	used for analysis
	471	^{55}Mn n(4,2)	13	used for analysis
	803	^{55}Mn n(8,4)	18	
	931	^{55}Mn n(2,0)	22	used for analysis
	1214	^{55}Mn n(7,2)	28	
	1316	^{55}Mn n(3,0)	33	used for analysis
	1408	^{55}Mn n(4,0)	38	see also Fe
	1918	^{55}Mn n(5,0)	48	
Iron	126	^{56}Fe γ(3,2)	2	
	352	^{56}Fe p(3,1)	9	
	846	^{56}Fe p(1,0)	19	
	1224	^{57}Fe n(2,0)	29	
	1237	^{56}Fe p(2,1)	30	
	1377	^{57}Fe n(2,0)	37	
	1408	^{54}Fe p(1,0)	38	
	1757	^{56}Fe n(5,0)	44	
	1810	^{56}Fe p(3,1)	46	
	2133	^{57}Fe n(7,0)	51	

TABLE 3 (Continued)

Element	Gamma-ray Energy (keV)	Assignment	Peak number	Remarks
Cobalt	339	^{59}Co n(1,0)	8	used for analysis
	878	^{59}Co n(3,0)	20	used for analysis
	1189	^{59}Co n(4,0)	27	used for analysis
	1288	^{59}Co p(3,0)	32	see also Cr
	1337	^{59}Co n(6,1)	34	used for analysis
	1432	^{59}Co p(4,0)	39	
	1948	^{59}Co n(11,0)	49	used for analysis
Tantalum	136	^{181}Ta p(1,0)	3	
Tungsten	122	^{186}W p(1,0)	1	
Background	198	^{19}F p(2,1)	5	
	466	^{208}Pb	12	
	511	β^+	14	
	970	^{227}Ac	23	
	2614	^{208}Bi	53	

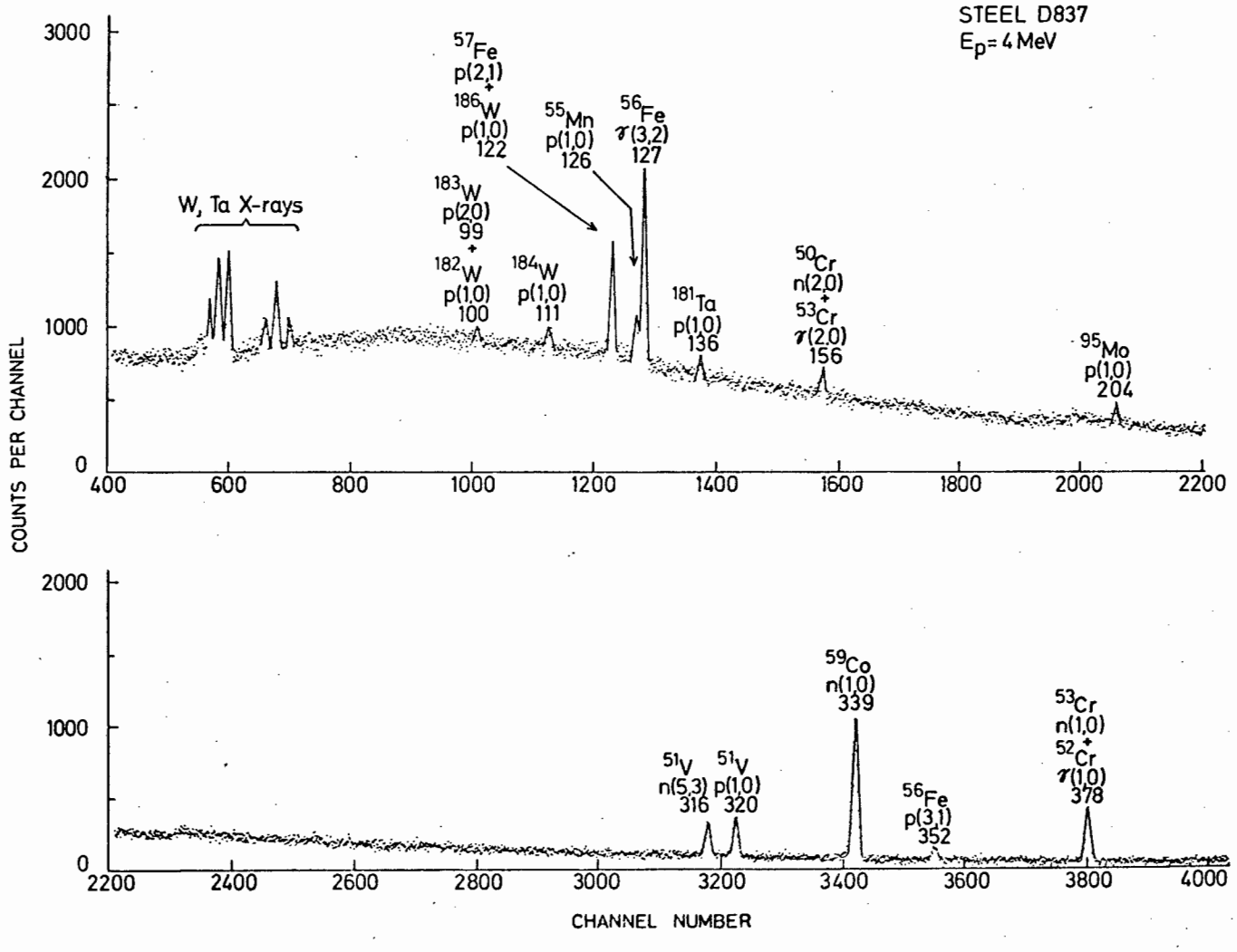

FIGURE 8 : Prompt photon spectrum of the same steel as that in Figure 7, but recorded with an intrinsic germanium detector

steel can be used for electric sheeting. The use of the 1779-keV ^{28}Si p(1,0) gamma-ray for the analysis of silicon had a good potential sensitivity. This gamma-ray was, therefore, used for the determination of silicon in steels, not as a separate study, but as part of the simultaneous analysis of the various components of steels.

Results and discussion

The most serious potential sources of interference with the 1779-keV gamma-ray was from proton-capture on ^{27}Al and the (p,αγ) reaction on ^{31}P, both of which could form excited ^{28}Si, and hence yield the same gamma-ray. However, aluminium and phosphorus were not present in the steels in any significant concentrations and therefore they did not pose any interference.

Because the stopping power of protons differs from one matrix to another it was required to correct the gamma-ray yields for the matrix effect. The $\underline{E}_m$ values (see page 13), needed to apply the method of average stopping power [Is 78a], were calculated from the excitation function for the production of the 1779-keV gamma-ray and are given in Table 4.

E_p (KeV)	E_m (KeV)	E_p (KeV)	E_m (KeV)
2500	2063	4000	3341
2600	2094	4100	3309
2700	2132	4200	3400
2800	2164	4300	3516
2900	2221	4400	3617
3000	2363	4500	3723
3100	2409	4600	3774
3200	2514	4700	3839
3300	2627	4800	3900
3400	2734	4900	3947
3500	2841	5000	4010
3600	2933	5100	4132
3700	3040	5200	4218
3800	3138	5300	4313
3900	3212		

TABLE 4 : $\underline{E}_m$ values for silicon determination

Precision, sensitivity and accuracy of the determination were evaluated from the analysis of 11 standard steel samples. The results, shown in Table 5, were the mean values of 4 or 5 replicate analyses on each steel. The known silicon content was the certified values obtained from the U.S. Bureau of Standards. In column 3 are the nett counts per millicoulomb of charge, being the mean value obtained from several irradiations. To compare the gamma-ray yield from different steels, the values in column 4 are expressed per unit silicon content.

The mean value obtained from 48 observations was 13796 ± 300 counts per mC for 1% Si by mass. This value was in agreement with the slope of the calibration line of 13780 counts per mC obtained by the method of least squares. The relative precision of the determination over the concentration range of 0.14 to 0.74 % Si by mass, was 2.1% as given by the relative standard error. A measure of the sensitivity of analysis could be obtained from the root mean square error of 0.0076 % which implied that the method might be used for Si concentrations to below 100 $\mu g.g^{-1}$. A comparison of the statistical data using 4000 keV and 4500 keV proton beams for analysis is given in Table 6.

Steel	Known (% Si)	Mean Count (mC^{-1})	Mean Count (mC^{-1} for 1% Si)	Number of Analyses	Found (% Si)	Error Absolute	Error Relative
D840	0.14	1 902	13 050	4	0.137	-0.003	-1.6
D841	0.16	2 180	13 627	4	0.158	-0.002	-1.1
D838	0.17	2 318	13 632	4	0.168	-0.002	-1.2
D839	0.21	2 953	14 061	4	0.213	+0.003	+1.8
1261	0.223	3 054	13 696	4	0.222	-0.001	-0.7
1262	0.390	5 326	13 657	4	0.386	-0.004	-1.0
1185	0.40	5 445	13 613	5	0.395	-0.005	-1.3
D837	0.53	7 463	14 089	5	0.541	+0.011	+2.1
1171	0.54	7 571	14 021	5	0.549	+0.009	+1.6
1172	0.59	8 269	14 015	5	0.599	+0.009	+1.6
1263	0.74	10 076	13 620	4	0.731	-0.009	-1.3

No. of Analyses	=	48
Mean count (mC^{-1} for 1% Si)	=	13 796 ± 300
Relative Standard Error (%)	=	2.1
Root Mean Square Error (%)	=	0.0076 Si by mass

TABLE 5 : Determination of silicon in standard steels using the gamma-ray of 1779 keV.

E_p		4000-keV	4500-keV
Relative Precision (%)	=	2.1	0.6
Accuracy (%)	=	- 0.126	0.013
Sensitivity ($\mu g.g^{-1}$)	=	76	28
Number of Analyses	=	48	40

TABLE 6 : Intercomparison of results for silicon determinations using two different bombarding energies.

The relative precision was much better at the higher bombarding energy. The improved sensitivity at the high bombarding energy confirmed the results shown in the sensitivity function, and the lower absolute values confirm the dependence of sensitivity on the counting conditions. Both precision and sensitivity were comparable with values normally associated with PIXE, even though silicon is not an element that can easily be determined by that method.

VANADIUM

By far the largest fraction of produced vanadium is used in the manufacture of steels where its incorporation, in concentrations ranging from 0.1 to about 3% by mass, improves rod hardness and reduces resistance wear. Because the steel industry has to cope with the analysis of large numbers of samples, rapid analytical techniques requiring minimal sample preparation receive preferential attention. Among the methods involving the use of nuclear beams it would appear, a priori, that the obvious

choice would be particle-induced X-ray emission (PIXE). However, this technique has the disadvantage that in complex materials where titanium,vanadium and chromium are likely to be present, inter-element effects are generally severe and impose serious restrictions on the determination of vanadium. In such systems the 4.93-keV K_β X-ray of titanium would interfere with the measurement of the 4.95-keV V k_αX-ray while the 5.43-keV V K_β X-ray is interfered with by the 5.91-keV Cr K_α radiation.

Even in the absence of titanium, a comparison of the spectrometric techniques for determining vanadium in steels by particle bombardment showed [Gi 80] that particle-induced prompt photon spectrometry using 5000 keV alpha particles was superior to PIXE in precision and sensitivity. The gamma-ray excited under such bombardment was the 320-keV ^{51}V $\alpha(1,0)$, and measurement was virtually free from interference, except for silver, if present in concentrations of 10% or more by mass [Gi 78b]. Generally speaking, prompt gamma-ray spectrometry using protons is more sensitive than with alpha particles of the same energy as was verified in this survey and [Bo 78]. For this reason, the application of proton-induced prompt gamma-ray spectrometry was investigated for the determination of vanadium in steels.

Results and discussion

Listed in Table 7 are the gamma-rays best suited for quantitative analysis together with their corresponding yields and obtainable sensitivities. The relatively large number of suitable gamma-rays pointed to the possibility of applying the technique for the determination of vanadium in many different types of samples, because it is unlikely that the sources of interference, also listed in Table 7, could affect the use of all the available gamma-rays.

The possible sources of interference included elements which yielded gamma-rays within an interval of ± 2keV of that of the gamma-ray concerned. This information was condensed from the

Energy keV	Identity	Yield quanta sr^{-1} pC^{-1}	Sensitivity $\mu g.g^{-1}$	Possible source of interference
316	n(5,3)	3.31	540	As, Se, Sn, Hg
320	p(1,0)	4.10	370	Ti, Zn, Ga, Br, Nb, Pd, Ag, In, I, Ba, Gd, Lu, Hf
609	p(2,1)	3.61	920	Ge[a], Br, Ru, In, Ba, Ho, Hg
750	n(1,0)	16.6	210	B, Cu, Ni, I, Ba
808	n(6,1)	5.24	600	S, Fe[a], Cu, Zn, Nb, I, Tl
929	p(2,0)	4.06	730	Cl, Ti, Mn[a], Ga, Br Ag
1148	n(10,3)	1.41	450	O
1165	n(3,0)	14.2	210	Mn, I
1353	n(4,0)	3.41	790	F, Cu, I
1481	p(5,0)	2.96	880	Co

a) Serious interference as discussed in text.

TABLE 7 : Prompt gamma-rays suitable for vanadium analysis from ^{51}V.

detailed Catalogue of Gamma-rays in Appendix II. It should be noted that interference was possible even from less intense gamma-rays if the corresponding target elements was a major constituent in the matrix under investigation.

When proton-induced prompt gamma-ray spectrometry was used for the determination of vanadium in steel, the relatively feeble 812-keV ^{58}Fe p(1,0) gamma-ray constituted serious interference for the 808-keV vanadium gamma-ray, because the high concentration of iron in the steels resulted in a sufficiently large peak, the base of which overlapped the peak of the vanadium gamma-ray in the spectrum. For this reason, iron was included as a source of interference even though its gamma-ray energy was outside the stipulated range.

In matrices containing appreciable concentrations of manganese such as in manganese nodules or manganese-rich steels, the excitation of the 931-keV ^{55}Mn n(2,0) gamma-ray seriously interfered with the use of the 929-keV vanadium gamma-ray for quantitative analysis.

Germanium was included as a possible source of interference on the 609-keV ^{51}V p(2,1) gamma-ray. The interfering gamma-ray was induced by neutrons generated at the target and interacting with the Ge(Li) detector to produce the 608-keV ^{74}Ge n(2,1) gamma-rays by neutron inelastic scattering. Interference from the source was expected whenever germanium detectors were used for spectrometry and the extent of interference would be determined by the neutron yield from the bombarded target.

The attainable sensitivity calculated from thick target vanadium spectra was used to construct a sensitivity function for each selected γ-ray, showing the variation of sensitivity with bombarding energy. A typical fit is shown in Figure 9 for the case of the 750-keV ^{51}V n(1,0) gamma-ray. Similar fits were obtained for each gamma-ray listed in Table 7 and the values of the coefficients are given on page 62. Included in the latter table

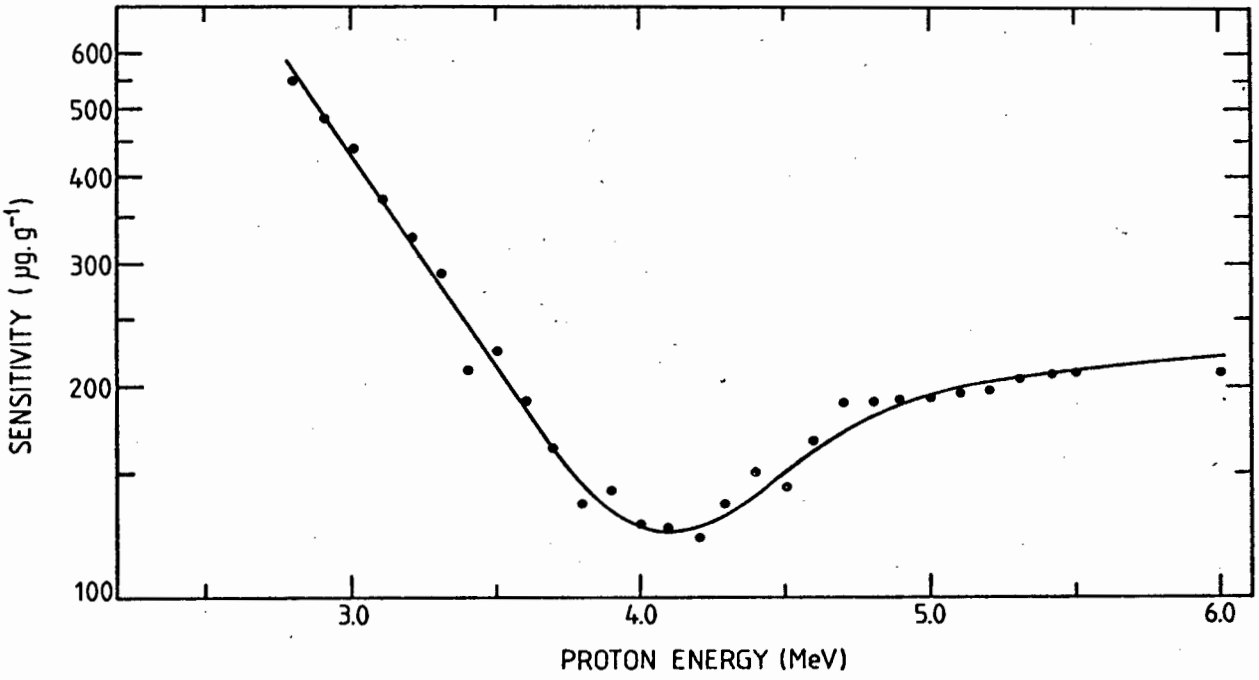

FIGURE 9 : Sensitivity function for the 750-keV ^{51}V n(1,0) gamma-ray. The curve was the best polynomial of degree 3 fitted by the method of least squares.

are the proton energies at which the best sensitivities may be expected and the corresponding sensitivities attainable at those energies. To make use of all the suitable gamma-rays, irradiations were carried out with protons of 4000 and 4500 keV as compromise energies giving acceptable overall results.

When absolute vanadium determinations were to be made in thick target matrices, accurate results required correction of the yields to be made, because of differences in the stopping power of protons from one matrix to another. To correct for this effect, the method of average stopping power [Is 78a] was used. Excitation functions were measured for the production of the vanadium gamma-rays listed in Table 7. A typical excitation function is shown in Figure 10 for the 750-keV gamma-ray.

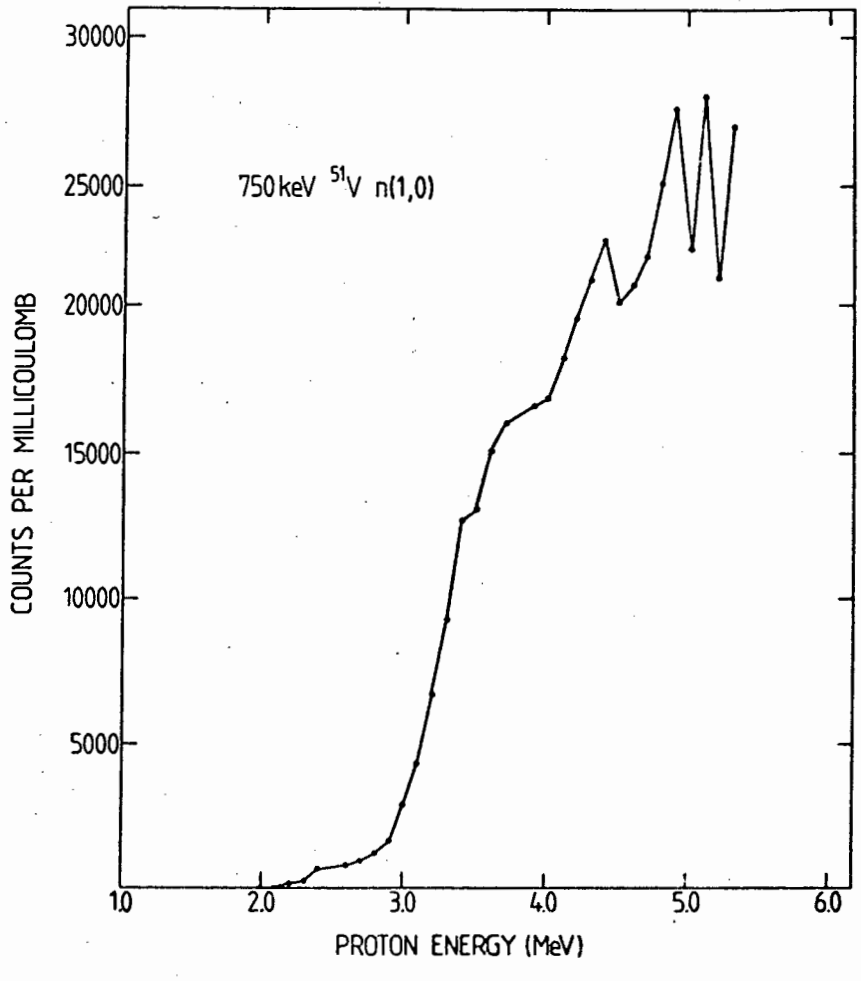

FIGURE 10 : Excitation function for the production of the 750-keV ^{51}V n(1,0) gamma-ray obtained from a foil of vanadium metal 5 µm thick.

From measured excitation functions, $\underline{E}_m$ values were calculated and the values for 2500 keV < E_p < 5300 keV, (where E_p was the energy of the bombarding protons) are given in Table 8 for each of the gamma-rays listed in Table 7. These values are applicable for all matrices.

A typical set of analytical results obtained from the yield of the 750-keV gamma-ray for eight standard reference steels is given in Table 9.

TABLE 8 : $\underline{E}_m$ values for vanadium determinations

E_γ /keV =	316	320	609	750	808	929	1148	1165	1353	1481
Proton Energy/keV										
2500	2344	2223	2336	2313	2280	2054	2006	2129	2187	2065
2600	2348	2308	2404	2320	2348	2110	2062	2234	2296	2138
2700	2406	2377	2479	2412	2420	2186	2146	2341	2359	2224
2800	2461	2466	2574	2452	2486	2212	2215	2394	2428	2291
2900	2543	2554	2660	2496	2568	2244	2278	2457	2501	2373
3000	2626	2622	2746	2577	2635	2371	2345	2530	2577	2447
3100	2708	2711	2818	2695	2708	2453	2427	2591	2640	2530
3200	2789	2779	2886	2807	2796	2522	2488	2674	2708	2606
3300	2872	2845	2961	2932	2878	2598	2570	2740	2781	2674
3400	2956	2914	3047	3024	2945	2693	2638	2819	2850	2753
3500	3023	2982	3129	3116	3027	2749	2719	2902	2923	2842
3600	3081	3045	3207	3124	3118	2817	2785	2968	2989	2915
3700	3140	3107	3289	3212	3184	2875	2859	3051	3048	2983
3800	3237	3175	3361	3241	3245	2924	2931	3117	3107	3090
3900	3331	3267	3422	3298	3312	3007	3019	3193	3211	3173
4000	3408	3335	3504	3435	3406	3075	3086	3259	3294	3236
4100	3510	3399	3565	3554	3468	3162	3157	3342	3361	3303
4200	3586	3481	3647	3722	3532	3230	3229	3408	3467	3386
4300	3665	3549	3722	3787	3599	3295	3290	3491	3540	3459
4400	3741	3617	3790	3817	3682	3374	3362	3558	3603	3550
4500	3819	3698	3876	3930	3749	3460	3426	3641	3670	3632
4600	3908	3766	3968	3938	3816	3545	3508	3709	3737	3705
4700	3966	3834	4036	3953	3875	3632	3580	3792	3823	3779
4800	4015	3883	4085	4011	3938	3720	3647	3860	3919	3852
4900	4104	3969	4167	4043	4030	3798	3719	3943	3995	3911
5000	4153	4053	4225	4131	4095	3886	3810	4011	4088	4015
5100	4198	4111	4309	4257	4162	3942	3896	4086	4181	4086
5200	4261	4189	4397	4388	4248	4030	3958	4155	4248	4168
5300	4320	4273	4483	4467	4307	4104	4003	4213	4304	4109

E_p = 4 000 keV Eγ = 750 keV

Steel	Known V content (% by mass)	Mean Count (mC^{-1})	Mean Count (mC^{-1} for 1% V)	Number of Analyses	Found % V	Error Absolute (% V)	Error Relative (%)
1264	0.10	713.4	7134	4	0.099	- 0.001	- 1.0
1263	0.31	2193	7073	4	0.290	- 0.020	- 6.5
D836	0.63	4476	7104	3	0.641	+ 0.011	+ 1.7
D841	1.13	8160	7221	3	1.124	- 0.006	- 0.6
D838	1.17	8399	7179	3	1.179	+ 0.009	+ 0.8
D839	1.50	10595	7063	3	1.531	+ 0.031	+ 2.1
D840	2.11	15228	7217	3	2.107	- 0.004	- 0.2
D837	3.04	21687	7134	3	3.046	+ 0.006	+ 0.2

No. of Analyses = 26

Mean Count/ mC^{-1} for 1% V = 7157 ± 301

Relative Standard Error = 4.2%

Root Mean Square Error = 0.027% V by mass

TABLE 9 : Typical results for vanadium determination in steels

The vanadium content ranged from 0.10 to 3.04% by mass. Over this concentration range, the precision of the method was 4.2% given by the relative standard deviation; the sensitivity was taken as the root mean square error and the accuracy was assumed to be represented by the mean relative deviation from the certified concentration. These parameters are listed in Table 9.

A summary of the same parameters obtained, using the yields of the selected gamma-rays for which no interferences were detected from the steel matrix, are given in Table 10 for proton bombarding energies of 4000 and 4500 keV as measured with a Ge(Li) detector. Also included in the table are the data obtained from the yields

E_γ /keV	316	320	750	1148	1165	1353	1480
^{51}V γ-rays	n(5,3)	p(1,0)	n(1,0)	n(10,3)	n(3,0)	n(4,0)	n(5,0)
Ge(Li) E_p=4000 keV							
Relative Precision/%		2.4	4.2	6.1	4.0	3.7	8.3
Accuracy/%		-0.21	-0.19	-0.10	0.06	-0.10	0.03
Sensitivity/μg.g^{-1}		400	270	510	590	1020	650
No. of Analyses		26	26	26	26	26	26
Ge(Li) E_p=4500 keV							
Relative Precision/%		3.7	2.4	8.1	4.1	6.3	4.8
Accuracy/%		-1.74	-0.03	0.11	0.04	0.06	-0.35
Sensitivity/μg.g^{-1}		720	320	680	410	940	490
No. of Analyses		23	23	23	23	23	23
Intrinsic germanium E_p=4000 keV							
Relative Precision / %	10.0	3.8					
Accuracy/%	-0.97	-3.3					
Sensitivity/μg.g^{-1}	980	700					
No. of Analyses	24	24					

TABLE 10 : Summary of the analytical parameters for vanadium determinations.

of the 316- and 320-keV gamma-rays as determined separately by the use of an intrinsic germanium detector. As was expected, the sensitivities measured for the steel matrix were worse than those listed for pure vanadium (see page 62) because of the increased intensity of the Compton continuum in the spectra from components of the matrix. This will not be the case with inert matrices or with thin targets where better sensitivities are expected.

CHROMIUM

Chromium is usually incorporated into steels in order to improve the tensile strength and to increase resistance to abrasive wear, while at the same time retaining good ductility and fatigue

Eγ (keV)	Identity	Yield (quanta $sr^{-1}nC^{-1}$)	Sensitivity ($\mu g.g^{-1}mC^{-1}$)	Possible Source of Interference
378	$^{52}Cr\ \gamma(1,0)$ + $^{53}Cr\ n(1,0)$	8 050	260	Co, Sc, Fe, Se, Rb, Rh, Cd
783	$^{50}Cr\ p(1,0)$	3 060	1 100	Pd, Cd, Er
911	$^{52}Cr\ \gamma(2,1)$ + $^{53}Cr\ n(2,1)$	1 750	1 800	Cu, Zn, Ge, Ag
1288	$^{52}Cr\ \gamma(2,0)$ + $^{53}Cr\ n(2,0)$	2 300	1 300	Sc, Co
1440	$^{52}Cr\ p(1,0)$ + $^{53}Cr\ n(3,0)$	36 600	140	Th
1619	$^{53}Cr\ n(4,1)$	660	3 200	Ti

TABLE 11 : Prompt gamma-rays suitable for chromium determinations.

analysis. The most serious interference on the 911-keV gamma-ray from chromium would be the 912-keV photon of copper but since the latter element was either absent or was present in the steels in much lower concentrations than chromium, the contribution of the copper gamma-ray would be minimal.

The $\underline{E}_m$ values for the analytically useful gamma-rays from chromium are given in Table 12. The excitation functions were measured with a 5 μm thick chromium foil bombarded with proton energies between 2500 and 5300 keV in steps of 100 keV.

E_p (KeV)	E_m values at Eγ values (KeV) for:-					
	378	785	911	1288	1440	1619
2500	2371	2440	2318	2349	2342	2317
2600	2398	2571	2409	2439	2416	2362
2700	2460	2620	2433	2517	2442	2439
2800	2484	2756	2490	2634	2468	2573
2900	2589	2950	2496	2732	2490	2634
3000	2619	2986	2593	2783	2510	2698
3100	2862	3170	2640	2904	2521	2758
3200	2892	3217	2767	2963	2565	2841
3300	2920	3335	2808	3109	2632	2912
3400	2971	3416	2849	3217	2673	2933
3500	3044	3536	2851	3354	3159	3107
3600	3104	3607	2867	3366	3162	3243
3700	3243	3699	2894	3395	3184	3366
3800	3246	3704	2927	3396	3218	3485
3900	3469	3864	2983	3575	3445	3525
4000	3479	3943	3103	3603	3519	3609
4100	3495	4093	3274	3611	3535	3671
4200	3662	4190	3288	3690	3851	3734
4300	3710	4200	3374	3832	3909	3807
4400	3885	4234	3393	4000	4057	3845
4500	4000	4280	3463	4044	4148	3905
4600	4024	4290	3514	4094	4215	3940
4700	4084	4326	3598	4132	4236	3987
4800	4145	4379	3673	4283	4386	4109
4900	4195	4384	3819	4377	4583	4263
5000	4247	4466	3917	4441	4594	4293
5100	4268	4491	4031	4454	4627	4371
5200	4290	4572	4132	4492	4675	4418
5300	4325	4654	4276	4536	4682	4473

TABLE 12 : E_m values for chromium determinations.

Detailed results obtained for chromium analysis in steels using the 378-keV gamma-ray at a proton bombarding energy of 4000 keV are given in Table 13. The chromium content of the steels ranged from 0.30 to 18.45 % by mass and over this concentration range, the precision of the method, given by the relative standard deviation was 1.3%. The root mean square error, 0.118% Cr by mass, was indicative of the sensitivity of analysis and the accuracy was assumed to be represented by the

Steel	Known Cr Content (% by mass)	Mean Count (mC^{-1})	Mean Count (mC^{-1} for 1% Cr)	Number of Analyses	Found (% Cr)	Error Absolute (% Cr)	Error Relative (%)
1262	0.30	2 351	7 835	3	0.294	-0.006	-2.0
1261	0.69	5 417	7 843	3	0.703	+0.013	+1.9
1263	1.31	10 409	7 946	3	1.330	+0.020	+1.6
D840	2.12	16 535	7 780	3	2.106	-0.014	-0.7
D839	2.72	21 336	7 844	3	2.717	-0.003	-0.2
D841	4.20	32 812	7 812	3	4.179	-0.021	-0.5
D838	4.66	36 472	7 827	3	4.649	-0.011	-0.3
D837	7.79	60 888	7 817	3	7.763	-0.027	-0.4
1185	17.09	135 395	7 922	3	17.242	+0.152	+1.0
1133	18.45	145 014	7 860	3	18.471	+0.021	+0.2

No. of Analyses	=	30
Mean Count (mC^{-1} for 1% Cr)	=	7 851 ± 103
Relative Standard Error	=	1.3%
Root Mean Square Error	=	0.118% Cr by mass

TABLE 13 : Results for chromium determinations using the 378-keV gamma-ray from a proton bombarding energy of 4000 keV

mean relative deviation from the certified concentrations. Summarized results for the chromium gamma-rays used are given in Table 14 for proton-bombarding energies of 4000 and 4500 keV as measured with a Gi(Li) detector. Results obtained when the 378-keV gamma-ray was measured when an intrinsic germanium detector was used, is also included. Most of the sensitivities that were obtained for the steel matrix were worse than the calculated sensitivities, which were measured from a pure chromium target (see page 63) This was expected because of increased contribution of the Compton background due to the presence of other gamma-rays from the various components of steels.

E_γ (keV)	378	783	911	1440	1619
Assignment	$^{52}Cr\ \gamma(1,0)$ + $^{53}Cr\ n(1,0)$	$^{56}Cr\ p(1,0)$	$^{52}Cr\ \gamma(2,1)$ + $^{53}Cr\ n(2,1)$	$^{52}Cr\ p(1,0)$ + $^{53}Cr\ n(3,0)$	$^{53}Cr\ n(4,1)$
Ge(Li) E_p = 4000-keV					
Relative Precision (%)	1.3	2.1	4.3	0.8	1.5
Accuracy (%)	0.90	1.66	- 2.71	- 0.06	1.04
Sensitivity ($\mu g.g^{-1}$)	1 180	1 740	2 670	160	1 270
Number of Analyses	30	30	30	30	30
Ge(Li) E_p = 4500-keV					
Relative Precision (%)	1.6	3.2	3.7	1.3	3.4
Accuracy (%)	0.40	- 0.11	1.40	0.14	2.27
Sensitivity ($\mu g.g^{-1}$)	1 220	2 110	3 170	110	990
Number of Analyses	43	43	43	43	43
InGe E_p = 4000-keV					
Relative Precision (%)	3.1				
Accuracy (%)	0.33				
Sensitivity ($\mu g.g^{-1}$)	3 390				
Number of Analyses	30				

TABLE 14 : Summary of the analytical parameters for chromium determinations.

Besides, the mean optimum bombarding energy calculated for those gamma-rays which show a poorer sensitivity, was 3700 keV with a result that, better sensitivities could be expected if the analysis was performed at a lower bombarding energy. The obvious choice of a gamma-ray for analysis for chromium would be the 1440-keV photon. As can be seen from the analytical results, a sensitivity of 110 $\mu g.g^{-1}$ could be obtained with a proton bombarding energy of 4500 keV. An optimum bombarding energy for maximum sensitivity was calculated (see page 63) to be about 5700 keV therefore it was expected that with increasing bombarding energy the sensitivity would improve. The poor

sensitivity obtained when the intrinsic germanium spectrometer was used, was due to the fact that the detector efficiency had dropped substantially in the energy region of the 378-keV gamma-ray.

MANGANESE

Manganese is usually introduced into steels to increase the coefficient of thermal expansion and for other applications where high tensile strength is required. However, the concentration of manganese is relatively lower than that of other alloying elements. Commonly the concentration lies between 0.1 and 3% manganese by mass. Over this range of concentration the technique of prompt photon emission during charge particle bombardment offers a rapid, precise and non-destructive method of analysis. A comparison between proton-induced X-rays and alpha-induced gamma-rays [Gi 80] spectrometry showed the latter method to be superior for the analysis of a steel matrix. Quantitative results obtained for manganese in this investigation (see page 64) showed that proton-induced gamma-rays offer better sensitivities than those obtained with alphas [Gi 78a] of a few MeV. For this reason the application of proton-induced prompt gamma-ray spectrometry for the determination of manganese in steels was investigated.

A recent review [Bo 80] of the present state of the art summarizes data for protons, tritons, alpha particles and heavy particles. However, with reference to protons the literature on the determination of manganese was confusing due to the variety of bombarding conditions preferred by various authors. Published values of sensitivities using protons, were not defined in a consistent manner and the clear distinction that should have been drawn between detection sensitivity and the sensitivity for analytical determination [Cu 68] was not always strictly maintained. The first reference [De 78] merely stated that the estimated limit of detection was 5 $\mu g.g^{-1}$ with 2500 keV protons, using the 931-keV gamma-ray. However, conditions for analysis were not

defined nor was any basis for the estimation cited. This claim need not therefore be discussed any further. A reported sensitivity of 15 $\mu g.g^{-1}$ for the 126-keV gamma-ray excited with 4000 keV beams was based on highly idealised conditions and represented the extrapolated limit of 0.1 counts per μC from a target of a thin film of vacuum deposited manganese on tantalum, a material which produces an exceptionally low Compton continuum in the gamma-ray spectrum (see page271) The only example of a gamma-ray spectrum given in that work [C1 75] emphasised the very high background in the region of the 126-keV gamma-ray and necessitated the use of a different gamma-ray even though the reported concentration of manganese was 1238 $\mu g.g^{-1}$. In the present survey a more realistic sensitivity for analytical determination was found to be 90 $\mu g.g^{-1}$ for the 931-keV gamma-ray induced by 4500 keV protons on a thick target of pure metallic manganese and calculated by the previously reported method [Cu 68].

Results and discussion

The gamma-rays most useful for manganese determination are listed in Table 15, together with the yields and the analytical

Energy (KeV)	Identity	Yield quanta $sr^{-1}nc^{-1}$	Sensitivity ($\mu g.g^{-1}$ mC^{-1})	Possible source of interference
126	p(1,0)	5900	250	Fe, Ru, Re, W,I
412	n(1,0)	7600	190	Mn, Fe, Ru, I, Hg
477	n(4,2)	6000	270	Li, Ni, Br, Os
803	n(8,4)	2400	950	I
931	n(2,0)	3400	90	Ci, Ti, V, I, Cu
1316	n(3,0)	13400	210	Ni
1370	n(9,2)	1900	550	Ma, Mg, Al, Cu, Mo,Pr
1408	n(4,0)	5400	450	Fe, Sc, I

TABLE 15 : Prompt gamma-rays from ^{55}Mn suitable for manganese analysis.

sensitivity attainable.

Gamma-rays were considered to be possible sources of interference if they were generated during proton bombardment and had energies that lay ±2keV from that of the gamma-ray considered for analysis. The extent of such interference could be deduced from the comprehensive Catalogue of Gamma-Rays in Appendix II. Although several elements could interfere with the use of the 126-keV ^{55}Mn p(1,0) gamma-ray for analysis, the interfering elements most likely to be present in steelswere iron and tungsten. Since these elements were usually present in concentrations much higher than that of manganese, the interference was serious despite the much lower yields of the corresponding gamma-rays. For this reason, the 126-keV gamma-ray could not be used with a Ge(Li) detector. When an intrinsic germanium detector with its greater resoltuion was used, the 2-keV interference range no longer applied. The 122-keV ^{186}W p(1,0) and ^{57}Fe p(2,1) gamma-rays were entirely resolved from that of the 126-keV gamma-ray (see Figure 8) and were no longer a source of interference. The 127-keV ^{59}Fe α(3,2) gamma-ray could be stripped in order to obtain the manganese yield.

The 412-keV gamma-ray from iron was produced with such poor intensity that its interference with the intense 412-keV manganese gamma-ray was small, and could be neglected as part of the background when the iron concentrations in a series of steels did not vary appreciably. Nickel was the only element which was likely to interfere with the 477-keV gamma-ray. But here again, the nickel gamma-ray was of very low intensity and was ignored as a serious source of interference. If it were necessary to make use of the 803-keV gamma-ray for analysis, a good resolution Ge(Li) detector would completely resolve this gamma-ray from the photon from iodine. Both the 931-keV and 1316-keV gamma-rays could be considered interference-free because all other gamma-rays in the same energy region have very low intensities. The 1370-keV and 1408-keV gamma-rays were not used for analysis because of major interference from 1367-keV

^{27}Al p(3,1) (from the construction material of the scattering chamber) and from 1408-keV ^{54}Fe p(1,0) gamma-rays.

Since the analytical sensitivity attainable depended not only on the yield of a gamma-ray but also on the level of the background continuum against which the gamma-ray had to be measured, it was necessary to determine the sensitivity limit experimentally as a function of the bombarding energy. A typical sensitivity function for the case of the 412-keV ^{55}Mn n(1,0) gamma-ray is shown in Figure 11. The figure shows a rapid improvement of sensitivity as the bombarding energy increased from 2500 to about 4500 keV, as a result of increasing reaction cross-section. Thereafter with increasing energy there was a gradual deterioration due to increasing intensities of the Compton continuum from higher energy gamma-rays. Similar curves were obtained for all the analytically significant gamma-rays. On page 65 are listed the co-efficients of polynomials fitted to the corresponding sensitivity functions. Analyses were carried out with 4000 and 4500 keV protons because over this energy range the best sensitivities were attained.

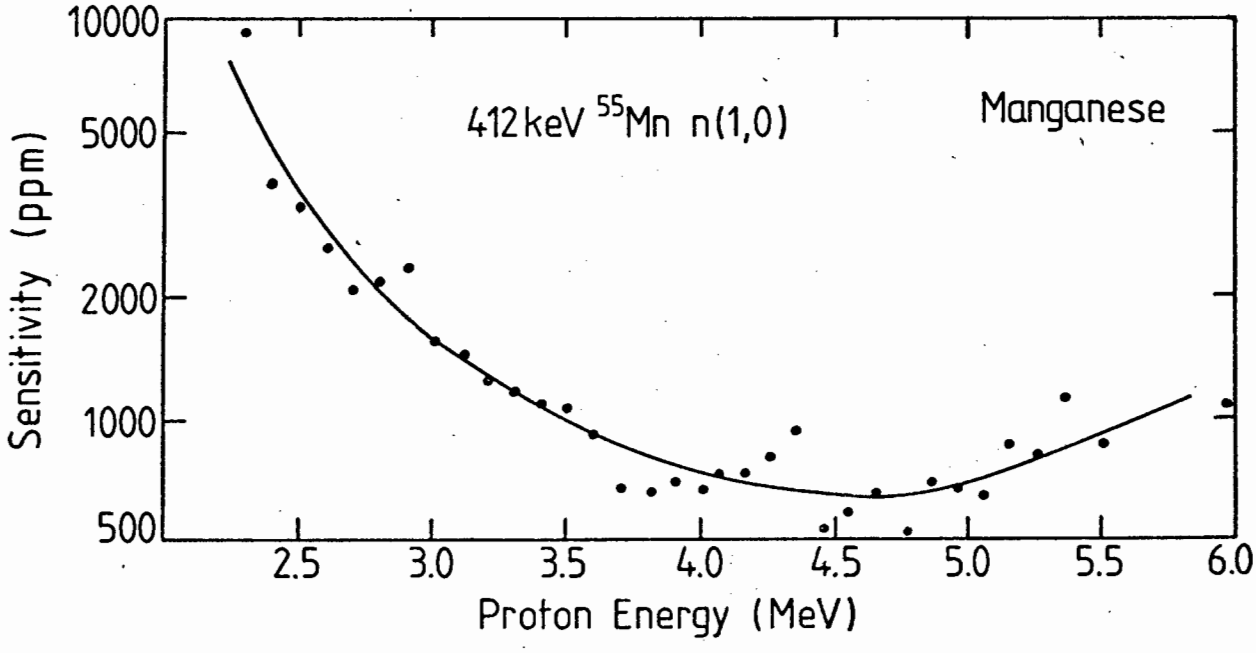

FIGURE 11 : Sensitivity function for the 412-keV ^{55}Mn n(1,0) gamma-ray. The curve was the best polynomial of degree 3 fitted by the method of least squares.

Foils of 5µm thick manganese mounted on permanent supports of epoxy resin were bombarded with protons over an energy range from 2300 to 5700 keV in steps of 100 keV to yield the excitation functions of the analytically significant gamma-rays. From these curves mean bombarding energies could be calculated and the method of average stopping powers [Is 78a] could be used to correct for the variation in composition of the analysed steels. The values of $\underline{E}_m$ are given in Table 16.

TABLE 16 : $\underline{E}_m$-values for manganese determinations

E_p	$\underline{E}_m$- values at Eγ values (KeV) of							
(KeV)	126	412	477	803	931	1316	1370	1408
2500	2401	2284	2273	2137	2374	2039	2574	2174
2600	2457	2416	2375	2204	2402	2084	2641	2220
2700	2505	2520	2453	2271	2515	2159	2732	2267
2800	2572	2649	2516	2363	2624	2225	2793	2350
2900	2615	2785	2591	2426	2707	2293	2857	2413
3000	2670	2801	2682	2508	2791	2361	2924	2459
3100	2744	2862	2764	2576	2864	2463	3012	2531
3200	2783	2887	2828	2635	2947	2554	3059	2630
3300	2853	2948	2901	2702	3035	2641	3120	2713
3400	2901	2965	2983	2784	3108	2727	3191	2784
3500	2948	3092	3074	2847	3184	2794	3257	2832
3600	3014	3155	3146	2931	3251	2876	3301	2881
3700	3089	3285	3224	2992	3297	2943	3368	2954
3800	3135	3334	3285	3059	3353	3029	3449	3035
3900	3202	3363	3370	3145	3387	3108	3530	3098
4000	3271	3438	3434	3212	3435	3194	3593	3169
4100	3356	3493	3525	3300	3496	3267	3634	3235
4200	3417	3556	3598	3367	3577	3353	3678	3307
4300	3500	3621	3695	3436	3621	3436	3733	3355
4400	3584	3683	3788	3503	3688	3503	3792	3417
4500	3647	3747	3855	3569	3726	3576	3864	3475
4600	3690	3808	3937	3658	3782	3658	3929	3544
4700	3762	3871	4004	3749	3828	3716	3992	3650
4800	3823	3934	4071	3817	3884	3779	4063	3721
4900	3900	3991	4153	3903	3925	3828	4126	3804
5000	3963	4053	4220	3989	3990	3901	4174	3868
5100	4031	4122	4284	4095	4031	3983	4256	3940
5200	4098	4178	4368	4202	4065	4055	4316	4001
5300	4186	4255	4473	4288	4167	4126	4393	4066
5400	4253	4332	4536	4355	4215	4193	4459	4125
5500	4319	4410	4603	4461	4260	4260	4536	4173
5600	4396	4511	4652	4528	4323	4341	4594	4267
5700	4459	4596	4717	4574	4367	4412	4663	4363

An example of a typical set of results using the 477-keV gamma-ray is shown in Table 17. Although mean values of the results are given for each SRM steel, the statistical data at the foot of the table werecalculated from the individual measurements.

E_p = 4000 keV E_γ = 477 keV

Steel	Known Mn content (% by mass)	Mean Count (mC^{-1})	Mean Count (mC^{-1} for 1% Mn)	Number of analyses	Found % Mn	Error Absolute (% Mn)	Error Relative (%)
D840	0.15	543.8	3625	5	0.153	+ 0.003	+ 2.0
D839	0.18	646.0	3588	4	0.181	+ 0.001	+ 0.6
D838	0.20	732.3	3661	4	0.205	+ 0.005	+ 2.5
1264	0.25	912.8	3651	4	0.256	+ 0.006	+ 2.4
D841	0.27	947.3	3508	4	0.266	- 0.004	- 1.5
D837	0.48	1671.6	3483	5	0.467	- 0.013	- 2.7
1261	0.66	2313	3505	4	0.654	- 0.006	- 0.9
1262	1.04	3732	3589	4	1.048	+ 0.008	+ 0.7
1185	1.22	4360	3574	5	1.224	+ 0.004	+ 0.3
1263	1.50	5239	3492	4	1.471	- 0.029	- 2.0
1172	1.76	6194	3519	5	1.740	- 0.020	- 1.2
1171	1.80	6401	3556	5	1.796	- 0.004	- 0.2

No of analyses = 53

Mean count/mC^{-1} for 1% = 3561 ± 116

Relative standard error = 3.3%

Root mean square error = 0.030 % Mn by mass

TABLE 17 : Results for manganese determination using the 477-keV gamma-ray from a bombarding energy of 4000-keV protons.

These data and the data using other gamma-rays are summarized in Table 18. Most of the data were obtained using a Ge(Li) detector but a batch of analyses could be carried out using the

E_γ/keV	126	412	477	931	1316
^{55}Mn gamma-rays	p(1,0)	n(1,0)	n(4,2)	n(2,0)	n(3,0)
Ge(Li) E_p = 4000 keV					
Relative precision/%		1.6	3.3	2.3	3.0
Accuracy/%		0.06	- 0.05	0.04	- 0.03
Sensitivity/mg.g^{-1}		0.19	0.30	0.54	0.25
Number of analyses		50	53	52	52
Ge(Li) E_p = 4500 keV					
Relative precision/%		2.2	3.7	3.0	4.9
Accuracy/%		0.03	- 0.03	- 0.03	0.04
Sensitivity/mg.g^{-1}		0.11	0.26	0.25	0.17
Number of analyses		40	40	40	40
I.G. E_p = 4000 keV					
Relative precision/%	8.2				
Accuracy/%	- 0.23				
Sensitivity/mg.g^{-1}	0.31				
Number of analyses	30				

TABLE 18 : Summary of the analytical parameters for manganese determinations.

126-keV gamma-ray when the resolution was sufficient to eliminate the interference of the iron gamma-ray. The relative precision of about 1.5 to 3.0 % by mass was readily obtainable. The poor precision obtained with an intrinsic germanium detector was due to the small size of the spectrometer used and was not a fair reflection of attainable precision.

COBALT

The inclusion of cobalt in steels not only improves its retention of hardness but also increases the coersive forces between atoms with a result that cobalt constitutes an appropriate alloy element for permanent magnets. Therefore simple rapid techniques for the analysis of cobalt would be of interest to the steel industry.

While there is no doubt that PIXE can be used, the difficulty encountered using that technique is that iron, the major component of steels, produces the very intense 7.057-keV k_β X-ray which overlaps with the 6.930-keV k_α X-ray of cobalt. The lesser intense k_β X-ray of cobalt would therefore have to be utilised.

From a survey [Bo 80] of prompt gamma-rays induced by various charged particles, it was deduced that the only appropriate beams that could be used to yield cobalt gamma-rays of reasonable intensity were 3.5 MeV tritons and 55-MeV ^{35}Cl particles. However, the theoretical sensitivities which were calculated on the gamma-rays generated by these specialised beams compared very favourable with the sensitivities measured for the cobalt gamma-rays (see page 67) using simple proton beams of appropriate energies as in the present study. The method was thus tested for the determination of this element in steels.

Results and discussion

Eγ (keV)	Identity	Yield (quanta $sr^{-1}nC^{-1}$)	Sensitivity ($\mu g.g^{-1}mC^{-1}$)	Possible Source of Interference
339	^{59}Co n(1,0)	14 800	80	Ni, Nb, Cd, Cs, Hf, W, Au, Tl
878	^{59}Co n(3,0)	2 210	710	Se, Rh, Cd
1189	^{59}Co n(4,0)	4 920	360	
1190	^{59}Co p(2,0)			
1337	^{59}Co n(6,1)	3 730	380	Ga, Sn, Th
1432	^{59}Co p(4,0)	3 380	390	Sc, V, Cr
1948	^{59}Co n(11,0)	1 200	640	

TABLE 19 : Prompt gamma-rays from ^{59}Co suitable for cobalt determinations

Listed in Table 19 are the most intense gamma-rays, generated from proton bombardment of cobalt. Included in the table are the relative yields and sensitivities together with the elements which would produce gamma-rays that could interfere with the analytical photopeaks.

With the exception of the 1432-keV gamma-ray , all the intense photons were considered as being interference-free because the elements that could affect these gamma-rays were not commonly present in steels.

A 5µm foil of cobalt was bombarded with protons of 2500 to 5300 keV in steps of 100 keV in order to obtain the excitation functions of the analytically useful gamma-rays. From these

excitation functions it was possible to calculate the $\underline{E}_m$ values so that the stopping power corrections could be applied for the various steel samples. The calculated values are listed in Table 20.

From the spectra of cobalt obtained at selected bombarding energies, it was possible to calculate the analytical sensitivities attainable for the potentially useful gamma-rays. Co-efficients of the polynomials fitted to the sensitivity functions were calculated (see page 68).

The precision, sensitivity and accuracy of the analytical procedure was tested by determining cobalt in 8 standard steel samples. The results, for the use of the intense 339-keV ^{59}Co n(1,0) gamma-ray measured for the steels under proton bombardment of 4000 keV, are given in Table 21.

E_p	$\underline{E}_m$ values at $E\gamma$ values (KeV) of					
(KeV)	339	878	1190	1337	1432	1948
2500	2107	2273	2016	2321	2064	2304
2600	2189	2336	2093	2392	2093	2373
2700	2243	2363	2168	2438	2147	2398
2800	2374	2407	2227	2449	2212	2471
2900	2482	2453	2289	2518	2263	2550
3000	2509	2591	2346	2563	2294	2576
3100	2581	2680	2472	2675	2338	2695
3200	2643	2772	2538	2760	2394	2722
3300	2739	2837	2603	2844	2443	2743
3400	2814	2963	2661	2935	2497	2801
3500	2865	3043	2728	3001	2563	2863
3600	2948	3128	2787	3073	2592	2972
3700	3047	3194	2843	3114	2660	3009
3800	3093	3237	2917	3180	2698	3045
3900	3147	3328	3039	3245	2745	3119
4000	3205	3449	3138	3298	2829	3194
4100	3267	3538	3186	3374	2963	3245
4200	3374	3616	3225	3429	3041	3311
4300	3430	3681	3273	3491	3139	3363
4400	3499	3759	3309	3501	3219	3420
4500	3546	3840	3435	3575	3283	3464
4600	3617	3938	3572	3649	3362	3590
4700	3712	4015	3643	3713	3427	3667
4800	3737	4091	3680	3828	3585	3717
4900	3904	4182	3727	3945	3638	3824
5000	4040	4240	3873	4007	3776	3865
5100	4173	4363	3956	4091	3869	3974
5200	4278	4427	4084	4163	3943	4081
5300	4314	4478	4103	4219	4018	4138

TABLE 20 : $\underline{E}_m$-values for cobalt determinations

Steel	Known (% Si)	Mean Count (mC^{-1})	Mean Count (mC^{-1} for 1% Si)	Number of Analyses	Found (% Si)	Error Absolute	Error Relative
1171	0.10	533	5 332	5	0.099	-0.001	-1.0
1172	0.12	641	5 343	5	0.122	+0.002	+1.7
1264	0.15	802	5 345	4	0.149	-0.001	-0.7
1262	0.30	1 619	5 397	4	0.296	-0.004	-1.3
D837	2.9	15 593	5 377	5	2.89	-0.010	-0.4
D838	4.9	26 445	5 397	4	4.92	+0.020	+0.4
D839	7.8	42 111	5 419	4	7.76	-0.040	-0.5
D840	11.8	63 710	5 399	5	11.85	+0.050	+0.4

No. of Analyses	=	36
Mean Count (mC^{-1} for 1% Co)	=	5 375 ± 126
Relative Standard Error	=	2.3%
Root Mean Square Error	=	0.092% Co by mass

TABLE 21 : Results for cobalt determination using the 339-keV gamma-ray from a proton bombarding energy of 4000 keV

The measured count refers to the nett integrated count under the peak in the gamma-ray spectrum corresponding to 339 keV calculated for a bombarding current of 1 nA This value was then expressed as the yield per mC per unit cobalt content in order to compare the gamma-ray yields from different steels. The mean value obtained from 36 analyses on the 8 steels is 5375 ± 126 counts per mC for 1% Co by mass.

The precision of the analysis over the cobalt concentration range of about 0.1 to 12% by mass was 2.3%. The accuracy of the method, through the use of the 339-keV gamma-ray, may be deduced from the mean relative deviation of the certified concentration. The root mean square error was 0.092% Co by mass. A summary of the same parameters as in Table 21 of the selected gamma-rays for which no interferences were detected from the steel matrix, are given in Table 22 for proton bombarding energies of 4000 and

4500 keV as measured with the Ge(Li) detector. A set of analyses similar to that listed in Table 21 were also obtained with an intrinsic germanium detector and summarised data are included in Table 22.

E_γ (keV) ^{59}Co γ-RAYS	339 n(1,0)	878 n(3,0)	1189 + 1190 n(4,0) + p(2,0)	1337 n(6,1)	1948 n(11,0)
Ge(Li) E_p = 4000-keV					
Relative Precision (%)	2.3	2.8	3.4	1.9	3.0
Accuracy (%)	-0.335	0.13	0.23	-0.31	0.12
Sensitivity (μg.g^{-1})	920	1 160	720	840	630
Number of Analyses	36	36	36	36	36
Ge(Li) E_p = 4500-keV					
Relative Precision (%)	3.8	2.9	1.4	3.7	3.4
Accuracy (%)	-0.001	0.08	-0.18	0.04	-0.24
Sensitivity (μg.g^{-1})	340	980	410	710	570
Number of Analyses	27	27	27	27	27
InGe E_p = 4000-keV					
Relative Precision (%)	2.2				
Accuracy (%)	-0.04				
Sensitivity (μg.g^{-1})	780				
Number of Analyses	23				

TABLE 22 : Summary of the analytical parameters for cobalt determinations.

CONCLUSION

PIPPS has been shown to be suitable for the determination of minor components in thick targets of matrices such as steels. Advantages of the method are that the experimental procedure is simple; that there is virtually no need for sample preparations than to provide a flat surface for analysis; that it is a non-destructive method, as is usually the case with nuclear

CHAPTER 5

CEMENT ANALYSIS

The process of cement manufacture involves the incorporation of geological material from different sources to form a homogeneous mixture. The geological components are essentially lime, silica, alumina, magnesium oxide and ferrous-bearing materials [Le 70] which make up the bulk of the raw material while minor constituents such as fluorspar,sodium oxide and phosphorus pentoxide may also be included.

A complete test whether the cement meets the required specification can only be carried out after production. In order to control production, the elemental composition of the intermediate stages of the process has to be known. It is thus not surprising that the cement industry makes extensive use of multi-element analytical tehcniques, both destructive and non-destructive. Since PIPPS is, in principle, a rapid, non-destructive and experimentally simple technique for multi-element analysis, the application of this technique was tested on standard cement samples. In addition, analyses were performed using a bombarding beam of 5000-keV alpha-particles [Gi 79c], not only to verify the results obtained by PIPPS but also to test the possibility of extending the range of elements analysed.

RESULTS AND DISCUSSION

Samples were analysed for the major components; calcium, silicon and aluminium and the minor components fluorine, sodium, magnesium and phosphorus. The spectrum from the bombardment of the standard cement, SRM 633 with protons of 4000 keV is shown in Figure 12. The identities of the numbered peaks are listed below the spectrum in Table 23.

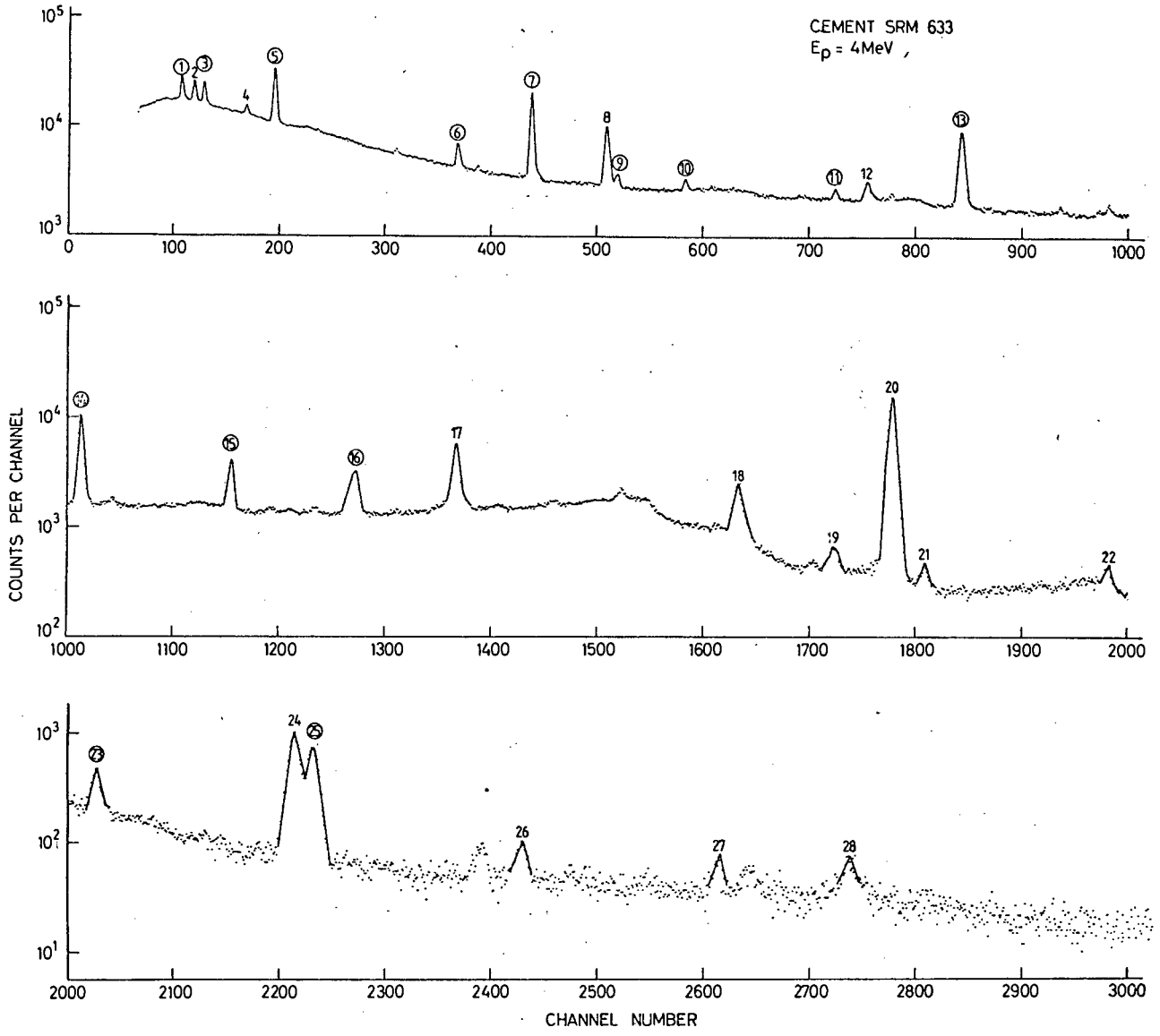

FIGURE 12 : Prompt gamma-ray spectrum from the irradiation of the standard cement SRM 633 with 4000-keV protons measured with a Ge(Li) detector. The identity of peaks as marked in the figure, are given in Table 23.

TABLE 23 : Identify of peaks as marked in Figure 12.

Element	Gamma-ray Energy KeV	Assignment	Peak number	Remarks
Oxygen	1982	^{18}O p(1,0)	22	
Fluorine	110	^{19}F p(1,0)	1	used for analysis
	197	^{19}F p(2,1)	5	used for analysis
Sodium	440	^{23}Na p(1,0)	7	used for analysis
	1637	^{23}Na p(2,1)	18	
Magnesium	585	^{25}Mg p(1,0)	10	used for analysis
	1367	^{24}Mg p(1,0)	17	see also Al
	1809	^{26}Mg p(1,0)	21	

Table 23 (Continued)

Element	Gamma-ray Energy KeV	Assignment	Peak number	Remarks
Aluminium	171	^{27}Al p(2,1)	4	
	844	^{27}Al p(1,0)	13	used for analysis
	1015	^{27}Al p(2,0)	14	used for analysis
	1367	^{27}Al p(3,1)	17	see also Mg
	1779	^{27}Al Y(1,0)	20	see also Si, P
	2210	^{27}Al p(3,0)	24	
	2734	^{27}Al p(4,0)	28	
Silicon	756	^{29}Si p(2,1)	12	
	1273	^{29}Si p(1,0)	16	used for analysis
	1779	^{28}Si p(1,0)	20	see also Al, P
	2030	^{29}Si p(2,0)	23	
	2430	^{29}Si p(3,0)	26	
Phosphorus	1779	^{31}P α(1,0)	20	see also Al, Si
	2230	^{31}P p(2,0)	25	see also S
Sulphur	1719	^{32}S	19	(2230 - m_e)
	2230	^{32}S p(1,0)	25	see also P
Calcium	121	^{48}Ca n(2,1)	2	
	131	^{48}Ca n(2,0)	3	used for analysis
	373	^{43}Ca p(1,0)	6	used for analysis
	520	^{48}Ca n(4,3)	9	used for analysis
	727	^{43}Ca n(5,1)	11	used for analysis
	1157	^{44}Ca p(1,0)	15	used for analysis
Background	511	$\beta^{\pm}$	8	
	2614	^{208}Bi	27	radioactivity

Although oxygen constituted one of the major elements in cement, the element could not be determined because the high background continuum in the spectrum, rendered the 1982-keV gamma-ray useless for analysis. On the other hand, flourine, a minor component in cements could easily be determined using the interference-free gamma-rays of 110-and 197-keV.

The obvious choice for sodium determination was the intense 440-keV gamma-ray and since the 1637-keV gamma-ray from this element was interference-free, it was also selected for analysis.

No elements commonly present in cements interferred with the intense 585-keV ^{25}Mg p(1,0) gamma-ray and this was used for magnesium determination. The choice for aluminium determination was the 844- and 1015-keV gamma-rays, although if it was necessary the less intense gamma-rays of 2210 and 2734 keV could also be used.

Silicon was determined using the 1273-keV gamma-ray instead of the more intense 1779-keV gamma-ray because both aluminium and phosphorus produced photons of the latter energy.

Phosphorus, a minor element, in cements was determined using the 2230-keV ^{31}P p(2,0) gamma-ray.

Calcium, the major constituent of cements offered a number of interference-free gamma-rays that could be used for analysis.

Sodium as sodium chloride, phosphorus as mercurous phosphate, fluorine as calcium fluoride and calcium as calcium hydroxide, deposited on tantalum discs, were bombarded with protons over an energy range of 2500 to 5300 keV in steps of 100 keV to yield the excitation functions of the analytically significant gamma-rays. A typical curve, for the 440-keV ^{23}Na p(1,0) gamma-ray is shown in Figure 13. Similar curves were obtained when 5 µm

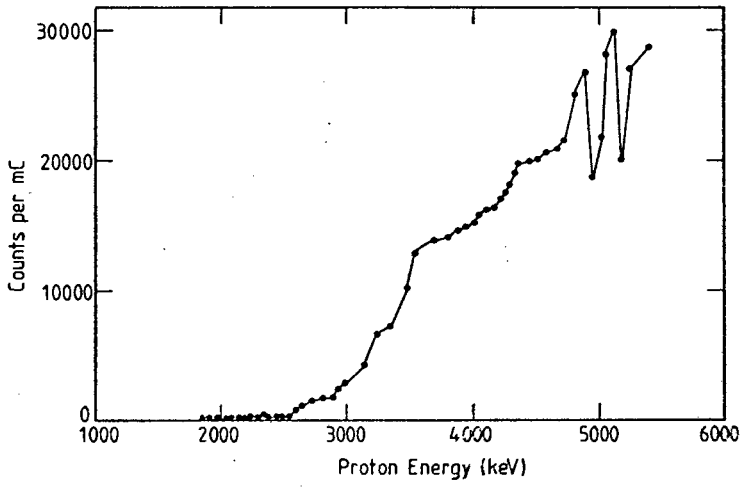

FIGURE 13 : Excitation function for the production of the 440-keV sodium gamma-ray obtained from the bombardment of vacuum-deposited NaCl on a tatalum disc.

thick foils of magnesium, aluminium and silicon were bombarded with protons over the same energy range. From the curves, $\underline{E}_m$ values were calculated and the method of average stopping power [Is 78 a]was used to correct for the variation in composition of the analysed samples. The values of $\underline{E}_m$ are given in Tables 24 and 25.

TABLE 24 : $\underline{E}_m$-values for cement analysis

E_p (keV)	$\underline{E}_m$ values at E_γ values (keV) of :-					
	F		Na	Mg	Al	
	110	197	440	585	844	1 015
2500	2 326	2 269	2 266	2 225	2 176	2 334
2600	2 382	2 274	2 343	2 298	2 184	2 406
2700	2 391	2 309	2 409	2 364	2 229	2 457
2800	2 393	2 367	2 416	2 410	2 305	2 565
2900	2 395	2 377	2 486	2 468	2 474	2 701
3000	2 511	2 426	2 502	2 557	2 543	2 752
3100	2 556	2 499	2 529	2 632	2 674	2 808
3200	2 645	2 568	2 562	2 789	2 698	2 840
3300	2 646	2 604	2 644	2 850	2 743	2 879
3400	2 707	2 605	2 713	2 945	2 891	2 906
3500	2 723	2 653	2 724	3 077	2 909	2 933
3600	2 798	2 665	2 763	3 078	3 047	3 093
3700	2 887	2 668	2 849	3 084	3 165	3 115
3800	2 903	2 771	2 888	3 156	3 199	3 156
3900	3 077	2 787	2 941	3 350	3 306	3 293
4000	3 150	2 893	3 001	3 379	3 323	3 312
4100	3 196	2 898	3 048	3 407	3 471	3 556
4200	3 219	2 947	3 107	3 471	3 569	3 760
4300	3 241	3 069	3 166	3 488	3 674	3 940
4400	3 370	3 090	3 416	3 545	3 800	4 052
4500	3 530	3 173	3 475	3 615	3 949	4 187
4600	3 538	3 263	3 482	3 689	4 017	4 281
4700	3 539	3 302	3 632	3 790	4 155	4 296
4800	3 621	3 356	3 832	3 929	4 234	4 314
4900	3 777	3 453	3 839	4 011	4 304	4 379
5000	3 867	3 713	3 963	4 041	4 378	4 437
5100	4 056	3 744	4 027	4 112	4 466	4 845
5200	4 091	3 824	4 099	4 233	4 509	4 903
5300	4 173	3 926	4 123	4 525	4 613	5 086

TABLE 25 : $\underline{E}_m$-values for cement analysis

E_p (keV)	$\underline{E}_m$ values at E_γ values (keV) of :-					
	Si	Ca				
	1 273	131	373	520	729	1 157
2500	2 107	2 196	2 093	2 304	2 163	2 177
2600	2 234	2 217	2 143	2 401	2 197	2 243
2700	2 319	2 243	2 247	2 469	2 269	2 279
2800	2 347	2 296	2 286	2 515	2 445	2 309
2900	2 368	2 319	2 341	2 663	2 563	2 378
3000	2 474	2 324	2 390	2 768	2 646	2 416
3100	2 515	2 404	2 443	2 774	2 737	2 531
3200	2 624	2 518	2 473	2 881	2 813	2 633
3300	2 711	2 641	2 554	2 923	2 947	2 721
3400	2 763	2 667	2 620	2 973	3 197	2 807
3500	2 841	2 753	2 785	3 017	3 321	2 913
3600	2 873	2 884	2 897	3 104	3 483	3 114
3700	2 942	2 920	3 001	3 193	3 542	3 201
3800	3 004	2 941	3 117	3 313	3 619	3 347
3900	3 096	3 017	3 214	3 497	3 664	3 418
4000	3 174	3 063	3 369	3 549	3 725	3 523
4100	3 263	3 119	3 394	3 757	3 853	3 663
4200	3 314	3 227	3 421	3 843	3 945	3 719
4300	3 419	3 237	3 449	4 017	4 124	3 783
4400	3 501	3 313	3 556	4 068	4 251	3 813
4500	3 619	3 490	3 615	4 147	4 473	3 932
4600	3 694	3 541	3 650	4 293	4 543	4 041
4700	3 742	3 679	3 724	4 404	4 663	4 172
4800	3 891	3 787	3 817	4 536	4 717	4 243
4900	3 921	3 831	3 963	4 693	4 843	4 291
5000	3 974	3 903	4 065	4 741	4 953	4 317
5100	3 993	4 019	4 242	4 843	5 063	4 339
5200	4 013	4 161	4 394	4 919	5 178	4 418
5300	4 160	4 347	4 574	5 018	5 201	4 425

In order to perform multi-elemental analysis of cements, the optimum bombarding energy, chosen as a compromise for best attainable sensitivities for the various gamma-rays used, was 4750 keV.

An example of a typical set of results for aluminium using the 1015-keV ^{27}Al p(2,0) gamma-ray is shown in Table 26. Precision, sensitivity and accuracy of the determination of aluminium was evaluated from the analysis of 7 standard cement samples having an aluminium concentration range of about 1.6 to 3.5%. Three or four replicate analyses were performed in each standard and a mean count from 27 observations of 70386 ± 529 counts per mC for 1% Al by mass was obtained. This value was in agreement with the slope of the calibration line of 70309 counts per mC obtained by the method of least squares. The relative standard error of less than 1% gave an indication

E_p = 4750 KeV γ-Ray used : ^{27}Al p(2,0) - 1015 KeV

SRM Cement	Known Al Content (% by mass)	Mean Count (mC^{-1})	Mean Count mC^{-1} for 1% Al	Found % Al	Number of Analyses	Error Absolute	Error Relative %
636	1.60	112031	70106	1.591	4	-0.009	-0.6
637	1.74	122281	70439	1.737	4	-0.003	-0.2
633	2.00	140915	70422	2.002	4	+0.002	+0.1
639	2.27	159339	70349	2.264	4	-0.006	-0.1
638	2.36	166250	70593	2.262	3	+0.002	+0.1
634	2.76	193336	70126	2.747	4	-0.013	-0.5
635	3.33	234713	70569	3.335	4	+0.005	+0.2

No of Analyses	=	27
Mean count (mc^{-1} for 1% Al)	=	70386 ± 529
Relative Standard Error	=	0.75%
Root Mean Square Error	=	0.0015% Al by mass

TABLE 26 : Typical analytical results for aluminium determination in cements

of the precision of analysis over the cited concentration range. The root mean square error of 0.0015% indicated that the method can be used for aluminium determinations in concentration ranges usually associated with the PIXE technique. This is particularly interesting because aluminium is usually difficult to determine with the latter analytical technique. A summary of the analytical parameters from the other gamma-rays in cements is given in Table 27.

Gamma-ray keV	Identity	Precision (%)	Sensitivity ($\mu g.g^{-1}$)
110	^{19}F p(1,0)	2,1	17
197	^{19}F p(2,0)	1,1	7
440	^{23}Na p(1,0)	6,4	480
583	^{25}Mg p(1,0)	3,3	370
844	^{27}Al p(1,0)	1,0	175
1015	^{27}Al p(2,0)	1,0	15
1273	^{29}Si p(1,0)	2,1	210
2230	^{31}P p(1,0)	1,9	120
131	^{48}Ca n(1,0)	2,7	9000
371	^{43}Ca p(1,0)	1,8	720
520	^{48}Ca n(4,3)	2,0	8900
729	^{43}Ca n(5,1)	8,5	9000
1157	^{44}Ca p(1,0)	2,9	70

TABLE 27 : Summary of the results of cement analysis with proton-bombarding beams

Differences in the precision obtained from the use of the respective gamma-rays reflect the statistical errors in counting, the intensities of corresponding backgrounds and the relative intensities of the gamma-rays.

CEMENT ANALYSIS USING ALPHA BEAMS

A spectrum obtained from the bombardment of a typical standard cement sample with 5000-keV alpha particles is shown in Figure 14 [Gi 79c].

The 110- and 197-keV Coulomb-excited gamma-rays from fluorine again feature prominently and were used for the determination of that element.

The 351-keV ^{18}O n(1,0) gamma-ray was interference-free and was selected for the determination of oxygen. Magnesium was determined using the Coulomb-excited gamma-ray of 585-keV. This gamma was interferred with by the 583-keV ^{19}F n(1,0) photon, with the result that the contribution of the interferring gamma-ray had to be calculated from the relative intensities of the fluorine gamma-rays as obtained in the survey[Gi 79a] of alpha-induced prompt gamma-rays.

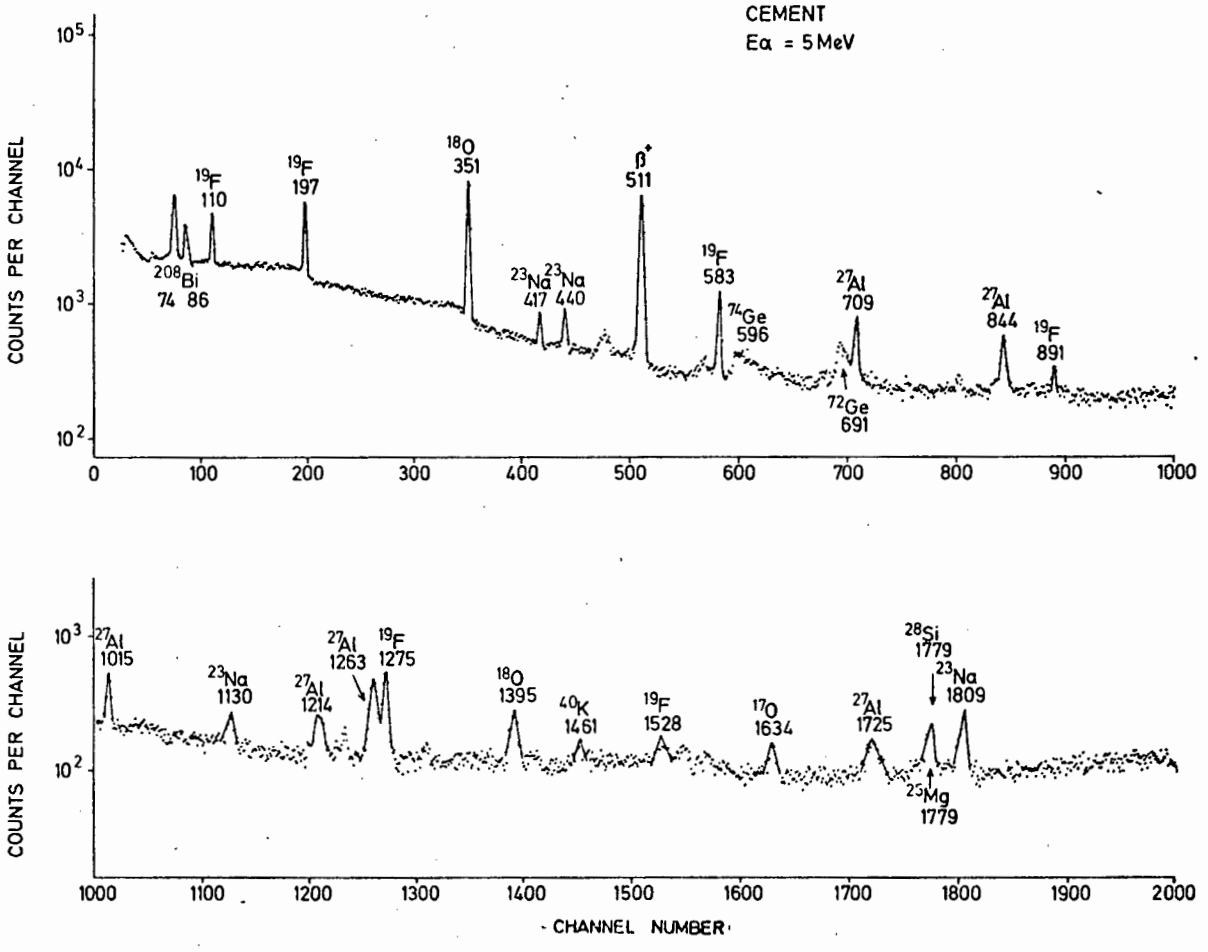

FIGURE 14 : Alpha-induced prompt gamma-ray spectrum obtained from a cement sample

The determination of sodium was carried out using both the reaction gamma-ray of 417-keV and the 440-keV Coulomb-excited gamma-ray.

For aluminium determination, only the 1015-keV gamma-ray was used. Here again, corrections for the contribution of the interferring magnesium gamma-ray had to be made by considering the relative intensities of the magnesium gamma-rays as obtained from the measurement of a pure elemental target [Gi 78a]. Summarized results of the analysis of the cement samples are given in Table 28.

Gamma-ray keV	Identity	Precision (%)	Sensitivity ($\mu g.g^{-1}$)
351	^{18}O n(1,0)	2,5	730
110	^{19}F α(1,0)	1,0	27
197	^{19}F α(2,0)	1,5	12
417	^{23}Na n(2,0)	2,6	360
440	^{23}Na α(1,0)	2,4	740
583	^{25}Mg α(1,0)	1,7	1940
1015	^{27}Al α(2,0)	2,2	970

TABLE 28 : Summary of the results of cement analysis with alpha-bombarding beams.

Oxygen, which could not be determined under proton bombardment, was measured under alpha bombardment with good precision and acceptable sensitivity. In the case of fluorine, sodium and magnesium, the precision using alpha particles was better than with protons, while the sensitivities were comparable. Protons were preferred for aluminium analysis. For calcium and phosphorus which were determined with protons, comparable results were not available because the sensitivities attainable under alpha bombardment were too poor.

CONCLUSION

PIPPS has been shown to play a useful role in the analysis of both major and minor components. In cements, under suitable conditions, the method may serve as a multi-element technique. In cases where interferences occurred either the use of alternate gamma-ray could be made or data from the survey could be used to correct for the contribution from the interferring element. It was demonstrated that duplicate analysis but with different beams proved beneficial by extending the range of elements analysed.

CHAPTER 6

ARCHAEOLOGICAL STUDY

Little is known of the pre-written history of South West Africa/ Namibia even over the past half millennium. Of particular interest is to establish the prehistoric routes of trade and exchange of the early inhabitants. In this context the chemical analysis of the trace element composition of artefacts could play an important role, especially if unique patterns of elemental concentrations could be recognised in source materials. As an essential preliminary it is required to compile data on widely different artefacts from all over the country and to extend the analytical data over as wide a range of elements as possible. Nuclear analytical methods are particularly suited to the analysis of trace and minor components in archaeological specimens such as potsherds and stone artefacts not only because the techniques are simple, multi-elemental and non-destructive but also because the matrix of silica, alumina and other light elements mostly do not interfere with the determinations. Accordingly, it has been possible to amass a large amount of data on trace element concentrations, which have become available for characterisation and identification purposes.

A difficult aspect of such archaeological studies in South West Africa/Namibia is the scarcity of artefacts of well-established origin. This problem is compounded by the fact that most artefacts were produced from widely-occurring ores and clays, the sources of which have mostly not been charted and therefore are not accessible to systematic chemical analysis. Since artefacts need not have been manufactured near the sites where they were found, the method for characterisation has relied upon the establishment of groupings of objects with similar chemical compositions as the first stage of classification. Earlier studies [Bo 77] have shown that well-defined groups could occur at an isolated site even though nearby sites contained specimens of mixed origins which characterise regions of sustained population movements.

Within the area of the Brandberg, a circular granite mountain ranging 20-30 km across, clay-like sediments were found that could have served as source material for pottery for any settlements established in the vicinity. Such pottery was expected to show trace element composition similar to that of the source material but different if produced elsewhere and transported to the area. A similar approach can be used with artefacts made from ores that are not widely-occurring. Such ores are soapstones which occur in relatively few isolated deposits and which are known to have been used for pipes, tuyeres and pendants. Correlations between trace element patterns of such artefacts and the source materials would be useful indicators of communication between the site of the source material and the site of discovery of the artefact.

MATHEMATICAL APPROACH

When multi-elemental analysis is carried out on a suite of samples, the tabulated results may be considered as defining each sample by a point in m-dimensional space, the coordinates of which correspond to the concentrations of the m elements determined. The relationship between the samples of the suite as given by the distances between the respective points in the defined space may readily be calculated, but in exploratory data analysis it may be much more instructive to obtain a global picture of the information contained in the data matrix [Gr 78]. Indeed, once such a picture is obtained, it may provide the answers to a classification problem and may make further data manipulation unnecessary. For this purpose a variety of mathematical techniques of descriptional statistics were applied to the multi-elemental analytical data. Such mathematical techniques were summarised in a recent review [Gr 81]. Inferential statistical techniques were not employed because the required distributional assumptions were not necessarily satisfied by the experimental data.

When n objects are analysed for m elements, the nxm matrix of data is a profile matrix $\underline{x}$, the component X_{ij} of which represents the concentration of element j in object i. From this matrix an nxn proximity matrix, D, can be constructed containing inter-object dissimilarities such that D_{ij} represents the dissimilarity between objects i and j. Single linkage, or nearest neighbour, cluster analysis [Sn 57] operates on the proximity matrix D to produce a dendogram which displays the levels of similarity among the objects and clusters of objects. At this stage in the construction of the dendogram the two most similar objects are located and fused to form a cluster. The dissimilarities between the two objects are deleted and a new set of dissimilarities is computed between the new cluster and the remaining objects or clusters. The process is then continued until all the objects are grouped in a single cluster. The application of this technique to activation analysis data has already been described [Op 77].

Finding the minimum spanning tree (MST) is equivalent to performing a single linkage cluster analysis, and very efficient algorithms exist [Go 69] for carrying out these calculations. Earlier classification of South West African potsherds made extensive use of this approach [Bo 77, Bo 79b].

Non-linear mapping [Sa 69] (NLM) is a technique that is intuitively easy to grasp, and is probably the simplest approach to representing the n-dimensional picture in a 2-dimensional plot. Interpoint distances in the solution configuration, d_{ij}, approximate the interobject dissimilarities, D_{ij}, in the proximity matrix, D. In non-linear mapping, the inter-object dissimilarities are weighted in such a way that smaller distances are fitted relatively more accurately than larger distances. The iterative method used to construct the non-linear map searches for the configuration for which

$$T = \sum_{ij} (d_{ij} - D_{ij})^2 / D_{ij} \qquad (30)$$

is a minimum. This technique has been applied to archaeological classification of potsherds [Bo 79c] using analytical data obtained from PIXE and neutron activation analysis.

In non-metric multidimensional scaling [Kr 64] (MDS) the constraint that interpoint distances must approximate inter-object dissimilarities is weakened by merely requiring that the rank order of the interpoint distances in the solution configuration should approximate the rank order of the original inter-object dissimilarities. The mathematical objective of this approach is to find the configuration which minimises

$$S = \sum_{ij} (d_{ij} - \hat{d}_{ij})^2 / \sum d_{ij}^2 \qquad (31)$$

where $\hat{d}_{ij}$ are the monotonic regression of d_{ij} on D_{ij}. A description of monotonic regression and algorithms for the calculation of $\hat{d}_{ij}$ have been published [Kr 68,Ba 72]

Correspondance analysis [Gr 78, Br 73] (CA) involves a subtle mathematical decomposition of the profile matrix into axes or dimensions, in such a way that the groups of objects which are most distinct, as well as the variables that separate them, are at the extremes of the first axis. Increasingly less important separations are displayed on the second and subsequent axes. If the first two axes of the correspondance analysis are plotted, a two-dimensional display is obtained in which both objects and variables are features. In this display inter-object and inter-variable distances are known as chi-square distances and are a generalisation of the familiar Euclidean distances, but it is not permissble to interpret object-variable distances. However, equations known as the 'transition formulae' relate the object coordinates to the variable coordinates, in such a way that an object that has a high value in a particular variable, and conversely, a low value, is repelled away from that point. The full mathematical description of this method has recently been reviewed [Gr 78, Gr 81] and the procedure for its application is summarised in Table 29.

TABLE 29 : Procedure for the application of correspondance analysis. [Lu 81]

Let X be the n x m matrix with positive elements to be subjected to correspondance analysis.

1. Compute $x = \sum_i \sum_j x_{ij}$

2. Let $P_{ij} = \frac{x_{ij}}{x}$, so that all the elements of the matrix P sum to unity.

3. Compute the vector of row sums $\underset{\sim}{r} = P\underset{\sim}{1}$ where $\underset{\sim}{1}$ is a column vector of 1's

4. Compute the vector of column sums $\underset{\sim}{c} = p^T\underset{\sim}{1}$ where p^T denotes the transpose of the matrix P.

5. Let $Q = P - \underset{\sim}{r}\,\underset{\sim}{c}^T$

6. Let the square matrices D_r and D_c be diagonal matrices with the elements of $\underset{\sim}{r}$ and $\underset{\sim}{c}$ respectively down the main diagonal.

7. Let $R = D_r^{-\frac{1}{2}}\ Q\ D_c^{-\frac{1}{2}}$

8. Find the singular value decomposition of R, i.e. find matrices M and N and a diagonal matrix D_μ such that

$$R = M\ D_\mu\ N^T$$

The singular value decomposition can be found using one of the eigenvalue/eigenvector packages.

9. The rank p approximation of X is then given by $M_{[p]}\ D_{\mu\,[p]}\ N^T_{\ [p]}$ where $M_{[p]}$, $N_{[p]}$ denotes the first p columns of M and N and $D_{\mu\,[p]}$ denotes the first p rows and columns of D_μ.

10. The rows and columns of the correspondance analysis of X in p dimensions are then given by the rows of an nxp matrix F and an mxp matrix G where

$$F = D_r^{-\frac{1}{2}}\ M_{[p]}\ D_{\mu[\,p]} \qquad \text{and} \qquad G = D_c^{-\frac{1}{2}}\ N_{[p]}\ D_{\mu\,[p]}$$

If p is chosen to be 2, we have the correspondance analysis in 2 dimensions, and the rows of F and G give the co-ordinates of the objects (e.g. potsherds, artefacts) and variables (e.g. chemical elements) respectively. The justification for plotting the objects and variables on the same axes lies in the transition formulae; which link F and G :

$$F = D_r^{-1}\ P\ G\ D_{\mu\,[p]}^{-1}$$

$$G = D_c^{-1}\ p^T\ F\ D_{\mu\,[p]}^{-1}$$

RESULTS AND DISCUSSION

The materials submitted for analysis consisted of 35 samples of artefacts and 5 samples of source materials as described in Table 30. In addition to the Si(Li) detector used for X-ray spectrometry, a Ge(Li) detector was placed behind the ladder on which the specimens were mounted, at 45° to the direction of the beam, for simultaneous analysis by PIPPS. The distance between the Ge(Li) detector and the target was varied in order to ensure that the dead-time of the gamma-ray measuring system did not exceed 10%.

The elements that were determined by PIXE were K, Ca, Ti, Fe, Cu, Zn, Ga, Rb, Sr and Zr, while those determined by gamma-ray spectrometry were B, F, Na, Mg, Al, Si and Cu.

A bombarding beam of 4000-keV protons was used. This beam was more energetic than was normally used to excite prompt X-rays, but this energy was chosen to increase the yield of X-rays of medium weight elements while at the same time approximating to optimal conditions for prompt gamma-ray excitation.

Label	Number of specimens	Locality	Raw material	Artefact or type
0	1	Brandberg	Soapstone	Pendant
1	14	Brandberg	Soapstone	Pipes and waste
2	3	Windhoek	Soapstone	Tuyere
3	2	Windhoek	Soapstone	Source material
4	2	Brandberg	Soapstone	Pipe
5	1	Northern Natal	Soapstone	Source material
6	14	Brandberg	Baked clay	Pottery
7	2	Brandberg	Loamy clay	Source material
9	1	Windhoek	Soapstone	Pipe

TABLE 30 : Archaeological data of the analysed materials.

The same analytical data were subjected to the following multivariate statistical techniques:

(a) cluster analysis using nearest neighbour data to produce a minimum spanning tree or a similarity dendogram,

(b) multi-dimensional scaling using metric or non-metric approaches to produce mappings of the proximity matrix,

(c) correspondance analysis which produces a mapping, of the samples that were analysed and of the chemical elements that were determined, in which their inter-relationship is shown.

TRANSFORMATION OF DATA

Because the main purpose of the analyses was to facilitate the classification of the specimens, it was acceptable to express the elemental concentrations either absolutely or in relative terms as counts, or as ratios relative to a selected component, provided that the same component was expressed in a similar manner for all the specimens. The significance of a component for classification purposes need, however, not be related to its absolute concentration. For this reason it was necessary to transform the concentration parameters in such a manner that major or minor components would not dominate trace components in the numerical calculations.

There exist several methods of transforming data to allow each component to have a comparable significance. In this work the concentration parameters were subjected to two kinds of transformations. In the first, the concentration was expressed by its logarithm. This method had the advantage that equal relative changes in high and in low concentration components had an equal affect on the grouping of specimens, but in practice this transformation tended to reduce the role of major components.

The second type of transformation altered the concentration parameter, a, to the value, a^n, where $0<n<1$ and where usually $n = 0.5$. This method tended to equalise the role of trace components.

An important problem of multivariate analysis is the need to cope with missing data points. In this work a datum may be missing when an element was absent in the analysed sample or was present in concentrations below the limit of determination [Cu 68]. As a first approximation, the multivariate analyses were carried out with the missing data points taken to be zero. Subsequently the calculations were repeated, in which estimates were made of the missing values by assuming the element to have been present at a concentration of half the limit of determination [Cu 68], i.e. 1.5 times the standard deviation of the background against which the peak would have been measured. In practice, this correction had little effect on the grouping of specimens.

Single-linkage Cluster Analysis

(a) The minimum spanning tree (MST)

The MST obtained from the analytical data of the 40 samples is shown in Figure 15. These samples can be separated

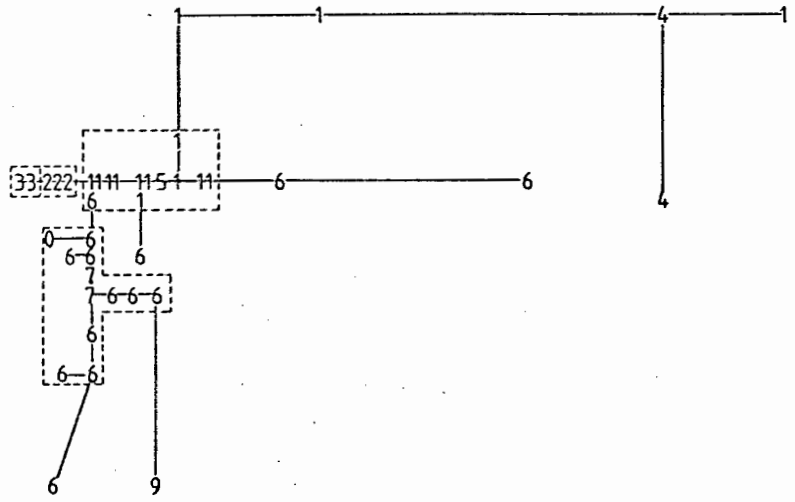

FIGURE 15 : The Minimal Spanning Tree for 40 samples based on the analysis of 10 elements. The numbers refer to the locality and type of samples as listed in Table 30.

into four groups, shown enclosed in broken lines in the figure, and outliers, whose composition was not sufficiently akin to other samples to be grouped in a similar manner. Label 1 represents a collection of soapstone pipes and waste which had been recovered from where they had been mined, manufactured and rejected either as fragments of waste or because of breakage during manufacture. Most of the samples form a compact group. The sample labelled 5 is from a soapstone source several thousand kilometers away which had a similar composition of the elements K, Ca, Ti, Fe and Cu, but in which the heavier elements are much lower in concentration. The inclusion of this sample in the group labelled 1 points to a weakness in the MST method because low concentration components play a slight role in determining the nearest neighbour. Similarly the apparent outliers 1 contain somewhat elevated concentrations of Ca and Ti. The separated groups labelled 2 and 3 are from the Windhoek area, the former consisting of three fragments, presumably of a single tuyere, while the latter is a pair of samples from a soapstone source. The group consists of potsherds from the Brandberg area, and group 7 is from deposits of clay found in the same vicinity. The close correlation between group 7 and most of group 6 strongly indicates that the pottery was manufactured from clays of the locality. The outliers of group 6 had markedly different compositions from those within the boundary and it is thus likely that these outliers were made elsewhere even though discovered at the same site.

(b) Similarity dendogram

A similarity dendogram based on PIXE analysis of the archaeological samples defined in Table 30 is shown in Figure 16. At the 68% similarity level two subgroups were separated, the one consisted of a one outlier labelled 6 and the other included all samples labelled 2, 3 and 5. Further examination of the latter subgroup

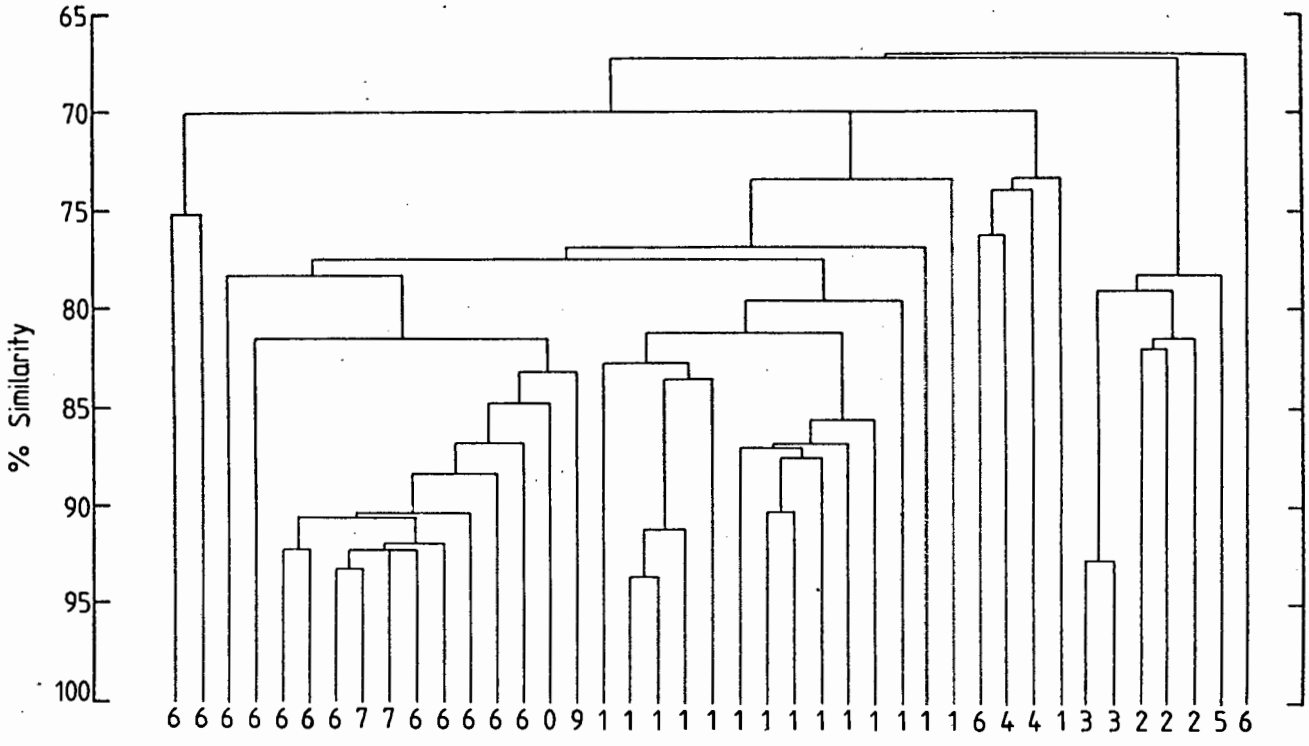

FIGURE 16 : Similarity dendogram for archaeological specimens using PIXE analytical data. The sample lables are those defined in Table 30.

showed that subsequent group separation resulted in three groups, each uniquely labelled. From the remaining suite of samples, a lone outlier labelled 1 and a pair of samples labelled 6 were separated at the 75% similarity level, while at 78% similarity the large group of samples labelled 1 was hived off. Further subdivision occurred for greater similarities.

The advantage of the similarity dendogram lay in the fact that a quantitative measure of similarity was obtained even for samples that were not closest neighbours, while the MST gave meaningful quantitative data only for the two points directly linked. Qualitative separation of groups was, however, more obvious in the latter.

Multidimensional Scaling

(a) Non-linear mapping (NLM)

The NLM obtained from the PIXE data is shown in Figure 17. As before, sample labels are those listed in Table 30. The disadvantage of the NLM is the difficulty of fixing group boundaries without sample identification. The information gained from the MST is thus essential and the two approaches should be used to compliment each other. Group boundaries may be drawn to enclose samples with the same label. It may be noted that the group 5 sample has been excluded from group 1. The close similarity between group 7 and most of group 6 is again emphasised, while the outliers of group 6 are clearly separated. An examination of the analytical data with respect to the positioning of the sample on the NLM in Figure 17, showed that while increasing concentrations corresponded to increased values of the calculated X-coordinates, no such simple correlation existed for the Y-coordinates.

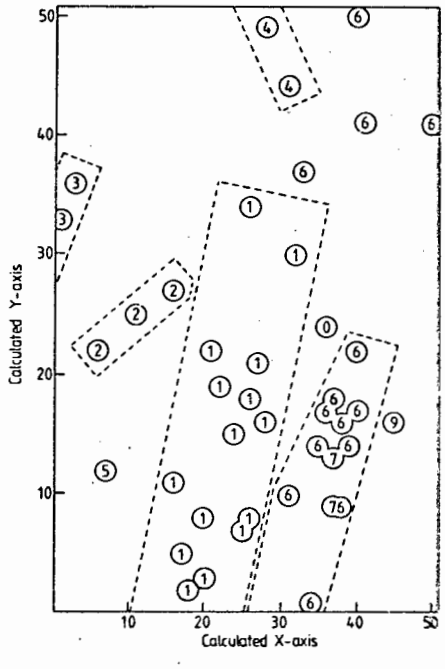

FIGURE 17 : Non-Linear Mapping of the samples, using the PIXE analytical data. The rings around the labels represent the estimate of a positional error caused by errors in analysis. Groups are shown enclosed in dotted lines.

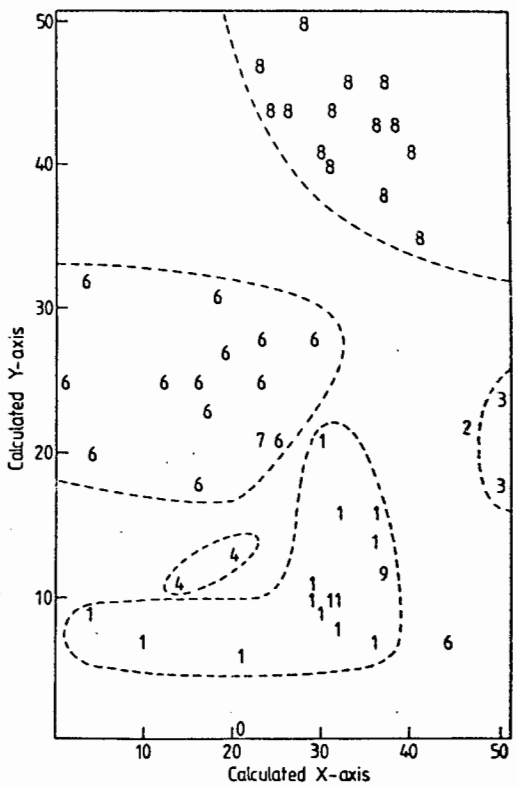

FIGURE 18 : Non-linear Mapping of archaeological specimens using PIPPS analytical data. Samples are labelled as in Table 30, but some specimens were not analysed.

Increased concentrations of the lighter elements K, Ca and Ti tended to produce lower values in the Y-coordinate, whilst the opposite was true for the heavier elements.

Thus the position of group 1 covering a region from low to relatively high Y-values could indicate a possible division of the group into three subgroups, and a measure of inhomogeneity in the samples.

The non-linear mapping of the samples using the data obtained from PIXE analysis was compared with a similar mapping (see Figure 18) in which data obtained from PIPPS was used. The arrangement of the data points in Figure 18

differ from those plotted from PIXE data because the component vectors represent the concentration of minor components whereas previously, trace components were used. However, despite this difference the groups as indicated in Figure 18 were essentially the same as before.

A separate group of samples, labelled 8, and not connected with the main suite of specimens, was included in the NLM to show the validity of this form of representation. As before, samples labelled 1 and 6 were isolated into separate groups, but the one outlier labelled 6 included in this plot remained isolated from the main group. It was again noted that the sample labelled 7 retained its affinity with group 6.

These results showed that the method of group characterisation was not necessarily confined to the use of sensitive multi-elemental analysis of trace elements, but could also be used with data for minor (and major) components.

(b) Multidimensional scaling (MDS)

Non-metric MDS plots of the PIXE data are shown in Figure 19. The plot obtained after the data had been subjected

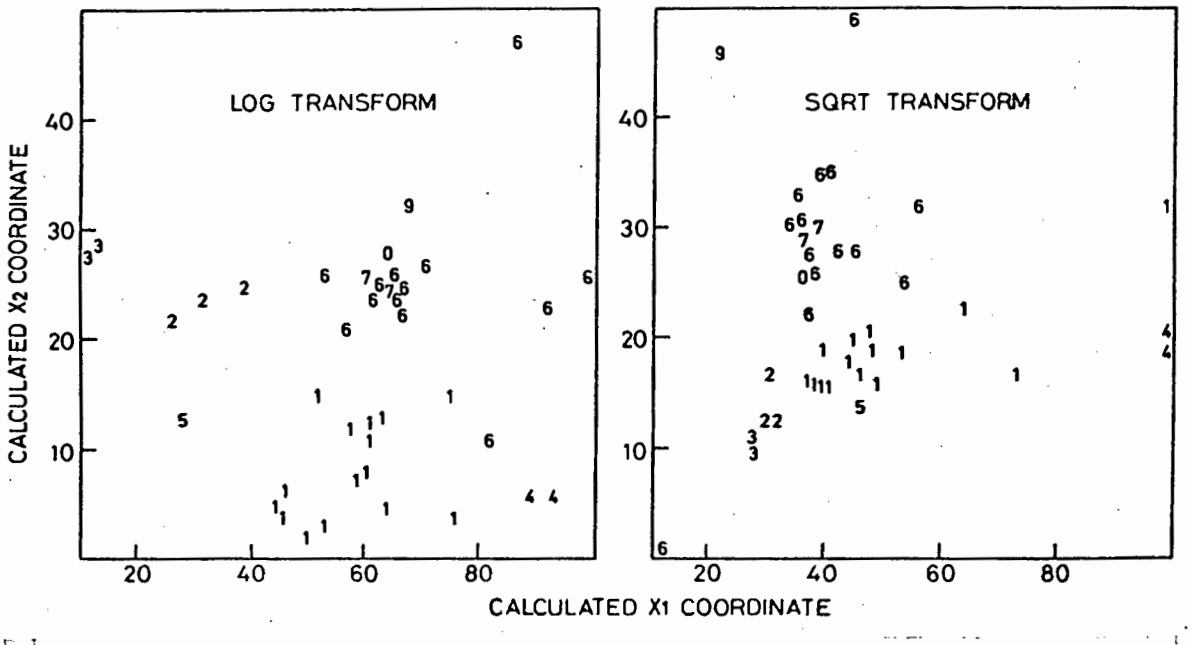

FIGURE 19 : Non-metric multidimensional scaling using PIXE data represented by their logarithms (left) and square-root (right). The numerical labels refer to the same specimens as before.

to a logarithm transformation shows a tight set of group 6, which included the two group 7 specimens (except for the outliers), while the plot showed a spread of group 1. When a a^n-transform was used, the groups became tighter with increasing values of n in the range $0<n<1$, but the most suitable representation was obtained with n = 0.5. In this case the group 1 was more concentrated than with the log-transformation but group 6 was spread out to a greater extent. Although the appearance of the plots was different, the same groupings were obtained even with a severe transformation as logarithms.

Correspondance analysis(CA)

A plot of the correspondance analysis of the first two dimensions, is shown in Figure 20 in which the same PIXE data was used and square-root transformation was applied. From this plot groups 1 and 6 are again separated, while group 6 again includes group 7. There is a slight spread of groups 2 and 4, while group 3 is compact and remote.

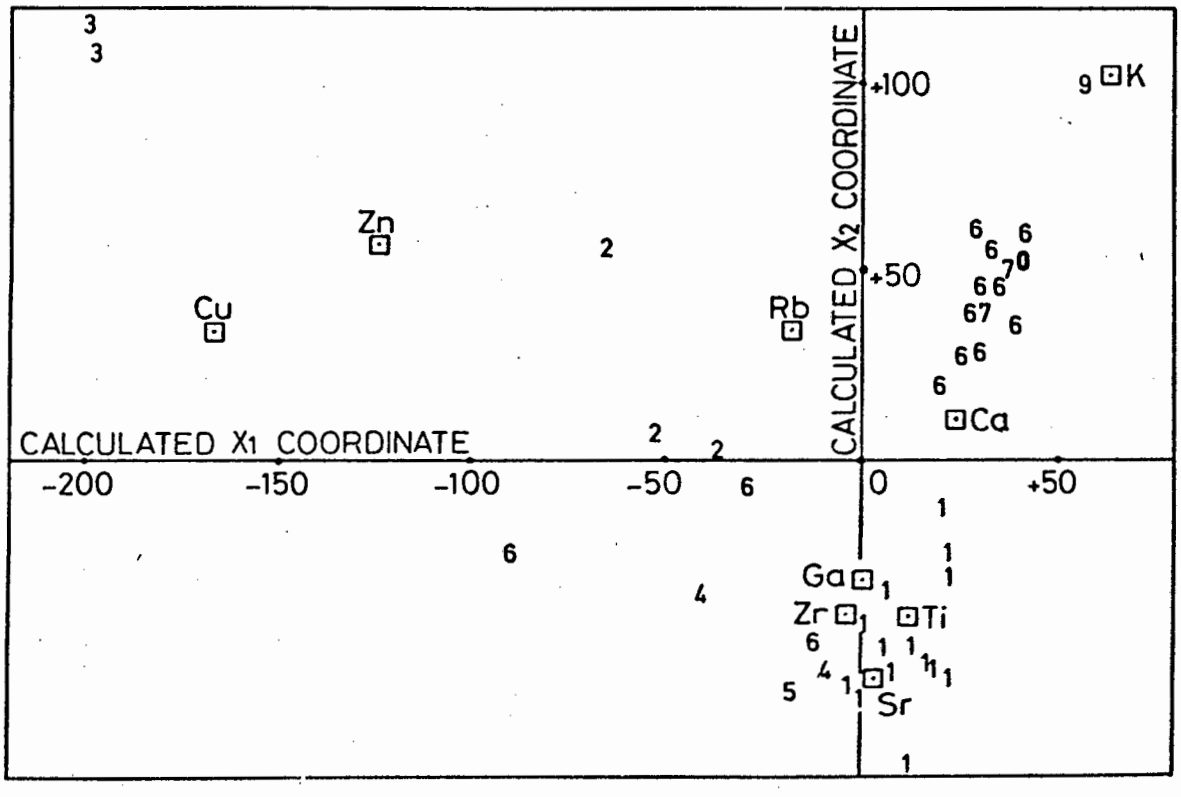

FIGURE 20 : Plot of the first two dimensions of a correspondance analysis showing the groupings of samples and possible correlation between the analysed elements. A square-root transformation was applied to the measured data.

Since this representation also included points representing the analysed elements it was possible to derive the information that there existed a form of correlation between the elements Ti,Ga, Zr and Sr, between the elements Cu and Zn and between Ca and K. In the last mentioned case, both elements were plotted along a similar direction from the origin, but the distant position of K represented a larger spread in the K-coordinates of the sample points.

The positioning of the points of group 3 implied that this group was characterised by high concentration of Cu and Zn. Similarly, group 6 had a higher content of Ca and K than group 1 but a lower content of Ti ,Ga, Zr and Sr. The outliers of group 6 contained decreased concentrations of K, but moderate levels of Cu, Zn and Ti, Ga, Zr and Sr.

The correlation that existed in the elements Ti, Ga, Zr and Sr was confirmed by a CA in which the Ti-component was omitted, but which yielded virtually unchanged groupings.

EXTENT OF SAMPLE HOMOGENEITY

In order to estimate the sample homogeneity, soapstone specimens cut into appropriate sizes (see page 20), were scanned with proton-beams at intervals of 5 mm.

Each spot analysed in the scans of the soapstones was considered as a separate sample and the data were analysed. It was found that the Windhoek soapstone (group 3) was more homogeneous than that from Natal (group 5), but the variability of each was comparable with the differences between individual samples from the corresponding ores. In the case of the Natal soapstones, the analysed spots clustered into three groups depending largely on the Cr and Zn content. Subsequent examination showed that spots with high Cr and low Zn fell either wholly or partly on green streaks in the ore. In cases of streaked soapstones therefore, several analyses on different spots should be carried out for characterisation purposes.

ARCHAEOLOGICAL SIGNIFICANCE

The specimens submitted consisted either of soapstones or of clays as described in Table 30. Group 1 represented a collection of soapstone pipes and waste which had been recovered many years ago from the actual quarry where they had been mined. As the original quarry had not been relocated it was assumed that these samples represented that part of the deposit which the miners considered as most suitable for making into pipes. Group 3 represented two samples from a soapsone source in quite a different geological setting and group 5 a sample from several thousand kilometers away. The three groups separated out very well and group 1 was relatively homogeneous. However, the apparent homogeneity of a group and the relative distance between two groups depended on the transformation used in the statistical analysis, as for example, the proximity of group 5 to group 1 in Figure 19. In this connection it may be noted that although group 5 is close to group 1 in the CA of Figure 20, this similarity is destroyed when the third dimension is taken into account. Group 2 was made up of three samples from a single tuyere, which displayed a certain amount of variability of composition. Group 4 consisted of two small pipe fragments, not necessarily of the same pipe, and appear to have a close relationship with the group 1 source material.

The specimens and artefacts of clay were confined to groups 6 and 7. Group 6 represented a suite of pottery samples from a number of sites within the Brandberg Mountain. Group 7 consisted of two clay-like sediments from the same area. All the described methods of analysis showed that most of the group 6 and both group 7 samples formed a single cluster, but a few of group 6 samples separated as outliers. Since the mountain was composed of uniform granite, the clays resulting from the weathering of the parent material reflected the same uniformity. The analytical results thus provided extra evidence that most of the pottery that was probably manufactured outside this area and was carried was manufactured within the mountain area. The outliers of group 6 represent pottery that was probably manufactured outside this area and was carried in either by people carrying their possessions from site to site or as a result of a trade network.

CONCLUSIONS

Several methods of multivariate analysis have been shown useful for characterisation of archaeological material. The different approaches result in similar groupings, even though different methods of elemental analysis were used and different elements were determined. It should, however, be noted that no method should be used in isolation because the various methods contribute different aspects of statistical information.

From an archaeological point of view the results showed that it was possible to distinguish a limited number of soapstone sources, while the close correspondence between the Brandberg clay source and most of the pottery samples indicated that the pottery was probably made in the area in which they were found.

CHAPTER 7

DETERMINATION OF LITHIUM

The minerals of the osumulite group are hexagonal and orthorhombic silicates of the general formula

$A_{1-2}B_{1-2}C_3Z_{12}O_{30}\cdot nH_2$

with A = Ba, Ca, K, Na
B = Fe^{+2}, Li, Mg, Mn^{+2}, Na, Sn, Ti, Zn, Zr
C = Al, Be, Li, Mg, Fe^{+3}, Fe
Z = Si, Al

A violet mineral of gem quality was discovered at the Wessels mine in the Kalahari manganese field in 1973 and was subsequently identified [Ba 78] as being the mineral *sogdianite*. A recent re-examination of the material [Du 80] however, indicated that the original identification had been incorrect and that the mineral in question was *sugilite*. The formulae for the type material of sogdianite [Mu 76] and sugilite [Du 68] are:

Sogdianite:

$(K_{1.1}Na_{0.9})(Li_2)(Li_{0.61}Fe^{+2}_{0.2}Fe^{+2}_{0.6}Al_{0.2}Ti_{0.2})(Zr_{0.8}Ti_{0.2})Si_{12}O_{30}$

Sugilite:

$(K_{0.81}Na_{0.19})(Na_{0.64}(H_2O)_{0.91})(Fe_{1.35}Na_{0.59}Ti_{0.06})(Li_{2.02}Al_{0.59}Fe_{0.29})Si_{12}O_{30}$

and both are members of the osumulite group of minerals with very similar and overlapping physical properties. A complete chemical analysis was thus needed for accurate identification.

Because of the economic value of the gem material in question, non-destructive techniques, such as the use of the electron microprobe, were used to determine the elements Z > 8 present. The results of previous analyses are summarised in Table 31. An important component, and one that had previously been calculated by difference, [Du 80], was lithium, which was not included in the Z > 8 elements that had been determined. Accordingly non-destructive nuclear methods using the spectrometry of prompt products, were applied to the determination of lithium.

	Ref [Mu 76]	Ref [Ba 78]	Ref [Co 81]
SiO_2	71.38	69.6	67.91
TiO_2	0.51	0.0	0.01
Al_2O_3	2.97	0.0	0.09
Fe_2O_3	12.76	13.9(b)	15.16
FeO	0.19	(a)	(a)
MgO	(a)	0.0	0.82
CaO	0.0	0.0	0.25
MnO	(a)	1.9	0.92
K_2O	3.76	4.7	3.95
Na_2O	4.37	6.0	5.77
Li O	3.14	3.9(c)	(a)

(a) Not reported

(b) Determined as total Fe

(c) Determined by difference

TABLE 31 : Chemical composition of sugilite mineral

PROMPT ALPHA SPECTROMETRY

The nuclear reaction $^7Li(p,\alpha)^4He$ is highly exoergic with a Q-value of 17 347 keV. Accordingly energetic alpha particles are emitted suitably for analytical spectrometry. Furthermore, because of the low coulomb barrier of lithium, the reaction can be induced with relatively low energy protons. Accordingly, protons that are backscattered from the target can easily be stopped in an absorber of suitable thickness, but one which will still allow the alpha particles to penetrate with sufficient energy for spectrometry and for the determination of lithium [01 74].

PIPPS

At proton energies above 2370 keV the nuclear reaction $^{7}Li(p,n\gamma)^{7}Be$ can occur with sufficient energy to produce the product nucleus in its first excited state, the decay of which proceeds through the emission of a 429-keV gamma-ray. From the survey (see page 37) it is evident that at proton energies between 3500 and 6000 keV, there are emitted two prompt gamma-rays of sufficient intensity, the 429-keV ^{7}Li n(1,0) and the 479-keV ^{7}Li p(1,0) gamma-rays, both of which are suitable for lithium analysis in thick samples.

The present investigation describes the determination of lithium under proton bombardment using both alpha spectrometry and PIPPS.

RESULTS AND DISCUSSION

Because differences in the composition of the matrix of a standard and that of the sample under investigation cause differences in the ranges of the bombarding charged particle beams, corrections are usually applied, based on the stopping powers of the targets [Is 78a]. To obviate the need of such corrections, a simulated gem mineral matrix were prepared by mixing the appropriate weights of SiO_2, Fe_2O_3, NaCl and KBr in a Siebtechnik mill with a wide barrel and grinding stone, to approximate to the composition of the major components of the mineral. Components present in the original mineral in a concentration of less than 1% by mass were not taken into account because their affect on the stopping power for the proton beam was considered to be negligible. To finely ground portions of the simulated mineral, known weights of lithium carbonate were added and the mixtures again milled to attain optimal homogeneity. The standards covered a range of lithium concentrations from 0.43 to 3.68% by mass as Li_2O. Finally, 3-5 pellets of each mixture were prepared under pressure in vacuum.

SELECTION OF IRRADIATION CONDITIONS

Calculations of the kinematics for the reactron $^{7}Li(p,\alpha)^{4}He$ showed that the energy of the product alpha particles did not vary appreciably with proton energy over the range 250 to 5000 keV, as shown diagrammatically in Figure 21.

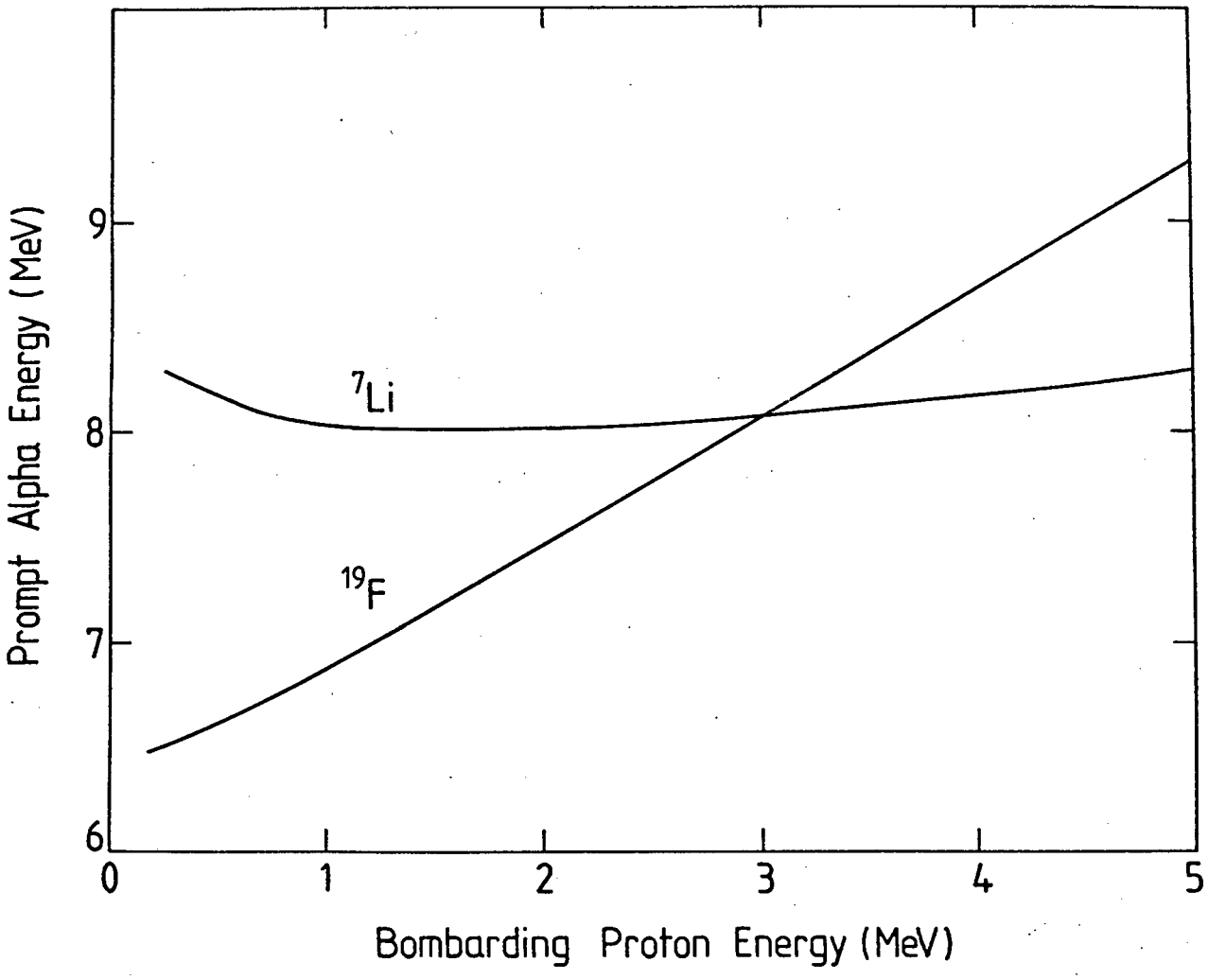

FIGURE 21 : The variation of the prompt alpha particle energy with the proton bombarding energy calculated from the kinematics of the nuclear reaction $^{7}Li(p,\alpha)^{4}He$ and $^{19}F(p,\alpha)^{16}O$.

Since the energy of the backscattered protons is directly proportional to the bombarding energy, and because protons penetrate the absorber material more readily than alpha particles, an absorber selected to stop protons of more than 2000 keV, will also effectively absorb the prompt alpha particles. For prompt alpha spectrometry, therefore, it would be advantageous to use the lowest convenient proton bombarding energy so as to be able to use the thinnest possible absorber.

Preliminary tests had shown that the simulated mineral matrix contained traces of fluoride contamination. This impurity is

the most likely element to cause interference in the alpha spectrometric analysis for lithium through the nuclear reaction $^{19}F(p,\alpha)^{16}O$ for which the Q-value is 8114 keV. The The variation in energy, of the prompt alpha particles from this reaction, with proton bombarding energy is also shown in Figure 21. Because thick targets would yield alpha particles covering a wider energy region below the maximum energy calculated by the kinematics, interference by fluoride would best be minimised by the use of the lowest convenient proton energy too.

For both these reasons it was decided, for prompt alpha spectrometry, to irradiate with protons of 1000 keV, the lowest energy at which the accelerator could maintain a constant beam current. At this bombarding energy the 479-keV ^{7}Li p(1,0) gamma-ray could also be used for analysis by PIPPS to give a simultaneous, but independent duplicate result.

At higher proton bombarding energies, the possibility of also using the 429-keV ^{7}Li n(1,0) gamma-ray became feasible. For this reason protons of 4500 keV were selected for the determination of lithium by PIPPS using both available gamma-rays.

PROMPT ALPHA SPECTROMETRY

Typical prompt alpha spectra obtained during bombardment with 1000 keV protons are shown in Figure 22. The agreement in the shapes of the spectra, obtained from a thick target of a prepared lithium standard and that measured from the gem, is readily evident. Also shown in the figure is the spectrum obtained from a thin layer of calcium fluoride deposited on a tantalum backing. A similar result was obtained from the simulated mineral containing no lithium, thus proving the presence of traces of fluoride impurity.

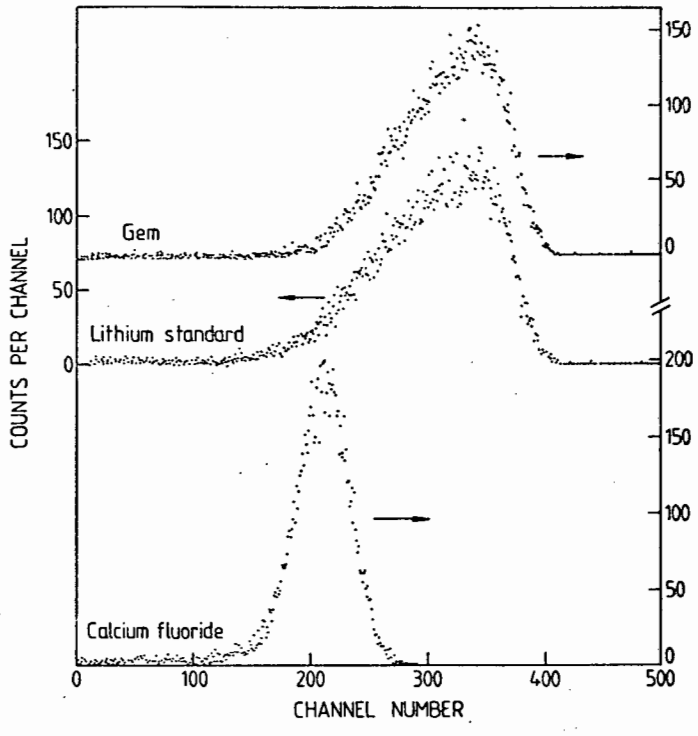

FIGURE 22 : Prompt alpha particle spectra of the gem mineral, and synthesized lithium standard and a deposit of calcium flouride on tantalum, obtained during the bombardment of 1000-keV protons and measured at 135°

If the broad peak from lithium were integrated *in toto*, any fluoride impurity in the sample would cause interference. However, under the conditions of the experiment the maximum count rate from lithium occurred at an energy well above that corresponding to the base of the leading edge of the peak representing fluoride. Accordingly the integrated count representing the lithium content was summed from this energy to the maximum energy of the peak representing lithium.

Precision of alpha spectrometry

Repeat and replicate analyses were carried out on both the standards and the gem in order to detect inhomogeneity. Repeat analyses on each target showed that the relative error was exactly that expected from the statistical errors of counting. Replicate analyses on different targets of the same material showed a relative standard error of about 2.2% which was accepted

as the precision of the method. Included in this value was the statistical errors of counting which amounted to about 1%. It thus followed that all targets were acceptably homogeneous.

PIPPS

The spectrum shown in Figure 23 was obtained during the irradiation of lithium standard with 1000 keV protons. The spectrum is dominated by the single intense peak corresponding to the 479-keV ^{7}Li p(1,0) gamma-ray. At low energies two small peaks were identified as representing the 110-and 197-keV gamma-rays from fluorine-19, thereby confirming the presence of this impurity as indicated with alpha particle spectrometry of the blank. Similar spectra, but without any trace of peaks due to fluorine, were obtained from the gem.

When 4500 keV protons were used the spectra from the standards and the gem indicated the presence of the 429-keV ^{7}Li n(1,0)

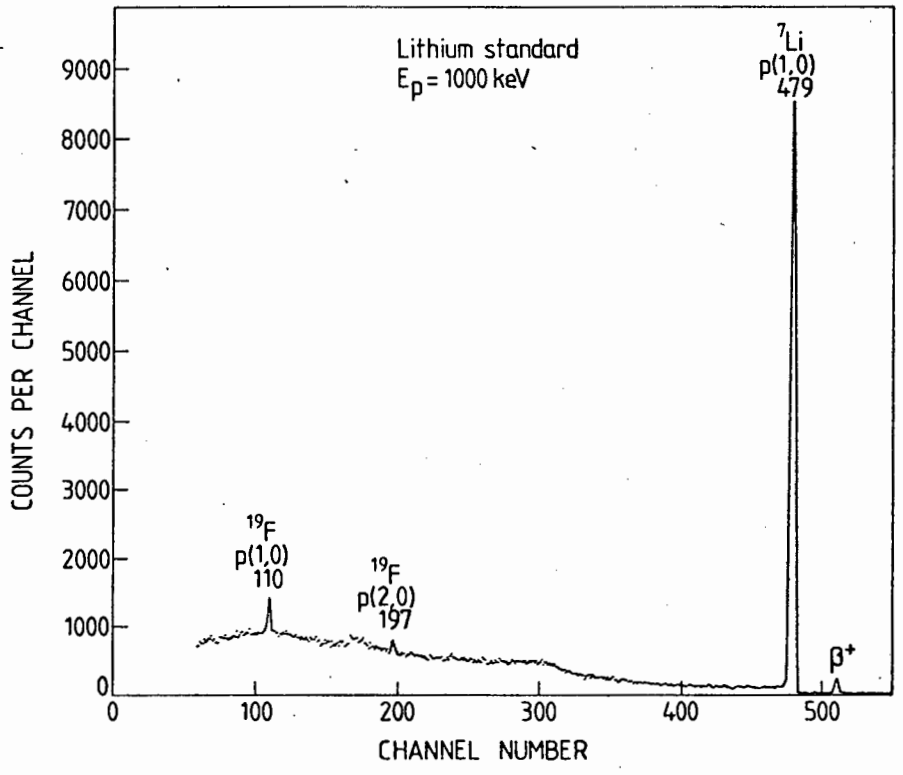

FIGURE 23 : Prompt gamma-ray spectrum obtained during the irradiation of the lithium standard with 1000-keV protons. The presence of small amounts of flourine contamination is indicated.

gamma-ray that could not be excited at the lower bombarding energy. The spectrum (see Figure 24) also showed an intense peak due to sodium corresponding to the 439-keV ^{23}Na p(1,0) gamma-ray. Although this peak is seen to overlap the base of the 429-keV gamma-ray peak of lithium, the resolution of the detector was sufficient to separate the two and even the slight overlap could be stripped by a computer programme without affecting the precision of measurement.

From a knowledge of the composition of the standards and the gem and from the survey data it was deduced that the only gamma-ray that could interfere with the use of the two lithium gamma-rays for analysis, was the 477-keV ^{79}Br n(9,3) gamma-ray, from bromine present in the standards. The intensity of this gamma-ray, observed in a blank after a long irradiation, was negligibly low at the concentration of bromine in the standard.

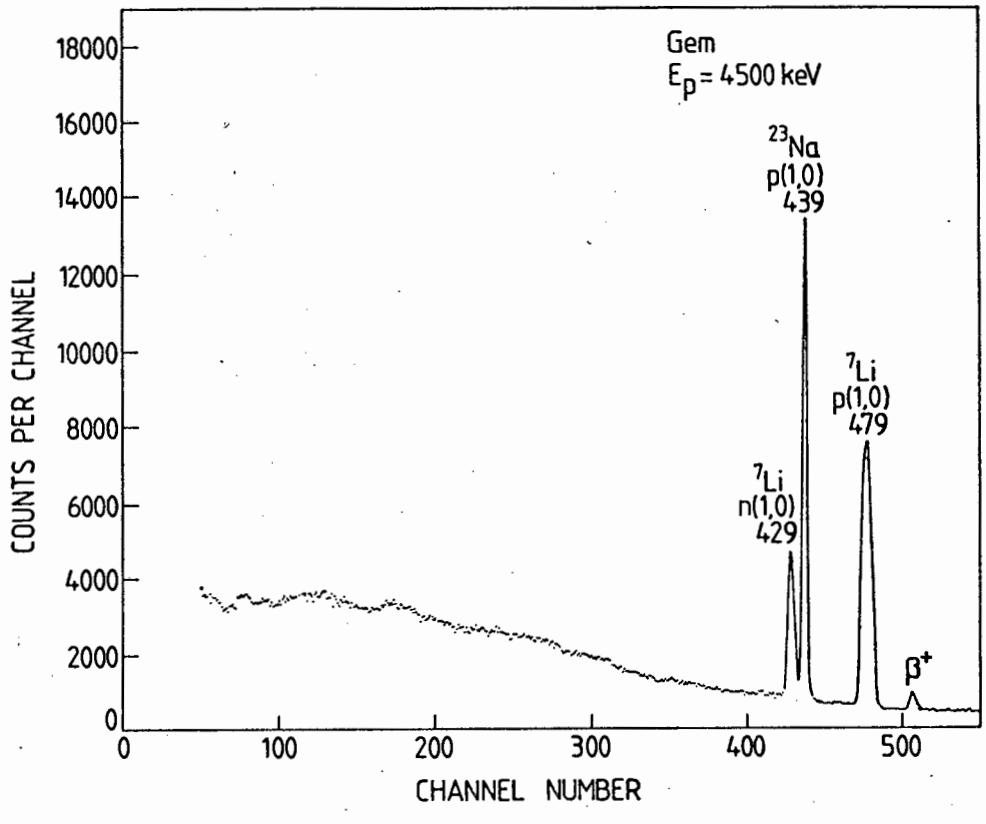

FIGURE 24 : Prompt gamma-ray spectrum obtained from the irradiation of the gem mineral with 4500-keV protons. The presence of sodium, a known component of the mineral, is clearly indicated.

CONCLUSION

A summary of all the analytical results obtained by the different methods is given in Table 32. The reported errors refer to actual experimental errors from a number of different determinations. The weighted mean and the error on the weighted mean were calculated by the standard method [Ba 73]. The lithium content thus obtained was 3.72 ± 0.06% by mass as Li_2O. The relative precision was about 1.6%.

TABLE 32 : Analytical results of sugilite mineral

Proton Energy keV	Measured species	% Li_2O by mass	Error	
			Absolute	Relative %
1000	Prompt alpha	3.76	0.20	2.8
1000	E_γ = 479 keV	3.42	0.20	5.9
4500	E_γ = 479 keV	3.77	0.11	2.9
4500	E_γ = 429 keV	3.66	0.24	6.6
Weighted mean		3.72	0.06	1.6

APPENDIX I

ATLAS OF PROMPT GAMMA-RAY SPECTRA

OF THE 77 STABLE NON-GASEOUS ELEMENTS
ARRANGED IN ORDER OF ATOMIC NUMBER

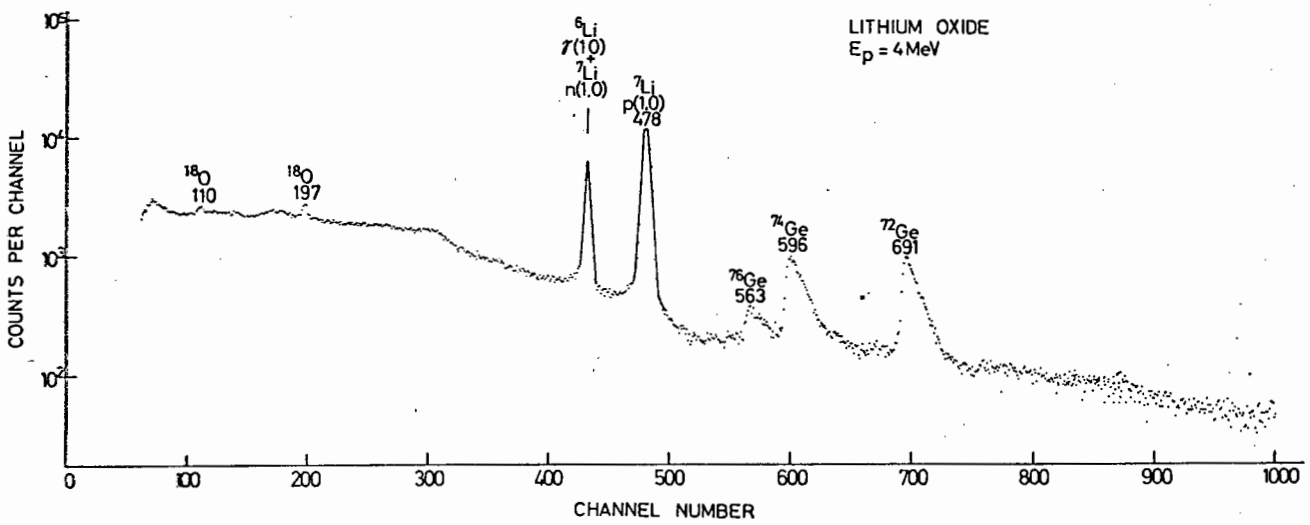
LITHIUM OXIDE
E_p = 4 MeV
^{6}Li γ(1.0)
^{7}Li n(1.0)
^{7}Li p(1.0) 478
^{18}O 110
^{18}O 197
^{76}Ge 563
^{74}Ge 596
^{72}Ge 691
COUNTS PER CHANNEL
CHANNEL NUMBER
0
100
200
300
400
500
600
700
800
900
1000

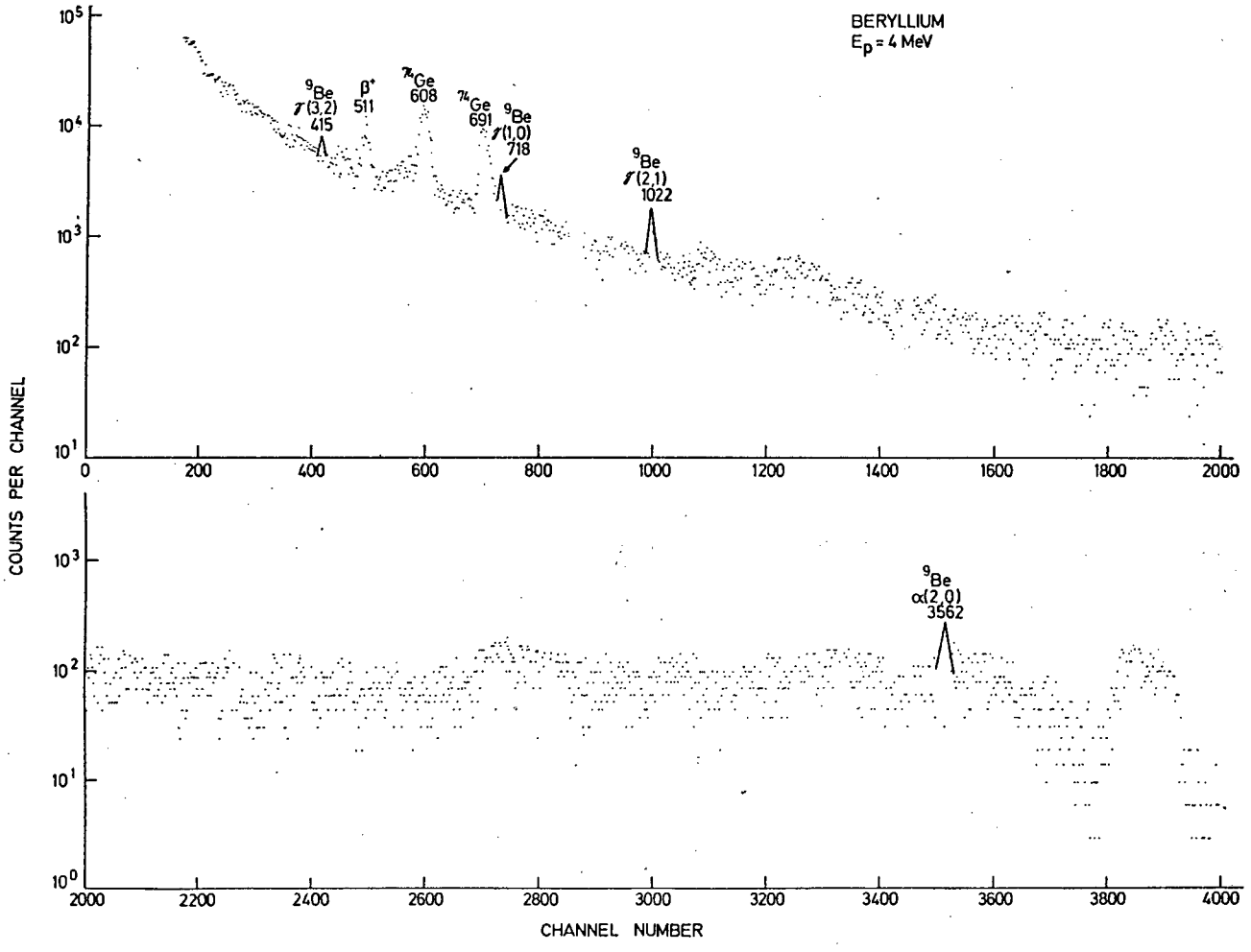
BERYLLIUM
E_p = 4 MeV
^{9}Be γ(3,2) 415
β⁺ 511
^{74}Ge 608
^{74}Ge 691
^{9}Be γ(1,0) 718
^{9}Be γ(2,1) 1022
^{9}Be α(2,0) 3562
COUNTS PER CHANNEL
CHANNEL NUMBER

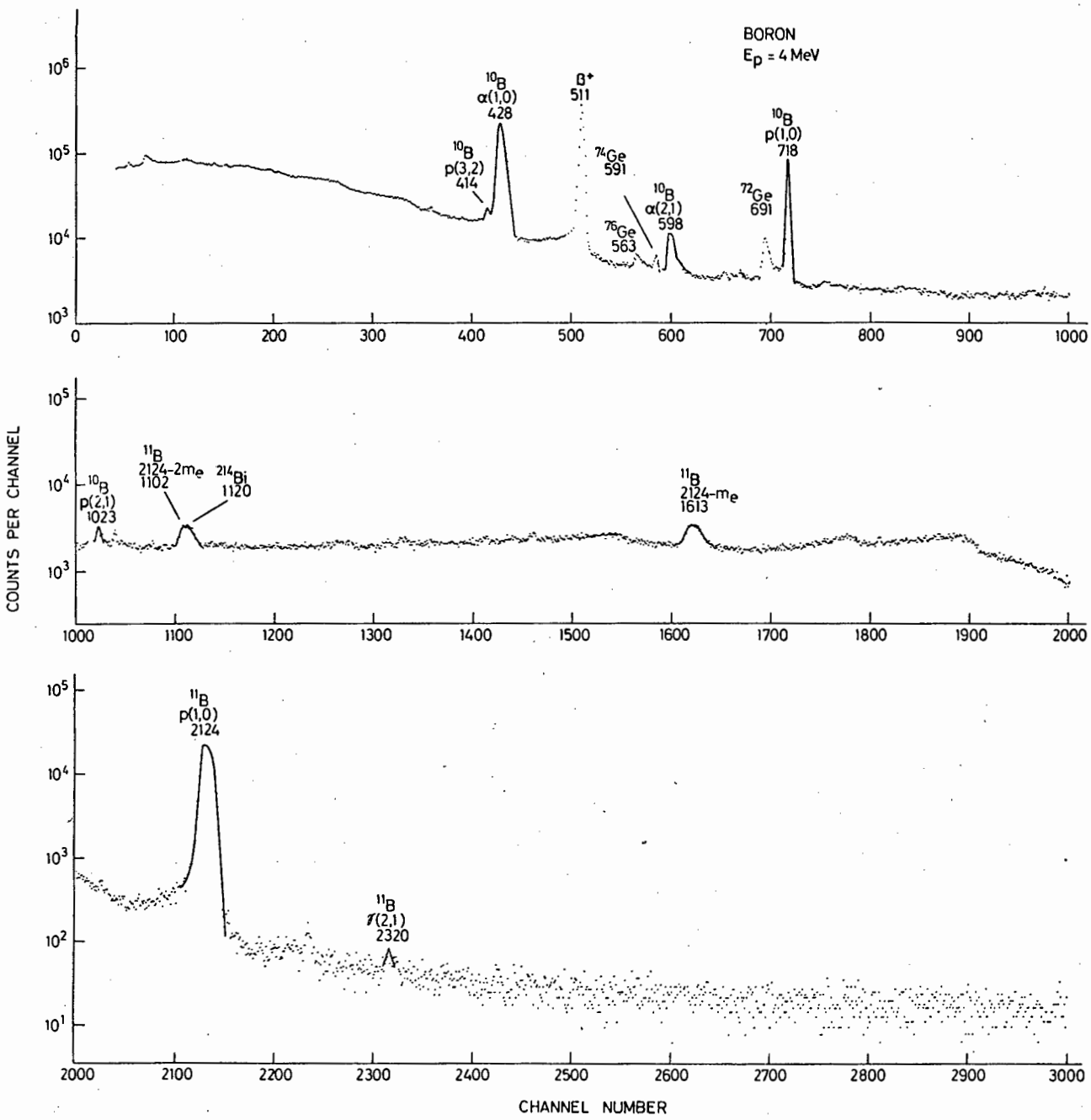
BORON
E_p = 4 MeV
^{10}B α(1,0) 428
β+ 511
^{10}B p(3,2) 414
^{74}Ge 591
^{10}B α(2,1) 598
^{76}Ge 563
^{72}Ge 691
^{10}B p(1,0) 718
^{10}B p(2,1) 1023
^{11}B 2124-2m$_e$ 1102
^{214}Bi 1120
^{11}B 2124-m$_e$ 1613
^{11}B p(1,0) 2124
^{11}B γ(2,1) 2320
COUNTS PER CHANNEL
CHANNEL NUMBER

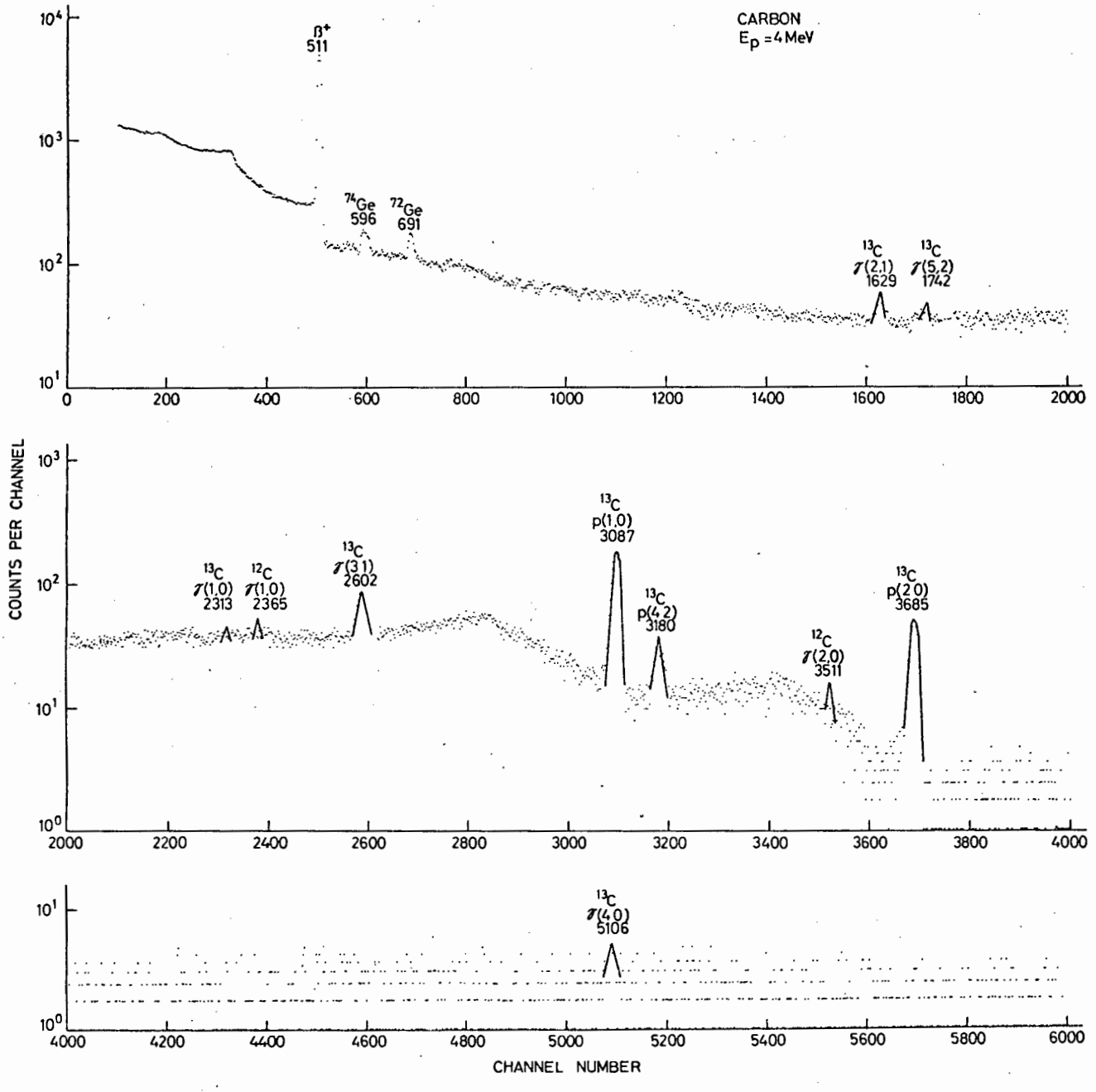
CARBON
E_p = 4 MeV
β^+ 511
^{74}Ge 596
^{72}Ge 691
^{13}C γ(2,1) 1629
^{13}C γ(5,2) 1742
^{13}C γ(1,0) 2313
^{12}C γ(1,0) 2365
^{13}C γ(3,1) 2602
^{13}C p(1,0) 3087
^{13}C p(4,2) 3180
^{12}C γ(2,0) 3511
^{13}C p(2,0) 3685
^{13}C γ(4,0) 5106
COUNTS PER CHANNEL
CHANNEL NUMBER

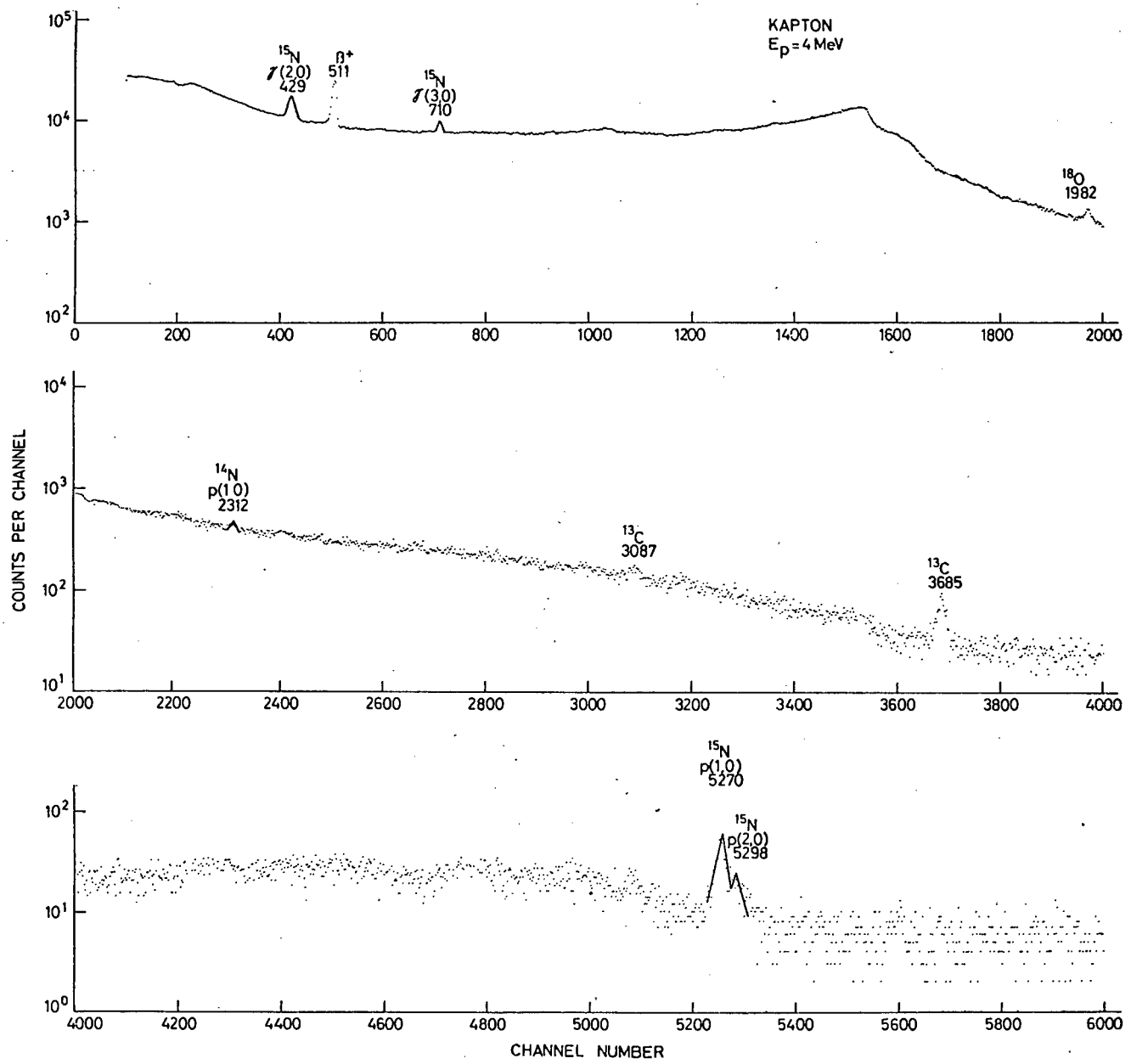
KAPTON
E_p = 4 MeV
^{15}N γ(2,0) 429
β+ 511
^{15}N γ(3,0) 710
^{18}O 1982
^{14}N p(1,0) 2312
^{13}C 3087
^{13}C 3685
^{15}N p(1,0) 5270
^{15}N p(2,0) 5298
COUNTS PER CHANNEL
CHANNEL NUMBER

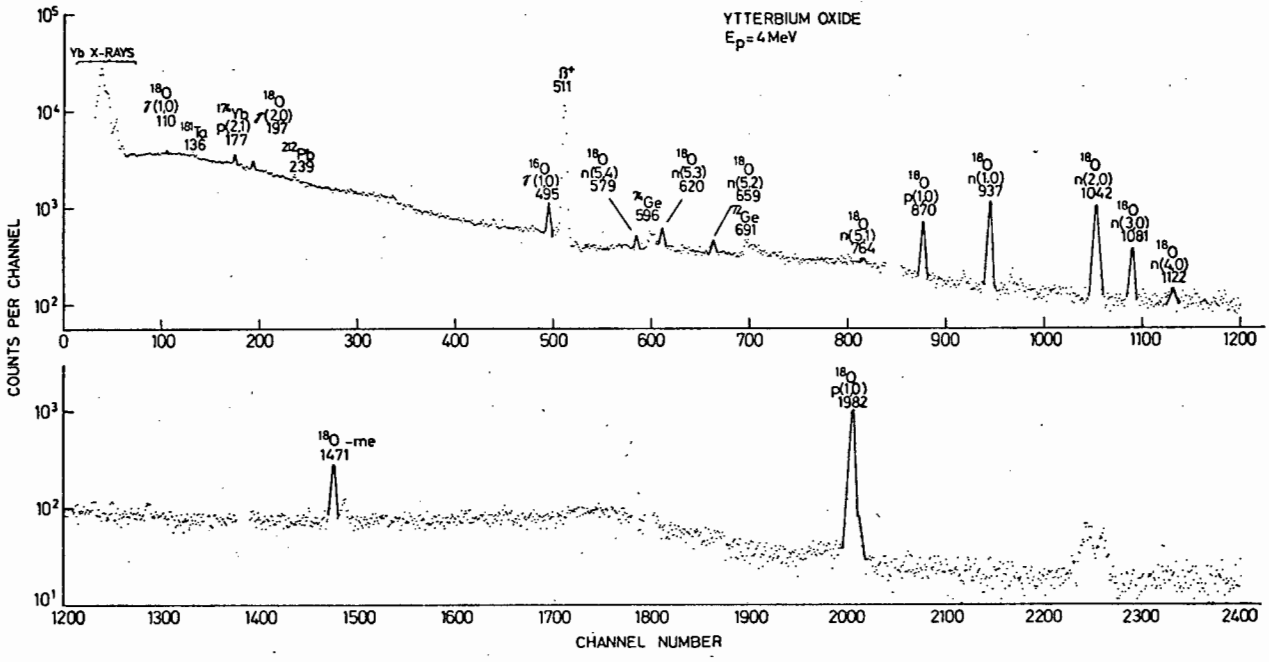
YTTERBIUM OXIDE
E_p = 4 MeV
Yb X-RAYS
^{18}O γ(1,0) 110
^{181}Ta 136
^{17}Yb p(2,1) 177
^{18}O γ(2,0) 197
^{22}Pb 239
β+ 511
^{16}O γ(1,0) 495
^{18}O n(5,4) 579
^{74}Ge 596
^{18}O n(5,3) 620
^{18}O n(5,2) 659
^{74}Ge 691
^{18}O n(5,1) 764
^{18}O p(1,0) 870
^{18}O n(1,0) 937
^{18}O n(2,0) 1042
^{18}O n(3,0) 1081
^{18}O n(4,0) 1122
^{18}O -me 1471
^{18}O p(1,0) 1982
COUNTS PER CHANNEL
CHANNEL NUMBER

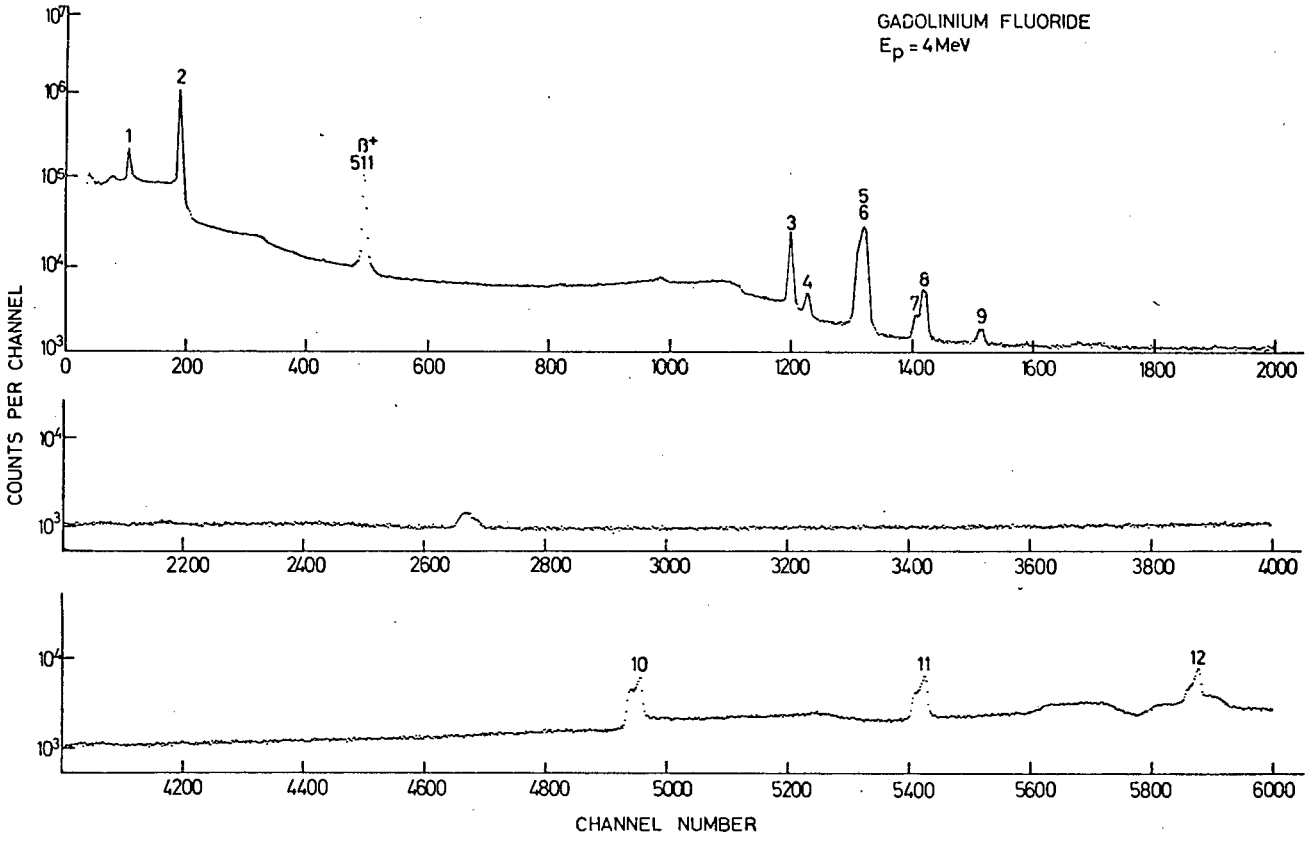

Peak	E_γ keV	Assignment
1	110	^{19}F p(1,0)
2	197	^{19}F p(2,0)
3	1236	^{19}F p(3,1)
4	1261	^{19}F p(4,2)
5	1346	^{19}F p(3,0)
	1349	^{19}F p(4,1)
6	1356	^{19}F p(5,2)
7	1444	^{19}F p(5,1)
8	1457	^{19}F p(4,0)
9	1554	^{19}F p(5,0)
10	6130	^{19}F α(2,0)
11	6720	^{19}F α(3,0)
12	7117	^{19}F α(4,0)

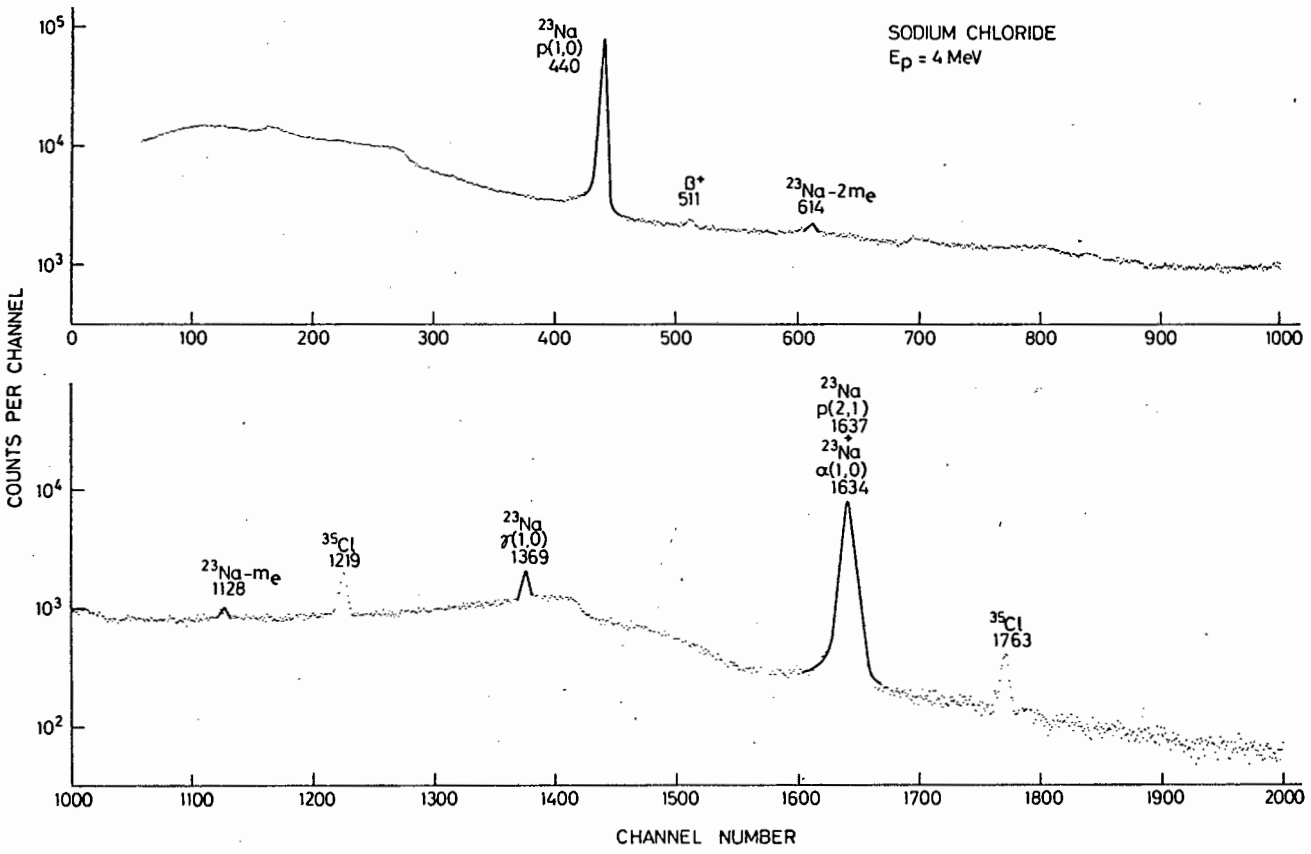
SODIUM CHLORIDE
E_p = 4 MeV
^{23}Na p(1,0) 440
β+ 511
^{23}Na - 2m$_e$ 614
^{23}Na - m$_e$ 1128
^{35}Cl 1219
^{23}Na γ(1,0) 1369
^{23}Na p(2,1) 1637
+
^{23}Na α(1,0) 1634
^{35}Cl 1763
COUNTS PER CHANNEL
CHANNEL NUMBER

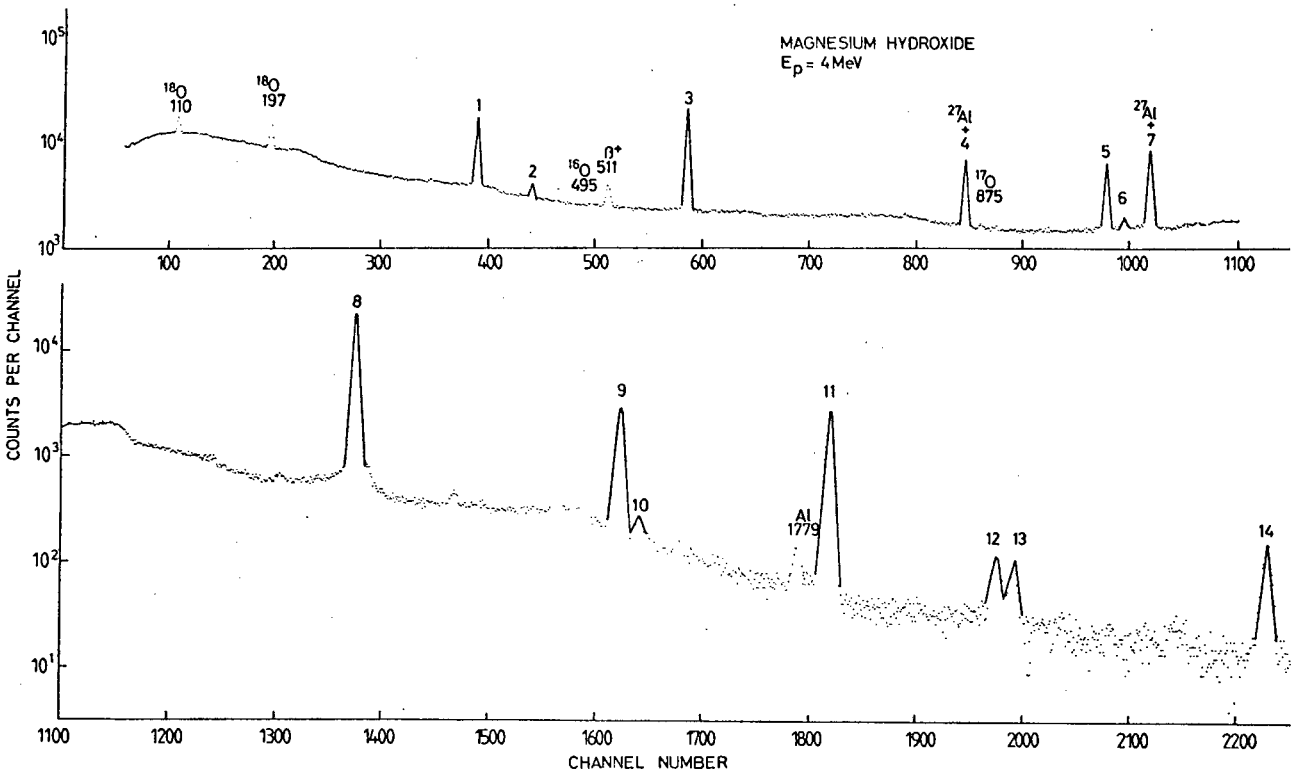

Peak	E_γ keV	Assignment
1	390	^{25}Mg p(2,1)
2	440	^{26}Mg α(1,0)
3	585	^{25}Mg p(1,0)
4	844	^{26}Mg γ(1,0)
5	975	^{25}Mg p(2,0)
6	990	^{25}Mg p(4,2)
7	1014	^{26}Mg γ(2,0)
8	1369	^{24}Mg p(1,0)
	1369	^{26}Mg γ(3,1)
9	1612	^{25}Mg p(3,0)
10	1637	^{26}Mg α(2,1)
11	1809	^{26}Mg p(1,0)
12	1965	^{25}Mg p(4,0)
13	1979	^{25}Mg p(5,1)
14	2210	^{26}Mg γ(3,0)

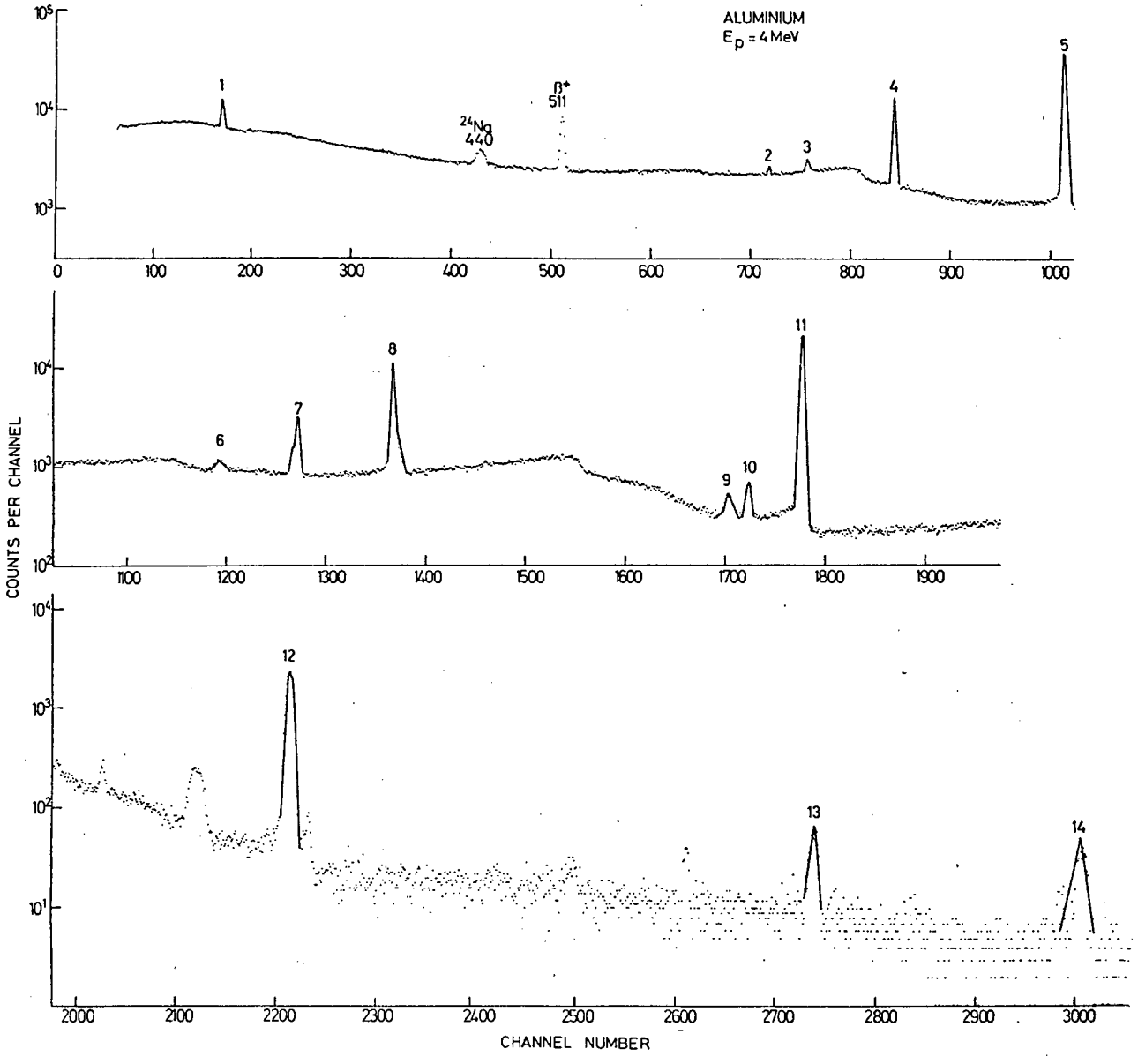

Peak	E_γ keV	Assignment
1	171	^{27}Al p(2,1)
2	720	^{27}Al p(6,1)
3	754	^{27}Al - $2m_e$
4	844	^{27}Al p(1,0)
5	1015	^{27}Al p(2,0)
6	1196	^{27}Al p(3,2)
7	1268	^{27}Al - m_e
8	1367	^{27}Al p(3,1)
9	1699	^{27}Al - m_e
10	1720	^{27}Al p(4,2)
11	1779	^{27}Al γ(1,0)
12	2210	^{27}Al p(3,0)
13	2735	^{27}Al p(4,0)
14	2982	^{27}Al p(5,0)

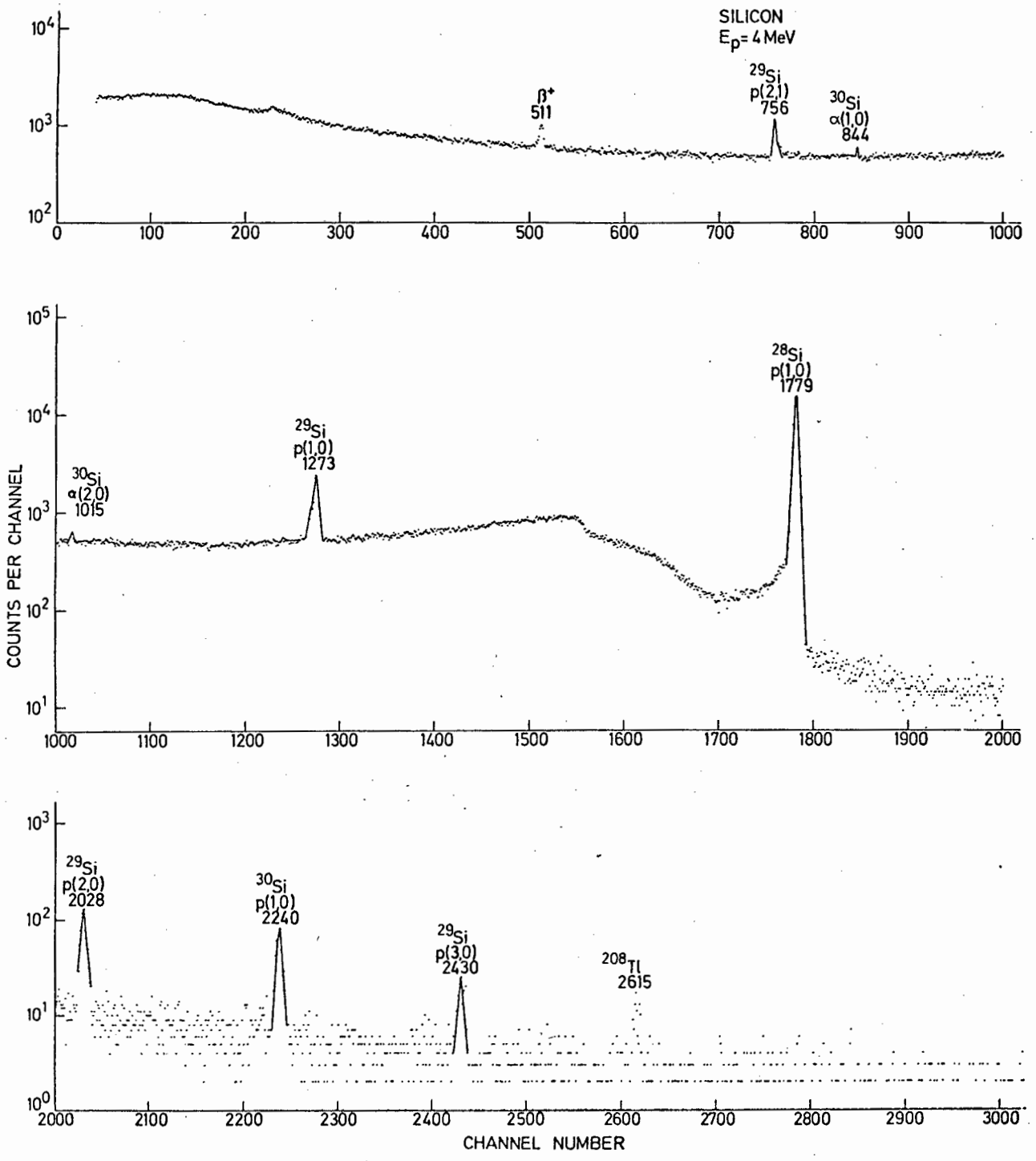
SILICON
E_p = 4 MeV
β^+ 511
^{29}Si p(2,1) 756
^{30}Si α(1,0) 844
^{30}Si α(2,0) 1015
^{29}Si p(1,0) 1273
^{28}Si p(1,0) 1779
^{29}Si p(2,0) 2028
^{30}Si p(1,0) 2240
^{29}Si p(3,0) 2430
^{208}Tl 2615
COUNTS PER CHANNEL
CHANNEL NUMBER

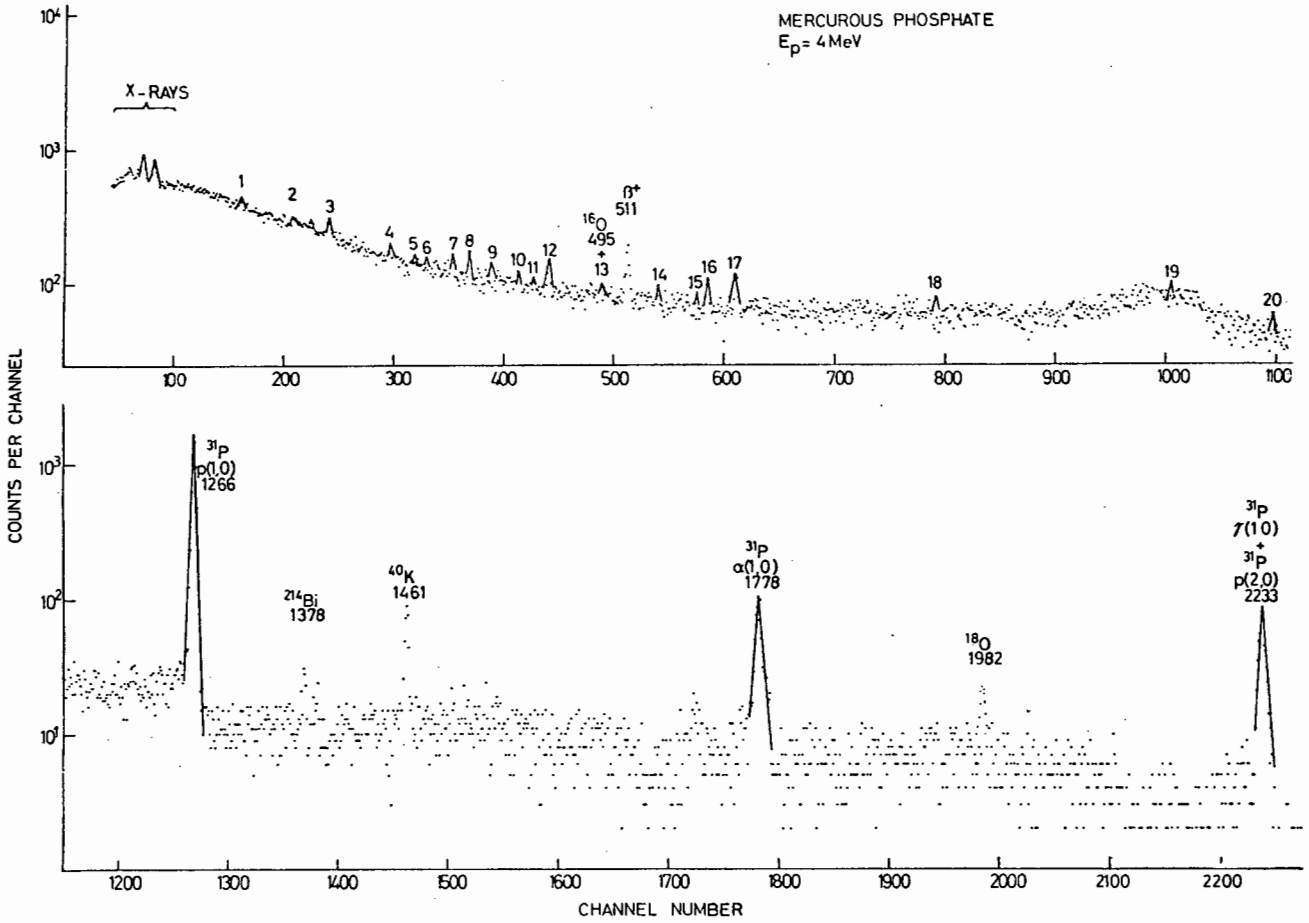

Peak	Eγ keV	Assignment	Peak	Eγ keV	Assignment
1	158	^{199}Hg p(1,0)	11	426	^{196}Hg p(1,0)
2	208	^{199}Hg p(2,0)	12	440	^{202}Hg p(1,0)
3	248	^{199}Hg p(5,2)	13	491	^{202}Hg p(4,0)
4	285	^{199}Hg p(6,2)		491	^{202}Hg n(4,0)
5	315	^{202}Hg n(2,0)	14	543	^{203}Hg p(4,0)
6	331	^{201}Hg n(1,0)	15	579	^{200}Hg p(2,1)
7	351	^{202}Hg n(3,0)	16	588	^{201}Hg n(3,1)
8	364	^{202}Hg γ(4,0)	17	608	^{196}Hg γ(2,0)
	367	^{198}Hg γ(1,0)		611	^{196}Hg p(2,1)
	367	^{199}Hg n(1,0)	18	787	^{202}Hg γ(4,1)
	368	^{200}Hg p(1,0)	19	1029	^{200}Hg p(3,0)
9	386	^{196}Hg γ(1,0)	20	1121	^{199}Hg n(3,0)
10	412	^{198}Hg p(1,0)			

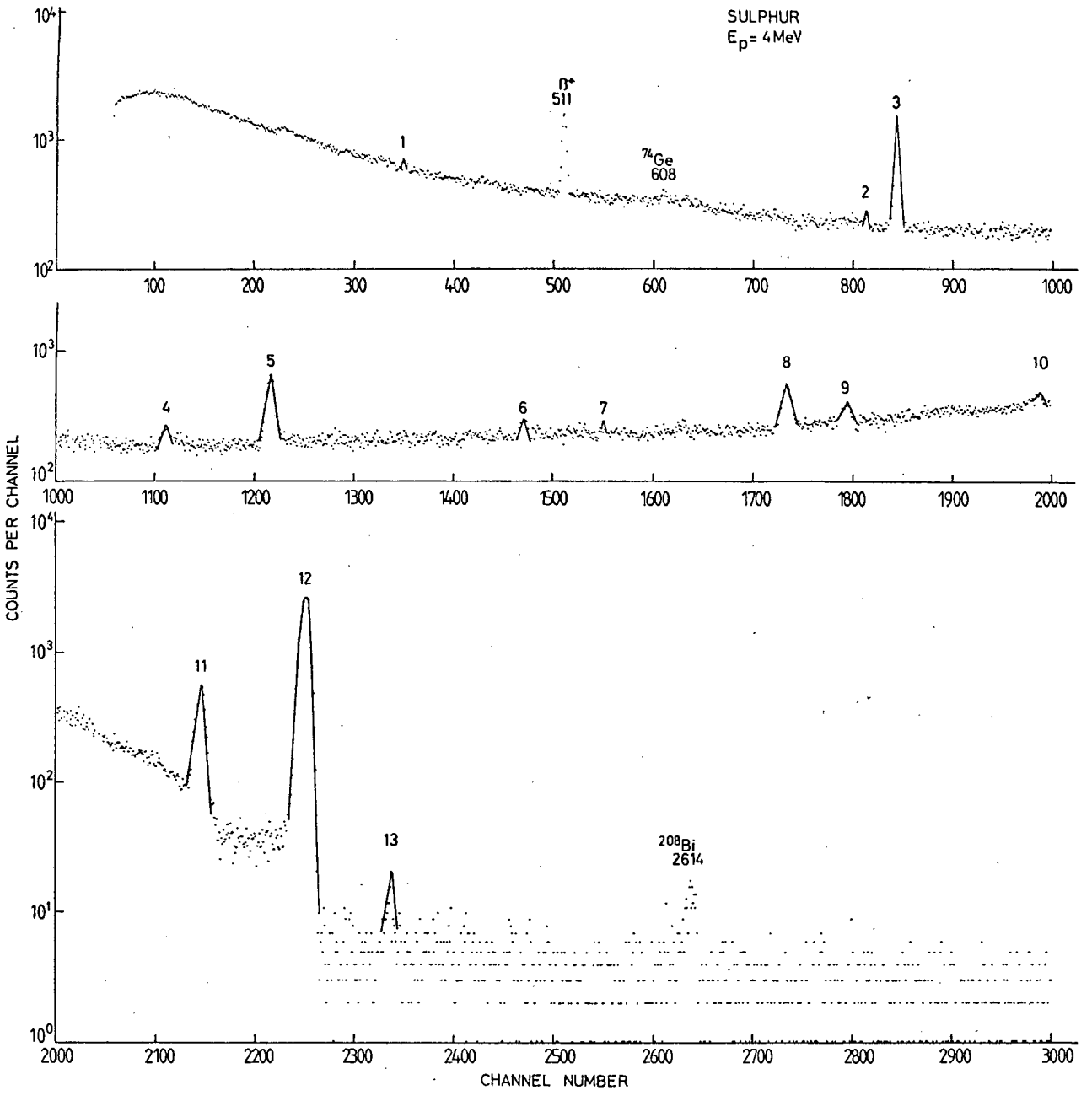

Peak	Eγ keV	Assignment
1	346	^{33}S p(3,2)
2	811	^{32}S γ(1,0)
3	841	^{33}S p(1,0)
4	1107	^{36}S α(1,0)
5	1208	^{32}S - $2m_e$
6	1472	^{33}S p(3,1)
7	1543	^{32}S p(2,1)
8	1719	^{32}S - m_e
9	1787	^{34}S p(3,1)
10	1966	^{33}S p(2,0)
11	2127	^{34}S p(1,0)
12	2229	^{32}S p(4,1)
	2230	^{32}S p(1,0)
13	2313	^{33}S p(3,0)

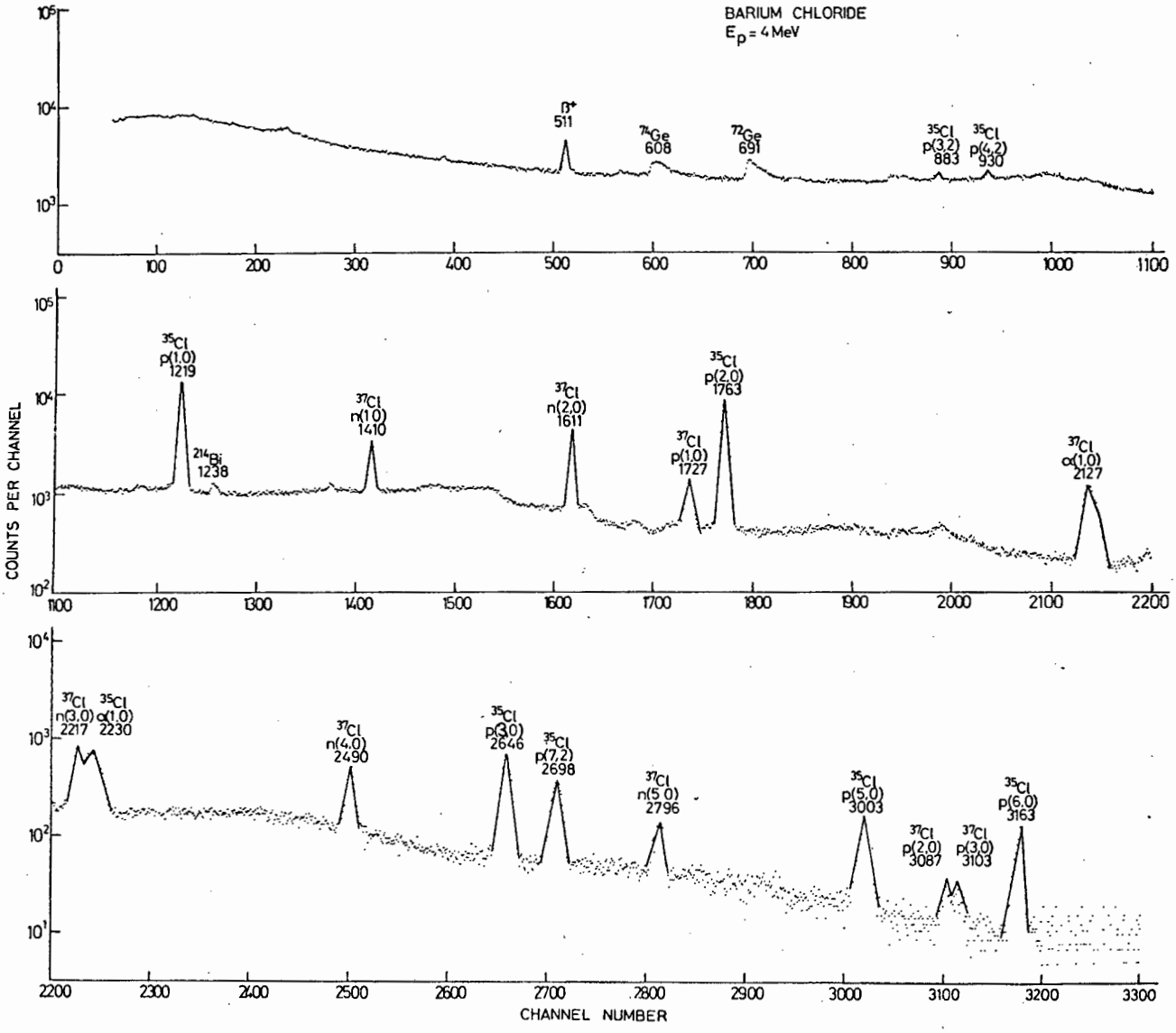
BARIUM CHLORIDE
E_p = 4 MeV
β^+ 511
^{74}Ge 608
^{72}Ge 691
^{35}Cl p(3,2) 883
^{35}Cl p(4,2) 930
^{35}Cl p(1,0) 1219
^{214}Bi 1238
^{37}Cl n(1,0) 1410
^{37}Cl n(2,0) 1611
^{37}Cl p(1,0) 1727
^{35}Cl p(2,0) 1763
^{37}Cl α(1,0) 2127
^{37}Cl n(3,0) 2217
^{35}Cl α(1,0) 2230
^{37}Cl n(4,0) 2490
^{35}Cl p(3,0) 2646
^{35}Cl p(7,2) 2698
^{37}Cl n(5,0) 2796
^{35}Cl p(5,0) 3003
^{37}Cl p(2,0) 3087
^{37}Cl p(3,0) 3103
^{35}Cl p(6,0) 3163
COUNTS PER CHANNEL
CHANNEL NUMBER

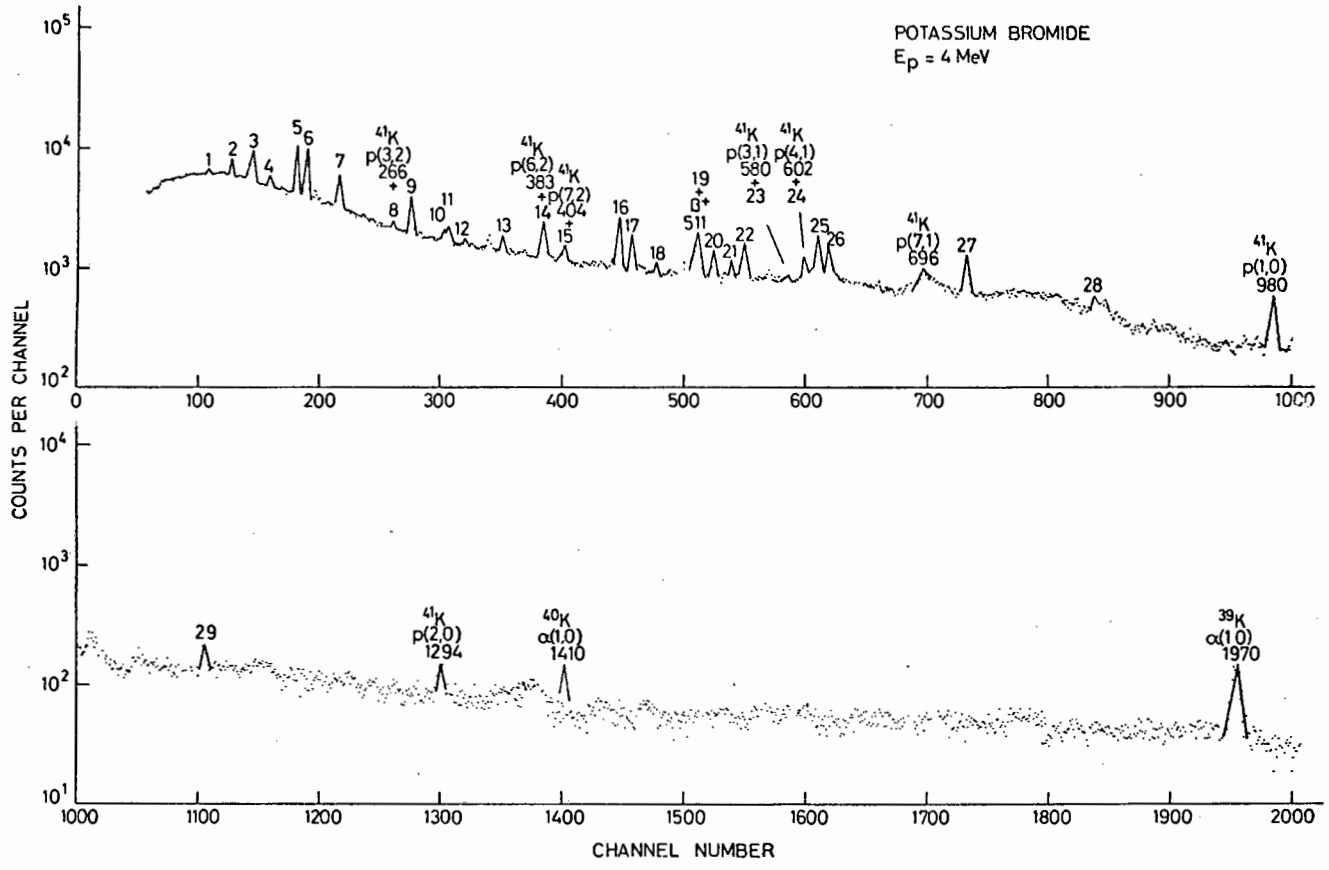

Peak	Eγ keV	Assignment
1	111	^{79}Br n(6,4)
2	130	^{79}Br n(1,0)
3	144	^{79}Br n(4,2)
	147	^{79}Br n(2,0)
4	161	^{79}Br n(4,1)
5	183	^{79}Br n(3,0)
6	190	^{81}Br n(1,0)
7	217	^{79}Br p(2,0)
	219	^{79}Br n(6,3)
8	262	^{79}Br p(3,0)
9	276	^{81}Br p(1,0)
	276	^{79}Br n(9,5)
10	303	^{79}Br n(7,2)
11	306	^{79}Br p(4,0)
12	320	^{79}Br n(7,1)
13	351	^{79}Br n(8,3)
14	384	^{79}Br n(5,0)
	385	^{79}Br n(10,4)
15	402	^{79}Br n(6,0)

Peak	Eγ keV	Assignment
16	445	^{81}Br n(8,3)
	446	^{81}Br n(5,1)
17	457	^{81}Br n(2,0)
18	477	^{79}Br n(9,3)
19	511	^{81}Br n(6,1)
	512	^{79}Br n(12,3)
	513	^{79}Br n(9,2)
20	523	^{79}Br p(6,0)
21	537	^{81}Br n(8,2)
	538	^{81}Br p(3,0)
22	549	^{81}Br n(3,0)
23	569	^{81}Br n(9,2)
24	605	^{79}Br p(7,0)
	608	^{81}Br n(4,0)
25	616	^{79}Br γ(1,0)
26	695	^{79}Br n(12,0)
27	729	^{81}Br n(7,1)
28	835	^{81}Br n(9,1)
	837	^{81}Br p(7,0)
29	1107	^{81}Br n(10,0)

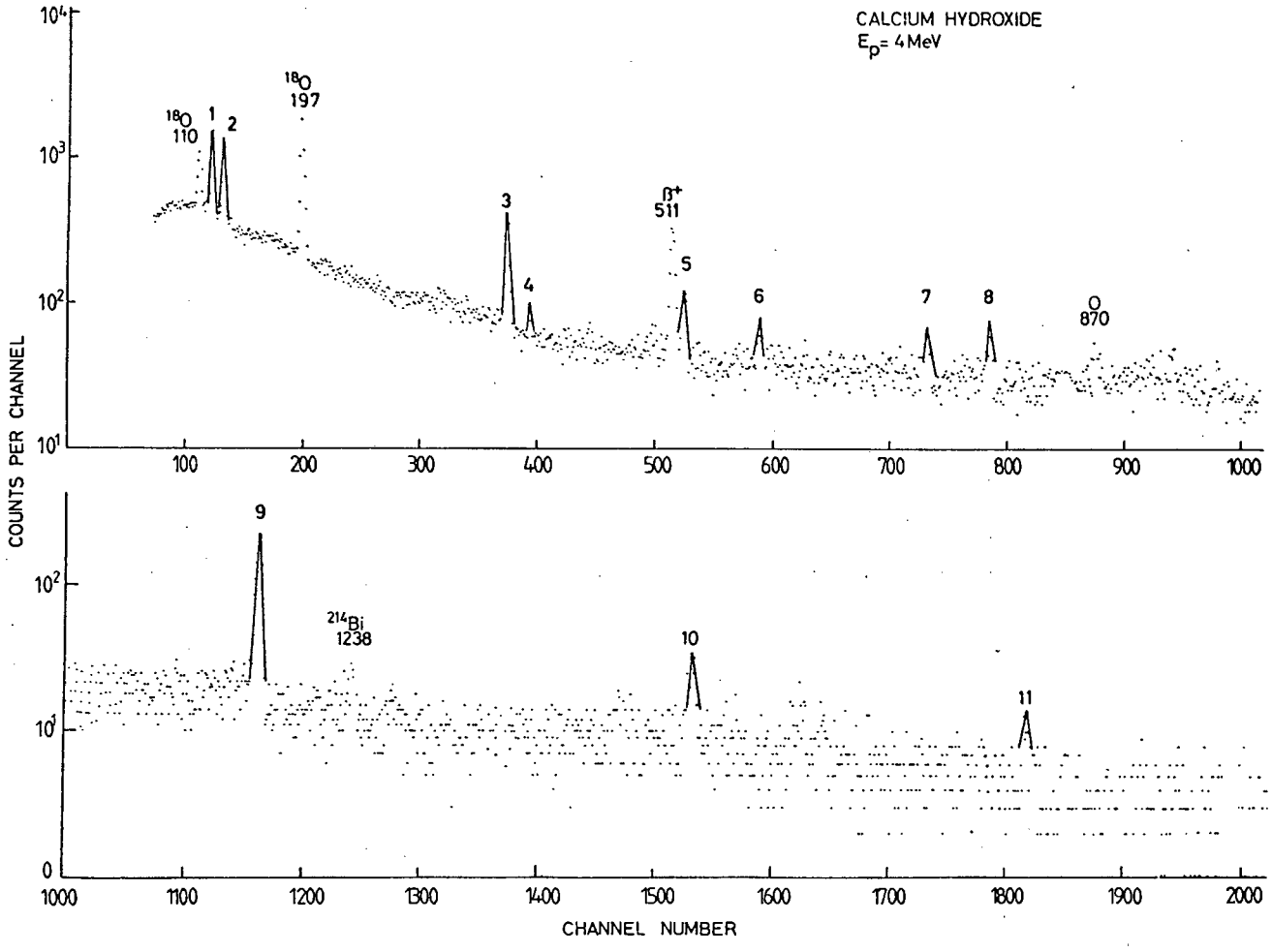

Peak	Eγ keV	Assignment
1	121	^{48}Ca n(2,1)
2	131	^{48}Ca n(1,0)
3	373	^{43}Ca p(1,0)
	376	^{44}Ca γ(2,0)
4	397	^{43}Ca p(3,2)
5	520	^{48}Ca n(4,3)
6	593	^{43}Ca p(2,0)
7	729	^{43}Ca n(5,1)
8	787	^{40}Ca p(6,3)
9	1157	^{44}Ca p(1,0)
10	1525	^{42}Ca p(1,0)
11	1811	^{48}Ca n(8,2)

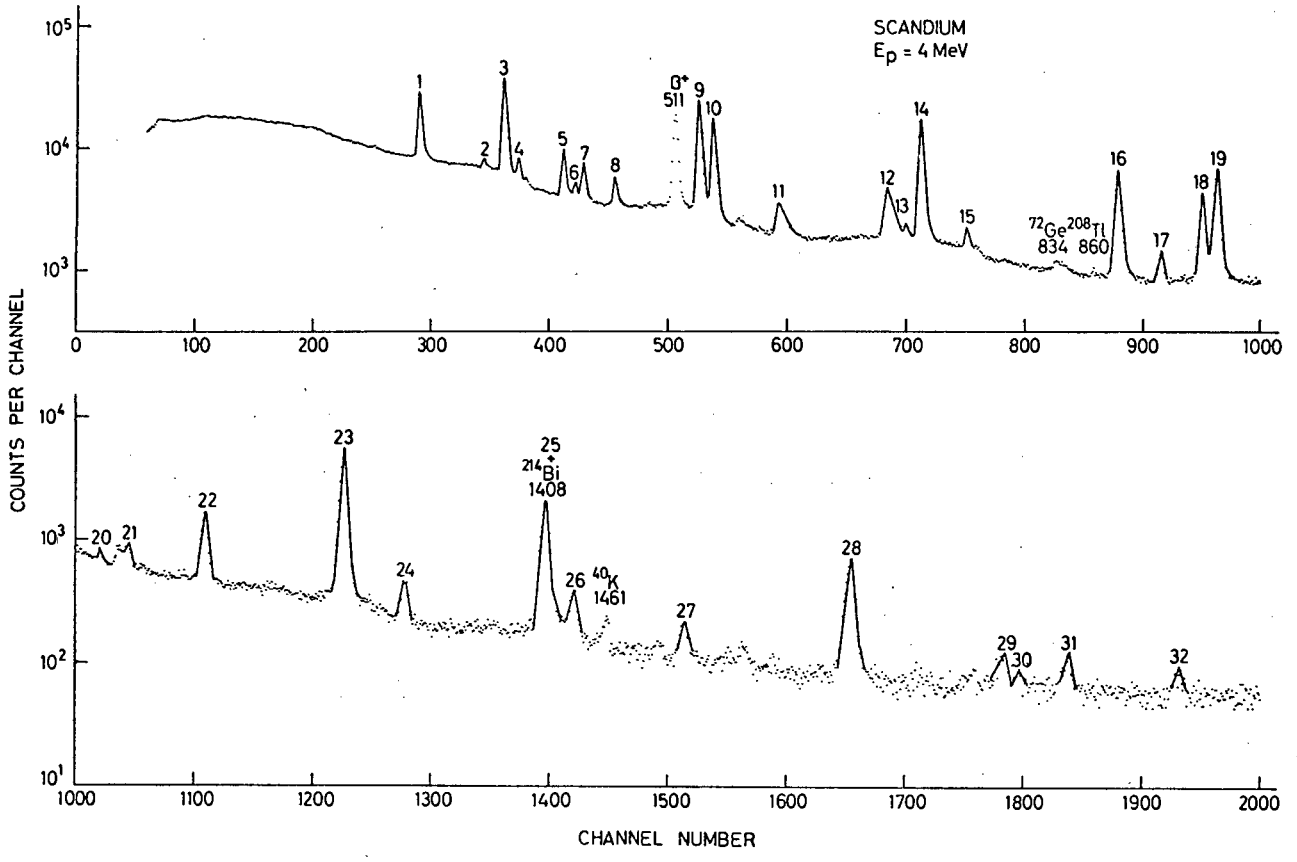

Peak	Eγ keV	Assignment
1	293	^{45}Sc n(3,1)
2	347	^{45}Sc p(7,4)
3	364	^{45}Sc p(2,1)
4	377	^{45}Sc p(2,0)
5	415	^{45}Sc n(4,2)
6	425	^{45}Sc p(13,8)
7	432	^{45}Sc p(6,3)
8	459	^{45}Sc p(11,6)
9	531	^{45}Sc p(3,1)
10	543	^{45}Sc p(3,0)
11	597	^{45}Sc p(15,11)
12	689	^{45}Sc p(10,4)
	692	^{45}Sc p(7,2)
13	707	^{45}Sc n(4,1)
14	720	^{45}Sc p(4,0)
15	760	^{45}Sc p(9,3)
16	889	^{45}Sc γ(1,0)
	890	^{45}Sc γ(1,0)

Peak	Eγ keV	Assignment
17	927	^{45}Sc p(5,0)
18	962	^{45}Sc p(6,1)
19	974	^{45}Sc p(6,0)
20	1033	^{45}Sc p(10,2)
21	1056	^{45}Sc p(16,6)
22	1121	^{45}Sc γ(2,1)
23	1237	^{45}Sc p(8,0)
24	1290	^{45}Sc p(9,0)
25	1409	^{45}Sc p(10,0)
26	1434	^{45}Sc p(11,0)
27	1525	^{45}Sc α(1,0)
28	1662	^{45}Sc p(13,0)
29	1788	^{45}Sc p(14,1)
30	1800	^{45}Sc p(14,0)
31	1837	^{45}Sc α(2,0)
32	1936	^{45}Sc p(15,0)

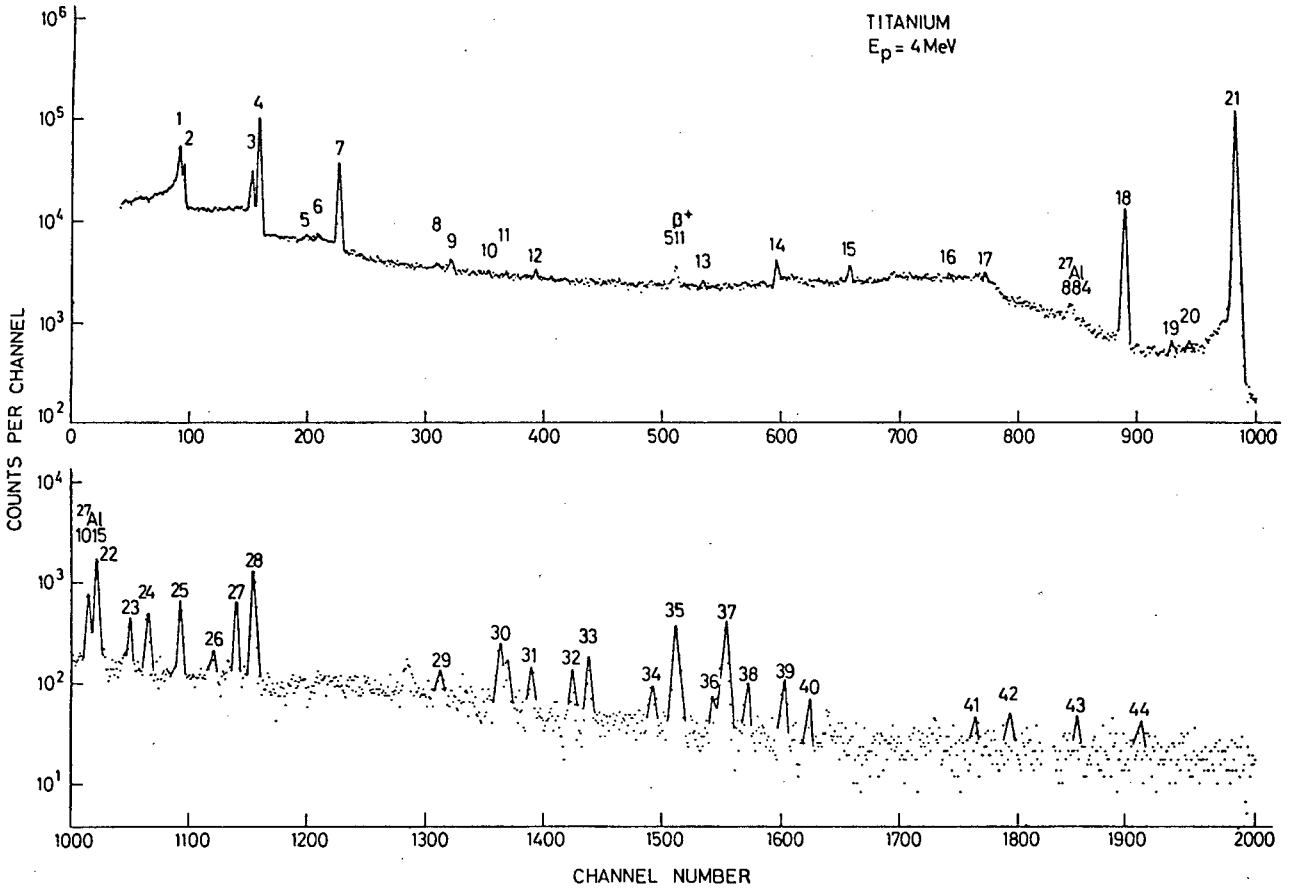

Peak	Eγ keV	Assignment
1	88	^{47}Ti n(1,0)
	88	^{46}Ti γ(1,0)
	90	^{49}Ti n(1,0)
	90	^{48}Ti γ(1,0)
2	94	^{50}Ti n(2,1)
	98	^{48}Ti n(4,2)
3	152	^{49}Ti n(2,0)
	152	^{46}Ti γ(2,0)
	152	^{48}Ti γ(2,0)
4	159	^{47}Ti p(1,0)
	160	^{49}Ti p(2,1)
5	204	^{49}Ti p(3,1)
6	210	^{47}Ti γ(3,1)
7	226	^{50}Ti n(1,0)
	227	^{49}Ti α(1,0)
8	308	^{48}Ti n(1,0)
	308	^{47}Ti γ(1,0)
9	320	^{50}Ti γ(1,0)
	320	^{50}Ti n(2,0)
10	354	^{48}Ti α(2,1)
11	368	^{48}Ti α(2,0)
12	393	^{48}Ti γ(5,3)
	393	^{49}Ti n(5,3)
13	543	^{48}Ti α(3,0)
14	595	^{49}Ti n(3,2)
	595	^{48}Ti γ(3,2)
15	657	^{48}Ti γ(3,1)
	657	^{49}Ti n(3,1)
	661	^{46}Ti γ(4,0)
16	748	^{48}Ti γ(3,0)
17	774	^{50}Ti α(1,0)
18	889	^{46}Ti p(1,0)
19	928	^{48}Ti p(4,2)
	929	^{50}Ti γ(2,0)
20	945	^{48}Ti p(5,2)
21	984	^{48}Ti γ(5,2)
	984	^{48}Ti p(1,0)
	986	^{49}Ti n(5,2)
22	1021	^{48}Ti γ(4,0)
	1021	^{49}Ti n(4,0)
23	1049	^{45}Ti p(5,2)
	1049	^{49}Ti n(5,1)
	1049	^{48}Ti γ(5,1)
24	1065	^{48}Ti p(7,2)
	1065	^{49}Ti n(6,1)
25	1092	^{47}Ti p(2,1)
26	1121	^{46}Ti p(2,1)
27	1140	^{48}Ti γ(5,0)
	1140	^{49}Ti n(5,0)
28	1155	^{48}Ti γ(6,0)
	1155	^{49}Ti n(6,0)
29	1312	^{48}Ti p(2,1)
30	1361	^{49}Ti n(7,2)
	1361	^{49}Ti γ(7,2)
31	1394	^{47}Ti p(4,1)
32	1424	^{48}Ti γ(7,1)
	1424	^{49}Ti n(7,1)
33	1438	^{48}Ti p(3,1)
34	1491	^{48}Ti γ(8,2)
	1491	^{48}Ti n(8,2)
	1492	^{50}Ti γ(3,1)
35	1509	^{48}Ti γ(9,2)
	1512	^{49}Ti n(7,0)
	1512	^{48}Ti γ(7,0)
	1512	^{49}Ti n(8,1)
36	1542	^{49}Ti p(2,0)
37	1553	^{48}Ti γ(8,1)
	1554	^{50}Ti p(1,0)
38	1570	^{46}Ti p(11,2)
	1571	^{49}Ti n(10,1)
	1571	^{48}Ti γ(10,1)
39	1601	^{47}Ti n(9,2)
	1602	^{48}Ti n(8,0)
	1602	^{49}Ti γ(8,0)
40	1623	^{49}Ti p(4,0)
41	1762	^{49}Ti p(6,0)
42	1796	^{48}Ti γ(11,0)
43	1841	^{46}Ti γ(12,1)
44	1903	^{48}Ti γ(12,0)

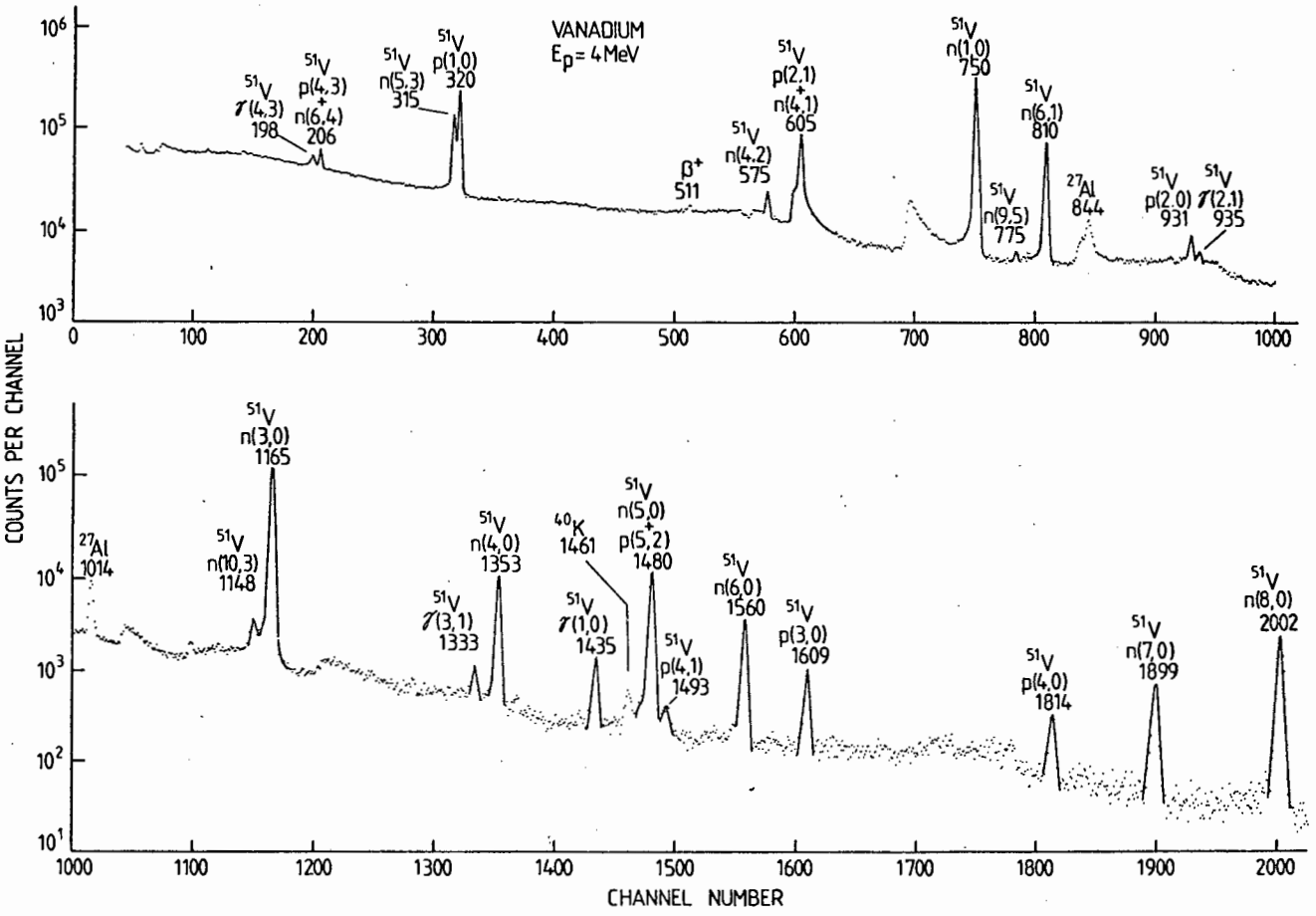
VANADIUM
E_p = 4 MeV
^{51}V γ(4,3) 198
^{51}V p(4,3) + n(6,4) 206
^{51}V n(5,3) 315
^{51}V p(1,0) 320
β+ 511
^{51}V n(4,2) 575
^{51}V p(2,1) + n(4,1) 605
^{51}V n(1,0) 750
^{51}V n(9,5) 775
^{51}V n(6,1) 810
^{27}Al 844
^{51}V p(2,0) 931
^{51}V γ(2,1) 935
^{27}Al 1014
^{51}V n(10,3) 1148
^{51}V n(3,0) 1165
^{51}V γ(3,1) 1333
^{51}V n(4,0) 1353
^{40}K 1461
^{51}V γ(1,0) 1435
^{51}V n(5,0) + p(5,2) 1480
^{51}V p(4,1) 1493
^{51}V n(6,0) 1560
^{51}V p(3,0) 1609
^{51}V p(4,0) 1814
^{51}V n(7,0) 1899
^{51}V n(8,0) 2002
COUNTS PER CHANNEL
CHANNEL NUMBER

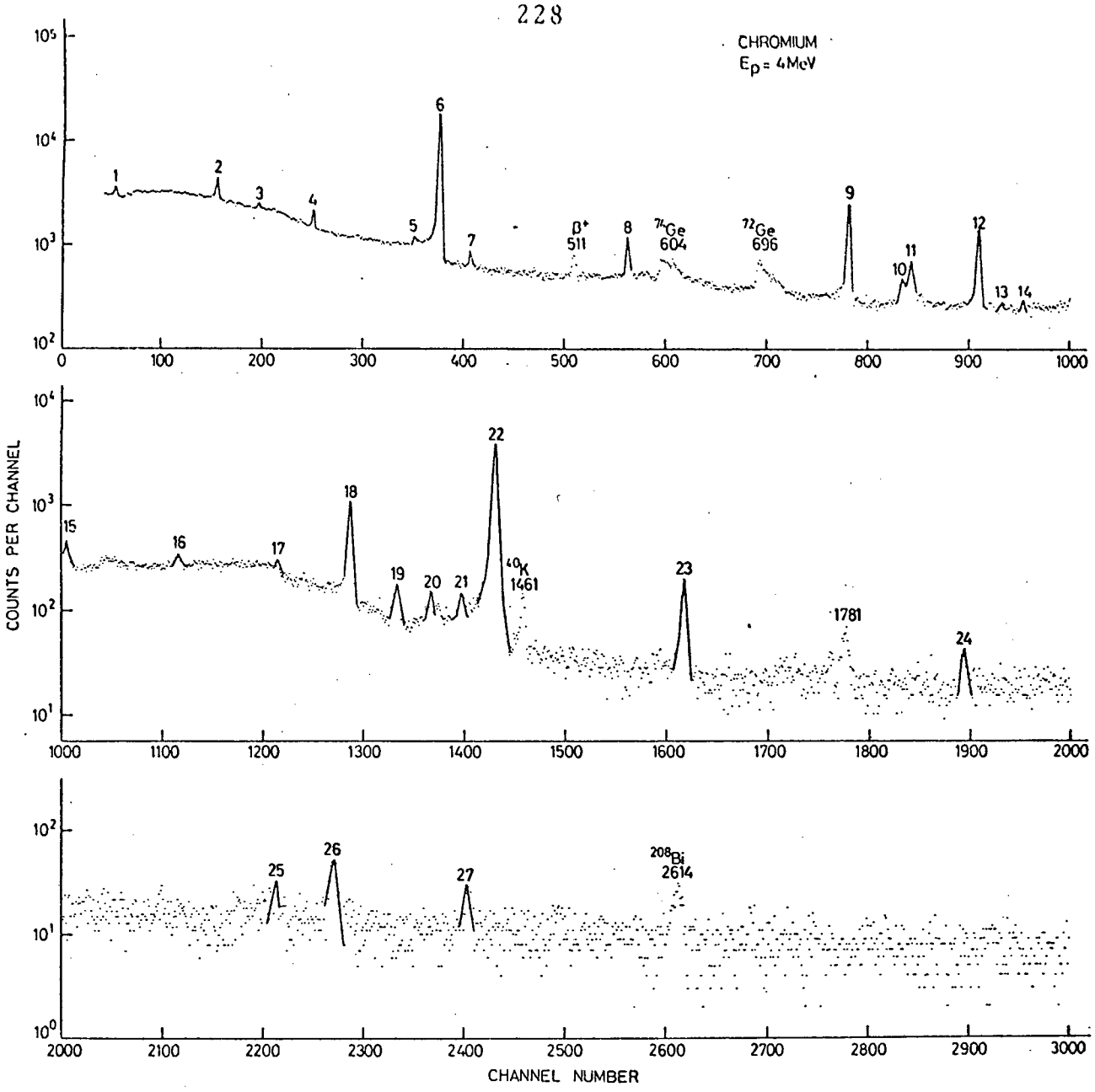

Peak	Eγ keV	Assignment	Peak	Eγ keV	Assignment
1	55	^{54}Cr n(1,0)	14	955	^{54}Cr n(6,1)
	55	^{53}Cr γ(1,0)		955	^{53}Cr γ(6,1)
2	154	^{52}Cr α(2,0)	15	1006	^{53}Cr p(2,0)
	156	^{54}Cr n(2,0)	16	1116	^{53}Cr n(6,2)
	156	^{53}Cr γ(2,0)	17	1213	^{52}Cr p(3,1)
3	211	^{54}Cr n(3,2)	18	1288	^{53}Cr n(2,0)
	211	^{53}Cr γ(3,2)		1288	^{52}Cr γ(2,0)
4	250	^{54}Cr n(4,2)	19	1332	^{52}Cr p(4,1)
	250	^{53}Cr γ(4,2)		1335	^{53}Cr γ(8,1)
5	353	^{53}Cr γ(4,1)	20	1375	^{53}Cr γ(7,0)
6	378	^{53}Cr n(1,0)	21	1400	^{53}Cr γ(9,1)
	378	^{52}Cr γ(1,0)	22	1434	^{52}Cr p(1,0)
7	406	^{54}Cr n(4,0)		1440	^{53}Cr n(3,0)
	406	^{53}Cr γ(4,0)	23	1619	^{53}Cr n(4,0)
8	564	^{53}Cr p(1,0)	24	1894	^{53}Cr n(5,1)
9	783	^{50}Cr p(1,0)		1894	^{52}Cr γ(5,1)
10	839	^{54}Cr n(5,0)	25	2194	^{53}Cr n(7,1)
	839	^{53}Cr γ(5,0)		2194	^{52}Cr γ(7,1)
11	854	^{54}Cr n(6,2)	26	2274	^{52}Cr γ(5,0)
	854	^{53}Cr γ(6,2)		2274	^{53}Cr n(5,0)
12	911	^{53}Cr n(2,1)	27	2405	^{53}Cr n(6,0)
	912	^{52}Cr γ(2,1)		2405	^{52}Cr γ(6,0)
13	935	^{52}Cr p(2,1)			

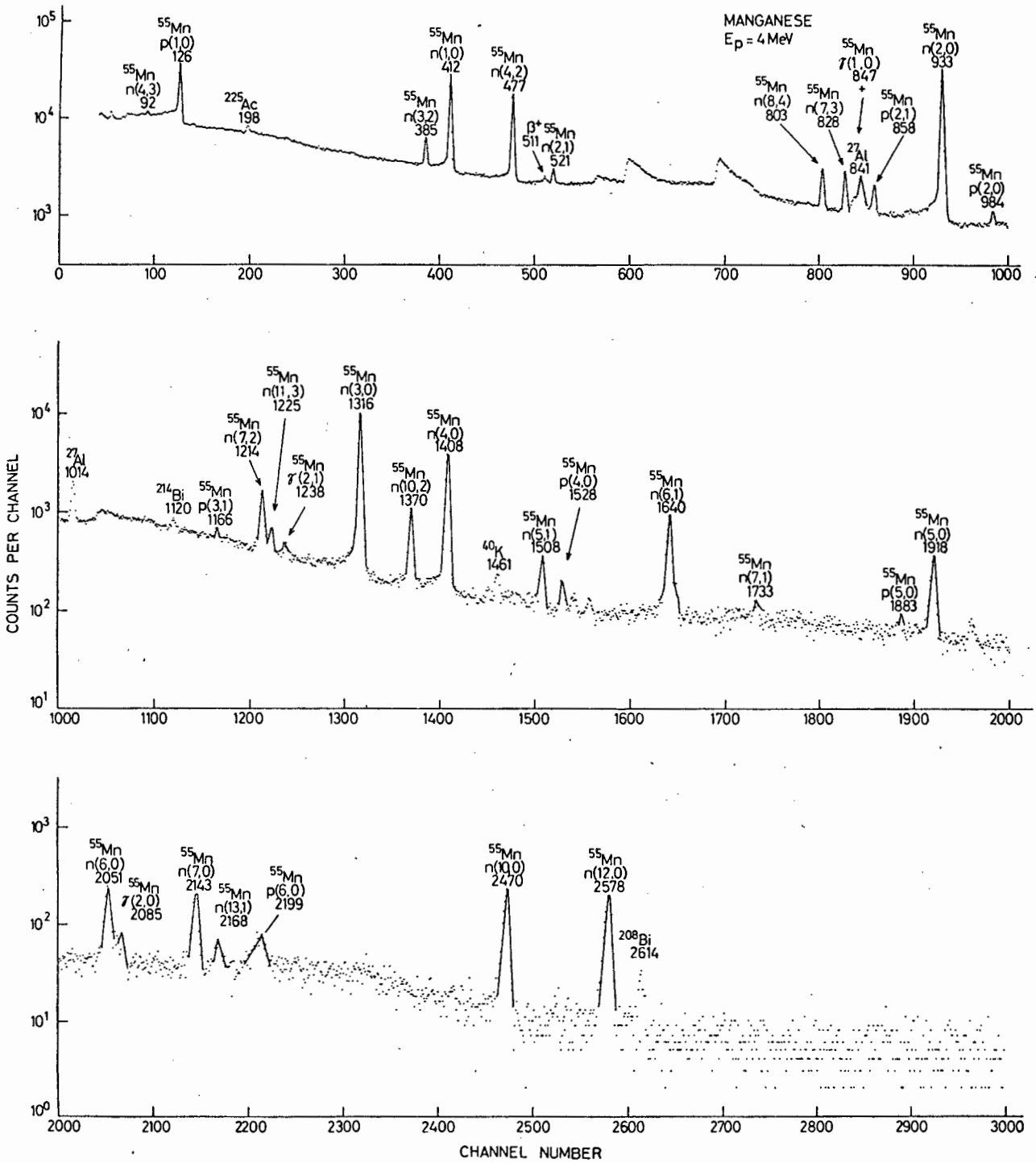
MANGANESE
E_p = 4 MeV
^{55}Mn n(4,3) 92
^{55}Mn p(1,0) 126
^{225}Ac 198
^{55}Mn n(3,2) 385
^{55}Mn n(1,0) 412
^{55}Mn n(4,2) 477
β^+ 511 ^{55}Mn n(2,1) 521
^{55}Mn n(8,4) 803
^{55}Mn n(7,3) 828
^{55}Mn γ(1,0) 847
^{27}Al 841
^{55}Mn p(2,1) 858
^{55}Mn n(2,0) 933
^{55}Mn p(2,0) 984
^{27}Al 1014
^{214}Bi 1120
^{55}Mn p(3,1) 1166
^{55}Mn n(7,2) 1214
^{55}Mn n(11,3) 1225
^{55}Mn γ(2,1) 1238
^{55}Mn n(3,0) 1316
^{55}Mn n(10,2) 1370
^{55}Mn n(4,0) 1408
^{40}K 1461
^{55}Mn n(5,1) 1508
^{55}Mn p(4,0) 1528
^{55}Mn n(6,1) 1640
^{55}Mn n(7,1) 1733
^{55}Mn p(5,0) 1883
^{55}Mn n(5,0) 1918
^{55}Mn n(6,0) 2051
^{55}Mn γ(2,0) 2085
^{55}Mn n(7,0) 2143
^{55}Mn n(13,1) 2168
^{55}Mn p(6,0) 2199
^{55}Mn n(10,0) 2470
^{55}Mn n(12,0) 2578
^{208}Bi 2614
COUNTS PER CHANNEL
CHANNEL NUMBER

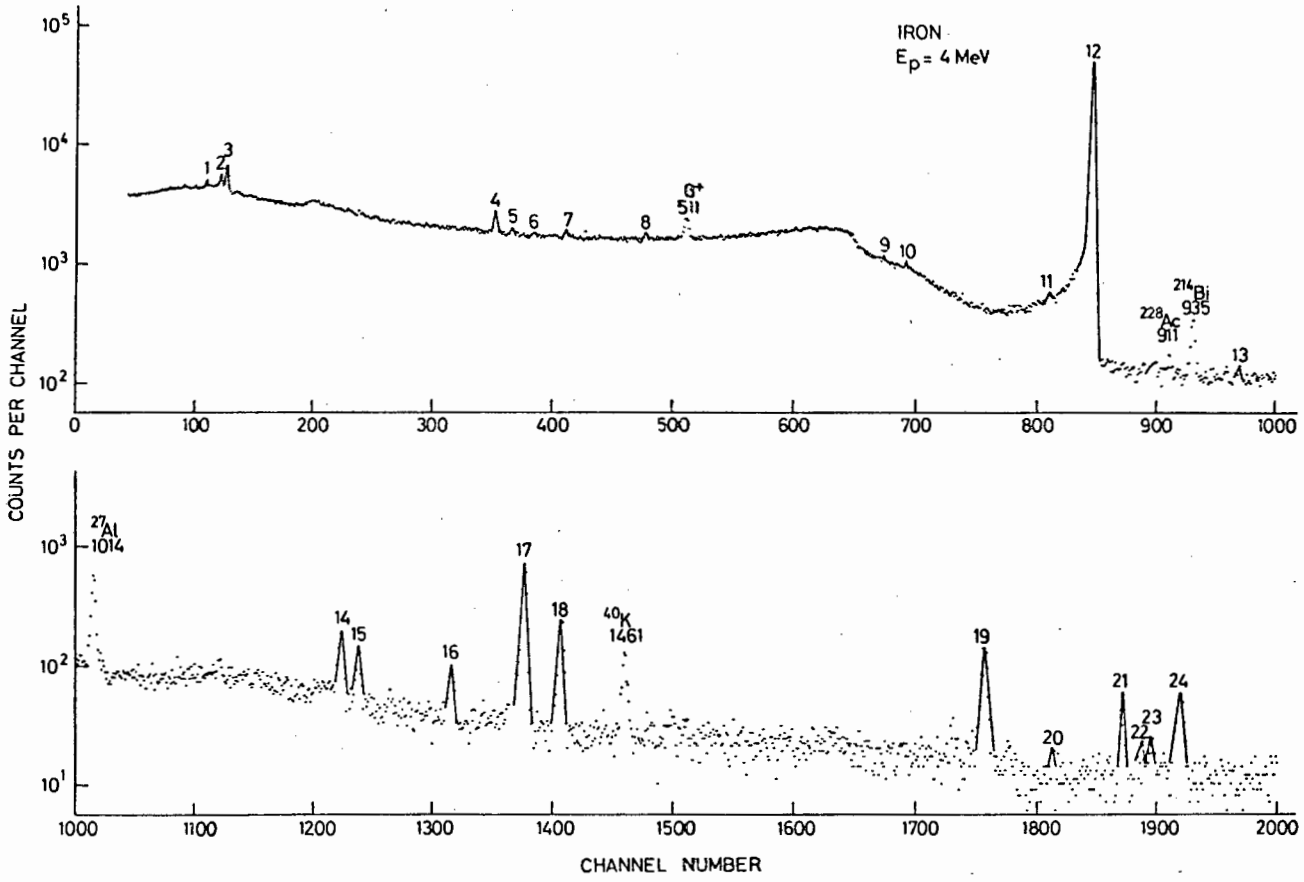

Peak	Eγ keV	Assignment
1	112	^{57}Fe γ(3,0)
	112	^{58}Fe n(3,0)
2	123	^{57}Fe p(2,1)
3	127	^{56}Fe γ(3,2)
	127	^{57}Fe n(3,2)
4	352	^{57}Fe p(3,1)
5	366	^{57}Fe γ(4,0)
	366	^{58}Fe n(4,0)
	367	^{57}Fe p(3,0)
6	380	^{56}Fe γ(5,2)
	380	^{57}Fe n(5,2)
7	412	^{54}Fe p(4,2)
8	466	^{56}Fe γ(4,1)
	466	^{57}Fe n(4,1)
9	673	^{56}Fe γ(6,1)
	673	^{57}Fe n(6,1)
10	692	^{57}Fe p(4,1)
11	812	^{58}Fe p(1,0)

Peak	Eγ keV	Assignment
12	847	^{56}Fe p(1,0)
13	970	^{56}Fe n(4,0)
14	1224	^{56}Fe γ(1,0)
	1224	^{57}Fe n(1,0)
15	1238	^{56}Fe p(2,1)
16	1328	^{58}Fe α(4,2)
17	1377	^{56}Fe γ(2,0)
	1377	^{57}Fe n(2,0)
18	1408	^{54}Fe p(1,0)
19	1757	^{56}Fe γ(5,0)
	1757	^{57}Fe n(5,0)
20	1810	^{56}Fe p(3,1)
21	1897	^{56}Fe γ(6,0)
	1897	^{57}Fe n(6,0)
22	1918	^{57}Fe n(7,0)
	1919	^{56}Fe γ(7,0)
23	2111	^{56}Fe p(4,1)
24	2133	^{56}Fe γ(8,0)
	2133	^{57}Fe n(8,0)

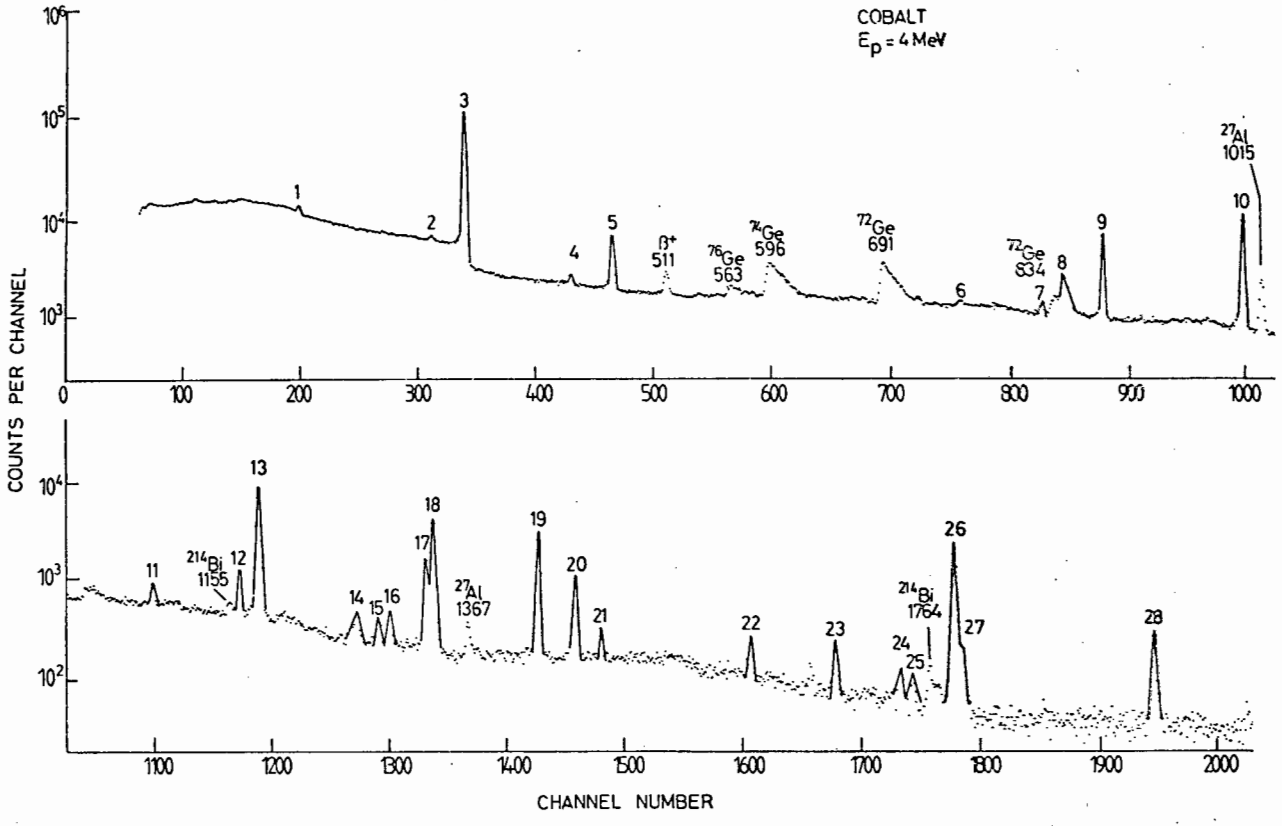

Peak	E_γ keV	Assignment	Peak	E_γ keV	Assignment
1	197	^{59}Co p(3,1)	15	1291	^{59}Co p(3,0)
2	312	^{59}Co n(4,3)	16	1301	^{59}Co n(5,0)
3	339	^{59}Co n(1,0)	17	1332	^{59}Co γ(1,0)
4	430	^{59}Co n(8,5)	18	1337	^{59}Co n(6,1)
5	465	^{59}Co n(2,0)	19	1432	^{59}Co p(4,0)
6	760	^{59}Co n(11,4)	20	1461	^{59}Co p(5,0)
7	826	^{59}Co γ(2,1)	21	1480	^{59}Co p(6,0)
8	842	^{59}Co α(1,0)	22	1608	^{59}Co n(11,1)
9	878	^{59}Co n(3,0)	23	1680	^{59}Co n(7,0)
10	997	^{59}Co n(5,1)	24	1735	^{59}Co n(8,0)
11	1099	^{59}Co p(1,0)	25	1746	^{59}Co n(9,0)
12	1173	^{59}Co γ(3,1)	26	1773	^{59}Co α(9,2)
13	1189	^{59}Co n(4,0)	27	1778	^{59}Co n(10,0)
	1190	^{59}Co p(2,0)	28	1948	^{59}Co n(11,0)
14	1272	^{59}Co n(8,2)			

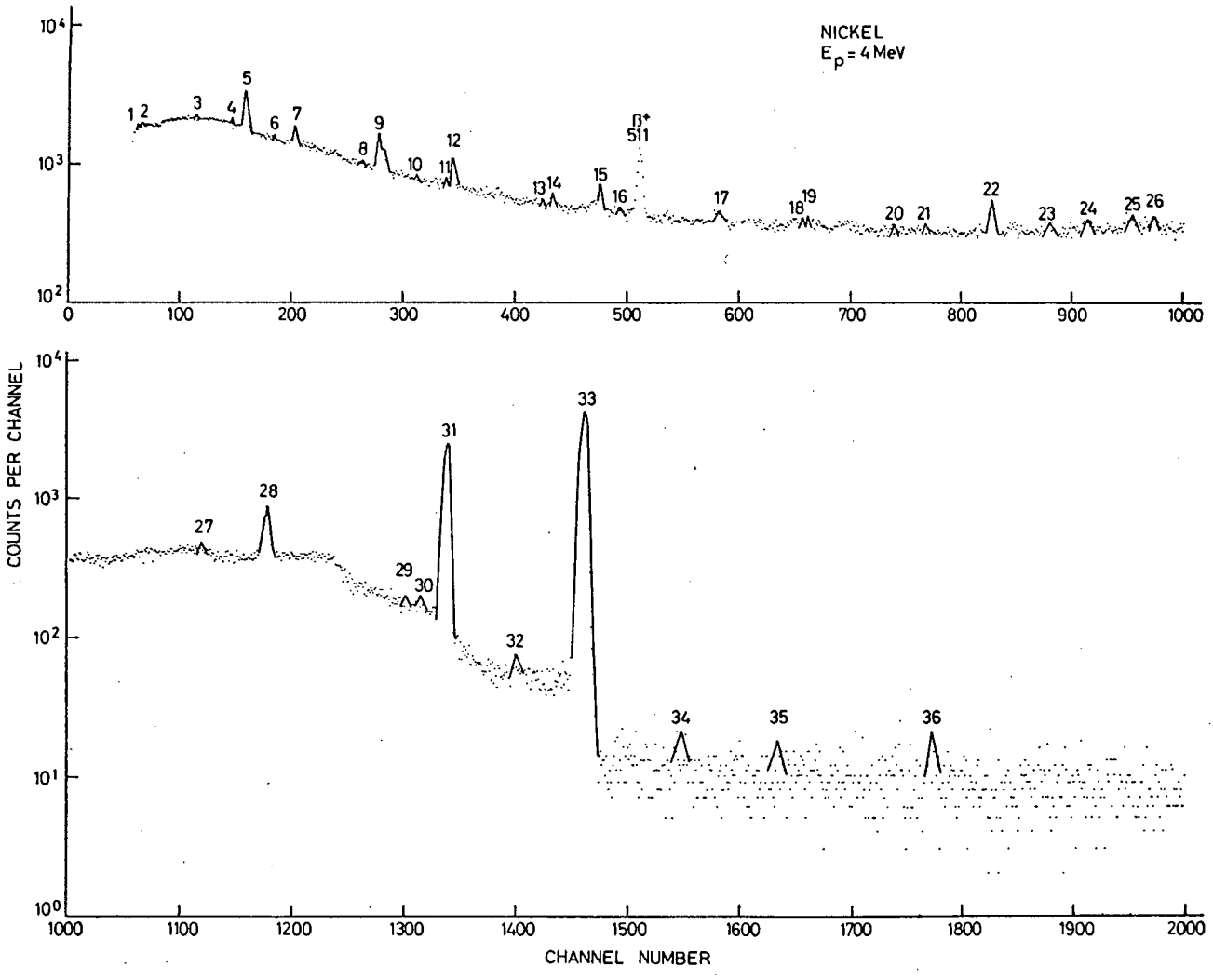

Peak	Eγ keV	Assignment	Peak	Eγ keV	Assignment
1	53	^{61}Ni α(1,0)	20	750	^{62}Ni p(6,3)
2	59	^{61}Ni α(3,2)	21	771	^{64}Ni γ(1,0)
3	111	^{61}Ni α(3,0)	22	826	^{60}Ni p(2,1)
4	147	^{62}Ni n(4,2)	23	870	^{62}Ni p(2,1)
5	159	^{64}Ni n(1,0)		873	^{61}Ni n(3,1)
6	185	^{64}Ni n(3,1)	24	914	^{58}Ni γ(2,0)
7	197	^{62}Ni α(2,1)	25	961	^{62}Ni γ(2,0)
8	265	^{61}Ni n(5,4)	26	970	^{60}Ni γ(2,0)
9	274	^{64}Ni n(2,0)	27	1027	^{64}Ni p(1,0)
10	313	^{61}Ni α(4,2)	28	1173	^{62}Ni p(1,0)
11	341	^{62}Ni α(4,1)	29	1314	^{61}Ni n(3,0)
12	349	^{62}Ni n(4,1)	30	1321	^{58}Ni p(3,1)
13	373	^{61}Ni p(3,2)	31	1333	^{60}Ni p(1,0)
14	423	^{58}Ni γ(2,1)	32	1412	^{62}Ni γ(4,0)
15	477	^{61}Ni n(1,0)	33	1454	^{58}Ni p(1,0)
16	491	^{58}Ni γ(1,0)	34	1547	^{62}Ni γ(5,0)
17	588	^{61}Ni p(3,1)	35	1640	^{61}Ni γ(5,0)
18	659	^{61}Ni p(3,0)	36	1774	^{58}Ni γ(6,1)
19	669	^{63}Ni γ(1,0)			

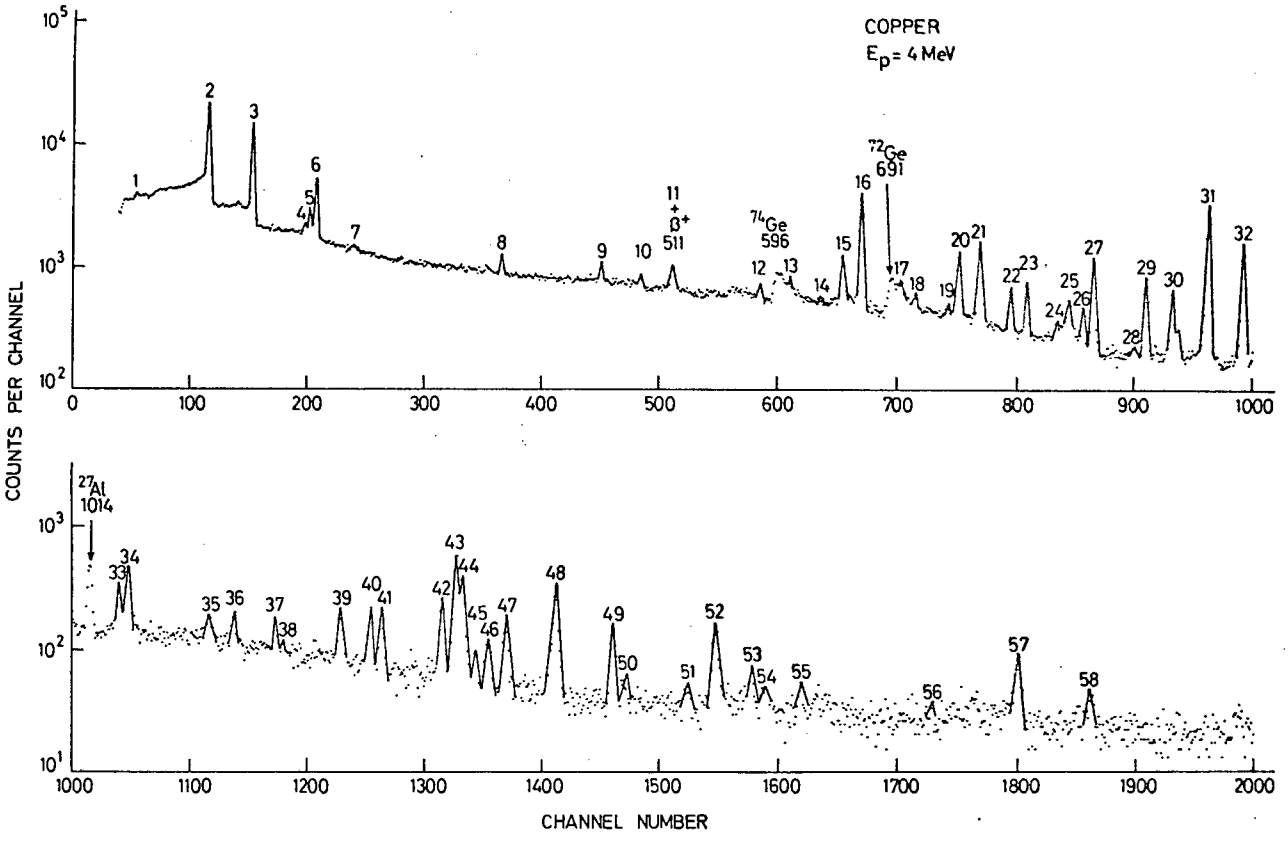

Peak	Eγ keV	Assignment	Peak	Eγ keV	Assignment	Peak	Eγ keV	Assignment
1	54	^{65}Cu n(1,0)	21	769	^{65}Cu n(4,0)	39	1229	^{65}Cu n(12,2)
	55	^{63}Cu n(2,1)		771	^{65}Cu p(1,0)	40	1254	^{65}Cu n(13,2)
2	115	^{65}Cu n(2,0)	22	795	^{65}Cu n(6,2)	41	1263	^{65}Cu n(4,3)
3	153	^{65}Cu n(3,1)	23	808	^{63}Cu γ(2,1)		1264	^{65}Cu n(11,0)
4	194	^{63}Cu n(1,0)	24	831	^{63}Cu α(2,1)	42	1310	^{63}Cu γ(2,1)
5	201	^{65}Cu n(8,6)	25	840	^{65}Cu α(2,1)	43	1327	^{63}Cu p(3,0)
6	207	^{65}Cu n(3,0)	26	852	^{65}Cu p(4,1)	44	1329	^{63}Cu α(1,0)
7	249	^{63}Cu n(2,0)		856	^{65}Cu n(7,1)	45	1343	^{63}Cu p(7,1)
8	365	^{63}Cu p(3,1)	27	865	^{65}Cu n(5,0)		1344	^{65}Cu n(12,0)
	369	^{65}Cu p(3,1)	28	899	^{63}Cu p(6,2)	46	1355	^{65}Cu n(14,2)
9	450	^{63}Cu p(4,2)	29	910	^{65}Cu n(6,0)	47	1370	^{65}Cu n(13,0)
10	484	^{65}Cu n(9,4)	30	932	^{65}Cu n(8,2)	48	1412	^{63}Cu p(4,0)
11	509	^{65}Cu p(4,2)	31	962	^{63}Cu p(2,0)	49	1463	^{63}Cu α(5,1)
12	585	^{63}Cu p(5,2)	32	992	^{63}Cu γ(1,0)	50	1470	^{65}Cu n(14,0)
13	611	^{65}Cu p(5,2)	33	1039	^{65}Cu γ(1,0)		1473	^{65}Cu n(16,2)
14	639	^{63}Cu n(4,0)	34	1048	^{65}Cu n(8,0)	51	1523	^{65}Cu n(15,1)
15	652	^{63}Cu n(5,0)		1048	^{65}Cu n(10,3)	52	1547	^{63}Cu p(5,0)
	654	^{65}Cu n(4,2)		1049	^{63}Cu p(7,2)	53	1577	^{65}Cu n(15,0)
16	670	^{63}Cu p(1,0)	35	1114	^{65}Cu p(2,0)	54	1588	^{65}Cu n(16,0)
17	703	^{65}Cu n(6,3)		1119	^{63}Cu p(9,2)	55	1623	^{65}Cu p(4,0)
18	715	^{65}Cu n(4,1)	36	1137	^{65}Cu n(12,3)	56	1725	^{65}Cu p(5,0)
19	742	^{63}Cu p(4,1)		1138	^{65}Cu n(10,2)	57	1799	^{65}Cu γ(2,0)
20	752	^{65}Cu n(5,4)	37	1174	^{65}Cu α(1,0)	58	1861	^{63}Cu p(6,0)
	754	^{63}Cu p(9,3)	38	1177	^{63}Cu α(4,1)			

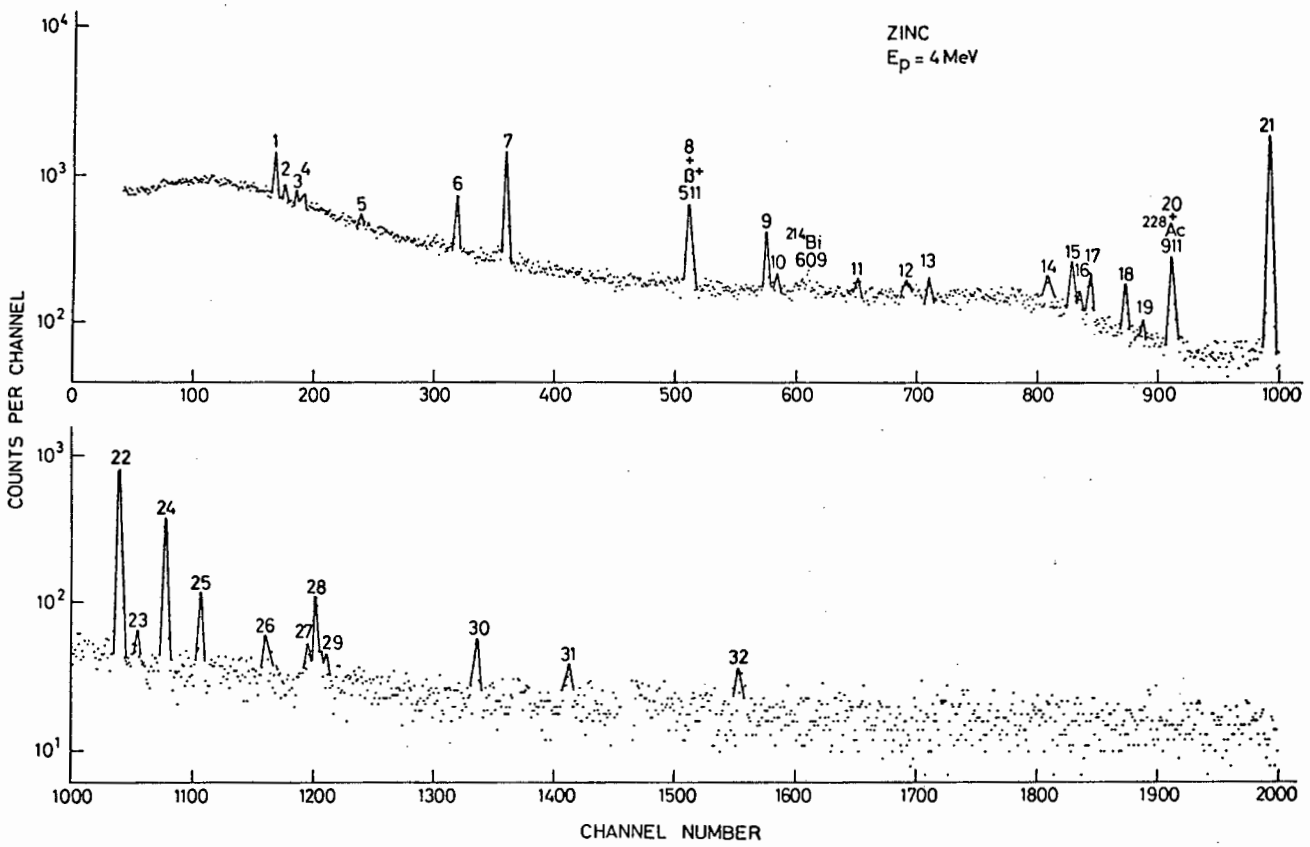

Peak	Eγ keV	Assignment	Peak	Eγ keV	Assignment	Peak	Eγ keV	Assignment
1	169	^{66}Zn γ(1,0)	10	585	^{68}Zn n(8,0)	23	1053	^{67}Zn n(6,2)
	169	^{67}Zn n(1,0)	11	651	^{70}Zn n(2,0)	24	1077	^{68}Zn p(1,0)
2	175	^{67}Zn γ(1,0)	12	691	^{70}Zn n(3,0)	25	1107	^{68}Zn γ(5,0)
	175	^{68}Zn n(1,0)	13	710	^{68}Zn γ(4,1)		1107	^{70}Zn γ(7,0)
3	185	^{67}Zn p(2,0)	14	807	^{68}Zn p(3,1)	26	1160	^{67}Zn n(7,2)
4	193	^{64}Zn γ(1,0)		809	^{64}Zn p(2,1)	27	1196	^{67}Zn n(8,2)
5	237	^{68}Zn γ(5,3)	15	828	^{67}Zn n(3,0)	28	1202	^{69}Zn n(5,0)
6	320	^{68}Zn γ(1,0)	16	834	^{66}Zn p(2,1)	29	1206	^{68}Zn γ(7,1)
	321	^{68}Zn n(5,1)	17	843	^{67}Zn n(5,2)	30	1333	^{66}Zn p(3,1)
	321	^{67}Zn γ(5,1)	18	871	^{67}Zn p(5,0)		1335	^{68}Zn γ(6,0)
				871	^{68}Zn γ(3,0)	31	1412	^{66}Zn p(4,1)
	324	^{67}Zn γ(2,0)	19	888	^{67}Zn p(6,0)		1413	^{67}Zn n(6,0)
7	360	^{67}Zn n(2,0)	20	910	^{70}Zn γ(5,0)	32	1555	^{67}Zn n(8,0)
8	508	^{70}Zn n(1,0)		911	^{67}Zn n(4,0)			
9	574	^{68}Zn γ(2,0)	21	992	^{64}Zn p(1,0)			
	578	^{68}Zn p(2,1)	22	1039	^{66}Zn p(1,0)			

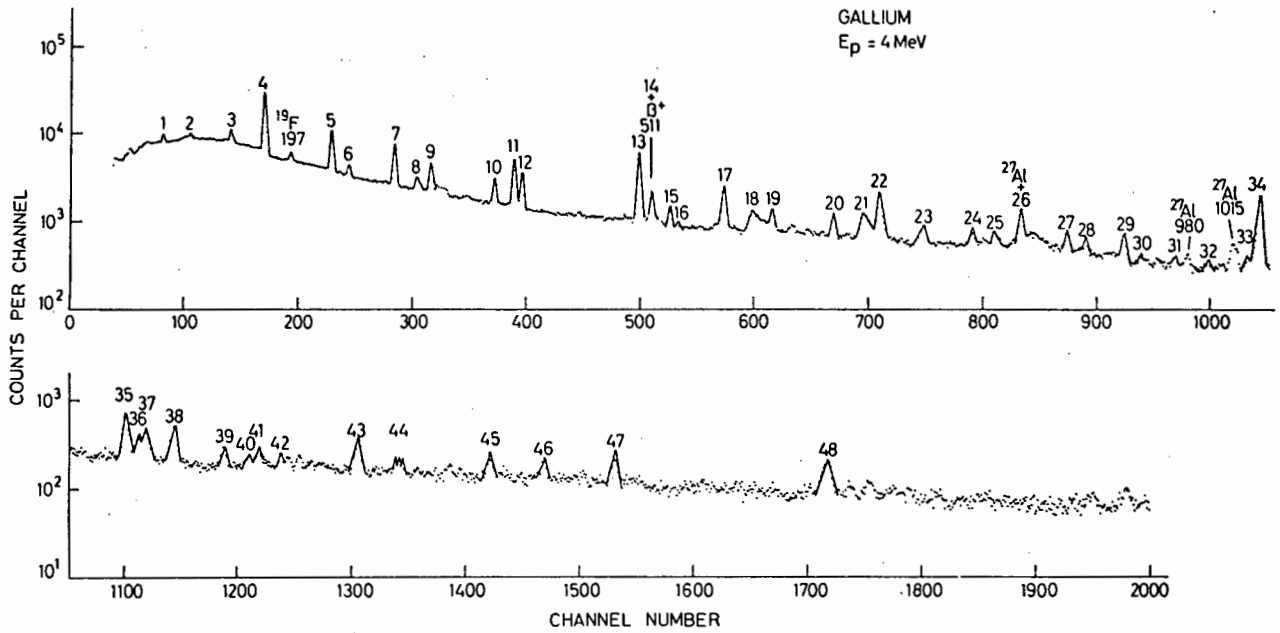

Peak	Eγ keV	Assignment	Peak	Eγ keV	Assignment	Peak	Eγ keV	Assignment
1	87	^{69}Ga n(1,0)	18	596	^{71}Ga p(6,3)	34	1040	^{69}Ga γ(1,0)
2	113	^{71}Ga γ(8,6)	19	620	^{71}Ga p(6,2)	35	1099	^{69}Ga γ(11,3)
3	143	^{71}Ga γ(2,1)	20	668	^{69}Ga γ(3,1)	36	1106	^{69}Ga p(5,0)
	146	^{69}Ga n(2,1)	21	691	^{71}Ga γ(1,0)	37	1113	^{69}Ga γ(4,1)
4	176	^{69}Ga γ(2,1)	22	708	^{69}Ga p(4,1)	38	1140	^{69}Ga γ(6,1)
5	233	^{69}Ga n(2,0)	23	744	^{69}Ga γ(8,3)	39	1182	^{69}Ga n(13,2)
6	247	^{69}Ga p(13,9)	24	786	^{71}Ga γ(8,4)	40	1208	^{69}Ga p(7,1)
7	287	^{69}Ga n(3,2)		788	^{69}Ga p(5,1)	41	1216	^{69}Ga γ(2,0)
8	307	^{69}Ga p(6,4)	25	812	^{69}Ga n(5,0)	42	1230	^{71}Ga γ(5,2)
9	318	^{69}Ga p(1,0)	26	834	^{71}Ga γ(2,0)	43	1307	^{69}Ga n(12,0)
10	374	^{69}Ga n(3,0)	27	872	^{69}Ga p(3,0)	44	1332	^{69}Ga γ(13,4)
11	390	^{71}Ga p(1,0)	28	894	^{71}Ga γ(4,2)		1336	^{69}Ga p(6,0)
12	398	^{69}Ga n(4,0)	29	927	^{69}Ga n(9,2)		1339	^{69}Ga γ(9,3)
13	500	^{69}Ga p(7,4)	30	941	^{69}Ga γ(4,2)	45	1412	^{69}Ga γ(8,1)
14	512	^{71}Ga p(3,0)	31	965	^{71}Ga p(5,0)	46	1464	^{71}Ga γ(3,0)
15	521	^{71}Ga p(4,1)	32	995	^{69}Ga n(8,0)	47	1527	^{69}Ga p(7,0)
16	532	^{69}Ga p(5,2)	33	1027	^{69}Ga p(4,0)	48	1708	^{69}Ga γ(3,0)
17	574	^{69}Ga p(2,0)						

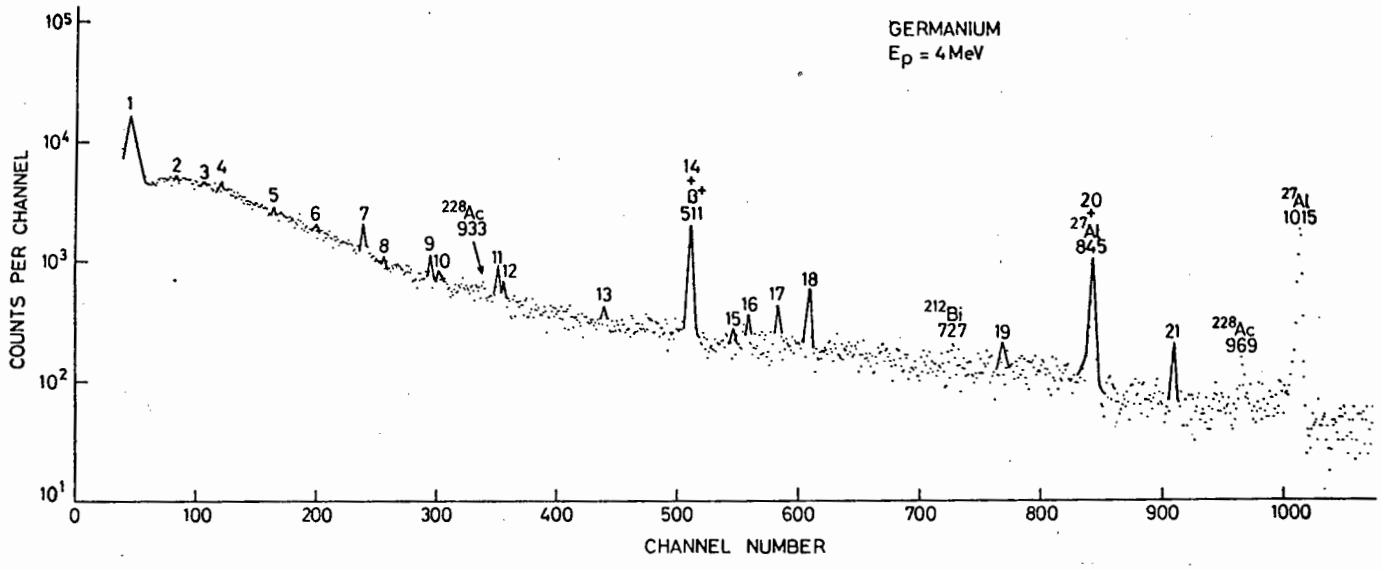

Peak	Eγ keV	Assignment
1	46	^{76}Ge n(1,0)
2	87	^{76}Ge n(2,0)
3	109	^{76}Ge p(6,5)
4	121	^{76}Ge n(3,0)
5	166	^{76}Ge n(4,0)
6	202	^{74}Ge n(3,0)
7	236	^{76}Ge n(8,3)
8	254	^{73}Ge n(3,0)
9	295	^{73}Ge p(5,3)
10	302	^{76}Ge p(3,2)
11	351	^{73}Ge p(5,1)
12	354	^{73}Ge p(4,0)
13	442	^{73}Ge n(5,1)
14	510	^{73}Ge n(5,0)
15	546	^{76}Ge p(2,1)
16	563	^{76}Ge p(1,0)
17	578	^{73}Ge n(7,0)
18	609	^{74}Ge p(2,1)
19	770	^{73}Ge n(10,0)
20	847	^{76}Ge p(3,1)
21	911	^{76}Ge p(6,2)

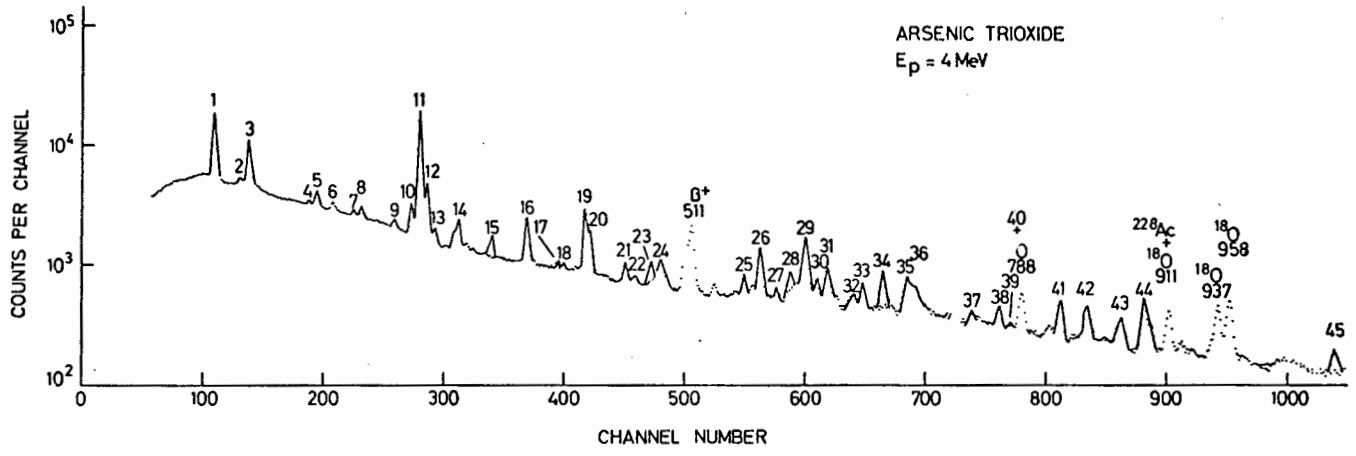

Peak	Eγ keV	Assignment	Peak	Eγ keV	Assignment	Peak	Eγ keV	Assignment
1	113	^{75}As n(1,0)	19	418	^{75}As p(13,6)	29	603	^{75}As p(12,2)
2	133	^{75}As n(2,0)		418	^{75}As p(9,1)		607	^{75}As p(13,3)
	136	^{75}As p(5,2)	20	426	^{75}As p(14,9)	30	615	^{75}As n(7,0)
3	141	^{75}As n(5,3)		428	^{75}As n(5,0)		618	^{75}As p(9,0)
4	189	^{75}As p(6,3)	21	460	^{75}As p(11,5)	31	621	^{75}As p(13,2)
5	199	^{75}As p(1,0)	22	466	^{75}As p(12,5)		623	^{75}As p(10,1)
6	203	^{75}As p(5,1)		469	^{75}As p(6,0)	32	643	^{75}As p(14,5)
	204	^{75}As p(6,2)	23	471	^{75}As p(14,7)	33	657	^{75}As γ(3,1)
7	229	^{75}As n(13,7)	24	486	^{75}As p(13,5)	34	662	^{75}As p(11,1)
8	236	^{75}As n(9,5)	25	557	^{75}As p(11,4)		666	^{75}As p(12,1)
9	265	^{75}As p(2,0)		557	^{75}As p(10,2)	35	688	^{75}As p(13,1)
10	280	^{75}As p(3,0)		558	^{75}As γ(1,0)	36	691	^{75}As α(1,0)
11	287	^{75}As n(3,0)		561	^{75}As p(12,4)	37	740	^{75}As p(14,4)
12	293	^{75}As n(4,0)		563	^{75}As γ(2,1)	38	764	^{75}As p(14,3)
13	304	^{75}As p(4,0)	26	572	^{75}As p(7,0)	39	772	^{75}As γ(4,1)
14	314	^{75}As p(13,7)		575	^{75}As p(14,6)	40	778	^{75}As p(14,2)
	316	^{75}As n(5,1)	27	581	^{75}As p(11,3)	41	822	^{75}As p(10,0)
15	338	^{75}As p(9,3)		582	^{75}As p(13,4)	42	845	^{75}As p(14,1)
16	374	^{75}As p(7,1)		585	^{75}As p(12,3)	43	861	^{75}As p(11,0)
17	397	^{75}As p(12,6)		586	^{75}As n(6,0)		865	^{75}As p(12,0)
18	401	^{75}As p(5,0)	28	596	^{75}As p(11,2)	44	886	^{75}As p(13,0)
						45	1044	^{75}As p(14,0)

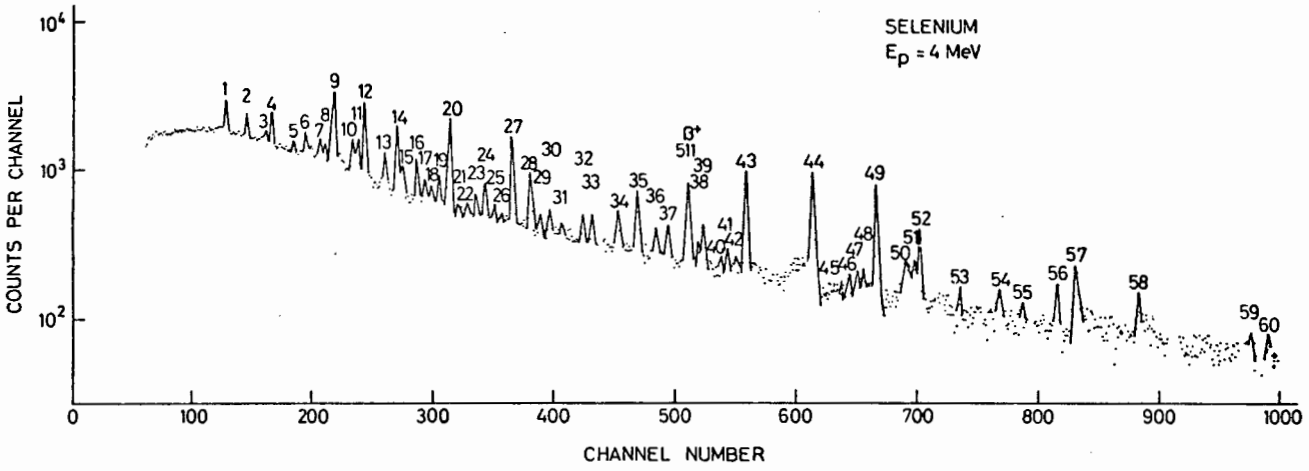

Peak	Eγ keV	Assignment	Peak	Eγ keV	Assignment	Peak	Eγ keV	Assignment
1	133	^{74}Se γ(1,0)	22	327	^{76}Se α(5,1)	40	538	^{80}Se γ(3,0)
2	148	^{74}Se α(2,0)		329	^{80}Se n(7,1)	41	543	^{82}Se α(2,1)
	149	^{77}Se n(4,0)		331	^{82}Se n(4,1)	42	552	^{80}Se γ(8,1)
	149	^{78}Se n(4,1)	23	336	^{78}Se n(12,1)	43	559	^{76}Se p(1,0)
3	158	^{77}Se α(1,0)	24	343	^{80}Se n(8,1)		561	^{80}Se γ(9,1)
4	162	^{77}Se p(1,0)		344	^{76}Se α(6,2)		563	^{76}Se p(2,1)
5	170	^{76}Se α(4,2)	25	347	^{82}Se n(5,2)	44	614	^{78}Se p(1,0)
6	195	^{80}Se α(1,0)		351	^{82}Se γ(7,2)	45	635	^{74}Se p(1,0)
	197	^{80}Se n(9,5)	26	357	^{82}Se γ(1,0)		638	^{82}Se n(8,0)
7	207	^{77}Se α(6,0)		359	^{74}Se α(3,1)	46	646	^{82}Se n(9,1)
8	212	^{80}Se n(10,5)		361	^{76}Se α(6,1)	47	650	^{80}Se γ(5,0)
9	216	^{80}Se α(2,0)	27	366	^{80}Se n(7,0)	48	655	^{82}Se p(1,0)
10	219	^{80}Se n(3,1)	28	377	^{82}Se n(4,0)	49	666	^{80}Se p(1,0)
	219	^{74}Se p(2,1)	29	391	^{77}Se n(13,0)	50	681	^{74}Se α(4,1)
11	234	^{80}Se n(4,1)	30	393	^{76}Se α(5,0)		684	^{82}Se γ(2,0)
	235	^{76}Se α(5,3)		398	^{82}Se n(6,2)	51	693	^{78}Se p(2,1)
12	244	^{80}Se n(5,1)	31	407	^{80}Se n(16,6)		696	^{82}Se γ(8,1)
	247	^{82}Se n(3,1)	32	425	^{82}Se n(5,0)	52	701	^{82}Se n(16,3)
13	261	^{80}Se γ(2,1)		425	^{76}Se α(7,2)	53	728	^{74}Se p(4,1)
14	269	^{76}Se α(6,3)	33	428	^{76}Se α(6,0)	54	767	^{80}Se γ(6,0)
	271	^{80}Se n(4,2)		430	^{82}Se n(6,1)	55	783	^{80}Se p(2,1)
15	276	^{80}Se γ(1,0)		432	^{80}Se n(9,1)	56	813	^{80}Se p(3,1)
16	286	^{76}Se α(8,4)	34	456	^{80}Se n(10,1)	57	828	^{80}Se γ(7,0)
17	290	^{80}Se γ(4,1)	35	467	^{80}Se n(9,0)		830	^{74}Se α(4,0)
	293	^{82}Se n(3,0)		470	^{82}Se n(7,2)		830	^{82}Se p(11,0)
	294	^{80}Se n(8,2)	36	484	^{74}Se α(8,3)		831	^{74}Se α(7,2)
18	299	^{82}Se n(4,2)	37	492	^{80}Se γ(6,1)	58	886	^{78}Se p(3,1)
19	308	^{82}Se γ(5,2)		493	^{80}Se n(10,0)	59	978	^{74}Se α(7,0)
	309	^{76}Se α(5,2)	38	521	^{77}Se p(7,0)	60	988	^{82}Se γ(5,0)
20	315	^{80}Se n(6,0)	39	525			991	^{74}Se α(8,0)
21	323	^{74}Se α(4,3)						

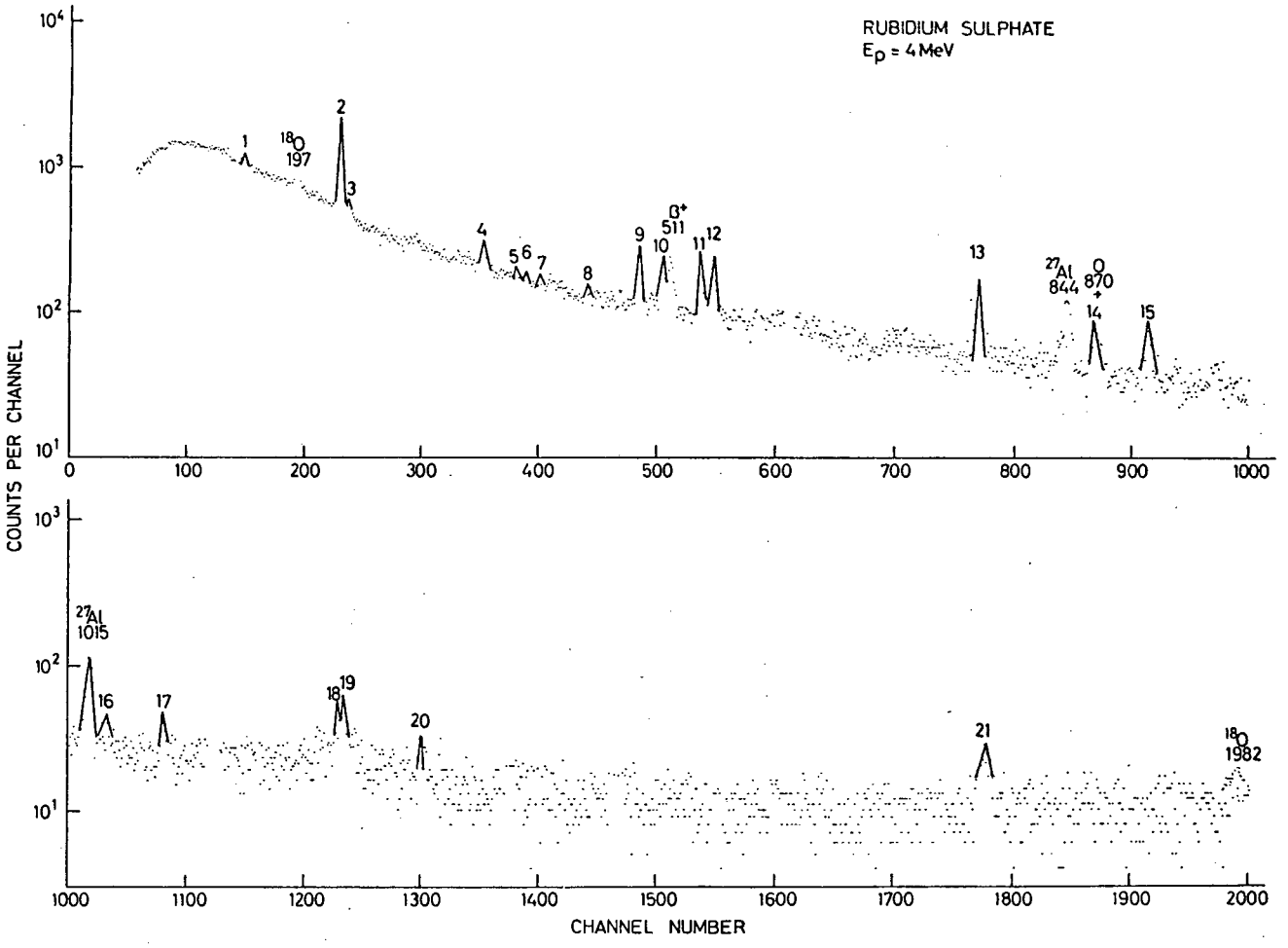

Peak	E_γ keV	Assignment	Peak	E_γ keV	Assignment
1	151	^{85}Rb p(1,0)	10	504	^{85}Rb n(3,2)
2	232	^{85}Rb n(1,0)	11	537	^{85}Rb n(5,1)
3	239	^{85}Rb n(2,0)	12	550	^{85}Rb n(9,5)
4	355	^{87}Rb n(3,2)	13	769	^{85}Rb n(5,0)
	355	^{85}Rb p(3,2)	14	865	^{87}Rb n(4,1)
5	380	^{85}Rb γ(6,3)	15	914	^{85}Rb n(8,0)
	381	^{87}Rb n(4,2)	16	1031	^{85}Rb n(9,1)
6	388	^{87}Rb n(1,0)	17	1077	^{85}Rb γ(1,0)
7	403	^{87}Rb p(1,0)	18	1229	^{87}Rb n(3,0)
8	439	^{85}Rb γ(8,4)	19	1238	^{87}Rb n(7,2)
9	484	^{87}Rb γ(4,2)	20	1296	^{87}Rb n(8,2)
	485	^{87}Rb n(2,1)	21	1771	^{87}Rb n(5,0)

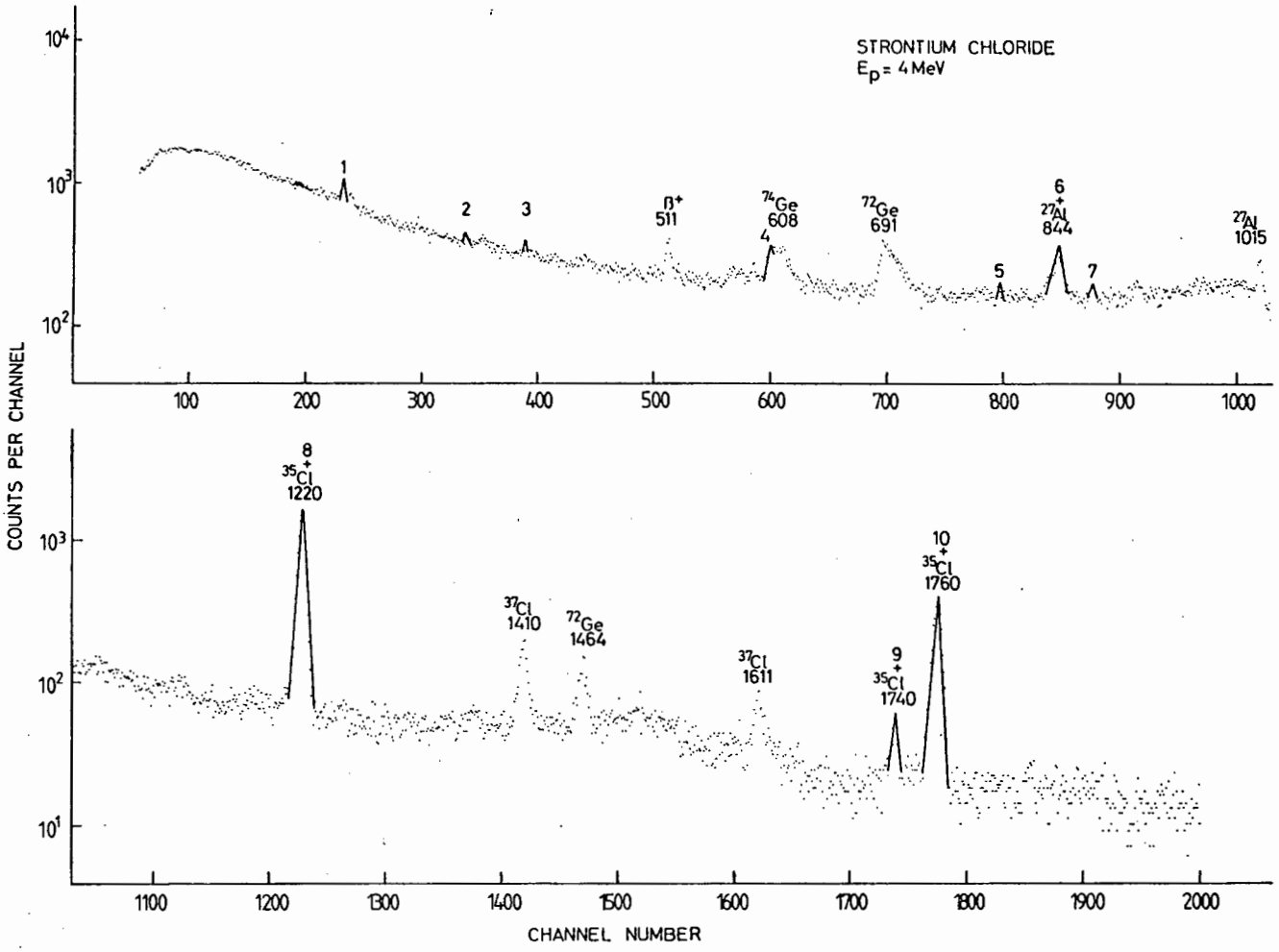

Peak	E_γ keV	Assignment
1	232	^{87}Sr γ(1,0)
	232	^{88}Sr n(1,0)
2	336	^{88}Sr p(5,3)
3	388	^{87}Sr p(1,0)
4	602	^{84}Sr p(4,2)
5	792	^{86}Sr γ(2,0)
	792	^{87}Sr n(2,0)
	793	^{84}Sr n(1,0)
	793	^{84}Sr p(1,0)
6	843	^{87}Sr γ(7,0)
	843	^{88}Sr n(7,0)
7	873	^{87}Sr p(2,0)
8	1229	^{87}Sr p(3,0)
9	1740	^{87}Sr p(5,0)
10	1771	^{87}Sr p(7,0)

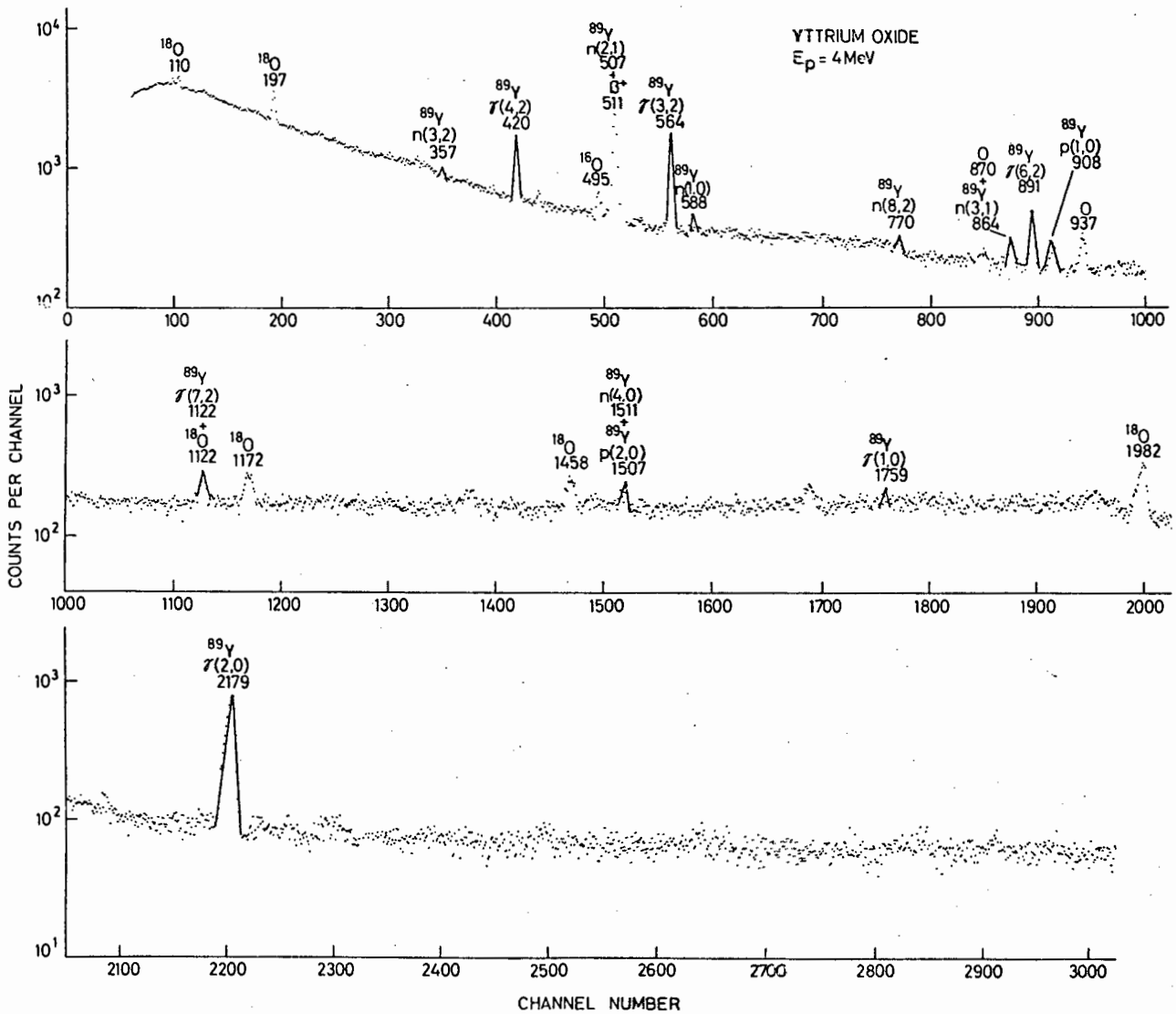
YTTRIUM OXIDE
E_p = 4 MeV
^{18}O 110
^{18}O 197
^{89}Y n(3,2) 357
^{89}Y γ(4,2) 420
^{89}Y n(2,1) 507
0+ 511
^{89}Y γ(3,2) 564
^{16}O 495
^{89}Y n(1,0) 588
^{89}Y n(8,2) 770
O 870
^{89}Y n(3,1) 864
^{89}Y γ(6,2) 891
^{89}Y p(1,0) 908
O 937
^{89}Y γ(7,2) 1122
^{18}O 1122
^{18}O 1172
^{18}O 1458
^{89}Y n(4,0) 1511
^{89}Y p(2,0) 1507
^{89}Y γ(1,0) 1759
^{18}O 1982
^{89}Y γ(2,0) 2179
COUNTS PER CHANNEL
CHANNEL NUMBER

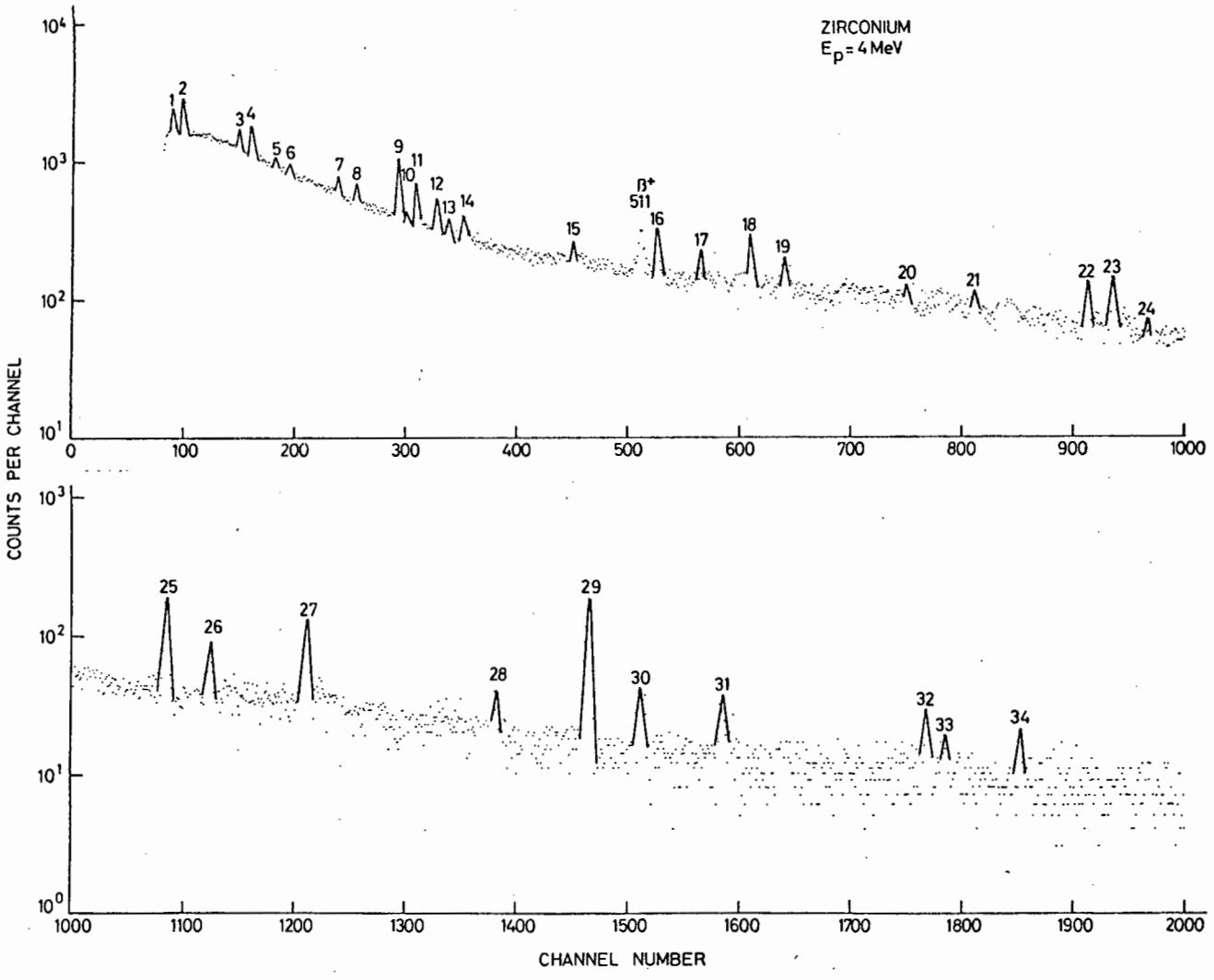

Peak	Eγ keV	Assignment	Peak	Eγ keV	Assignment
1	92	^{92}Zr n(2,1)	17	560	^{92}Zr p(3,1)
2	105	^{91}Zr n(1,0)	18	616	^{96}Zr p(4,1)
3	151	^{92}Zr n(3,1)	19	642	^{94}Zr n(10,0)
4	163	^{90}Zr n(3,1)	20	751	^{94}Zr p(4,1)
	164	^{96}Zr p(2,1)	21	804	^{92}Zr n(9,3)
	165	^{92}Zr n(5,2)	22	918	^{94}Zr p(1,0)
5	180	^{96}Zr n(2,0)	23	934	^{92}Zr p(1,0)
6	195	^{92}Zr n(6,3)	24	979	^{93}Zr n(7,0)
7	233	^{96}Zr n(3,0)	25	1083	^{91}Zr n(2,1)
	234	^{94}Zr γ(1,0)	26	1129	^{90}Zr p(6,3)
8	253	^{94}Zr n(6,2)	27	1205	^{91}Zr p(1,0)
9	293	^{94}Zr n(7,1)	28	1385	^{92}Zr p(2,0)
10	305	^{96}Zr p(4,3)	29	1466	^{91}Zr p(2,0)
11	311	^{96}Zr p(3,1)	30	1508	^{91}Zr n(5,1)
12	329	^{94}Zr n(10,4)	31	1594	^{96}Zr p(1,0)
13	344	^{94}Zr n(7,0)	32	1758	^{96}Zr p(2,0)
14	357	^{92}Zr n(4,0)		1761	^{90}Zr p(1,0)
15	452	^{96}Zr p(4,2)	33	1778	^{92}Zr p(3,0)
16	535	^{96}Zr p(6,3)	34	1848	^{92}Zr p(4,0)

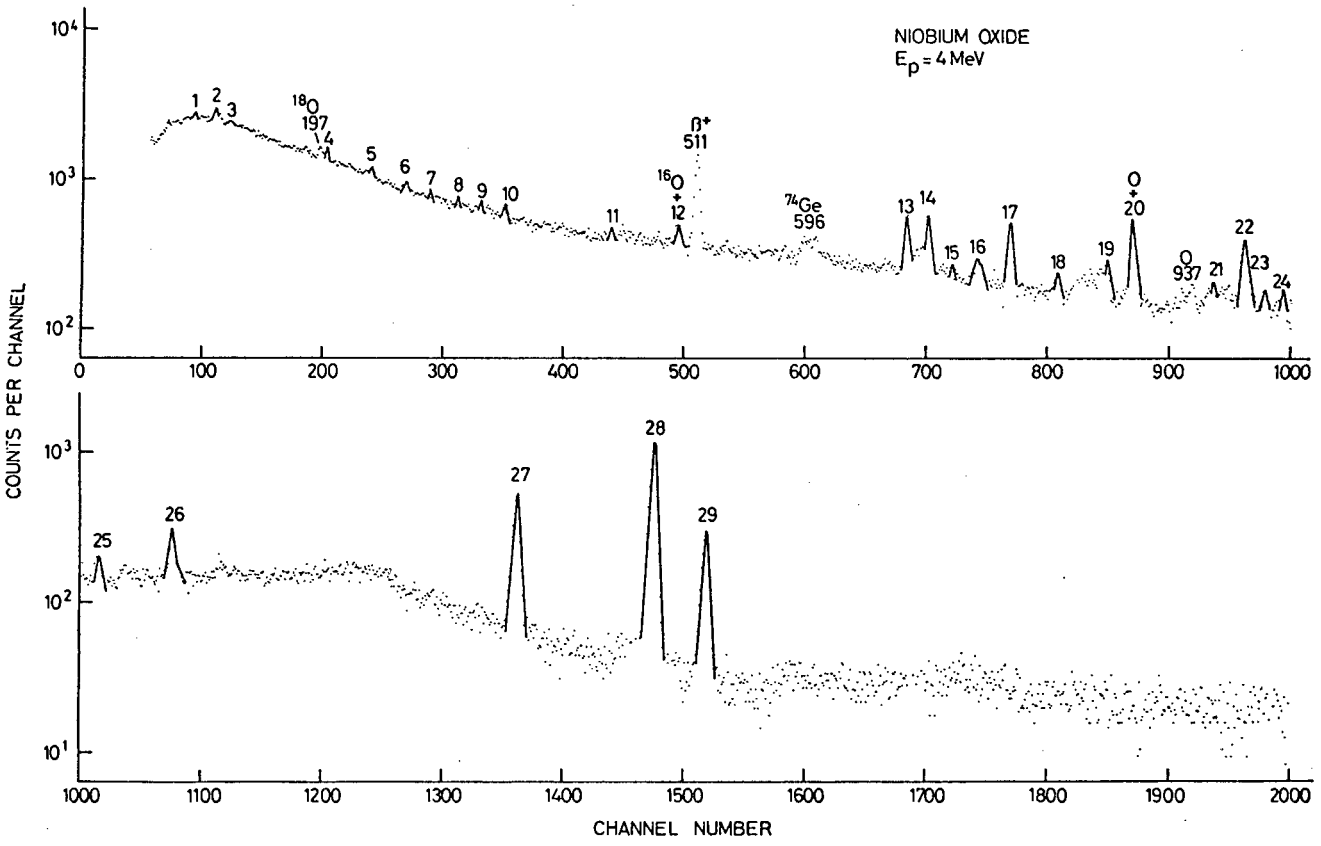

Peak	Eγ keV	Assignment	Peak	Eγ keV	Assignment
1	93	^{93}Nb γ(6,5)	15	726	^{93}Nb γ(5,2)
2	110	^{93}Nb n(3,2)	16	744	^{93}Nb p(3,0)
3	123	^{93}Nb γ(7,5)	17	780	^{93}Nb p(4,1)
4	203	^{93}Nb γ(4,3)	18	809	^{93}Nb p(4,0)
	204	^{93}Nb p(7,4)	19	850	^{93}Nb γ(7,2)
5	235	^{93}Nb p(7,3)	20	871	^{93}Nb γ(1,0)
6	268	^{93}Nb γ(9,5)	21	944	^{93}Nb n(1,0)
7	291	^{93}Nb γ(3,2)	22	950	^{93}Nb p(6,0)
8	318	^{93}Nb p(8,3)	23	979	^{93}Nb γ(3,1)
9	326	^{93}Nb γ(6,4)	24	993	^{93}Nb γ(4,1)
10	339	^{93}Nb p(5,1)	25	1034	^{93}Nb p(8,1)
11	436	^{93}Nb γ(5,3)	26	1083	^{93}Nb p(8,0)
12	494	^{93}Nb γ(4,2)	27	1364	^{93}Nb n(2,0)
13	686	^{93}Nb p(2,0)	28	1429	^{93}Nb γ(5,1)
14	703	^{93}Nb γ(2,1)	29	1530	^{93}Nb γ(6,1)
	704	^{93}Nb γ(9,3)			

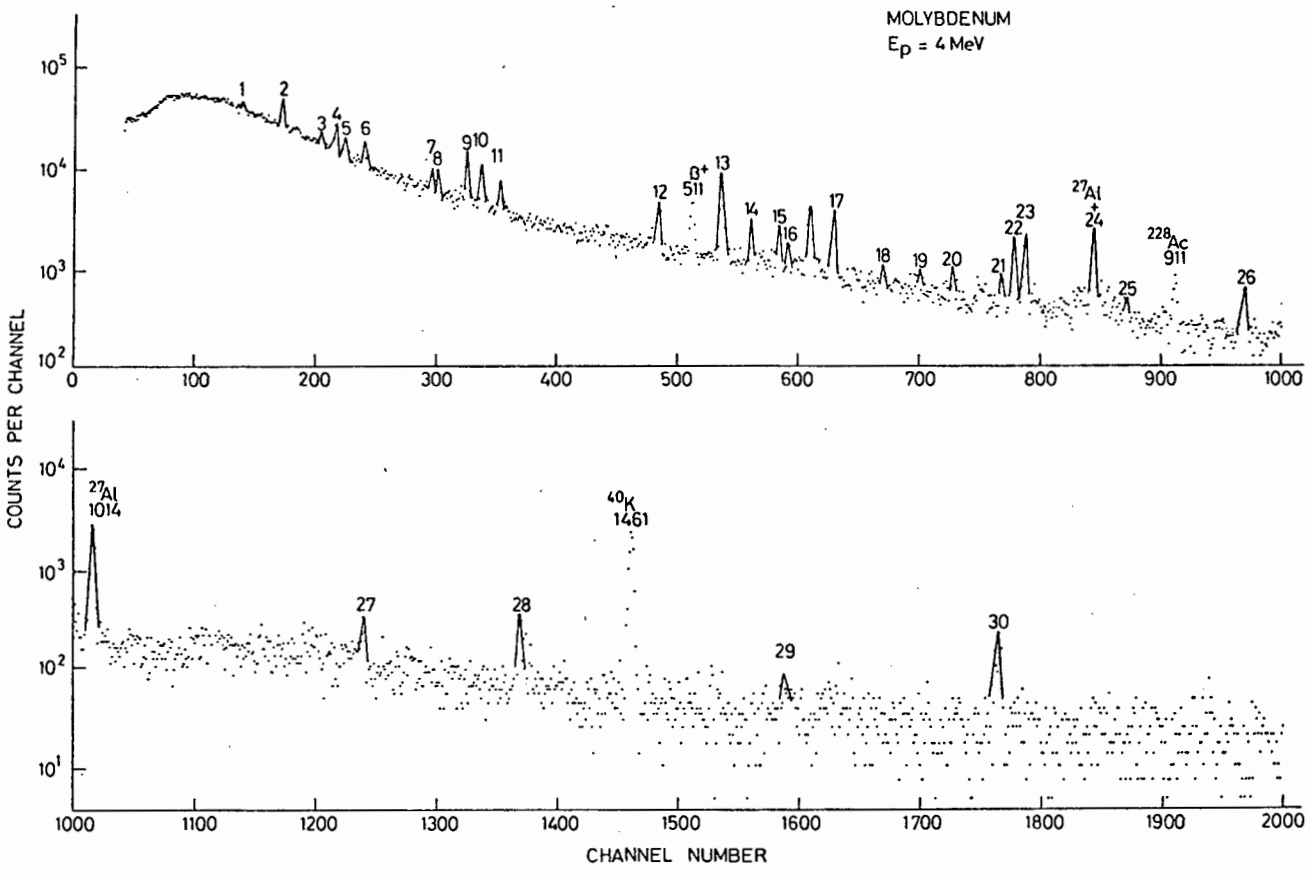

Peak	Eγ keV	Assignment	Peak	Eγ keV	Assignment
1	139	^{98}Mo n(5,0)	14	567	^{95}Mo p(2,1)
	140	^{98}Mo γ(1,0)	15	585	^{95}Mo γ(3,1)
2	181	^{90}Mo γ(3,0)	16	592	^{95}Mo p(3,1)
3	203	^{95}Mo n(4,3)	17	630	^{95}Mo n(3,0)
	204	^{95}Mo p(1,0)		630	^{94}Mo γ(3,0)
4	216	^{96}Mo γ(2,0)	18	669	^{97}Mo n(10,6)
	216	^{96}Mo n(2,0)	19	703	^{94}Mo p(2,1)
	216	^{96}Mo γ(2,0)	20	723	^{98}Mo p(3,1)
5	228	^{96}Mo γ(3,1)	21	767	^{95}Mo p(2,0)
6	242	^{92}Mo p(3,2)		773	^{92}Mo p(2,1)
7	294	^{95}Mo n(3,2)	22	778	^{96}Mo p(1,0)
8	298	^{94}Mo γ(2,1)	23	786	^{95}Mo p(3,0)
9	324	^{96}Mo γ(3,0)		787	^{98}Mo p(1,0)
	324	^{97}Mo n(3,0)	24	843	^{96}Mo p(2,1)
10	336	^{95}Mo n(2,0)	25	871	^{94}Mo p(1,0)
	336	^{94}Mo γ(2,0)	26	972	^{98}Mo p(4,1)
11	353	^{98}Mo n(9,0)	27	1230	^{96}Mo p(5,1)
12	480	^{92}Mo p(10,7)	28	1372	^{100}Mo p(5,1)
	481	^{97}Mo p(1,0)	29	1583	^{92}Mo p(7,1)
13	537	^{100}Mo p(1,0)	30	1760	^{98}Mo p(4,0)

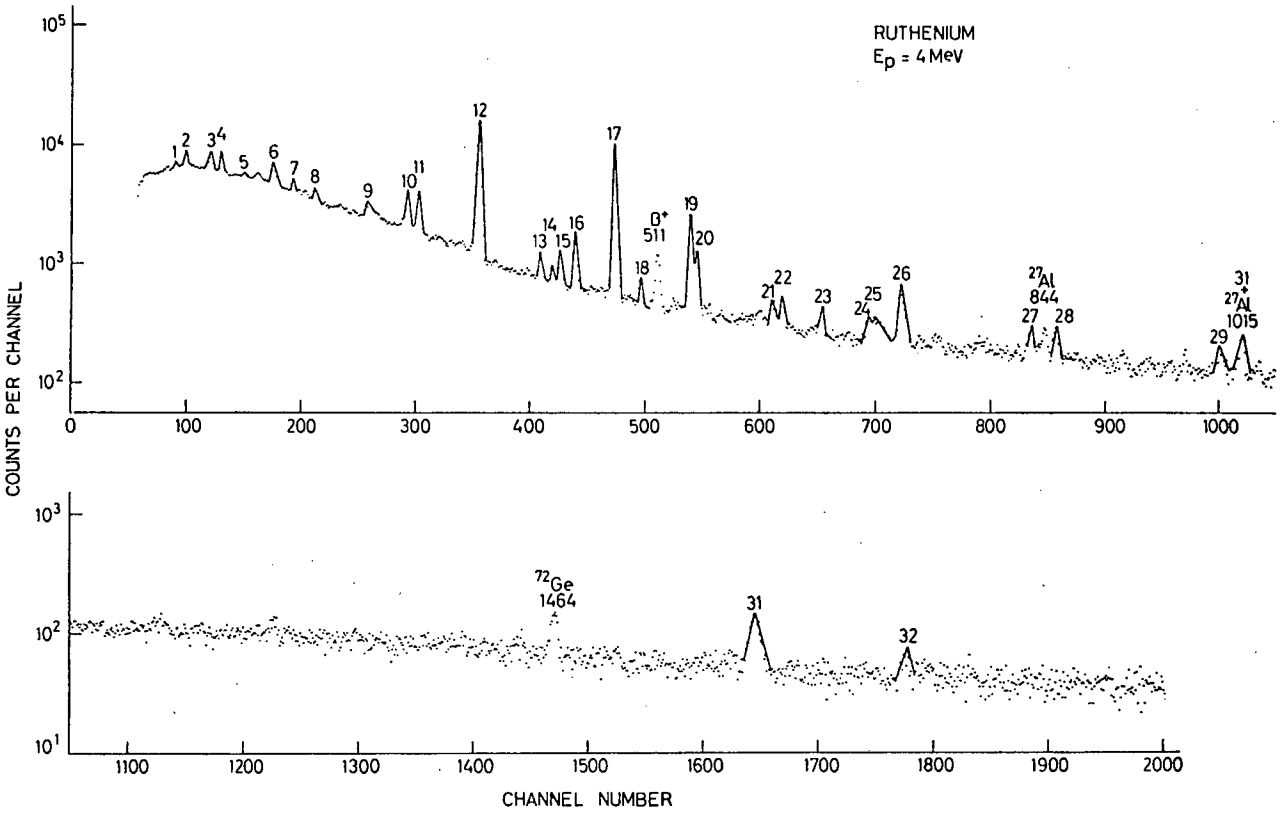

Peak	Eγ keV	Assignment
1	89	^{99}Ru p(1,0)
2	97	^{104}Ru n(2,0)
3	120	^{96}Ru n(6,4)
4	127	^{101}Ru p(1,0)
	129	^{104}Ru n(3,0)
	130	^{104}Ru γ(1,0)
5	151	^{99}Ru γ(3,0)
6	181	^{104}Ru n(4,0)
	182	^{101}Ru n(2,0)
	182	^{100}Ru γ(2,0)
7	197	^{101}Ru n(3,1)
	197	^{100}Ru γ(3,1)
	198	^{101}Ru p(4,1)
8	217	^{96}Ru p(5,4)
9	264	^{99}Ru n(4,2)
	264	^{98}Ru γ(4,2)
10	297	^{102}Ru γ(3,0)
11	305	^{101}Ru n(3,0)
	305	^{100}Ru γ(3,0)
	307	^{101}Ru p(2,0)
12	355	^{101}Ru n(4,0)
	355	^{100}Ru γ(4,0)
	358	^{104}Ru p(1,0)
13	410	^{104}Ru γ(4,0)
14	422	^{101}Ru p(6,0)
15	427	^{99}Ru n(3,0)
	427	^{98}Ru γ(3,0)
16	441	^{96}Ru p(6,5)
17	475	^{102}Ru p(1,0)
18	496	^{101}Ru n(7,3)
	496	^{100}Ru γ(7,3)
19	540	^{100}Ru p(1,0)
20	545	^{101}Ru p(10,0)
	546	^{101}Ru n(7,2)
	546	^{100}Ru γ(7,2)
21	610	^{102}Ru γ(6,0)
22	616	^{101}Ru p(11,0)
	617	^{99}Ru p(6,0)
23	653	^{98}Ru p(1,0)
24	690	^{100}Ru p(3,1)
25	694	^{101}Ru n(7,1)
	694	^{100}Ru γ(7,1)
26	719	^{99}Ru p(8,0)
	720	^{101}Ru p(16,0)
27	826	^{100}Ru p(4,1)
28	851	^{101}Ru n(7,0)
	851	^{100}Ru γ(7,0)
29	1004	
30	1013	^{96}Ru n(4,1)
31	1645	
32	1756	^{96}Ru p(6,1)

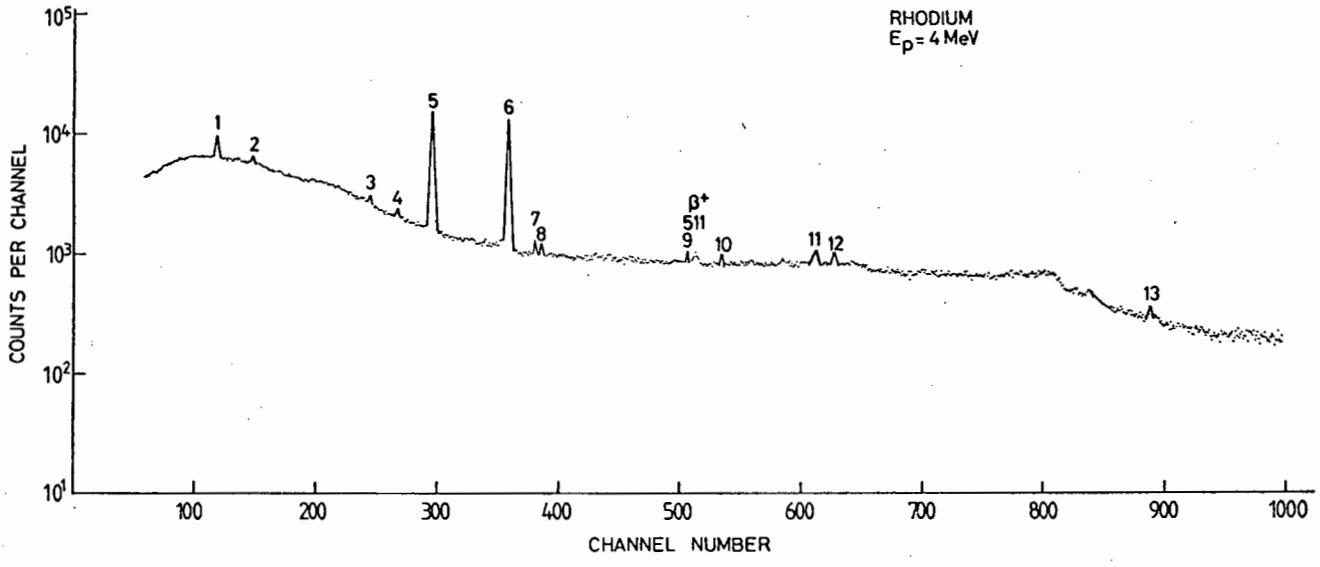

Peak	E_γ keV	Assignment
1	119	^{103}Rh n(1,0)
2	148	^{103}Rh n(3,1)
3	244	^{103}Rh n(2,0)
4	267	^{103}Rh n(3,0)
5	295	^{103}Rh p(3,0)
6	357	^{103}Rh p(4,0)
7	380	^{103}Rh n(4,1)
8	385	^{103}Rh n(5,1)
9	504	^{103}Rh n(5,0)
10	532	^{103}Rh n(6,0)
11	608	^{103}Rh p(7,1)
12	626	^{103}Rh n(7,0)
13	880	^{103}Rh p(5,0)

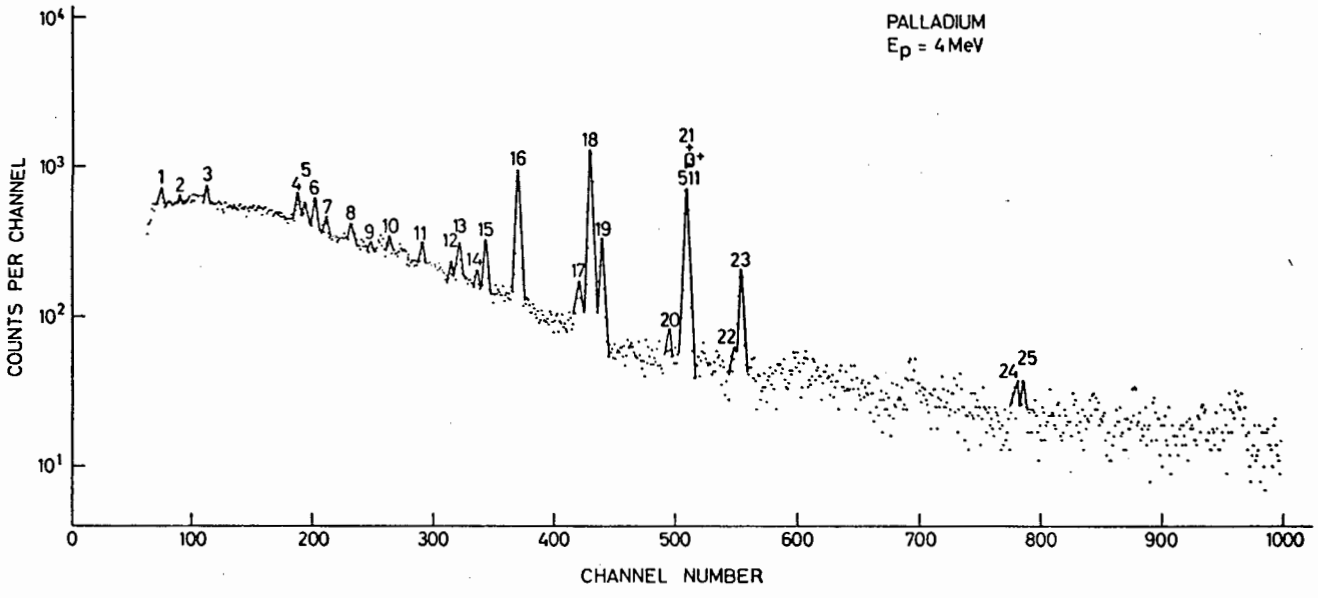

Peak	Eγ keV	Assignment
1	79	^{106}Pd n(1,0)
2	93	^{106}Pd γ(2,0)
	93	^{110}Pd γ(1,0)
3	113	^{109}Pd p(1,0)
4	189	^{109}Pd p(2,0)
	191	^{110}Pd n(2,0)
	193	^{108}Pd n(4,0)
5	195	^{106}Pd γ(3,1)
6	198	^{110}Pd n(3,0)
7	206	^{106}Pd n(3,0)
8	235	^{110}Pd n(4,0)
	237	^{110}Pd n(5,0)
9	248	^{110}Pd n(6,0)
10	267	^{110}Pd n(7,0)
11	281	^{105}Pd p(1,0)
12	321	^{104}Pd γ(3,1)
13	325	^{106}Pd γ(3,0)
14	345	^{105}Pd p(4,0)
15	347	^{105}Pd n(3,0)
16	378	^{110}Pd p(1,0)
17	423	^{105}Pd γ(4,0)
18	433	^{105}Pd p(5,0)
	433	^{105}Pd n(5,0)
	434	^{108}Pd p(1,0)
19	442	^{105}Pd p(6,0)
20	498	^{108}Pd p(2,1)
21	512	^{106}Pd p(1,0)
22	550	^{106}Pd γ(8,4)
23	556	^{104}Pd p(1,0)
	556	^{102}Pd p(1,0)
24	768	^{104}Pd p(2,1)
25	786	^{104}Pd p(4,1)
	786	^{106}Pd γ(5,0)

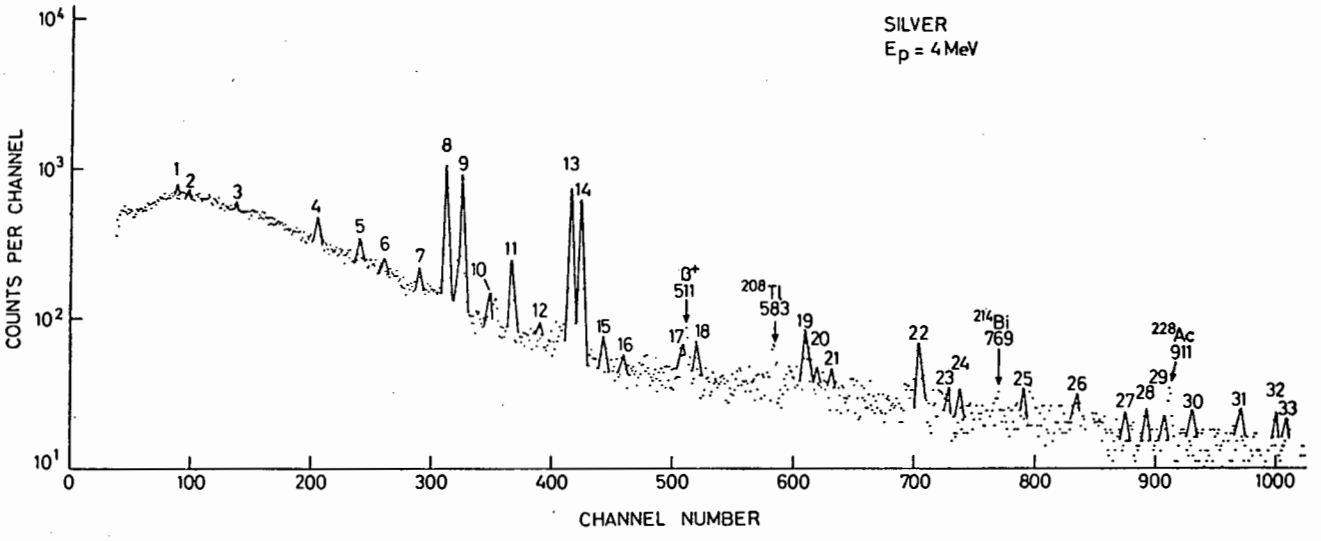

Peak	Eγ keV	Assignment	Peak	Eγ keV	Assignment
1	93	^{107}Ag p(1,0)	17	505	^{107}Ag n(4,0)
2	98	^{107}Ag p(3,2)	18	526	^{107}Ag p(5,3)
3	144	^{109}Ag n(2,1)	19	614	^{109}Ag n(7,1)
4	203	^{109}Ag n(2,0)	20	623	^{109}Ag n(6,0)
	205	^{107}Ag n(1,0)		625	^{107}Ag p(5,2)
5	247	^{109}Ag n(7,4)	21	633	^{107}Ag γ(1,0)
6	259	^{109}Ag n(5,2)	22	702	^{109}Ag p(5,0)
7	285	^{109}Ag p(5,4)	23	722	^{109}Ag n(8,0)
	288	^{109}Ag n(3,1)		724	^{107}Ag p(7,3)
8	311	^{109}Ag p(3,0)	24	738	^{107}Ag p(8,3)
9	325	^{107}Ag p(2,0)	25	786	^{107}Ag p(4,0)
	325	^{107}Ag n(2,0)	26	832	^{109}Ag n(10,1)
10	348	^{109}Ag n(3,0)		834	^{107}Ag p(8,2)
11	362	^{107}Ag p(4,3)	27	872	^{107}Ag p(2,1)
	366	^{107}Ag n(3,0)	28	891	^{109}Ag n(10,0)
	367	^{109}Ag n(4,1)	29	909	^{109}Ag p(9,4)
12	391	^{109}Ag p(5,3)	30	927	^{109}Ag n(11,0)
13	415	^{109}Ag p(4,0)	31	974	^{107}Ag p(6,0)
14	423	^{107}Ag p(3,0)	32	997	^{109}Ag n(13,0)
	426	^{109}Ag n(4,0)	33	1013	^{107}Ag p(9,3)
15	447	^{109}Ag p(6,4)			
16	462	^{107}Ag p(4,2)			
	462	^{109}Ag n(5,0)			

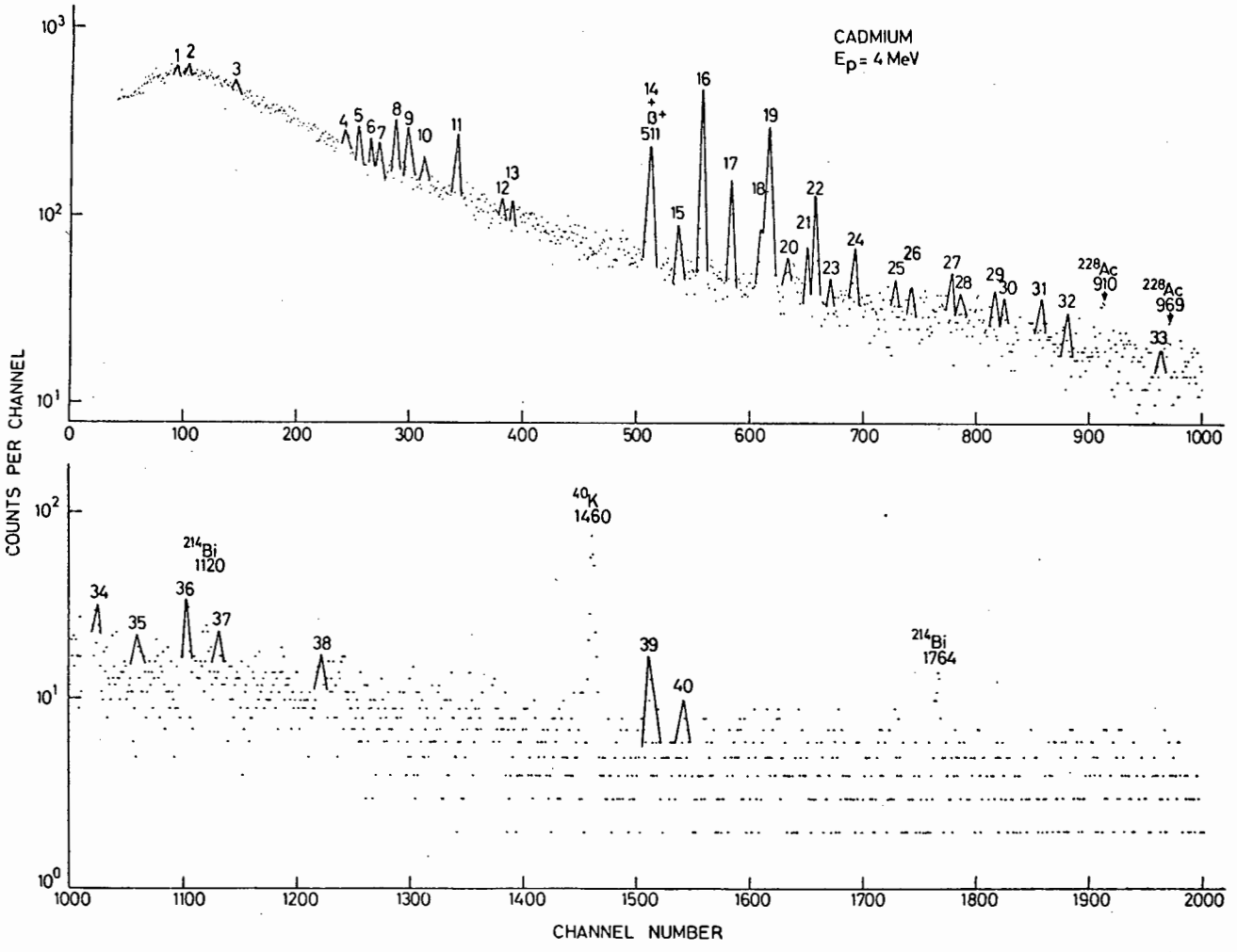

Peak	Eγ keV	Assignment	Peak	Eγ keV	Assignment	Peak	Eγ keV	Assignment
1	96	^{111}Cd p(2,1)	15	536	^{110}Cd γ(1,0)	30	826	^{114}Cd n(9,0)
2	102	^{106}Cd p(4,2)		536	^{111}Cd n(1,0)		826	^{113}Cd γ(9,0)
3	145	^{106}Cd p(7,5)	16	559	^{114}Cd p(1,0)	31	858	^{111}Cd p(7,0)
4	246	^{111}Cd p(1,0)	17	584	^{113}Cd p(5,0)	32	881	^{116}Cd n(6,0)
5	255	^{112}Cd γ(2,1)	18	616	^{106}Cd p(2,1)			
	255	^{113}Cd n(2,1)		617	^{112}Cd p(1,0)	33	963	^{112}Cd n(10,0)
6	264	^{113}Cd p(1,0)	19	621	^{111}Cd p(4,0)		963	^{111}Cd γ(10,0)
7	278	^{114}Cd n(2,0)	20	633	^{106}Cd p(1,0)	34	1026	^{112}Cd γ(3,0)
	278	^{113}Cd γ(2,0)		633	^{108}Cd p(1,0)		1026	^{113}Cd n(3,0)
8	289	^{116}Cd n(9,1)	21	650	^{111}Cd n(5,1)		1026	^{108}Cd n(3,0)
				650	^{110}Cd γ(5,1)	35	1063	^{108}Cd γ(12,1)
9	299	^{113}Cd p(2,0)		650	^{108}Cd γ(1,0)	36	1101	^{111}Cd n(3,0)
10				650	^{114}Cd p(3,1)		1101	^{110}Cd γ(3,0)
	311	^{114}Cd γ(2,1)	22	658	^{110}Cd p(1,0)	37	1132	^{112}Cd γ(4,0)
	316	^{113}Cd p(3,0)		660	^{116}Cd γ(3,0)		1132	^{113}Cd n(4,0)
11	342	^{111}Cd p(2,0)	23	671	^{108}Cd γ(6,1)	38	1218	^{111}Cd n(6,0)
			24	695	^{112}Cd p(2,1)		1218	^{110}Cd γ(6,0)
	345	^{114}Cd γ(3,1)	25	730	^{114}Cd n(7,0)		1220	^{116}Cd p(2,0)
12	377	^{114}Cd n(5,0)		730	^{113}Cd γ(7,0)	39	1509	^{108}Cd p(2,0)
	377	^{113}Cd γ(5,0)	26	742	^{111}Cd γ(8,0)	40	1542	^{111}Cd n(9,0)
13	392	^{112}Cd γ(1,0)		742	^{112}Cd n(8,0)		1542	^{110}Cd γ(9,0)
	392	^{113}Cd n(1,0)	27	770	^{116}Cd p(4,1)			
14	513	^{111}Cd p(7,2)	28	782	^{106}Cd p(8,2)			
	514	^{116}Cd p(1,0)	29	818	^{110}Cd p(2,1)			

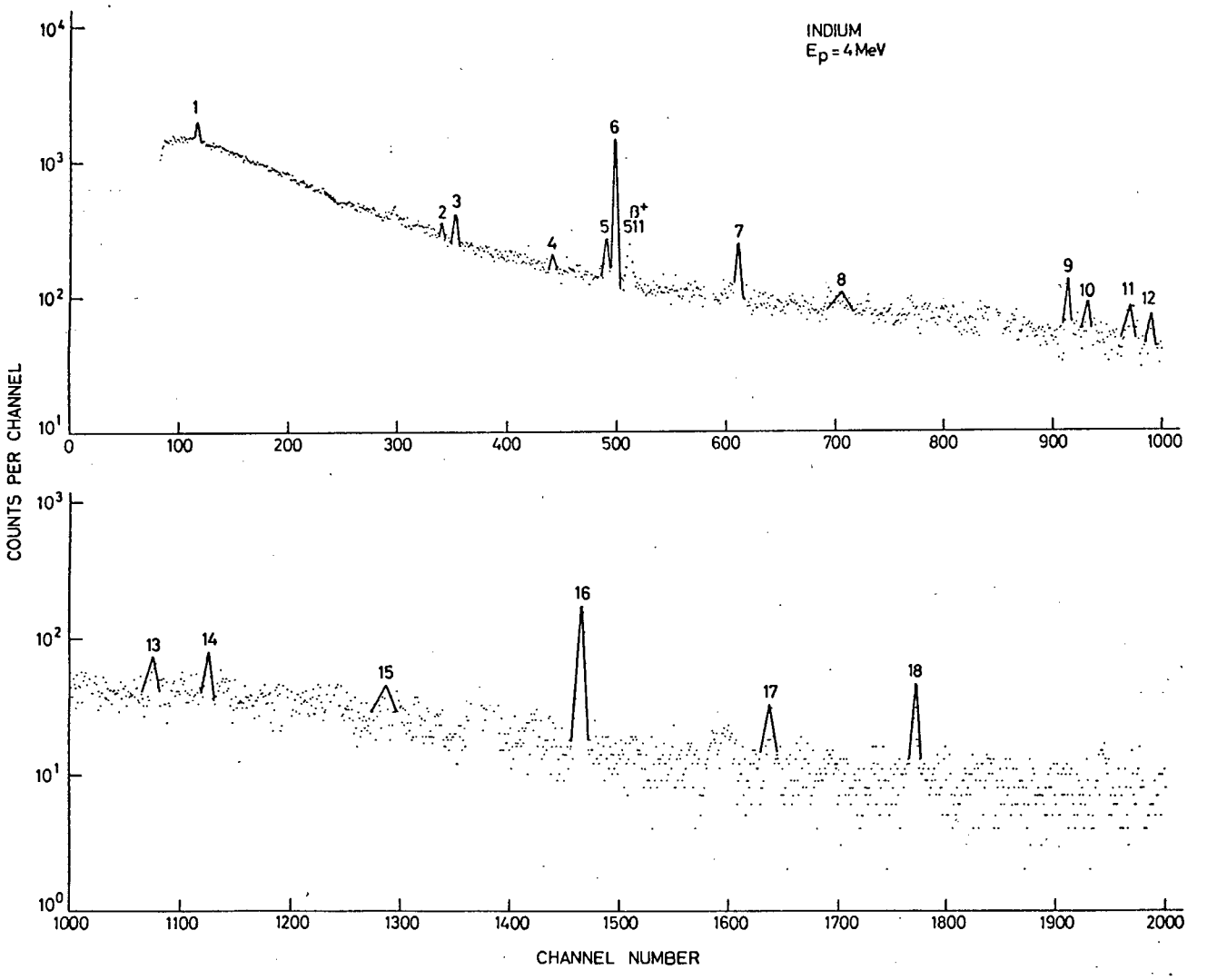

Peak	E_γ keV	Assignment
1	115	^{115}In n(2,1)
2	336	^{115}In p(1,0)
3	355	^{115}In γ(4,2)
4	444	^{115}In p(7,2)
5	489	^{115}In n(4,1)
6	496	^{113}In n(4,0)
	497	^{115}In n(1,0)
7	613	^{115}In n(2,0)
8	705	^{115}In n(7,1)
9	719	^{115}In n(3,0)
10	934	^{115}In p(5,0)
11	972	^{115}In γ(5,1)
12	986	^{115}In n(4,0)
13	1078	^{115}In p(4,0)
14	1133	^{115}In p(9,0)
15	1280	^{115}In n(5,0)
16	1463	^{115}In p(14,0)
17	1633	^{115}In n(7,0)
18	1757	^{115}In γ(2,0)

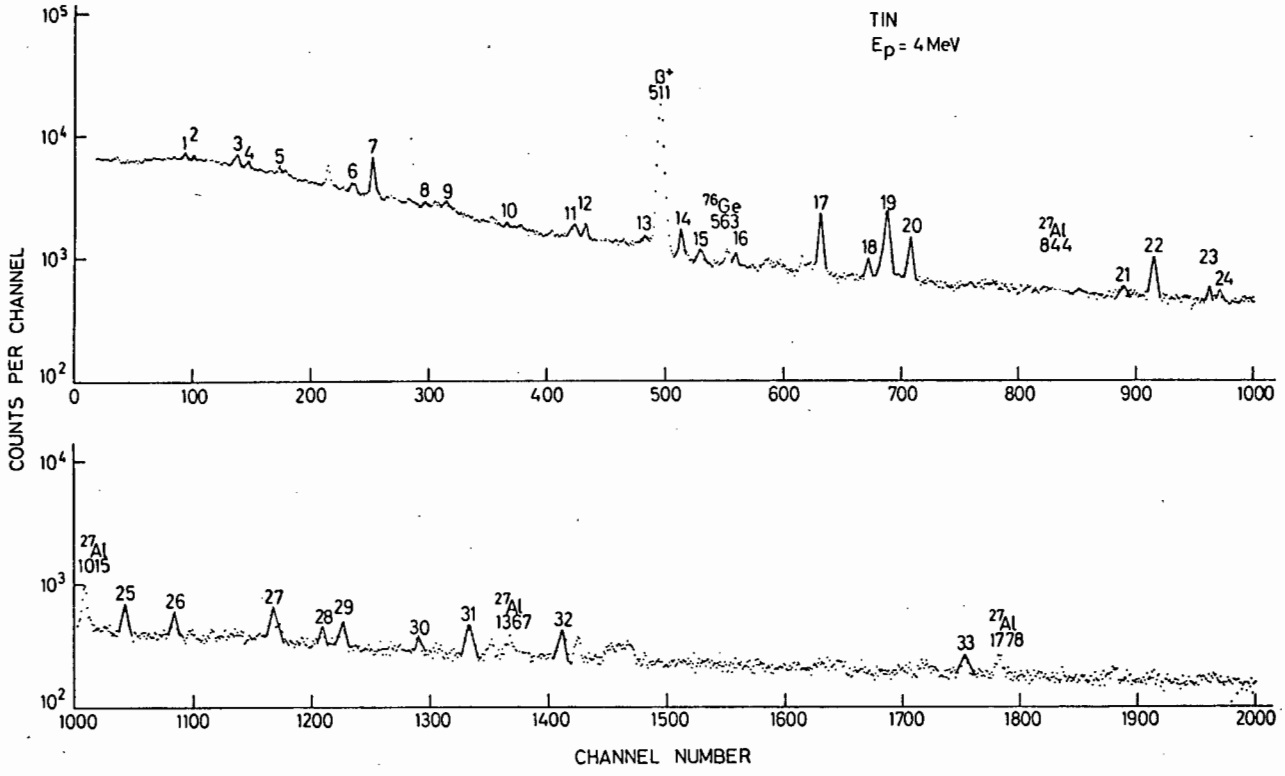

Peak	E_γ keV	Assignment
1	115	^{122}Sn n(7,2)
	116	^{115}Sn p(2,1)
2	122	^{122}Sn n(3,0)
3	159	^{117}Sn p(1,0)
	160	^{122}Sn γ(1,0)
4	167	^{122}Sn n(6,0)
5	194	^{122}Sn n(9,1)
6	256	^{122}Sn n(9,0)
7	270	^{119}Sn n(1,0)
	273	^{117}Sn n(2,1)
	273	^{116}Sn γ(2,1)
8	315	^{116}Sn γ(1,0)
9	332	^{124}Sn γ(1,0)
10	382	^{122}Sn γ(2,1)
11	439	^{120}Sn γ(4,2)
12	447	
13	497	^{115}Sn p(1,0)
14	527	^{117}Sn n(1,0)
15	542	^{122}Sn γ(2,0)
16	573	^{120}Sn γ(3,0)
17	643	^{124}Sn γ(2,0)
	644	^{119}Sn n(2,0)

Peak	E_γ keV	Assignment
18	683	^{119}Sn n(7,2)
19	700	^{119}Sn n(3,0)
20	719	^{117}Sn n(2,0)
	724	^{115}Sn n(1,0)
21	897	^{119}Sn p(4,1)
	898	^{119}Sn p(5,1)
22	921	^{119}Sn p(4,0)
	923	^{117}Sn n(3,0)
23	970	^{114}Sn p(6,1)
	971	^{119}Sn n(4,0)
24	987	^{115}Sn p(4,0)
25	1049	^{119}Sn n(5,0)
26	1090	^{119}Sn p(7,0)
27	1172	^{120}Sn p(1,0)
28	1213	^{119}Sn n(6,0)
29	1230	^{118}Sn p(1,0)
30	1293	^{116}Sn p(1,0)
	1300	^{114}Sn p(1,0)
31	1339	^{119}Sn n(8,0)
32	1413	^{119}Sn n(9,0)
33	1750	^{119}Sn n(12,0)

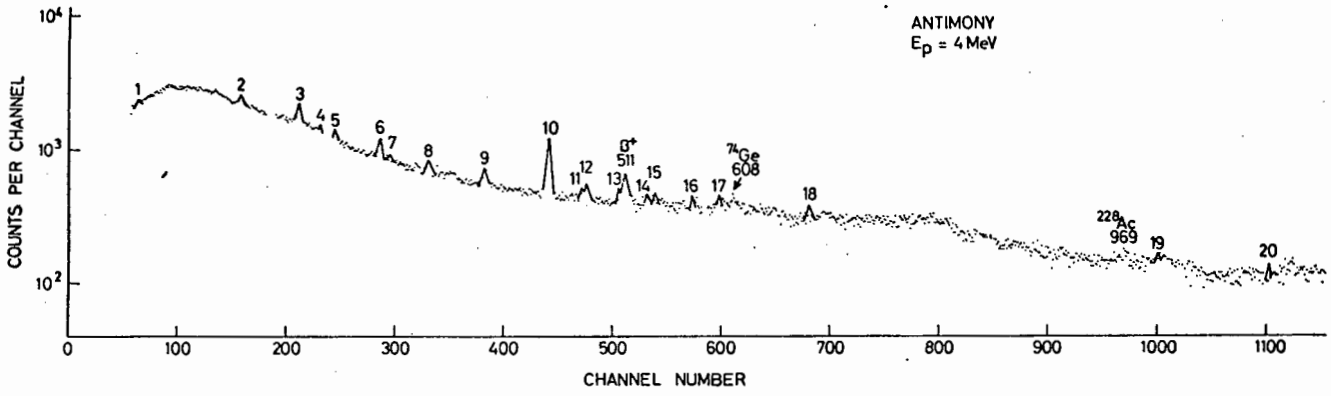

Peak	Eγ keV	Assignment	Peak	Eγ keV	Assignment
1	65	^{123}Sb n(5,3)	10	438	^{121}Sb n(4,0)
	66	^{121}Sb p(3,2)		440	^{123}Sb n(3,0)
2	159	^{123}Sb n (1,0)	11	464	^{121}Sb n(6,0)
	160	^{123}Sb p(1,0)		470	^{121}Sb p(2,1)
3	212	^{121}Sb n(1,0)	12	475	^{121}Sb n(7,0)
4	231	^{121}Sb n(5,1)	13	507	^{121}Sb p(2,0)
5	245	^{121}Sb n(2,0)	14	532	^{121}Sb n(8,0)
	248	^{123}Sb n(2,0)	15	537	^{121}Sb p(3,1)
6	281	^{123}Sb n(3,1)		542	^{123}Sb p(2,0)
7	294	^{121}Sb n(3,0)	16	573	^{121}Sb p(3,0)
8	332	^{121}Sb p(4,1)	17	594	^{121}Sb n(9,0)
9	382	^{123}Sb p(2,1)	18	681	^{121}Sb n(10,0)
	382	^{121}Sb n(9,1)	19	1000	^{121}Sb p(5,1)
			20	1102	^{121}Sb p(6,1)

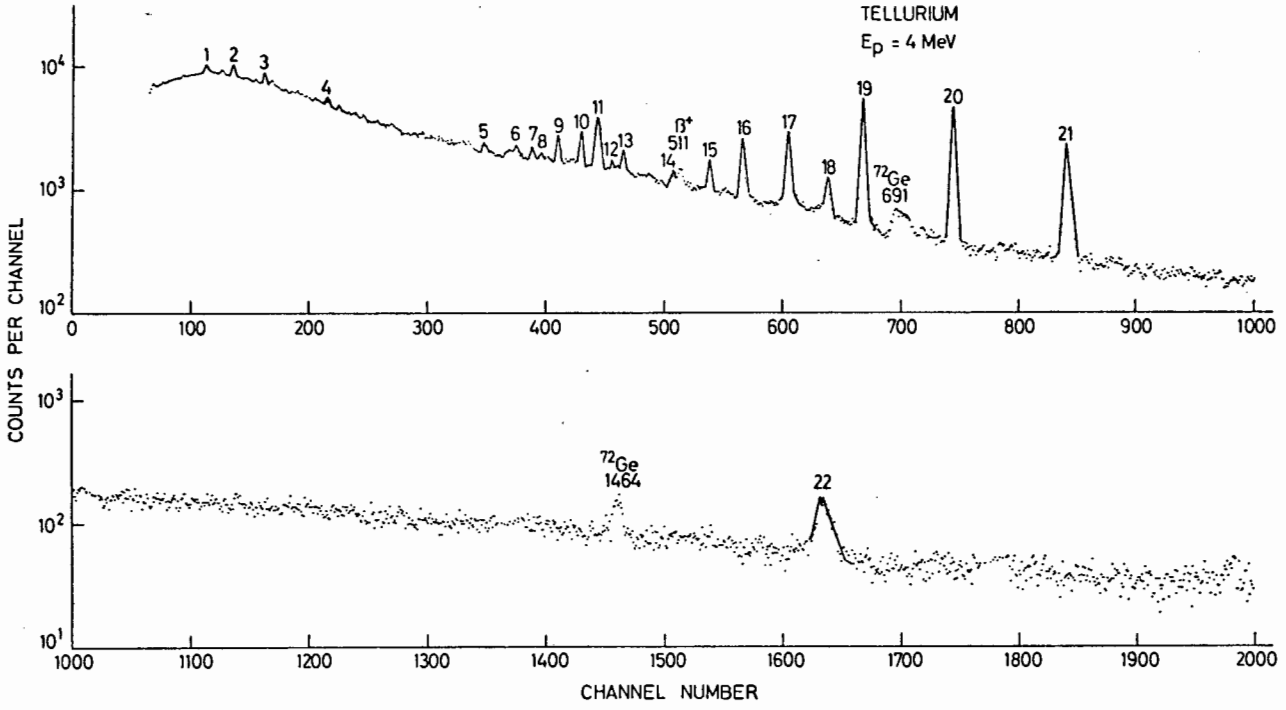

Peak	E_γ keV	Assignment
1	109	^{125}Te p(2,1)
	114	^{125}Te n(1,0)
2	133	^{120}Te γ(2,0)
3	173	^{125}Te p(7,5)
	176	^{125}Te p(3,0)
4	211	^{125}Te n(6,3)
5	349	^{130}Te p(6,3)
6	372	^{125}Te n(4,0)
7	384	^{130}Te γ(6,2)
8	393	^{130}Te p(6,2)
9	408	^{125}Te p(4,1)
10	428	^{125}Te p(5,1)
11	443	^{125}Te p(4,0)
12	452	^{130}Te γ(3,1)
	454	^{125}Te n(5,0)

Peak	E_γ keV	Assignment
13	463	^{125}Te p(5,0)
14	505	^{123}Te p(5,0)
15	539	^{123}Te p(6,1)
16	560	^{120}Te p(1,0)
	564	^{122}Te p(1,0)
17	603	^{124}Te p(1,0)
	603	^{130}Te γ(3,0)
18	636	^{125}Te n(6,4)
19	667	^{126}Te p(1,0)
20	743	^{128}Te p(1,0)
21	839	^{130}Te p(1,0)
22	1633	^{130}Te p(3,0)

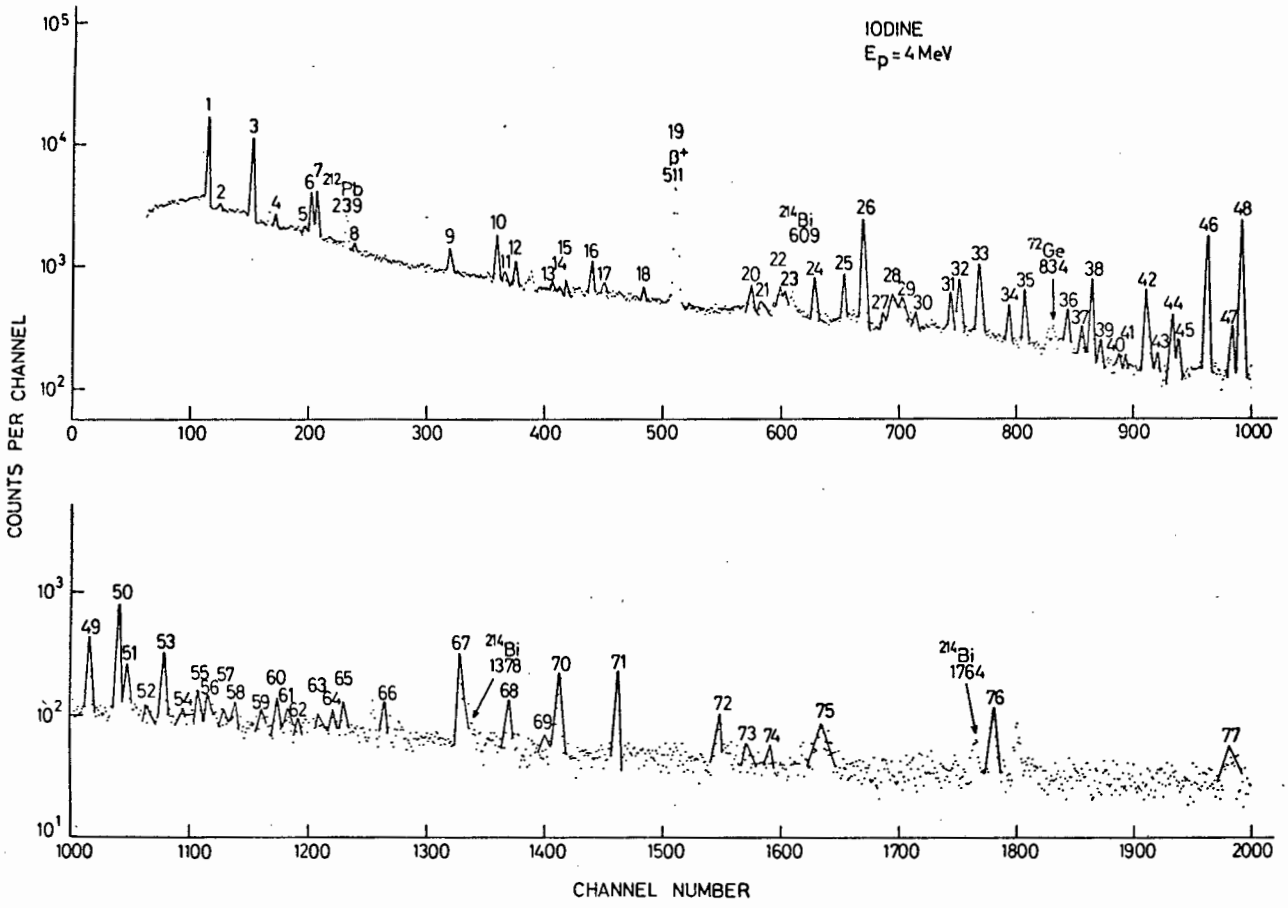

Peak	Eγ	Assignment	Peak	Eγ	Assignment	Peak	Eγ	Assignment
1	114	^{127}I n(4,2)	26	677	^{127}I p(12,4)	51	1054	^{127}I α(5,1)
2	125	^{127}I n(1,0)	27	687	^{127}I p(4,1)	52	1066	^{127}I p(13,1)
3	146	^{127}I p(2,1)	28	695	^{127}I α(7,4)	53	1070	^{127}I n(7,1)
4	173	^{127}I n(2,1)	29	706	^{127}I p(13,4)	54	1095	^{127}I p(12,0)
	173	^{127}I p(3,2)	30	717	^{127}I p(8,0)	55	1110	^{127}I n(9,4)
5	196	^{127}I n(3,1)		720	^{127}I p(12,3)	56	1124	^{127}I p(13,0)
6	201	^{127}I p(5,4)	31	745	^{127}I p(9,0)		1125	^{127}I p(14,1)
	204	^{127}I p(2,0)	32	749	^{127}I p(13,3)	57	1139	^{127}I p(24,3)
7	216	^{127}I p(4,2)	33	765	^{127}I p(14,4)	58	1143	^{127}I γ(3,1)
8	244	^{127}I p(5,3)	34	788	^{127}I p(10,2)	59	1161	^{127}I p(15,1)
9	317	^{127}I p(3,1)	35	804	^{127}I n(6,1)	60	1178	^{127}I n(8,1)
	321	^{127}I n(3,0)		808	^{127}I p(14,3)	61	1183	^{127}I p(14,0)
10	360	^{127}I p(4,1)	36	841	^{127}I p(11,2)	62	1196	^{127}I n(7,0)
11	370	^{127}I p(9,3)	37	856	^{127}I p(18,4)	63	1213	^{127}I n(10,3)
12	375	^{127}I p(3,0)	38	865		64	1219	^{127}I p(15,0)
13	411	^{127}I n(4,0)	39	874	^{127}I n(7,4)	65	1230	^{127}I p(16,0)
14	413	^{127}I p(5,2)	40	892	^{127}I n(8,4)	66	1261	^{127}I n(11,4)
15	418	^{127}I p(4,0)	41	898	^{127}I n(11,2)	67	1326	^{127}I n(18,3)
16	443	^{127}I p(12,7)	42	908	^{127}I p(25,9)	68	1350	^{127}I p(19,1)
17	462	^{127}I n(5,1)	43	920	^{127}I p(13,2)	69	1394	^{127}I n(20,4)
18	490	^{127}I p(17,9)	44	929	^{127}I n(9,8)	70	1409	^{127}I n(10,1)
19	513	^{127}I p(8,2)	45	933	^{127}I p(10,1)	71	1453	^{127}I n(12,4)
20	571	^{127}I p(6,1)	46	970	^{127}I γ(2,1)	72	1535	^{127}I n(10,0)
21	587	^{127}I n(5,0)	47	987	^{127}I p(11,1)	73	1582	^{127}I n(18,0)
22	594	^{127}I p(7,1)	48	991	^{127}I p(10,0)	74	1585	^{127}I n(17,1)
23	600	^{127}I p(15,5)	49	1016	^{127}I p(15,2)	75	1629	^{127}I n(22,2)
24	629	^{127}I p(6,0)	50	1037	^{127}I p(12,1)	76	1778	^{127}I n(12,0)
25	659	^{127}I p(8,1)		1044	^{127}I p(11,0)	77	1975	^{127}I n(23,0)

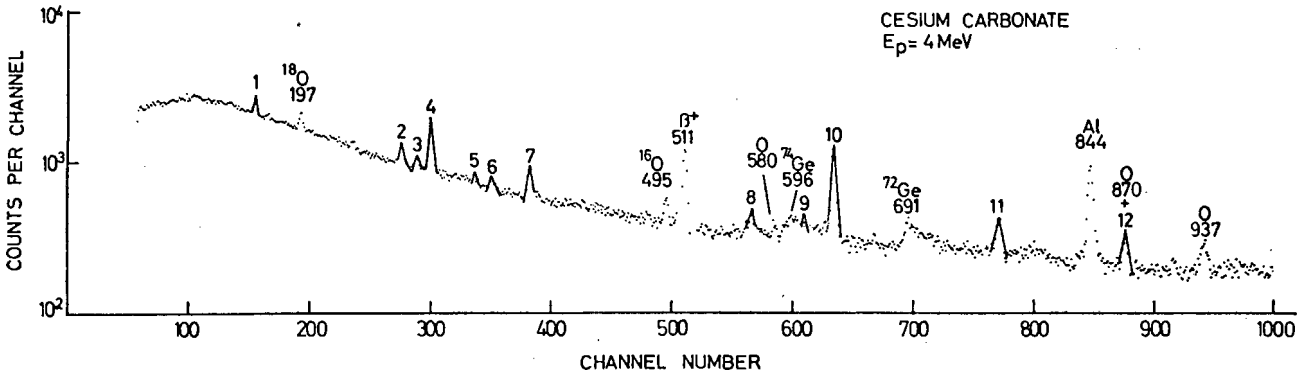

Peak	E_γ keV	Assignment
1	161	^{133}Cs p(2,0)
2	276	^{133}Cs p(4,2)
	276	^{133}Cs n(2,1)
3	279	^{133}Cs n(3,1)
	286	^{133}Cs n(5,3)
	290	^{133}Cs n(4,1)
	291	^{133}Cs n(3,0)
4	302	^{133}Cs n(4,0)
	303	^{133}Cs p(3,1)
5	339	^{133}Cs n(6,3)
6	356	^{133}Cs p(4,1)
7	384	^{133}Cs p(3,0)
8	560	^{133}Cs p(7,1)
	564	^{133}Cs n(5,1)
9	605	^{133}Cs p(5,0)
10	633	^{133}Cs p(6,0)
11	769	^{133}Cs p(10,0)
12	872	^{133}Cs p(13,0)

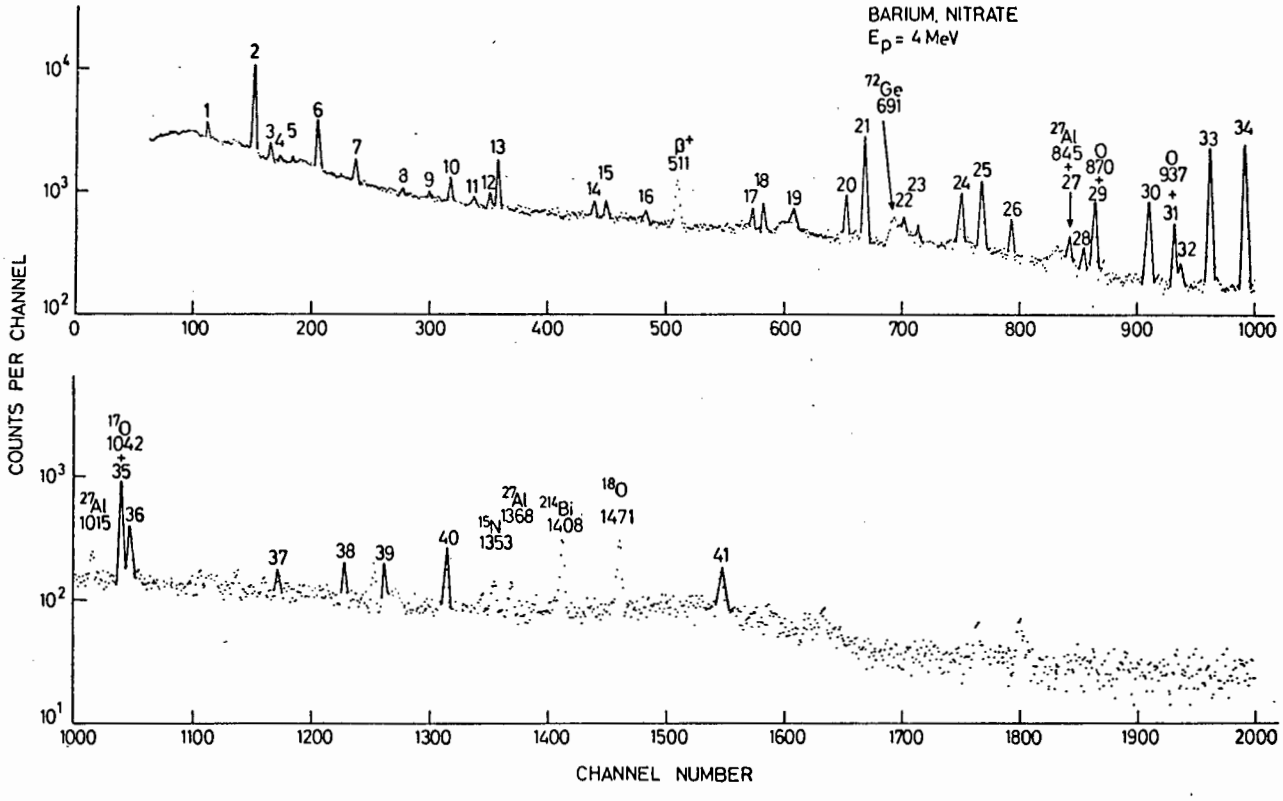

Peak	Eγ keV	Assignment	Peak	Eγ keV	Assignment
1	120	^{135}Ba n(1,0)	22	707	^{138}Ba n(16,5)
2	155	^{132}Ba n(1,0)	23	717	^{135}Ba p(5,0)
3	170	^{130}Ba γ(3,1)	24	751	^{137}Ba γ(14,1)
4	177	^{138}Ba n(6,2)		753	^{134}Ba γ(12,1)
5	182	^{132}Ba n(2,0)		753	^{135}Ba n(12,1)
6	207	^{135}Ba γ(2,0)	25	761	^{136}Ba p(3,1)
7	245	^{130}Ba γ(6,3)	26	796	^{134}Ba p(3,2)
8	279	^{137}Ba p(1,0)	27	842	^{138}Ba n(15,0)
9	304	^{130}Ba γ(4,0)	28	855	^{135}Ba p(6,0)
10	310	^{138}Ba n(9,4)	29	866	^{138}Ba n(20,4)
11	336	^{130}Ba γ(8,4)	30	908	^{130}Ba p(3,0)
12	341	^{138}Ba n(7,1)	31	936	^{138}Ba n(16,0)
13	357	^{130}Ba p(1,0)	32	941	^{138}Ba n(19,2)
14	438	^{138}Ba n(9,1)	33	961	^{136}Ba n(19,0)
15	448	^{137}Ba n(2,0)	34	990	^{132}Ba p(2,0)
16	481	^{135}Ba p(3,0)	35	1039	^{134}Ba p(4,1)
	481	^{136}Ba n(2,0)	36	1048	^{136}Ba p(4,1)
17	576	^{136}Ba n(12,3)	37	1173	^{130}Ba γ(11,0)
18	588	^{135}Ba p(4,0)	38	1235	^{136}Ba p(6,1)
19	605	^{134}Ba p(1,0)	39	1261	^{136}Ba p(7,1)
20	654	^{135}Ba p(7,1)	40	1309	^{136}Ba p(8,1)
21	671	^{130}Ba γ(9,0)	41	1550	^{136}Ba p(2,0)
	671	^{136}Ba p(9,2)			

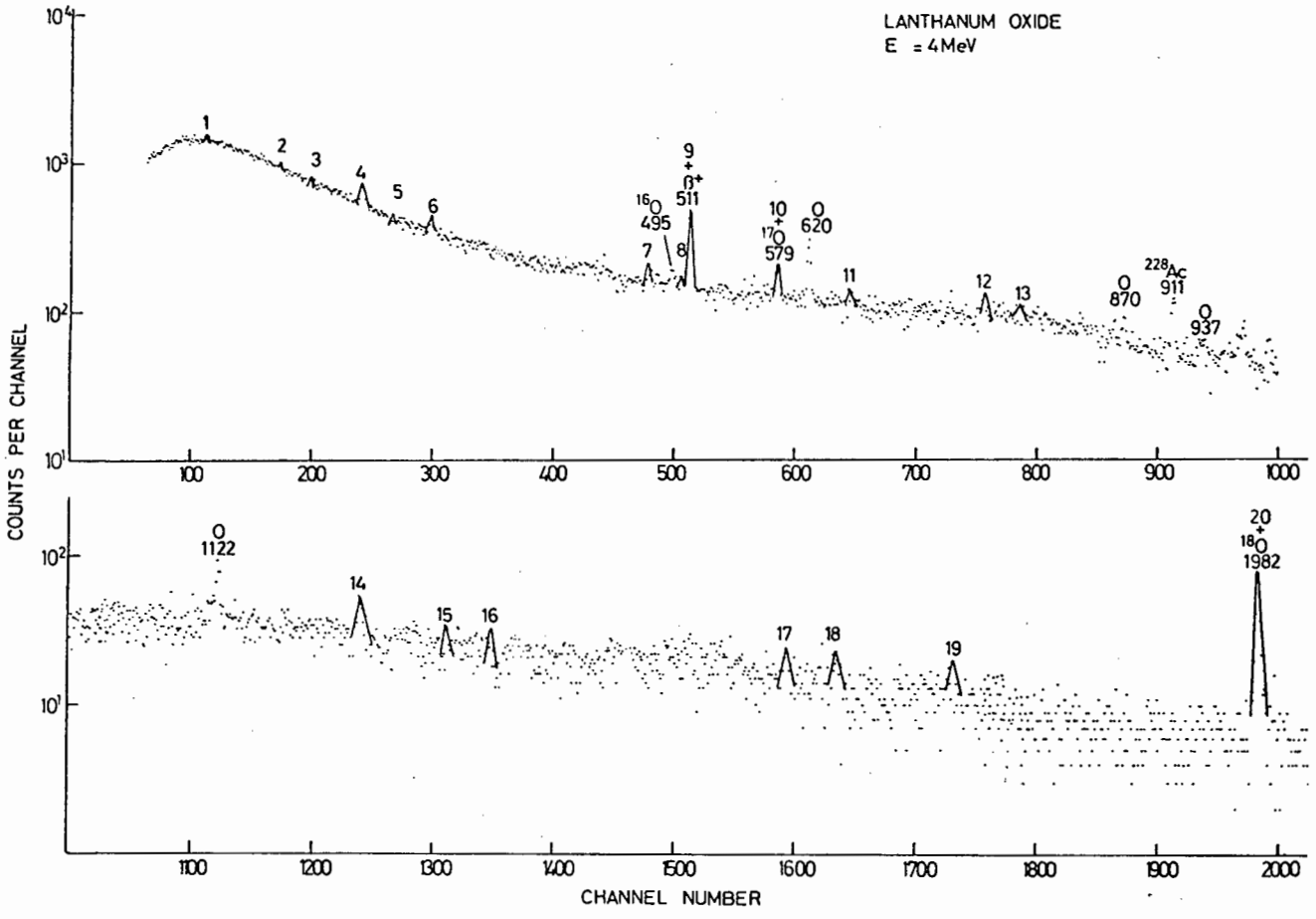

Peak	Eγ keV	Assignment	Peak	Eγ keV	Assignment
1	116	^{138}La p(2,0)	13	789	^{138}La n(1,0)
2	139	^{139}La γ(1,0)	14	1231	^{139}La n(12,3)
3	195	^{138}La γ(2,1)		1231	^{138}La γ(12,3)
4	230	^{138}La p(5,0)	15	1320	^{139}La n(5,0)
5	255	^{139}La n(1,0)		1320	^{138}La γ(5,0)
	255	^{138}La γ(1,0)	16	1347	^{139}La n(6,0)
6	290	^{139}La n(5,4)		1347	^{138}La γ(6,0)
	290	^{139}La γ(5,4)	17	1597	^{138}La n(7,0)
7	479	^{138}La p(8,0)		1597	^{139}La γ(7,0)
8	500	^{139}La n(3,1)	18	1631	^{139}La n(8,0)
	500	^{138}La γ(3,1)		1631	^{138}La γ(8,0)
9	511	^{138}La p(9,0)	19	1730	^{139}La n(12,1)
10	580	^{139}La n(4,2)		1730	^{138}La γ(12,1)
	580	^{138}La γ(4,2)	20	1985	^{139}La n(12,0)
11	642	^{138}La p(11,0)		1985	^{138}La γ(12,0)
12	754	^{139}La n(3,0)			
	754	^{138}La γ(3,0)			

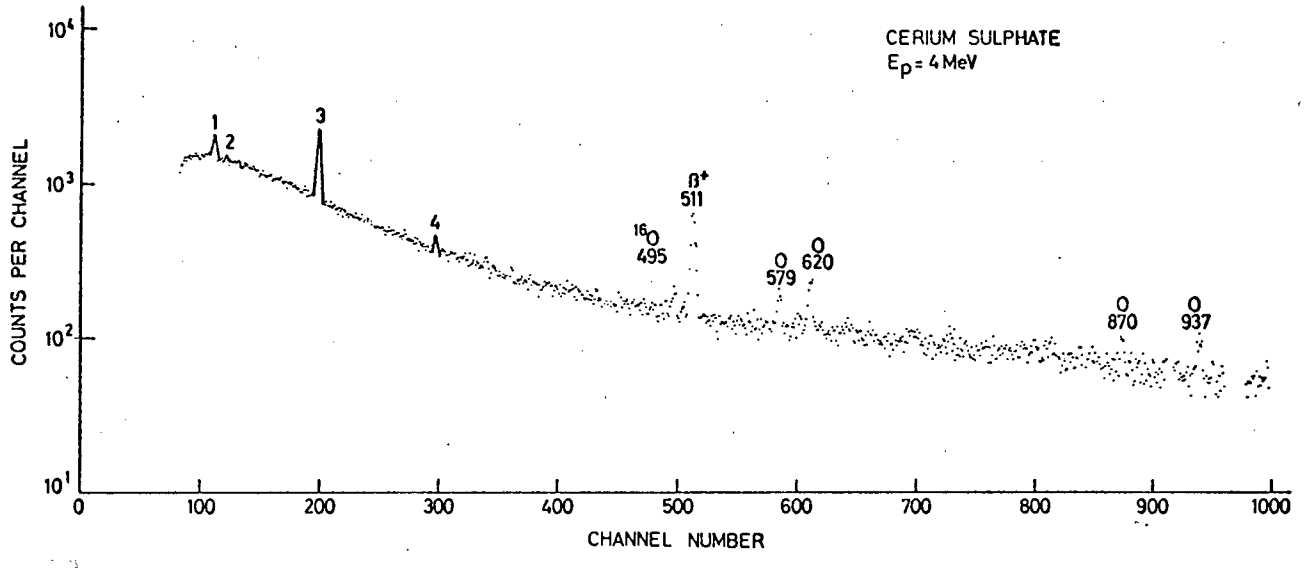

Peak	Eγ keV	Assignment
1	109	^{136}Ce n(3,1)
2	124	^{142}Ce n(7,0)
	126	^{138}Ce n(3,2)
3	200	^{138}Ce n(2,0)
4	295	^{136}Ce n(5,1)

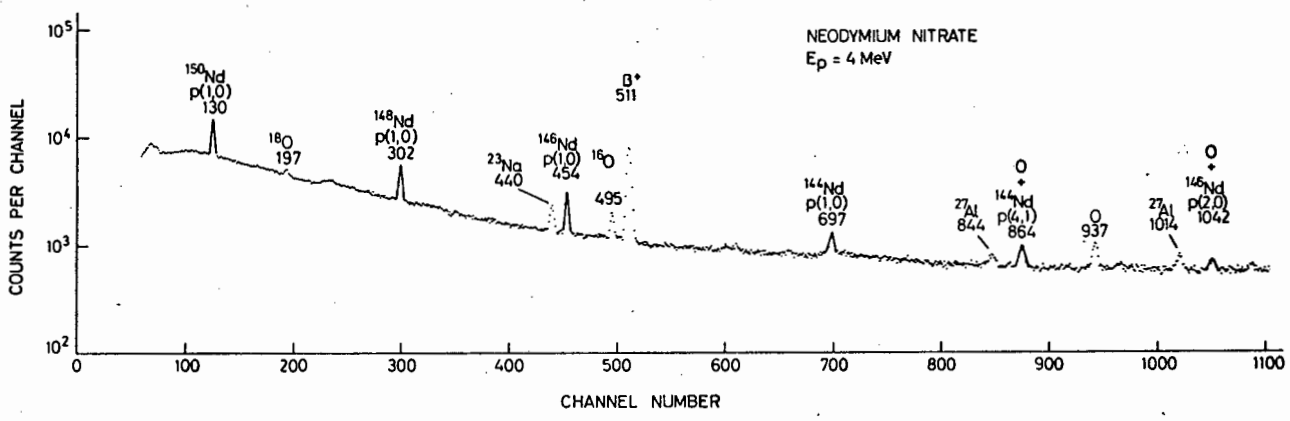
NEODYMIUM NITRATE
E_p = 4 MeV
COUNTS PER CHANNEL
CHANNEL NUMBER
10^5
10^4
10^3
10^2
0
100
200
300
400
500
600
700
800
900
1000
1100
^{150}Nd p(1,0) 130
^{18}O 197
^{148}Nd p(1,0) 302
^{23}Na 440
^{146}Nd p(1,0) 454
^{16}O 495
β+ 511
^{144}Nd p(1,0) 697
^{27}Al 844
O + ^{144}Nd p(4,1) 864
O 937
^{27}Al 1014
O + ^{146}Nd p(2,0) 1042

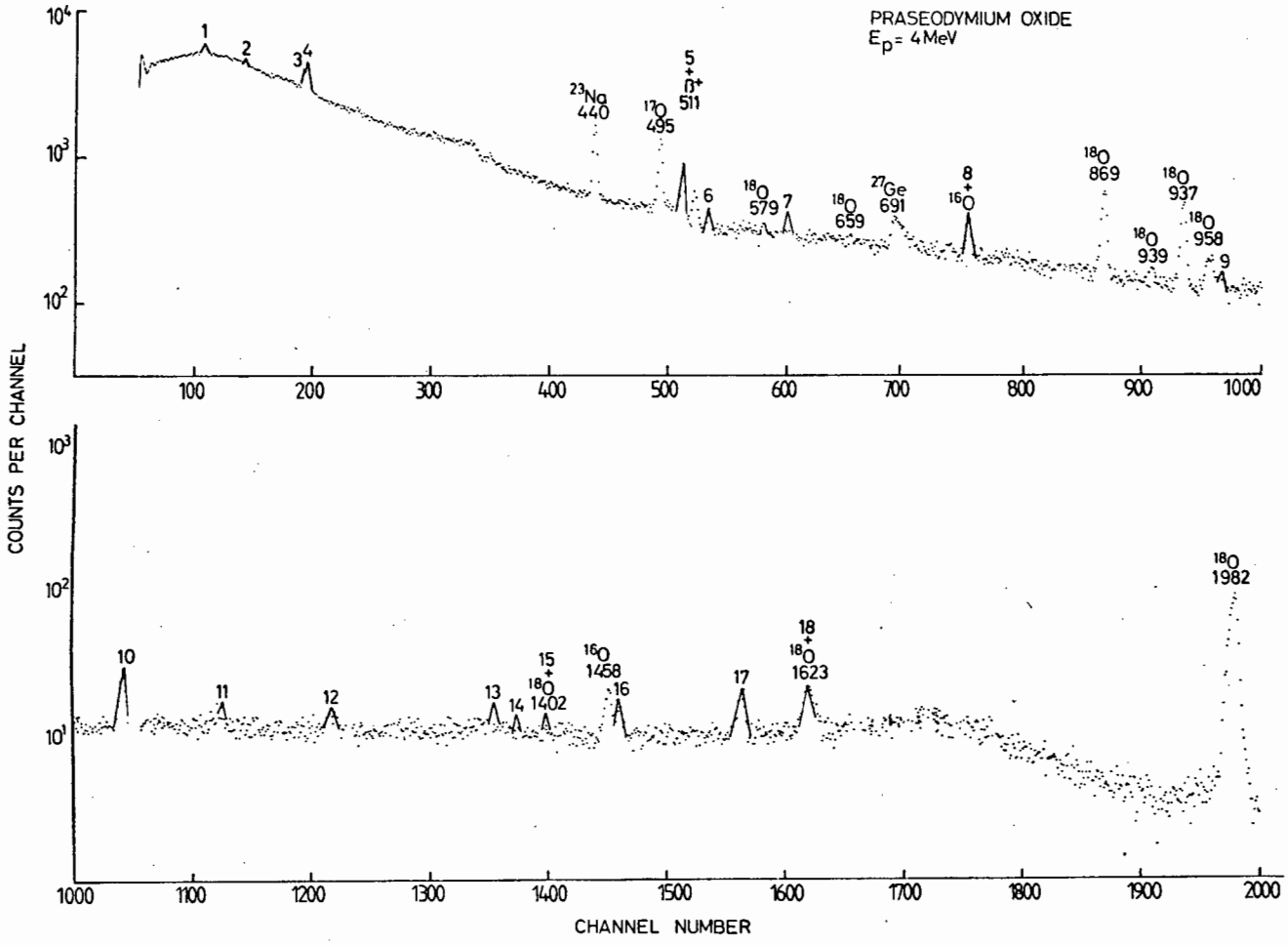

Peak	Eγ keV	Assignment
1	108	^{141}Pr γ(4,2)
2	145	^{141}Pr p(1,0)
3	194	^{141}Pr n(1,0)
4	197	^{141}Pr n(5,3)
5	508	^{141}Pr γ(2,1)
6	525	^{141}Pr γ(3,1)
7	597	^{141}Pr n(9,3)
8	757	^{141}Pr n(2,0)
9	971	^{141}Pr p(2,1)
10	1036	^{141}Pr γ(5,4)
11	1127	^{141}Pr p(3,0)
12	1223	^{141}Pr n(3,0)
13	1345	^{141}Pr n(4,0)
14	1371	^{141}Pr n(5,1)
15	1403	^{141}Pr n(7,1)
16	1470	^{141}Pr γ(15,1)
17	1576	^{141}Pr γ(1,0)
18	1626	^{141}Pr n(9,1)

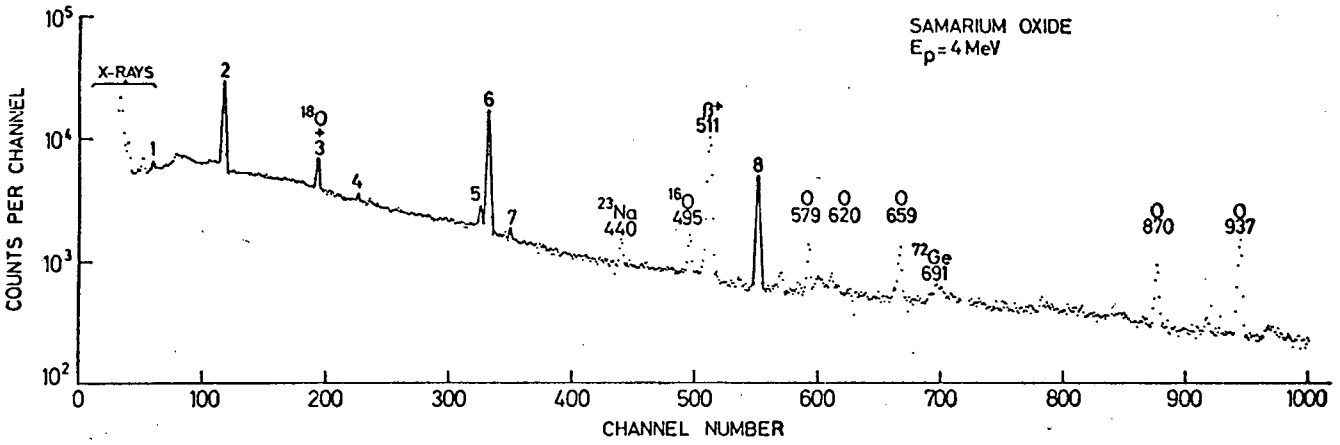

Peak	Ey keV	Assignment
1	68	^{154}Sm n(1,0)
2	121	^{147}Sm p(1,0)
	122	^{152}Sm p(1,0)
3	197	^{147}Sm p(2,0)
4	229	^{147}Sm n(1,0)
5	328	^{149}Sm p(3,1)
6	333	^{144}Sm n(1,0)
	334	^{150}Sm p(1,0)
7	350	^{149}Sm p(3,0)
8	550	^{146}Sm p(1,0)

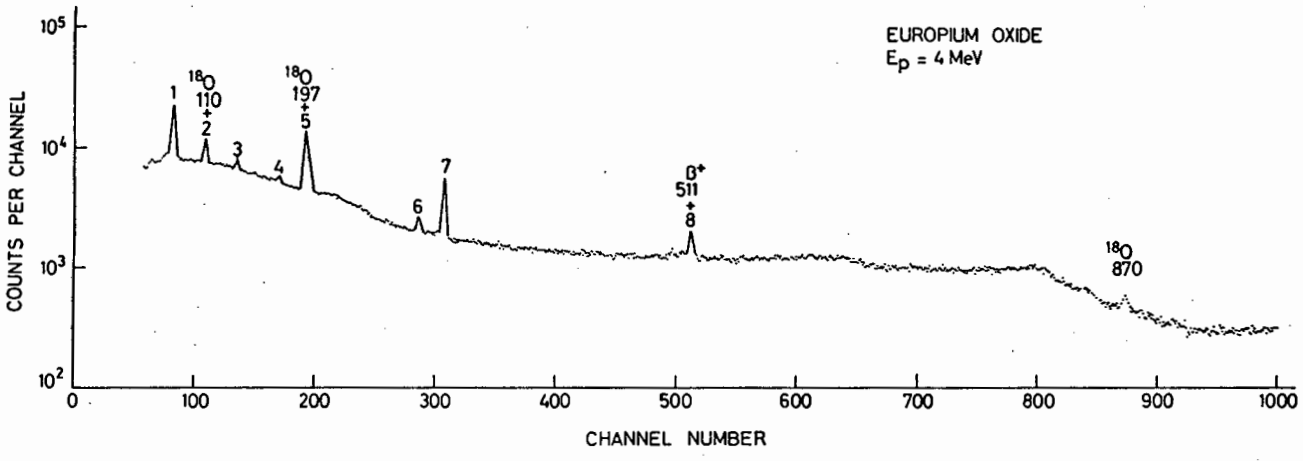

Peak	E_γ keV	Assignment
1	84	^{153}Eu p(1,0)
2	110	^{151}Eu p(3,0)
	110	^{151}Eu p(4,2)
3	135	^{151}Eu n(5,0)
4	175	^{151}Eu p(2,1)
5	197	^{151}Eu p(2,0)
6	286	^{151}Eu p(4,1)
7	308	^{151}Eu p(4,0)
8	512	^{151}Eu n(7,1)

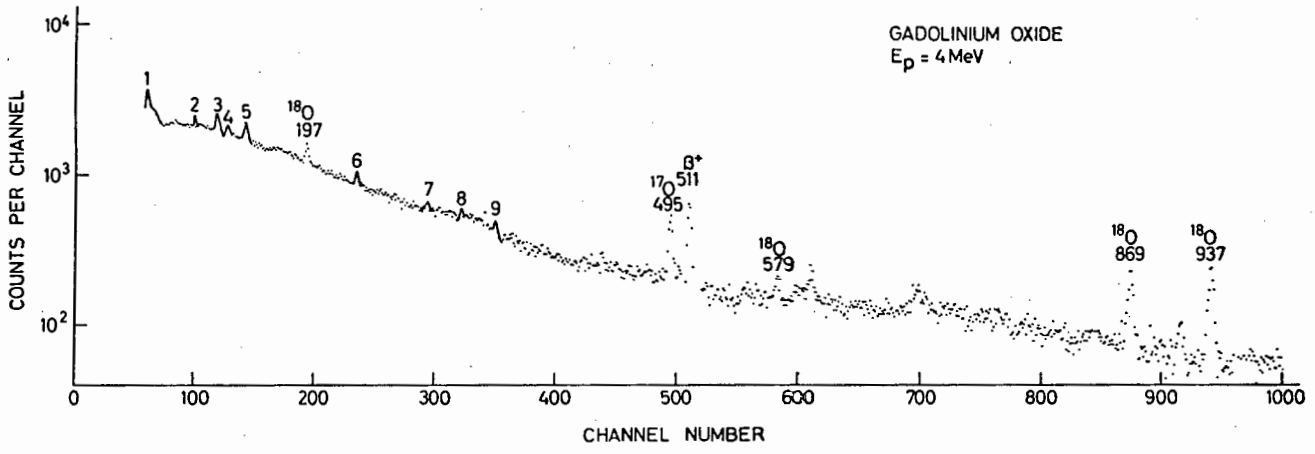

Peak	E_γ keV	Assignment
1	65	^{155}Gd n(1,0)
2	105	^{155}Gd p(3,2)
3	123	^{154}Gd p(1,0)
4	131	^{157}Gd p(2,0)
5	146	^{155}Gd p(2,0)
6	232	^{154}Gd p(6,4)
7	296	^{156}Gd p(3,2)
8	322	^{155}Gd p(4,0)
9	347	^{154}Gd p(3,2)

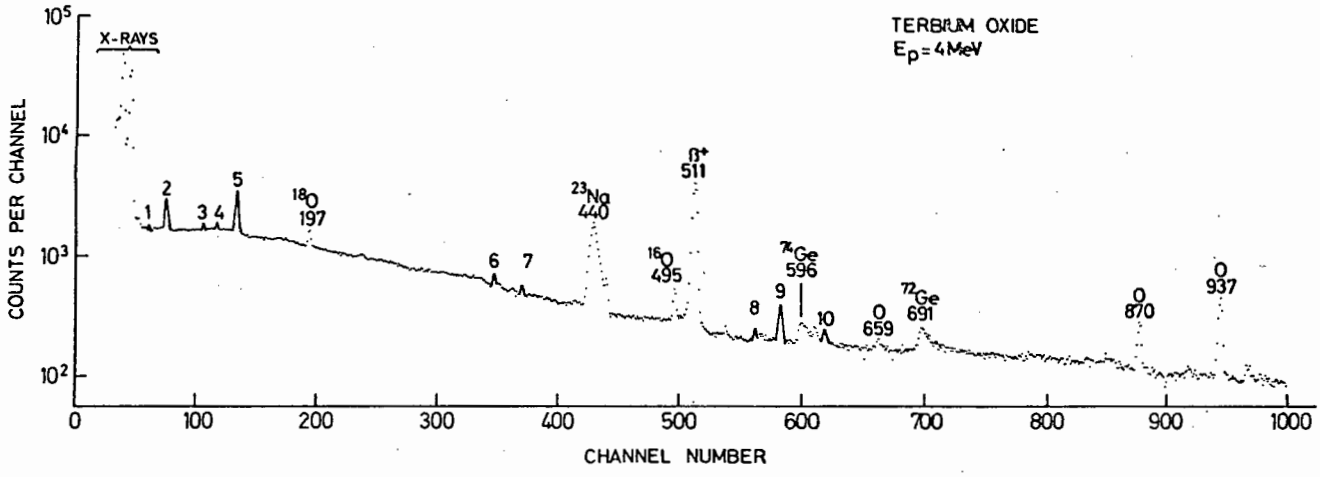

Peak	E_γ keV	Assignment
1	57	^{159}Tb n(1,0)
	58	^{159}Tb p(1,0)
2	80	^{159}Tb p(2,1)
	80	^{159}Tb n(2,1)
3	104	^{159}Tb p(3,2)
4	121	^{159}Tb n(3,1)
	122	^{159}Tb p(5,3)
5	136	^{159}Tb n(2,0)
	138	^{159}Tb p(2,0)
6	348	^{159}Tb p(4,0)
7	371	^{159}Tb p(6,1)
8	560	^{159}Tb p(9,1)
9	580	^{159}Tb p(8,0)
10	617	^{159}Tb p(9,0)

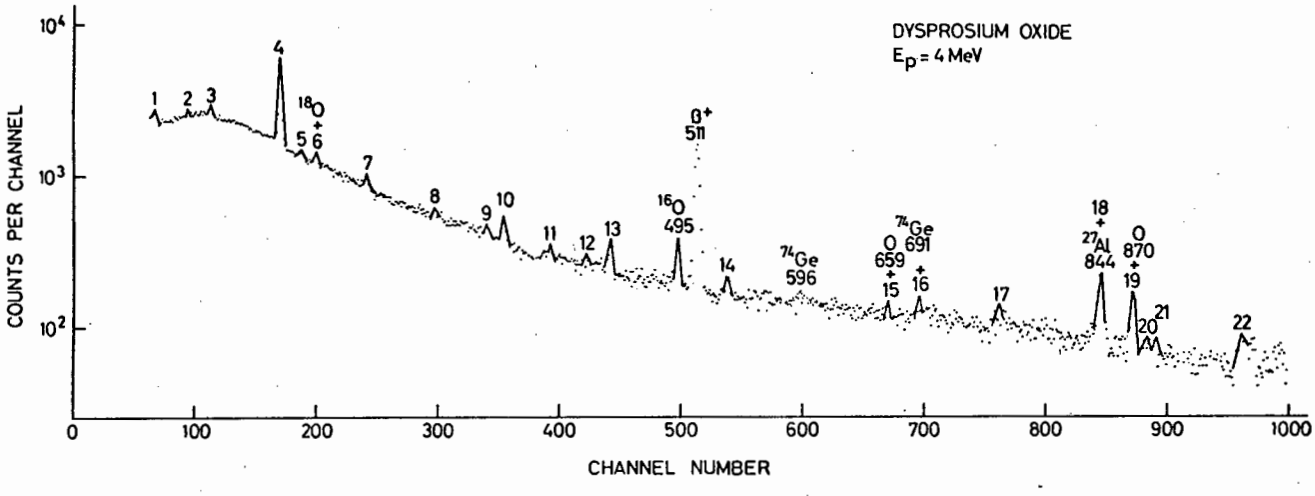

Peak	Eγ keV	Assignment	Peak	Eγ keV	Assignment
1	73	^{164}Dy p(1,0)	11	390	^{163}Dy p(5,0)
2	94	^{163}Dy p(2,1)	12	422	^{163}Dy p(7,0)
	95	^{163}Dy n(1,0)	13	440	^{163}Dy n(3,0)
3	114	^{163}Dy p(3,2)	14	538	^{156}Dy p(3,1)
4	167	^{163}Dy p(2,0)	15	674	^{164}Dy p(6,2)
	169	^{164}Dy p(2,1)	16	689	^{164}Dy p(4,1)
5	185	^{162}Dy p(2,1)	17	762	^{164}Dy p(4,0)
6	197	^{160}Dy p(2,1)	18	643	^{164}Dy p(6,1)
7	242	^{164}Dy p(2,0)	19	871	^{160}Dy p(7,2)
8	297	^{160}Dy p(3,1)	20	884	^{156}Dy p(7,1)
	298	^{163}Dy n(2,0)	21	891	^{156}Dy p(6,0)
9	342	^{164}Dy p(5,3)	22	962	^{160}Dy p(6,1)
10	351	^{163}Dy p(4,0)			

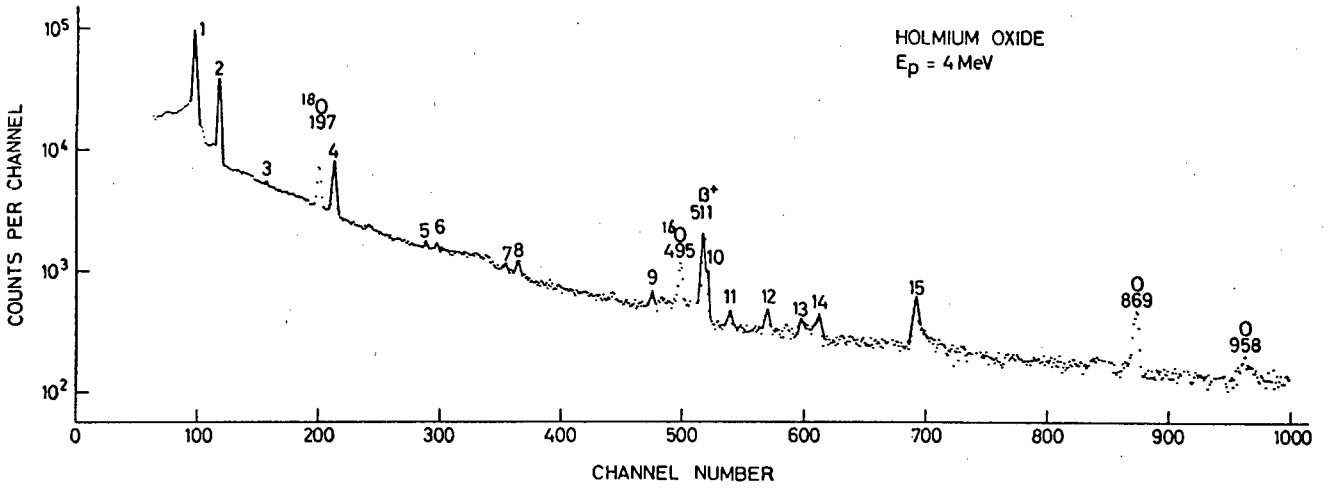

Peak	E_γ keV	Assignment
1	95	^{165}Ho p(1,0)
2	115	^{165}Ho p(2,1)
3	154	^{165}Ho p(5,3)
4	210	^{165}Ho p(2,0)
5	289	^{165}Ho p(5,2)
6	296	^{165}Ho n(6,0)
7	357	^{165}Ho n(8,0)
8	361	^{165}Ho p(4,0)
9	472	^{165}Ho p(7,1)
10	516	^{165}Ho p(6,0)
11	535	^{165}Ho n(13,0)
12	567	^{165}Ho p(7,0)
13	594	^{165}Ho p(10,2)
14	608	^{165}Ho n(15,0)
15	689	^{165}Ho p(10,0)

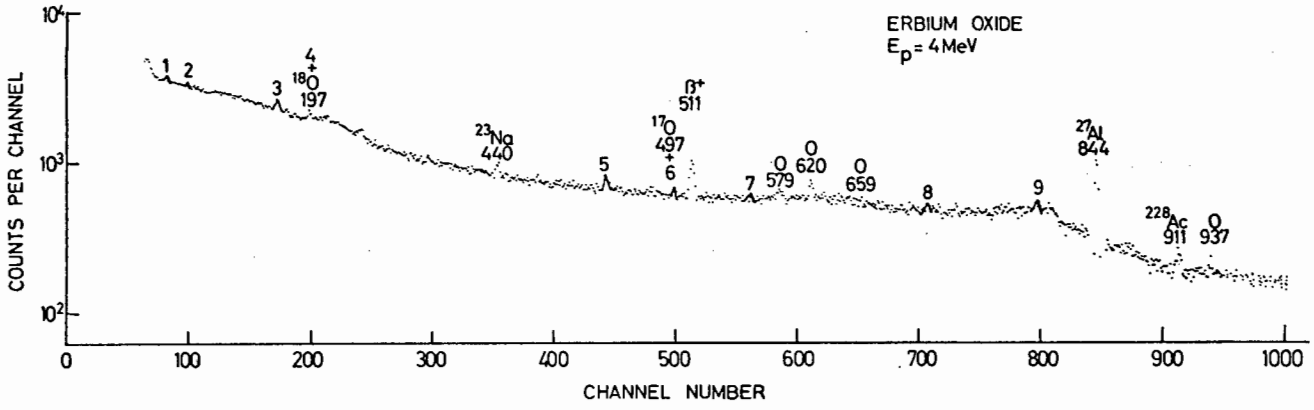

Peak	E_γ keV	Assignment
1	78	^{164}Er n(3,0)
	79	^{170}Er p(1,0)
	79	^{167}Er p(1,0)
	80	^{168}Er p(1,0)
	81	^{166}Er p(1,0)
2	90	^{164}Er p(1,0)
3	178	^{167}Er p(2,0)
	178	^{162}Er n(5,0)
4	200	^{164}Er p(2,1)
5	495	^{167}Er p(6,1)
6	532	^{167}Er p(5,0)
7	562	^{167}Er p(7,1)
8	705	^{166}Er p(4,1)
9	786	^{166}Er p(4,0)

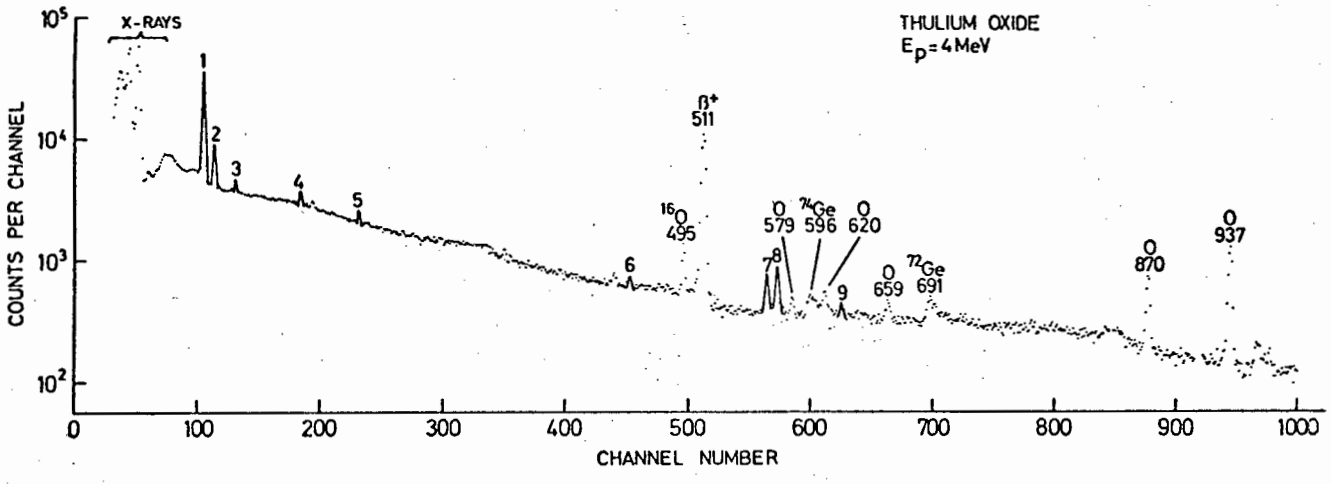

Peak	E_γ keV	Assignment
1	110	^{169}Tm p(2,1)
2	118	^{169}Tm p(2,0)
3	130	^{169}Tm p(3,2)
4	193	^{169}Tm p(4,3)
5	228	^{169}Tm p(5,2)
6	453	^{169}Tm p(6,2)
7	563	^{169}Tm p(6,1)
8	571	^{169}Tm p(6,0)
9	625	^{169}Tm p(7,1)

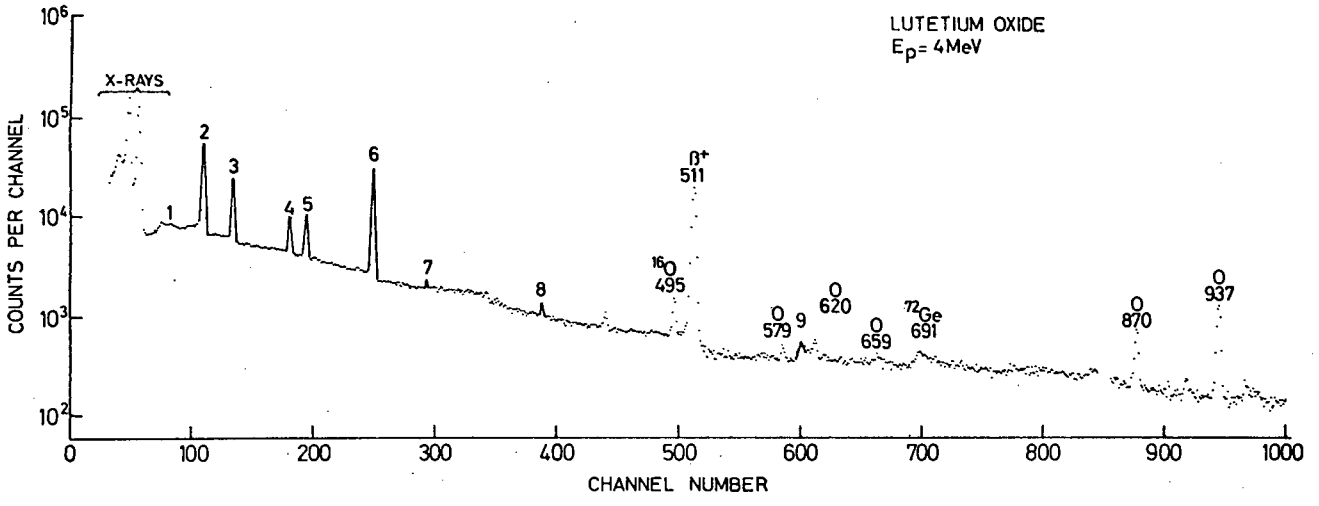

Peak	Eγ keV	Assignment
1	82	^{175}Lu n(1,0)
	82	^{176}Lu p(1,0)
2	114	^{175}Lu p(1,0)
3	138	^{175}Lu p(2,1)
4	186	^{175}Lu n(3,0)
5	190	^{176}Lu p(2,1)
6	252	^{175}Lu p(2,0)
7	293	^{176}Lu p(3,2)
8	390	^{176}Lu p(4,2)
9	597	^{175}Lu p(4,0)

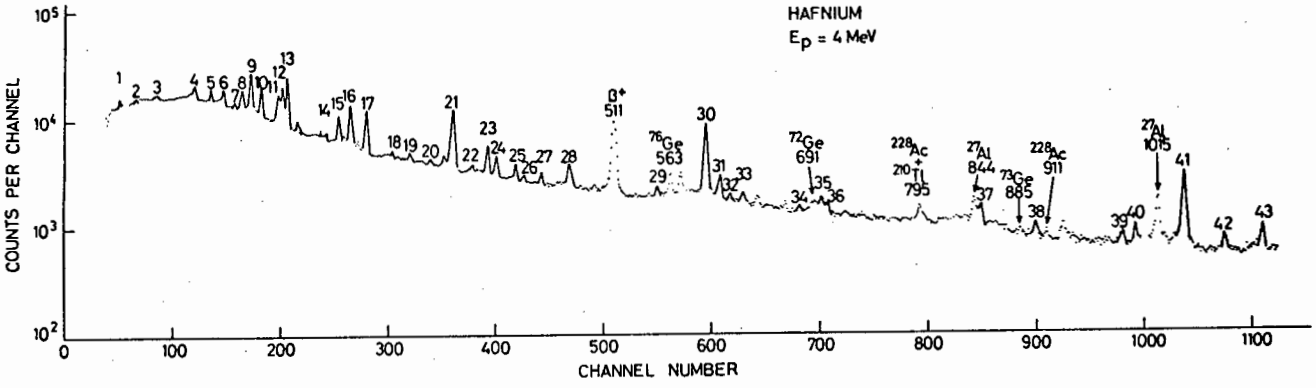

Peak	Eγ keV	Assignment	Peak	Eγ keV	Assignment	Peak	Eγ keV	Assignment
1	51	^{174}Hf γ(2,0)	10	181	^{178}Hf γ(3,0)	22	375	^{179}Hf p(5,0)
2	66	Hf k_β		181	^{179}Hf n(3,0)	23	390	^{177}Hf p(5,0)
	69	^{174}Hf γ(3,0)	11	202	^{176}Hf p(2,1)	24	401	
	71	^{176}Hf γ(1,0)		203	^{180}Hf γ(5,2)	25	421	^{179}Hf p(6,0)
	71	^{177}Hf n(1,0)	12	207	^{174}Hf p(2,1)	26	426	^{178}Hf p(4,3)
3	87	^{174}Hf γ(4,1)		208	^{177}Hf p(3,1)		427	^{177}Hf p(7,0)
	88	^{176}Hf p(1,0)		210	^{178}Hf γ(6,2)	27	445	
	91	^{174}Hf p(1,0)	13	215	^{180}Hf p(2,1)	28	520	
	93	^{178}Hf p(1,0)	14	237	^{178}Hf γ(4,0)	29	548	^{180}Hf p(3,1)
	93	^{180}Hf p(1,0)		237	^{179}Hf n(4,0)	30	597	^{176}Hf p(3,0)
4	123	^{179}Hf p(1,0)	15	249	^{177}Hf p(2,0)	31	608	^{174}Hf p(3,0)
	124	^{174}Hf γ(1,0)	16	269	^{179}Hf p(3,0)	32	615	^{180}Hf γ(9,0)
5	131	^{177}Hf n(3,0)	17	277	^{177}Hf p(5,1)	33	632	^{178}Hf p(3,0)
	131	^{176}Hf γ(3,0)	18	301	^{180}Hf γ(4,0)	34	680	^{179}Hf p(15,0)
	133	^{179}Hf n(2,0)		306	^{178}Hf p(2,0)	35	701	^{179}Hf p(16,0)
	134	^{178}Hf γ(2,0)	19	321	^{177}Hf p(3,0)	36	708	^{176}Hf p(4,2)
	136	^{180}Hf γ(2,0)	20	338	^{180}Hf p(3,2)	37	849	^{180}Hf p(6,2)
	137	^{177}Hf p(2,1)		339	^{180}Hf γ(5,0)	38	892	^{180}Hf p(9,2)
6	146	^{179}Hf p(3,1)		344	^{179}Hf n(6,0)	39	983	^{180}Hf p(11,2)
7	159	^{180}Hf γ(3,0)		344	^{178}Hf γ(6,0)	40	991	^{180}Hf p(4,1)
8	165	^{180}Hf γ(4,2)	21	356	^{178}Hf γ(7,0)	41	1046	^{180}Hf p(5,1)
9	172	^{176}Hf γ(4,0)		356	^{179}Hf n(7,0)	42	1090	^{180}Hf p(7,1)
	172	^{177}Hf n(4,0)				43	1107	^{180}Hf p(9,1)

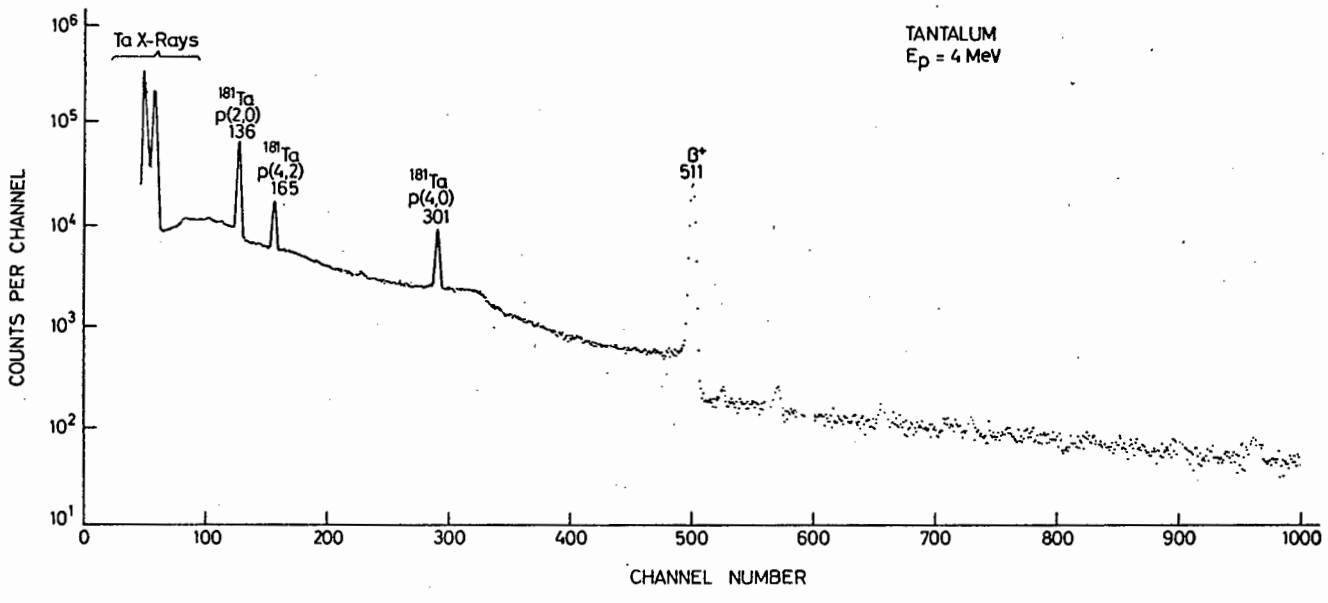
Ta X-Rays
181Ta p(2,0) 136
181Ta p(4,2) 165
181Ta p(4,0) 301
β+ 511
TANTALUM
Ep = 4 MeV
COUNTS PER CHANNEL
CHANNEL NUMBER
10^6
10^5
10^4
10^3
10^2
10^1
0
100
200
300
400
500
600
700
800
900
1000

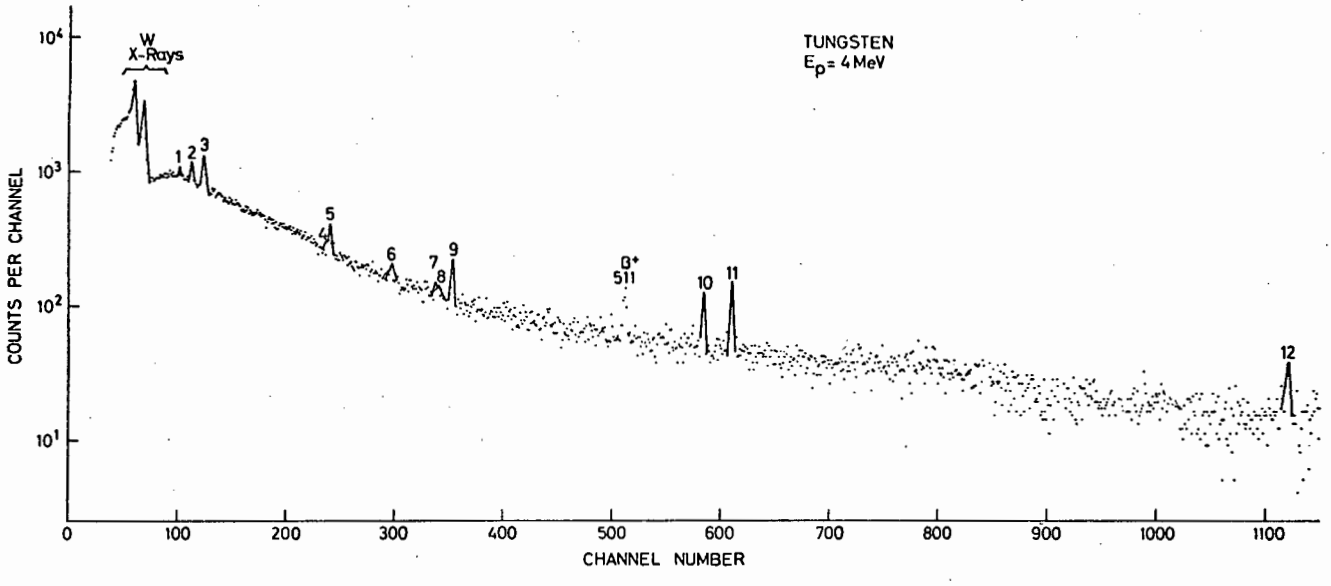

Peak	Eγ keV	Assignment
1	99	^{183}W p(2,0)
	100	^{182}W p(1,0)
	104	^{180}W p(1,0)
2	111	^{184}W p(1,0)
3	122	^{186}W p(1,0)
4	234	^{180}W p(2,1)
5	236	^{184}W n(6,0)
6	292	^{183}W p(4,0)
7	338	^{180}W p(2,0)
8	341	^{186}W p(3,2)
9	351	^{182}W p(3,2)
10	585	^{180}W p(3,1)
11	615	^{186}W p(3,1)
12	1121	^{182}W p(4,1)

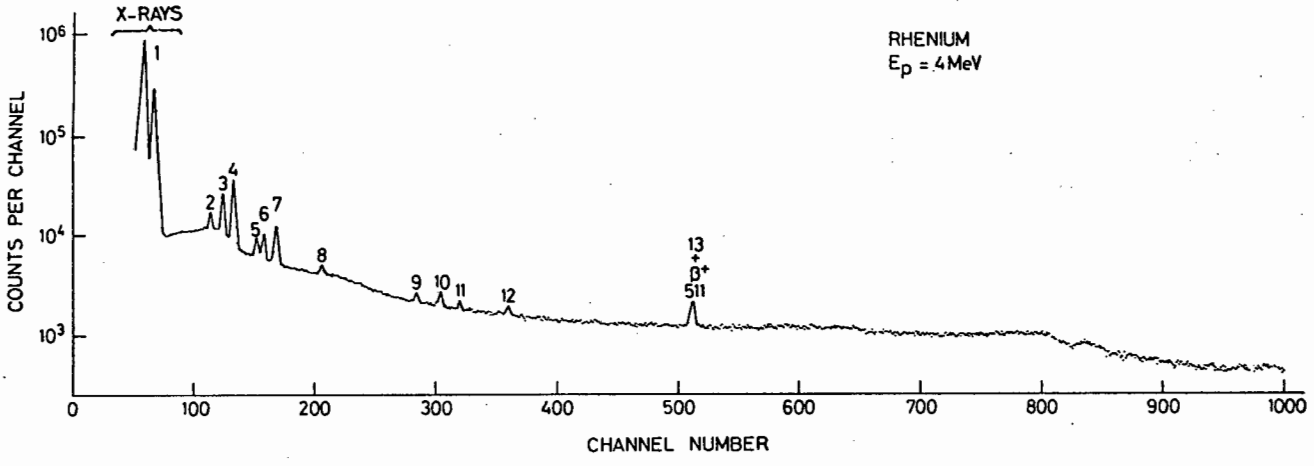

Peak	Eγ keV	Assignment
1	70	Re kβ
	72	^{187}Re p(2,1)
2	116	^{187}Re n(5,0)
3	125	^{185}Re p(1,0)
4	134	^{187}Re p(1,0)
	137	^{185}Re γ(1,0)
5	155	^{187}Re γ(1,0)
	157	^{187}Re n(4,3)
6	159	^{185}Re p(2,1)
7	167	^{187}Re p(3,1)
8	206	^{187}Re p(2,0)
9	285	^{185}Re p(2,0)
10	301	^{187}Re p(3,0)
11	323	^{187}Re γ(2,1)
12	359	^{187}Re n(8,3)
13	512	^{187}Re p(6,0)

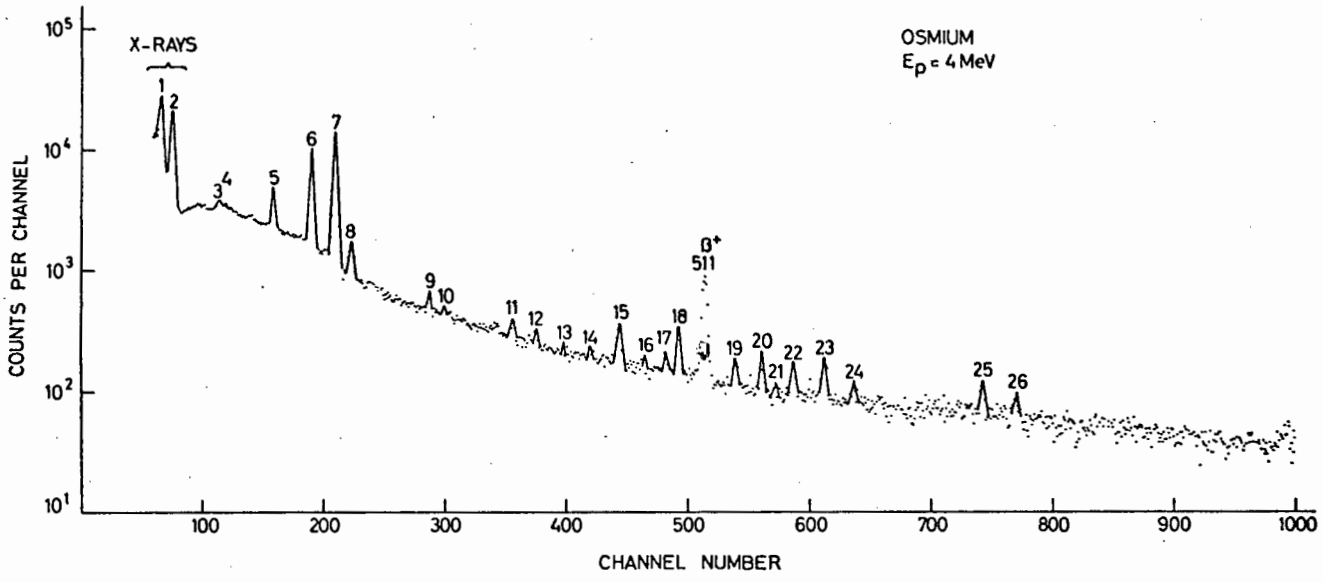

Peak	keV	Assignment
1	65	Os kα
	65	^{187}Os p(2,1)
2	70	^{189}Os p(2,0)
	72	^{189}Os n(6,4)
	73	^{187}Os p(2,0)
	74	Os k_β
3	112	^{187}Os p(5,1)
	114	^{189}Os n(2,0)
4	120	^{184}Os p(1,0)
5	155	^{188}Os p(1,0)
	157	^{187}Os p(8,4)
6	187	^{189}Os n(4,2)
	187	^{188}Os γ(4,2)
	187	^{190}Os p(1,0)
	187	^{187}Os n(3,0)
	187	^{186}Os γ(3,0)
	187	^{187}Os p(6,0)
	188	^{188}Os n(3,0)
	188	^{187}Os γ(3,0)
	189	^{187}Os p(7,0)
	189	^{189}Os p(4,1)
7	206	^{192}Os p(1,0)
8	219	^{189}Os p(4,0)
	223	^{189}Os n(5,1)
9	281	^{188}Os n(5,0)
	281	^{187}Os γ(5,0)
	283	^{192}Os p(2,1)
10	297	^{186}Os p(2,1)
11	354	^{186}Os p(12,7)
12	375	^{192}Os p(3,1)
13	396	^{190}Os p(5,3)
14	420	^{192}Os p(5,2)
15	435	^{186}Os p(4,2)
16	462	^{188}Os p(4,2)
17	478	^{188}Os p(3,1)
18	487	^{188}Os p(5,2)
	487	^{188}Os n(7,0)
	487	^{187}Os γ(7,0)
	489	^{192}Os p(2,0)
	490	^{186}Os p(11,6)
	491	^{187}Os p(8,1)
19	530	^{187}Os n(13,5)
	530	^{186}Os γ(13,5)
20	557	^{186}Os p(12,6)
	558	^{190}Os p(3,0)
21	568	^{190}Os p(4,1)
	569	^{192}Os p(12,8)
22	580	^{192}Os p(6,2)
23	608	^{189}Os n(11,1)
	608	^{188}Os γ(11,1)
24	630	^{186}Os p(3,1)
	633	^{188}Os p(3,0)
25	743	
26	767	^{190}Os p(5,1)
	767	^{186}Os p(3,0)

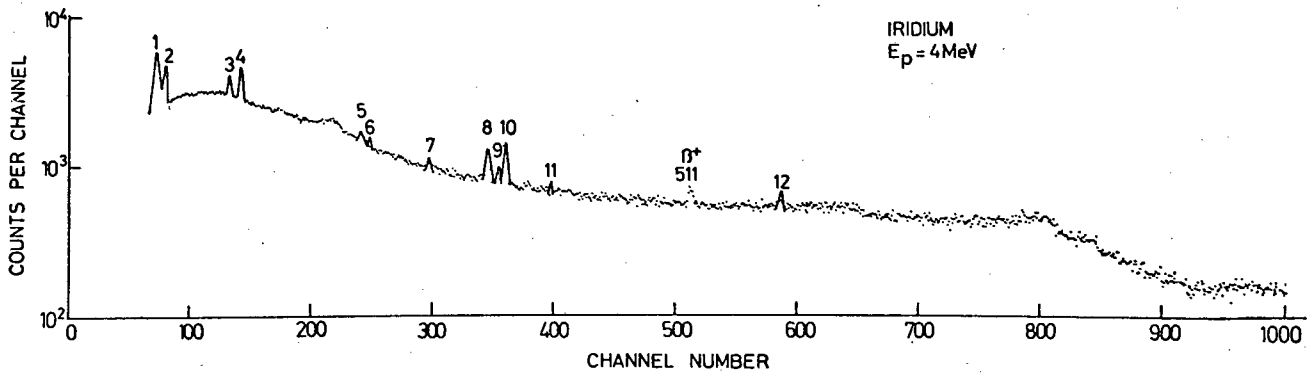

Peak	Eγ keV	Assignment
1	67	^{193}Ir p(3,1)
2	73	^{193}Ir p(1,0)
3	129	^{191}Ir p(2,0)
4	139	^{193}Ir p(3,0)
5	214	^{191}Ir p(4,2)
6	219	^{193}Ir p(5,2)
7	299	^{193}Ir p(5,0)
8	343	^{191}Ir p(5,0)
9	351	^{191}Ir p(6,0)
10	358	^{193}Ir p(6,0)
11	391	^{191}Ir p(7,0)
12	588	^{191}Ir p(9,0)

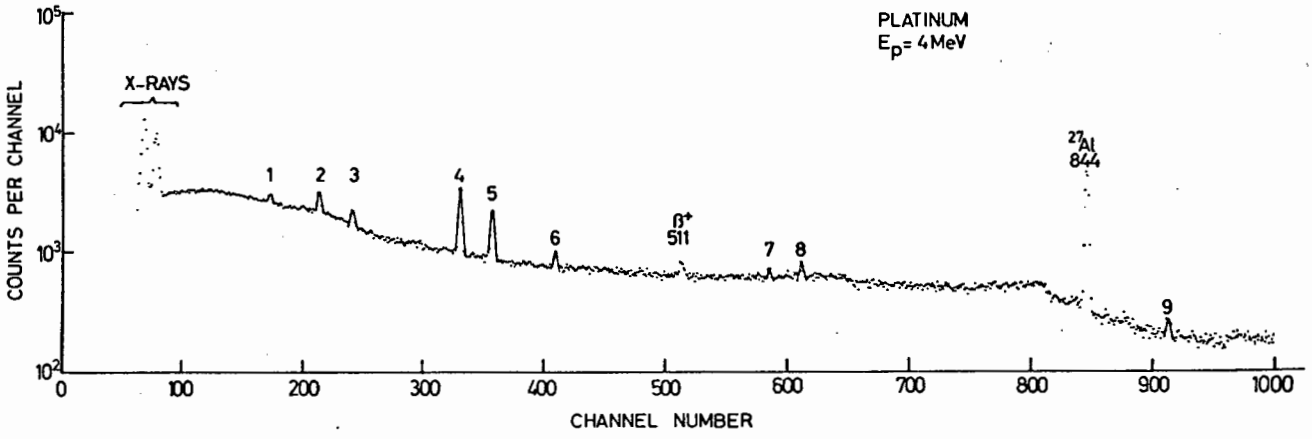

Peak	Eγ keV	Assignment
1	173	^{192}Pt p(3,2)
2	211	^{195}Pt p(4,0)
3	239	^{195}Pt p(5,0)
4	329	^{194}Pt p(1,0)
5	356	^{196}Pt p(1,0)
6	407	^{198}Pt p(1,0)
7	587	^{192}Pt p(5,2)
8	608	^{194}Pt p(5,2)
	612	^{192}Pt p(2,0)
9	908	^{196}Pt p(6,1)

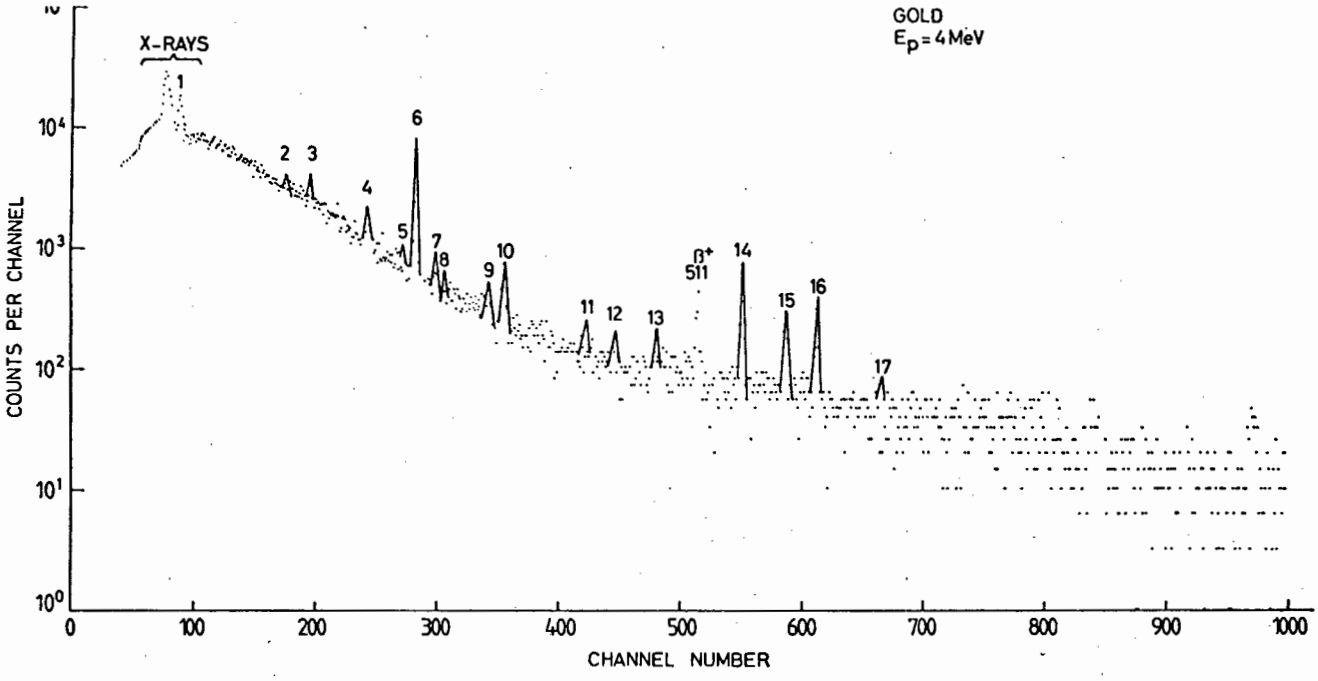

Peak	Eγ keV	Assignment
1	77	^{197}Au p(1,0)
	78	Au k_β
2	174	^{197}Au n(4,1)
3	193	^{197}Au p(2,1)
4	249	^{197}Au n(3,0)
5	269	^{197}Au p(6,3)
	269	^{197}Au p(2,0)
6	279	^{197}Au p(6,2)
	279	^{197}Au p(3,0)
7	299	^{197}Au n(4,0)
8	308	^{197}Au n(5,0)
9	341	^{197}Au n(7,1)
10	354	^{197}Au n(11,2)
11	426	^{197}Au n(9,5)
12	444	^{197}Au n(9,2)
13	475	^{197}Au n(7,0)
14	548	^{197}Au p(6,0)
15	585	^{197}Au n(10,0)
16	619	^{197}Au p(7,2)
17	667	^{197}Au p(8,2)

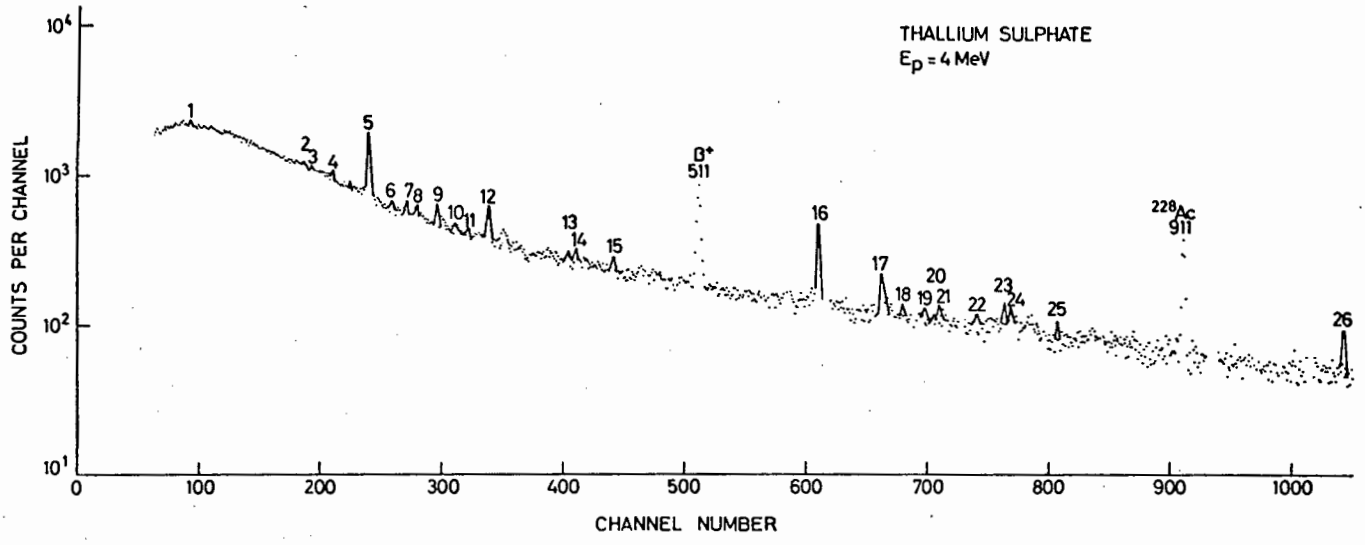

Peak	Eγ keV	Assignment
1	89	^{203}Tl γ(9,8)
2	185	^{205}Tl n(5,3)
	187	^{203}Tl n(2,0)
3	209	^{203}Tl γ(4,3)
4	225	^{203}Tl n(4,3)
5	236	^{205}Tl γ(6,4)
6	261	^{205}Tl n(2,1)
7	272	^{203}Tl n(6,3)
8	279	^{203}Tl p(1,0)
9	296	^{205}Tl n(8,4)
10	308	^{203}Tl γ(5,2)
11	317	^{205}Tl γ(7,4)
12	338	^{203}Tl n(8,3)
13	401	^{203}Tl p(2,1)
14	409	^{203}Tl n(3,2)

Peak	Eγ keV	Assignment
15	441	^{205}Tl n(4,2)
16	619	^{205}Tl p(2,0)
17	663	^{203}Tl γ(4,1)
	663	^{205}Tl γ(4,1)
18	680	^{203}Tl n(6,2)
	681	^{203}Tl p(2,0)
19	699	^{203}Tl n(5,1)
20	710	^{203}Tl n(7,2)
21	740	^{203}Tl n(6,1)
22	761	^{205}Tl n(4,0)
23	765	^{203}Tl p(3,1)
24	770	^{203}Tl n(7,1)
25	803	^{205}Tl γ(1,0)
26	1663	^{203}Tl γ(7,0)

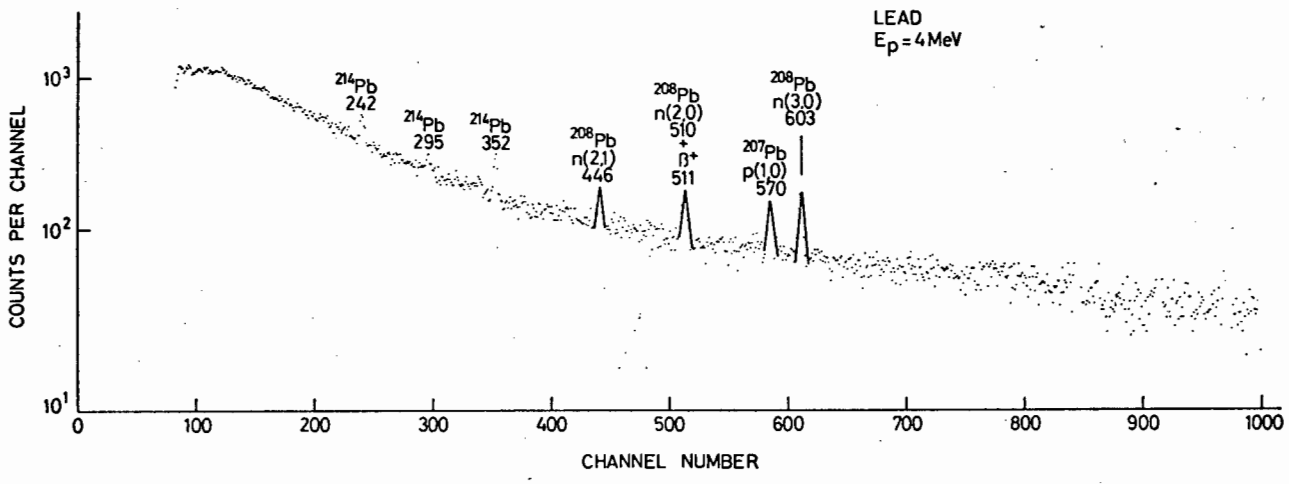
LEAD
$E_p = 4$ MeV
^{214}Pb 242
^{214}Pb 295
^{214}Pb 352
^{208}Pb n(2,1) 446
^{208}Pb n(2,0) 510 + β^+ 511
^{207}Pb p(1,0) 570
^{208}Pb n(3,0) 603
COUNTS PER CHANNEL
10^3
10^2
10^1
0
100
200
300
400
500
600
700
800
900
1000
CHANNEL NUMBER

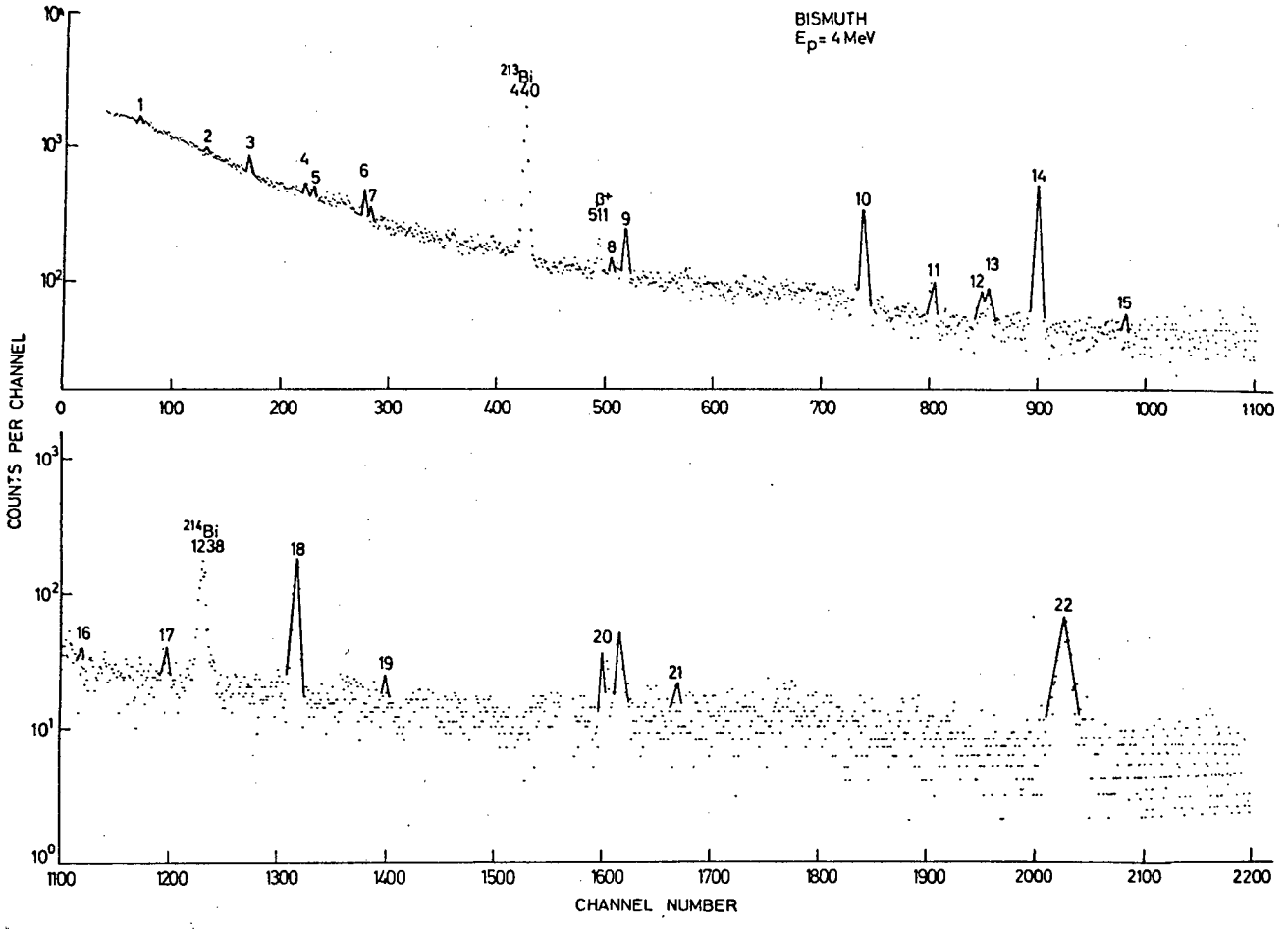

Peak	E_γ keV	Assignment
1	80	^{209}Bi γ(4,3)
	82	^{209}Bi n(6,5)
2	146	^{209}Bi n(8,5)
3	195	^{209}Bi n(9,5)
	195	^{209}Bi n(6,4)
4	242	^{209}Bi n(7,3)
5	246	^{209}Bi γ(2,1)
6	292	^{209}Bi γ(3,1)
7	297	^{209}Bi n(8,3)
8	520	^{209}Bi n(12,7)
9	545	^{209}Bi n(1,0)
10	753	^{209}Bi γ(5,2)
11	816	^{209}Bi n(13,3)
12	863	^{209}Bi n(6,1)
13	873	^{209}Bi n(7,1)
14	896	^{209}Bi p(1,0)
15	992	^{209}Bi p(6,2)
16	1139	^{209}Bi γ(7,1)
17	1213	^{209}Bi n(4,0)
18	1327	^{209}Bi n(5,0)
19	1418	^{209}Bi n(7,0)
20	1609	^{209}Bi p(2,0)
21	1687	^{209}Bi p(5,1)
22	2061	^{209}Bi n(15,0)

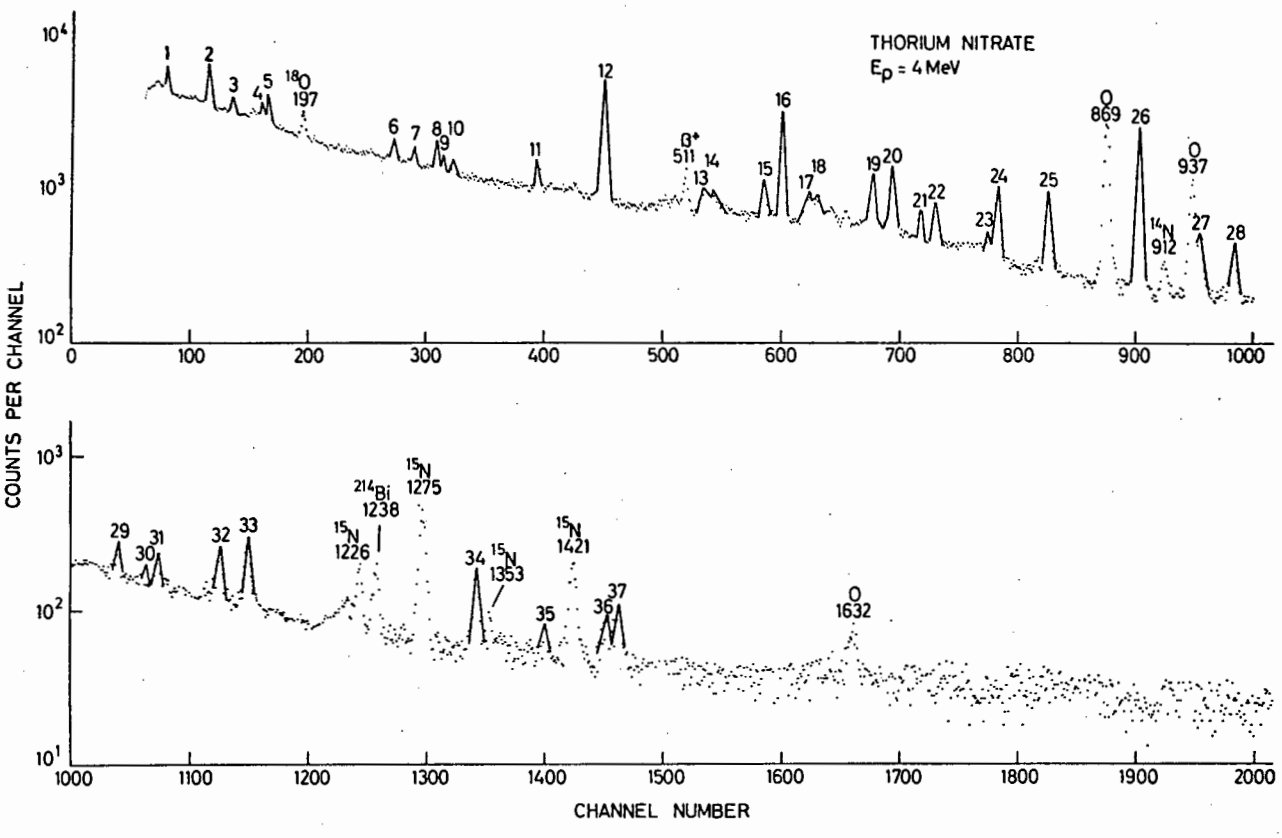

Peak	Eγ keV	Assignment	Peak	Eγ keV	Assignment
1	64	^{232}Th γ(3,1)	20	681	^{232}Th p(5,1)
2	113	^{232}Th p(2,1)	21	714	^{232}Th p(4,0)
3	131	^{232}Th γ(12,3)	22	725	^{232}Th p(6,1)
4	163	^{232}Th γ(8,0)	23	774	^{232}Th p(6,0)
5	169	^{232}Th γ(9,0)	24	780	^{232}Th p(8,0)
6	273	^{232}Th γ(16,0)	25	824	^{232}Th p(9,1)
7	290	^{232}Th γ(17,0)	26	890	^{232}Th p(12,0)
8	304	^{232}Th γ(20,0)	27	973	^{232}Th p(13,2)
9	310	^{232}Th γ(23,2)	28	981	^{232}Th p(19,2)
10	320	^{232}Th γ(24,4)	29	1029	^{232}Th p(15,1)
11	380	^{232}Th γ(27,3)	30	1056	^{232}Th p(20,1)
12	447	^{232}Th γ(26,0)	31	1076	^{232}Th p(18,1)
13	519	^{232}Th γ(30,1)	32	1122	^{232}Th p(18,0)
14	529	^{232}Th γ(31,0)	33	1143	^{232}Th p(21,0)
15	569	^{232}Th γ(34,0)	34	1338	^{232}Th p(26,1)
16	586	^{232}Th γ(36,0)	35	1392	^{232}Th p(32,2)
17	612	^{232}Th p(6,2)	36	1440	^{232}Th p(30,1)
18	627	^{232}Th p(12,3)	37	1448	^{232}Th p(37,2)
19	665	^{232}Th p(4,1)			

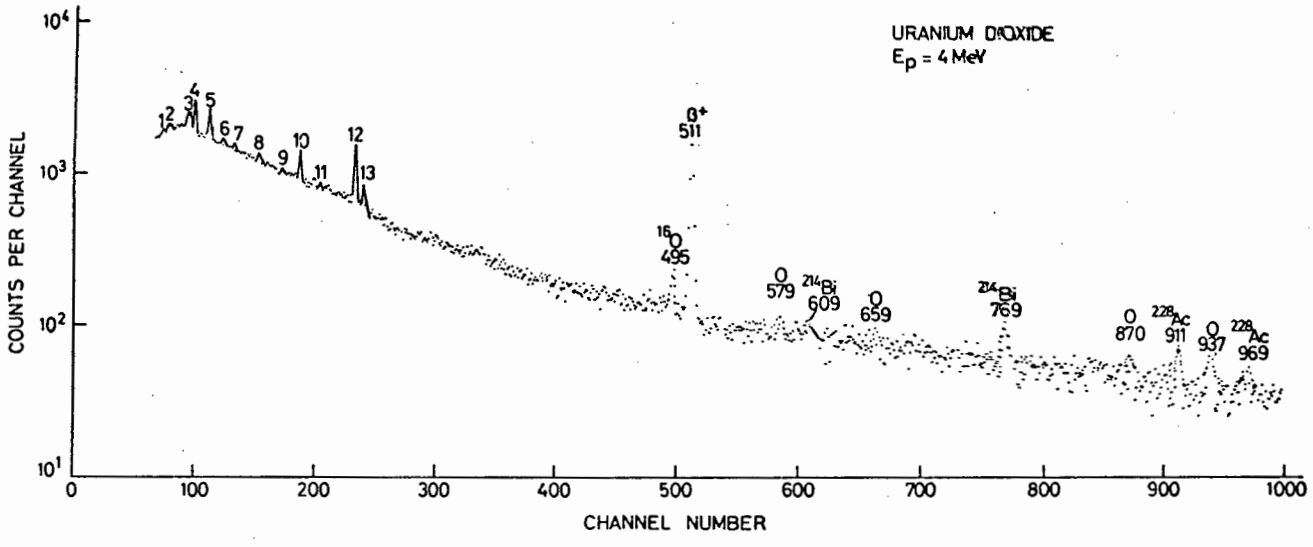

Peak	Eγ keV	Assignment
1	68	^{235}U n(7,6)
	68	^{234}U γ(7,6)
2	79	^{235}U n(3,0)
	79	^{234}U γ(3,0)
3	92	^{235}U n(4,0)
	92	^{234}U γ(4,0)
4	98	^{235}U n(6,2)
	98	^{234}U γ(6,2)
	98	U kα
	99	^{235}U n(5,1)
	99	^{234}U γ(5,1)
5	109	^{235}U n(7,4)
	109	^{234}U γ(7,4)
6	113	^{235}U n(6,1)
	113	^{234}U γ(6,1)
	113	U k_β

Peak	Eγ keV	Assignment
7	122	^{235}U n(7,3)
	122	^{234}U γ(7,3)
8	133	^{235}U n(5,0)
	133	^{234}U γ(5,0)
	152	^{235}U n(7,2)
	152	^{234}U γ(7,2)
9	167	^{235}U n(7,1)
	167	^{234}U γ(7,1)
10	189	^{235}U p(25,13)
11	201	^{235}U n(6,0)
	201	^{234}U γ(6,0)
12	232	
13	241	^{238}U γ(9,0)

A P P E N D I X II

CATALOGUE OF ALL OBSERVED GAMMA-RAYS

ARRANGED IN ORDER OF INCREASING ENERGY

Eγ keV	Assignment	Yield. quanta $sr^{-1}nC^{-1}$	Sensitivity $\mu g.g^{-1}mC^{-1}$
46,1	Ge-76 n(1,0)	290	5500
51,4	Hf-174 g(2,0)	140	54600
52,8	Ni-61 a(1,0)	6,3	93000
53,2	Pb-214 4n + 2	r.a.	
53,9	Cu-65 n(1,0)	5	76000
	Cr-53 g(1,0)		
54,7	Cr-54 n(1,0)	380	4800
55,0	Cu-63 n(2,1)	5	76000
56,0	Hf k_α x-ray		
56,8	Tb-159 n(1,0)	26	22600
57,0	Ta k_α x-ray		
57,9	Tb-159 p(1,0)	26	22600
58,6	Ni-61 a(3,2)	7,4	69000
59,0	W k_α x-ray		
61,1	Re k_α x-ray		
63,0	Hf k_β x-ray	290	4050
63,0	Os k_α x-ray	3360	2490
63,9	Th-232 g(3,1)	180	6300
64,6	Os-187 p(2,1)	3300	240
65,0	Gd-155 n(1,0)	25	21700
65,4	Sb-123 n(5,3)	15	12200
65,6	Sb-121 p(3,2)	15	12200
66,0	Ta k_β x-ray		
66,0	Pt k_α x-ray		
66,8	Ir-193 p(3,1)	5400	110
67,0	W k_β x-ray		
68,0	U -235 n(7,4)	4,7	53200
	U -234 g(7,4)		
68,2	Sm-147 n(1,0)	50	8300
68,9	Hf-174 g(3,0)	290	4050

Eγ keV	Assignment	Yield. quanta $sr^{-1}nC^{-1}$	Sensitivity $\mu g.g^{-1}mC^{-1}$
69,0	Au k_α x-ray		
69,3	Re k_β x-ray	1630	460
69,5	Os-189 p(2,0)	3020	460
70,0	Hg k_α x-ray		
	Hf-176 g(1,0)		
70,9	Hf-177 n(1,0)	290	4050
71,7	Os-189 n(6,4)	3020	460
72,0	Os k_β x-ray	3020	460
72,0	Re-187 p(2,1)	1630	880
73,0	Ir-193 p (1,0)	1760	330
73,4	Dy-164 p(1,0)	100	4300
74,0	Bi-208;Pb-212	r.a.	
74,3	Os-187 p(2,0)	3020	460
75,0	Pt k_β x-ray		
77,3	Au-197 p(1,0)	4300	180
78,0	Au k_β x-ray	4300	180
78,3	Er-164 n(3,0)	11	28900
79,0	U -235 n(3,0)	7,5	44900
	U -234 g(3,0)		
79,0	Er-170 p(1,0)	11	28900
79,1	Pd-108 n(2,0)	17	54300
79,3	Er-167 p(1,0)	11	28900
79,5	Tb-159 p(2,1)	220	2700
79,8	Er-168 p(1,0)	11	28900
79,9	Tb-159 n(1,0)	220	2700
80,0	Bi-209 g(4,3)	3,2	101000
80,1	Hg k_β x-ray	470	620
80,6	Er-166 p(1,0)	11	28900
82,0	Bi-209 n(6,5)	3,2	101000
82,1	Hg-200 p(3,2)	420	620

Eγ keV	Assignment	Yield. quanta $sr^{-1}nC^{-1}$	Sensitivity $\mu g.g^{-1}mC^{-1}$
82,2	Lu-175 n(1,0)	4	98500
82,2	Lu-175 p(1,0)	4	98500
83,4	Eu-153 p(1,0)	480	1100
86,0	Bi-208;Pb-212	r.a.	
86,8	Ge-76 n(2,0)	23	21800
86,8	Ga-69 n(1,0)	230	2300
87,3	Hf-174 g(4,1)	420	3300
87,5	Ti-47 n(1,0)	2890	420
	Ti-46 g(1,0)		
88,4	Hf-176 p(1,0)	420	3300
89,3	Tl-203 g(9,3)	37	10900
89,4	Ru-99 p(1,0)	25	15400
90,0	Er-164 p(1,0)	2,4	75800
90,0	Ti-49 n(1,0)	2890	420
	Ti-48 g(1,0)		
91,0	Hf-174 p(1,0)	420	3300
	U -234 g(4,0)		
91,6	U -235 n(4,0)	85	4800
91,9	Mn-55 n(4,3)	3400	7800
92,0	Zr-92 n(2,1)	200	2000
92,2	Ac-228	r.a.	
92,9	Nb-93 g(6,5)	1,6	95800
93,0	Hf-178 p(1,0)	420	3300
93,0	Hf-180 p(1,0)	420	3300
93,0	Ag-107 p(1,0)	17	14500
93,1	Pd-106 g(1,0)	74	14100
93,1	Pd-110 g(1,0)	74	14100
93,2	Hf-178 p(1,0)	420	3300
93,9	Dy-163 p(2,1)	15	11300
94,1	Ti-50 n(2,1)	560	2200

Eγ keV	Assignment	Yield. quanta $sr^{-1}nC^{-1}$	Sensitivity $\mu g.g^{-1}mC^{-1}$
94,7	Ho-165 p(1,0)	115	4900
95,0	Dy-163 n(1,0)	15	11300
95,5	Cd-111 p(2,1)	8,3	7000
97,1	Ru-104 n(2,0)	20	19300
97,7	U -235 n(6,2)	140	2900
	U -234 g(6,2)		
98,0	Ti-48 n(4,2)	560	2200
98,2	Ag-107 p(3,2)	1,7	93300
98,3	U k_α x-ray	140	2900
98,8	U -235 n(5,1)	140	2900
98,8	U -234 g(5,1)	140	2900
98,8	W -183 p(2,0)	105	3200
100,1	W -182 p(1,0)	105	3200
102,0	Cd-106 p(4,2)	8,9	5300
102,0	Cd-106 p(4,2)	8,9	5300
103,6	W -180 p(1,0)	105	3200
104,1	Tb-159 p(3,2)	14	25800
104,5	Zr-91 n(1,0)	350	1100
105,0	Gd-155 p(3,2)	3,7	94600
108,0	Pr-141 g(4,2)	3,7	45600
108,8	Ge-76 p(6,5)	0,3	968000
109,0	U -235 n(7,4)	150	2400
	U -234 g(7,4)		
109,3	Te-125 p(2,1)	32	24100
109,8	O -18 g(1,0)	21	11700
109,8	Eu-151 p(3,0)	120	3500
109,8	Tm-169 p(2,1)	520	550
109,9	F -19 p(1,0)	84500	70
110,0	F -19 n,n'(1,0)		
110,2	Nb-93 n(3,2)	6,6	56300

E_γ keV	Assignment	Yield. quanta $sr^{-1}nC^{-1}$	Sensitivity $\mu g.g^{-1}mC^{-1}$
110,5	Eu-151 p(4,2)	120	3500
111,0	Br-79 n(6,4)	115	4700
111,0	W -184 p(1,0)	300	1300
111,4	Ni-61 a(3,0)	64	52000
	Fe-57 g(3,0)		
111,5	Fe-58 n(3,0)	5,6	90500
112,4	Os-187 p(5,1)	5,9	47000
112,5	As-75 n(1,0)	3200	270
	U -234 g(6,1)		
112,5	U -235 n(6,1)	150	2100
112,6	U k_β x-ray	150	2100
112,8	Th-232 p(2,1)	250	2800
113,0	Ga-71 g(8,6)	100	4400
113,0	Pd-109 p(1,0)	105	8300
113,6	Te-125 n(1,0)	32	24100
113,8	Os-189 n(2,0)	5,9	47000
113,8	Lu-175 p(1,0)	730	470
114,1	I -127 n(4,2)	2620	280
114,2	Dy-163 p(3,2)	30	5800
114,9	Sn-122 n(7,2)	3,4	18700
115,1	Cu-65 n(2,0)	6400	390
115,1	Ho-165 p(2,1)	220	2800
115,4	In-115 n(2,1)	150	2000
115,5	Re-187 n(5,0)	310	2310
115,9	Sn-115 p(2,1)	3,4	18700
116,2	La-138 p(2,1)	5,3	29100
118,2	Tm-169 p(2,0)	93	2500
118,7	Rh-103 n(1,0)	620	950
119,5	Ba-135 n(1,0)	11	62100
119,8	Os-184 p(1,0)	5,8	50400

Eγ keV	Assignment	Yield. quanta $sr^{-1}nC^{-1}$	Sensitivity $\mu g.g^{-1}mC^{-1}$
120,0	Ru-96 n(6,4)	2,8	26200
120,6	Ge-76 n(3,0)	0,3	880000
120,8	Tb-159 n(3,1)	19	17400
121,3	Sm-147 p(1,0)	380	790
121,2	Sn-122 n(3,0)	1,7	27600
121,5	Ca-48 n(2,0)	290	630
121,6	Tb-159 p(5,3)	19	17400
121,8	Sm-152 p(1,0)	380	790
121,8	U -235 n(7,3)	23	10400
	U -234 g(7,3)		
122,3	W -186 p(1,0)	480	700
122,5	Fe-57 p(2,1)	8,3	72400
122,7	Hf-179 p(1,0)	510	1850
123,0	Gd-154 p(1,0)	16	21900
123,4	Nb-93 g(7,5)	510	18590
123,7	Hf-174 g(4,0)	510	1850
124,7	I -127 n(1,0)	160	3900
125,4	Re-185 p(1,0)	1040	780
125,9	Mn-55 p(1,0)	5900	250
127,2	Ru-101 p(1,0)	50	9100
	Fe-56 g(3,2)		
127,6	Fe-57 n(3,2)	79	10200
129,0	Ru-104 n(3,0)	50	9100
129,0	Ac-228	r.a.	
129,4	Ir-191 p(2,0)	61	4900
129,6	Ru-104 g(1,0)	50	9100
130,0	Tm-119 p(3,2)	6,7	30400
130,0	Br-79 n(1,0)	420	2200
130,1	Nd-150 p(1,0)	110	1800
130,9	Ca-48 n(1,0)	310	590

Eγ keV	Assignment	Yield. quanta $sr^{-1}nC^{-1}$	Sensitivity $\mu g.g^{-1}mC^{-1}$
131,0	Hf-177 n(3,0) }	180	4620
	Hf-176 g(3,0) }		
131,0	Hf-157 p(2,0)	2,5	100100
131,0	Th-232 g(12,3)	27	18100
132,5	Se-74 g(1,0)	81	9300
132,8	Te-120 g(2,0)	43	18700
133,0	U -235 n(5,0) }	14	15400
	U -234 g(5,0) }		
133,2	As-75 n(2,0)	148	4100
133,8	Hf-179 n(2,0)	180	4620
	Hf-178 g(2,0)		
134,2	Re-187 p(1,0)	1200	440
134,7	Eu-151 n(5,0)	49	6300
136,0	As-75 p(5,2)	148	4100
136,2	Ta-181 p(2,0)	810	1020
136,3	Hf-180 g(2,0)	180	4620
136,4	Tb-159 n(2,0)	181	1800
136,8	Hf-177 p(2,1)	180	46200
137,2	Re-185 g(1,0)	1200	440
137,5	Tb-159 p(2,0)	181	1800
137,7	Lu-175 p(2,1)	290	1000
139,0	Ir-193 p(3,0)	115	2200
139,0	Mo-98 n(5,0)	13	20600
139,0	La-139 g(1,0)	3,4	37400
140,4	Mo-98 g(1,0)	13	20600
141,3	As-75 n(5,3)	1380	570
143,0	Ga-71 g(2,1)	330	1300
143,7	Ag-109 n(12,1)	1,9	84300
144,0	Br-79 n(4,2)	740	1300
145,0	Pr-141 p(1,0)	2,6	61000

Eγ keV	Assignment	Yield. quanta $sr^{-1}nC^{-1}$	Sensitivity $\mu g.g^{-1}mC^{-1}$
145,8	Bi-209 n(8,5)	52	5900
145,9	Ga-69 n(2,1)	330	1300
146,0	Gd-155 p(2,0)	13	29000
146,1	Hf-179 p(3,1)	740	1150
146,3	I -127 p(2,1)	1200	450
146,8	Ni-62 n(4,2)	1,3	217000
147,0	Br-79 n(2,0)	740	1300
147,5	Se-74 a(2,0)	12	51400
148,2	Rh-103 n(3,1)	150	3100
148,5	Se-77 n(4,0)	12	51400
148,5	Se-78 n(4,1)	12	51400
151,0	Zr-92 n(3,1)	120	2600
151,3	Ru-99 g(3,0)	2,0	45700
151,4	Rb-85 p(1,0)	71	2600
151,9	U -235 n(7,2)	25	7500
	U -234 g(7,2)		
152,0	Ti-46 g(2,0)	475	1200
152,0	Ti-49 n(2,0)	475	1200
	Ti-48 g(2,0)		
153,0	Cu-63 n(3,1)	4800	580
154,0	Cr-52 a(2,0)	540	2600
154,2	Ho-165 p(5,3)	690	700
155,1	Os-188 p(1,0)	65	4600
155,1	Re-187 g(1,0)	180	2350
155,4	Ba-132 n(1,0)	6,6	75600
156,3	Cr-54 n(2,0)	540	2600
	Cr-53 g(2,0)		
156,7	Os-187 p(8,4)	65	4600
156,9	Re-187 n(4,3)	180	2350
158,2	Se-77 a(1,0)	15	39200

Eγ keV	Assignment	Yield. quanta $sr^{-1}nC^{-1}$	Sensitivity $\mu g.g^{-1}mC^{-1}$
158,4	Hg-199 p(1,0)	20	9800
158,7	Sn-117 p(1,0)	5,3	9400
158,7	Hf-180 g(3,0)	260	6700
159,0	Sb-123 n(1,0)	220	4500
159,0	Re-185 p(2,1)	205	1960
159,3	Ni-64 n(1,0)	130	2800
159,4	Ti-47 p(1,0)	2110	350
160,0	Ti-49 p(2,1)	2110	350
160,2	Sn-122 g(1,0)	5,3	9400
160,2	Sb-123 p(1,0)	220	4500
160,9	Cs-133 p(2,0)	65	6600
161,0	Br-79 n(4,1)	120	4000
161,8	Se-77 p(1,0)	67	9700
162,9	Zr-90 n(3,1)	160	1700
163,3	Th-232 g(8,0)	600	1100
164,0	Zr-96 p(2,1)	160	1700
165,0	Zr-92 n(5,2)	160	1700
165,1	Ta-181 p(4,2)	110	6300
165,2	Hf-180 g(4,2)	320	5300
166,0	Ge-76 n(4,0)	8	400000
166,7	U -235 n(7,1) U -234 g(7,1)	22	10200
166,8	Re-187 p(3,1)	360	1180
167,0	Sn-122 n(6,0)	20	17900
167,3	Dy-163 p(2,0)	330	1640
168,8	Dy-164 p(2,1)	330	1640
169,2	Th-232 g(9,0)	160	3400
169,5	Ba-130 g(3,1)	18	24900
169,5	Se-76 a(4,2)	63	10000

Eγ keV	Assignment	Yield. quanta $sr^{-1}nC^{-1}$	Sensitivity $\mu g.g^{-1}mC^{-1}$
169,5	Zn-67 n(1,0)	290	3500
170,8	Al-27 p(2,1)	660	1760
	Hf-176 g(4,0)		
172,2	Hf-177 n(4,0)	1520	490
172,5	I -127 n(2,1)	300	1200
172,5	I -127 p(3,2)	300	1200
172,6	Te-125 p(7,5)	62	11700
173,0	Pt-192 p(3,2)	53	10800
173,8	Au-197 n(4,1)	25	6900
174,7	Eu-151 p(2,1)	38	9400
	Zn-67 g(1,0)		
174,9	Zn-68 n(1,0)	1210	1200
176,1	Ga-69 g(2,1)	2250	140
176,3	Te-125 p(3,0)	62	11700
176,8	Yb-174 p(2,1)	11	16300
176,8	Ba-138 n(6,2)	11	41300
178,0	Er-167 n(5,0)	32	20600
180,0	Zr-96 n(2,0)	32	7500
180,0	Ru-104 n(4,0)	74	5200
180,9	Hf-179 n(3,0)	2100	380
	Hf-178 g(3,0)		
181,0	Mo-98 g(3,0)	180	2400
181,8	Ru-101 n(2,0)	74	5200
	Ru-100 g(2,0)		
182,1	Ba-132 n(2,0)	8,6	52000
182,3	U -238 n(6,0)		
183,0	Br-79 n(3,0)	1020	760
184,6	Ni-64 n(3,1)	1,3	212000
184,6	Zn-67 p(2,0)	110	10300
185,0	Dy-162 p(2,1)	13	11500

Eγ keV	Assignment	Yield. quanta $sr^{-1}nC^{-1}$	Sensitivity $\mu g.g^{-1}mC^{-1}$
185,2	Tl-205 n(5,3)	19	19500
185,8	Lu-175 n(3,0)	105	2400
186,0	Ra-226	r.a.	
186,2	Os-187 n(3,0)	160	2000
186,7	Os-189 n(4,2)	160	2000
186,7	Tl-205 n(5,3)	19	19500
186,7	Os-190 p(1,0)	160	2000
187,0	Os-187 p(6,0)	160	2000
187,5	Os-187 p(7,0)	160	2000
187,6	Os-188 n(3,0)	160	2000
188,6	Os-189 p(4,1)	160	2000
189,0	Pd-109 p(2,0)	215	6900
189,0	U -235 p(25,13)	70	5100
189,2	As-75 p(6,3)	32	14600
189,6	Lu-176 p(2,1)	110	2100
190,1	Br-81 n(1,0)	1040	760
191,3	Pd-110 n(2,0)	215	6900
191,3	Au-197 p(2,1)	36	4700
192,8	Zn-64 g(1,0)	100	12400
192,8	Pd-108 n(4,0)	215	6900
194,0	Sn-122 n(9,1)	10	34100
193,0	Tm-169 p(4,3)	7,6	28900
193,7	Pr-141 n(1,0)	4,8	34200
194,0	Cu-63 n(1,0)	290	4800
194,5	Pd-106 g(1,0)	17	65100
195,0	Bi-209 n(9,5)	27	12100
195,0	Zr-92 n(6,3)	29	9100
195,0	Se-80 a(1,0)	68	8400
195,2	Bi-209 n(6,4)	27	12100
195,3	La-138 g(2,1)	3,1	36100

Eγ keV	Assignment	Yield. quanta $sr^{-1}nC^{-1}$	Sensitivity $\mu g.g^{-1}mC^{-1}$
196,2	I -127 n(3,1)	43	10000
196,5	Eu-151 p(2,0)	250	1420
196,6	Ni-62 a(2,1)	38	7800
197,0	F -19 n,n'(2,0)		
197,0	Co-57 p(3,1)	72	7400
197,0	Se-80 n(9,5)	68	8400
197,0	Ru-100 g(3,1) Ru-101 n(3,1)	10	19300
197,0	Pr-141 n(5,3)	4,6	36100
197,1	Dy-160 p(2,1)	13	11200
197,2	O -18 g(2,0)	73	2700
197,2	F -19 p(2,1)	483000	10
197,4	Sm-147 p(2,0)	53	4600
197,8	Ru-101 p(4,1)	10	19300
198,0	V -51 g(4,3)	380	1800
198,4	Pd-110 n(3,0)	275	4400
198,6	As-75 p(1,0)	190	3300
200,0	Er-164 p(2,1)	1,1	152900
200,5	I -127 p(5,4)	210	1900
201,0	U -235 n(6,0) U -234 g(6,0)	8,3	27200
201,0	Cu-65 n(8,6)	740	2600
201,7	Hf-176 p(2,1)	2560	300
202,1	Ge-74 n(3,0)	0,5	651000
202,8	Hf-180 g(5,2)	2560	300
202,8	As-75 p(5,1)	48	12100
203,1	Mo-95 n(4,3)	80	3100
203,2	Nb-93 g(4,3)	25	15100
203,3	Ag-109 n(2,0)	87	2600
203,5	I -127 p(2,0)	210	1900

Eγ keV	Assignment	Yield. quanta $sr^{-1}nC^{-1}$	Sensitivity $\mu g.g^{-1}mC^{-1}$
203,8	Ti-49 p(3,1)	12	19200
203,8	Mo-95 p(1,0)	80	3100
203,9	Nb-93 n(6,4)	25	15100
204,0	Nb-93 p(7,4)	25	15100
204,0	V -51 n(6,4)	710	3300
204,0	As-75 p(6,2)	48	12100
205,0	Ag-107 n(1,0)	87	2600
205,8	Os-192 p(1,0)	230	1400
205,9	Pd-106 n(3,0)	140	8600
206,0	V -51 p(4,3)	710	3300
206,2	Re-187 p(2,0)	380	950
206,5	Se-77 a(6,0)	830	1000
206,5	Hf-174 p(2,1)	3370	240
206,5	Ba-134 g(2,0)	18	26500
207,0	Cu-63 n(3,0)	380	2700
208,0	Hf-177 p(3,1)	3370	240
208,0	Hf-178 p(3,1)	3370	240
208,2	Hg-199 p(2,0)	2,7	43300
209,1	Tl-203 g(4,3)	100	5800
209,7	Ho-165 p(2,0)	130	2900
210,2	Hf-178 g(6,2)	3370	240
210,4	Ti-47 g(3,1)	8	30500
211,0	Te-125 n(6,3)	23	28500
211,0	Cr-54 n(3,2) } Cr-53 n(3,2) }	75	16600
211,3	Pt-195 p(4,0)	290	1870
211,6	Se-80 n(10,5)	150	4600
212,2	Sb-121 n(1,0)	540	1900
213,7	Ir-191 p(4,2)	51	6200
215,3	Hf-180 p(2,1)	830	910

Eγ keV	Assignment	Yield. quanta $sr^{-1}nC^{-1}$	Sensitivity $\mu g.g^{-1}mC^{-1}$
215,5	I -127 p(4,2)	240	1800
215,6	Se-80 a(2,0)	1030	820
	Mo-96 g(2,0)		
216,0	Mo-97 n(2,0)	50	6000
216,0	Mo-96 g(2,0)	50	6000
217,0	Ru-96 p(5,4)	45	7700
217,3	Br-79 p(2,0)	210	2200
219,0	Br-79 n(6,3)	210	2200
219,0	Se-74 p(2,1)	1030	820
219,1	Se-80 n(3,1)	1030	820
219,1	Ir-193 p(5,2)	57	5700
219,4	Os-189 p(4,0)	21	12600
223,3	Os-189 n(5,1)	21	12600
224,9	Tl-203 n(4,3)	65	7300
226,0	Ti-50 n(1,0)	1570	420
227,0	Ti-49 a(3,0)	1570	420
227,5	Mo-96 g(3,1)	6	40000
228,3	Tm-169 p(5,2)	7,3	33000
229,3	Sm-147 n(1,0)	7,4	30800
229,4	As-75 n(13,7)	50	11300
230,4	La-138 p(5,0)	13	23200
230,9	Sb-121 n(3,1)	110	7700
231,7	Rb-85 n(1,0)	1300	240
	Sr-87 g(1,0) }		
231,9	Sr-88 n(1,0) }	300	530
232,0	Gd-154 p(6,4)	18	19000
232,0	U -238 n(14,5)	60	5200
232,7	Ga-69 n(2,0)	790	400
233,0	Zr-96 n(3,0)	3,5	68300
234,0	Zr-94 g(1,0)	3,5	68300

Eγ keV	Assignment	Yield. quanta $sr^{-1}nC^{-1}$	Sensitivity $\mu g.g^{-1}mC^{-1}$
234,2	Se-80 n(4,1)	22	17300
234,3	W -180 p(2,1)	12	13900
234,9	Se-76 a(5,3)	22	17300
235,0	Pd-110 n(4,0)	150	8100
235,1	Nb-93 p(7,3)	27	16300
236,0	Tl-205 g(6,4)	63	7500
236,0	Ge-76 n(8,3)	41	4000
236,1	As-75 n(9,5)	110	5500
236,3	W -184 n(6,0)	1	149000
236,6	Hf-179 n(4,0)	60	7900
	Hf-178 g(4,0)		
236,8	Pd-110 n(5,0)	150	8100
237,0	Zn-68 g(5,3)	44	16700
238,7	Rb-85 n(2,0)	28	10000
239,0	Pb-212;Pb-214	r.a.	
239,0	Pt-195 p(5,0)	170	2500
241,0	U -238 g(9,0)	30	17300
242,0	Dy-164 p(2,0)	18	8600
242,0	Mo-92 p(3,2)	22	34800
242,3	Bi-209 n(7,3)	50	6100
243,6	I -127 p(5,3)	12	34000
244,0	Rh-103 n(2,0)	100	3800
244,1	Se-80 n(5,1)	225	3700
244,8	Sb-121 n(2,0)	560	1900
244,8	Ba-130 g(6,3)	35	16900
246,0	Bi-209 g(2,1)	2,8	150000
246,3	Cd-111 p(1,0)	8,4	6900
246,9	Ag-109 n(7,4)	7,4	24700
247,0	Ga-69 p(13,9)	110	3100
247,0	Se-82 n(3,1)	225	3700

Eγ keV	Assignment	Yield. quanta $sr^{-1}nC^{-1}$	Sensitivity $\mu g.g^{-1}mC^{-1}$
247,6	Hg-199 p(5,2)	18	12700
247,8	Sb-123 n(2,0)	560	1900
248,0	Pd-110 n(6,0)	105	10100
249,0	Cu-63 n(2,0)	80	25000
249,0	Hf-177 p(2,0)	570	1300
249,3	Au-197 n(3,0)	15	9800
249,9	Cr-54 n(4,2)	210	6300
251,5	Lu-175 p(2,0)	560	500
253,0	Zr-94 n(6,2)	55	5500
254,0	Ge-73 n(3,0)	34	12000
254,7	La-139 n(1,0)	5,8	26800
	La-138 g(1,0)		
255,0	Sn-122 n(9,0)	30	14500
	Cd-112 g(2,1)		
255,1	Cd-113 n(2,1)	18	3100
258,7	Ag-109 n(5,2)	16	12800
260,5	Tl-205 n(2,1)	120	4300
260,5	Se-80 g(2,1)	4,6	97500
261,5	Br-79 p(3,0)	44	10600
	Ru-98 g(4,2)		
263,6	Ru-99 n(4,2)	31	11200
264,0	Cd-113 p(1,0)	23	2800
264,6	As-75 p(2,0)	71	7200
265,0	Ni-61 n(5,4)	1,5	188000
266,7	K -41 p(3,2)	22	27300
266,8	Pd-110 n(7,0)	85	12200
266,9	Rh-103 n(3,0)	83	5200
268,0	Nb-93 g(9,5)	64	11500
268,5	Au-197 p(6,3)	18	9270

Eγ keV	Assignment	Yield. quanta $sr^{-1}nC^{-1}$	Sensitivity $\mu g.g^{-1}mC^{-1}$
268,7	Au-197 p(2,0)	18	9270
268,8	Hf-197 p(3,0)	570	1270
269,1	Se-76 a(6,3)	150	4800
270,0	Sn-119 n(1,0)	150	3200
270,5	Sn-115 n(1,0)	150	3200
271,2	Se-80 n(4,2)	22	35500
271,5	Tl-203 n(6,3)	92	5000
273,0	Sn-117 n(2,1)	150	3200
273,1	Th-232 g(16,0)	320	1800
274,0	Ni-64 n(2,0)	140	3100
275,9	Br-81 p(1,0)	145	3300
276,0	Se-80 g(1,0)	24	25200
276,0	Br-79 n(9,2)	145	3300
276,0	Cs-133 n(2,1)	16	17300
276,4	Cs-133 p(4,2)	16	17300
277,0	Hf-177 p(5,1)	620	1080
277,0	Tl-208;Ac-228	r.a.	
278,0	Cd-114 n(2,0) Cd-113 g(2,0)	12	4300
278,8	Au-197 p(6,2)	240	650
278,8	Cs-133 n(3,1)	16	17300
279,0	Au-197 p(3,0)	240	650
279,0	Ac-228	r.a.	
279,1	Tl-208 p(1,0)	125	3600
279,2	Ba-137 p(1,0)	23	24900
279,5	As-75 p(3,0)	330	1400
280,5	Pd-105 p(1,0)	180	7100
280,5	Os-188 n(5,0)	4,7	56400
281,2	Sb-123 n(3,1)	220	4700
283,2	Os-192 p(2,1)	4,7	56400

Eγ keV	Assignment	Yield. quanta $sr^{-1}nC^{-1}$	Sensitivity $\mu g.g^{-1}mC^{-1}$
284,8	Re-185 p(2,0)	39	8200
284,9	Hg-199 p(6,2)	22	8500
285,0	Bi-214	r.a.	
285,0	Ag-109 p(5,4)	29	5900
286,0	Se-76 a(8,4)	36	20200
286,0	Cs-133 n(5,3)	18	14200
286,1	Eu-151 p(4,1)	275	1310
286,6	As-75 n(3,0)	4900	100
287,2	Ga-69 n(3,2)	970	450
287,8	Ag-109 n(3,1)	29	5900
289,0	Cd-116 n(9,1)	45	1300
289,3	Ho-165 p(5,2)	4,7	86000
290,0	Th-232 g(17,0)	140	4700
290,0	La-139 n(5,4) }	3,2	42000
	La-138 g(5,4) }		
290,1	Cs-133 n(4,1)	18	14200
290,2	Nb-93 g(3,2)	8,3	39600
290,2	Se-80 g(4,1)	18	41100
291,1	Cs-133 n(3,0)	18	14200
291,8	W -183 p(4,0)	3	63900
292,0	Bi-209 g(3,1)	13	24300
292,8	Sc-45 n(3,1)	4000	300
292,8	As-75 n(4,0)	470	1200
293,0	Se-82 n(3,0)	18	41100
293,1	Lu-176 p(3,2)	4,4	58800
293,2	Zr-94 n(7,1)	190	1500
293,8	Sb-121 n(3,0)	250	4400
294,0	Mo-95 n(3,2)	36	5800
294,3	Se-86 n(8,2)	18	41100
295,1	Rh-103 p(3,0)	590	710

Eγ keV	Assignment	Yield. quanta $sr^{-1}nC^{-1}$	Sensitivity $\mu g.g^{-1}mC^{-1}$
295,2	Ge-73 p(5,3)	28	9300
295,7	Tl-205 n(8,4)	41	9900
296,0	Tl-210;Pb-214	r.a.	
296,0	Gd-156 p(3,2)	22	17300
296,1	Ho-165 n(6,0)	6,1	68000
296,8	Os-186 p(2,1)	2,2	94100
297,0	Ru-102 g(3,0)	100	3800
297,3	Bi-209 n(8,3)	4,9	80400
297,4	Dy-160 p(3,1)	14	11700
297,5	Mo-94 g(2,1)	22	16300
298,0	Dy-163 n(2,0)	14	11700
298,6	Cd-113 n(2,0)	18	3100
298,9	Au-197 n(4,0)	15	9600
299,0	Se-82 n(4,2)	5,4	84800
299,4	Ir-193 p(5,0)	23	8400
301,0	Re-187 p(3,0)	74	5000
301,4	Ta-181 p(4,0)	170	4500
301,4	Hf-180 g(4,0)	50	8300
301,7	Nd-148 p(1,0)	73	2800
302,0	Ge-76 p(3,2)	11	25000
302,2	Cs-133 n(4,0)	44	7800
302,8	Cs-133 p(3,1)	44	7800
303,0	Br-79 n(7,2)	130	5800
303,7	Ba-130 g(4,0)	24	24400
303,8	Th-232 g(20,0)	130	3700
303,9	As-75 p(4,0)	8	58000
305,0	Zr-96 p(4,3)	6,7	43100
305,3	Ru-101 n(3,0) }	110	3400
	Ru-100 g(3,0) }		
306,4	Br-79 p(4,0)	15	61800

Eγ keV	Assignment	Yield. quanta $sr^{-1}nC^{-1}$	Sensitivity $\mu g.g^{-1}mC^{-1}$
306,6	Hf-178 p(2,0)	50	8300
306,8	Ru-101 p(2,0)	110	3400
307,0	Ga-69 p(6,4)	100	3400
307,5	Eu-151 p(4,0)	190	2100
307,8	Au-197 n(5,0)	8,6	13000
307,9	Se-82 g(5,2)	12	48200
308,2	Tl-203 g(5,2)	12	9900
	Ti-47 g(1,0) }		
308,3	Ti-48 n(1,0) }	18	33200
309,4	Se-76 a(5,2)	12	48200
310,0	Th-232 g(23,3)	55	10700
311,0	Zr-96 p(3,1)	105	2800
311,0	Cd-114 g(2,0)	19	5100
311,3	Ag-109 p(3,0)	230	930
312,0	Co-56 n(4,3)	110	10000
312,8	Ni-61 a(4,2)	4,3	72000
314,0	As-75 p(13,7)	315	2000
314,7	Se-80 n(6,0)	150	5700
315,0	Hg-202 n(2,0)	43	3100
315,6	V -51 n(5,3)	3315	540
315,8	As-75 n(5,1)	315	2000
316,2	Cd-113 p(3,0)	19	5100
317,0	Tl-205 g(7,4)	9,1	13400
317,3	I -127 p(3,1)	200	2400
318,3	Ba-137 g(9,4)	19	31900
318,4	Ga-69 p(1,0)	250	1800
318,4	Nb-93 p(8,3)	7,4	42300
320,0	Zn-68 g(1,0)	930	2200
320,0	Ti-50 g(1,0)	64	11200

Eγ keV	Assignment	Yield. quanta $sr^{-1}nC^{-1}$	Sensitivity $\mu g.g^{-1}mC^{-1}$
320,0	Br-79 n(7,1)	50	12500
320,0	Th-232 g(24,4)	73	7900
320,1	V -51 p(1,0)	4100	370
320,2	Ti-50 n(2,0)	64	11200
321,0	Zn-68 n(5,1)	930	2200
	Zn-67 g(5,1)		
321,3	I -127 n(3,0)	200	2400
321,3	Hf-177 p(3,0)	40	13000
321,4	Pd-104 g(3,1)	9,6	88700
321,5	Gd-155 p(4,0)	33	12100
322,5	Se-74 a(4,3)	3,8	101200
322,9	Re-187 g(2,1)	31	11200
324,0	Zn-67 g(2,0)	930	2200
324,0	Mo-97 n(3,0)	105	3900
	Mo-96 g(3,0)		
324,8	Pd-106 g(3,0)	130	9900
324,8	Ag-107 p(2,0)	290	830
324,8	Ag-107 n(2,0)	290	830
325,6	Nb-93 g(6,4)	8,8	38100
326,9	Se-76 a(5,1)	1,9	150600
328,0	Sm-149 p(3,1)	22	12200
328,0	Ac-228	r.a.	
328,5	Pt-194 p(1,0)	1410	390
329,1	Zr-94 n(10,4)	84	3500
329,1	Se-80 n(7,1)	1,9	150600
331,0	Se-82 n(4,1)	1,9	150600
331,2	Hg-201 n(1,0)	39	3400
331,9	Sn-124 g(1,0)	25	15900
331,9	Sb-121 p(4,1)	210	4500

Eγ keV	Assignment	Yield. quanta $sr^{-1}nC^{-1}$	Sensitivity $\mu g.g^{-1}mC^{-1}$
333,2	Sm-144 n(1,0)	500	550
333,9	Sm-150 p(1,0)	500	550
335,5	Sr-88 p(5,3)	7	64300
335,6	Ba-130 g(8,4)	15	38200
335,7	Se-78 n(12,1)	17	27400
336,0	Mo-95 n(2,0)	135	2500
336,3	In-115 p(1,0)	7,4	28700
336,4	Mo-94 g(2,0)	135	2500
337,9	W -180 p(2,0)	3	50500
338,0	Hf-180 p(3,2)	80	5800
338,1	As-75 p(9,3)	180	3600
338,2	Tl-203 n(8,3)	7,4	17300
338,6	Nb-93 p(5,1)	12	32800
338,6	Cs-133 n(6,3)	38	10500
339,0	Ac-228	r.a.	
339,1	Co-59 n(1,0)	14800	80
339,0	Hf-180 g(5,0)	80	5800
340,7	Ni-62 a(4,1)	47	6600
340,8	Ba-138 n(7,1)	13	41900
341,0	Au-197 n(7,1)	5,4	15400
341,0	W -186 p(3,2)	3	50500
341,9	Cd-111 p(2,0)	22	2900
342,2	Dy-164 p(5,3)	20	8600
343,2	Ir-191 p(5,0)	34	5700
343,4	Se-80 n(8,1)	24	23600
343,6	Se-76 a(6,2)	24	23600
344,0	Hf-179 n(6,0) } Hf-178 g(6,0) }	80	5800
344,2	Zr-94 n(7,0)	16	17600
344,5	Cd-116 g(3,1)	22	2900

Eγ keV	Assignment	Yield. quanta $sr^{-1}nC^{-1}$	Sensitivity $\mu g.g^{-1}mC^{-1}$
344,6	Pd-105 p(4,0)	26	39500
346,2	S -33 p(3,2)	3	336000
346,7	Gd-154 p(3,2)	10	42800
346,9	Pd-105 n(3,0)	26	39500
347,0	Se-82 n(5,2)	4,3	95700
347,4	Sc-45 p(7,4)	270	3700
347,5	Ag-109 n(3,0)	43	4300
347,7	Tb-159 p(4,0)	15	7200
348,6	Te-130 p(6,3)	72	13400
349,0	Ni-62 n(4,1)	6,5	51800
350,0	Sm-149 p(3,0)	11	20900
350,6	Se-82 g(7,2)	4,3	95700
350,7	Ge-73 p(5,1)	14	20000
351,0	Br-79 n(8,3)	150	4400
351,0	Hg-202 n(3,0)	21	8800
351,1	W -182 p(3,2)	12	12200
351,1	Dy-163 p(4,0)	25	6500
351,2	Ir-191 p(6,0)	30	6600
352,0	Pb-214	r.a.	
352,3	Fe-56 p(3,1)	88	8900
353,0	Mo-98 n(9,0)	17	20900
353,2	Cr-53 g(4,1)	210	6300
353,5	Os-186 p(12,7)	3,9	61500
353,5	Ge-73 p(4,0)	3	65000
354,0	Ti-48 a(2,1)	8	112000
354,1	Au-197 n(11,2)	9,3	15100
355,1	Rb-85 p(3,2)	51	7200
355,1	Rb-87 n(3,2)	51	7200
355,3	Ru-101 n(4,0) } Ru-100 g(4,0) }	500	800

Eγ keV	Assignment	Yield. quanta $sr^{-1}nC^{-1}$	Sensitivity $\mu g.g^{-1}mC^{-1}$
355,4	In-115 g(4,2)	2,3	83300
355,9	Pt-196 p(1,0)	960	490
356,4	Hf-179 n(7,0)	280	2100
	Hf-178 g(7,0)		
356,5	Cs-133 p(4,1)	14	26100
356,7	Se-82 g(1,0)	1,9	162800
356,8	Ho-165 n(8,0)	60	8400
357,0	Zr-92 n(4,0)	22	12700
357,1	Y -89 n(3,2)	5,3	32400
357,3	Ba-130 p(1,0)	21	25300
357,4	Rh-103 p(4,0)	690	700
357,7	Ru-104 p(1,0)	500	800
358,0	Ir-193 p(6,0)	66	3300
358,8	Se-74 a(3,2)	1,9	162800
359,1	Re-187 n(8,3)	51	7100
360,0	Zn-67 n(2,0)	1540	980
360,3	I -127 p(4,1)	240	2800
361,0	Ho-165 p(4,0)	45	10400
361,1	Se-76 a(6,1)	1,9	162800
362,2	Se-74 a(3,1)	1,9	162800
362,3	Ag-107 p(4,3)	140	1300
364,0	Hg-202 g(4,0)	190	1400
364,4	Sc-45 p(2,1)	3200	340
365,0	Cu-63 p(3,1)	960	3600
365,6	Ag-107 n(3,0)	140	1300
366,0	Fe-58 n(4,0)	19	44900
	Fe-57 g(4,0)		
366,3	Se-80 n(7,0)	160	5200
366,7	Fe-57 p(3,0)	19	44900
366,7	Ag-109 n(4,1)	140	1300

Eγ keV	Assignment	Yield. quanta $sr^{-1}nC^{-1}$	Sensitivity $\mu g.g^{-1}mC^{-1}$
366,9	Hg-199 n(1,0)	190	1400
	Hg-198 g(1,0)		
367,5	Ti-48 a(2,0)	10	89800
367,9	Hg-200 p(1,0)	190	1400
369,0	Cu-65 p(3,1)	960	3600
369,8	I -127 p(9,3)	61	8300
370,6	Tb-159 p(6,1)	9,1	33000
372,1	Te-125 n(4,0)	45	24600
372,8	Ca-43 p(1,0)	180	930
373,0	Ni-61 p(3,2)	20	19600
373,7	As-75 p(7,1)	460	1300
373,9	Ga-69 n(3,0)	300	1200
374,5	Os-192 p(3,1)	2,9	84700
374,7	I -127 p(3,0)	84	7500
375,0	Hf-179 p(5,0)	82	6400
376,8	Cd-114 n(5,0)	5,3	11200
	Cd-113 g(5,0)		
376,8	Ca-44 g(2,0)	180	930
376,9	Sc-45 p(2,0)	380	2500
377,0	Se-82 n(4,0)	42	13900
377,5	Cr-53 n(1,0)	8050	260
	Cr-52 g(1,0)		
378,3	Pd-110 p(1,0)	1290	1100
380,0	Rb-85 g(6,3)	43	7900
380,0	Rh-103 n(4,1)	95	4100
380,2	Th-232 g(27,3)	220	3800
380,4	Fe-57 n(5,2)	31	29600
	Fe-56 g(5,2)		
380,6	Rb-87 n(4,2)	43	7900
381,6	Sn-122 g(2,1)	5,7	78900

E_γ keV	Assignment	Yield. quanta $sr^{-1}nC^{-1}$	Sensitivity $\mu g.g^{-1}mC^{-1}$
381,6	Sb-123 p(2,1)	180	3600
382,2	Sb-121 n(9,1)	180	3600
383,6	Cs-133 p(3,0)	12	30400
383,6	K -41 p(6,2)	230	2500
384,0	Te-130 g(6,2)	21	31600
384,0	Br-79 n(5,0)	490	1700
385,0	Br-79 n(10,4)	490	1700
385,1	Mn-55 n(3,2)	930	1800
385,4	Rh-103 n(5,1)	71	5400
385,6	Hg-196 g(1,0)	4,4	45000
388,4	Rb-87 n(1,0)	39	8000
388,4	Sr-87 p(1,0)	15	22600
389,7	Mg-25 p(2,1)	1260	620
389,8	Dy-163 p(5,0)	15	9600
390,0	Ga-71 p(1,0)	560	700
390,0	Hf-177 p(5,0)	300	2000
390,3	Lu-176 p(4,2)	11	21300
390,8	Se-78 n(13,0)	3,2	112400
390,9	Ir-191 p(7,0)	4	90500
390,9	Ag-109 p(5,3)	1,3	90500
391,7	Cd-112 g(1,0) Cd-113 n(1,0)	8,1	9400
393,0	Ti-48 g(5,3) Ti-49 n(5,3)	26	30900
393,4	Te-130 p(6,2)	14	48400
393,9	Se-76 a(5,0)	3,4	111200
396,0	Os-190 p(5,2)	1,4	160000
396,6	As-75 p(12,6)	13	39400
396,9	Ca-43 p(3,2)	6,9	94200
397,9	Ga-69 n(4,0)	540	750

E_γ keV	Assignment	Yield. quanta $sr^{-1}nC^{-1}$	Sensitivity $\mu g.g^{-1}mC^{-1}$
398,0	Se-82 n(6,2)	3,4	111200
400,6	As-75 p(5,0)	25	18300
401,0	Hf	220	2700
401,3	Tl-203 p(2,1)	15	8700
402,0	Br-79 n(6,0)	180	3900
402,6	Rb-87 p(1,0)	12	24800
404,1	K -41 p(7,2)	52	15400
406,4	Cr-54 n(4,0)	160	9300
407,1	Se-80 n(16,6)	5,2	87300
407,2	Pt-198 p(1,0)	160	3500
408,0	Te-125 p(4,1)	27	24500
408,6	Tl-203 n(3,2)	13	8500
410,0	Ru-104 g(4,0)	23	13200
411,2	I -127 n(4,0)	6,4	73000
411,5	Mn-55 n(1,0)	7600	190
411,6	Fe-54 p(4,2)	82	12800
411,8	Hg-198 p(1,0)	120	2400
414,0	B -10 p(3,2)	490	2400
414,5	Sc-45 n(4,2)	1900	570
414,9	I -127 p(5,2)	6,1	71000
415,0	Be-9 g(3,2)	14	43700
415,1	Ag-109 p(4,0)	260	730
417,6	As-75 p(13,6)	9	40500
417,6	As-75 p(9,1)	9	40500
418,3	I -127 p(4,0)	12	55000
420,0	Y -89 g(4,2)	46	5300
420,4	Os-192 p(5,2)	1,7	152000
420,7	Hf-179 p(6,0)	80	6500
421,8	Dy-163 p(7,0)	5,8	23800

Eγ keV	Assignment	Yield. quanta $sr^{-1}nC^{-1}$	Sensitivity $\mu g.g^{-1}mC^{-1}$
422,0	Ru-101 p(6,0)	12	23100
423,0	Ni-58 g(2,1)	22	17200
423,1	Pd-106 g(4,0)	130	7300
423,1	Ag-107 p(3,0)	280	805
425,0	Se-82 n(5,0)	21	41300
425,3	Sc-76 a(7,2)	21	41300
425,4	Sc-45 p(13,8)	250	3400
425,7	Au-197 n(9,5)	3,8	30800
426,2	As-75 p(14,9)	830	820
426,2	Ag-109 n(4,0)	280	805
426,3	Hg-196 p(1,0)	96	1800
426,3	Hf-178 p(4,3)	160	3400
426,7	Hf-177 p(7,0)	160	3400
427,3	Ru-98 g(3,0) Ru-99 n(3,0)	48	7000
427,8	As-75 n(5,0)	830	820
427,9	Te-125 p(5,1)	46	15600
428,0	B -10 a(1,0)	26600	90
428,1	Se-76 a(6,0)	9,8	52300
429,0	N -15 g(2,0)	710	1880
429,2	Li-6 g(1,0)	154300	13
429,2	Li-7 n(1,0)	154300	13
430,0	Se-82 n(6,1)	9,8	52300
430,0	Co-59 n(8,5)	153	6000
431,7	Sc-45 p(6,3)	530	1900
432,2	Se-80 n(9,1)	9,8	52300
433,2	Pd-105 p(5,0)	2700	260
433,2	Pd-105 n(5,0)	2700	260
433,9	Pd-108 p(1,0)	2700	260

Eγ keV	Assignment	Yield. quanta $sr^{-1}nC^{-1}$	Sensitivity $\mu g.g^{-1}mC^{-1}$
434,8	Os-186 p(4,2)	3,2	95900
435,8	Nb-93 g(5,3)	12,3	27300
437,9	Ba-138 n(9,1)	31	21200
438,4	Sb-121 n(4,0)	1460	770
439,3	Rb-85 g(8,4)	47	9400
439,4	Sn-120 g(4,2)	4,2	121000
439,6	Hg-202 p(1,0)	240	1300
439,8	Na-23 p(1,0)	92600	16
439,8	Mg-26 a(1,0)	130	6720
440,0	Dy-163 n(3,0)	6,2	19500
440,2	Sb-123 n(3,0)	1460	770
440,6	Tl-205 n(4,2)	45	3100
441,0	Ru-96 p(6,5)	89	5400
442,3	Ge-73 n(5,1)	15	22300
442,3	Pd-105 p(5,0)	470	2100
443,1	I -127 p(12,7)	600	8700
443,1	I -127 g(1,0)	600	8700
443,3	Te-125 p(4,0)	93	8600
444,0	Au-197 n(9,2)	3,8	26800
444,3	In-115 p(7,2)	17	15200
445,0	Hf	120	5000
445,1	Br-81 n(8,3)	490	1600
446,0	Pb-208 n(1,0)	20	6980
446,2	Br-81 n(5,1)	490	1600
446,5	Th-232 g(26,0)	240	3100
447,0	Sn	35	13400
447,3	Ag-109 p(6,4)	2,2	73100
448,3	Ba-137 n(1,0)	31	20100
449,6	Cu-93 p(4,2)	270	4900
452,0	Zr-96 p(4,2)	35	8200

Eγ keV	Assignment	Yield. quanta $sr^{-1}nC^{-1}$	Sensitivity $\mu g.g^{-1}mC^{-1}$
452,3	Te-130 g(3,1)	13	50200
452,8	Tm-169 p(6,2)	10	22100
453,6	Nd-146 p(1,0)	100	2200
453,8	Te-125 n(5,0)	13	50200
455,7	Se-80 n(10,1)	15	32300
456,8	Br-81 n(2,0)	240	2100
459,2	Sc-45 p(11,6)	470	2300
460,2	As-75 p(11,5)	130	4500
461,8	I -127 n(5,1)	66	10200
461,9	Os-188 p(4,2)	2,9	92700
461,9	Ag-107 p(4,2)	14	12600
462,0	Ag-109 n(5,0)	14	12600
463,0	Ac-228	r.a.	
463,4	Te-125 p(5,0)	34	22200
464,2	Sb-121 n(6,0)	130	7600
464,9	Co-59 n(2,0)	910	1200
465,5	As-75 p(12,5)	45	11300
	Fe-56 g(4,1)		
466,0	Fe-57 n(4,1)	74	13800
466,8	Se-80 n(9,0)	100	9900
468,7	As-75 p(6,0)	45	11300
470,0	Se-82 n(7,2)	100	9900
470,5	Sb-121 p(2,1)	130	7600
471,2	As-75 p(14,7)	45	11300
472,1	Ho-165 p(7,1)	15	43000
475,0	Ru-102 p(1,0)	330	910
475,0	Au-197 n(7,0)	2,9	12800
475,2	Sb-121 n(7,0)	210	4800
477,0	Ni-61 n(1,0)	43	10100
477,0	Br-79 n(9,3)	63	10700

Eγ keV	Assignment	Yield. quanta $sr^{-1}nC^{-1}$	Sensitivity $\mu g.g^{-1}mC^{-1}$
477,1	Mn-55 n(4,2)	6000	270
478,0	Li-7 p(1,0)	521800	5
478,1	Os-188 p(3,1)	2,6	108000
479,3	La-138 p(8,0)	3,7	38000
480,0	Mo-92 p(10,7)	70	5900
480,6	Ba-135 p(3,0)	29	22500
480,9	Ba-136 n(2,0)	34	16500
480,9	Mo-97 p(1,0)	70	
484,0	Cu-63 n(9,4)	470	8500
484,3	Se-74 a(8,3)	9,2	85600
484,4	Rb-87 g(4,2)	340	980
484,9	Rb-87 n(2,1)	340	980
485,6	As-75 p(13,5)	120	5000
487,0	Os-188 p(5,2)	9,4	42600
487,3	Os-188 n(7,0)	9,4	42600
489,0	Os-192 p(2,0)	9,4	42600
489,3	In-115 n(4,1)	51	5800
489,8	Os-186 p(11,6)	9,4	42600
490,0	I -127 p(17,9)	62	11100
490,5	Hg-202 n(4,0)	22	9900
490,5	Hg-202 p(4,0)	22	9900
491,0	Ni-58 g(1,0)	11	35900
491,0	Os-187 p(8,1)	9,4	42600
491,7	Se-80 g(6,1)	3,9	112500
492,8	Se-80 n(10,0)	3,9	112500
493,6	Nb-93 g(4,2)	8,2	43300
494,5	Er-167 p(6,1)	11	21800
495,3	O -16 g(1,0)	270	850
496,4	Ru-101 n(7,3) } Ru-100 g(7,3) }	31	14200

Eγ keV	Assignment	Yield. quanta $sr^{-1}nC^{-1}$	Sensitivity $\mu g.g^{-1}mC^{-1}$
496,5	In-113 n(4,0)	870	340
498,0	Pd-108 p(2,1)	93	11100
497,3	In-115 n(1,0)	870	340
497,4	Sn-115 p(1,0)	45	7800
	La-138 g(3,1)		
499,7	La-139 n(3,1)	3,1	41000
500,0	Ga-69 p(7,4)	950	490
504,0	Rb-85 n(3,2)	440	820
504,2	Rh-103 n(5,0)	30	16500
505,0	Te-123 p(5,0)	43	11700
505,4	Ag-107 n(4,0)	31	9300
506,4	Y -89 n(2,1)	280	940
507,6	Sb-121 p(2,0)	110	8600
508,0	Pr-141 g(2,1)	3,4	48600
508,2	Zn-70 n(1,0)	1270	1000
509,0	Cu-65 p(4,2)	5450	2500
510,0	Ge-73 n(5,0)	1530	230
510,0	Pb-208 n(2,0)	110	1380
510,5	La-138 p(9,0)	74	4800
510,9	Br-81 n(6,1)	900	720
511,0	β^+	r.a.	
511,6	Ga-71 p(3,0)	180	2300
511,7	Re-187 p(6,0)	510	890
511,7	Pd-105 p(1,0)	2025	630
511,8	Eu-151 n(7,1)	500	1000
512,0	Br-79 n(12,3)	900	720
513,0	Br-79 n(9,2)	900	720
513,0	I -127 p(8,2)	860	1000
513,1	Cd-116 p(1,0)	125	670
513,1	Cd-111 p(7,2)	125	670

Eγ keV	Assignment	Yield. quanta $sr^{-1}nC^{-1}$	Sensitivity $\mu g.g^{-1}mC^{-1}$
515,5	Ho-165 p(6,0)	12	47000
518,9	Th-232 g(30,1)	57	13600
520,0	Hf	250	2500
520,3	Ca-40 n(4,3)	64	5700
520,3	Bi-209 n(12,7)	3,5	99000
520,5	Ga-71 p(4,1)	370	1100
520,8	Mn-55 n(2,1)	310	5800
521,0	Se-71 p(7,0)	6,4	92600
522,8	Br-79 p(6,0)	92	7800
524,6	Pr-141 g(3,1)	8,1	24500
525,0	Se	5,2	90000
526,5	Ag-107 p(5,3)	1	122000
527,3	Sn-117 n(1,0)	85	5600
529,0	Th-232 g(31,0)	76	10200
530,0	Os-187 n(13,5)	0,6	179000
530,7	Sc-45 p(3,1)	3800	300
531,7	Sb-121 n(8,0)	79	10200
531,9	Rh-103 n(6,0)	66	9700
532,0	Er-167 p(5,0)	1,9	126400
532,4	Ga-69 p(5,2)	91	4400
535,0	Zr-96 p(6,3)	105	3100
535,3	Ho-165 n(13,0)	5,3	110000
535,6	Mo-100 p(1,0)	15	22400
535,9	Sb-121 p(3,1)	82	9400
537,3	Rb-85 n(5,1)	320	1200
537,4	Br-81 n(8,2)	98	7700
537,6	Dy-156 p(3,1)	7,9	11300
538,0	Cd-111 n(1,0)	19	2900
538,1	Se-80 g(3,0)	82	8100

Eγ keV	Assignment	Yield. quanta $sr^{-1}nC^{-1}$	Sensitivity $\mu g.g^{-1}mC^{-1}$
538,2	Br-81 p(2,0)	98	7700
538,5	Te-123 p(6,1)	74	9100
539,6	Ru-100 p(1,0)	140	3300
541,8	Sn-122 g(2,0)	35	12700
541,8	Sb-123 p(2,0)	82	9400
542,5	Se-82 a(2,1)	68	6200
542,9	Ti-48 a(3,0)	8	100000
543,0	Hg-203 p(4,0)	58	4200
543,1	Sc-45 p(3,0)	2700	420
544,9	Ru-101 p(10,0)	12	10300
545,0	Bi-209 n(1,0)	5,2	61600
545,6	Ge-76 p(2,1)	1	214000
546,4	Ru-101 n(7,2) }	12	10300
	Ru-100 g(7,2) }		
547,5	Au-197 p(6,0)	160	790
547,6	Hf-180 p(3,1)	100	6000
549,1	Br-81 n(3,0)	370	2100
550,0	Rb-85 n(9,5)	360	1100
550,3	Sm-148 p(1,0)	240	1200
550,4	Pd-106 g(8,4)	130	7500
551,6	Se-80 g(8,1)	84	8300
555,8	Pd-104 p(1,0)	560	2300
556,4	Pd-102 p(1,0)	560	2300
556,9	As-75 p(11,4)	75	8100
557,0	Os-186 p(12,6)	4	73400
557,2	As-75 p(10,2)	75	8100
557,8	Os-190 p(3,0)	4	73400
558,1	As-75 g(1,0)	75	8100
558,5	Cd-114 p(1,0)	120	640
559,3	Se-76 p(1,0)	210	5000

Eγ keV	Assignment	Yield. quanta $sr^{-1}nC^{-1}$	Sensitivity $\mu g.g^{-1}mC^{-1}$
559,9	Cs-133 p(7,1)	14	32700
560,0	Tb-159 p(9,1)	7,7	38900
560,0	Zr-92 p(3,1)	14	21900
560,4	Te-120 p(1,0)	120	5600
561,4	Se-80 g(9,1)	210	5000
561,4	As-75 p(12,4)	75	8100
561,5	Er-167 p(7,1)	2,1	121600
562,0	Mo-95 p(2,1)		
562,7	Tm-169 p(6,1)	25	9500
563,0	Ge-76 n,n'(1,0)		
563,0	Ge-76 p(1,0)	0,7	258000
563,0	Se-76 p(2,1)	210	5000
563,2	As-75 g(2,1)	75	8100
563,5	Y -89 g(5,2)	73	2600
564,0	Cr-53 p(1,0)	700	3400
564,4	Te-122 p(1,0)	120	5600
564,7	Cs-133 n(5,1)	14	32700
566,8	Ho-165 p(7,0)	6,1	108000
567,0	Mo-95 p(2,1)	55	8200
568,0	Os-190 p(4,1)	1,2	210000
568,6	Br-81 n(9,2)	83	8500
569,0	Os-192 p(12,8)	1,2	210000
569,0	Th-232 g(34,0)	82	8700
570,0	Pb-207 p(1,0)	2,3	42300
570,9	I -127 p(6,1)	65	10300
571,0	Tm-169 p(6,0)	30	8300
572,3	As-75 p(7,0)	285	2400
573,0	Sb-121 p(3,0)	105	6700
573,1	Sn-120 g(3,0)	25	15700
573,9	Ga-69 p(2,0)	400	1230

Eγ keV	Assignment	Yield. quanta $sr^{-1}nC^{-1}$	Sensitivity $\mu g.g^{-1}mC^{-1}$
574,0	Zn-68 g(2,0)	400	7100
574,8	As-75 p(14,6)	285	2400
575,6	V -51 n(4,2)	550	4400
576,4	Ba-136 n(12,3)	35	19300
578,0	Ge-73 n(7,0)	15	21000
578,6	Zn-68 p(2,1)	400	7100
578,9	O -18 n(5,4)	62	3800
579,3	Hg-200 p(2,1)	8,3	23300
579,9	K -41 p(3,1)	30	4960
	La-138 g(4,2)		
580,0	La-139 n(4,2)	4,5	46000
580,2	Tb-159 p(8,0)	50	5300
580,3	Os-192 p(6,2)	9,4	48300
581,3	As-75 p(11,3)	28	19000
582,4	As-75 p(13,4)	28	19000
583,7	Cd-113 p(5,0)	21	3500
584,8	As-75 p(12,3)	28	19000
585,0	Cu-63 p(5,2)	530	7100
585,0	Mo-94 g(3,1)	25	8300
585,0	Zn-68 n(8,0)	100	19700
585,1	Mg-25 p(1,0)	3200	310
585,2	Au-197 p(10,0)	10	12300
585,2	W -180 p(3,1)	1,4	126000
585,6	As-75 n(6,0)	28	19000
585,5	Th-232 g(36,0)	390	2400
586,7	I -127 n(5,0)	46	12100
587,9	Ba-135 p(4,0)	21	27900
587,8	Ir-191 p(9,0)	7	49000
588,0	Ni-61 p(3,1)	29	18900
588,0	Y -89 n(1,0)	260	1200

Eγ keV	Assignment	Yield quanta $sr^{-1}nC^{-1}$	Sensitivity $\mu g.g^{-1}mC^{-1}$
588,6	Pt-192 p(5,2)	21	31500
588,8	Hg-201 n(3,1)	12	16700
592,0	Mo-95 p(3,1)	11	16300
593,4	Ca-43 p(2,0)	38	8500
593,8	Ho-165 p(10,2)	40	17900
593,9	I -127 p(7,1)	83	8800
594,1	Sb-121 n(9,0)	95	9500
595,0	Ti-49 n(3,2) }	170	6800
	Ti-48 g(3,2) }		
596,0	Ge-74 n,n'(1,0)		
596,1	Ga-71 p(6,3)	250	1800
596,2	As-75 p(11,2)	120	4980
597,0	Hf-176 p(3,0)	510	700
597,0	Lu-175 p(4,0)	14	19200
597,1	Pr-141 n(9,3)	21	14200
597,4	Sc-45 p(15,11)	530	2300
598,2	B -10 a(2,1)	1200	1310
600,2	I -127 p(15,5)	180	3900
601,7	K -41 p(4,1)	35	5900
602,0	Sr-84 p(4,2)	13	22800
602,0	Te-124 p(1,0)	110	6300
602,1	Te-130 g(1,0)	110	6300
602,7	I -127 a(1,0)	180	3900
603,0	Pb-208 n(3,0)	4,5	30400
603,2	As-75 p(12,2)	670	1100
603,4	V -51 n(4,1)	3570	860
604,7	Ba-134 p(1,0)	22	23400
605,2	Cs-133 p(5,0)	42	11300
605,4	Br-79 p(7,0)	420	2200
606,9	As-75 p(13,3)	670	1100

Eγ keV	Assignment	Yield. quanta $sr^{-1}nC^{-1}$	Sensitivity $\mu g.g^{-1}mC^{-1}$
607,6	Os-189 n(11,1)	11,4	43900
607,6	Pt-194 p(5,2)	17	37300
607,6	Rh-103 p(7,1)	65	10600
608,0	Ge-74 n,n'(2,1)		
608,2	Hg-196 g(2,0)	4,8	76700
608,3	Br-81 n(4,0)	420	2200
608,3	Hf-174 p(3,0)	250	2100
608,4	Ho-165 n(15,0)	16	42100
608,5	Ge-74 p(2,1)	30	11400
608,9	V -51 p(2,1)	3610	920
609,0	Bi-214	r.a.	
610,0	Ru-102 g(6,0)	9,6	13300
610,6	Hg-196 p(2,1)	4,8	76700
611,0	Cu-65 p(5,2)	280	11600
611,9	Th-232 p(6,2)	84	11400
612,4	Pt-192 p(2,0)	17	37300
612,8	In-115 n(2,0)	4	6900
613,6	Ag-109 n(7,1)	27	10200
613,6	Se-78 p(1,0)	1240	930
614,0	Na-23 1637-2Me	690	2400
615,0	Hf-180 g(9,0)	220	2100
615,0	W -186 p(3,1)	19	10600
615,1	As-75 n(7,0)	85	6600
616,0	Zr-96 p(4,1)	10	33800
616,1	Cd-106 p(2,1)	92	900
616,2	Br-79 g(1,0)	120	6100
616,3	Ru-101 p(11,0)	62	5900
617,0	Tb-159 p(9,0)	15	19300
617,4	Ru-99 p(6,0)	62	5900
617,4	Cd-112 p(1,0)	92	900

Eγ keV	Assignment	Yield. quanta $sr^{-1}nC^{-1}$	Sensitivity $\mu g.g^{-1}mC^{-1}$
617,6	As-75 p(9,0)	85	6600
619,4	Au-191 p(7,2)	12	8400
619,4	Tl-205 p(2,0)	7,8	17400
619,9	O -17 g(5,3)	130	2100
620,0	Ga-71 p(6,2)	120	4200
620,6	Cd-110 p(4,0)	270	590
621,3	As-75 p(13,2)	230	2900
623,1	Ag-109 n(6,0)	14	20800
623,3	As-75 p(10,1)	230	2900
624,9	Ag-107 p(15,2)	14	20800
625,0	Tm-169 p(7,1)	9,3	26300
625,9	Rh-103 n(7,0)	52	14000
627,3	Th-232 p(12,3)	72	13200
628,5	I -127 p(6,0)	140	5200
630,0	Mo-95 n(3,0)	175	2100
630,2	Os-186 p(3,1)	1,4	210000
632,0	Hf-178 p(3,0)	96	6500
632,8	Cd-106 p(1,0)	20	4000
632,8	Cs-133 p(6,0)	140	3900
632,9	Cd-108 p(1,0)	20	4000
633,0	Ag-107 g(1,0)	8,4	32200
633,1	Os-188 p(3,0)	1,4	210000
634,8	Se-74 p(1,0)	24	21400
636,0	Te-125 n(6,4)	63	11300
638,0	Se-82 n(8,0)	24	21400
639,0	Cu-63 n(4,0)	400	6800
641,7	Zr-94 n(10,0)	92	4400
642,0	La-138 p(11,0)	5,8	33800
643,0	Sn-124 g(2,0)	190	2600

Eγ keV	Assignment	Yield. quanta $sr^{-1}nC^{-1}$	Sensitivity $\mu g.g^{-1}mC^{-1}$
643,2	As-75 p(14,5)	88	6700
644,0	Sn-119 n(2,0)	190	2600
646,0	Se-82 n(9,1)	4,2	114300
650,0	Cd-111 n(5,1) }	21	2400
	Cd-110 g(5,1) }		
650,1	Cd-108 g(1,0)	21	2400
650,2	Se-80 g(5,0)	4,8	105900
650,2	Cd-114 p(3,1)	21	2400
651,2	Zn-70 n(2,0)	83	22600
652,0	Cu-63 n(5,0)	2560	1900
653,0	Ru-98 p(1,0)	190	3200
653,6	Ba-135 p(7,1)	24	27300
654,0	Cu-65 n(4,2)	2560	1900
654,7	Se-82 p(1,0)	19,2	32800
655,8	Ni-61 p(3,0)	3,4	115000
657,0	As-75 g(3,1)	130	4500
657,7	Cd-110 p(1,0)	39	1600
658,0	Ti-49 n(3,1)	120	11900
658,8	O -18 n(5,2)	120	2400
659,0	I -127 p(8,1)	240	2200
659,8	Cd-116 g(3,0)	39	1600
660,3	Ti-46 g(4,0)	120	11900
662,2	As-75 p(11,1)	32	15600
663,8	Tl-203 g(4,1)	10	61800
663,9	Tl-205 g(4,1)	10	61800
664,9	Th-232 p(4,1)	465	2100
666,0	Bi-214	r.a.	
666,2	Se-80 p(1,0)	310	3300
666,2	As-75 p(12,1)	32	15600

Eγ keV	Assignment	Yield. quanta $sr^{-1}nC^{-1}$	Sensitivity $\mu g.g^{-1}mC^{-1}$
666,5	Te-126 p(1,0)	390	1900
666,9	Au-197 p(8,2)	1,2	85300
668,0	Ga-69 g(3,1)	100	5200
669,0	Mo-97 n(10,6)	40	9600
669,0	Ni-63 g(1,0)	3,2	161000
669,8	Cu-63 p(1,0)	12300	770
670,7	Cd-108 g(6,1)	4	13700
671,2	Ba-130 g(9,0)	26	24600
671,3	Ba-136 p(9,2)	26	24600
	Fe-56 g(6,1) }		
673,5	Fe-57 n(6,1) }	34	39700
673,7	Dy-164 p(6,2)	10	11200
677,0	I -127 p(12,4)	1490	700
680,0	Hf-179 p(15,0)	105	6900
680,1	Tl-203 n(6,2)	22	35400
680,5	Tl-203 p(2,0)	22	35400
680,9	Th-232 p(5,1)	2500	390
681,0	Sb-121 n(9,0)	53	14900
681,3	Se-74 a(4,1)	44	20800
683,2	Sn-119 n(7,2)	30	16100
684,0	Se-85 g(2,0)	44	20800
686,0	Nb-93 p(2,0)	110	6200
687,0	I -127 p(9,1)	90	15800
687,7	As-75 p(13,1)	250	2800
688,5	Dy-164 p(4,1)	10	9200
688,6	Ho-165 p(10,0)	22	37000
688,9	Sc-45 p(10,4)	940	1500
690,0	Ru-100 p(3,1)	35	17400
691,0	Ge-72 n,n'(1,0)		
691,0	Zn-70 n(3,0)	170	13100

Eγ keV	Assignment	Yield. quanta $sr^{-1}nC^{-1}$	Sensitivity $\mu g.g^{-1}mC^{-1}$
691,1	Sc-45 p(7,2)	940	1500
691,2	Ga-71 g(1,0)	230	2500
691,2	As-75 a(1,0)	125	5500
692,0	Fe-57 p(4,1)	42	33200
693,0	Se-78 p(2,1)	66	13700
694,4	Ru-101 n(7,1) } Ru-100 g(7,1) }	35	17400
695,0	Br-79 n(12,0)	140	7900
695,0	I -127 a(7,4)	200	5700
695,1	Cd-112 p(2,1)	20	3400
696,0	K -41 p(7,1)	92	2600
696,5	Nd-144 p(1,0)	51	6900
696,9	Se-82 g(8,1)	66	13700
698,7	Tl-203 n(5,1)	4,7	40000
699,9	Sn-119 n(3,0)	240	2500
700,5	Se-82 n(16,3)	59	17300
701,0	Hf-179 p(16,0)	200	4000
702,0	Ag-109 p(5,0)	43	7300
702,6	Mo-94 p(2,0)	60	6200
702,6	Nb-93 g(2,1)	106	2500
703,8	Nb-93 g(9,3)	106	6700
705,3	In-115 n(7,1)	6,9	43000
705,3	Er-166 p(4,1)	16	22600
705,7	I -127 p(13,4)	230	5500
706,5	Ba-138 n(16,5)	35	18100
707,2	Sc-45 n(4,1)	250	5000
708,0	Ga-69 p(4,1)	420	1400
708,0	Hf-176 p(4,2)	200	3700
710,0	N -15 g(3,0)	340	4320
710,0	Zn-68 g(4,1)	24	42400

E_γ keV	Assignment	Yield. quanta $sr^{-1}nC^{-1}$	Sensitivity $\mu g.g^{-1}mC^{-1}$
710,4	Tl-203 n(7,2)	30	24500
714,2	Th-232 p(4,0)	49	20200
714,7	Cu-65 n(4,1)	640	6800
716,6	I -127 p(8,0)	81	22300
717,0	Ba-135 p(5,0)	33	18900
718,0	B -10 p(1,0)	15300	120
718,0	Be-9 g(1,0)	5,3	90300
719,2	Ru-99 p(8,0)	442	13100
719,3	In-115 n(6,0)	3,7	78600
719,4	Sn-117 n(2,0)	100	5800
719,8	I -127 p(12,3)	81	22300
720,1	Ru-101 p(16,0)	42	13100
720,3	Sc-45 p(4,0)	3800	400
720,3	Nb-93 g(5,3)	22	28800
720,4	Al-27 p(6,1)	21	120300
721,7	Ag-109 p(8,0)	16	18500
723,0	Mo-98 p(3,1)	30	12100
723,6	Sn-115 n(1,0)	100	5800
723,7	Ag-107 p(7,3)	16	18500
724,7	Th-232 p(6,1)	105	8600
727,0	Bi-212	r.a.	
728,4	Se-74 p(4,1)	47	10400
728,7	Ca-43 n(5,1)	35	9100
729,2	Br-81 n(7,1)	430	2100
730,0	Cd-114 n(7,0)	6	11300
	Cd-113 g(7,0)		
738,0	Ag-107 p(8,3)	12,8	23200
739,9	Tl-203 n(6,1)	30	24600
	Cd-111 g(8,0)		
742,0	Cd-112 n(8,0)	7	9600

Eγ keV	Assignment	Yield. quanta $sr^{-1}nC^{-1}$	Sensitivity $\mu g.g^{-1}mC^{-1}$
742,0	Cu-63 p(4,1)	170	2100
743,2	Te-128 p(1,0)	400	1980
743,8	Ga-69 g(8,3)	68	5500
744,4	Nb-93 p(3,0)	11	12600
744,6	I -127 p(9,0)	460	2900
748,1	Ti-48 g(3,0)	12	124000
749,0	V -51 n(1,0)	3380	210
749,2	I -127 p(13,3)	650	1800
750,0	Ni-62 p(6,3)	10	62000
750,5	Zr-94 p(4,1)	85	5100
750,8	Ba-137 g(14,1)	37	18400
751,9	Cu-65 n(5,4)	3800	1200
	Ba-134 g(12,1)		
752,8	Ba-135 n(12,1)	37	18400
753,0	Bi-209 g(5,2)	68	7500
754,3	Al-27 1776,2-2me	33	112500
754,4	La-139 n(3,0)	18	23000
	La-138 g(3,0)		
754,4	Cu-63 p(9,3)	3800	1200
756,0	Si-29 p(2,)	720	2100
756,7	Pr-141 n(2,0)	32	7100
760,0	Co-59 n(11,4)	120	12200
760,2	Sc-45 p(9,3)	250	4800
760,6	Ba-136 p(3,1)	41	15800
761,4	Tl-205 n(4,0)	35	11700
761,7	Dy-164 p(4,0)	11	12400
763,7	O -18 n(5,1)	22	13100
764,3	As-75 p(14,3)	75	8100
764,7	I -127 p(14,4)	630	2200
765,4	Tl-203 p(3,1)	27	20200

Eγ keV	Assignment	Yield. quanta $sr^{-1}nC^{-1}$	Sensitivity $\mu g.g^{-1}mC^{-1}$
767,0	Se-80 g(6,0)	28	29700
767,0	Os-190 p(5,1)	2,1	185000
767,0	Mo-95 p(2,0)	80	4200
767,4	Os-186 p(3,0)	2,1	185000
767,7	Pd-104 p(2,1)	25	46300
768,7	Cs-133 p(10,0)	20	23500
769,0	Bi-214	r.a.	
769,0	Rb-85 n(5,0)	270	1510
769,1	Cu-65 n(4,0)	4520	970
770,0	Ge-73 n(10,0)	6	57000
770,0	Y -89 n(8,2)	15	11800
770,0	Mo-96 p(1,0)	80	4200
770,4	Tl-203 n(7,1)	28	26300
770,6	Cu-65 p(1,0)	4520	970
770,8	Ni-64 g(1,0)	12	43400
771,8	As-75 g(4,1)	70	8500
773,0	Mo-92 p(2,1)	80	4200
774,0	Ti-50 a(1,0)	13	110000
774,1	Th-232 p(6,0)	800	1400
775,4	V -51 n(9,5)	150	5100
778,0	As-75 p(14,2)	12	43700
778,0	Mo-96 p(1,0)	100	4500
779,7	Nb-93 p(4,1)	230	2600
780,2	Th-232 p(8,0)	890	1300
782,0	Cd-106 p(8,2)	2	36100
783,3	Cr-50 p(1,0)	3060	1100
783,3	Se-80 p(2,1)	4,6	96900
785,6	Pd-104 p(4,1)	85	14600
785,9	Er-166 p(4,0)	3,4	97600
786,0	Mo-95 p(3,0)	6,7	49700

Eγ keV	Assignment	Yield. quanta $sr^{-1}nC^{-1}$	Sensitivity $\mu g.g^{-1}mC^{-1}$
786,1	Pd-106 g(5,0)	85	14600
786,4	Ga-71 g(8,4)	70	7700
786,5	Ag-107 p(4,0)	10	30200
786,8	Hg-202 g(9,1)	14	18300
787,0	Mo-98 p(1,0)	6,7	49700
787,2	Ca-40 p(6,3)	29	10600
787,7	Ga-69 p(5,1)	70	7700
788,2	I -127 p(10,2)	180	6600
788,7	La-138 n(1,0)	2,7	58000
792,0	Sr-87 n(2,0)	18	20700
792,0	Sr-84 n(1,0)	18	20700
793,4	Sr-84 p(1,0)	18	20700
794,8	Cu-65 n(6,2)	1360	2900
795,0	Tl-210;Ac-228	r.a.	
795,3	Ba-134 p(3,1)	40	16100
803,0	Mn-55 n(8,4)	2400	950
804,0	Zr-92 n(9,3)	8,6	44800
804,0	Tl-205 g(1,0)	41	25500
804,2	I -127 n(6,1)	300	4200
806,9	Zn-68 p(3,1)	480	5800
807,5	Cu-63 g(2,1)	1000	3600
807,9	V -51 n(6,1)	5240	600
808,3	I -127 p(24,9)	300	4200
808,5	Zn-64 p(2,1)	480	5800
808,9	Nb-93 p(4,0)	14	31400
810,7	S -32 g(1,0)	105	71090
811,8	Fe-58 p(1,0)	36	27600
812,2	Ga-69 n(5,0)	280	2100
812,6	Se-80 p(3,1)	50	18400
815,6	Bi-209 n(13,3)	20	23100

Eγ keV	Assignment	Yield. quanta $sr^{-1}nC^{-1}$	Sensitivity $\mu g.g^{-1}mC^{-1}$
817,8	Cd-110 p(2,1)	4	16900
821,9	As-75 p(10,0)	125	5100
823,6	Th-232 p(9,1)	420	2400
826,0	Ru-100 p(4,1)	28	14800
826,1	Co-59 g(2,1)	88	13500
	Cd-113 g(9,0)		
826,4	Cd-114 n(9,0)	8	8000
826,4	Ni-60 p(2,1)	100	6200
827,8	Mn-55 n(7,3)	1700	1300
828,0	Zn-67 n(3,0)	64	1900
828,2	Se-80 g(7,0)	12	56500
830,3	Se-82 p(11,0)	12	56500
830,3	Se-74 a(4,0)	12	56500
830,6	Se-74 a(7,2)	12	56500
831,0	Cu-63 a(2,1)	530	6300
832,2	Ag-109 n(10,1)	20	13300
834,0	Ge-72 n,n'(2,0)		
834,0	Ga-71 g(2,0)	280	2000
834,0	Ag-107 p(8,2)	20	13300
834,4	Zn-66 p(2,1)	220	8600
835,0	Mn-54	r.a.	
835,1	Br-81 n(9,1)	91	8400
836,5	Br-81 p(7,0)	91	8400
838,7	Cr-54 n(5,0)	690	3700
	Cr-53 g(5,0)		
840,0	Cu-65 a(2,1)	950	4100
840,5	I -127 p(11,2)	55	19800
840,7	S -33 p(1,0)	1400	620
842,0	Co-59 a(1,0)	140	12100
842,7	Ba-138 n(15,0)	45	13400

Eγ keV	Assignment	Yield. quanta $sr^{-1}nC^{-1}$	Sensitivity $\mu g.g^{-1}mC^{-1}$
842,9	Sr-88 n(7,0) } Sr-87 g(7,0) }	42	5650
843,0	Zn-67 n(5,2)	200	10200
843,0	Mo-96 p(2,1)	26	11600
843,2	Dy-164 p(6,1)	12	11900
843,7	Al-27 p(1,0)	8080	390
843,7	Mg-26 g(1,0)	350	3800
844,0	Si-30 a(1,0)	150	19100
845,2	As-75 p(14,1)	500	1400
846,6	Fe-56 p(1,0)	21800	40
846,7	Mn-55 g(1,0)	670	4100
847,2	Ge-76 p(3,1)	160	2300
849,0	Hf-180 p(6,2)	160	1600
849,7	Nb-93 g(7,2)	20	21900
851,4	Ru-101 n(7,0) } Ru-100 g(7,0) }	4,3	31200
852,0	Cu-65 p(4,1)	870	3700
853,5	Cr-54 n(6,2) } Cr-53 g(6,2) }	760	3300
854,9	Ba-135 p(6,0)	44	14800
855,8	Cu-65 n(7,1)	870	3700
856,2	I -127 p(18,4)	35	27300
856,3	As-75 p(12,0)	130	4800
858,0	Cd-111 p(7,0)	5	11400
858,2	Mn-55 p(2,1)	1100	1800
861,0	Tl-208	r.a.	
863,1	As-75 p(11,0)	105	5800
863,3	Bi-209 n(6,1)	5,6	84900
863,5	Y -89 n(3,1)	13	19400
864,4	Nd-144 p(4,1)	45	6400

Eγ keV	Assignment	Yield. quanta $sr^{-1}nC^{-1}$	Sensitivity $\mu g.g^{-1}mC^{-1}$
864,6	Cu-65 n(5,0)	4300	900
865,0	I -127	560	2200
865,4	Rb-87 n(4,1)	130	3800
865,6	Ba-138 n(20,4)	44	14600
870,0	Ni-62 p(2,1)	29	24100
870,1	O -17 p(1,0)	380	700
870,9	Zn-67 p(5,0)	300	7400
871,0	Dy-160 p(7,2)	12	11800
871,0	Zn-68 g(3,0)	300	7400
871,1	Nb-93 g(1,0)	90	7800
871,1	Mo-94 p(1,0)	77	22200
871,8	Cs-133 p(13,0)	10	37600
872,0	Ga-69 p(3,0)	110	4300
872,0	Ag-107 p(2,1)	9,9	90000
872,7	Bi-209 n(7,1)	31	16300
873,0	Sr-87 p(2,0)	14	24600
873,4	Ni-61 n(3,1)	29	24100
874,0	I -127 n(7,4)	36	28200
877,8	Co-59 n(3,0)	2210	710
879,9	Rh-103 p(12,0)	4	142000
880,7	Cd-116 n(6,0)	3	24800
882,5	Cl-35 p(3,2)	72	14600
884,0	Dy-156 p(7,1)	16	6900
886,0	Se-78 p(3,1)	40	17200
886,3	As-75 p(13,0)	210	3100
888,0	Zn-67 p(6,0)	130	12600
889,0	Sc-45 g(1,0)	2100	640
889,2	Ti-46 p(1,0)	1990	560
889,9	Sc-45 p(11,3)	2100	640
890,4	Th-232 p(12,0)	730	1300

Eγ keV	Assignment	Yield. quanta $sr^{-1}nC^{-1}$	Sensitivity $\mu g.g^{-1}mC^{-1}$
890,8	Dy-156 p(6,0)	14	8700
891,0	Ag-109 n(10,0)	14	17900
891,0	Y -89 g(6,2)	12	15800
892,0	Hf-180 p(9,2)	115	5400
892,0	I -127 n(8,4)	5,4	124600
894,0	Ge-72 n,n'(4,2)		
894,3	Ga-71 g(4,2)	72	6300
896,3	Bi-209 p(1,0)	82	6300
896,6	Sn-119 p(4,1)	15	32600
897,5	Sn-119 p(5,1)	15	32600
897,9	I -127 n(11,2)	52	22100
899,1	Cu-63 p(6,2)	480	6800
907,5	Pt-190 p(6,1)	20	32000
907,9	Ba-130 p(2,0)	43	14900
908,0	Y -89 p(1,0)	20	10900
908,2	I -127 p(25,9)	480	2200
909,0	Ag-109 p(9,4)	20	25300
909,8	Cu-63 n(7,0)	2800	1500
910,2	Zn-70 g(5,0)	79	3200
910,8	Cr-53 n(2,1)	1750	1800
911,0	Ac-228	r.a.	
911,0	Zn-67 n(4,0)	79	3200
911,4	Ge-76 p(6,2)	18	17000
913,6	Rb-85 n(8,0)	190	2200
914,0	Ni-58 g(2,0)	72	10100
918,9	Zr-94 p(1,0)	18,7	17300
920,1	I -127 p(13,2)	39	32500
920,5	Sn-119 p(4,0)	105	6000
923,3	Sn-117 n(3,0)	105	6000

Eγ keV	Assignment	Yield. quanta $sr^{-1}nC^{-1}$	Sensitivity $\mu g.g^{-1}mC^{-1}$
926,8	Sc-45 p(5,0)	350	3300
927,0	Ag-109 n(11,0)	11	22800
927,3	Ga-69 n(9,2)	140	3800
928,4	Ti-48 p(4,2)	20	49200
929,0	Ti-50 g(2,0)	20	49200
929,0	I -127 n(9,0)	320	3200
929,0	V -51 p(2,0)	410	1730
930,3	Cl-35 p(4,2)	81	14300
931,4	Mn-55 n(2,0)	3400	90
932,4	Cu-65 n(8,2)	2500	1600
933,4	I -127 p(10,1)	330	3200
933,7	Zr-92 p(1,0)	60	6500
933,8	In-115 p(5,0)	33	8900
934,5	Cr-52 p(2,1)	180	13500
935,0	Bi-214	r.a.	
935,0	V -51 g(2,1)	320	2200
936,2	Ba-136 n(16,6)	44	14500
939,9	O -18 n(1,0)	900	280
941,0	Ga-69 g(4,2)	140	3300
941,3	Ba-138 n(19,2)	57	10300
943,0	Th-232 p(13,2)	540	1610
944,0	Nb-93 n(1,0)	40	16900
945,1	Ti-48 p(5,2)	40	22800
950,1	Nb-93 p(6,0)	110	4900
955,1	Cr-54 n(6,1)	22	120000
	Cr-53 g(6,1)		
961,0	Ni-62 g(2,0)	18	47000
961,4	Ba-138 n(18,0)	44	15400
962,0	Sc-45 p(6,1)	1400	860
962,2	Cu-63 p(2,0)	18800	500

Eγ keV	Assignment	Yield quanta $sr^{-1}nC^{-1}$	Sensitivity $\mu g.g^{-1}mC^{-1}$
962,3	Dy-160 p(6,1)	40	5600
963,0	Cd-112 n(10,0) }	2	67900
	Cd-111 g(10,0) }		
963,5	Zr-92 p(3,1)	6,9	53900
964,7	Ga-71 p(5,0)	44	10600
969,0	Ac-228	r.a.	
969,5	I -127 g(2,1)	2140	430
970,0	Sn-114 p(6,1)	20	23400
970,0	Ni-60 g(2,0)	10	91600
970,4	Fe-56 n(4,0)	35	25400
970,7	Sn-119 n(4,0)	20	23400
971,0	Pr-141 p(2,1)	80	2800
972,0	Mo-98 p(4,1)	2,7	53500
972,4	In-115 g(5,1)	10	35500
973,5	Ag-107 p(6,0)	8	31300
974,4	Sc-45 p(6,0)	2500	490
974,8	Mg-25 p(4,2)	1360	1290
978,1	Se-74 a(7,0)	54	12300
979,0	Nb-93 p(7,0)	46	14200
980,4	K -41 p(1,0)	135	1360
981,2	Th-232 p(19,2)	3700	270
982,6	Hf-180 p(11,2)	65	8500
983,5	Ti-48 p(1,0)	17700	54
985,0	Mn-55 n(9,3)	260	9000
985,0	Mn-55 p(2,0)	260	9000
986,0	Ti-49 n(5,2)	17700	54
986,5	Sn-115 p(4,0)	10	33400
986,4	In-115 n(4,0)	30	11200
986,5	Sn-115 p(4,0)	10	33400

Eγ keV	Assignment	Yield. quanta $sr^{-1}nC^{-1}$	Sensitivity $\mu g.g^{-1}mC^{-1}$
986,8	I -127 p(11,1)	240	4400
987,9	Se-82 g(5,0)	14	49300
990,0	Ba-132 p(2,0)	45	15100
990,1	Mg-25 p(4,2)	290	4800
990,6	Se-74 a(8,0)	14	49300
990,8	Hf-180 p(4,1)	300	1250
991,0	I -127 p(10,0)	1980	480
991,5	Zn-64 p(1,0)	10200	210
991,5	Cu-63 g(1,0)	4400	900
992,0	Bi-209 p(6,2)	6,8	43000
993,1	Nb-93 g(4,1)	14	32600
994,5	Ga-69 n(8,0)	23	22500
997,0	Co-59 n(5,1)	4500	370
997,3	Ag-109 n(13,0)	7,3	29300
1000,0	Sb-121 p(5,1)	15	30900
1004,0	Ru	5,7	35600
1006,0	Cr-53 p(2,0)	430	6000
1012,9	Ag-109 p(9,3)	4,8	35600
1013,0	Ru-96 n(4,1)	55	5300
1014,4	Mg-26 g(2,0)	820	2200
1014,5	Al-27 p(2,0)	22700	110
1015,0	Si-30 a(2,0)	460	7500
1015,7	I -127 p(15,2)	100	10200
1021,0	Ti-48 g(4,0) Ti-49 n(4,0)	470	1800
1022,0	Be-9 g(2,1)	2,1	120400
1023,0	B -10 p(2,1)	2140	860
1026,0	Cd-113 n(3,0) Cd-112 g(3,0)	16	3200
1026,1	Cd-108 n(3,0)	16	3200

Eγ keV	Assignment	Yield. quanta $sr^{-1}nC^{-1}$	Sensitivity $\mu g.g^{-1}mC^{-1}$
1027,0	Ga-69 p(4,0)	1540	381
1027,4	Ni-69 p(1,0)	5,1	174000
1029,3	Th-232 p(15,1)	3750	260
1029,4	Hg-200 p(3,0)	6,7	52300
1031,0	Rb-85 n(9,1)	75	3600
1032,8	Sc-45 p(10,2)	63	7300
1034,0	Nb-93 p(5,4)	85	6800
1035,6	Pr-141 g(5,4)	110	2200
1037,0	I -127 p(12,1)	980	1400
1038,5	Ba-134 p(4,1)	75	6400
1039,2	Zn-66 p(1,0)	5220	320
1039,4	Cu-65 g(1,0)	650	5500
1039,5	Ga-69 g(1,0)	600	970
1041,9	O -18 n(2,0)	1230	230
1042,0	Nd-146 p(2,0)	15	8800
1043,8	As-75 p(14,0)	74	9100
1044,4	I -127 p(11,0)	980	1400
1047,5	Cu-65 n(8,0)	2600	1700
1047,7	Ba-136 p(4,1)	82	6100
1048,0	Cu-65 n(10,3)	2600	1700
1048,4	Hf-180 p(5,1)	160	3800
1048,5	Sn-119 n(5,0)	65	8900
1048,8	Ti-46 p(5,2)	88	8700
1049,0	Ti-49 n(5,1) Ti-48 g(5,1)	88	8700
1049,4	Cu-63 p(7,2)	2600	1700
1053,0	Zn-67 n(6,2)	100	10300
1054,0	I -127 a(5,1)	48	14100
1056,1	Sc-45 p(16,6)	310	4400
1056,2	Th-232 p(20,1)	310	2800

Eγ keV	Assignment	Yield. quanta $sr^{-1}nC^{-1}$	Sensitivity $\mu g.g^{-1}mC^{-1}$
1062,8	Cd-108 g(12,1)	7	12200
1065,0	Ti-48 p(7,2)	110	7100
1065,0	Ti-49 n(6,1)	110	7100
1066,0	I -127 p(13,1)	4,6	106100
1070,0	I -127 n(7,1)	100	9900
1072,5	Th-232 p(18,1)	1120	1000
1076,8	Rb-85 g(1,0)	66	7200
1077,3	Zn-68 p(1,0)	1630	1100
1077,7	In-115 p(4,0)	50	7200
1080,9	O -18 n(3,0)	270	960
1082,5	Zr-91 n(2,1)	205	1900
1082,5	Nb-93 p(8,0)	120	4400
1090,0	Hf-180 p(7,1)	120	7000
1090,0	Sn-119 n(7,0)	50	10600
1092,0	Ti-47 p(2,1)	180	4200
1094,5	I -127 p(12,0)	110	10000
1098,7	Ga-69 g(11,3)	260	2200
1098,9	Co-59 p(1,0)	270	5700
1101,1	Cd-110 g(3,0) Cd-111 n(3,0)	33	2200
1102,0	B -11 2124-1Me	1960	1470
1102,0	Sb-121 p(6,1)	27	23800
1106,0	Ga-69 p(5,0)	120	1400
1107,0	Br-81 n(10,0)	73	12000
1107,0	Zn-68 g(5,0)	320	7800
1107,1	S -36 a(3,1)	8	146000
1107,2	Hf-180 p(9,1)	250	2500
1107,5	Zn-70 g(1,0)	320	7800
1110,0	I -127 n(9,4)	39	19500
1113,0	Ga-69 g(4,1)	84	1800

E_γ keV	Assignment	Yield. quanta $sr^{-1}nC^{-1}$	Sensitivity $\mu g.g^{-1}mC^{-1}$
1114,0	Cu-65 p(2,0)	600	7000
1116,0	Cr-53 n(6,2)	460	6600
1119,4	Cu-63 p(9,2)	600	7000
1120,0	Bi-214	r.a.	
1120,6	Ti-46 p(2,1)	50	15400
1121,0	Sc-45 p(4,1)	280	4500
1121,0	Hg-199 n(3,0)	8,4	46000
1121,4	W -182 p(4,1)	3	38800
1121,8	Th-232 p(18,0)	110	10000
1121,8	O -18 n(4,0)	43	6900
1122,4	Y -89 g(7,2)	22	14700
1124,0	I -127 p(13,0)	41	19300
1125,0	I -127 p(14,1)	41	19300
1127,0	Pr-141 p(3,0)	27	10200
1128,0	Na-23 1637-Me	780	10400
1129,0	Zr-90 p(6,3)	23	18800
	Cd-112 g(4,0)		
1132,0	Cd-113 n(4,0)	11	15700
1132,6	In-115 p(9,0)	26	11800
1137,0	Cu-65 n(12,3)	710	5000
1137,8	Cu-65 n(10,2)	710	5000
1139,0	I -127 p(24,3)	37	16300
1139,0	Bi-209 g(7,1)	33	12400
	Ti-48 g(5,0)		
1140,0	Ti-49 n(5,0)	165	4800
1140,0	Ga-69 g(6,1)	190	1750
1143,0	Th-232 p(21,0)	460	1900
1143,0	I -127 g(3,1)	23	22100
1147,9	V-51 n(10,3)	420	1800
1155,0	Bi-214	r.a.	

Eγ keV	Assignment	Yield. quanta $sr^{-1}nC^{-1}$	Sensitivity $\mu g.g^{-1}mC^{-1}$
	Ti-48 g(6,0)		
1155,0	Ti-49 n(6,0)	380	1900
1156,9	Ca-44 p(1,0)	560	500
1160,0	Zn-67 n(7,2)	230	4300
1161,0	I -127 p(15,1)	38	16800
1164,5	V -51 n(3,0)	1420	210
1166,0	Mn-55 p(3,1)	50	59000
1171,5	Sn-120 p(1,0)	60	8200
1172,8	Ni-62 p(1,0)	350	3000
1173,0	Ba-130 g(11,0)	93	5900
1173,1	Cu-65 a(1,0)	590	6500
1173,2	Co-59 g(3,1)	410	6900
1177,0	Cu-63 a(4,1)	420	8000
1177,7	I -127 n(8,1)	270	4300
1182,4	Ga-69 n(13,2)	42	6700
1183,0	I -127 p(14,0)	370	2600
1189,4	Co-59 n(4,0)	4920	360
1190,2	Co-59 p(2,0)	4920	360
1196,0	Zn-67 n(8,2)	110	15000
1196,0	Al-27 p(3,2)	280	9400
1196,0	I-127 n(7,0)	250	5100
1202,0	Zn-69 n(5,0)	450	4000
1204,9	Zr-91 p(1,0)	175	2300
1206,0	Zn-68 g(7,1)	12	32600
1208,0	Ga-69 p(7,1)	16	17900
1208,0	S -32 2230-2Me	620	2030
1212,7	Sn-119 n(6,0)	15	28400
1212,8	Cr-52 p(3,1)	140	24400
1213,0	Bi-209 n(4,0)	23	11500
1213,0	I -127 n(10,3)	9,3	42000

Eγ keV	Assignment	Yield. quanta $sr^{-1}nC^{-1}$	Sensitivity $\mu g.g^{-1}mC^{-1}$
1213,7	Mn-55 n(7,2)	1800	1300
1215,6	Ga-69 g(2,0)	39	7300
	Cd-110 g(6,0)		
1218,0	Cd-111 n(6,0)	11	6100
1218,6	I -127 p(15,0)	6,7	91300
1219,3	Cl-35 p(1,0)	10500	130
1220,0	Cd-116 p(2,0)	11	6100
1223,0	Na-24	r.a.	
1223,3	Pr-141 n(3,0)	21	10600
1223,6	Fe-57 n(2,0)	44	15900
	Fe-56 g(2,0)		
1225,2	Mn-55 n(11,3)	990	2300
1228,5	Rb-87 n(3,0)	150	3600
1228,8	Cu-65 n(12,2)	1500	2500
1229,0	Sr-87 p(3,0)	16	22240
1229,5	I -127 p(16,0)	190	4400
1230,0	Mo-98 p(5,1)	4,6	38300
1230,1	Ga-71 g(5,2)	15	17800
1230,2	Sn-118 p(1,0)	45	12600
1230,5	La-139 n(12,3)	4,4	75900
	La-138 g(12,3)		
1234,6	Ba-136 p(6,1)	120	4700
1235,8	F -19 p(3,1)	55000	130
1237,0	Fe-56 p(2,1)	190	2900
1237,1	Sc-45 p(8,0)	3200	360
1237,5	Rb-87 n(7,2)	17	23900
1238,0	Bi-214	r.a.	
1238,0	Mn-55 g(2,1)	2800	6600
1254,3	Cu-65 n(13,2)	1900	1700
1260,8	I -127 n(18,3)	200	3900

E_γ keV	Assignment	Yield. quanta $sr^{-1}nC^{-1}$	Sensitivity $\mu g.g^{-1}mC^{-1}$
1261,0	F -19 p(4,2)	62	10600
1261,0	Ba-136 p(7,1)	66	7100
1263,0	Cu-65 n(14,3)	1300	2200
1263,9	Cu-65 n(11,0)	1300	2200
1266,1	P -31 p(1,0)	39100	25
1267,9	Al-27 1779-Me	340	6700
1272,0	Co-59 n(8,2)	96	12600
1273,0	Si-29 p(1,0)	3600	750
1275,0	Na-24	r.a.	
1280,0	In-115 n(5,0)	29	10500
1288,4	Cr-53 n(2,0)	2300	1300
1289,6	Sc-45 p(9,0)	120	7500
1291,2	Co-59 p(3,0)	95	12800
1293,3	Sn-116 p(1,0)	25	20600
1293,6	K -41 p(2,0)	69	2980
1296,0	Rb-87 n(8,2)	52	10000
1300,0	Sn-114 p(1,0)	25	20600
1301,0	Co-59 n(5,0)	150	7200
1307,0	Ga-69 n(12,0)	140	2200
1309,4	Ba-136 p(8,1)	260	2900
1310,0	Cu-63 g(2,1)	910	3900
1312,2	Ti-48 p(2,1)	160	4700
1314,0	Ni-61 n(3,0)	20	29500
1316,4	Mn-55 n(3,0)	13400	210
	La-138 g(5,0) }		
1320,0	La-139 n(5,0) }	7,1	24600
1321,2	Ni-58 p(3,1)	10	41100
1325,9	I -127 n(18,3)	180	5400
1326,9	Bi-209 n(5,0)	38	8700

Eγ keV	Assignment	Yield. quanta $sr^{-1}nC^{-1}$	Sensitivity $\mu g.g^{-1}mC^{-1}$
1327,0	Cu-63 p(3,0)	9900	950
1327,5	Fe-58 a(4,2)	86	5100
1329,0	Cu-63 a(1,0)	5600	960
1332,0	Cr-52 p(4,1)	230	10500
1332,0	Co-59 g(1,0)	750	1290
1332,2	Ga-69 g(13,4)	78	36700
1332,5	Ni-60 p(1,0)	2100	320
1333,0	Zn-66 p(3,1)	180	8800
1333,0	V -51 g(3,1)	35	12000
1335,0	Zn-68 g(6,0)	180	8800
1335,0	Cr-53 g(8,1)	230	10500
1336,2	Ga-69 p(6,0)	78	36700
1337,0	Co-59 n(6,1)	3730	380
1338,0	Th-232 p(26,1)	150	6100
1338,7	Sn-119 n(8,0)	50	12200
1339,4	Ga-69 g(9,3)	78	36700
1342,6	Cu-63 p(7,1)	550	5300
1343,8	Cu-65 n(12,0)	550	5300
1345,0	Pr-141 n(4,0)	15	13200
1345,7	F -19 p(3,0)	2400	330
1347,4	La-139 n(6,0)	6,4	33700
	La-138 g(6,0)		
1348,6	F -19 p(4,1)	2400	330
1350,2	I -127 p(19,1)	170	2500
1353,0	V -51 n(4,0)	1120	790
1354,8	Cu-65 n(14,2)	1200	2500
1356,9	F -19 p(5,2)	2,2	128000
1361,0	Ti-49 n(7,2)	20	37100
	Ti-48 g(7,2)		
1364,0	Nb-93 n(2,0)	1270	610

Eγ keV	Assignment	Yield. quanta $sr^{-1}nC^{-1}$	Sensitivity $\mu g.g^{-1}mC^{-1}$
1366,7	Al-27 p(3,1)	10300	230
1366,7	Mg-26 g(3,1)	21800	86
1368,6	Mg-24 p(1,0)	21800	86
1369,0	Na-24 g(1,0)	42	34900
1369,6	Cu-65 n(13,0)	1300	2400
1370,0	Mn-55 n(10,2)	1900	550
1371,0	Pr-141 n(5,1)	241	1100
1372,0	Mo-100 p(5,1)	21	20500
1375,3	Cr-53 g(7,0)	130	19500
1377,3	Fe-57 n(2,0) }	590	860
	Fe-56 g(2,0) }		
1378,0	Bi-214	r.a.	
1384,5	Zr-92 p(2,0)	28	11900
1392,3	Th-232 p(32,2)	230	3900
1393,8	I -127 n(20,4)	20	42800
1394,0	Ti-47 p(4,1)	55	12700
1399,6	Cr-53 g(9,1)	135	18700
1403,1	Pr-141 n(7,1)	10	16900
1408,0	Bi-214	r.a.	
1408,2	Fe-54 p(1,0)	530	900
1408,3	Mn-85 n(4,0)	5400	450
1409,0	I -127 n(10,1)	210	3800
1409,1	Sc-45 p(10,0)	1500	730
1409,8	K -40 a(1,0)	78	2130
1409,8	Cl-37 n(1,0)	1950	640
1411,8	Cu-63 p(4,0)	4300	770
1412,0	Ni-62 g(4,0)	7,1	44300
1412,0	Ga-69 g(8,1)	63	4300
1412,0	Zn-66 p(4,1)	160	12400
1412,5	Zn-67 n(6,0)	160	12400

Eγ keV	Assignment	Yield, quanta $sr^{-1}nC^{-1}$	Sensitivity $\mu g.g^{-1}mC^{-1}$
1413,2	Sn-119 n(9,0)	55	11500
1417,7	Bi-209 n(7,0)	16	30100
1423,0	Ti-49 n(7,1) }	15	33300
	Ti-48 g(7,1) }		
1428,9	Nb-93 g(5,1)	1420	420
1432,0	Co-159 p(4,0)	3380	390
1433,6	Sc-45 p(11,0)	160	5200
1434,1	Cr-52 p(1,0)	36600	140
1434,5	V -51 g(1,0)	500	1400
1437,8	Ti-48 p(3,1)	370	1700
1440,1	Th-232 p(30,1)	870	1400
1440,1	Cr-53 n(3,0)	36600	140
1444,2	F -19 p(5,1)	176	3800
1447,5	Th-232 p(37,2)	290	2400
1453,0	I -127 n(12,4)	154	10900
1454,0	Ni-58 p(1,0)	4360	110
1458,6	F -19 p(4,0)	298	2300
1461,0	Co-59 p(5,0)	680	1560
1461,0	K -40	r.a.	
1463,0	Cu-63 a(5,1)	370	7200
1463,0	In-115 p(14,0)	21	13600
1464,0	Ga-71 g(3,0)	33	7300
1466,3	Zr-91 p(1,0)	24	15400
1469,9	Cu-65 n(14,0)	170	15000
1470,0	Pr-141 g(15,1)	90	2600
1471,0	O -18 1982-Me	340	810
1471,8	S -33 p(3,1)	870	11000
1473,0	Cu-65 n(16,2)	170	15000
1479,0	Co-59 p(6,0)	190	5900
1480,3	V -51 p(5,2)	4960	880

Eγ keV	Assignment	Yield. quanta $sr^{-1}nC^{-1}$	Sensitivity $\mu g.g^{-1}mC^{-1}$
1480,3	V -51 n(5,0)	4960	880
	Ti-48 g(8,2)		
1491,0	Ti-49 n(8,2)	50	14100
1492,0	Ti-50 g(3,1)	50	14100
1493,0	V -51 p(4,1)	410	1300
1507,0	Y -89 p(2,0)	58	2200
1507,5	Mn-55 n(5,1)	510	3700
1508,0	Zr-91 n(5,1)	86	4400
1508,5	Ti-48 g(9,2)	195	3400
1509,0	Bi-214	r.a.	
1509,0	Cd-108 p(2,0)	4	14600
1511,0	Y -89 n(4,0)	58	2200
1512,0	Ti-49 n(7,0)	195	3400
1512,0	Ti-49 n(8,1)	195	3400
1523,3	Cu-65 n(15,1)	290	10000
1524,6	Ca-42 p(1,0)	140	1540
1524,6	Sc-45 a(1,0)	130	5700
1527,0	Ga-69 p(7,0)	64	4100
1528,0	Mn-55 p(4,0)	290	2900
1529,9	Nb-93 g(6,1)	1360	530
1535,0	I -127 n(10,0)	220	3800
1542,0	Cd-111 n(9,0)	4	10600
	Cd-110 g(9,0)		
1542,0	Ti-49 p(2,0)	15	48500
1543,0	S -32 p(2,1)	27	52000
1547,0	Ni-62 g(5,0)	8,1	45000
1547,0	Cu-63 p(5,0)	2160	1300
1550,5	Ba-136 p(2,0)	230	3500
1553,0	Ti-48 g(8,1)	315	2400

E_γ keV	Assignment	Yield. quanta $sr^{-1}nC^{-1}$	Sensitivity $\mu g.g^{-1}mC^{-1}$
1554,0	Ti-50 p(1,0)	315	2400
1554,0	F -19 p(5,0)	56	11100
1555,0	Zn-67 n(8,0)	130	14700
1557,6	V -51 n(6,0)	1020	2100
1570,0	Ti-46 p(11,2)	50	12300
	Ti-48 g(10,1) }		
1570,7	Ti-49 n(10,1) }	50	12300
1575,7	Pr-141 g(1,0)	25	8400
1577,2	Cu-65 n(15,0)	590	4800
1582,0	I -127 n(18,0)	9,6	46500
1583,0	Mo-92 p(7,1)	12	28100
1585,0	I -127 n(17,1)	4,5	105200
1588,0	Ac-228	r.a.	
1588,2	Cu-65 n(16,0)	670	3700
1592,0	Bi-208	r.a.	
1594,0	Zr-96 p(1,0)	66	4900
	La-138 g(7,0) }		
1597,1	La-139 n(7,0) }	4,3	34400
1601,0	Ti-47 n(9,2)	65	8700
1602,0	Ti-49 n(8,0) }	65	8700
	Ti-48 g(8,0) }		
1608,0	Co-59 n(11,1)	440	2100
1608,0	V -51 p(3,0)	750	3400
1608,9	Bi-209 p(3,0)	39	14000
1611,3	Cl-37 n(2,0)	2660	420
1611,7	Mg-25 p(3,0)	2790	470
1613,0	B -11 2124-Me	3100	1480
1619,0	Cr-53 n(4,0)	660	3200
1622,6	Ti-49 p(4,0)	10	46700

Eγ keV	Assignment	Yield. quanta $sr^{-1}nC^{-1}$	Sensitivity $\mu g.g^{-1}mC^{-1}$
1623,0	Cu-63 p(4,0)	150	18000
1625,0	Ac-228	r.a.	
1626,7	Pr-141 n(9,1)	8	36600
1629,4	I -127 n(22,2)	35	30300
1629,6	C -13 g(2,1)	15	47400
	La-138 g(8,0) }		
1630,6	La-139 n(8,0) }	4,2	46964
1632,8	Te-130 p(3,0)	220	6500
1633,4	In-115 n(7,0)	48	6500
1633,8	Na-23 a(1,0)	80600	37
1636,5	Mg-26 a(2,1)	27	34000
1636,6	Na-23 p(2,1)	80600	37
1640,0	Ni-61 g(5,0)	8,2	30400
1640,4	Mn-55 n(6,1)	1700	1300
1645,0	Ru	8,6	32100
1661,9	Sc-45 p(13,0)	770	950
1663,0	Tl-203 g(7,0)	43	22700
1680,0	Co-59 n(7,0)	240	3800
1687,0	Bi-209 p(5,1)	5,6	82600
1693,0	Bi-214	r.a.	
1699,0	Al-27 2210-Me	530	5700
1708,2	Ga-69 g(3,0)	82	3700
1719,0	S -32 2230-Me	950	2300
1719,5	Al-27 p(4,2)	610	4200
1725,0	Cu-65 p(5,0)	60	91000
1726,6	Cl-37 p(1,0)	750	1000
1730,2	La-139 n(12,1) }	2,6	54600
	La-138 g(12,1) }		
1732,0	Bi-214	r.a.	
1732,9	Mn-55 n(7,1)	1480	11000

Eγ keV	Assignment	Yield. quanta $sr^{-1}nC^{-1}$	Sensitivity $\mu g.g^{-1}mC^{-1}$
1735,0	Co-59 n(8,0)	170	6200
1739,9	Sr-87 p(5,0)	13	20960
1741,8	C -13 g(5,2)	19	39600
1746,0	Co-59 n(9,0)	39	18000
1749,7	Sn-119 n(12,0)	30	26300
1756,0	Ru-96 p(6,1)	13	23800
1757,1	In-115 g(2,0)	6,9	49300
1757,4	Fe-57 n(5,0) }	220	2560
	Fe-56 g(5,0) }		
1758,0	Zr-96 p(2,0)	25	15200
1759,0	Y -89 g(1,0)	11	29700
1760,0	Mo-98 p(4,0)	14	24600
1760,7	Zr-90 p(1,0)	25	15200
1761,9	Ti-49 n(6,0)	8,3	67400
1763,3	Cl-35 p(2,0)	7420	180
1764,0	Bi-214	r.a.	
1770,5	Rb-87 n(5,0)	72	10600
1770,5	Sr-87 p(7,0)	14	17970
1773,0	Co-59 a(9,2)	710	1120
1774,0	Ni-58 g(6,1)	12	18900
1778,0	Co-59 n(10,0)	650	1700
1778,0	I -127 n(12,0)	40	15600
1778,0	P -31 a(1,0)	7720	140
1778,0	Zr-92 p(3,0)	17	19400
1778,9	Al-27 g(1,0)	760	4500
1779,0	Si-28 p(1,0)	31900	75
1787,0	S -34 p(3,1)	140	10400
1788,0	Sc-45 p(14,1)	8,3	55000
1796,0	Ti-48 g(11,0)	20	34200
1799,4	Cu-63 g(2,0)	430	5400

Eγ keV	Assignment	Yield. quanta $s^{-1}nC^{-1}$	Sensitivity $\mu g.g^{-1}mC^{-1}$
1800,1	Sc-45 p(14,0)	68	10500
1808,7	Mg-26 p(1,0)	410	2430
1810,0	Fe-56 p(3,1)	33	14500
1811,0	Ca-48 n(8,2)	35	8300
1814,0	V -51 p(4,0)	930	1000
1837,3	Sc-45 a(2,0)	51	14900
1847,7	Zr-92 p(4,0)	6,6	43300
1850,0	Bi-214	r.a.	
1861,2	Cu-63 p(6,0)	620	3200
1883,0	Mn-55 p(5,0)	1250	10000
1894,0	Cr-53 n(5,1)	115	15900
	Cr-52 g(5,1)		
1897,0	Fe-57 n(6,0)	18	20800
	Fe-56 g(6,0)		
1899,3	V -54 n(7,0)	630	3100
1903,0	Ti-48 g(12,0)	10	63000
1917,9	Mn-55 n(5,0)	930	2100
	Fe-56 g(7,0)		
1919,7	Fe-57 n(7,0)	115	4100
1935,5	Sc-45 p(15,0)	9,7	50100
1948,0	Co-59 n(11,0)	1200	640
1964,8	Mg-25 p(4,0)	180	3400
1966,3	S -33 p(2,0)	35	46300
1970,0	K -39 a(1;0)	110	1470
1975,0	I -127 n(23,0)	25	59800
1978,8	Mg-25 p(5,1)	110	6100
1982,1	O -18 p(1,0)	2950	120
1984,0	La-139 n(12,0)	3,6	17100
	La-138 g(12,0)		
2001,5	V -51 n(8,0)	1050	1300

Eγ keV	Assignment	Yield. quanta $sr^{-1}nC^{-1}$	Sensitivity $\mu g.g^{-1}mC^{-1}$
2028,0	Si-29 p(2,0)	690	1600
2051,2	Mn-55 n(6,0)	690	2400
2061,0	Bi-209 n(15,0)	18	19900
2103,0	Bi-208	r.a.	
2111,0	Fe-56 p(4,1)	44	10200
2124,4	B -11 p(1,0)	47800	50
2127,3	Cl-37 a(1,0)	1780	560
2127,3	S -34 p(1,0)	830	2000
	Fe-56 g(8,0) }		
2133,0	Fe-57 n(8,0) }	59	7600
2143,0	Mn-55 n(7,0)	1700	1100
2168,0	Mn-55 n(12,1)	1090	6600
2179,0	Y -89 g(2,0)	110	1700
2194,0	Cr-53 n(7,1) }	95	18000
	Cr-52 g(7,1) }		
2199,0	Mn-55 p(6,0)	1210	5800
2204,0	Bi-214	r.a.	
2210,4	Mg-26 g(3,0)	530	1540
2210,4	Al-27 p(3,0)	8750	200
2217,4	Cl-37 n(3,0)	400	2240
2228,5	S -32 p(4,1)	15700	80
2230,1	S -32 p(1,0)	15700	80
2230,1	P -31 g(1,0)	7600	40
2230,2	Cl-35 a(1,0)	6,7	49600
2233,8	P -31 p(2,0)	7600	40
2240,0	Si-30 p(1,0)	570	1700
2243,0	Na-24	r.a.	
2274,0	Cr-53 n(5,0) }	490	4050
	Cr-52 g(5,0) }		
2312,6	S -33 p(3,0)	17	22100

E_γ keV	Assignment	Yield. quanta $sr^{-1}nC^{-1}$	Sensitivity $\mu g.g^{-1}mC^{-1}$
2312,6	N -14 p(1,0)	520	1850
2312,9	C -13 g(1,0)	24	36300
2313,0	O -17 a(1,0)	10	16300
2319,7	B -11 p(2,1)	42	4100
2365,3	C -12 g(1,0)	29	27500
2405,0	Cr-53 n(6,0) } Cr-52 g(6,0) }	180	13100
2430,0	Si-29 p(3,0)	170	4900
2469,7	Mn-55 n(10,0)	980	1800
2490,5	Cl-37 n(4,0)	190	3100
2575,0	C -13 3086-Me		
2578,0	Mn-55 n(12,0)	1290	1200
2605,0	C -13 g(3,1)	47	13700
2614,0	Bi-208;Tl-208	r.a.	
2645,6	Cl-35 p(3,0)	950	640
2693	Cl-35 p(4,0)	290	1420
2698,4	Cl-35 p(7,2)	290	1420
2734,9	Al-27 p(4,0)	310	7200
2754,0	Na-24	r.a.	
2796,1	Cl-37 n(5,0)	230	2100
2981,3	Al-27 p(5,0)	44	27300
3002,5	Cl-35 p(5,0)	8,4	32500
3086,6	Cl-37 p(2,0)	290	1370
3087,0	C -13 p(1,0)	54	16600
3162,5	Cl-35 p(6,0)	34	9500
3179,6	C -13 p(4,2)	26	27300
3511,0	C -12 g(2,0)	75	21500
3562,0	Be-9 a(2,0)	11	40300
3685,0	C -13 p(2,0)	30	31100
5105,9	C -13 g(4,0)	12	11700
5270,4	N -15 p(1,0)	63	13700

$E\gamma$ keV	Assignment	Yield, quanta $sr^{-1}nC^{-1}$	Sensitivity $\mu g.g^{-1}mC^{-1}$
5298,9	N -15 p(2,0)	72	7370
6130,4	F -19 a(2,0)	880	1800
6720,0	F -19 a(3,0)	860	1900
7116,9	F -19 a(4,0)	710	2900

REFERENCE INDEX

Ah 77 M. Ahlberg, *Nucl. Instr. Meth.*, 142 (1977) 61.

Al 56 K.L. Alder, A.Bohr, T. Huus, B.Mottelson and A. Winther *Revs. Mod. Phys.*, 28 (1956) 432.

An 76 Anon, *Anal. Chem.* 48 (1976) 2294.

An 81 A. Anttila, R. Hänninen and J. Räisänen, J. *Radioanal. Chem.*, 62 (1981) 293.

Au 77 R.L. Auble, *Nucl. Data Sheets*, 20 (1977) 253.

Ba 78 H.Bank, A. Banerjee, J. Pense, W. Scheinder and W. Schrander, *Z. Deut. Gemmol. Ges.*, 27 (1978) 104.

Ba 72 R.E. Barlow, D.J. Bartholomew, J.M. Bremer and H.D. Brunk, 'Statistical Interference under Order restrictions', Wiley, New York (1972).

Ba 73 H.J. Bartsch, 'Taschenbuch Mathematischer Formaln', Verlag Harri Deutsch, Frankfurt, (1973) p. 451.

Be 55 J. Bent, Bonner and McCrary, *Phys. Rev.* 98 (1955) 1325.

Bi 78 J.R. Bird, B.L. Campbell and R.J. Cawley, Australian Atomic Energy Commission Report, AAEC/E 443 May, 1978, ISBN) 642 59650 6.

Bo 78 B. Borderie and J.N. Barrandon, *Nucl. Instru. Meth.*, 156 (1978) 483.

Bo 79a B. Borderie, J.N. Barrandon, B. Delaunay and M. Basutcu, *Nucl. Instr. Meth.*, 163 (1979) 441.

Bo 80 B. Borderie, *Nucl. Instr. Meth.*, 175 (1980) 465.

Bo 77 G.J. Boulle and M. Peisach, *J. Radioanal. Chem.*, 39 (1977) 33.

Bo 79b G.J. Boulle, M. Peisach and L. Jacobson, *S. Afr. J. Sci.*, 75 (1979) 215.

Bo 79c G.J. Boulle and M. Peisach, *J. Radioanal. Chem.*, 50 (1979) 205

Br 73 J.P. Brezéeri *et al*, 'L'Analyse de Données Vol. 2, 'L'Analyse des correspondances', Dunod, Paris (1973)

Ch 72 J.F. Chemin, J. Roturier, B. Saboya and G.Y. Petit, *J. Radioanal. Chem.*, 12 (1972) 221.

Cl 75 P.J. Clark, G.F. Neal and R.O. Allen, *Anal Chem.*, 47 (1975) 650.

Co 81 D.H. Cornell and A Uttley, Dept. of Geology, University of Stellenbosch (private communications) 1981.

Co 74 C.W. Cottrell, *J. Phys.* (London), A7 (1974) 100.

Cu 68 L.A. Currie, *Anal. Chem.*, 40 (1968) 586.

De 78 G. Demortier, *J. Radioanal. Chem.*, 45 (1978) 459.

Do 59 I. Dostrovsky, Z. Fraenkel and G. Friedlander, *Phys. Rev.*, 116 (1959) 683.

Du 80 P.J. Dunn, J.J. Brummer and H. Belsky, *Can. Mineral*, 18 (1980) 37.

Du 68 V.D. D-smatov, A.F. Efimov, Z.T. Kataeva, L. Khordshilova and Y. Yanulov, Doklady Akad. Nauk. S.S.S.R., 182 (1968) 1176.

En 79a P.M. Endt, *Atomic Data and Nuclear Data Tables*, 23 (1979) 3.

En 79b P.M. Endt, *Atomic Data and Nuclear Data Tables*, 23 (1979) 547.

En 81 P.M. Endt, *Atomic Data and Nuclear Data Tables*, 26 (1981) 47.

En 65 C. Engelmann, Proceedings of the Symposium on Radiochemical Methods of Analysis, IAEA, Vienna, 1 (1965) 405

Ev 55 R.D. Evans, 'The Atomic Nucleus', New York, Toronto, London, McGraw-Hill Book Co. (1955).

Fa 63 U. Fano, *An. Rev. Nucl. Sci.*, 13 (1963) 1.

Gi 78a I.S. Giles, Elemental Analysis by alpha-induced prompt gamma-ray Spectrometry, Thesis, University of Cape Town (1978).

Gi 78b D. Gihwala, I.S. Giles and M. Peisach, *J. Radioanal. Chem.*, 47 (1978) 145.

Gi 79a I.S. Giles and M. Peisach, *J. Radioanal. Chem.*, 50 (1979) 307.

Gi 79b D. Gihwala and M. Peisach, *S. Afr. J. Chem.*, 33 (1979) 4.

Gi 79c I.S. Giles and M. Peisach, *Cement and Concrete Research*, 9 (1979) 591.

Gi 80 D. Gihwala and M. Peisach, *S. Afr. J. Chem.*, 33 (1980) 4.

Go 57 R. Gold and C.H. Stone, AECU-3505 (1957) 1.

Go 72a N.B. Gove and A.H. Wapstra, Nuclear Reaction Q-values, *Nucl. Data Tables*, Sect. A. II (1972) 127.

Go 72b I. Golicheff, M. Loeuillet and C. Engelmann, *J. Radioanal. Chem.*, 12 (1972) 233.

Go 69 J.C. Gower and G.J.S. Ross, *Appl. Statistics*, 18 (1969) 54.

Gr 78 M.J. Greenacre, 'Some Objective Methods of Graphical Display of a Data Matrix', Special Report, University of South Africa, Pretoria, (1978).

Gr 81 M.J. Greenacre, 'Topics in Applied Multivariate Analysis'. ed. D.M. Hawkins, Report TWISK 193, National Research Institute for Mathematical Sciences, Pretoria, (1981).

Ha 77 B. Harmatz, *Nucl. Data Sheets*, 20 (1977) 73.

Ha 62 B.G. Harvey,'Introduction to Nuclear Physics and Chemistry', p. 107. Prentice-Hall International, London, (1962).

Ho 61 J. Hoste, F. Bouten and F. Adams, *Nucleonics*, 19 (1961) No. 3, 118.

Is 78a K. Ishii, M. Valladon and J.L. Debrun, *Nucl. Instr. Meth.*, 150 (1978) 213.

Is 78b K. Ishii, C. Sastri, M. Valladon, B. Borderie and J. Debrun, *Nucl. Instr. Meth.*, 153 (1978) 507.

Ko 76 D.C. Kocher, *Nucl. Data Sheets*, 18 (1976) 463.

Kr 64 J.B. Kruskal, *Psychometrika*, 29 (1964) 1.

Kr 68 J.B. Kruskal, 'How to use M-D-SCAL, a programme to do multidimensional scaling and multidimensional unfolding.', Bell Telephone Laboratories report, 1968.

La 66 T. Lauristen and F. Ajzenberg-Selove, *Nucl. Phys.* 78 (1966) 1.

Le 72 F.M. Lea, 'The Chemistry of Cements and Concrete', Edward Arnold (publishers) Ltd, Glasgow (1972).

Mu 76 N. Murakami, E. Kato, Y. Miura and F. Hirowatari, *Mineral J.*(Japan), 8 (1976) 110.

Ol 74 C. Olivier and T.B. Pierce, *Radiochem. Radioanal. Letters*, 17 (1974) 335.

Op 77 J. Op de Beeck, *J. Radioanal. Chem.*, 37 (1977) 213.

Pe 72 M. Peisach, *J. Radioanal Chem.*, 12 (1972) 251.

Pe 81a M. Peisach, *J. Radioanal. Cehm.*, 61 (1981) 243.

Pe 81b M. Peisach, 'Nondestructive Activation Analysis', ed., S. Amiel. Elsevier Scientific Publishing Co., Amsterdam, Oxford, New York, 1981.

Pi 65 T.B. Pierce, P. Peck and W. Henry, *Analyst*, 90 (1965) 339.

Ra 81 H. Ras, Simultaneous determination of boron-10 and boron-11 under proton bombardment. M.Sc Thesis, University of Stellenbosch, 1981.

Ri 65 E. Ricci and R. Hahn, *Anal. Chem.*, 37 (1965) 742.

Ri 67 E. Ricci and R. Hahn, *Anal. Chem.*, 39 (1967) 794.

Ri 68 E. Ricci and R. Hahn, *Anal. Chem.*, 40 (1968) 54.

Ro 72 R.L. Robinson, F.K. McGowan, W.T. Milner and P.L. Stelson, *Nucl. Phys.*, A 193 (1972) 14.

Ro 69 J. Routti and S. Prussin, *Nucl. Instr. Meth.*, 72 (1969) 125.

Ru 57 S. Rubin, T.O. Passel and L.E. Bailey, *Anal. Chem.*, 29 (1957) 736.

Sa 69 J.W. Sammon, I.E.E.E. Trans. Computers, 18 (1969) 401.

Sc 78 M.R. Schmorak, *Nucl. Data Sheets*, 25 (1978) 193.

Sh 73 L. Shabason and B.L. Cohen, *Anal Chem.*, 45 (1973) 284.

Sn 57 P.H.A. Sneath, *J. Gen. Microbiol.* 17 (1957) 201.

Th 67 B.V. Thosar, R.P. Sharma, K.G. Prasad and V.R. Pandharipande, Contrib. Intern. Conf. Nucl. Struct., Tokyo, p. 153 (1967).

Un 81 L.G. Underhill, Dept. of Mathematical Statistics, University of Cape Town (private communications) 1981.

Wo 75 E.A. Wolicki, 'New Uses of Ion Accelerators', ed. J.F. Ziegler, Plenum Press, New York, London, (1975) 159.

Zi 77 J.F. Zeigler, 'The Stopping and Ranges in Matter, Vol. 1-4', Pergamon Press Inc., Elmsford, New York (1977).

Zi 78 J. Ziegler *et al*, *Nucl. Instr. Meth.*, 149 (1978) 19.